

**50 years**  
**University of Mining and Geology**  
**“St. Ivan Rilski”**  
**( 1953 – 2003 )**

**A N N U A L**  
**OF THE**  
**UNIVERSITY OF MINING AND**  
**GEOLOGY**  
**“ST. IVAN RILSKI” – SOFIA**

***PART III: MECHANIZATION,***  
***ELECTRIFICATION AND AUTOMATION***  
***IN MINES***

Vol. 46

2003



**Publishing House “St. Ivan Rilski”**  
**Sofia**  
**2003**

**ISSN 1312-1820**

## **EDITORIAL BOARD:**

Assoc. Prof. Michael Michaylov, PhD – editor-in-chief  
Assoc. Prof. Strashimir Strashimirov, PhD – deputy editor-in-chief  
Assoc. Prof. Radi Radichev, PhD – chairman of editorial council  
Prof. Nikola Marhov, PhD – chairman of editorial council  
Assoc. Prof. Krastyo Dermendjiev, PhD – chairman of editorial council  
Prof. Atanas Stamatov, DSc – chairman of editorial council  
Eng. Mariana Svilarova  
Eng. Teodora Hristova

## **EDITORIAL COUNCILS:**

### **PART III: MECHANIZATION, ELECTRIFICATION AND AUTOMATION IN MINES**

Prof. Nikola Marhov, PhD – chairman  
Prof. Slavcho Donchev, DSc  
Assoc. Prof. Kancho Ivanov, PhD  
Assoc. Prof. Velichka Angelova, PhD  
Assoc. Prof. Maria Mincheva, DSc

## CONTENTS

|   |   |        |
|---|---|--------|
| Tsv. Damyanov, E. Asenov<br>Z. Mihalkov, P. Nedyalkov | Gallery support manipulator – dynamical research  | ...1   |
| Sv. Tokmakchiev                                       | Determining the load on RKS-type tangential picks   | ...5   |
| Sv. Deevski<br>K. Shehadi                             | Threshold levels of shifting and speeds in discrete regulation of mine belt conveyors   | ...9   |
| K. Shehadi  | About maximum utilization of supporting capacity of mine belt conveyors   | ...13  |
| I. Iochev<br>E. Kartzelin                             | Technical diagnostics of major components of mine winding machines  | ...17  |
| A. Yaneva   | Optimizing the selection of a hoist rope in the design and operation of shaft hoists  | ...21  |
| A. Yaneva<br>I. Iochev                                | Ways of increasing the service life of the steel ropes in the mine hoists   | ...25  |
| V. Pojidaeva  | Wear in sliding bearings from mining and ore-processing machines  | ...29  |
| N. Perenovski, A. Yaneva<br>I. Minin, Tsv. Damyanov   | A linear structural analysis of the leading sheaves of shaft hoists by the finite element method  | ...33  |
| V. Tenchev  | On the velocity of an optional point of crank mechanism connecting rod  | ...37  |
| B. Grigirov<br>St. Asparuhov                          | Trajectory investigation of a hydraulically driven manipulator  | ...41  |
| E. Asenov, E. Bosilkov<br>R. Dimitrov, Tsv. Damyanov  | Kinematics and dynamics of working mechanism of hydraulic excavator   | ...47  |
| E. Asenov,<br>M. Yancheva<br>R. Vucheva               | Research of centrifugal-impact-vibrating mill /CIVM/ working process  | ...51  |
| Sl. Donchev<br>V. Pojidaeva                           | Studying some of the tribo-characteristics of mineral grinding  | ...55  |
| Sl. Donchev<br>G. Takov                               | An electrophysical technology for improvement of the durability (under wear) of the cutters of the cutter-loaders   | ...59  |
| V. Tasev  | Application of centrifugal ball clutch to the drive of a mill fan at the “Bobov Dol” power plant  | ...63  |
| A. Smilianov<br>F. Kuzmanov                           | On the probabilistic character of haulage for routes with movable railroads   | ...67  |
| A. Smilianov  | Theoretical investigation of the applicability Manevich-Pavlenko model for determining the strength of extraction of a single traverse from the ballast prism of a movable railroad | ...71  |
| P. Zlatanov<br>A. Smilianov<br>F. Kuzmanov            | Technical condition of movable railroads and effect on technological parameters of combined operation of railroad haulage and bucket wheel excavators                               | ...81  |
| N. Cristea<br>G. Gherman<br>G. Cristea                | Sampling device adaptable to the high capacity conveyer – belts   | ...87  |
| J. Zaimov   | Ventilation of zones of potentially explosive gas atmosphere  | ...91  |
| K. Djustrov, D. Kostov<br>M. Menteshhev               | Dc mains insulation resistance control in electrolysis shops  | ...95  |
| A. Zabchev  | Topographical method for solving problems of three-phase circuits   | ...99  |
| St. Stefanov<br>A. Zabchev                            | Analyses of one electrostatic problem and its application in measurement of the electrostatic field parameters  | ...103 |
| V. Tasev<br>I. Iordanov                               | Transformation of mine battery locomotive 4,5 ARP into a trolley locomotive   | ...107 |

|   |   |        |
|---|---|--------|
| K. Trichkov<br>B. Petrova   | About the temperature regime of an induction motor, supplied by a controlled inverter   | ...111 |
| N. Genadiev<br>V. Bagarov   | Investigation and estimation of higher harmonics in power network of charge station in underground coal mine "Ivan Rousev"              | ...113 |
| V. Bagarov<br>J. Stoyanov   | System of energy management of electricity consumption in the concentration plant "Elacite Med"   | ...117 |
| R. Vuicheva   | Energy absorption rate at the mechanical treatment of specularite from bulgarian deposits   | ...121 |
| Ts. Georgiev<br>T. Varbev   | Failurs of the power supply system of open – air mine "Hristo Botev" of mines "Bobov Dol" ltd.  | ...125 |
| T. Varbev   | Safety analysis of the power supply systems in open-air mines of Bulgaria   | ...129 |
| T. Varbev, Tz. Georgiev,<br>P. Petkova                              | Data failure analysis of power supply system in mine "Kremikovtzi"  | ...133 |
| S. Siderov, N. Matanov,<br>B. Boychev, V. Georgiev                  | Structure and operation of the microprocessor analyzer of the electromagnetic compatibility of electrical power systems                 | ...137 |
| S. Siderov, N. Matanov,<br>B. Boychev, V. Georgiev                  | Algorithm for evaluating the basic characteristics of the electromagnetic compatibility of electrical power systems by digital analyzer | ...143 |
| I. Stoilov, K. Djustrov<br>M. Menteshv, A. Trapov                   | System for measuring control and monitoring of power consumption at the dressing plant of the "Elatsite-Med" Co                         | ...149 |
| I. Stoilov, D. Tzvetkov<br>E. Filipov                               | Structure of power consumption of dressing plant at the "Elatsite – Med" Co   | ...155 |
| St. Chobanov, M.<br>Menteshev                                       | Innovations in CMC-C electroengineering   | ...161 |
| N. Stefanova<br>A. Zabchev<br>M. Mateev                             | Scheme and technical means for automated control of the compressor station in quarry first of may – marble and granite corporation      | ...165 |
| D. Tasheva<br>S. Iliiev   | Mathematical models with improved characteristics in the control systems of wheel excavators  | ...171 |
| V. Hristov<br>St. Garabotov   | E-engineering: a project for mechanical constructions design over internet  | ...177 |
| T. Kisiova  | Applying multifactor logico-probabilistic functions in local ecological monitoring  | ...181 |
| N. Janev, K. Ivanov<br>V.Karagiozov, I. Starbanova<br>Y. Anastasova | Opportunities for implementation of web interface in data base works in the mining industry   | ...185 |
| M. Radovonovic  | Organizations and manufacturers in field of laser   | ...191 |
| V. Angelov  | Neutral equations with polynomial nonlinearities arising in transmission lines  | ...197 |
| V. Angelov  | On the neutral lossless transmission line equations with tunnel diode and a lumped parallel capacitance                                 | ...201 |
| V. Angelov<br>D. Angelova<br>L. Georgiev                            | Nonlinear circuits with polynomial resistive elements   | ...205 |
| J. Dimitrov   | Automatic recognition of scales, grids and tables in scanned mechanical drawing   | ...209 |

|   |  |        |
|---|--|--------|
| E. Kartzelin,<br>R. Istalianov, P. Petrov,<br>S. Vasilev, L. Todorov,<br>N. Nikolov | Electric power supply of underground mines for machine production of coal  | ..213  |
| A. Kotlyarov ,N. Matvienko<br>E. Kartzelin, R. Istalianov                           | Rising a level of safety work of miners – the main direction of activity of the publicly held company “Krasny Metallist”         | ..219  |
| I. Antonov  | Two-phase turbulent flows. Methods for description and numerical modeling  | ...221 |
| V. Dimova<br>P. Lalov   | Stationary stream of viscose fluid in a pipe with finite length  | ...225 |
| M. Michaylov, N. Marhov<br>E. Vlaseva, Z. Dinchev                                   | Risk analysis of mine equipment  | ...227 |
| M. Michaylov  | Modeling of gas jet distribution in porous environment   | ...233 |
| N. Nikolov  | Issues of noise of mine fans   | ...241 |
| N. Nikolov  | Reververations in large areas  | ...245 |
| V. Tomov  | Dynamics evaluation of risk factors  | ...247 |
| Y. Podobnaja,<br>P. Molchanov, T. Holieva   | Accident risk assessment at the electrical engineering objects on the linguistic   | ...253 |
| L. Popesku<br>O. Olaru<br>F. Grofu  | Speed control systems of the electrical motors<br>Which are driving the mechanism of the ERC port-wheel excavators               | ...259 |
| O. Olaru<br>L. Popesku<br>G. Gidei  | Applications of stepping motors in mining appliances   | ...265 |
| N. Nedić, R. Petrović,<br>L. Dubonjić   | Dynamic behavior of servo controlled hydrostatic power transmission system with long transmission line                           | ...267 |
| O. Daniela, C. Vasile<br>P. Ovidiu  | The possibility of aplying the selsines in commanding the cupe wheel excavators  | ...273 |
| C. Vasile, O. Daniela,  | About the magnetical characteristics of the synchronous motor, proposed in activating the conveyors from the lignite mine shafts | ...279 |

## GALLERY SUPPORT MANIPULATOR – DYNAMICAL RESEARCH

**Tsvetan Damyanov**

**Emil Assenov**

**Zahari Mihalkov**

**Patar Nedyalkov**

University of Mining and Geology  
"St. Ivan Rilski"  
Sofia, 1700 Bulgaria

TU  
Sofia, Bulgaria

University of Mining and  
Geology "St. Ivan Rilski"  
Sofia, 1700 Bulgaria

University of Mining and  
Geology "St. Ivan Rilski"  
Sofia, 1700 Bulgaria

### ABSTRACT

The results of kinematic and dynamic study of gallery support manipulator are shown. A methods for 3D SolidWorks modeling and the Dynamic Designer simulation is created. The results present the telescope velocity and acceleration and dynamic reaction in the linkage of the arm and the jib, the jib, and column forces and the force of the hydraulic cylinder.

### INTRODUCTION

Forming of steady support gallery is an important part in technological process. It has an advantage as high level of technical security of support and good technical and economical parameters. The object of study is a manipulator that was created by the author team from "Minsstroy". This manipulator as similar as "Maschinen-fabrik – Moeminghoff's" manipulator. It causes of – vertical rotated column, two telescopic job, a special catch unit with local structure with two degree of freedom. The manipulator can work with heavy beton element with weight of 500 – 1000 kg and create the gallery with diameter -  $\varnothing$  4,0 - 4,5m.

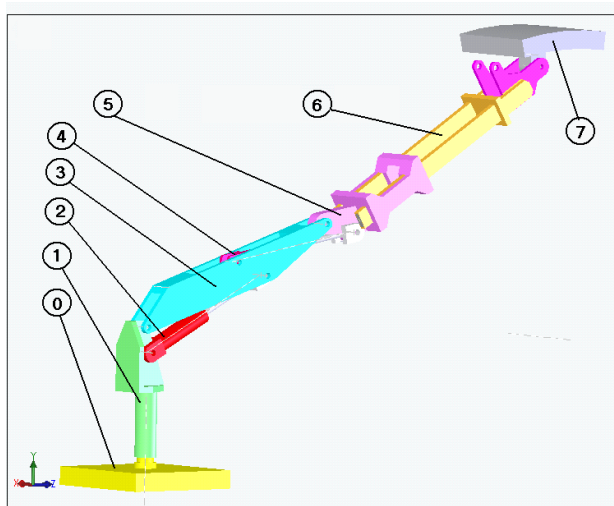


Figure 1 Scheme of the manipulator

A scheme of the manipulator is show in Fig. 1, where:

- 0 – base;
- 1 – column with vertical rotated R linkage;
- 2 – leading cylinder for jib;
- 3 – jib;
- 4 – leading cylinder for arm;
- 5 – arm with horizontal R linkage;

6 – telescopic arm with translation T linkage with the arm;

7 – support element;

The manipulator technical parameters are given in Table 1.  
Table 1

| No | parameter  | dimen sion | value          |
|----|--|------------|----------------|
| 1  | Load – minimal   | kN         | 10             |
| 2  | Stroke of the telescope – $S_3$  | mm         | 1100           |
| 3  | Angle of rotation of vertical column -   | deg        | 210°           |
| 5  | Angle between arm and job – $\beta$<br>minimal -<br>maximal -                          | deg        | 40°<br>185°    |
| 6  | Angle of rotation of support element perpendicular to the axis of the job - $\alpha_z$ | deg        | 45°            |
| 7  | Angle of rotation of sup. elem-ent around of the job axis - $\alpha_x$                 | deg        | 360°           |
| 8  | Maximum rotation moment of the catch mechanism   | Nm         | 1200           |
| 9  | Distance between axis of the manipulator rotation and the catch mechanism              | mm         | 3560 -<br>4660 |
| 10 | Working pressure   | MPa        | 20             |
| 11 | Width of beton element   | mm         | 800            |
| 12 | Mass of the manipulator  | kg         | 1000           |

The manipulator is part on the loader 2PNB-2, and the machine has high effectiveness.

The dynamical study of the manipulator is important because of high weight of the beton element (1000 kg) and weight of the manipulator elements creates large dynamical forces in the unestablished work rates. Also of the fact that operator work, so we have a biotechnical control system in changeable work cycles and conditions.

The aim of this works is to:

1. Make a computer modeling of a parameters of high loaded manipulator elements;
2. Define the conditions of kinematical scheme, driving system, manipulator metrics and object and special feature of technological process;
3. Create 3D – assembly model in Solid Works with correct kinematical linkages between moving;
4. Define the dynamic parameters in Dynamic Designer environment;
5. Structure of the computing module and decision of the dynamical purpose, in conformity with nominated methodics for development.

GEOMETRICAL MODEL

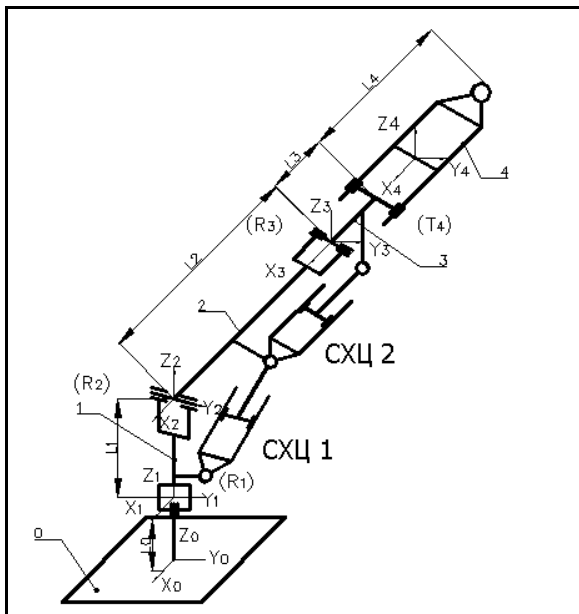


Figure 2 – Kinematical scheme of the manipulator

The kinematical scheme of the geometric model is shown in Fig.2. There are shown relations between parts. This type of scheme allows mathematical purpose of the kinematical parameters for all parts related to the base. The shown parts are:

- 0 – base grounded part;
- 1 – column with rotatory (R<sub>1</sub>) linkage to the base and vertical axis (Z<sub>0</sub>) of relative rotation (φ<sub>1</sub>);
- 2 – jib with rotatory (R<sub>2</sub>) linkage to the column (1) and horizontal axis (Y<sub>2</sub>) of relative rotation (φ<sub>2</sub>);
- 3 – arm with rotatory (R<sub>3</sub>) linkage to the jib (2) and horizontal axis (Y<sub>3</sub>) of relative rotation (φ<sub>3</sub>);
- 4 – telescope with translation (T<sub>4</sub>) linkage to the arm (3) and relative translation (x<sub>4</sub>) on axis (X<sub>4</sub>).

This kinematic scheme is plane opened and work when the linkage base – column is blocked with base manoeuvre  $m_6 = 0$ , with general manoeuvre  $m_0 = -2$ . The characteristic of this kinematic scheme shows that the manipulator requires global and local structure. That is mean to the limited possibility for operation only with the global structure.

For mathematical developing (Fu, 1989; Nakano, 1989) of the problem we accept that:

1. The length of parts  $l_0, l_1, l_2, l_3$  and  $l_4$  are known;
2. Coordinate systems  $R_0, R_1, R_2, R_3, R_4$  have origine to point  $O, O_1$  to  $O_4$ , respectively, where the linkage between parts are.
3. The axes  $X_1, X_2, X_3$  and  $X_4$  are parallel

With these conditions the problem is divided to two parts:

1. Define the  $O_4$  and  $O_5$  coordinates to coordinate system  $R_0$ ;
2. Define the orientation of the vector  $\overrightarrow{O_4O_5}$  in  $R_0$ .

To make this we need to define the transformation matrixes (Ekserov 1989).

The rotation  $R_1$  toward  $R_0$  around  $Z_0$  in angle  $\phi_1$  is responsible to matrix:

$$M_0^1 = \begin{vmatrix} \cos 1 & \sin 1 & 0 \\ -\sin 1 & \cos 1 & 0 \\ 0 & 0 & 1 \end{vmatrix}$$

The rotation  $R_2$  toward  $R_1$  around  $X_2$  in angle  $\phi_2$  is responsible to matrix:

$$M_1^2 = \begin{vmatrix} 1 & 0 & 0 \\ 0 & \cos 2 & \sin 2 \\ 0 & -\sin 2 & \cos 2 \end{vmatrix}$$

The rotation  $R_3$  toward  $R_2$  around  $X_3$  in angle  $\phi_3$  is responsible to matrix:

$$M_2^3 = \begin{vmatrix} 1 & 0 & 0 \\ 0 & \cos 3 & \sin 3 \\ 0 & -\sin 3 & \cos 3 \end{vmatrix}$$

The translation  $T_4$  toward  $R_3$  on axis  $X_4$  in distance  $T_4$  is responsible to matrix:

$$M_3^4 = \begin{vmatrix} 1 & 0 & 0 \\ 0 & 1 & 0 \\ 0 & 0 & 1 \end{vmatrix}$$

Matrix for the transition to base  $R_0$  are:

$$\begin{aligned} |M_0^2| &= |M_0^1| \times |M_1^2| \\ |M_0^3| &= |M_0^1| \times |M_1^2| \times |M_2^3| \\ |M_0^4| &= |M_0^1| \times |M_1^2| \times |M_2^3| \times |M_3^4| \end{aligned}$$

After simplifying (for simplifying we put  $T_0 = l_3 + l_4 + T_4$ ,  $L = l_0 + l_1$ ) we have equation for the positions and orientations of the mechanism's part:

$$x_5 = \sin 1 * [l_2 * \cos 2 + T_0 * \cos(2 + 3)] \quad i_4^{x_0} = \cos 1$$

$$\begin{aligned}
 y_5 &= \cos 1 * [l_2 * \cos 2 + T_0 * \cos(2 + 3)] & i_4^{y_0} &= -\sin 1 \\
 z_5 &= L - l_2 * \sin 2 - T_0 * \sin(2 + 3) & i_4^{z_0} &= 0 \\
 j_4^{x_0} &= \sin 1 * \cos(2 + 3) & k_4^{x_0} &= \sin 1 * \sin(2 + 3) \\
 j_4^{y_0} &= \cos 1 * \cos(2 + 3) & k_4^{y_0} &= \cos 1 * \sin(2 + 3) \\
 j_4^{z_0} &= -\sin(2 + 3) & k_4^{z_0} &= -\cos(2 + 3)
 \end{aligned}$$

Deduction equations are geometric model, with short type is:

$$\vec{X}_{R_0} = F(\vec{\varphi} - \vec{\varphi}_0)$$

or be the system:

$$\begin{aligned}
 x_5 &= [l_2 * \cos 2 + T_0 * \cos(2 + 3)] * \sin 1 \\
 y_5 &= [l_2 * \cos 2 + T_0 * \cos(2 + 3)] * \cos 1 \\
 z_5 &= L - l_2 * \sin 2 - T_0 * \sin(2 + 3) \\
 j_4^{y_0} &= \cos 1 * \cos(2 + 3) .
 \end{aligned}$$

### METHODS

The research method corresponds to those entire told upper.

We examine virtual model, created by CAD system we have some requests (Assenov, 2002). In view of the fact there are important requirements to the CAD model:

- maximum and accurately fulfillment of the forms, dimensions of the all manipulator's parts;
- maximum and accurately fulfillment of the linkage between the manipulator's parts and linkage between them and hydraulic cylinders.

After 3D SolidWorks modeling we put the model in the Dynamic Designer environment. After that we check the linkage property. This is shown on Fig.3.

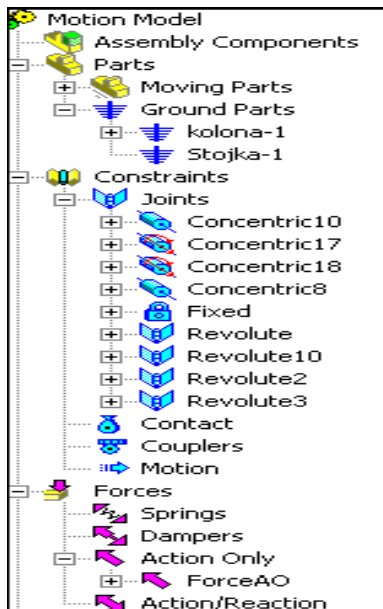


Figure 3 Dynamic Designer feature manager.

We set the maximum load beton element of 10 kN, and we set motion to be complex from movement of the jib and arm. Then we set motion – constant velocity of the hydraulic cylinders of the and arm equal to 10 mm/s and 33 mm/s. The

mode of the motion we set is similar as usual mode in the simplified unregulated hydraulic leading. All this is made as assigning parameters of the linkage. An example the setting the constant velocity of the hydraulic cylinder is shown on Figure 4.

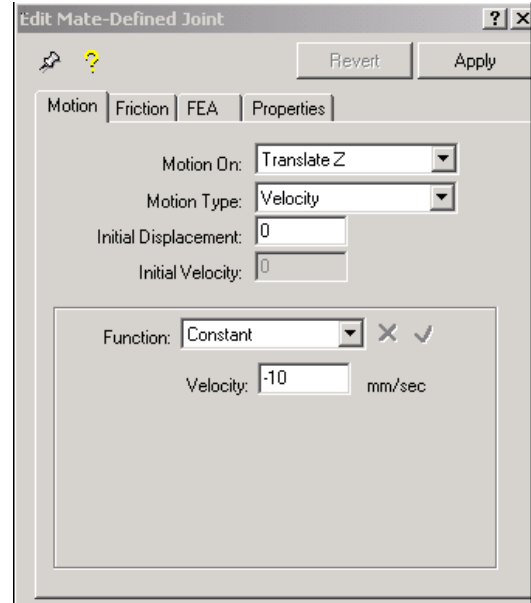


Figure A window for setting the joint parameters

When all parameters are assigned we run simulation process.

### RESULTS AND DECISIONS

The simulation results are shown graphically

1. The ideal reaction in cylindrical joint between jib and the arm is shown on Fig.5.

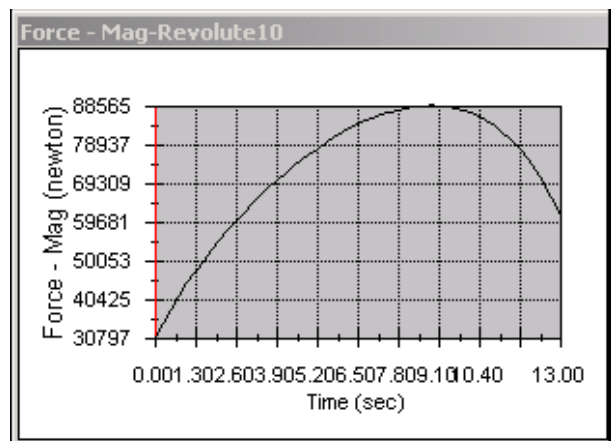


Figure 5 Reaction in joint jib – arm.

2. The ideal reaction in cylindrical joint between the and the column is shown on Fig.6.

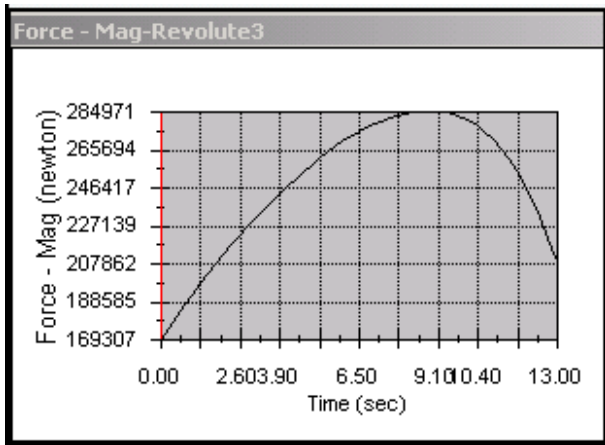


Figure 6 Reaction force in joint - column

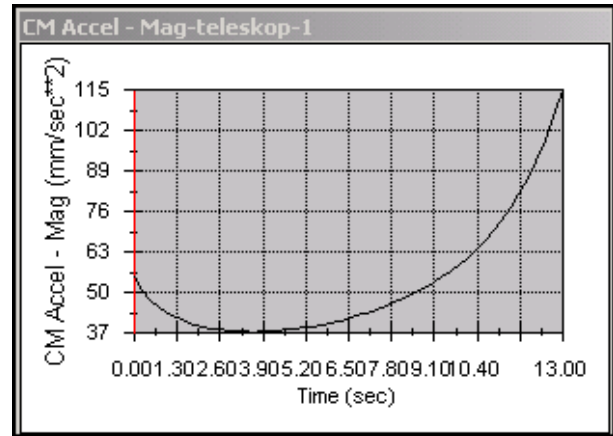


Figure 9 Acceleration of the mass center of the telescope

3. The force in hydraulic cylinder of jib is shown on Fig.7.

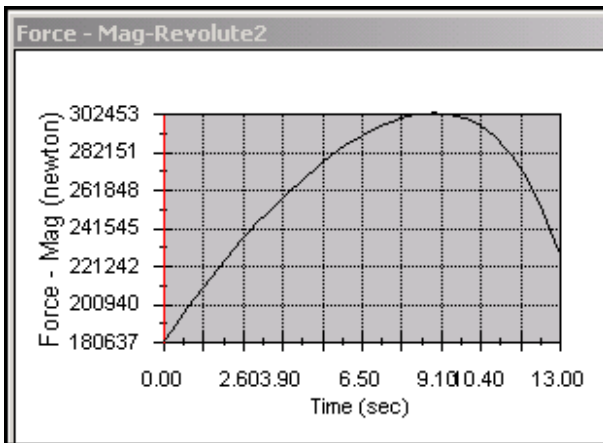


Figure 7. Force variation of the hydraulic cylinder of the jib.

4. The manipulator's parts kinematic parameters are shown in Fig.8 and Fig.9

- The velocity of mass center of the telescope is shown in Fig. 8 and in Fig. 9 is shown acceleration of the mass center of the telescope.

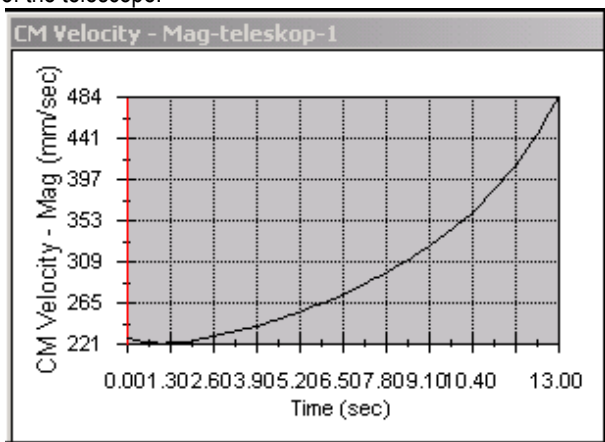


Figure 8 Velocity of mass center of the telescope

## CONCLUSIONS

Methods for kinematic and dynamic study of gallery support manipulator are made. These methods are based on combination of 3D CAD modeling and dynamic simulation.

The gallery support manipulator is studied by the constant velocity of the jib and the arm hydraulic cylinders and to maximum load.

The results can be used for the manipulator's elements optimization for minimum mass and increasing the security coefficient

The results can be used for improving control rate of the hydraulic system, as we optimize transition process of hydro distributing elements.

Methodic for development of the dynamic loading will be improved, as we use opportunities of "spline" option for entering of leading velocity  $\omega(t)$ . We can enter for some part of trajectory leading velocity  $\omega(t) = 0$ . This enables us to study in characteristic points only static load of manipulator's elements.

## REFERENCE

- Fu K.S, R.C.Gonzalez, C.S.Lee Robotics: Control, Sensing, Vision and Intelligence, McGraw - Hill NY1989
- Nakano E. Introduce in robotics, Moskva, Mirr 1989
- Assenov E. SolidWorks manual, Sofia, 2002
- Ekserov P. Hosting manipulators and robots, Sofia, Tehnika 1989

Recommended for publication by Department of Mine mechanization, Faculty of Mining Technology

## DETERMINING THE LOAD ON RKS-TYPE TANGENTIAL PICKS

Svetlozar Tokmakchiev

University of Mining and Geology  
 "St. Ivan Rilski"  
 Sofia 1700, Bulgaria

### ABSTRACT

The article deals with the issue of determining the load on RKS-type tangential picks under lab conditions. The tests were performed with three specially prepared RKS-type cutting tools. The cutting force components and resultant values were determined for each type. It was found that the change in the cutting angle from 70° to 110° has a weak effect on the ratios between the individual forces.

A test stand shown in Fig. 1 was used to determine the load on RKS-type tangential picks. The shearing drum is a strain-measuring head by which it is possible to measure and record the resultant cutting force and its components. The test stand consists of a frame 1, a welded structure made of steel sections and sheet iron. The casket 5 and the hydraulic system 11 are mounted on it. The hydraulic cylinder 7 feeds the strain-measuring head 6 to the casket 5 where the rock fragment is

fixed. The driving screw 12 is used to move the casket horizontally for a new sickle and the straight-line movement of the cutting tool is achieved by supports 2 and 9, slides 8 and guides 13. The stand is fitted with limit switches 4 serving to protect the strain-measuring head and the cutting tool against inadmissible overloads. The hydraulic cylinder is fixed on the panel 10 thus obtaining the necessary rigidity and stability of the structure.

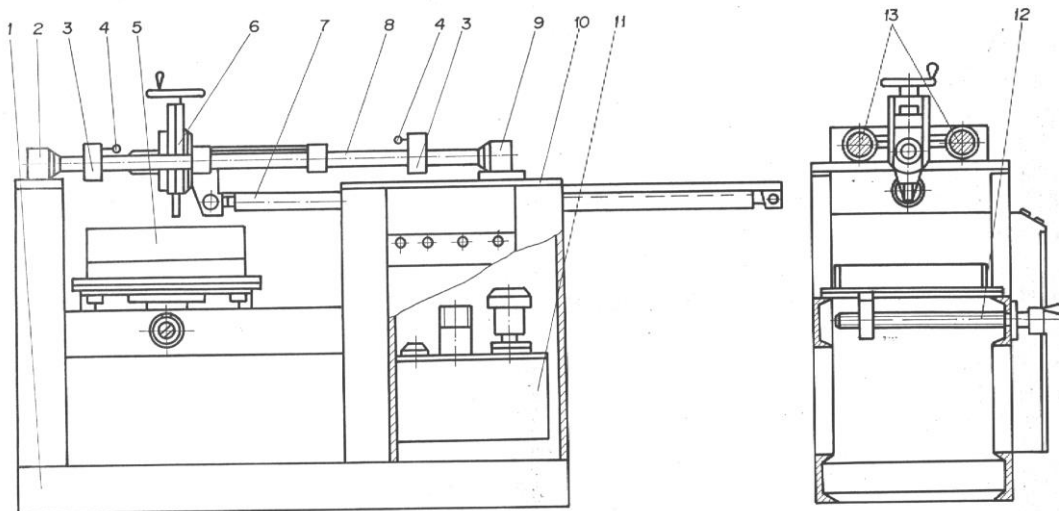


Figure 1

The cutting force components are oriented along the axes of the spatial rectangular coordinate system designated by  $P_x$ ,  $P_y$  and  $P_z$ , respectively, where  $P_x$  is the side cutting force,  $P_y$  is the vertical cutting force and  $P_z$  is the tangential force. The

resultant cutting force is designated by  $P_{res}$  and is determined by the analytical relationship

$$P_{res} = \sqrt{P_x^2 + P_y^2 + P_z^2} \quad (1)$$

After making observations under the conditions of the Babino Mine at Bobov Dol we found that the broken mining mass comes in contact not only with the hard alloy plate (the pin) but also with the head (holder) of the cutting tool. In order to determine what part of the cutting force is exerted on the pin and what part is taken up by the holder, a series of long-term measurements were carried out in the lab. As an object of breakage we used representative fragments of material from the Babino Mine and the cutting tools were prepared in accordance with the picks shown in Fig. 2. Fig. 2a presents an original RKS1pick and Fig. 2b depicts a pick with an elongated

head, in which the cutting force is exerted on the hard alloy pin. The sample shown in Fig. 2b is without a hard alloy pin. The cutting force in that tool is distributed only on the head (holder). The tests were performed under the following operating conditions: blocked cutting along a smooth surface; thickness of sickles  $h = 10$  mm; cutting angle  $\beta$  from  $70^\circ$  to  $110^\circ$  changing within the range of  $10^\circ$ ; material strength from 2.5 to 3 by Protodyakonov's scale and rate of feeding the tool  $V_p = 20$  mm/s.

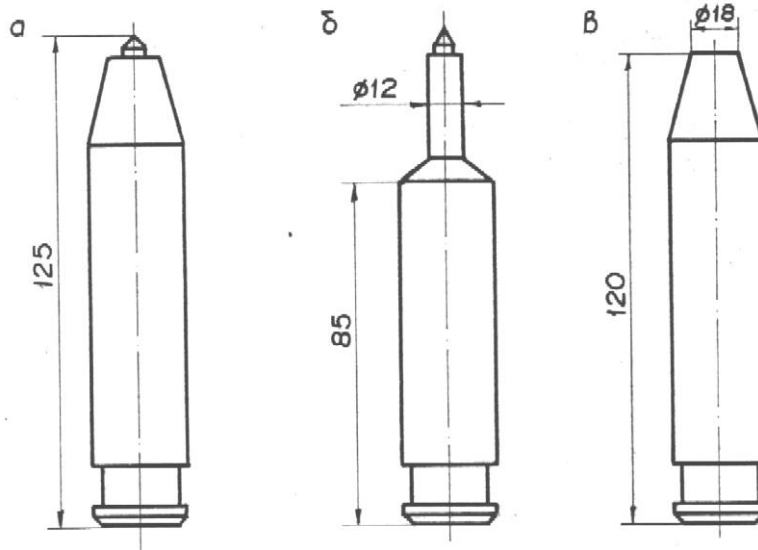


Figure 2 Experimental RKS1picks  
 a – original pick; b – pick with elongated head;  
 c – pick without head

The experimental studies were necessitated by the heavy conditions of cutting tool operation at Babino Mine. Due to the higher rock hardness, the hard alloy pin of some picks is broken from the very beginning and they cut the mining mass only with their holders thus causing a negative effect on the whole machine.

The results of the experimental studies are presented in Table 1. The same table gives in percentage the ratios between the resultant cutting forces for each type of tested pick. The graphic dependencies of the test results obtained are shown in Fig. 3

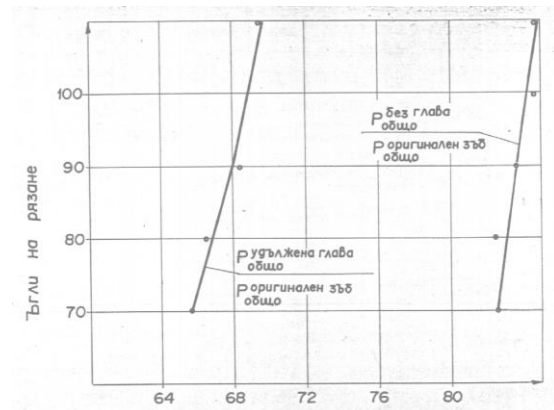


Figure 3

Table 1

| Cutting angle $\beta$ | Cutting forces, N |       |       |           |                  |       |       |           |                          |       |       |           | Ratio between resultant cutting forces, % |                 |
|-----------------------|-------------------|-------|-------|-----------|------------------|-------|-------|-----------|--------------------------|-------|-------|-----------|---|-----------------|
|                       | Original pick     |       |       |           | Pick without pin |       |       |           | Pick with elongated head |       |       |           | $P_{wp}/P_{or}$                           | $P_{eh}/P_{or}$ |
|                       | $P_x$             | $P_y$ | $P_z$ | $P_{res}$ | $P_x$            | $P_y$ | $P_z$ | $P_{res}$ | $P_x$                    | $P_y$ | $P_z$ | $P_{res}$ |   |                 |
| 70                    | 0.22              | 1.28  | 1.53  | 2.01      | 0.06             | 0.54  | 1.21  | 1.32      | 0.14                     | 0.98  | 1.33  | 1.66      | 82.5                                      | 65.7            |
| 80                    | 0.23              | 1.29  | 1.57  | 2.04      | 0.07             | 0.55  | 1.24  | 1.36      | 0.17                     | 1.01  | 1.35  | 1.69      | 82.2                                      | 66.7            |
| 90                    | 0.25              | 1.33  | 1.61  | 2.10      | 0.09             | 0.57  | 1.27  | 1.38      | 0.19                     | 1.03  | 1.41  | 1.76      | 83.8                                      | 68.6            |
| 100                   | 0.27              | 1.34  | 1.64  | 2.14      | 0.10             | 0.59  | 1.29  | 1.47      | 0.21                     | 1.05  | 1.44  | 1.79      | 84.8                                      | 68.9            |
| 110                   | 0.28              | 1.37  | 1.69  | 2.19      | 0.10             | 0.61  | 1.31  | 1.51      | 0.22                     | 1.07  | 1.49  | 1.85      | 84.4                                      | 69.3            |

The results showed that the resultant cutting force in the original picks is determined by the forces acting on the hard alloy pin and the body. Furthermore, the greater part of that force is taken up by the central pin (approx. 80-85%), whereas 15-20% of it is taken up by the body. A different picture can be observed with respect to the vertical ( $P_y$ ) and side ( $P_x$ ) forces, which can be explained by the profile of the groove formed by the pin as well as by the fact that these two forces have considerably lower values.

In general we can conclude that the change in the angle of cutting from 70° to 110° has a weak effect on the ratios between the individual forces discussed above.

#### REFERENCES

- Pozin, E.Z. Coal breaking by coal-cutters. Nedra. Moscow.1987 (In Russian)  
 Skorobogatov, S.V. A study on the wear-out of picks in rock cutting. *Mining Machines Journal* 1. 1988 (In Russian)

## THRESHOLD LEVELS OF SHIFTING AND SPEEDS IN DISCRETE REGULATION OF MINE BELT CONVEYORS

**Prof.S.Deevski**

University of Mining and Geology "St. Ivan Rilski"  
Sofia 1700, Bulgaria

**Eng. Katerina Shehadi**

University of Mining and Geology "St. Ivan Rilski"  
Sofia 1700, Bulgaria

### ABSTRACT

The probability characteristics of load flow of the main belt conveyor of Assarel Mine are determined and the optimal levels of shifting and motion speed in discrete regulation of the speed are found. Regulation of the belt speed will be driven to considerably increase of mine belt conveyors lifetime.

### 1. INTRODUCTION

One of the possible ways to make economies when mine loads are hauled with belt conveyors is to put controlled conveyor drive. The following advantages are achieved:

1. Drawing in the energy consumption for transportation;
2. Decreasing wearing of rotating parts and increasing their lifetime;
3. Increasing the lifetime of conveyor bearing structure as a result of decreasing of dynamic shocks.

Controlled driving could be continuous or discrete depending on technical means used for its realization.

Continuous regulation changes uninterruptedly the speed of conveyor belt depending on the intensity of load flow. In discrete the speed shifting is made only when the flow intensity reaches determined edge values.

The modern technique offers comparatively cheap and enough effective equipment for continuous and discrete speed regulation.

We will consider the discrete regulation method in this report because the equipment is cheaper and more available. Discrete regulation could be realized by mechanical devices (switchable gearing) or by using of planet reducers, as well as by electrical means: switching the way of connection of electrical motors or the number of their poles, direct frequency regulation etc.

### 2. PROBABILITY CHARACTERISTICS OF MINE LOAD FLOWS

Numerous investigations show that intensity of mine load flows is a probability quantity [Schahmaister etc., 1983]. That is due to inhomogeneity of mined mineral resources, breaking off the mining in order to displace machines, fulfillment of different technological requirements etc.

The load flow intensity could be divided in some sub-flows:

- Flow of entry load with different intensity;
- Flow of discontinuity (pauses) in feed of the load;
- Flow of load feel duration;
- Flow of pause durations, etc.

Only the first sub-flow is considered in this report because it has relation with the change of belt speed. Investigations show, that it is well approximated with normal probability distribution.

The main characteristics of normal distribution of the material flow, hauled by belt conveyor are:

- density of probabilities

$$f(Q) = \frac{1}{\sigma\sqrt{2\pi}} \exp\left[-\frac{(Q-a)^2}{2\sigma^2}\right] \quad (1)$$

- distribution function

$$F(Q) = \frac{1}{\sigma\sqrt{2\pi}} \int_0^Q \exp\left[-\frac{(Q_i-a)^2}{2\sigma^2}\right] dQ_i \quad (2)$$

- mathematical expectation

$$a = \frac{\sum m_i Q_i}{n} \quad (3)$$

- dispersion

$$D(Q) = \frac{\sum (Q_i - Q)^2 m_i}{n} \quad (4)$$

- quadratic mean deviation

$$\sigma = \sqrt{D(Q)} \quad (5)$$

where  $Q_i$  is conveyor productivity in the moment  $i$ ,

$m_i$  - frequency of the  $Q_i$  intervals.

3. THRESHOLD LEVELS OF SPEED SHIFTINGS

In discrete regulation of belt speeds a control system keep abreast a load flow intensity and unevenly change of the belt speed when the load flow crosses the any of the preliminary defined levels. Regulation will be normal, i.e. with minimum energy losses, if the levels are determined so as to obtain a minimal belt run in load haulage. Determination of optimal levels is made as follows:

We assume that control system is of three-step type. Material flow loaded on the conveyor is changed during the time casually as it is shown on fig. 1 a.



Figure 1.

When the material is loaded on the belt the speed  $v_1$  is turned on, if the flow rate increases to level  $Q_1$  the speed  $v_2$  is turned on and if it reaches and gets beyond  $Q_2$  the speed  $v_3$  is turned on (Fig.1, b).

Probabilities the belt to moves with speeds  $v_1, v_2$  и  $v_3$  are:

$$P_1 = P[0 < Q(t) \leq Q_1] = F(Q_1); \tag{6}$$

$$P_2 = P[Q_1 < Q(t) \leq Q_2] = F(Q_2) - F(Q_1);$$

$$P_3 = P[Q_2 < Q(t) \leq Q_3] = F(Q_3) - F(Q_2),$$

where  $Q(t)$  is the load flow intensity in the moment  $t$ .

The average speed of the belt is:

$$v_{cp} = v_1 P_1 + v_2 P_2 + v_3 P_3, m/s. \tag{7}$$

becausef

$$v_1 = \frac{Q_1}{q}; v_2 = \frac{Q_2}{q}; v_3 = \frac{Q_3}{q}, \tag{8}$$

- where  $q = S\rho$  is linear mass of loaded on the belt material, kg/m;

$S$  - maximal section of the material on the belt, m<sup>2</sup>;

$\rho$  - density of the transported material, kg/m<sup>3</sup>,

$$v_{cp} = \frac{Q_1}{q} \int_0^{Q_1} f(Q)dQ + \frac{Q_2}{q} \int_{Q_1}^{Q_2} f(Q)dQ + \frac{Q_3}{q} \int_{Q_2}^{Q_3} f(Q)dQ. \tag{9}$$

The level  $Q_3$  is equal to the maximal productivity of the belt conveyor. Levels  $Q_1$  and  $Q_2$  are variable and in order to find their optimal quantities we determine the partial derivatives of equation (9) toward  $Q_1$  and  $Q_2$  nullify them.

$$\frac{\partial v_{cp}}{\partial Q_1} = F(Q_1) + (Q_1 - Q_2)f(Q_1) = 0 \tag{10}$$

$$\frac{\partial v_{cp}}{\partial Q_2} = F(Q_2) + (Q_2 - Q_3)f(Q_2) = 0$$

So we are able to subtract the equation of optimal level of regulation if the control system is with  $n$  degrees

$$F(Q_{n-1}) + (Q_{n-1} - Q_n)f(Q_{n-1}) = 0. \tag{11}$$

4.CALCULATION RESULTS

A determination of threshold levels of the speed is made on the base of data of loading of the main belt conveyor in Assarel mine for the period from 11 to 17 February, 2002 in order to obtain practical results of utilization of the mentioned above formulas. Computer, who controls the belt line, records the data. The curve of loading is average for every half of hour in order to obtain numerical data.

The calculations were made using computer program "Mathematica" for Windows, created by Stephen Wolfram.

The probability characteristics of the haulaged by the belt conveyor load are calculated by using the sub-program Descriptive Statistics, which use the formulas (3)-(5). The calculation results are the following:

Mathematical expectation  $a=2177$  t/h

Dispersion  $D=5626$  t/h

Quadratic mean deviation  $\sigma =474$  t/h

Using the obtained data and solving the equations (10) and (11) for degree numbers from 1 to 5, i.e. with different number of equations, we find the levels of speed shifting. The upper productivity limit is set to be the maximal productivity of the conveyor  $Q_{max}=4000$  t/h.

Using the obtained levels of shifting and dependences (8) we calculate the necessary speeds. The average speed of belt motion is determined according to the formula (9). Calculation results are given in Table 1.

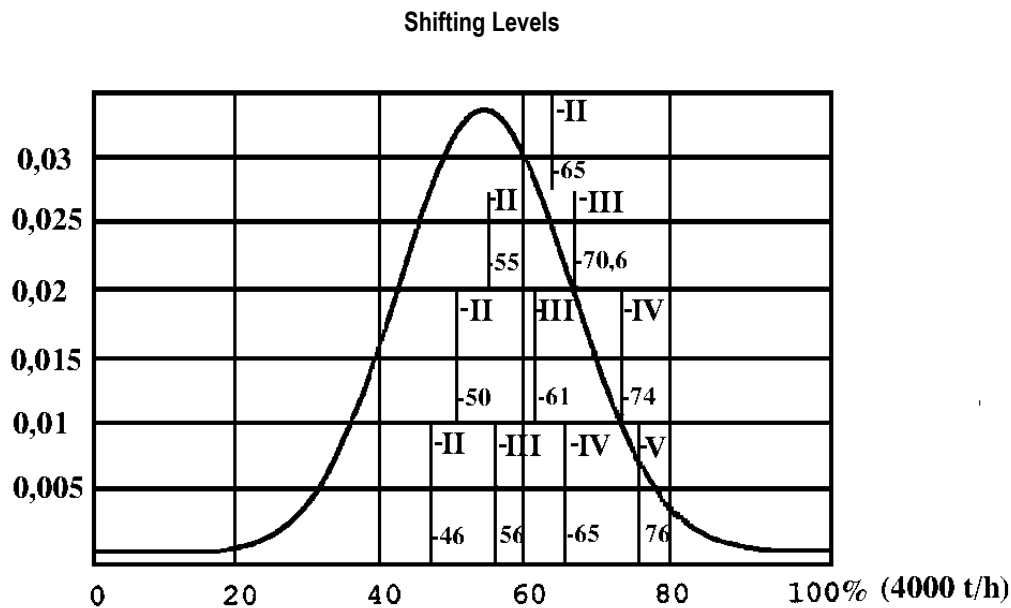


Figure 2.

Table 1 Shifting levels and motion speeds in different number of speed degrees

| Number of degrees | Shifting levels, t/h |                     |                     |                     |                   | Average speed $v_{cp,m/s}$ |
|-------------------|----------------------|---------------------|---------------------|---------------------|-------------------|----------------------------|
|                   | Motion speeds, m/s   |                     |                     |                     |                   |                            |
|                   | $\frac{Q_1}{v_1}$    | $\frac{Q_2}{v_2}$   | $\frac{Q_3}{v_3}$   | $\frac{Q_4}{v_4}$   | $\frac{Q_5}{v_5}$ |                            |
| 2                 | $\frac{2592}{2,6}$   | $\frac{4000}{4}$    |                     |                     |                   | 2,84                       |
| 3                 | $\frac{2202}{2,2}$   | $\frac{2823}{2,8}$  | $\frac{4000}{4}$    |                     |                   | 2,58                       |
| 4                 | $\frac{1995}{2}$     | $\frac{2444}{2,44}$ | $\frac{2949}{2,95}$ | $\frac{4000}{4}$    |                   | 2,48                       |
| 5                 | $\frac{1859}{1,86}$  | $\frac{2233}{2,23}$ | $\frac{2587}{2,59}$ | $\frac{3035}{3,03}$ | $\frac{4000}{4}$  | 2,4                        |

### CONCLUSIONS

The following results could be made on the base of data, obtained in Table 1:

1.The results are an product of probability calculations and are concerned to the load flow with determined characteristics. For each particular case it is necessary to make calculations using corresponding statistical data.

2.The threshold levels for different speed degrees are not identical and depend on their place on the curve of probability distribution. (Figr.2).

3.The average speed of belt motion depends on the number of speed degrees. As many are the degrees so lower is the average speed. It is not arithmetical mean of speeds in particular degrees because duration of motion on different levels is different and depends on the interval size  $F(Q_i)$ .

4.If the conveyor speed without regulation is 100%, in two-degree regulation it will be it will drop to 71% and in five-degree – to 60% With such value will drop the run of the belt and turnover of the rotating parts It should be lead to prolongation of conveyor lifetime. .

### REFERENCES

- Deevski,S., 1996. Analytical Investigations of Main Parameters of Mine Belt Conveyors.- *Dissertation thesis for obtaining of Doctor Degree in Technical Sciences. (In Bulgarian)*
- Schahmaister L.G., V.G.Dmitriev.,1938 r, *Probability methods of calculation of Transporting machines .M.,Machinostroenie. (in Russian)*

## ABOUT MAXIMUM UTILIZATION OF SUPPORTING CAPACITY OF MINE BELT CONVEYORS

**Katerina Shehadi**

University of Mining and Geology  
"St. Ivan Rilski",  
Sofia 1700, Bulgaria

### ABSTRACT

Possibilities to increase the productivity of belt conveyors without considerable change of their construction are treated. Calculations of the area of conveyor cross sections of transported material for five different forms of the belt and their protective widths with belt width  $B=1600$  mm are made. The results show, that productivity could be increased about 40%.

### 1. INTRODUCTION

Belt conveyors are used in mining industry for haulage of bulk freight mineral resources and rock mass.

Increasing productivity of mining machines – combines, excavators etc. the belt conveyors are the only transporting machines that could cope with increased load flows. That is why their utilization in mining is great.

Possibilities to increase the productivity of belt conveyors without considerable change of their construction will be treated in this report. Capacity productivity of conveyors depends on two quantities: cross section area of the material, that is on the belt  $F$ ,  $m^2$ , and motion speed of the belt  $V$ ,  $m/s$ , i.e.

$$Q = F \cdot v, \text{ m}^3/\text{s} \quad (1)$$

The belt speed is regular and depends on the type of conveyor. For conveyors, used in underground mines the speed is 1,5 - 2 m/s, and for open cast mines - 4 - 6 m/s.

The cross section area of the material on the belt depends on the width, the type and the construction of supporting roller bearing.

In the belt conveyors theory [Schahmaister etc., 1978] it is the custom, that loaded in the belt material do not gain the belt ends in order to get protective strips, which avoid lateral falling of the material. It is assumed also that the upper surface of the material is in the form of triangular prism with inclination of side faced  $\varphi$  (Fig.1). The angle  $\varphi$  is side to be the natural slope in transportation and is about a half of the angle of natural slope of the material at steady state.

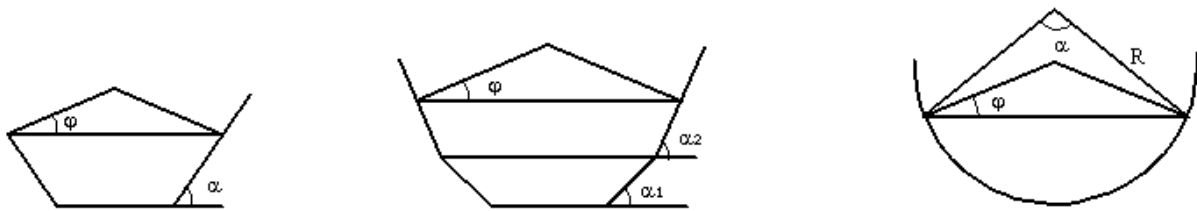


Figure 1.

### 2. DETERMINATION OF MAXIMAL AREA OF MATERIAL SECTION

We investigate loading of four types belt conveyors, used in "Maritsa – Istok" [Stoev, Marhor, 1991]. Two of them are with three-roller supports and angles of inclination of side rollers  $\alpha$  respectively  $30^\circ$  and  $36^\circ$  (Fig.1, a), and the other two are with

five-roller supports and angles of setting of side rollers  $\alpha_1$  and  $\alpha_2$  respectively  $\alpha_1 = 31^\circ$  and  $\alpha_2 = 38^\circ$  and  $\alpha_1 = 36^\circ$   $\alpha_2 = 43^\circ$  (Fig.1, b).

Sectional areas of the material are determined by using of the formula, subtracted by Prof. S. Deevski [Deevski, 1996]:

- for three-roller supports:  
 $F_3=(x_1^2-x_0^2)tg \alpha + x_1^2 \cdot tg \varphi, m^2, \quad (2)$

- for five roller supports:  
 $F_5=(x_1^2-x_0^2)tg \alpha + (x_2^2-x_1^2) \cdot tg \alpha + x_2^2 \cdot tg \varphi, m^2; \quad (3)$

where  $x_0, x_1$  and  $x_2$  are the lengths of segments, obtained by projecting of cross section angles on the abscissa (Fig.2).

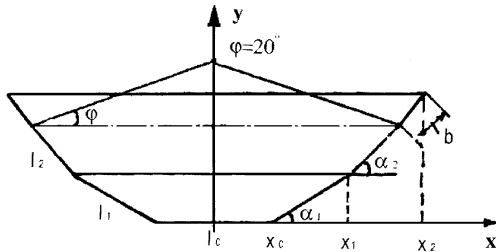


Figure 2.

The lengths of the segments are::

$$x_0 = \frac{l_0}{2},$$

$$x_1 = x_0 + l_1 \cdot \cos \alpha_1,$$

$$x_2 = x_1 + l_2 \cdot \cos \alpha_2,$$

where  $l_0, l_1$  and  $l_2$  are the lengths of cross section of the belt, m.

In order to compare obtained results, we determine maximal area that could be obtained if the belt is supported by infinitely number of rollers. According to the Lullie theorem that says: "From all plan figures, which contour has the l, the greatest area has the circle" we assume that the belt is bended on circular curve with radius R (Fig.1, b). The form of the material section is circular segment with a triangle on top, which area is:

$$F_0 = \frac{R^2}{2} \left( \frac{\pi \alpha}{180} - \sin \alpha \right) + \frac{1}{4} a^2 tg \varphi, \quad (4)$$

where  $\alpha$  is the central angle,  
 R – circle radius, m;  
 a - chord of the figure, m.

The central angle  $\alpha$ , in which the figure of the material has maximal area, is  $180^\circ$ . It is determined by investigation of

maximum of the function (4) according to the method of digit-by-digit approximation.

### 3.DETERMINATION OF THE PROTECTIVE WIDTHS

When the belt conveyors are designed, the size of the protective widths is determined according to the following dependences:

- for conveyors with small productivity

$$\Delta b_1 = 0,1 \cdot B, m \quad (5)$$

- for conveyors with great productivity

$$\Delta b_2 = 0,05 \cdot B + 0,025, m \quad (6)$$

Recommended by formulas (5) and (6) protective widths are subtracted as a result of empirical obstructions [1].

Prof. Deevski [1996] subtracts formulas for determination of the needed protective widths and assumes that the upper surface of the triangle prism becomes plane and it draw level with the edge of the pan-like belt as a result of shaking down during the material motion.

The formulas of protective widths are:

$$\Delta b_3 = \frac{B - \sqrt{B^2 - 4AC}}{2A}, m, \quad (7)$$

where  $A = \cos \alpha_n \cdot \sin \alpha_n + \cos \alpha_n \cdot tg \varphi$ ;

$$B = a \cdot (\sin \alpha_n + \cos \alpha_n \cdot tg \varphi);$$

$$C = \frac{1}{4} a^2 tg \varphi;$$

$\alpha_n$  is inclination of the highest side rollers,  $^\circ$ ;  
 a – distance between upper edges of pan-like belt, m.

### 4.CALCULATION RESULTS

Calculation results of areas of cross sections of transported material for different belt forms by using the formulas (2), (3) and (4) and their protective widths, determined by using the formulas (5), (6) and (7) for belt width  $B= 1600$  mm and angle of the natural slope during the transportation  $\varphi = 20^\circ$  are given in Table 1.

Table 1

| Type of roller support   | Protective widths<br>$\Delta b, mm$ | Area of the material |      |
|--|-------------------------------------|----------------------|------|
|  |                                     | F, m <sup>2</sup>    | F, % |
| Three-roller support with inclination of side rollers $\alpha = 30^{\circ}$                              | $\Delta b_1 = 160$                  | 0,276                | 68   |
|  | $\Delta b_2 = 105$                  | 0,331                | 81   |
|  | $\Delta b_3 = 186$                  | 0,253                | 62   |
| Three-roller support with inclination of side rollers $\alpha = 36^{\circ}$                              | $\Delta b_1 = 160$                  | 0,291                | 71   |
|  | $\Delta b_2 = 105$                  | 0,348                | 85   |
|  | $\Delta b_3 = 162$                  | 0,290                | 71   |
| Five-roller support with inclination of side rollers $\alpha_1 = 31^{\circ}$ and $\alpha_2 = 38^{\circ}$ | $\Delta b_1 = 160$                  | 0,309                | 76   |
|  | $\Delta b_2 = 105$                  | 0,367                | 90   |
|  | $\Delta b_3 = 154$                  | 0,317                | 78   |
| Five-roller support with inclination of side rollers $\alpha_1 = 36^{\circ}$ and $\alpha_2 = 43^{\circ}$ | $\Delta b_1 = 160$                  | 0,317                | 78   |
|  | $\Delta b_2 = 105$                  | 0,376                | 92   |
|  | $\Delta b_3 = 138$                  | 0,342                | 84   |
| Semi-circular (ideal) section  | $\Delta b_1 = 160$                  | 0,335                | 82   |
|  | $\Delta b_2 = 105$                  | 0,390                | 96   |
|  | $\Delta b_3 = 90$                   | 0,407                | 100  |

## 5. CONCLUSIONS

Calculation result allows us to make the following conclusions:

1. When conveyors are fully loaded their productivity could be increased about 40% without change of their constructions only by replacement of roller support with such ones, which makes pan-like belt deeper. The driving power should be confirmed with increased productivity.

2. For most cases, protective widths calculated by using the formulas (5) (6) and are prove to be insufficient to avoid the material falling from side edges of the belt. That is why it should to be used the formula (7) when determine the limits of loading.

As the most of the protective widths, calculated by using the formulas (5) and (6) are inadmissible from exploitation point of

view, comparison of the results concerning material areas is right only for these areas who corresponds to the protective widths calculated by using the formula (7).

## REFERENCES

- Deevski, S., 1996. Analytical Investigations of Main Parameters of Mine Belt Conveyors.- *Dissertation thesis for obtaining of Doctor Degree in Technical Sciences. (In Bulgarian)*
- Lusternic, L.A., 1984. Bulging figures and polyhedrons. – *Nauka I iskustvo (In Bulgarian)*
- Stoev, S., Marhov, N. etc. 1991, Sofia. – Catalogue for unification of roller stations of rubber conveyor belts, excavators and spreaders in "Maritsa-Isrok" (in Bulgarian).
- Schahmaister L.G., V.G.Dmitriev., 1978r, Theory and Calculations of belt conveyors. *M., Machinostroenie. (in Russian)*

## TECHNICAL DIAGNOSTICS OF MAJOR COMPONENTS OF MINE WINDING MACHINES

**Iliia Yochev**

Rudmetal JSC  
Rudozem 4960, Bulgaria

**Evtim Kartzelin**

University of Mining and Geology "St. Ivan  
Rilski Sofia 1700, Bulgaria

### ABSTRACT

Quality technical diagnostic is of major importance for reliable and safe operation of mine winding machines.

The paper presents summarize criteria for winding machine diagnostics. Limit wear norms are established for major components and units. Guidelines are presented for inspection of winding machines after long periods of operation.

### INTRODUCTION

One of the most effective and practically the only means of vertical transport of people, materials and mineral resources, and simultaneously one of the most important units in the technological sequence of underground mining, are mine winding facilities (MWF). Their technical conditions impact not only the rhythmic and efficient work of the mining company as a whole but also the safety of all underground workers.

Technical condition means the set of machine parameters chaining in the process of its operation and at any given time defined by technical specifications. Various factors influence the change of MWF status such as mining conditions, structure and quality of units and components, level and quality of operation and maintenance, etc.

MWF technical condition depends on the quality of machine components. Establishment of individual component quality generally means inspection of the degree of change of geometrical form and dimensions, roughness and physico-mechanical properties of surfaces. Establishment of MWF technical conditions calls for precise inspection, micro-measurements, defect-finding of most important components and by means of all possible diagnostic methods – vibrometrical, acoustic, functional diagnostics method, oil analysis method, etc.

Technical status of components and machines is usually represented by the following conditions: normal, admissible and boundary. A boundary condition means that, due to various requirements, the respective component should not be operated any more. The boundary technical condition is defined by means of technical and economic criteria related to labor safety.

### INSPECTION OF TECHNICAL STATUS OF ROPE WINDING DEVICE

Conditionally, rope winding device is split into to major parts – steel structure and brake fields. Inspection of technical status can be carried out in the sequence shown below:

#### Steel structure

- Measurement of actual values of maximal static loads and of static difference between individual rope branches. Results are compared with admissible design parameters of the respective machine and, if such parameters do not exist, they can be calculated using the equations in Yochev (2002).
- Inspection of drum for cracks. If cracks are found these should be welded. Cracks of length over 200 mm are not allowed.
- Inspection of bolt, rivet and weld joints. This is done by visual inspection and hammering. Loose bolts and rivets emit specific sound. No loose or cracked joints are allowed.
- Inspection of splint joints. This is done by visual inspection and hammering. No loose or deformed splints are allowed. Axial drum displacement in respect of the main winding machine shaft is not allowed. The latter shall be measured as provided by the Technical Survey Instruction (1969).
- Inspection of flanges. No cracks are allowed and internal surface should be smooth and free of grooves and protuberances. In case of double- or multi-layer winding, the uppermost flange section should be spaced from the rope at 2.5 times its diameter as a minimum.
- Inspection of transition section from one winding layer to the other, in case of multi-layer rope winding. Inspection of the special pin as provided in Underground Mining Safety Regulations (1969) in cases of multi-layer rope winding. The surface should be smooth, free of deformations and worn-out sections exceeding 10% of design dimensions. Check for compliance with factory or design requirements.

design dimensions. Check for compliance with factory or design requirements.

- Check of drum locking device. No cracks in welding seams are allowed or loose bolts, or cracks in supporting concrete.
- Inspection of drum lacing. This should be discarded if the state of wear is such that channel bottom is located at a distance of 3-5 mm from fixing bolt heads. With multi-rope MWF the lacing should be replaced where its height under the rope is 0,8-1,0 time the rope diameter. With bi-cylindrical – conical winding devices no deformations or cracks in raceways are allowed or wear in excess of 20% the initial thickness.
- Measurement of radial gaps in the free drum bearings. This is carried out by means of gap-measuring plates or by means of two measuring clocks and jacking up the free drum. One clock measures radial gap and the other one records radial displacement of the main shaft. The first clock readings are taken until the second one starts operation (the latter is due to the radial gap of the main bearings of the winding machine. Boundary values of radial gaps are shown in table 1

Table 1. Boundary values of radial gap for friction bearings

| Main shaft diameter of winding machine, mm. | Boundary value , mm |
|---|---------------------|
| 50 - 120                                    | 0,8                 |
| 120 - 260                                   | 1,0                 |
| 260 - 500                                   | 1,2                 |
| 500 - 800                                   | 1,5                 |
| Над 800                                     | 2,0                 |

Boundary values of radial gaps for antifriction bearings are 0,2 – 0,3 mm for brand new winding machines and 0,8 mm for machines in operation.

**Brake fields**

- Inspection of working surfaces and thickness of brake fields. The work surface should be smooth and free of cracks or grooves. The maximum admissible groove depth is 0,1mm. Minimal thickness wear of brake fields is 15% the nominal dimension. Micro-cracks are admissible if not reaching the brake field end.
- Measurement of radial displacement of brake fields. This is carried out by means of measuring clock. The drum is rotated with speed of 0,2-0,3 m/s without using the brake in order to prevent reading of rum bearing gaps. Admissible values of radial displacement for drums of diameters greater than 3500 mm is 1,2 mm . For all other machines - 0,8 mm .
- Inspection of heating temperature. It should be noted that the braking system is not used for stopping (except for emergency stops) but rather for locking the winding machine. Therefore, no burnt-out paint shall be present near the fields or blue-grey field sections signifying overheating. Presence of such signs is due to faulty dynamic braking system and presence of protuberances on field surface or maladjusted brake. The admissible temperature of brake field heating is e 70 - 80 ° C .

**INSPECTION OF BRAKING SYSTEM STATUS**

The braking system comprises three components – braking device, drive and control system.

**Braking device .**

Fig. 1 shows the most common braking device.

- Inspection of brake cover plates. The inspection is visual and by measurements. No operation is allowed with broken cover plates. During replacement of cover plates, the contact area of the new ones should be at least 50% of their total surface area.
- Measurement of cover plate wear. The most worn-out plates shall be removed and their thickness – measured. The admissible cover plate wear is the one where the distance from the working surface to the most protruding part of supporting structure is 5 mm for pressed plates, and 10 mm - for timber ones.
- Inspection of supports and foundation under the brake beams. No cracks in foundation are allowed.

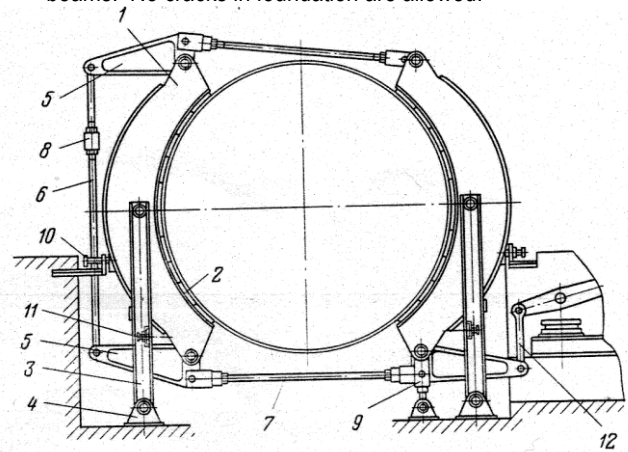


Figure 1. Braking device of double drum winding machine

- Inspection of degree of wear of finger joints. Finger joints should be dismantled first and micro-measurement should be carried out. Radial gaps shall be measured, the values whereof are shown in Table 2.

Table 2. Boundary value of radial gaps in finger joints of braking device

| Gap, mm  | Nominal diameter of joint opening, mm |           |           |           |           |           |
|----------|---------------------------------------|-----------|-----------|-----------|-----------|-----------|
|          | 18 - 30                               | 30 - 50   | 50 - 80   | 80-120    | 120-180   | 180-260   |
| Nominal  | 0,06-0,13                             | 0,07-0,15 | 0,08-0,18 | 0,09-0,21 | 0,10-0,24 | 0,12-0,28 |
| Boundary | 0,25                                  | 0,30      | 0,35      | 0,42      | 0,50      | 0,60      |

### Brake drive

Most common brake drives for winding machines are shown on fig.2 and fig.3.

- Inspection of frame and foundation for cracks. No cracks are allowed in the metal section or concrete.
- Inspection of working surfaces of cylinders and pistons of working and emergency brakes. No scratches, grooves, channels or visible wear are allowed.
- Inspection of finger joint wear. This is carried out by means of micro-measurements. Radial joint gaps are measured, the values whereof are shown in Table 2. Measurement of distance between brake loads in end position and surrounding structure. In lower end position, the minimal distance between loads and pit bottom should be 300 mm. Minimal lateral distance is 10 mm for steel walls and 25 mm for concrete walls.
- Establishment of degree of wear of load supporting bar. Maximal admissible wear of bar diameter is 0,4 – 0,5 mm. Inspection of spring block in case of spring-load drives. No operation is allowed with broken or deformed springs or pins with defective thread.

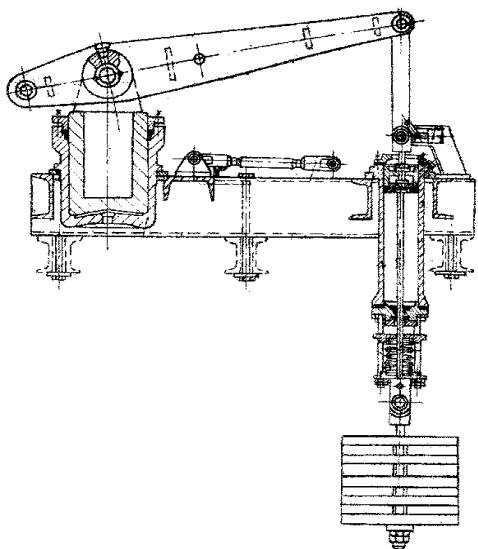


Figure 2. Pneumatic-load drive

It is recommended to replace old spring regulators with spring-less ones.

- Inspection of plunger couple (for all types of pressure regulators). Visual inspection for scratches or grooves. Regulator should be first disassembled and micro-measurements should be carried out. Unstable regulator operation accompanied by strong vibration is a clear sign of wear – air passes from one chamber to another. Regulators with worn-out plunger couple shall not be operated. Admissible gap in plunger couple is 0,02 mm .

Recording of pressure regulator parameters. A graph should be developed of the relationship of working cylinder pressure and control coil current. Current varies from 30mA (+-10mA) to 160mA (+- 20mA) and back. For RDBV regulators, 25 stable phases should be recorded. For RDU regulator, 50 stable phases should be recorded.

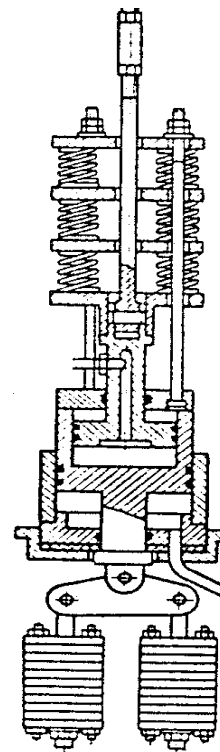


Figure 3. Pneumatic-spring-load drive

### Brake control system

It is sufficient to inspect basic system components – pressure regulators and valves.

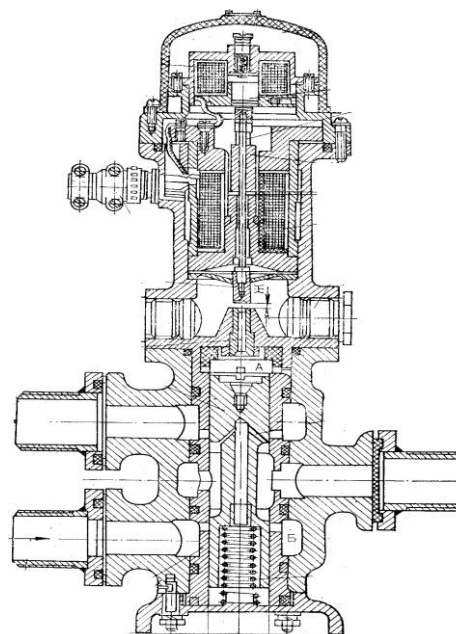


Figure 4. Spring-less regulators RDU- 1M.

### CONCLUSION

MWF technical diagnostic involves quality measurement and inspection of all major components, details and units.

Boundary technical condition is established on the basis of technical, economic and safety criteria. For mine winding facilities, the economic criterion is not the most important one.

For technical diagnostics of some of the most important MWF components, such as rope winding device and braking system, it is recommended to use the above boundary wear norms.

For inspection of serviceability and safety after along operation periods of mine winding facilities, in addition to above-described actions, it is necessary, to inspect the technical condition of the following major components:

- Reducing gear ;
- Suspension ropes of hoisting skips;
- Hoisting skips;
- Winding ropes;
- Shaft reinforcement;

- All ancillary mechanisms;
- MWF electric units.

#### REFERENCES

- Бежок В. Р. , Чайка Б. Н. , Кузьменко Н. Ф. 1982. Руководство по ревизии , наладке и испытанию шахтных подъемных установок , Москва , "Недра" .
- Yochev I.S. 2002. Technical Diagnostics and Selection of Solution for Modernization of Mine Winding Facilities in Gorubso Mines, Dissertation, St. Ivan Riski UMG
- Marhov N. 1991. Mine Equipment Maintenance, Sofia, Technica
- Underground Mining Safety Regulations. 1969. B-01-02-04), Sofia , Technica.
- Technical Survey Instruction. 1969 . Sofia , Technica

*Recommended for publication by Department of  
Mine Mechanization, Faculty of Mining Electromechanics*

## OPTIMIZING THE SELECTION OF A HOIST ROPE IN THE DESIGN AND OPERATION OF SHAFT HOISTS

Antoaneta Yaneva

University of Mining and Geology "St. Ivan Rilski"  
Sofia1700

### ABSTRACT

This paper deals with the selection of an optimal hoist rope design with preserving the hoist parameters in terms of geometry, need for changing the effective load or lift height in the design process, deepening the vertical shaft or reconstructing the shaft hoist by replacing the hoist vessel. Variants and recommendations are proposed for the selection of each parameter in compliance with the Labor Safety Regulations and underground mine design norms.

### INTRODUCTION

Hoist shafts are used for vertical haulage of minerals and ores, waste rock, elements of mining and transport mechanization, ancillary, i.e. blasting and support materials, cables, pipes, etc. They are also used for man riding in two directions for the shift personnel, mine construction, erection and repair workers. In the design process it is normal to preset the lift height – H, annual mine output, shaft hoist function, mineral type, extraction levels, configuration of the surface technological complex.

The sequence of calculating and selecting each hoist device is as follows:

- selecting the hoist vessel (HV) according to the hourly output;
- selecting the hoist rope;
- designing the shaft reinforcement;
- calculating the shaft frame;
- selecting the hoist (HM) – a rope winding device – by diameter and width;
- calculating the hoist kinematics and dynamics;
- selecting the electric drive, brake system and protection equipment.

The aim of this paper is: A) to check the bearing capacity of various hoist rope designs and propose an optimal variant for a constant rope diameter  $d_r = \text{const}$  that also determines a constant diameter of the hoist  $D_{HM} = \text{const}$  and a possibility for variable hoist vessels -  $Q_P = \text{var}$  - to have variable effective load; B) or for  $Q_P = \text{const}$ , variable lift height  $H = \text{var}$ , i.e. to check the maximum capacities of the hoist ropes in shaft hoist design as well as their strength reserve when changes are required during operation.

### STUDY PARAMETERS

The main performance characteristics that have an effect on the hoist rope design are as follows:

- hoist type and location of hoist drum mounting – on the surface or a friction sheave – on the surface or in the hoist frame;
- shaft hoist function – materials (skip) or materials and men (non-tipping skip);
- lift height and number of levels;
- HV guiding – rigid or flexible;
- conditions in vertical shaft – presence of dampness; air flow direction;
- maximum rate of motion; acceleration and delay rates; type of rope vibrations at starting and stopping;
- ratio of HV effective to dead weight;
- shaft hoist output – hourly, daily;
- allowable rope tensile force;
- ratio of hoist diameter, leading and angle sheaves to  $d_r$ ; lining of leading sheaves,
- friction sheaves or drum;
- contact stress in the rope cross-section.

Two variants are considered focusing on the most important parameters listed above.

A) Design: the lift height is preset  $H = \text{const}$ ; the maximum effective load is sought  $Q_{P \max}$  for  $d_r = \text{const}$  and  $D_{HM} = \text{const}$  - various hoist rope designs are considered – with variable linear weights ( $p = \text{var}$ ) and a braking force ( $S_{br} = \text{var}$ ) that provide higher strength within the allowable working diameter of the hoist.

B) Operation: the effective load is known  $Q_{HM} = \text{const}$  and the lift height can vary  $H = \text{var}$  – deepening of the shaft.  $H_{\max}$  is sought for preserved rope diameter  $d_r = \text{const}$  and hoist parameters  $D_{HM} = \text{const}$ . We check the various rope designs –  $p = \text{var}$  whose tensile strength increases within certain limits. According to the safety requirements for rope bending [1], [2], the hoist diameter should be  $D_{\min} = 79 \cdot d_r$  and the standard  $D_{\max}$  is given in the manufacturing plant catalogues, most of which contain data on the maximum  $d_r$  of the respective hoist according to its design, type of lining, etc.

The study made is limited for depths of  $H \leq 500$  m as are most vertical shafts in Bulgaria for hoists with a constant

winding radius – drums with one-layer winding and friction sheaves – one- or multi-rope. The results can be applied for all shafts hoists operating in Bulgaria. An object of a further separate study can be the capacities of hoist ropes in vertical shafts of great depths (up to 1000 m for Bulgaria). We consider a shaft hoist only for load – mineral, especially ore for the more complicated case as compared with coal. We work with high density  $\rho = 1.8 - 1.9 \text{ t/m}^3$ . The hoist vessels as effective and dead weight are larger than those used for men and materials (non-tipping skips) so that the conditions observed for them and the hoist rope selection will be valid with a high reserve factor for the others as well.

Two sets of calculations are made – of the lift height  $H = 400 \text{ m}$  and  $H = 500 \text{ m}$ . The complete height for which the rope is dimensioned is: where we assume

$$H_0 = H + h' + h'', \text{ m}, \quad (1)$$

$h'$  – the height from elevation 0'00 to the axis of the leading sheaves;

$h''$  - maximum value of sagging in the presence of a lower balance rope with linear weight ( $q = p$ ).

The hoist ropes are selected by linear weight “ $p$ ” according to the following formula [3],

$$p = \frac{Q_0}{\frac{\sigma_0}{k_s \cdot \gamma_0} - H_0}, \text{ N/m} \quad (2),$$

where:  $Q_0 = Q_P + Q_D, \text{ N}$ , ( $Q_D$  – dead load of HV);  
 $\sigma_0 = 1770 \text{ kN/mm}^2$  – as assume;  
 $k_s = 6, 5$  factor of safety (for a hoist only for materials);  
 $\gamma_0 = 100 \text{ N/m}^3$ .

Given the requirement for a constant rope diameter, its linear weight will depend only on its design – number of wires with variable diameters and total number of wires; number and shape of strands, type of core. From practice we know that for such heights and one-rope hoisting, we can expect a hoist with  $D_{HM} \geq 3.5 \text{ m}$  thus presupposing ropes with  $d_r \geq 40 \text{ mm}$ . In order to increase the capacities of the rope in terms of designs and forces, we select  $d_r = 45 \text{ mm}$  thus determining a standard drum diameter of  $4 \text{ m}$  [1].

We can calculate the drum width by the formula below [3] and check whether it is sufficient for the respective lift heights  $H = 400 \text{ m}$ ;  $H = 500 \text{ m}$

$$B_{HM} = \left( \frac{H + l_t}{\pi \cdot D_{HM}} + z_{fr} + z_l \right) \cdot (d_r + \varepsilon), \text{ m} \quad (3),$$

where:

$$l_t = 30 \text{ m};$$

$$z_{fr} + z_l = 6 \text{ windings};$$

$$\varepsilon = 3 \text{ mm}.$$

For standard two-drum hoists with  $D_{HM} = 4 \text{ m}$  the maximum width is  $B_{HM} = 2,3 \text{ m}$ , which is sufficient for  $H = 500 \text{ m}$ . From formula (2) we express the finite suspended load  $Q_s$ :

$$Q_0 = p \cdot \left( \frac{\sigma_0}{k_s \cdot \gamma_0} - H_0 \right), \text{ N} \quad (4)$$

On the other hand, the maximum static force by which we select the rope is:

$$F_{st} = Q_0 + p \cdot H_0 = \frac{Q_{bf}}{k_s}, \text{ N} \quad (5),$$

where  $Q_{bf}$  is the ultimate breaking force for the selected strength  $\sigma_0$  and was selected from a catalogue [2].

The sequence of calculations is given below and the results obtained are presented in Table 1.

1. We select 4 different designs of one-layer ropes with  $d_r = 45 \text{ mm}$  from [1]: graph 2, Table 1.
2. We calculate the maximum load they can carry by formula ( $F_{st}$ ) – in graph 5 from Table 1 and we subtract the natural weight of the rope  $p \cdot H_0$  – graph 6 for  $H = 400 \text{ m}$  and graph 7 for  $H = 500 \text{ m}$ .
3. The results obtained are plotted in graphs 8 and 9, respectively.
4. From reference data [3] for standard hoists in the mining industry we search and check for ones having maximum effective load  $Q_P = V \cdot \rho$  depending on  $Q_0$  and  $Q_D$  – graphs 10 and 11.

#### SUMMARY AND ANALYSIS OF RESULTS

For hoists with diameter  $D_{HM} = 4 \text{ m}$  and a rope with  $d_b = 45 \text{ mm}$  when lifting only materials (minerals and ores), the possibilities for maximum weight  $Q_P$  are as follows:

- a) for  $H = 400 \text{ m}$  and ore with  $\rho = 1.8 \text{ t/m}^3$  a standard tipping skip with a capacity of  $V = 7.5 \text{ m}^3$  and a hoist rope with triangular strands – design 1 from Table 1 can be used. For coal, due to its lower density  $\rho = 0.9 \text{ t/m}^3$ , the capacity can be increased up to  $11 \text{ m}^3$  for a single rope skip for  $Q_D = 87.3 \text{ kN}$ . We have reserve both from the density and the rope designs.
- b) for  $H = 500 \text{ m}$  and ore with  $\rho = 1.9 \text{ t/m}^3$  we can use a similar skip but with a capacity of  $V = 5 \text{ m}^3$  and all proposed rope designs so as to be able to select a lighter one – e.g. the fourth one with  $p = 68.86 \text{ N/m}$  since the allowable working static force  $F_{st}$  is much lower than the bearing capacity of the given ropes. For coal it is again possible to have  $V = 11 \text{ m}^3$  even for the lightest rope design.

B) For the conditions listed above and selected hoist vessels:  $V = 7.5 \text{ m}^3$ ,  $\rho = 1.8 \text{ t/m}^3$  tipping ore vessel; lift height  $H = 400 \text{ m}$  and a rope with  $d_r = 45 \text{ mm}$  and  $p = 80,05 \text{ N/m}$  with a  $6 \times 27$  design, triangular strands and the similar skip for  $H = 500 \text{ m}$  and  $V = 5 \text{ m}^3$  at  $\rho = 1.9 \text{ t/m}^3$  we check its capacities for taking an additional load from its natural weight in deepening the vertical shaft.

From formula (1) we determine inversely:

$$H_{\text{max}} = H_{0\text{max}} - (h' + h'') = H_{0\text{max}} - 40, \text{ m},$$

where:

$$H_{0\text{max}} = \frac{(F_{st} - Q_0)}{p}, \text{ m} \quad (6)$$

Table 1

|   | Rope constructions  | p, N/m | Q <sub>br</sub> , kN | F <sub>st</sub> , kN | p.H <sub>0</sub> , N<br>400 m | p.H <sub>0</sub> , N<br>500m | Q <sub>0 pos</sub> , kN<br>400m | Q <sub>0 pos</sub> , kN<br>500m | Q <sub>P+Q<sub>D</sub></sub> , kN<br>400m | Q <sub>P+Q<sub>D</sub></sub> , kN<br>500m |
|---|---------------------|--------|----------------------|----------------------|-------------------------------|------------------------------|---------------------------------|---------------------------------|---|---|
| 1 | 2                   | 3      | 4                    | 5                    | 6                             | 7                            | 8                               | 9                               | 10  | 11  |
| 1 | Δ - fascicles, 6x27 | 80,05  | 1520                 | 233,85               | 35,22                         | 43,22                        | 198,63                          | 190,63                          | 132+63,76                                 | 93,2+54,94                                |
| 2 | O - fascicles, 6x36 | 72,98  | 1410                 | 216,9                | 32,11                         | 39,41                        | 184,79                          | 177,49                          | 88,3+54,94                                | 88,3+54,94                                |
| 3 | O - fascicles, 6x29 | 71,5   | 1380                 | 212,3                | 31,46                         | 38,61                        | 180,84                          | 173,69                          | 88,3+54,94                                | 88,3+54,94                                |
| 4 | O - fascicles, 6x19 | 68,86  | 1330                 | 204,6                | 30,3                          | 37,18                        | 174,3                           | 167,42                          | 93,2+54,94<br>88,3+54,94                  | 93,2+54,94<br>88,3+54,94                  |

From Table 1 for the selected vessels we check the rope reserve. Besides the largest HV ( $H_{res} = 35m$  only), for all others we obtain sufficient reserve of length from 530 m (for rope 1 and  $H = 500$  m) to 225 m (for rope 4 and  $H = 500$ ), which may be considered double reserve. This is so because of the lack of standard HV with intermediate capacities or different designs. For the separate mines, depending on the mining technology, this can allow for entering in depth of 1 to 4 more levels.

In the coal skips the reserve rope lengths are shorter due to the more appropriately selected capacities. For example, for rope 1 and  $H = 500$  m, the reserve length for a skip with  $V = 11m^3$  will be 77 m.

From the calculations made for the selected hoist rope designs within the limits of  $d_r = 45mm$  with preserving the hoist diameter  $D_{HM} = 4$  m we can draw the following conclusions:

- The steel rope with triangular strands (1) gives the greatest possibilities in terms of tensile strength, which for variant (A) means maximum effective load  $Q_P$  – for the standard ore hoists used in Bulgaria – up to 7,5 m<sup>3</sup> capacity, and generally up to 8-9 m<sup>3</sup> depending on the vessel design and its dead weight; and for variant (B) – maximum lift height up to two additional extraction levels of 100 m each or four levels of 50 m each depending on the mining technology;

- The breaking force reserve for the same rope in operation can be used also for increasing the output for preserved height – or replacing the hoist vessel with one with a higher effective load; basically, it is important to preserve the other expensive hoist devices, mostly the shaft reinforcement; normally there should not be any problem because the standard skips are designed in such a way that every following size type increases its capacity at the expense of a change only in height.
- The study carried out can be a basis for creating a complete future methodology for selection of hoist ropes that can include all hoists with  $D_{HM} = 2 - 6m$  manufactured in Bulgaria as well as all possible depths, below 400 m down to 1000 m. Other rope designs can also be included – with a different number of strands and more than one layer.

#### REFERENCES

- Правилник по безопасност на труда при разработване нерудни и нерудни находища по подземен начин, 1982г.
- Thyssen katalogen – Stahlseile für den Bergbau
- Янева А., Переновски Н., "Ръководство за упражнения по РПУ", 2003г.София, Изд. къща МГУ.

Recommended for publication by Department of  
Mine Mechanization, Faculty of Mining Electromechanics

## WAYS OF INCREASING THE SERVICE LIFE OF THE STEEL ROPES IN THE MINE HOISTS

Antoaneta Yaneva

University of Mining and Geology "St. Ivan Rilski"  
Sofia 1700, Bulgaria

Ilia Yochev

"Rudmetal" AD  
Rudozem 4960, Bulgaria

### ABSTRACT

The purpose of the paper is to put forward ways of reducing the expenses on the hoisting ropes, which are a considerable part of the total expenses in the enterprises for underground mining of mineral resources. The preliminary measures were examined for extension of the steel ropes durability as early, as at the time of their manufacture, and also some suggestions on the choice of both the ropes and the pulleys are made. The kinds of procedures were systematized for increase of the service life chiefly of the hoisting ropes, and recommendations are given on the improvement of their operating conditions.

### INTRODUCTION

Among the main units of the mine hoists (MH) are the hoisting and balancing ropes. Their operation lifetime depends on how correctly they are chosen and used and it in turn has a strong effect on the financial condition of the whole mining enterprise.

The principal reason for the destruction of the steel ropes is their frequent folding when they are reeled and pass by the guide pulleys, under the continuous effect of variable tensile forces. Corrosion and mechanical wear and tear step up the aging processes. The ways of increasing the steel ropes operation lifetime can tentatively be divided into two groups: *research and development ways and operation related ways.*

The ropes durability can be varied as early as at their manufacture, and also when they are dimensioned at the MH designing. The good routine maintenance, cleaning, lubrication, inspection and technical checking, as well as the securing of normal operating conditions (with no additional dynamic load, adverse bending or inadmissible contact stress) are also a precondition for a reduction in the expenses.

### RESEARCH AND DEVELOPMENT WAYS

Activities involved in the rope production fall into this group, and also recommendations on their correct calculation and selection, as well as their combination with appropriate structural features of the hoisting machines, the guide pulleys and the suspension devices.

The physico-mechanical properties of the wires greatly influence the rope serviceability. The wire strength is determined by the chemical composition of the steel, its thermal treatment and the aggregate reduction in the cross section at cold drawing. Normally steels having C content from 0.4% to 1% are chosen. If its content is increased, or at larger differences in the cross section (a greater number of steps-

nozzles) higher strength can be achieved, however it is at the expense of a decreased flexibility and elasticity  $220 \text{ N/mm}^2$  is put forward as the optimal strength limit. In selecting hoisting ropes it is necessary to take into consideration the relationship illustrated in Fig.1, between the number of the bending cycles up to the point of destruction  $N$  and the tensile strength (the temporary tearing resistance)  $\sigma_s$ . It can be seen that the wire tensile strength increase at constant load does not lead to a serviceability increase, while with a constant safety factor  $n$  this parameter greatly worsens[3].

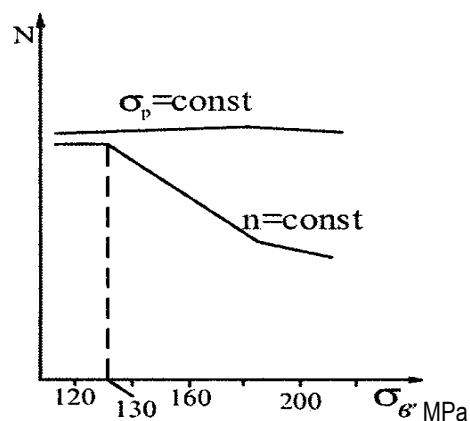


Figure 1.

Mn - from 0.3% to 1% is added to increase the wear resistance and an additional Zn coating is applied. In a normal operating medium the use of zinc-coated wires in a rope does not affect its durability. In a corrosive medium however such coating increases many times the rope life. If the zinc coating protection against corrosion is not sufficient, the wires should be made from corrosion resistant alloy steel. Up to 30% increase in the wire durability can be achieved if the hot rolled blanks having  $d \geq 5 \text{ mm}$  undergo 7-8 different processes of chemical heat treatment.

In recommending the choice of rope design, particular attention should be paid to the way of twist- parallel or reverse-

laid one. From the average statistical results in testing ropes at bending [6] it turns out that the ones with parallel twist withstand a considerably higher number of bends than those with reverselaid twist. Therefore the choice of parallel twist ropes is normally recommended for hoist ropes. Only with prevailing requirement for non-untwisting (e.g. big depths, multi-rope friction pulleys, etc.) is allowed the use of reverse-laid twist or of non-untwisting ropes. The parallel curve ropes have 20-30% higher service ability than the ones with reverse-laid twist, and at the presence of reverse bending (with the deflector pulleys of the multirope MH) such advantage augments.

In the modern structures round ropes are normally used with 6, 8 or 9 fascicles. The bending tests show that with one-layer winding, as a whole, the ropes with more fascicles take precedence. The reason for that is the reduced contact and bend stresses between the wires. With large-diameter pulleys and the presence of groove lining such advantage does not matter much. It was demonstrated [1] that when the ratio between the rope winding pitch and the fascicle winding pitch is an integer, then the number of the destruction inducing bending cycles reaches its maximum value - Fig.2.

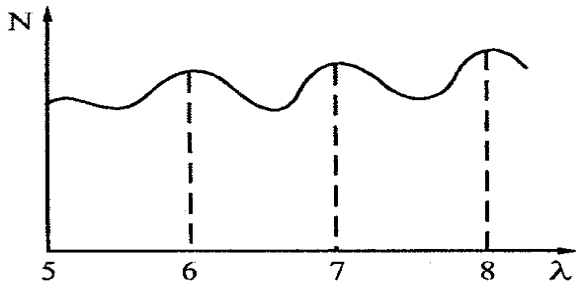


Figure 2.

The rope core serves to provide its round cross-section and for even taking up of the radial forces at the fascicle twisting along the helical line. Metal core is recommended with ropes operating in a very corrosive medium; high temperatures; need for small permanent elongation and large durability. Aluminium core has not been used in the latest structures due to the following shortcomings: fast corrosion, strain and penetration between the fascicles. The combined core has the highest strength parameters and durability - steel fascicles, bonded in polyamide medium or other medium. The rope tends to untwist diminishes, and so do the changes in its diameter at operation loads. The use of ropes (e.g. PK 8x26+7x17 turboplast, PK 8x26+4x17/4x7+1x7/ turbo-lift, etc.) can increase their serviceability more than twice.

Fig.3 shows the dependence of the number of bending cycles up to the point of destruction, on the ratio between the pulley diameter  $D$  and the rope diameter  $d$  and the magnitude of the tensile stresses  $\sigma$  [2]. Hence the conclusion comes that rope service-ability increases with the increase in the  $D/d$  ratio and the decrease of  $\sigma$ .

MPa

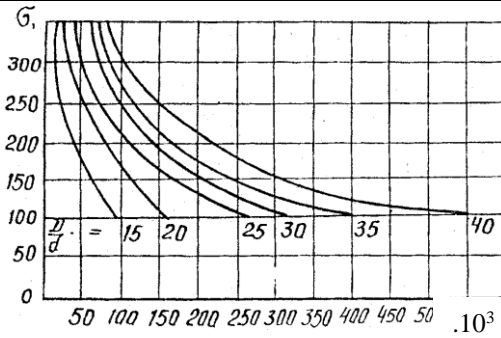


Figure 3.

The groove shape of the winding member of a hoisting machine - Fig.4 is crucial for the time of operation of a rope. A number of authors [2], [3], [5] and others recommend, with the aim of reducing the harmful residual stresses (which appear in the wires when the rope cross-section over the reel is formed), the following relationship:

$$r_k = (0.52 - 0.53) \cdot d \quad (1)$$

where:  $r_k$  is the groove radius, mm  
 $d$  is the rope diameter, mm

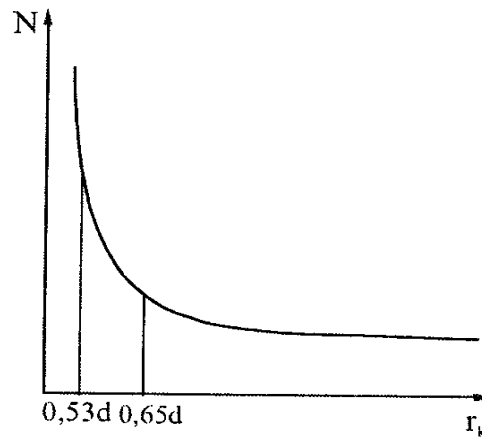


Figure 4.

If the groove radius increases up to  $0.65d$ , the rope serviceability strongly worsens. It is recommended, in order to reduce the secondary stresses, to cut at the groove bottom a narrow strip with  $b$  width, at the ratio of  $b/d = 0.15$  - Fig.5. That is easily feasible with grooves having no lining.

#### OPERATION RELATED WAYS

##### Respect for the general technical requirements of the routine maintenance (RM).

As soon as the hoisting ropes are purchased, it is necessary to subject them to tests at the relevant rope testing laboratories with the objective of finding their technical fitness. Rope rejection because of factory defects makes up 3-4% of all the reasons for that.

Upon their reception the ropes should be kept in dry stores, put on thick wood pads, thus being insulated from dampness. No substances aggressive to metals must be stored in such premises - salts, acids, etc.

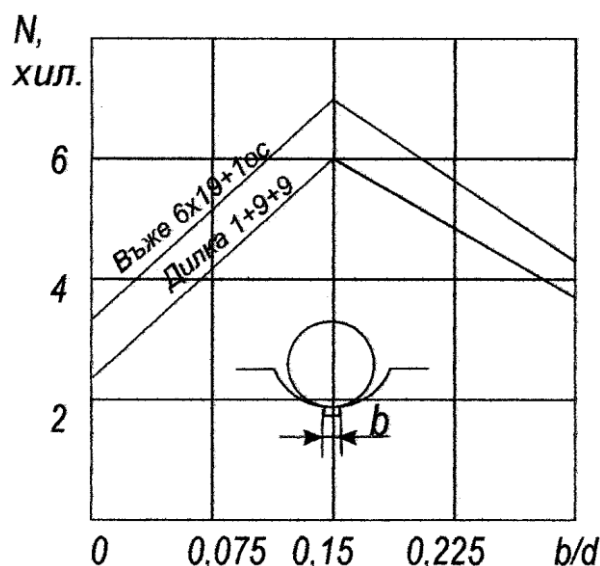


Figure 5.

When performing rewinding from factory reels, preparation for installation, or other operations, ropes must not be drawn axially, since that causes them to untwist, or to further twist, depending on the stitch direction. The phenomenon described above is particularly dangerous for MH with a friction winding member and with triangular fascicles. When they are untwisted, the triangular fascicle border comes out and intensively induces wear and tear both to the groove lining and to the rope itself - because of the irregular configuration in the cross-section. In spite of the lower resistance when tested for bending, compared to the round fascicle ropes, the ones with triangular fascicles are better suited to MH having multi-rope friction pulley and greater depths, due to their higher bearing capacity and lower trend to unwind.

The use of quality fastening elements further contributes to an increase in the hoisting ropes service life. The practical experience has been gradually giving up the use of the lever and wedge cells - KRG type - in that their members induce excessive stresses in the wires and the fascicles. The use of SKK type self-tightening cells and of still better KKB structures with built-in plastic rope fluctuation dampers is recommended.

With the multi-rope MH one should operate with equal winding diameters. The lining grooves are faced when a 0.5mm difference in the diameters has been reached.

To prevent the harmful effect of the mine environment - water, dust, various gases - is recommended the use of galvanized ropes (which are by 20-25% more expensive), and if that is impossible, regular lubrication must be carried out. It is recommended to be done at the areas of rope bending around pulleys, reels and other radiuses, in order to facilitate its penetration into the internals. Lubrication is basically intended to render easier the wires and fascicles reciprocal slip at the

rope bending. Just then it serves also as anticorrosive protection. In MH with a friction winding member are used lubricants guaranteeing normal values of the coefficient of friction between rope and coating. Particular attention should be paid to the "dead" tracts - the ones which do not pass by the guide pulleys or the winding member.

At the presence of two-layer winding, the critical tract (the place of transition from the first to the second layer of winding) must be changed in every two months by cutting out a length of the rope equal to a quarter of a turn. Such operation is carried out at the place of fastening the rope to the reel.

#### Control of the technical condition of the ropes.

The magnetic-inductive test of the ropes has been employed for years in the practice of a number of European and other countries, to find defects in their internals and on their surface. The destructionless check of the hoisting ropes for all MH types was not adopted formally in our country until recently. After it became possible (not however in the coal mines), the operation lifetime of most principal and balancing ropes of MH with friction winding member increased nearly twice. This means that for a long time ropes quite serviceable, but with expired rated service life of two years for the main ropes and four years for the balancing ropes, according to the old requirements of [4], were rejected. Therefore the methods of destructionless check of the technical condition of the hoisting ropes should be applied ever increasingly in the practical use for optimization of the capital and operating expenses for the ropes in MH.

An important point in the practice of the MH operation is the excellent knowledge of the kinds of rope defects, too. The types of damages, described in DIN 15020, and their fast and easy diagnosing by the mine technical staff, enables in a number of occasions further use of the ropes, without it involving risks for the underground workers.

#### REFERENCES

- Глушко М. Ф., Козаченко В. Д. 1968. "Критерий оптимизации параметров стальных канатов двойной свивки." Черная металлургия, бюлл. НТИ №6.
- Дворников И.В., Кърцелин Е.Р. 1997 "Теоретические основы динамики шахтного подъемного комплекса", София, МГУ ..
- Малиновский В.А. 2001 "Стальные канаты - часть I" Одесса, Астропринт,.
- Правилник по безопасност на труда при разработване на рудни и нерудни находища по подземен начин. В-01-02-04), София, Техника. 1982
- Ръководство с нормативи за подбора, доставката, държането на склад, манипулирането и експлоатацията на въжетата при шахтовите подедни уредби. София, ЦНИРПД при ДСО "Металургия и рудодобив". 1973.
- TAS - Technische Anforderungen an Schachtforderanlagen.

## WEAR IN SLIDING BEARINGS FROM MINING AND ORE-PROCESSING MACHINES

Viara Pozhidaeva

University of Mining and Geology "St. Ivan Rilski"  
Sofia 1700, Bulgaria

### ABSTRACT

The article treats a theoretical method for determination of the wear in self-aligning bearings from mining and ore-concentration machines. On the basis of parameters characterizing the wear in a "shaft - sliding bearing" friction pair, there have been obtained relationships for estimation of bearing wear, which gives possibility for prognostication of the bearings resource.

The conditions in which mining machines operate are characterized by higher dynamic loads, dust-loading of the working space and a number of other negative factors, which cause rapid wear of units and details in the mining machines. In this regard, of interest are the bearing units with self-aligning bearings in-built in a number of mining and ore-processing machines, such as bearing type EKG, KU, etc.

The wear in those units operating in the conditions of dry friction or border lubrication is an isolated case of the task of determining the wear in a friction pair "rotating cylinder – sleeve" [2] for  $\alpha_0 = \frac{\pi}{2}$ , where  $\alpha_0$  is the angle determining the dimensions of the contact surface according to the designations in Fig. 1.

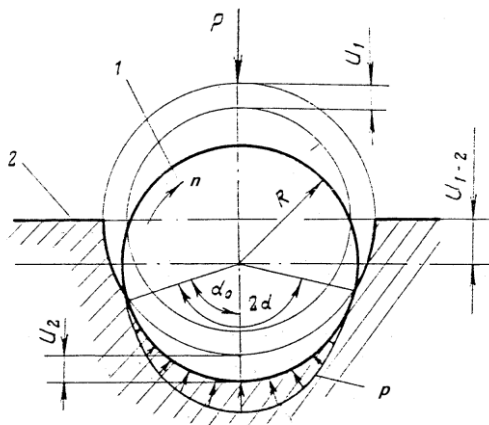


Figure 1. Wear in the shaft and bearing  
1 - shaft, 2 - bearing,  $U_1$  - wear in the shaft,  $U_2$  - wear in the sliding bearing,  $U_{1-2}$  - wear in the units

To determine the wear  $U_2$  and the wear intensity  $I_2$  in the bearing, it is necessary to determine wear  $U_{1-2}$  and wear rate  $I_{1-2}$  in the friction pair of two mutually perpendicular cross-sections. According to the general law of wear [1]

$$I_2 = k_2 p v \quad (1)$$

where:  $k_2$  - wear coefficient of the bearing material;  
 $p$  - pressure;  
 $v = 2\pi n R = \text{const}$  - speed of the friction surfaces.

The wear intensity in the bearing  $I_2$  depends on the pressure in the friction pair, and the latter on its part is a function of angle  $\alpha$ , i.e.

$$I_2 = I_{1-2} \cos \alpha - I_1 \quad (2)$$

where:  $I_1$  is wear rate in the shaft;  
 $I_{1-2}$  is wear rate in the unit.

The angle  $\alpha$  changes from  $-\alpha_0$  to  $+\alpha_0$ , and the quantities  $k_2, v, I_{1-2}$  and  $I_1$  are constant for the specific wear conditions. To determine the numerical values of  $I_{1-2}$  and  $I_1$ , a relationship between force  $P$  and pressure  $p$ , distributed over contact surface  $S$  has to be established:

$$P = \int_S p \cos \alpha ds = 2\pi \int_{y_1}^{y_2} p \cos \alpha \rho dy = 2\pi \cos^2 \alpha \int_{y_1}^{y_2} p y dy \quad (3)$$

where:  $y_1 = \frac{r}{\cos \alpha}$ ,  $y_2 = \frac{R}{\cos \alpha}$ ,  $\rho = y \cos \alpha$ ,  $dS = \ell_0 R d\alpha$ ,  
 $\ell_0$  - bearing length.

$$P = R \ell_0 \int_{-\alpha_0}^{\alpha_0} p \cos \alpha d\alpha = R \ell_0 \int_{-\alpha_0}^{\alpha_0} \frac{I_{1-2} \cos \alpha - I_1}{k_2 v} \cos \alpha d\alpha \quad (4)$$

After integration and transformation of (4), follows:

$$P = \frac{R\ell_0}{k_2 v} [I_{1-2}(0,5 \sin 2\alpha_0 + \alpha_0) - I_1 2 \sin \alpha_0] \quad (5)$$

From equation (5) for wear intensities  $I_{1-2}$  and  $I_1$ , follows

$$I_{1-2} = \frac{2\pi k_2 P n}{\ell_0 \left( 0,5 \sin \alpha_0 + \alpha_0 - \frac{k_1 \sin \alpha_0}{\pi k_2 + \alpha_0 k_1} \right)} \quad (6)$$

$$I_1 = I_{1-2} = \frac{k_2 \sin \alpha_0}{\pi k_2 + \alpha_0 k_1} \quad (7)$$

where  $k_1$  - wear coefficient of the shaft material

$n$  - circular shaft frequency,  $\text{min}^{-1}$ .

From equations (2) and (7) for bearing wear  $U_2$  and shaft wear  $U_1$  follows:

$$\begin{cases} U_1 = I_{1-2} \frac{k_1 \sin \alpha_0}{\alpha_0 k_1 + \pi k_2} \cdot t \\ U_2 = I_{1-2} \left( \cos \alpha - \frac{k_1 \sin \alpha_0}{\alpha_0 k_1 + \pi k_2} \right) \cdot t \end{cases} \quad (8)$$

Equations (6) and (8) were obtained in considering a diametral section of the bearings unit, but they are applicable in determining the wear over the whole friction surface if force  $P$  is applied centrally lengthwise of bearing  $\ell_0$ .

In this case, the wear in the axial cross-section of the bearing unit will be uniform and will be determined from equation (6), through the distributed load of a  $\frac{P}{\ell_0}$  unit of length from the bearing. If force  $P$  is not applied centrally, but with eccentricity  $x$  (Fig. 2), then the wear in the bearing unit will be determined from two parameters:

$$\begin{cases} U'_{1-2} = I_{1-2} \cdot t \\ U''_{1-2} = I_{1-2} \cdot t \end{cases} \quad (9)$$

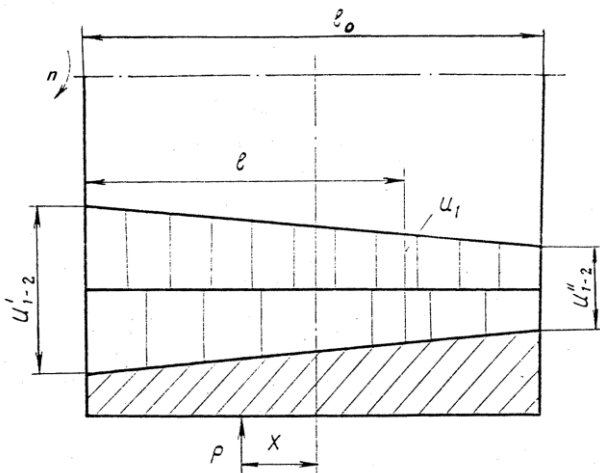


Figure 2. Wear in the units axial cross - section

The relationship between the wear in the friction surfaces and in the coupling will be obtained from the contact conditions of the friction surfaces, and namely:

$$U_1 + U_2 = U'_{1-2} \left( 1 - \frac{\ell}{\ell_0} \right) + U''_{1-2} \frac{\ell}{\ell_0} \quad (10)$$

and for wear intensity in the bearing unit, follows:

$$I_{1-2} = I_1 + I_2 = I'_{1-2} \left( 1 - \frac{\ell}{\ell_0} \right) + I''_{1-2} \frac{\ell}{\ell_0} \quad (11)$$

for  $\ell = 0$   $I_1 + I_2 = I'_{1-2}$

for  $\ell = \ell_0$   $I_1 + I_2 = I''_{1-2}$

As follows from formula (6), wear intensity  $I_{1-2}$  depends on the relative force  $\frac{P}{\ell_0}$  acting in a given cross-section. If we

designate with  $P_e$  the force of a unit of length from the axial cross-section, applied in a point with a  $\ell$  coordinate (Fig. 3), then:

$$I_{1-2} = \frac{P_e}{A} \quad (12)$$

where: 
$$A = \frac{k_2}{\left( 0,5 \sin 2\alpha + \alpha_0 - \frac{k_1 \sin \alpha}{\pi k_2 + \alpha_0 k_1} \right)}$$

After replacement in (11) and transformation, follows:

$$P_e = A \left[ I_{1-2} - \frac{\ell}{\ell_0} (I'_{1-2} - I''_{1-2}) \right] \quad (13)$$

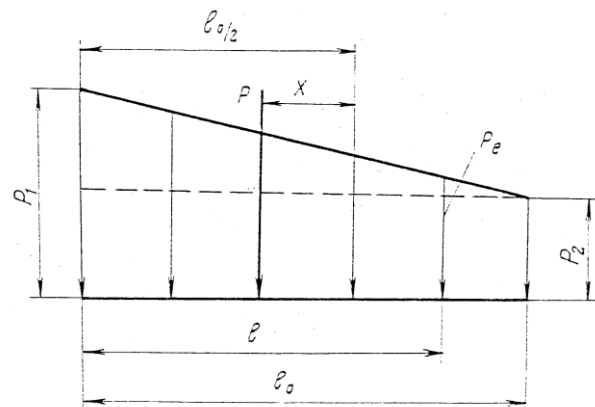


Figure 3. Pressure diagram in an axial cross - section

For a linear character of the pressure diagram in an axial cross-section, the relationship between the force  $P$  applied with eccentricity  $x$  and the force  $P_e$  in the cross section with coordinate  $\ell$  is:

$$P_e = \frac{p}{\ell_0} \left( 1 + \frac{6x}{\ell_0} - \frac{12x}{\ell_0^2} \cdot \ell \right) \quad (14)$$

If in equation (6), instead of  $\frac{P}{\ell_0}$  we substitute  $P_e$  from equation (14) for  $l_{1-2}$ , we obtain:

$$l_{1-2} = \frac{P_0 \left( \ell_0^2 + 6x\ell_0 - 12x\ell \right) 2\pi n k_2}{\ell_0 \left( 0,5 \sin 2\alpha_0 + \alpha_0 - \frac{k_1 \sin \alpha_0}{\pi k_2 + \alpha_0 k_1} \right)} \quad (15)$$

Shaft wear  $U_1$  and bearing wear  $U_2$  in an arbitrary point of the friction surface can be obtained from equation (8) after replacement of the  $l_{1-2}$  quantity estimated by equation (15).

Determination of shaft and bearing wear for two border values - minimal and maximal admissible - enables estimation of wear-resistance by formula (9) for each separate case of in-building and prognostication of the bearing resource.

#### REFERENCES

- Kragelskij I. V., Dobyjchin M.N., Kombalov V.S., Principles of friction and wear, M., *Mashinostroenie*, 1977.  
 Pronikov A.S., Machines Reliability, M., *Mashinostroenie*, 1978.

Recommended for publication by Department of Mine mechanization, Faculty of Mining Electromechanics

## A LINEAR STRUCTURAL ANALYSIS OF THE LEADING SHEAVES OF SHAFT HOISTS BY THE FINITE ELEMENT METHOD

**Nikolay Perenovski**

University of Mining and Geology "St. Ivan Rilski"  
Sofia 1700, Bulgaria

**Antoaneta Yaneva**

University of Mining and Geology "St. Ivan Rilski"  
Sofia 1700, Bulgaria

**Ivan Minin**

University of Mining and Geology "St. Ivan Rilski"  
Sofia 1700, Bulgaria

**Tzvetan Damianov**

University of Mining and Geology "St. Ivan Rilski"  
Sofia 1700, Bulgaria

### ABSTRACT

An analysis is made of the strain-stress state of the leading sheaves of shaft hoists. The finite element method and, in particular, its computer application is used. Simulation investigation of a previously designed model in a 3-D format has been performed. The approach has great advantages for large-size pieces that are extremely difficult to subject to investigation under industrial or laboratory conditions.

Minimum factors of safety are determined on the basis of the results obtained for the regions of highest stresses under different operating conditions. These have been analyzed and the possibilities assessed for improving the design-performance parameters of a leading sheave under specific shaft hoist conditions.

### INTRODUCTION

Leading sheaves in shaft hoists serve to take on the forces of the hoist ropes, i.e. their dead weight, suspended end load and all working and breaking dynamic loads. The sheaves direct the ropes along the axis of the vertical shaft and their accurate mounting determines the linear movement of the hoisting vessel. The leading sheaves are mounted on a special platform on the shaft frame. They consist of a ring with a groove for the hoist rope, a hub and spokes – steel sections or another connecting structure – side disks – Fig. 1. The leading sheave is keyed to an axle rotating freely on bearing supports. The standard size sheaves are designed with diameters of 2 – 5 m. In case of diameters larger than 3m the sheave ring is made of die steel in several segments. The ring type determines the leading sheave design – with a lining or with a replaceable one made of wear-resisting steel, rubber mix, plastics, metal ceramics, etc. The presence of lining produces up to a 30-40% higher flywheel moment and failure or dropping out of lining parts can cause the rope to come out of the groove and break.

Until now most studies on the 'leading sheave - rope' mechanical pair have been carried out with the aim of improving the operating conditions of the hoist rope, decreasing its wear, better contact between it and the sheave groove, higher durability. The aim of this study is to check the strength and strain characteristics of the leading sheave under maximum load on the hoist rope in view of optimizing its design. The relative strains of the groove and its wear also affect these rope parameters. By improving the design of the leading sheave we create better operating conditions for the rope.

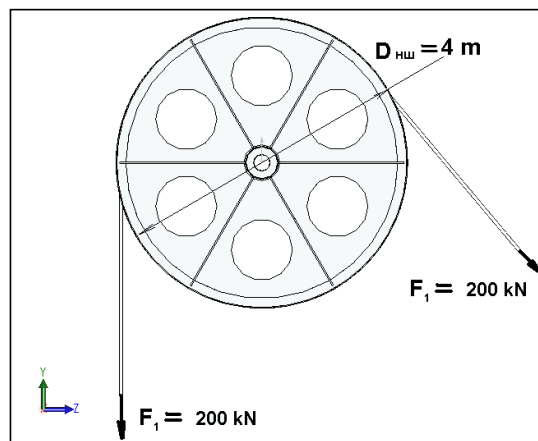


Figure 1

A leading sheave of welded design without lining, having a  $D = 4\text{ m}$  is selected. Two options for the cross-section of its groove are considered – Fig.2 – common semicircular with a wrapping angle of  $60^\circ$  (Fig. 2b) and semicircular with an undercut groove and a wrapping angle of  $90^\circ$  (Fig. 2a) [2]. The aim is to reach minimum stresses on the groove and the rope, respectively, by increasing the contact area between them.

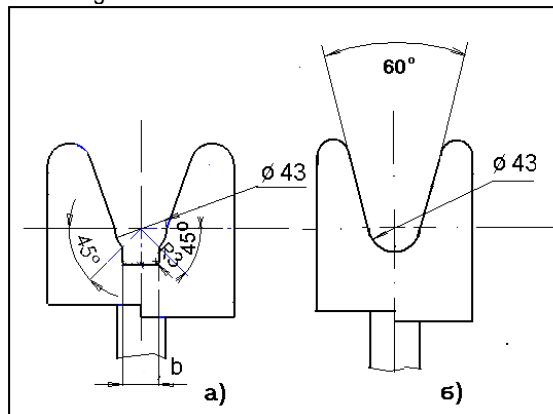


Figure 2

The working loads have been calculated for shaft hoists with a lift height  $H = 500\text{m}$ ; two hoisting vessels – skips with a suspended end load of  $160\text{ kN}$  (at maximum density of the mineral and  $V = 5\text{ m}^3$  for ore or  $V = 7\text{ m}^3$  for coal); a two-drum hoisting machine with a constant winding radius ( $D = 4\text{m}$ ). The hoist rope is round and has an open design with the following parameters: linear weight  $76.22\text{ N/m}$ ; diameter  $d = 46\text{ mm}$ ; maximum breaking force  $1470\text{ kN}$ . The maximum static load on the rope is  $200\text{ kN}$ .

The leading sheave is investigated under maximum dynamic loads, five times greater than the working static ones. They can occur when a rope is broken, a safety catch is actuated for seizure in stopping ropes; when a full skip comes out of the end stands; when the safety brake is actuated, etc. The results can be distributed for other operating conditions as well as other sheave designs.

The simulation modeling of the leading sheave is required because of its large size and mass. Computer simulation is applied by the finite element method. The leading sheave is presented as an object composed of a finite number of parts, called elements, which are connected at characteristic points – nodes. The interaction of the elements occurs only in the nodes. The behavior of the investigated design is judged by the displacement of a certain number of nodes. The process can be represented as a system of algebraic equations that in the problems of strain-stress analysis are static equilibrium equations.

## INVESTIGATION METHODS

**1. Computer simulation.** This is the first stage during which a three-dimensional computer model of the object is designed. The case refers to the leading sheave shown in Fig. 1 of sheet steel welded design and different rope groove configuration (Fig. 2). The simulation is performed in a Solid Works environment with the greatest possible details for the output data (the real object).

**2. Planning of the investigation.** A main point at this stage is the choice of a suitable software package based on the already specified finite element method. After carrying out a preliminary analysis of the possibilities to utilize the qualities of the programs Ansys, Cosmos M, Cosmos Works and Designer Space, the latter two were chosen. Several test studies were performed using these programs. As a result it was found that working with the Designer Space program is particularly difficult at the stage of “discretization of the object”, i.e. when a grid of finite elements is formed for such a large-size piece having a complex configuration of thin-walled elements. This is the reason why the program Cosmos Works 6 was chosen for the computer realization of the finite element method.

Since the capacities of the post-processor module of this program are widely utilized with respect to the results (parameters of the strain-stress state), for the purposes of this investigation only some of these will be used:

- equivalent stress according to von Mises;
- factor of safety according to the theories of Mises - Henkey and Treska;
- static strains (absolute; equivalent).

According to Mises – Henky the yield limit is determined by the ratio between the magnitude of Mises’ equivalent stress and that of the allowable stress  $\sigma$  [1]

$$\sigma_{von} \geq \sigma_{limit}$$

Mises’ stresses can be expressed by the three main stresses:

$$\sigma_{von} = \sqrt{\frac{(\sigma_1 - \sigma_2)^2 + (\sigma_2 - \sigma_3)^2 + (\sigma_1 - \sigma_3)^2}{2}} \quad (1)$$

The limit value of the stress  $\sigma_{limit}$  can be expressed as a function of the yield stress or material breaking stress. Hence, the factor of safety (FOS) according to von Mises is:

$$FOS = \frac{\sigma_{limit}}{\sigma_{von}} \quad (2)$$

and non-dimensionally - 
$$\frac{1}{FOS} = \frac{\sigma_{von}}{\sigma_{limit}}, \quad (3)$$

The maximum shear stress criterion, known as Treska’s criterion, is based on the theory of maximum shear stresses. According to this theory

$$\tau_{max} \geq \frac{\sigma_{limit}}{2},$$

where  $\tau_{max}$  can be  $\tau_{1,2}$  or  $\tau_{2,3}$  or  $\tau_{1,3}$ , and is therefore equal to:

$$\tau_{1,2} = \frac{\sigma_1 - \sigma_2}{2}; \tau_{2,3} = \frac{\sigma_2 - \sigma_3}{2}; \tau_{1,3} = \frac{\sigma_1 - \sigma_3}{2} \quad (4)$$

Hence: 
$$FOS = \frac{\sigma_{limit}}{2\tau_{max}} \quad (5)$$

and non-dimensionally - 
$$\frac{1}{FOS} = \frac{2\tau_{max}}{\sigma_{limit}}. \quad (6)$$

The factor of safety (FOS) is calculated automatically by the program and visualized in the “safety result” field on the basis of maximum local stresses in the investigated object and the values of the limit stresses in the material.

**3. Parametrization of a test study.** This is performed in a Cosmos Works 6 environment in the following sequence:

- Precise parametrization (presetting) of the accurate values of the material density, Young’s modulus ( $E$ ), Poisson’s ratio ( $\mu$ ). The material of the investigated object should be isotropic.
- Optimal presetting of the load and boundary conditions of the model so that they can reflect very precisely the actual compression forces and limitation of degrees of freedom in the global coordinate system. It is assumed that the function of load distribution is according to the cosine law. There must be a region of zero known displacements, i.e. static fixation. This is required even if the external loads are self-balanced. For the particular case the boundary conditions will be preset as a load distributed on the surface of the hoist rope groove at a wrapping angle of  $140^\circ$  and a region of zero displacements, fixed surface of the bearing shaft hole – Fig. 3.

- Validating the model by selecting finite elements that are appropriate in terms of their geometry and metrics and by generating the best possible grid. In this case we have in mind a regular-shaped grid of the elements and narrow limits of size variation.

### RESULTS AND ANALYSIS

The first investigation stage involves determination of the strain-stress pattern according to Fig. 2a, which is visualized in Figs. 3 and 4. Fig. 3 shows explicitly the discretization of the tetrahedral-shaped model of finite elements and parameters:  $b = 87.5$  mm,  $N_v = 45\ 195$  nodes and  $N_e = 23\ 007$  finite elements. The maximum values of Mises' equivalent stresses ( $\sigma = 7.2$  MPa) are localized around the mass-lighting holes of the sheave, whereas the stress values for the groove do not exceed  $\sigma_v = 15\text{-}20$  MPa. These values are considerably lower than the limit values for the material (structural alloy steel), which are:

- yield strength  $\sigma_s = 620$  MPa
- ultimate strength  $\sigma_B = 724$  MPa.

Objective evaluation of the equivalent stresses can be made by the pattern of distribution of Mises.

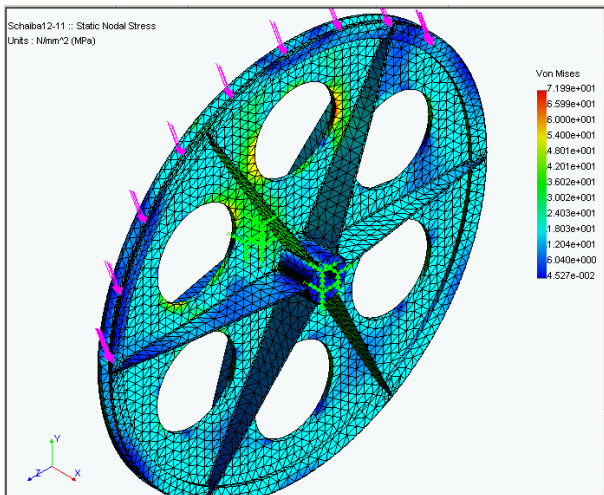


Figure 3

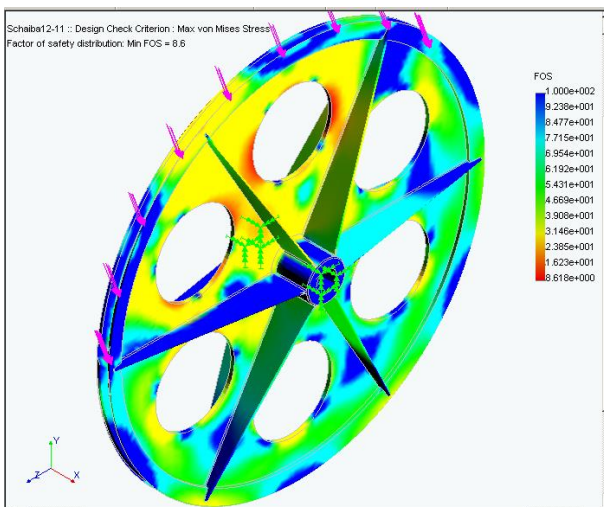


Figure 4

Factor of Safety (FOS) – Fig. 4. The lowest values for the investigated sheave are  $FOS = 0.6$  and are localized in the

same regions. These results show that the equivalent stresses in the groove from Fig. 2 do not exceed 30 MPa.

Fig. 5 presents a pattern of distribution of FOS for a groove version from Fig. 2a and parameter value  $b = 20$  mm. Here the possibilities of the Cosmos Works program were used for selective point representation of the results by the Probe results tool. The minimum FOS value is found in the region of point 1 ( $FOS_1=11$ ), which is at the interface of the holes. The highest value of the same parameter was calculated for the regions of point 2 and point 3 ( $FOS_2=26$  and  $FOS_3=100$ ), which are regions from the sheave groove.

Fig. 6 shows the pattern of distribution of the equivalent stresses and their highest values calculated for the sheave groove. It can be seen that the values vary within  $\sigma_s = 6 \div 18$  MPa.

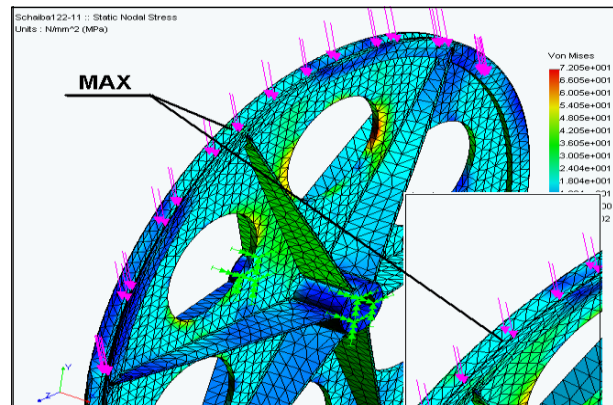


Figure 6

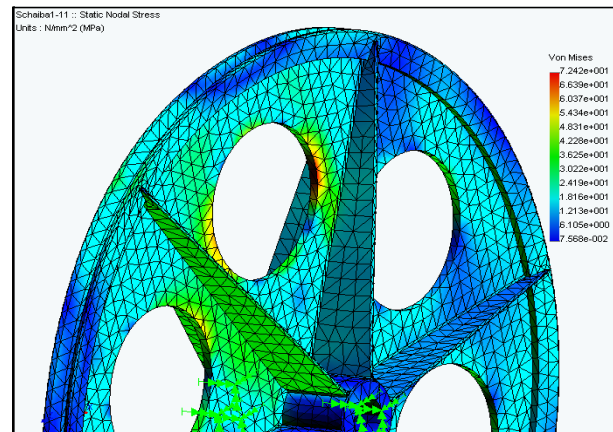


Figure 7

The results of the study on a leading sheave shaped like the groove according to Fig. 2b are presented in Fig. 7. Here we can also observe localization of the maximum values of the equivalent stress (up to 72 MPa) in regions remote from the sheave groove. For the groove itself these stresses vary within much lower limits from 6 to 30 MPa. The results of the calculations for the factor of safety are not presented since they are not very different from those of the previous investigated designs.

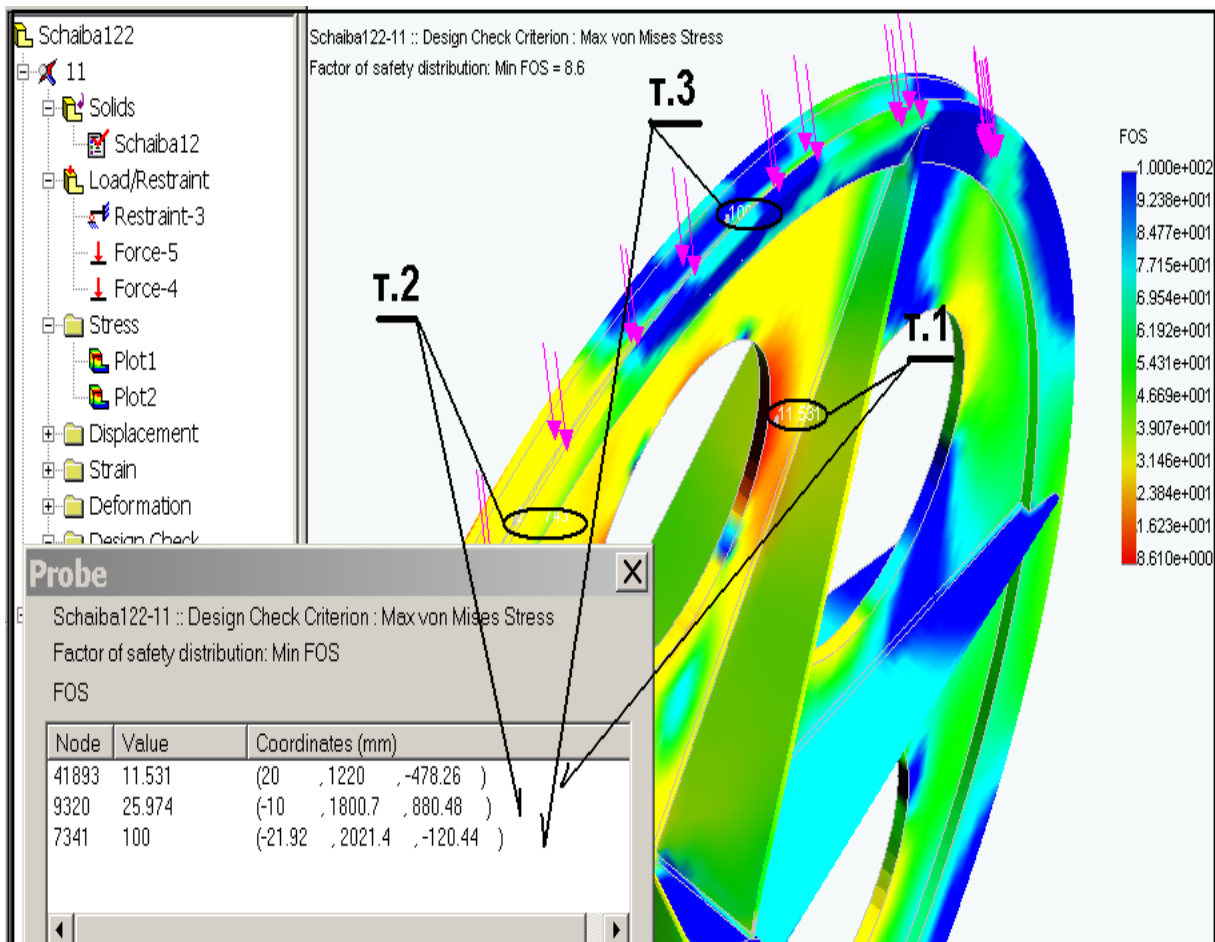


Figure 5

### CONCLUSIONS

1. The model rigidity can be investigated for loads different in size and distribution. Analytically this is very difficult and inaccurate and experimentally for large-size object it is practically impossible.

2. The retardation of the wear process of both the rope and the sheave groove for a stress value between the rope-groove interface preset within the allowable limits, depends also on the even distribution of the strains on that interface. Therefore, the minimization of the strains and stresses is an insufficient condition for improving the leading sheave design of shaft hoists.

3. When designing or improving leading or driving friction sheaves for shaft hoists it is necessary to perform a computer simulated structural analysis with the aim of optimizing the distribution of stresses and strains.

### REFERENCES

- Hibbeler R. C., Mechanics of Materials, Second edition, Prentice Hall, 1994  
 TAS – Technische Anforderungen an Schachtförderanlagen VDI – VDI-Verlag, Dusseldorf, 1984

## ON THE VELOCITY OF AN OPTIONAL POINT OF CRANK MECHANISM CONNECTING ROD

Vasko Tenchev

University of Mining and Geology "St. Ivan Rilski"  
 Sofia 1700, Bulgaria

**ABSTRACT**

The paper deals with evaluation of the velocity of an optional point of crank mechanism connecting rod, by applying the so-called secondary model of the mechanism (Piperkov, 1987). Short formulae for fast evaluation of point velocity have been synthesized for the case, when the point is center of mass of the connecting rod. These formulae can be used in the dynamical study of assemblies comprising such mechanisms.

Evaluation of the velocity of optional point of crank mechanism connecting rod is an already solved problem, which as analytical solution leads to voluminous results. The velocity of the point is evaluated in the present paper by means of the so-called *secondary model* of the mechanism, proposed by D. L. Piperkov (1987). With the aid of this model short formulae could be synthesized for calculation of point

velocity concerning the case that the point is center of mass of the connecting rod.

Fig. 1 shows arbitrary position of the axial crank mechanism  $OAB$ . For this position, the velocity  $V_S$  of the arbitrary point  $S$  of the symmetry axis of the connecting rod 2 is to be found, when applying the secondary model  $OAB'$  of the mechanism.

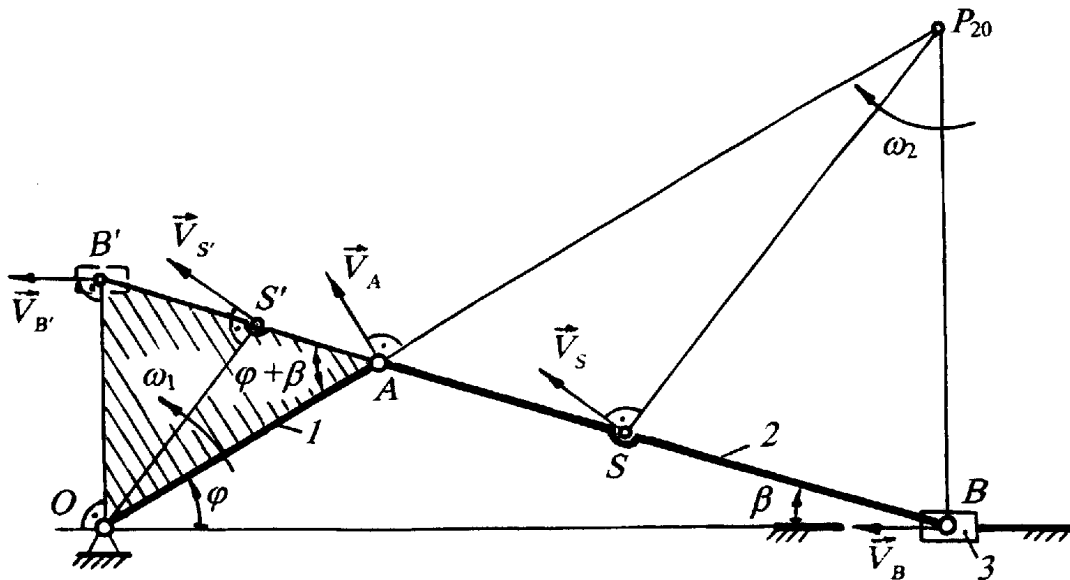


Figure 1

Point  $B'$  is intersection point of connecting rod direction 2 and the line passing through the axis  $O$  of the crank 1 and is perpendicular to the straight-line  $OB$ , which is the path of

movement of slider 3. Line segment  $AB'$  is called *image* of the line segment  $AB$ , representing the connecting rod 2, and points  $B'$  and  $S'$  - *images* of the corresponding points  $B$

and S from the connecting rod. For each arbitrary position of the mechanism the relationship (1) is valid:

$$\frac{AS'}{AB'} = \frac{AS}{AB} = \xi, \quad (1)$$

where  $\xi$  is a known constant.

In the considered position of the mechanism the secondary model  $OAB'$  represents a body (designated by shaded triangle), which rotates around the axis O with the known rotational speed  $\omega_1$  of the crank 1. In this case there is no problem to evaluate the velocity  $V_{S'}$  of image  $S'$ . The directrix of this velocity is perpendicular to the line segment  $OS'$ , and its direction corresponds to the direction of  $\omega_1$ . The magnitude of  $V_{S'}$  is

$$V_{S'} = \omega_1 \cdot OS' . \quad (2)$$

With the evaluation of  $V_{S'}$  the searched velocity  $V_S$  of the optional point S from the connecting rod 2 is also evaluated, because it comes out, that they are equal, i. e.

$$V_S = V_{S'} . \quad (3)$$

This statement can be proved, having in view, that the point  $P_{20}$  is the absolute instantaneous velocity center (IVC) for the connecting rod 2, and that triangles  $ABP_{20}$  and  $OAB'$  are similar. For the magnitude of the velocity  $V_S$  can be declared

$$V_S = \omega_2 \cdot P_{20}S , \quad (4)$$

where the rotational speed  $\omega_2$  of the connecting rod 2, expressed by the velocity of point A, is

$$\omega_2 = \frac{V_A}{P_{20}A} = \frac{\omega_1 \cdot OA}{P_{20}A} = \frac{\omega_1 \cdot OS'}{P_{20}S} . \quad (5)$$

Then

$$V_S = \omega_1 \cdot OS' . \quad (6)$$

$$V_S = V_S(\varphi) = r\omega_1 \sqrt{\frac{\xi^2 \cos^2 \varphi}{1 - \lambda^2 \sin^2 \varphi} + 1 - 2\xi \cos \varphi \left( \cos \varphi - \frac{\lambda \sin^2 \varphi}{\sqrt{1 - \lambda^2 \sin^2 \varphi}} \right)} . \quad (9)$$

It is important for the dynamical study of crank mechanism that we know how does proceed the variation of the gear ratio  $V_S/\omega_1$  as a function of  $\varphi$  at  $\omega_1 = \text{const}$ , particularly when  $V_S$  is the velocity of the mass center S of the connecting rod 2. Obviously, the answer is in the relationship (9), but for the requirements of practice it appears to be too complicated. The secondary model  $OAB'$  gives us the possibility to use the line segment  $OS'$  to notice easily the nature of change of this

After comparison of the expressions (6) and (2) is established, that velocities  $V_S$  and  $V_{S'}$  have equal magnitudes. The equivalence of directness and directions of these velocities follows from the parallelism of straight lines  $P_{20}S$  and  $OS'$ , and from the direction of rotational speeds  $\omega_2$  and  $\omega_1$ . By this means the statement (3) has been proved.

Creation of secondary model  $OAB'$  for each position of the crank mechanism  $OAB$  gives the possibility for graphic evaluation of the investigated velocity  $V_S$ . At the same time, this model permits a relatively easy way for determining the analytical expression of the function  $V_S = V_S(\varphi)$ , where  $\varphi$  is geometrical parameter, defining the rotation of the crank 1 related to the horizontal line in the side of slider 3. Using triangle  $OAS'$ , with the aid of the theorem of cosines, the line segment  $OS'$  is defined. This gives us the possibility to write down for the velocity  $V_S$  the following expression

$$V_S = V_{S'} = \omega_1 \cdot OS' = \omega_1 \sqrt{(AS')^2 + r^2 - 2AS' \cdot r \cos(\varphi + \beta)} . \quad (7)$$

Here for brevity is nominated  $r = OA$ , and  $\beta$  is the geometrical parameter, defining the rotation of connecting rod 2 against the horizontal line. Further, using the theorem of sines, from the triangle  $OAB'$  we determine

$$AB' = r \frac{\cos \varphi}{\cos \beta} . \quad (8)$$

Taking into consideration (1), after substituting (8) in (7), and using the equations  $\sin \beta = \lambda \sin \varphi$  (triangle  $OAB$  - theorem of sines) and  $\cos \beta = \sqrt{1 - \lambda^2 \sin^2 \varphi}$  (for brevity here is nominated  $\lambda = r/AB$ ), then for the function  $V_S = V_S(\varphi)$  we obtain the following analytical expression

quantity, as well as to find short analytical relationships for its description.

In fig. 2 is presented graphically the variation of the gear ratio  $V_S/\omega_1$  for the axial crank mechanism  $AOB$ , when  $\varphi$  varies from  $0^\circ$  to  $180^\circ$ . In the interval of change of  $\varphi$  from  $180^\circ$  to  $360^\circ$ , the variation is symmetrical to the straight line  $OB$ . As it can be seen, at  $\varphi = 0$  for the gear ratio could be obtained

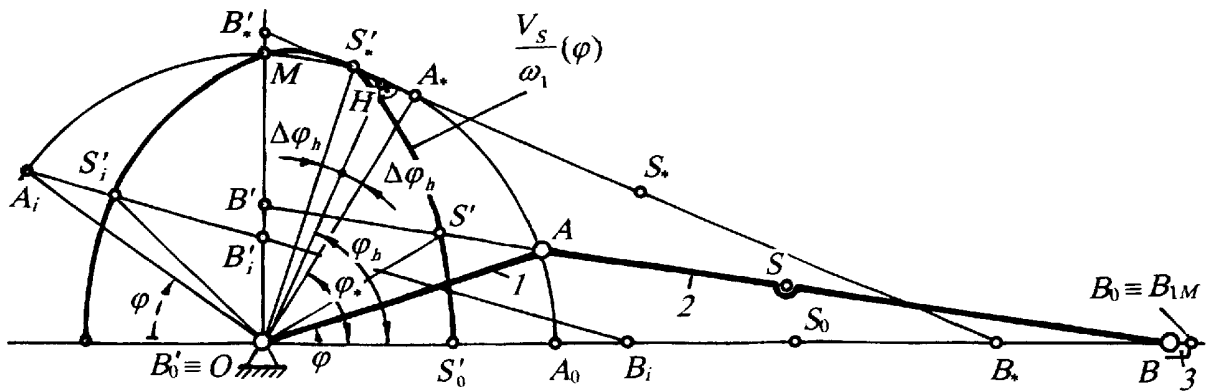


Figure 2

$$OS' = \frac{V_s}{\omega_1} = r - r \frac{A_0 S'_0}{A_0 B'_0} = r(1 - \xi). \quad (10)$$

The increase of  $\varphi$  leads to increment of the gear ratio  $V_s / \omega_1$  too. For one characteristic angle  $\varphi = \varphi_*$

$$OS' = \frac{V_s}{\omega_1} = r, \quad (11)$$

and after that

$$OS' = \frac{V_s}{\omega_1} > r. \quad (12)$$

At  $\varphi = 90^\circ$  the ratio  $V_s / \omega_1$  arrives at the value (11) again, after that it begins continuously to decrease, until it reaches at  $\varphi = 180^\circ$  its initial magnitude (10).

The characteristic angle  $\varphi_*$  is determined by the position  $OA_*B_*$  of the crank mechanism, where

$$OA_* = OS'_* = r. \quad (13)$$

The triangle  $OA_*S'_*$  is isosceles and its height  $OH$  with angular coordinate  $\varphi_h$  divides the central angle  $A_*OS'_*$  to two equal angles  $\Delta\varphi_h$ . Then for the characteristic angle  $\varphi_*$  can be written

$$\varphi_* = \varphi_h - \Delta\varphi_h. \quad (14)$$

Further the point  $S$  is regarded as mass center of the connecting rod 2. For the crank mechanism  $OAB$  very often  $\lambda = OA / AB < 1/3$ , and for the location of the mass center  $S$  is valid the condition  $\xi = AS / AB < 1/2$ . At these limitations we can assume with enough accuracy that

$$\varphi_h \approx \arctan \frac{A_*B_*}{OA_*} = \arctan \frac{1}{\lambda} \quad (15)$$

and

$$\frac{2\Delta\varphi_h}{90^\circ - \varphi_*} = \frac{A_*S'_*}{A_*M} \approx \frac{A_*S'_*}{A_*B'_*} = \xi, \quad (16)$$

from there

$$\Delta\varphi_h \approx \frac{\xi}{2} (90^\circ - \varphi_h). \quad (17)$$

After substitution of (15) and (17) in (14), for the characteristic angle  $\varphi_*$  is obtained

$$\varphi_* \approx \frac{2 \arctan \frac{1}{\lambda} - 90^\circ \xi}{2 - \xi}. \quad (18)$$

The variation of the gear ratio  $V_s / \omega_1$  in the interval of  $\varphi$  from  $0^\circ$  to  $180^\circ$ , which is graphically shown in fig. 2, can be described approximately in the sections with the aid of short trigonometrical relationships. Obviously these relationships should obtain the mentioned values of  $V_s / \omega_1$  for  $\varphi = 0^\circ, \varphi_*, 90^\circ, 180^\circ$ , as well as for the limit case  $\lambda = \xi = 0$ , at which, going out from (9) it appears, that  $V_s / \omega_1 = r$ . On the base of these requirements and the observation of the dimensional correspondence, as well as based on a lot of numerical experiments, aiming the achievement of a specific relative error, have been synthesized reasonably short trigonometrical relationships, given in table 1.

When the geometrical parameter  $\varphi$  of the crank 1 has been read from the horizontal line, which related to the axis  $O$  is situated on the opposite side of the slider 3 (in fig. 2 the parameter  $\varphi$  for that case is given with dash-line), the graphical form of the gear ratio

Table 1

|  |  |
|--|--|
| Limitations: $\lambda \leq \frac{1}{3}$ и $\xi \leq \frac{1}{2}$ |  |
| $0 \leq \varphi \leq \varphi_*$                                  | $\rightarrow \frac{V_s}{\omega_1} \approx r \left[ 1 - \xi \cos^2 \left( 90^\circ \frac{\varphi}{\varphi_*} \right) - 0,16\xi(2\lambda - \xi) \sin \left( 180^\circ \frac{\varphi}{\varphi_*} \right) \right]$ |
| $\varphi_* \leq \varphi \leq 90^\circ$                           | $\rightarrow \frac{V_s}{\omega_1} \approx r$   |
| $90^\circ \leq \varphi \leq 180^\circ$                           | $\rightarrow \frac{V_s}{\omega_1} \approx r \left[ 1 - \xi \cos^2 \varphi + 0,56 \frac{180^\circ - \varphi}{90^\circ} \xi^2 (3\lambda - \xi) \sin 2\varphi \right]$  |

$V_s / \omega_1$  as a function of  $\varphi$  (Fig. 2) is kept the same, but according to the new situation the characteristic angle  $\varphi_*$  is given with the expression

$$\varphi_* \approx 180^\circ - \frac{2 \arctan \frac{1}{\lambda} - 90^\circ \xi}{2 - \xi} \quad (19)$$

The short relationships from table 1 for this case are also subjected to changes. The formula (19) and the modified relationships are obtained correspondingly from the expression (18) and the relationships in table 1, when we substitute formally  $\varphi_*$  by  $180^\circ - \varphi_*$ , and  $\varphi$  by  $180^\circ - \varphi$ .

The relative error of the short relationships at values of  $\lambda$  in the limits of  $1/10 \leq \lambda \leq 1/3$  and the above said values of  $\xi$ , attains the magnitude 2%. These limits of variation of  $\lambda$  are mostly used in practice. At  $\lambda = 0$  and  $\xi = 1/2$  this error increases to 2,5%, but its sense is generally theoretical. Without the last summand in the first and the third formula of table 1 the relative error is higher, but it is not higher than 6% for the specified limitations of the parameters  $\lambda$  и  $\xi$ .

## CONCLUSION

Through the application of the secondary model of crank mechanism has been regarded the possibility of determination of the velocity of optional point from the axis of symmetry of connecting rod. Short formulae have been synthesized for the evaluation of velocity (gear ratio) of the mass center of connecting rod. The relative error of the obtained by these formulae results (in the limits of the parameters  $\lambda$  and  $\xi$ , where the mechanism is being used) is not higher than 2%.

## REFERENCES

- Piperkov, D. L. 1987. Secondary modeling in theoretical mechanics. *Author's summary of dissertation for doctor degree "candidate of technical sciences"*. Sofia, Technical University.

*Recommended for publication by Department of Mine Mechanization, Faculty of Mining Electromechanics*

## TRAJECTORY INVESTIGATION OF A HYDRAULICALLY DRIVEN MANIPULATOR

**Bojidar Grigorov**

Technical University - Sofia  
Sofia 1797, Bulgaria  
E-mail b.grigorov@vmei.acad.bg

**Stefan Asparuhov**

Technical University - Sofia  
Sofia 1797 Bulgaria

### ABSTARCT

The present work presents an investigation conducted in order to determine the abilities of loading manipulator to move a particular load along desired trajectory through space. Such a trajectory is defined via number of known path points (including initial and final positions). Each path point is represented as position and orientation of the load within the manipulator's working space according to some basic frame. The particular construction under consideration is hydraulically driven, five degree of freedom structure with revolute joints. Given the time elapsed between the path points, the necessary driving torques to counterbalance the system of external static and dynamic forces at each degree of freedom are computed. Such computations are performed using interactive Newton – Euler algorithm. The necessary flow output of the hydraulic pump to provide desired velocities of the manipulator's links is also determined. The computed required forces and flow are compared to the actual parameters of the manipulator in order to evaluate the capabilities of concrete installation to follow predefined trajectory in space.

Trajectory as stated in robotics refer to a time history of position, velocity and acceleration for each degree of freedom. These functions are determined by taking into account a number of known positions and orientations of the tool, load or the last link of manipulator, i.e. the basic problem is to move the manipulator from one initial to one final position. Note that, in general, this motion involves change in position, but change in orientation as well relative to some basic frame. Sometimes the trajectory can be specified in more details as sequence of "via points" are given in addition to the starting and ending positions. All the starting, ending locations as well as the "via points" are referred as "trajectory points". We can also include the time factor – a time interval required to complete the motion via the set of trajectory points.

It is obvious, that while in motion, the links of the manipulator are subjected to a system of external forces – both static and dynamic. This is quite true for heavy duty loading equipment, designed to lift and transport considerable loads. In such cases the mass of the links could not be negligible. The set of external forces produces reactions – three dimensional torque and force vectors at each joint. All components of these force and moment vectors are resisted by the structure of the mechanism itself, except for the torque about the joint axis, which is balanced by the hydraulic system actuators.

On the other hand, there is constant desire to intensify the working process mainly by increasing link's velocity and thus reducing the working cycle. This leads however to increasing accelerations and escalating dynamic forces and thus – to the greater stress upon the construction.

In general, the universal loading manipulators are intended to perform large scope of activities, including some purely technological tasks. This is why the structure and the

driving system are designed having in mind some general requirements, sometimes without regard to any specific applications. When going to specific tasks however, it is necessary to conduct some kind of investigations upon the given construction. Such investigation can be the study of the manipulator's ability to maintain given trajectory in space. This involves not only the ability of the driving system to generate the necessary forces (torques with revolute joints) and velocities at each joint, but the strength of the structure as well.

The present paper is dedicated to trajectory investigation of five degree of freedom, hydraulically driven loading manipulator with revolute joints as shown on Figure 1. The first and the fifth link rotate about vertical axes, while the others arms – about three parallel horizontal axes.

The trajectory investigations are conducted by means of computer simulation and treat the capacity of the existing driving system to:

- a/ generate the necessary driving forces (torques) in order to balance the set of external static and dynamic forces;
- b/ generate the necessary velocities of arms in order to maintain desired trajectory;
- c/ generate desired output power.

The acquired result from such a simulation could be easily utilized in wide area of additional research tasks, including stress analysis, which is out of the scope of this work.

Specifically we will consider transportation of a particular load with defined mass and dimensions from one starting location **S**, via some middle point **M** (without stopping there), to a particular final position **E**. For every one of these trajectory points, the position and orientation of the gravity center of the load in respect to the base coordinate system is known and given by transformation matrix:

$${}^0_Q T = \begin{pmatrix} \cos(\varphi) & -\sin(\varphi) & 0 & x_c \\ \sin(\varphi) & \cos(\varphi) & 0 & y_c \\ 0 & 0 & 1 & z_c \\ 0 & 0 & 0 & 1 \end{pmatrix}$$

Where  $x_c, y_c, z_c$  and are the coordinates of the load's center of gravity, while  $\varphi$  represents the rotational angle about the vertical axis passing through that center.

The solution of the present task will be achieved utilizing the Newton – Euler interactive algorithm, which regards the state of static equilibrium of each manipulator's link under arrangement of external static and dynamic forces and reactions in joints. Numbering the links in ascending order starting from the immobile base of the manipulator and placing the local frames (connected rigidly to respective arms) in accordance to some rules, we can apply the Denavit-Hartenberg's transformation which gives the description between two neighboring frames: - Denavit and Hartenberg, 1955

$${}^{i+1} T = \begin{pmatrix} {}^{i+1} R & {}^i \vec{P}_{i+1O} \\ 0 & I \end{pmatrix},$$

where  ${}^{i+1} R$  is rotational 3x3 matrix describing the orientation between  $i+1$ -th and  $i$ -th frames, and  ${}^i \vec{P}_{i+1O}$  is the  $i+1$  frame's origin vector described in respect to the  $i$  th coordinate system

The task of simulation will be performed in the following order:

- solving the inverse problem of manipulator kinematics. This will give a positional vector in joint space (five dimensional vector with particular values for each joint angle) corresponding to the starting middle and final trajectory points;
- generating time dependant functions for position, velocity and acceleration for each joint angle while passing between the trajectory points;
- applying the Newton – Euler interactive algorithm in order to determine the dual force-moment vectors acting in each joint.

Solving the inverse problem of manipulator kinematics is routine tasks and can be done considering the position and orientation of the fifth arm's coordinate system in respect to the base frame of the manipulator. The location of the load in this fifth frame has elementary description. One additional condition which somehow simplifies the solution is the fact that the load must be maintained in horizontal orientation during the motion. That condition could be ensured by different techniques (using the pantograph system for this particular example), and provides one simple dependency between joint variables.

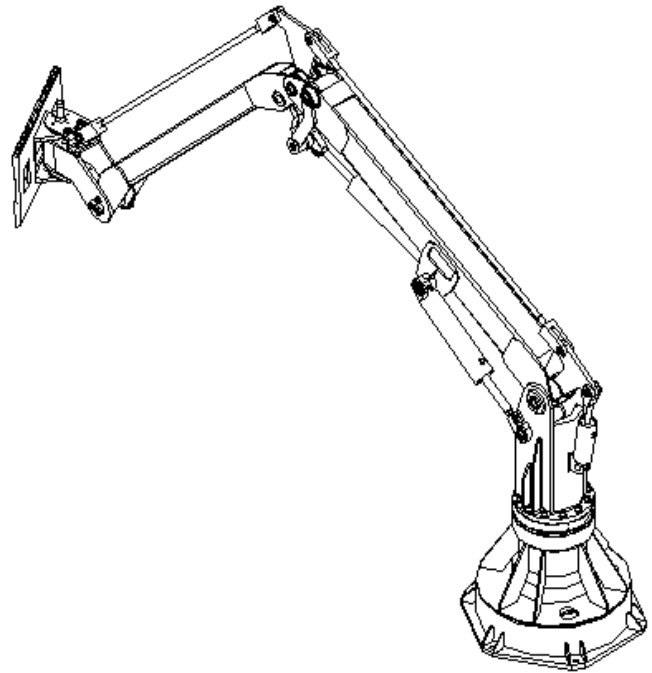


Figure 1. Five degree of freedom loading

The inverse problem solution produces as a result three values for each joint variable which values correspond to the given trajectory points. Hence the joint variable will vary  $\Theta_{Si} \leq \Theta \leq \Theta_M$  for the first section of the motion (from the start to the middle position) and  $\Theta_{Mi} \leq \Theta \leq \Theta_{Ei}$  for the second section.

The time elapsed between the trajectory points will be also considered as specified and we will denote  $0 \leq t \leq t_1$  for the first section and for  $0 \leq t \leq t_2$  the second section respectively.

To assure the smooth motion between the points, third order polynomials will be used to specify the time dependent position for each joint variable  $\Theta(t)$ .

$$\begin{aligned} \Theta_i(t) &= a_{i0} + a_{i1}.t + a_{i2}.t^2 + a_{i3}.t^3 \\ \dot{\Theta}_i(t) &= a_{i1} + 2.a_{i2}.t + 3.a_{i3}.t^2 \end{aligned} \tag{1}$$

The forth polynomial coefficients will be computed using the initial and final values of the function which are known:

- for the first section

$$\begin{aligned} \Theta(t=0) &= \Theta_S; \quad \dot{\Theta}(t=0) = 0 \\ \Theta(t=t_1) &= \Theta_M; \quad \dot{\Theta}(t=t_1) = \dot{\Theta}_M \end{aligned}$$

whence:

$$\begin{aligned}
 a_{10} &= \Theta_S; & a_{11} &= 0; \\
 a_{12} &= \frac{3 \cdot (\Theta_M - \Theta_S)}{t_1^2} - \frac{\dot{\Theta}_M}{t_1}; \\
 a_{13} &= -\frac{2 \cdot (\Theta_M - \Theta_S)}{t_1^3} + \frac{\dot{\Theta}_M}{t_1^2};
 \end{aligned} \quad (2)$$

- for the second section:

$$\begin{aligned}
 \Theta(t=0) &= \Theta_M; & \dot{\Theta}(t=0) &= \dot{\Theta}_M \\
 \Theta(t=t_2) &= \Theta_E; & \dot{\Theta}(t=t_2) &= 0
 \end{aligned}$$

whence

$$\begin{aligned}
 a_{20} &= \Theta_M; & a_{21} &= \dot{\Theta}_M; \\
 a_{22} &= \frac{3 \cdot (\Theta_E - \Theta_M)}{t_2^2} - \frac{2 \cdot \dot{\Theta}_M}{t_2}; \\
 a_{23} &= -\frac{2 \cdot (\Theta_E - \Theta_M)}{t_2^3} + \frac{\dot{\Theta}_M}{t_2^2};
 \end{aligned} \quad (3)$$

We can compute the desired velocity at the "via point" assuming the equality of the acceleration at the end of the first section and the beginning of the second section.

$$\begin{aligned}
 \ddot{\Theta}(t=t_1) &= \ddot{\Theta}(t=0) \\
 2 \cdot a_{12} + 6 \cdot a_{13} \cdot t_1 &= 2 \cdot a_{22}
 \end{aligned}$$

Substituting the coefficients for the middle point we obtain:

$$\dot{\Theta}_M = \frac{3 \cdot [t_2^2 \cdot (\Theta_M - \Theta_S) + t_1^2 \cdot (\Theta_E - \Theta_M)]}{2 \cdot t_1 \cdot t_2 \cdot (t_1 + t_2)}$$

As it was mentioned above, each link of the manipulator could be regarded as in equilibrium when subjected to a set of external forces and joint reactions. When a particular load is being transported, the masses of the load itself and manipulator's arms represent the static external forces. Additional dynamic components are applied at mass centers due to the acceleration of the arms. Considering the balance of the last arm from the kinematical chain we can write:

$$\begin{aligned}
 \vec{f}_5 &= -{}^5_0R \cdot ({}^0\vec{Q} + {}^0\vec{G}_5) + \vec{F}_Q + \vec{F}_5; \\
 \vec{m}_5 &= -\vec{P}_Q \times {}^5_0R \cdot {}^0\vec{Q} - \vec{P}_{G5} \times {}^5_0R \cdot {}^0\vec{G}_5 + \vec{M}_Q + \\
 &+ \vec{M}_5 + \vec{P}_Q \times \vec{F}_Q + \vec{P}_{C5} \times \vec{F}_{C5}
 \end{aligned} \quad (4)$$

In the above equation all force and moment vectors are expressed in terms of the coordinate system of the fifth link. Here the following notations are made:

$\vec{f}_5$  - force vector applied at the fifth frame origin;

$\vec{m}_5$  - moment vector applied at the fifth frame origin;

${}^0\vec{Q}$ ,  ${}^0\vec{G}_5$  - weights of the load and the link as vectors expressed in the base, motionless coordinate system;

$\vec{F}_Q$ ,  $\vec{F}_5$  - dynamic forces applied at the mass centers of the load and the fifth link owing to the linear acceleration of the link (three dimensional vectors);

$\vec{M}_Q$ ,  $\vec{M}_5$  - dynamic moments acting on the load and the link owing to the angular acceleration of the link (three dimensional vectors);

$\vec{P}_Q$ ,  $\vec{P}_{C5}$  - positional vectors specifying the gravity centers locations of the load and the fifth link, expressed in respect to the same coordinate system.

It is natural that the weights of the load and each arm of the manipulator are best known in the base coordinate system, where the Z axis points vertically upwards. Then we can write a simple description:  ${}^0\vec{Q} = [0 \quad 0 \quad -g \cdot m_Q]^T$ . In this case the rotational matrix  ${}^5_0R$  gives the description of these vectors in respect to the fifth coordinate system, which is in accordance to the equation requirements.

We will use the Newton-Euler equations to compute the dynamic force and moment, Craig (1991):

$$\begin{aligned}
 \vec{F}_5 &= m_5 \cdot \dot{v}_{c5}; & \vec{F}_Q &= m_Q \cdot \dot{v}_Q; \\
 \vec{M}_5 &= I_5 \cdot \dot{\omega}_5 + \omega_5 \times I_5 \cdot \omega_5; \\
 \vec{M}_Q &= I_Q \cdot \dot{\omega}_5 + \omega_5 \times I_Q \cdot \omega_5;
 \end{aligned} \quad (5)$$

where:

$\dot{v}_{c5}$ ,  $\dot{v}_Q$  - linear acceleration of the mass centers of the load and manipulator's link;

$I_5$ ,  $I_Q$  - inertia tensor of the load and the link in respect to the coordinate systems with origins at the mass centers, having the same orientation as the link's frame]

$\dot{\omega}_5$ ,  $\omega_5$  - angular acceleration and angular velocity of the link.

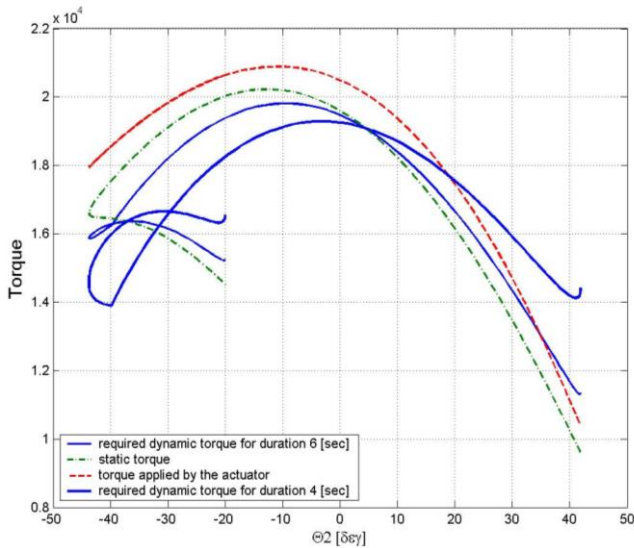


Figure 2 Static and dynamic torques at the second joint [N·m]

Using the inward iterations we can compute the force and moment vectors as reactions at each successive joint in descending order

$$4 \leq i \leq 1:$$

$$\begin{aligned} \vec{f}_i &= {}_{i+1}^i R \cdot \vec{f}_{i+1} + \vec{F}_i - {}_0^i R \cdot \vec{G}_i; \\ \vec{m}_i &= {}_{i+1}^i R \cdot \vec{m}_{i+1} + \vec{M}_i - \vec{P}_{Ci} \times {}_0^i R \cdot \vec{G}_i + \\ &\quad + \vec{P}_{i+1} \times {}_{i+1}^i R \cdot \vec{f}_{i+1} + \vec{P}_{CS} \times \vec{F}_i \end{aligned} \quad (6)$$

$$\begin{aligned} \vec{F}_i &= m_i \cdot \dot{v}_{ci}; \\ \vec{M}_i &= I_i \cdot \dot{\omega}_i + \omega_i \times I_i \cdot \omega_i; \end{aligned} \quad (7)$$

Linear and angular velocities and accelerations of each link can be determined by outward iterations, having in mind that their values for the base frame are equal to zero, Craig (1991). The values for the joint variables, their velocities and accelerations at each moment of time are taken from generated trajectories (third order polynomials) for each degree of freedom (formulas 1-3).

Between them vectors  $\vec{f}_i$  and  $\vec{m}_i$  have six components altogether. All these components are resisted by the structure of the mechanism itself except for the torque about the joint axis, which is to be counterbalanced by the driving system's actuator. As we place local Z axes along the axes of rotation between arms, the necessary torque, required to maintain the static equilibrium, will be determined by the dot product of the joint axis vector with the moment vector:

$$\tau_i = \vec{m}_i \cdot \vec{z}_i; \quad \vec{z}_i = [0 \ 0 \ 1]^T.$$

Figure 2 shows the necessary torques to be applied by the driving system at the second joint (rotation about the first horizontal axis), while moving the load along predetermined trajectory in space. Two sets of values are computed applying the above described simulation method (formulas 4 – 7) – one for the overall duration of the motion of 6 seconds

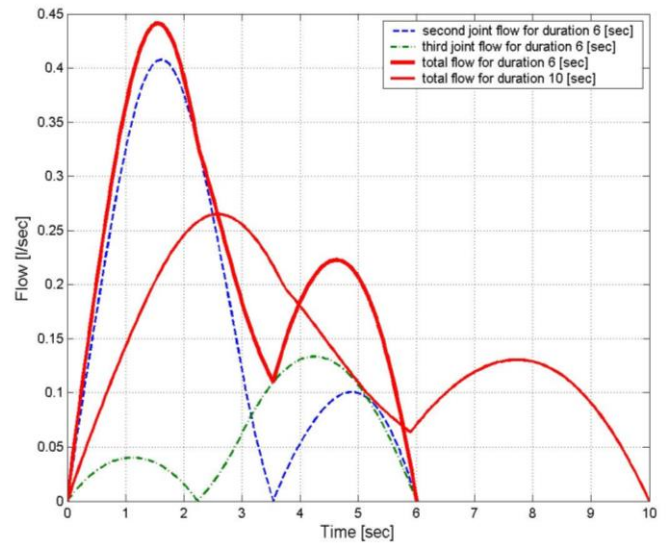


Figure 3 Desired overall flow [l/sec]

and one for the duration of 10 seconds. The necessary static torque as well as the actual torque, applied by the driving system's actuators are also shown there. It is clearly visible, that increasing the process by reducing the time elapsed leads to greater dynamic loads which can not be balanced by the existing driving system at some part of the trajectory and thus rendering such a trajectory unfeasible.

The ability of the driving system to provide desired link velocities (computed by formulas 1-3) depends mainly on the flow produced by the hydraulic pump, which usually generates flow needed to power several actuators at the same time. Determining the necessary flow requires transforming the angular velocities in joints to linear velocities of hydraulic actuators as soon as linear actuators are used to drive rotational joints. The schemes used to attach the linear actuators to the manipulator's arms (directly or using a kind of leverage) as well as the parameters of the attachments are paramount in such transformations. (Grigorov and Exsarov, 1981, Grigorov 1996).

Figure 3 gives graphical representation of the flow necessary to drive the second, third and fifth links of the manipulator while moving along the same trajectory. Analyzing the graphs, one can see that moving along the path in 6 seconds interval could not be achieved because the lack of the actual pump to supply desired flow.

The simulation presented is made by programming in Matlab mathematical package environment. The masses and center of gravity locations of the manipulator links as well as inertia tensors are determined through creating 3D models in Mechanical Desktop 6 CAD package

## CONCLUSIONS

- A method to investigate the capability of hydraulically driven manipulator to transport a load along given trajectory in space is presented. This method is based on comparing the actual driving torques applied by the hydraulic actuators in each joint to the torques necessary to counterbalance the sum of static and dynamic forces acting on links and the load during the motion. One additional comparison is made regarding the flow supplied

by the pump and the flow needed to provide desired velocities of the manipulator's links.

- This method can be used to investigate a real machine as well as in the design stage in order to choose suitable driving system parameters, provided a concrete application for the manipulator is given.

- Some additional results such as computing the reaction forces in each joint can be utilized for other purposes such as stress analysis or mechanical design of manipulator's links.

#### REFERENCES

- Григоров Б., Пл. Ексаров 1981. Относно избора на хидроцилиндър за задвижване на звената на товароподемен манипулатор от антропоморфен тип. *Машиностроене кн. 1*.
- Григоров, Б. 1996. Кинематично изследване на товароподемен манипулатор с хидравлично задвижване. *Машиностроене, кн. 9-10*.
- Craig, J.J. 1991. Introduction to Robotics - Mechanics and Control. – Addison-Wesley Publishing company.
- Denavit, J., R.S. Hartenberg. 1955. A Kinematic Notation for Lower-Pair Mechanisms Based on Matrixes. - *J. Applied Mechanics June 1955*.

*Recommended for publication by Department of  
Mine Mechanization, Faculty of Mining Electromechanics*

## KINEMATICS AND DYNAMICS OF WORKING MECHANISM OF HYDRAULIC EXCAVATOR

**Emil Assenov**

TU-Sofia  
Department "Logistics"  
Sofia 1756, Bulgaria  
E-mail:emil\_assenov@yahoo.com

**E. Bosilkov**

TU-Sofia  
Department "Logistics"  
Sofia 1756, Bulgaria  
E-mail:e\_bosilkov@mail.ru

**Radoslav Dimitrov**

TU-Sofia  
Department "Logistics"  
Sofia 1756, Bulgaria  
E-mail: radoslaff@hotmail.com

**Tzvetan Damianov**

UMG "St. Ivan Rilski"  
Sofia 1700  
Bulgaria

**ABSTRACT**

In this paper are studied kinematic and dynamic parameters of working mechanism of hydraulic excavator. The manipulator is designed by the SolidWorks, than with Dynamic Designer are simulated velocities and forces. As a result are derived the relationships for force in hydraulic cylinder, reaction force in joint between arm and jib.

**INTRODUCTION**

The study of kinematic and dynamic parameters of manipulator of hydraulic excavator is based. The mechanism of this manipulator is plane multilinkage, that consists of arms joined and hydraulic cylinders.

The aim of this paper is to create methodology for kinematic and dynamic parameters research of working mechanism of hydraulic excavator.

We consider the working mechanism as conjunction of jib, arm and bucket, that are joined by the cylindrical joints and hydraulic cylinders. The working process is based on rotation of arm to jib with hydraulic cylinder.

A model of arm and jib is shown in Fig.1.

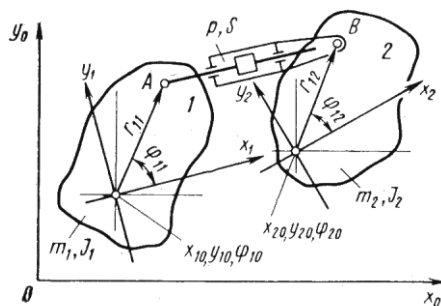


Figure 1. A model of mechanism arm – jib

The body 1 presents the jib, the body 2 – arm. They are joined in point A and point B with hydraulic cylinder. The pressure and area of the cylinder are known.

Simulation of such a mechanism is made by using Lagrange equation of the first type with unknown multipliers.

$$\left. \begin{aligned} m_i \ddot{x}_{i0} + \sum_{s=1}^p \lambda_s \frac{\partial \Phi_s}{\partial x_{i0}} &= Q_{xi}; \\ m_i \ddot{y}_{i0} + \sum_{s=1}^p \lambda_s \frac{\partial \Phi_s}{\partial y_{i0}} &= Q_{yi}; \\ J_i \ddot{\varphi}_{i0} + \sum_{s=1}^p \lambda_s \frac{\partial \Phi_s}{\partial \varphi_{i0}} &= Q_{\varphi i}; \end{aligned} \right\} \quad (1)$$

Where  $Q_{x1}, Q_{y1}$  are components of resultant force in Dekart's system for the i-body;  $Q_{\varphi i}$  – correspondingly moment;  $\lambda_s$  – unknown multipliers;  $F_s$  – joint function. Let's take symmetrical cylinder. This system is forced by the unconservative force  $F=pS$ . The pressure  $p$  is taken as known. To estimate the forces  $Q_i$  for equations (1) we consider elementary work

$$dA = Q_i dq_i \quad (2)$$

The cylinder length  $l$  is:

$$l = \sqrt{\{(x_{20} - x_{10}) + [r_{21} \cos(\varphi_{20} + \varphi_{21}) - r_{11} \cos(\varphi_{10} + \varphi_{11})]\}^2 + \{(y_{20} - y_{10}) + [r_{21} \sin(\varphi_{20} + \varphi_{21}) - r_{11} \sin(\varphi_{10} + \varphi_{11})]\}^2} \quad (3)$$

Then:

$$dA = pSdl = pS \left( \frac{\partial l}{\partial x_{10}} dx_{10} + \frac{\partial l}{\partial y_{10}} dy_{10} + \frac{\partial l}{\partial \varphi_{10}} d\varphi_{10} + \frac{\partial l}{\partial x_{20}} dx_{20} + \frac{\partial l}{\partial y_{20}} dy_{20} + \frac{\partial l}{\partial \varphi_{20}} d\varphi_{20} \right)$$

Let's assign  $L$  to equation (3), then the derivatives  $\partial l / \partial q_i$  are  $\frac{\partial l}{\partial q_i} = \frac{1}{2\sqrt{L}} \frac{\partial L}{\partial q_i}$ , and the forces (2) are:

$$\left. \begin{aligned} F_1^x &= pS \frac{1}{2\sqrt{L}}(-a); & F_1^y &= pS \frac{1}{2\sqrt{L}}(-b); \\ M_1 &= pS \frac{1}{2\sqrt{L}}L; & F_2^x &= -F_1^x; \\ F_2^y &= -F_1^y; & M_2 &= pS \frac{1}{2\sqrt{L}}M. \end{aligned} \right\} \quad (4)$$

For the moments  $M_1$  and  $M_2$  we have:

$$\begin{aligned} M_1 &= r_{11}[F_1^x \sin(\varphi_{10} + \varphi_{11}) - F_1^y \cos(\varphi_{10} + \varphi_{11})]; \\ M_1 &= r_{21}[-F_2^x \sin(\varphi_{20} + \varphi_{21}) + F_2^y \cos(\varphi_{20} + \varphi_{21})] \end{aligned}$$

Recognizing the friction force in the hydraulic cylinder, the force  $F_{1,2}$  is

$$F'_{1,2} = F_{1,2} + \mu F_{1,2} \text{sign} \dot{i} \quad (5)$$

The differential equation system is

|       |     |                       |  |
|-------|-----|-----------------------|--|
| $m_1$ | $I$ | $\ddot{x}_{10}$       | $F_{10}^x - F_7^x (1 + \mu \text{sign} \dot{i})$   |
| $m_1$ |     | $\ddot{y}_{10}$       | $F_{10}^y - F_7^y (1 + \mu \text{sign} \dot{i})$   |
| $J_1$ |     | $\ddot{\varphi}_{10}$ | $M_{10} + r_{11} [F_7^x (1 + \mu \text{sign} \dot{i}) \times \sin(\varphi_{10} + \varphi_{11}) - F_7^y (1 + \mu \text{sign} \dot{i}) \times \cos(\varphi_{10} + \varphi_{11})]$  |
| $m_2$ |     | $\ddot{x}_{20}$       | $F_{20}^x + F_2^x (1 + \mu \text{sign} \dot{i})$   |
| $m_2$ |     | $\ddot{y}_{20}$       | $F_{20}^y + F_2^y (1 + \mu \text{sign} \dot{i})$   |
| $J_2$ |     | $\ddot{\varphi}_{20}$ | $M_{20} + r_{21} [-F_2^x (1 + \mu \text{sign} \dot{i}) \times \sin(\varphi_{20} + \varphi_{21}) + F_2^y (1 + \mu \text{sign} \dot{i}) \times \cos(\varphi_{20} + \varphi_{21})]$ |

(6)

There is relation for cylinder area  $S$  when we calculate the forces  $F_{1,2}^x$  and  $F_{1,2}^y$

$$S = \frac{S_1}{2}(1 + \text{sign} \dot{i}) + \frac{S_2}{2}(1 - \text{sign} \dot{i}). \quad (7)$$

Where  $S_1$  – piston area;  $S_2$  – area behind the piston.

The methods for research the kinematic and dynamic parameters of working mechanism of hydraulic excavator consist of:

- 1) Create the 3-D Solidworks model
- 2) Use the Dynamic Designer program

An example for implementation of this methods is:

### EXPERIMENTAL WORK

- 1) We have created the 3-D SolidWorks model of working mechanism of hydraulic excavator

Caterpillar with 1m<sup>3</sup> bucket volume. This model is shown in Fig.2.

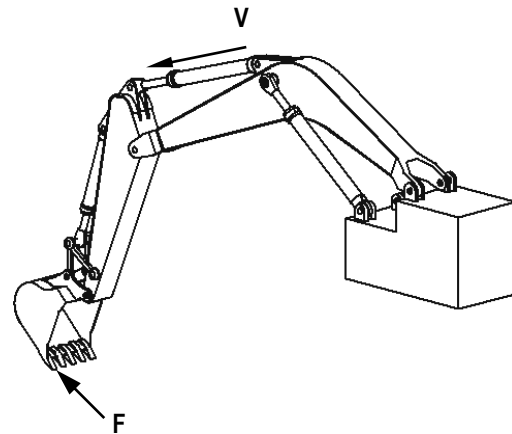


Figure 2. 3-D SolidWorks model

- 2) The Dynamic Designer program is started and the 3-D SolidWorks model is attached here.
  - 3) We check the joints that were created as SolidWorks model – here we have concentric joint in the hinge between the arm and the jib, the concentric joints in the hinges of hydraulic cylinder and the arm and the jib. There is also a translation joint between the cylinder body and the piston.
  - 4) In this study we assign the translation velocity of the piston to be constant and equal to 0,3 m/s.
  - 5) On the tooth of the bucket we put the constant resistant force  $F_{\text{bucket}} = 20000$  N. This is the force of scission of the ground.
- In the Fig.3 and Fig.4 are shown the Dynamic Designer work tree and property window respectively.

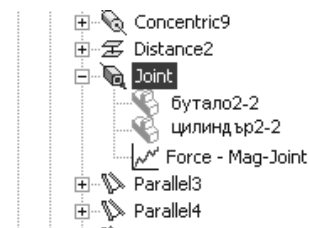


Figure 3. Dynamic Designer work tree

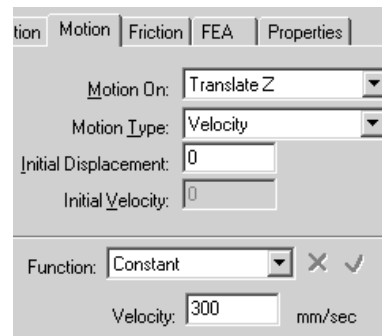


Figure 4. Dynamic Designer property window

- 6) The created dynamic model is simulated in the Dynamic Designer environment.

### RESULTS OF THE EXPERIMENT

The simulation results are shown in Fig.5., Fig.6. and Fig.7., where:

- Fig.5. represents the velocity of the mass center of the bucket;
- Fig.6. represents the piston force;
- Fig.7. represents the reaction force in the hinge between the arm and the jib.

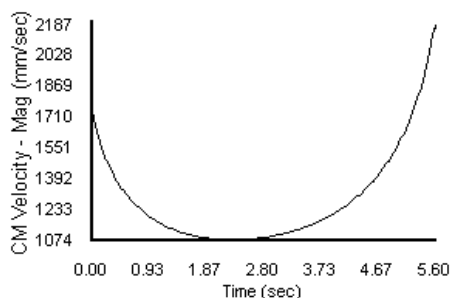


Figure 5. Velocity of the mass center of the bucket

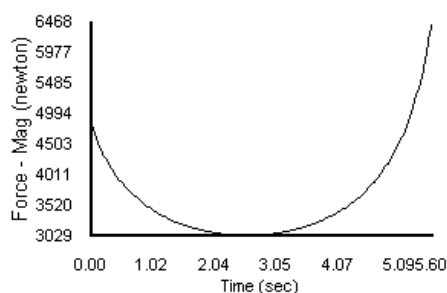


Figure 6. Piston force

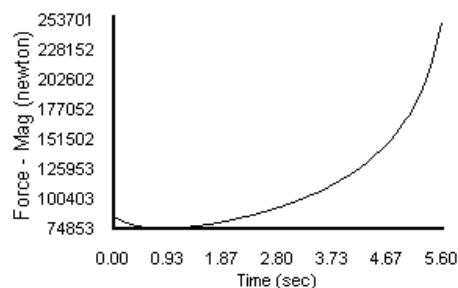


Figure 7. Reaction force in the hinge between the arm and the jib

### CONCLUSION

1. A method for study of the kinematic and dynamic parameters of working mechanism of the hydraulic excavator is created. This method includes jointly using the 3-D SolidWorks model and Dynamic Designer.
2. The study of the velocity of the mass center of the bucket, the force of the piston of the hydraulic cylinder and the reaction force in the hinge between the arm and the jib is carried out.
3. The results can be used for creation of a control system of the working process of the hydraulic excavator.

### REFERENCE

- Yaha P.K. and Skibiewski M.Y. "Cognitive force. Control of excavators" Journal of Aerospace Engineering (6) 2. 159-166. 93.
- Koivo A., J. Thoma, M. Cocaoglan, E. Andrede, "Cetto J. Modeling and control of excavator dynamics during digging operation" Journal of Aerospace Engineering 9(1) 10-18, 1996.
- H. P. Nguyen, D. C. Duzz and Whqte Robust "Imperrlance Control of Excavators" – The University of Sidney 2006 NSW Australia, 1998.
- Malinovski E. In. "Computer design and study of building and road machines", Moskva, Machinostroene, 1980.
- Assenov E. "SolidWorks – Main Course", Sofia, 2002

Recommended for publication by Department of Mine Mechanization, Faculty of Mining Electromechanics

## RESEARCH OF CENTRIFUGAL-IMPACT-VIBRATING MILL /CIVM/ WORKING PROCESS

**Emil Assenov**

TU – Sofia  
Department of logistics  
e\_mail:emil\_assenov@yahoo.com

**Marieta Yancheva**

TU – Sofia  
Department of logistics

**Raina Vucheva**

UMG "St. Ivan Rilski"  
Sofia 1700, Bulgaria

### ABSTRACT

In this paper is described working process of CIVM, that is protected by patent, using theoretical-experimental method. For objective function is chosen quality of final product and for ruling factors-weight of material in the mill, weight of grinding balls in the mill and time for grinding. A experimental plan is created for two level of the ruling factors. A statistical analys of the experimental resen is made.

### INTRODUCTION

CIVM is a mill for fine grinding of are and building materials. It is a new mill protected by patent (Assenov, 1977).

The aim of this paper is to represent the results of theoretical-experimental research of working process of CIVM.

CIVM is built [fig.1] of a rotate parabolic part 1 with vertical axis, a vertical shaft 2, the bearings 3, a plate 4, the springs 5, the base 6, fixed parabolic part 7, the columns 8. There are grinding balls 9 and are falling trough tube 10, and the grids 11.

CIVM is working as follows:

The grinding balls and material [are] to be milled are put into the parabolic part 1. The motor 12 rotate the part 1 and because of that grinding balls and ore are rotated and are raised by the centrifugal forces. These forces press the balls to the inner face of rotated part 1 and grinding the material [ore].

The rotated balls goes to the fixed parabolic part 7. There they press again the material. When the kinetic energy of balls decreases they falls on the bottom of part 1. Here the balls hit the material and crushed. The movement of flow of balls and material call forth the vibrations of the whole mill that is put on the springs 5. These vibrations crush the ore.

Thus the material is crushed by pressure originate from centrifugal forces, by slug of falling balls and finally by vibrations.

### BASE THEOTY AND EXPERIMENTAL WORK

The CIVM working process is studded by cybernetic theory of experiments (Assenov,1988; Bojanov,1973 etc) .

$X_i$  are the input parameters (ruling factors);  $Y_i$  – objective functions and  $\xi$  – disturbance.

In this study for objective function is chosen the quality of product that is measured by the sieve analysis. There is no information for the input parameters that is way, it is made the list of all parameters that would influence on quality. This list is:

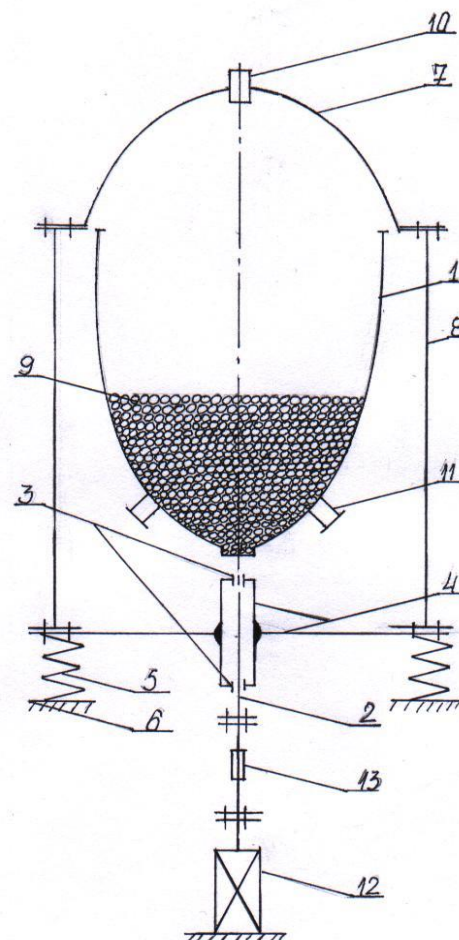


Figure 1. The model of CIVM

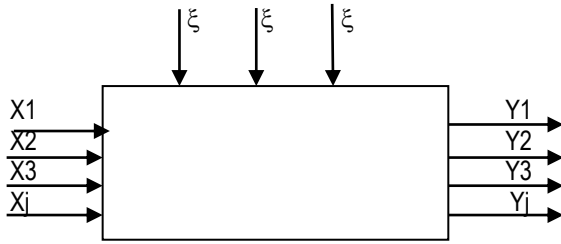


Figure 2. Cybernetic model of black box

- Gm- the weight of material [ore] to be grinder [kg];
- Gt – the weight of the grinding ball [kg];
- t – the time for grinding [min];
- n – the angular velocity of parabolic part 1 [min<sup>-1</sup>];
- c- the stiffness coefficient of the springs [N/m];
- dt – the ball is diameter [mm];
- m – sort of material-quartz sand;

An active experiment is made for the first 3 parameters and the another were constant:

c = 290 .10<sup>3</sup> [N/m]; n = 800 [ min<sup>-1</sup>]; dt = 15 [mm];  
dm = 0 ÷ 3 [mm];

The basic levels, intervals of the input parameters variation are given on table 1.

- Xi = 0 - Signbasic level
- λi - Interval
- Xi = -1 - Lower level
- Xi = +1 - Upper level

Table 1. Basic level for input parameters

| parameter | Xi = 0 | λi | Xi = -1 | Xi = +1 | Dimensi on |
|-----------|--------|----|---------|---------|------------|
| X1-Gm     | 4      | 1  | 3       | 5       | [kg]       |
| X2-Gt     | 4      | 1  | 3       | 5       | [kg]       |
| X3-t      | 2      | 1  | 1       | 3       | [min]      |

The matrix of the plan of experiments is 2<sup>3</sup>. The plane of experiments and the result are given in table 2.

Table 2. Matrix plan and experimental results

| No | X <sub>1</sub> code | X <sub>2</sub> code | X <sub>3</sub> code | Doubled experiment | Result Y |
|----|---------------------|---------------------|---------------------|--------------------|----------|
| 1  | -1                  | -1                  | -1                  | 80,20<br>78        | 79,1     |
| 2  | +1                  | -1                  | -1                  | 43,4<br>41,2       | 42,3     |
| 3  | -1                  | +1                  | -1                  | 52,7<br>49,8       | 51,25    |
| 4  | +1                  | +1                  | -1                  | 70,3<br>73,7       | 72       |
| 5  | -1                  | -1                  | +1                  | 54,8<br>51,3       | 53,05    |
| 6  | +1                  | -1                  | +1                  | 76,8<br>72,1       | 74,45    |
| 7  | -1                  | +1                  | +1                  | 73,1<br>79,3       | 76,2     |
| 8  | +1                  | +1                  | +1                  | 39,3<br>42,7       | 41       |

THE RESULTS AND DISCUSSIONS

The regression coefficients are calculated by the formulae (Assenov, 1977).

$$b_i = \sum f_{ij} \cdot Y_j / n \tag{1}$$

The coded regression equation is:

$$Y = 61.044 - 3.606X_1 - 0.931X_2 + 14.394X_3 + 0.25X_1X_2 + 1.387X_2X_3 - 0.406X_1X_3 \tag{2}$$

Statistical analyst:

There are doubled experiments and we can check hypothesis for homogeneous of dispersions by the Kochren criterion:

$$S_i = \frac{\sum \left( Y_{pq} - Y_p \right)^2}{l - 1} \tag{3} ; \quad l = 2 ;$$

The maximum dispersion was for the sixth experiment.

$$\frac{1}{G} = \frac{\sum S_i}{S_{max}} = \frac{11,045}{37,775} = 0,2924 \tag{4}$$

The table value of Kochren criterion is taken from table 5 (Bojanov, 1973) and have Gt= 0,6798.

Hence the dispersions are homogeneous.

We calculate the dispersion of experiment by condition of uniformity experiments and for degree of freedom v= 8.

The estimated dispersion is

$$Q_{\epsilon 1} = \sum_{p=1}^n \sum_{q=1}^v \left( Y_{pq} - Y_p \right)^2 = 37,775 \tag{5}$$

$$S^2_{\epsilon 1} = \frac{Q_{\epsilon \epsilon}}{Y_{\epsilon \epsilon}} = \frac{37,775}{8} = 4,722 \tag{6}$$

Significant regression coefficients are derived using Student’s criterion for confidence level α= 0,05 and degree of freedom df = 8. The student’s table value is tτ=2,896. We calculate the dispersion of regression coefficients as

$$S^2\{b_j\} = S^2_{\epsilon 1} / N = 4.722 / 16 = 0,295 \tag{7}$$

, than calculate multiplication: tτ \* S<sup>2</sup>{b<sub>i</sub>} = 1,579 (7’) Each coefficient that is grater than (7’) are significant. The final regression equation is

$$Y = 61,044 - 3,606X_1 + 14.394X_3 \tag{8}$$

We check the adequate equation with Fisher criterion.

$$F = S^2 / S^2_{\epsilon} = 5,7 / 4,722 = 1,207 \tag{9}$$

,where S<sup>2</sup>=Ql/vl is the estimated dispersion of insignificant; vl- degree of freedom.

$$QI = \sqrt{n} \cdot \sum \left( \frac{\hat{Y}_p - Y_p}{\hat{Y}_p} \right)^2 = 28,5 \quad (10)$$

The table value of  $F_t = 3,69$  is derived from table (Assenov, 1988; Bojnov, 1973 etc.) when  $\alpha=0.05; v_l=4; v_e=8$ . Hence the regression equation is adequate.

We have made another experiment, where the milling factors were:  $G_m$ ,  $n$  and  $t$ . The  $n$  is angular velocity of the rotated parabolic part 1. The factors were constant.

The basic level, the intervals of variation of the parameters are given on table 3.

- $X_i = 0$  - sign
- $\lambda_i$  - interval
- $X_i = -1$  - lower level
- $X_i = +1$  - upper level

Table 3. Basic level, intervals of parameters

| Para-Meter | $X_i = 0$ | $\lambda_i$ | $X_i = -1$ | $X_i = +1$ | Dimension            |
|------------|-----------|-------------|------------|------------|----------------------|
| $Z_1$      | 4         | 1           | 3          | 5          | [kg]                 |
| $Z_2$      | 1000      | 200         | 800        | 1200       | [min <sup>-1</sup> ] |
| $Z_3$      | 2         | 1           | 1          | 3          | [min]                |

The plane matrix and the results are given in table 4. The coded regression equation is

Table 4. Matrix plane and the second results

| No | $X_1$ | $X_2$ | $X_3$ | Experimental results -Y | Mean value Y |
|----|-------|-------|-------|-------------------------|--------------|
| 1  | -1    | -1    | -1    | 48,9<br>51,1            | 50,2         |
| 2  | +1    | -1    | -1    | 40,4<br>43,6            | 42           |
| 3  | -1    | +1    | -1    | 54,9<br>54,5            | 54,7         |
| 4  | +1    | +1    | -1    | 44,2<br>46              | 45,1         |
| 5  | -1    | -1    | +1    | 62,1<br>72,7            | 67,4         |
| 6  | +1    | -1    | +1    | 70,1                    | 72,7         |

|   |    |    |    |              |      |
|---|----|----|----|--------------|------|
|   |    |    |    | 74,6         |      |
| 7 | -1 | +1 | +1 | 81,5<br>84,1 | 82,8 |
| 8 | +1 | +1 | +1 | 72,8<br>76,0 | 74,9 |

The regression equation is

$$Y = 61,225 - 2,55X_1 + 3,15X_2 + 13,225X_3 - 1,825X_1X_2 + 1,25X_2X_3 + 1,9X_1X_3 \quad (11)$$

After statistical analysis is derived final equation

$$Y = 61,225 - 2,55.X_1 + 3,15.X_2 + 13,225.X_3 \quad (12)$$

### CONCLUSION

- From the equation (8) and (12) we draw a conclusion that when the weight of grinding material increases the quality of final product decrease. When the angular velocity of rotated parabolic part 1, and the grinding time increases the quality of final product also increases.
- When we increase the weight of grinding material  $G_m$  with 1 kg this decreases the quality with 2,55%.
- When we increase the angular velocity with 200 [tr/min] this increases the quality with 3,15 %.
- When we increase the grinding time with 1[min] the quality of final product increases with 13,25%.

### REFERENCES

- Assenov E. "Centrifugal impact-vibration mill " B02C17/14; №24842/07.02.77
- Assenov E. "Research of working process and parameters of vertical vibration mill"- dissertation 1988
- Bojanov E. "Statistical methods for modeling and optimizing of multiple objects" Technika -73.
- Shupov L. "The practical mathematical methods in ore dressing" Nedra-Moskva 74.
- Cohen M.L., Rolph J.E., Steffey D.L. "Statistics, Testing and Defense Acquisition: New Approaches and Methodological Improvements" 1998, National Academy Press, Washington DC.

Recommended for publication by Department of Mine Mechanization, Faculty of Mining Electromechanics

## STUDYING SOME OF THE TRIBO-CHARACTERISTICS OF MINERAL GRINDING

Slavtcho Dontchev

University of Mining and Geology "St. Ivan Rilski"  
Sofia 1700, Bulgaria

Viara Pojidaeva

University of Mining and Geology "St. Ivan Rilski"  
Sofia 1700, Bulgaria

### ABSTRACT

Functional responses of the coefficient of friction depending on the technological regime of machines for mineral grinding were tested. The coefficient of friction depending on the fullness of a drum mill was determined.

Key words: tribo-characteristics, mineral grinding, coefficient of friction.

### TASK:

Typical tribo-characteristics for determining the coefficient of friction  $\mu$  depending on the coefficient of fullness are tested for drum mills for mineral grinding.

### THEORETICAL ANALYSIS

Equation 1 from [1] allows the determination of the most general value of friction forces for mills working with different coefficients of fullness  $\varphi$  and different speed regimes.

$$N_{TP} = 19,7 \frac{\sqrt{D}}{\sqrt[4]{1+K^2}} f(\varphi, K) W_{\varphi} \operatorname{tg} \rho \left( \frac{1}{\sqrt{\sin \rho}} - 1 \right) (0,576 + \sin \theta), \text{ kW} \quad (1)$$

where

$D$  is the drum diameter, m;

$W_{\varphi}$  - weight of grinding bodies, moving along a circular trajectory;

$\varphi$  - coefficient of fullness;

$\theta$  - angle of deviation of the gravity centre;

$K = \frac{R_1}{R}$  radius of the drum and  $R_1$  (radius of the most

inner layer of grinding bodies);

$f(\varphi, K)$  - part of grinding bodies, moving along a circular trajectory;

$\rho$  - angle of friction.

A certain technologic regime in consideration of the theory of Levenson requires the determination of equations of the type:

$$N_{TP} = 10,1 \sqrt{D} W_{\varphi} \operatorname{tg} \rho \left( \frac{1}{\sin \rho} - 1 \right), \text{ kW.} \quad (2)$$

Preliminary considerations reveal that in case of equal  $D$ ,  $\varphi$  и  $W_{\varphi}$  the equations (2) have equal coefficients, 10, 1, which shows that their powers are equal, i.e. correctness of accepted equations is confirmed.

It is evident that in case of equal values of  $D$ ,  $D$ ,  $W_{\varphi}$ ,  $\theta$ ,  $\varphi$  and  $K$  the power of forces of friction depends on the expression:

$$y = \operatorname{tg} \rho \left( \frac{1}{\sin \rho} - 1 \right), \quad (3)$$

where  $\rho$  is the angle of friction.

In case of  $\rho = \frac{\pi}{2}$ , the expression is undefined.

An analysis of the following function reveals:

$$\begin{aligned} \lim_{\rho \rightarrow \frac{\pi}{2}} \operatorname{tg} \rho \left( \frac{1}{\sqrt{\sin \rho} - 1} \right) &= \lim_{\rho \rightarrow \frac{\pi}{2}} \frac{\operatorname{tg} \rho (1 - \sqrt{\sin \rho})}{\sqrt{\sin \rho}} = \\ &= \lim_{\rho \rightarrow \frac{\pi}{2}} \frac{\sin \rho}{\sqrt{\sin \rho}} \lim_{\rho \rightarrow \frac{\pi}{2}} \frac{1 - \sqrt{\sin \rho}}{\cos \rho} \end{aligned}$$

$$\text{but } \lim_{\rho \rightarrow \frac{\pi}{2}} \frac{\sin \rho}{\sqrt{\sin \rho}} = 1.$$

Then

$$\lim_{\rho \rightarrow \frac{\pi}{2}} \frac{1 - \sqrt{\sin \rho}}{\cos \rho} = \lim_{\rho \rightarrow \frac{\pi}{2}} \frac{-\frac{1}{2} \frac{\cos \rho}{\sqrt{\sin \rho}}}{-\sin \rho} = \lim_{\rho \rightarrow \frac{\pi}{2}} \left( -\frac{1}{2} \right) \frac{\cos \rho}{(\sin \rho)^{3/2}} = 0 \quad (4)$$

Theoretical considerations reveal that when friction becomes infinitely high there will not be any relative motion between grinding bodies and lining of the mill. Work of the forces of friction acquires the value of zero.

The expression  $\frac{1-\sqrt{\sin \rho}}{\cos \rho}$  can be transformed in the following way:

$$\frac{1-\sqrt{\sin \rho}}{\cos \rho} = \frac{1-\sqrt{\cos(\frac{\pi}{2}-\rho)}}{\sin(\frac{\pi}{2}-\rho)} = \frac{1-\sqrt{\cos \alpha}}{\sin \alpha} = \frac{1-\cos \alpha}{\sin \alpha(1+\sqrt{\cos \alpha})}$$

for  $\frac{\pi}{2}-\rho = \alpha$ , or

$$\frac{1-\cos \alpha}{\sin \alpha(1+\sqrt{\cos \alpha})} = \frac{2 \sin^2 \frac{\alpha}{2}}{2 \sin \frac{\alpha}{2} \cos \frac{\alpha}{2}(1+\sqrt{\cos \alpha})} = \frac{\operatorname{tg} \frac{\alpha}{2}}{1+\sqrt{\cos \alpha}}$$

then

$$\lim_{\rho \rightarrow \frac{\pi}{2}} \frac{1-\sqrt{\sin \rho}}{\cos \rho} = \lim_{\alpha \rightarrow 0} \frac{\operatorname{tg} \frac{\alpha}{2}}{1+\sqrt{\cos \alpha}} = 0 \quad (5)$$

The equation (3) is analyzed for determining the value of the angle  $\rho$ , when the work of the forces of friction acquires maximum value. It is evident that minimum work is acquired when  $\rho = \frac{\pi}{2}$  in the lack of relative sliding of milling bodies along the lining.

Or from (3)

$$y' = \frac{1}{\cos^2 \rho} \left( \frac{1}{\sqrt{\sin \rho}} - 1 \right) + \operatorname{tg} \rho \left( -\frac{1}{2} \frac{\cos \rho}{(\sin \rho)^{3/2}} \right) \quad (6)$$

$$y' = \frac{1}{\cos^2 \rho} \left( \frac{1}{\sqrt{\sin \rho}} - 1 \right) - \frac{1}{2} \operatorname{tg} \rho \frac{\cos \rho}{(\sin \rho)^{3/2}} \quad (7)$$

The maximum ( $y_{max}$ ) is acquired from the expression:

$$\frac{1}{\cos^2 \rho} \left( \frac{1}{\sqrt{\sin \rho}} - 1 \right) - \frac{1}{2} \frac{1}{\sqrt{\sin \rho}} = 0 \quad (8)$$

$$\frac{1}{\sqrt{\sin \rho}} \left( \frac{1}{\cos^2 \rho} - 1 \right) - \frac{1}{2} \frac{1}{\sqrt{\sin \rho}} = 0, \quad (9)$$

iif  $0 < \rho < \frac{\pi}{2}$  and  $\sqrt{\sin \rho} = t$

$$\frac{1}{\sqrt{\sin \rho}} (2 - \cos^2 \rho) - 2 = 0 \quad (10)$$

$$2 - \cos^2 \rho - 2\sqrt{\sin \rho} = 0 \quad (11)$$

$$1 - \sin^2 \rho - 2\sqrt{\sin \rho} = 0. \quad (12)$$

The equation is reduced to the following:

$$1 + t^4 - 2t = 0$$

$$f(t) = t^4 - 2t + 1 \quad (13)$$

it has two roots  $f(0) = 1$  and  $f(1) = 0$ .

It can be reduced to:

$$\rho(t) = t^3 - t^2 + t - 1 = 0. \quad (14)$$

The above equation has a real root and is solved with an accepted precision

$$t = 0,5437$$

$$t = \sqrt{\sin \rho} = 0,5437$$

$$\rho \approx 17^\circ 12' \text{ and } \mu = \operatorname{tg} \rho = 0,309, \quad (15)$$

i.e. when  $\mu = 0,309$ ,  $N_{mp}$  will possess the maximum value.

## RESULTS AND DISCUSSION

The theoretical analyses and adopted methodic directions allow the determination of some tribo-technologic characteristics of the process of grinding of mineral resources in drum mills. The functional dependence of the power of the coefficient of friction is shown in fig. 1. The figure shows increase of power under values of the coefficient of friction from 0,01 to 0,35 and sharp decrease to  $\mu = 0,4$ , then it remains almost constant in a wide range. It can be considered that this is a result of the integrated action of tested parameters and the change in the composition of grinding and grindable media. Results afford an opportunity for selection of effective technologic regime under given technologic parameters.

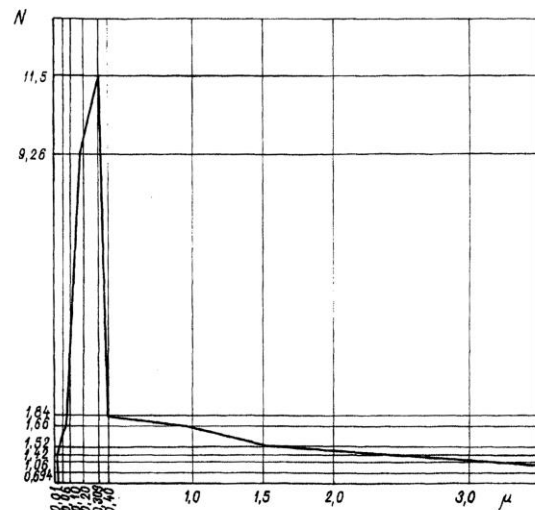


Figure 1.

REFERENCES

- Friction, wearing and lubrication. Handbook, vol. 1, vol. 2.  
Edited by Prof. DSc I. V. Kragelskii and Dr. V. V. Alisina,  
Moscow, Machinostroenie, 1979 (in Russian).
- Laricov E. A., Viliaevskaya T. I., Units and parts of mechanical  
apparatures. Moscow, Machinostroenie, 1974 (in Russian).

*Recommended for publication by Department of  
Mine Mechanization, Faculty of Mining Electromechanics*

## AN ELECTROPHYSICAL TECHNOLOGY FOR IMPROVEMENT OF THE DURABILITY (UNDER WEAR) OF THE CUTTERS OF THE CUTTER-LOADERS

**Slavtcho Dontchev**

University of Mining and Geology  
"St. Ivan Rilski"  
Sofia 1700, Bulgaria

**Genadi Takov**

University of Mining and Geology  
"St. Ivan Rilski"  
Sofia 1700, Bulgaria

### ABSTRACT

The high durability (under wear) of the cutting tools (cutters) determines both continuous and stable operation of the cutter loaders. The continuous contact of the teeth (cutters) to the material mass being destructed is to be characterized by significant impact loading, variable characteristics of the forces, and a highly expressed abrasion. In this comparative study, which was carried out under the field conditions of the pit "Babino" (the Bulgarian "Bobov dol" mines), a possibility for improvement of the durability (under wear) of the cutters by means of its preliminary treatment in the "MUS-1" device is to be commented, said device being replicated the action of a combined electrophysical method. The outcome of an investigation for long shows: decrease of the abrasion from two to two and a half folds for the teeth being preliminary treated in the "MUS-1" device; significant decrease of the number of the teeth being subject to wear following from fatigue (breakage and break off of the crowns).

### INTRODUCTION

In the underground exploitation and mining of the deposits are used high-performance machines, by means of which both significant increase of the productivity and decrease of the production costs is achieved.

The advantages possessed by the cutter-loaders, particularly in the case of the complex technological lines for mining of the (ores and) minerals, are determining the actuality of their enhancement and effective use. Of significant importance for the effective use of the cutter loaders is the resistance to wear (i.e. the durability) of the cutting tools- the cutters mounted to the cutting drum of the working head thereof.

The operation of the cutter-loaders is characterized by a continuous contact of the teeth (cutters) to the material mass being destructed. Each of the cutters draws a complex curve in the space during the cutting with a small cut (chip). The chips being cut from the separate cutters have different cross-sections, hence the loading of both individual cutters and the working head is uneven. The same effect results from the material mass when being none homogenous. Consequently, the total loading of the working head at a significant extent is defined from both cutting properties of its individual cutters and their durability (under wear).

The latter defines the purpose of this study, i.e. to increase the cutters' durability (under wear), and thus to enhance both cutting process stability and labor productivity by the application of a combined magnetic-ultrasound treatment.

### RESEARCH PROCEDURE

The cutter-loaders used in the underground pits separate (ores and) minerals from the mass and load it into a transport. The use of heading machines in the mine practice represents the most progressive means for working.

The present comparative study was accomplished under real production conditions in the pit "Babino" of the mines "Bobov dol" (Bulgaria) in the case of a type "ГПК-1С" heading machine featuring selective action of its working head [Инструкция за монтаж и експлоатация ...]. Usually, under service conditions the working head of the combined cutter-loader cuts in the destroyed layer and after that successively process the surface of the face, thus performing a rotary motion around its proper axis at a rotational speed  $n = 54 \text{ min}^{-1}$ , and a tilting motion in both horizontal and vertical plane thereof. To the working head in a suitable manner are mounted 39 pieces of tangential cutting teeth of the type "РКС-1И". The body (i.e. the gripping part of the cutting teeth) is made of the GOST grade "30Г5" manganese steel, and in the front conical part of the tooth (its head) is embedded the hard- alloy crown made of a monocarbide hard alloy of the type K40 (BK8).

The data for the section of the pass part of the work-mass are corresponding to hardness (abrasion) of  $10 \text{ m}^2$ , categorized as being of the IV<sup>th</sup> degree, according to Protodiakonov.

The teeth wear was given by the "weighing method" via measuring by means of a technical scales with an accuracy of 0,01 g. For this purpose, both initial mass,  $m_{in}$ , of the every tooth and its mass after 15-shift (120 hr.) service,  $m_{out}$ , were measured, thus the resulting difference giving their abrasive wear.

EXPERIMENTAL INVESTIGATIONS AND ANALYSIS OF THE OUTCOME OF THE TEST

The investigations for determining the wear resistance of both "standard" (i.e. untreated) and "treated" teeth (i.e. preliminary treated in the "MUS-1" device, see Fig. 1) by means of a combined electrophysical method [Македонски, А.; Makedonski A. et al.] were performed under strict observation of the requirements for the tools comparison during their service stage [Крџа, 1983; Башков и др., 1985].

With this purpose in view, the treated group of teeth were prepared for treatment in the "MUS-1" type apparatus (Fig. 1), said apparatus reproducing said combined electrophysical method.

The essence of said method consisting of a placement of the tooth in a constant magnetic field under preliminary given both magnitude of the current (i.e. field strength) and treatment time. At the same time, the tooth is submitted to the influence of a mechanical vibration energy with a frequency in the ultrasound range in direction parallel to that of the applied magnetic field. The method is carried out under room temperature and its impact is of short duration (from some seconds to few minutes). The mechanism of the exercised influence features complexity in its nature proper. The energy input in the materials treated by the method leads to their strengthening, the latter resulting from induced movements of defects and dislocations, which are bringing sometimes to both transformation of the crystal lattice and forming of new structure configurations.

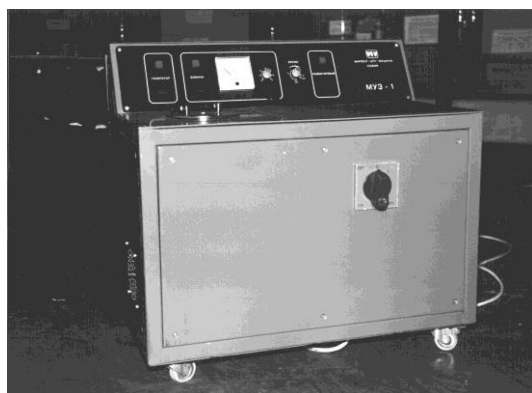


Figure 1. The MUS-1 device

During the drawing up of the matrix of the full factor experiment of the kind  $N = 2^2$  (Table № 1) and determination of the levels for the factors' variation- the amperage  $I$ , in [ A ] and the treatment time  $\tau$ , in [ s ]- the *a priori* information received in previous similar studies was considered [Makedonski A., 2001].

After treatment with subsequent demagnetizing in the MUS-1 apparatus, the teeth were mounted in the working head of the combined cutter-loader in the following succession: standard tooth – treated tooth – standard tooth, etc. Thus, the accidental factors, e.g. various composition of the (ores and) minerals, stability of the working head or that of the heading machine (i.e. the coal getter-loader) , etc., or all of the quantities entering in the generalized notion of the "working conditions"

have been considered, in order to eliminate the coarse errors in the final outcome from the research. On the other hand, again in order to minimize the experimental errors in every point of the factor's space, four or three teeth have been investigated, i.e. the condition for a recurring has been observed.

The duration of the teeth service was 15 shifts or 120 hr. work in the pit, after which the teeth were disassembled, brought to the ground surface and for every tooth was carried out a control in two directions:

- Measurement of the final weight (mass) thereof by means of a technical scales;
- Recording of the external changes occurred- deformation and cracking- deformation and cracking of the body, and breakage (tears off) in the hard-alloy working head (Fig.2).



Figure 2.

Both outcome of the measurements and calculated values are given in the Table 1.

From the statistical treatment of the experimental data, the following statistical model for the wear of the treated teeth,  $W$ , was obtained both in code and natural expression:

$$\hat{Y} = 2.468 - 0.075X_1 - 0.075X_2 - 0.016X_1X_2 \quad (1)$$

$$\bar{U} = e^{2.793} \cdot I^{-0.02} \cdot \tau^{-0.041} (I, \tau)^{-0.032} \quad (2)$$

The statistical analysis approves the reproducibility of the tests, the importance of the coefficients and the model adequacy.

Table 1

| Tooth Code | The code designation |    | The PMF + US Natural values |            | Outcome of the measurement |           | $\bar{U}$<br>g | $Y = \ln \bar{U}$ | $\hat{Y}$ |
|------------|----------------------|----|-----------------------------|------------|----------------------------|-----------|----------------|-------------------|-----------|
|            | X1                   | X2 | I [A]                       | $\tau$ [s] | M in [g]                   | M out [g] |                |                   |           |
| 1          | 1                    | 1  | 6                           | 60         | 460                        | 450       | 10             | 2.302             | 2.302     |
| 1'         |                      |    |                             |            |                            | 450       |                |                   |           |
| 1''        |                      |    |                             |            |                            | 450       |                |                   |           |
| 1'''       |                      |    |                             |            |                            | 449       |                |                   |           |
| 2          | -1                   | 1  | 2                           | 60         | 460                        | 449       | 12             | 2.485             | 2.484     |
| 2'         |                      |    |                             |            |                            | 448       |                |                   |           |
| 2''        |                      |    |                             |            |                            | 448       |                |                   |           |
| 2'''       |                      |    |                             |            |                            | 448       |                |                   |           |

|                 |    |    |   |    |     |            |          |       |       |
|-----------------|----|----|---|----|-----|------------|----------|-------|-------|
| 3               | 1  | -1 | 6 | 10 | 460 | 449        | 12       | 2.485 | 2.484 |
| 3'              |    |    |   |    |     | 448        |          |       |       |
| 3''             |    |    |   |    |     | 447        |          |       |       |
| 3'''            |    |    |   |    |     | 447        |          |       |       |
| 4               | -1 | -1 | 2 | 10 | 460 | 447        | 12,5     | 2.602 | 2.602 |
| 4'              |    |    |   |    |     | 447        |          |       |       |
| 4''             |    |    |   |    |     | 446        |          |       |       |
| 4'''            |    |    |   |    |     | 446        |          |       |       |
| 5               | 0  | 0  | 4 | 35 | 460 | 448        | 12       | 2.485 | 2.468 |
| 5'              |    |    |   |    |     | 448        |          |       |       |
| 5''             |    |    |   |    |     | 447        |          |       |       |
| 5'''            |    |    |   |    |     | 447        |          |       |       |
| Untreated teeth |    |    |   |    | 460 | 430<br>410 | 30<br>50 |       |       |

### TECHNICAL AND ECONOMICAL ANALYZIS

The technical-economical effect represents a generalized indicator for evaluation the outcome of this research. Bearing in mind the fact that this effect is a multilateral notion, its can be evaluated regarding different criteria, e.g.:

#### Providing for a high productivity

One of the factors providing a high productivity during machining is the enhanced tool life, or the durability (under wear) of the cutting tools, respectively.

From the results obtained after treatment of the teeth by the combined electrophysical method it is evident that its significantly reduces the wear thereof, also, break off (breakage) in the hard-alloy crowns which, on the one hand, improves the productivity- as a result of the created possibility for bigger number of teeth to take part to a greater extent in the cutting process-, and on the other hand, following the many times decreased auxiliary time for the tools change. All of this positively reflects on both stabilization of the work of the mining machine and cutting process as a whole.

#### Lowering of the (manufacturing) cost

Considering the essence of the process, i.e. cutting of a rocky mass without the requirement for accuracy and quality of the cut surface, to cut the cost is to be considered determining in the decision making process. The increase of the cutting tools life leads to a decrease of the number of the tools needed for a given process accomplishment This, in turns, contributes for lowering the cost of produced items.

From the research made in the "Bobov dol" mines and bearing in mind the production conditions in the pit "Babino", in particulars: number of combined cutter-loaders- four pieces, unit price per tooth-10 BGN, and assuming an yearly

consumption of 8,112 teeth, it turn out (to be) that the application of the process of magneto-ultrasound treatment of the teeth will bring to costs lowering thereof of the order of some 45,240 BGN.

Arriving at a conclusion, from the accomplished comparative study one may draw the following generalized deductions:

1. The wear resistance of the treated teeth is from two to two and half times higher than that of the standard (untreated) ones.
2. The typical breakage and break off of the hard-alloy crowns for the standard teeth are not observed in the case of treated ones (Fig. 2).
3. The technical- economical analysis of the results shows that under existing conditions, bearing in mind only the purchasing price of the cutters, the implementation of one apparatus of the type MUS-1 will have a return on investment period (ROI) from four to five months.
4. With a high degree of authenticity one may forecast the yearly need for teeth for every pit (mine), the latter being directly related to the effective management of the tool flows thereof.

### REFERENCES

- Инструкция за монтаж и експлоатация на галериен комбайн ГКП-С. Мини "Бобов-дол", Р.България.
- Македонски А., Повишаване трайността на режещите инструменти чрез предварителни енергийни въздействия. Дисертация к.т.н., София.
- Македонски А., Метод и технологи упрочнения инструментъй для механическа обработка на инсталация МУЗ-1. International Conference on Projektowanie Procesow technologicznych TPP98, p.p.87-91, Poznan.
- Makedonski A., B. Makedonski: An Electrophysical Method for Enhancing the Durability /Under Wear/ of Tools and Parts&Development and Deficas Thereof. 2-nd Asia-Pasific Forum PSFDT 2001, Conference proceedings, pp.253-57, Konkuk University, Seoul, Korea.
- Круга Г.К., 1983. Статистические методы в инженерных исследованиях. Москва. "Высшая школа".
- Башков В.М., Кацев П.Г., 1985. Испитания режущего инструмента на стойкость. Москва. Машиностроение.
- Makedonski A., 2001, Durability /Under Wear/ of the Cutters of the Cutter-Loaders After Treatment. Conference at Miskolc, Conference proceedings, pp.49-53, Miskolc, Hungary.

Recommended for publication by Department of  
Mine Mechanization, Faculty of Mining Electromechanics

## APPLICATION OF CENTRIFUGAL BALL CLUTCH TO THE DRIVE OF A MILL FAN AT THE "BOBOV DOL" POWER PLANT

Venelin Tasev

University of Mining and Geology "St. Ivan Rilski"  
Sofia 1700, Bulgaria  
E-mail: [lvasev@mail.bg](mailto:lvasev@mail.bg)

### ABSTRACT

The report discusses the results of replacement of ball-bearing clutches, used in the drives of mill fans of the combustion compartment of "Bobov dol" Thermal Power Plant with centrifugal ball clutches of 800 kW power. The disadvantages of the used ball-bearing clutches from a point of technical maintenance are indicated. Oscillograms are prepared, which indicate the low quality initial characteristics of the ball-bearing clutches. They are compared to the oscillograms of the transitional process, done with centrifugal ball clutches. The advantages of centrifugal ball clutches are apparent.

The centrifugal ball clutches are frictional mechanisms, which operation is fulfilled automatically by the centrifugal forces. Their kinematical connection and the frictional momentum is carried out by steel balls, freely placed in six operating chambers.

In their principle of operating, they do not practically differ from the various centrifugal clutches, in which the moment is transmitted by fluids, solid weights with permanent shape or graphitized powder.

In respect of initial characteristics they are similar to those of hydraulic clutches, as though they are capable to translate larger initial momentum at identical dimensions and weight, and ensure loss-free work for the established modes of operation. The hydraulic clutches, in the best case, operate with efficiency of 98-99, which in the case of transmitted power of 800 kW, means continuous loss of 8-16 kW. In comparison to the clutches with monolithic weights or powder filling, they differentiate by:

- constant initial parameters;
- high smoothness of the starting process;
- high stability upon heat supercharges.

In respect of maintenance characteristics, the centrifugal ball clutches are totally comparable to hydraulic clutches, as they practically have an equivalent resource.

In this aspect, they significantly better than other types of centrifugal ball clutches – with monolithic weights and with powder filling.

They achieve the good maintenance indexes, more than 10000 starts, owing to the use of high-quality steels during the last 10 years and active elements, operating in a proper oil medium. Their construction is not much more complicated than construction of the other types of centrifugal clutches and it is considerably more simplified than construction of hydraulic clutches.

The reasons for applying hydraulic ball clutches to the mill drives at "Bobov dol" Thermal Power Plant were the problems, which were brought about by clutches of "Pulvis" type, used before 1994. They were the less safe element of

the fan drive. Actually, mostly repairing and reconstruction of clutches occupied the maintenance department.

After fixing the problem, firstly an analytical check of the possibilities of the utilized asynchronous motor for running the machine without a starting clutch was done. The mill fan is an aggregate, which provides feeding of fuel mixture of coal dust and air into the furnace of the boiler. It provides simultaneously the filling-up of the necessary amount of air and coal, and in the same time grinds the coal to required size of the grain fragmentation. The operating body of the mill is a cylinder with diameter of 3,2 m and a weight about 10 t. Significant part of it is concentrated to the periphery of the cylinder, which defines an inertia momentum of about 14200 kgm<sup>2</sup>. The static resistivity momentum for the starting period without a coal feeding is 5 kNm.

The accomplished calculation showed that the common time for initiating the spinning of the mill fan is 47,58. This is inadmissible high, since practically through the whole starting period current flow of 6-7I<sub>n</sub> will flow, which may bring it out of order. Moreover, for the time of starting process, there is a significant overloading of the entire electricity supply system, and this may bring to worsening the electricity supply of all other consumers.

After proving the necessity of a starting clutch the issues related to the "Pulvis" type clutch that had been used before were investigated.

With the aim of specifying the problems during the exploitation of the powder clutches, an analysis of the existing clutches was made. It is based on the following:

1. Oscillography of the starting process with the existing drive, the inlet and outlets speeds are measured as well as current of the motor.

2. Analysis of the most frequent damages of the used clutches.

3. Investigation of the exploitation indexes of the centrifugal clutches with graphitized powder filling.

The practice of exploitation of clutches with graphitized powder filling showed:

- instability of initial characteristics, which are expressed by:

- change of the initial torque in the starting process;
- absence of repetition of characteristics for different starting processes.
- high sensitivity towards thermal overloading;
- fast wearing out of the active surfaces and friction junctions;
- granulation, densification and enlargement of the filling, bringing to obtaining of large forms and disbalance.
- adhesion of the filling to the active surfaces and blocking of the clutch.

Some of the reasons, bringing to the above phenomena, figure out to be the thermal-frictional phenomena in the area of friction. For clutches of discussed type and the particular case, the thermal flow through the active elements reaches from 2 to 2,5 MN/m<sup>2</sup>. Considering the bad thermal conduction properties of the mentioned filling and the relatively large duration of starting process, the expectation of a superficial layer (the place of frictional contact), where temperature reaches considerable values, which leads to melting and enlarging of fragments, as well as to unpredictable chemical reactions is logical. In any case, it is inevitable to expect an intense wearing out, change of the grain composition, chemical changes, unexpected alterations of the friction coefficient and therefore of initial starting torque.

An effective solution for decreasing the thermal loading and respectively the undesired above described phenomena, is the reduction of time for starting process. The only way of reducing the time of starting process is increasing the torque, developed by the clutch  $M_c$ . This opportunity is restricted also by the capacity of the motor.

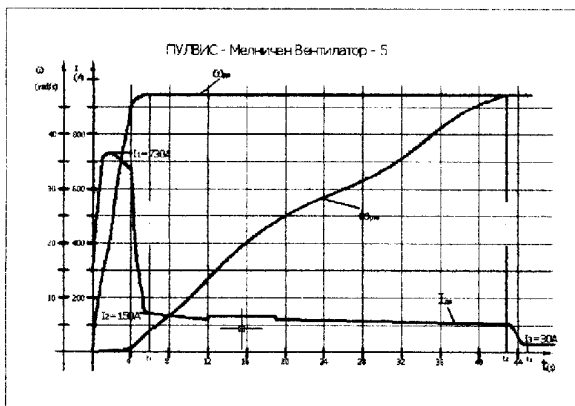


Figure 1

The oscillogram shown in fig.1 shows that the electrical current of the motor at the starting process is 2-2,5I<sub>n</sub>, which suggests utilizing the maximum feasible, "the critical" for the asynchronous motor torque. This method ensures a relatively stable operation of the clutch, but has some disadvantages, as follows:

- considerable electrical current of the motor at the time of starting;
- danger of "overturning" of the motor while an eventual change of drive parameters takes place.

Exactly the same case of "overturning" of the motor is shown in the oscillogram in fig.2.

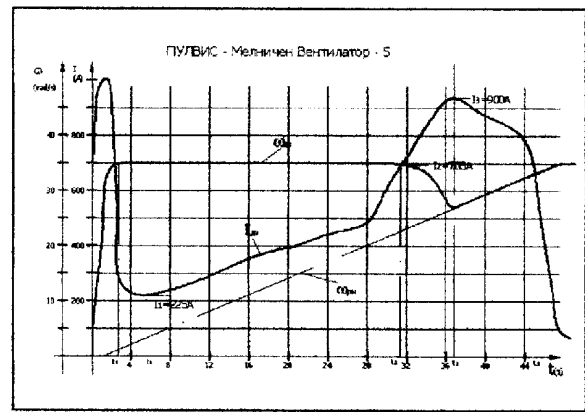


Figure 2

Through the figure is obvious, that because of the reasons connected to the above described processes in the friction contact, the momentum of the clutch increases, passes over the critical for the motor moment, as follows:

- abrupt decrease of the velocity of the motor;
- considerable increasing of motor current.

This occasion may be considered us a accidental one, because of its relation to the significant overloading of the overall kinematics of the drive of machine, as well as to a significant mechanical and current rush upon the motor and the current supply system.

The accomplished research and the negative experience in the maintenance of up-to-now used clutches of the "Pulvis" type, predetermine the application of centrifugal ball clutch (CBC). For this purpose a project for a proper CBC is accomplished. It was initiated by the following considerations:

1. Mill aggregate has relatively small static starting torque and there are no strict restrictions for the time of starting.
2. Motors are large and expensive aggregates, which permit only one switching per day.
3. Maximum care for the motor, by ensuring the minimum time for acceleration of the motor and accelerating of the system by the least possible current.

Starting process of drive accomplished by CBC and asynchronous motor is fulfilled as follows. When switched on, the motor begins to accelerate by a dynamic moment equal to the starting torque of the motor  $M_n$ . Together with rotations of the motor, the rotor of the CBC also rotates together with the balls filling. The momentum of CBC increases by the square of initial angle velocity ( $\omega_1$ ). At definite  $\omega_1$ ,  $M_c$  equalizes to the static resisting moment of the machine and it begins to driven into motion. This time is called initial time for rotation of the machine -  $t_n$ . From this moment on, the motor accelerates simultaneously with the mill fan, by different values of acceleration defined by their dynamic moments. This continues until the clutch comes to the natural characteristic of the motor. The motor ceases its acceleration and the momentum developed by CBC remains a permanent one. At this momentum of CBC the acceleration of the mill fan proceeds, so the size of this acceleration is determined by the dynamic moment  $M_n = M_c - M_p(\omega_1)$ . This continues until equalizing of the revolutions of incoming and outgoing shafts of the clutch. After their equalization the acceleration of motor is completed by "solid" clutch according to the natural curve of asynchronous motor until equaling of the momentum of the machine with the momentum of the motor.

After the design and constructing, the clutch was produced and mounted to mill fan № 5.

The clutch showed smooth, safe and noiseless acceleration of the whole system. The oscillography of the starting process (fig.3) shows the following:

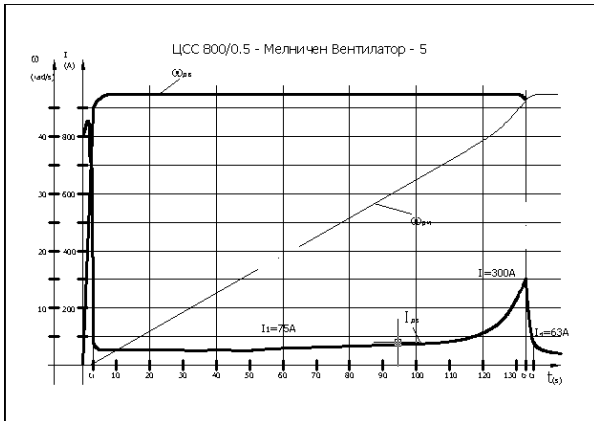


Figure 3

1. The motor runs to its nominal velocity in 3-4 sec.
2. The mill fan begins its acceleration after the motor has reached its nominal revolutions. The acceleration is smooth, almost linear, a certain increase is noticed at the end of the process. That is explained with the increase of the momentum developed by the CBC, during the decreasing of the relative velocity of slipping.
3. In the process of rotating the current of motor reaches a value of 800 A, for a period of time less then one second. After reaching the nominal velocity of the motor, the current drops to 75 – 80A. That value is determined by the outgoing momentum developed by CBC. It is selected in such a manner, as the motor is preserved to the maximum extent and the current supply throughout the starting process is not more than  $1,1-1,2I_n$ . This momentum ensures high smoothness of rotation and safety of drive and, at the same time keeps away from heavy overloading.

4. The total time of starting process is about 140 seconds. It is thoroughly acceptable for this kind of machines and does not make trouble for the technological process.

The achieved results unambiguously present the good starting capabilities of the CBC. The exploitation properties of clutches of CBC type may be judged by the almost nine years of failure-free operation of clutches installed in 1995. Up to now another twenty four clutches are installed to the mill fans at the “Bobov dol” Thermal Power Plant. They complying with requirements of drive and up to now operate in a failure-free mode.

\*TEPS – Thermo-Electric Power-Station

## ON THE PROBABILISTIC CHARACTER OF HAULAGE FOR ROUTES WITH MOVABLE RAILROADS

Atanas Smilianov

Philip Kouzmanov

University of Mining and Geology "St. Ivan Rilski"  
 Sofia 1700, Bulgaria

**ABSTRACT:**

Movable railroads are in both ends of routes of the technologic haulage: beginning – at overburdening or mining areas and ending – at dumping areas or receiving stations. It is shown how routes may be found at different levels of intensity depending on probability of working condition, which predetermines the probabilistic character of provoked deformations in movable roads.

The movable railroads are unique facilities, typical and applicable only to opencast mines equipped with technological railroad haulage. Their effect on continuity of haulage is crucial and depends on their technical condition. This is so, because it determines the speed of movement on them.

On the other hand, it is subjected to the probability of haulage on one and the same routes, where the movable railroads are at the both ends: beginning – in overburdening or faces and ends – dumping areas, depots in intermediate storage, receiving devices.

The overall efficiency of the performance of the large engineering system "opencast mine" is limited by the probability of failure-free performance of its subsystems, including the subsystem "railroad haulage". The probability of failure-free performance, according St. Irinkov in "Automation of technological processes in opencast mines" [1], may be presented as follows:

$$P_{\text{жсн}}(t) = P_{\text{нс}}(t) \cdot P_{\text{прп}}(t) \cdot P_{\text{мрп}}(t) \cdot P_{\text{мо}}(t) \cdot P_{\text{рп}}(t) \quad (1)$$

or

$$P_{\text{жсн}}(t) = k_1 \cdot e^{-\lambda_1 t} \cdot k_2 \cdot e^{-\lambda_2 t} \cdot k_3 \cdot e^{-\lambda_3 t} \cdot k_4 \cdot e^{-\lambda_4 t} \cdot k_5 \cdot e^{-\lambda_5 t} \quad (2)$$

where:

$P_{\text{жсн}}(t)$  – probability of failure-free performance of the subsystem railroad haulage, treated as an independent system;

$P_{\text{нс}}(t)$  – probability of failure-free performance of movable railroad haulage components – locomotives and cars;

$P_{\text{прп}}(t)$  – probability of failure-free performance of the railroad haulage caused by the constant railroads;

$P_{\text{мрп}}(t)$  – probability of failure-free performance of the railroad haulage caused by the movable railroads;

$P_{\text{мо}}(t)$  – probability of failure-free performance of the railroad haulage caused by maneuver operations;

$P_{\text{трп}}(t)$  – probability of failure-free performance of the railroad haulage caused by the loading and unloading stations;

$k_i$  – coefficient of readiness for operation for each separate detail of the transport system.

$$k_i = \frac{T_{\text{ср.р}}}{T_{\text{ср.р}} + T_{\text{ср.нр}}} = \frac{1}{1 + \frac{T_{\text{ср.нр}}}{T_{\text{ср.р}}}} = \frac{1}{1 + k_n} \quad (3)$$

where:

$T_{\text{ср.р}}$  – average time of efficiency of the independent subsystem railroad haulage (in a shift, in a month etc.);

$T_{\text{ср.нр}}$  – average idle time of trains caused by different reasons.

Equation (3) reveals the physical essence of the coefficient for readiness of the system. When

$$T_{\text{ср.нр}} > T_{\text{ср.р}}$$

the coefficient of readiness for  $k_i$  decreases, i.e. according the value  $k_i$  it may evaluate the level of maintenance and repair of all subsystems in the system railroad haulage.

Below, there is an illustration of an example of the railroads of "Kremikovtsi" mine for a more complete differentiation of the probability of railroad haulage – fig. 1.

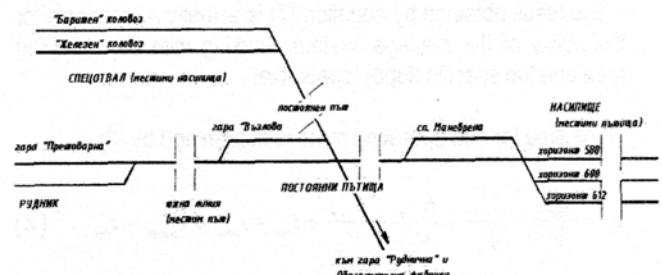


figure 1. Principle scheme of railroad network for "Kremikovtsi" mine

The scheme in fig. 1 corresponds to the real production program for the year 2002 and shows the active operating layers (two) of the dumping area and the special depot (called "spetsotval"), also shows two operating tracks – for barite and for ferrous ore.

If we set aside the transport of ore from the mine directly to the ore-dressing plant, there are available four actively operating routes from the mine: two for the layers 588 and 600 into the dumping area and two for the special depot "spetsotval".

The production capabilities of each of routes may be presented as follows:

$$V_{\tau} = \sum_{i=1}^n V_i t_{pi} \quad (4)$$

where:

$V_{\tau}$  – volume of transported ore aggregate for a respective period of time of duration  $\tau$ ;

$V_i$  – volume of ore aggregate in  $i$ -st train-composition (also a probabilistic quantity);

$n$  – number of train-compositions;

$t_{pi}$  – continuousness of time of traffic, i.e accomplishment of a real transport operation  $i$ -st train-composition.

If the probability of train-composition  $i$  being in an operating status is denoted by  $P(t_{pi})$ , then the probability to find the same in a non-operating status is  $1 - P(t_{pi})$ .

In such a case for the transport system, including "m" independent haulage flows, the probability to find it at "k" status is expressed by:

$$P(t_{pc})_k = \prod_{i=1}^s P(t_{pi}) \cdot \prod_{1+s}^m [1 - P(t_{pi})] \quad (5)$$

The permission ability of this haulage system in status "k" is:

$$V_{ok} = \sum_{i=1}^s V_i \quad (6)$$

In such case the volume of the operation done for a definite calendar period of time " $T_k$ " will be:

$$V_{kk} = V_{ok} \cdot T_k \cdot P(t_{pc})_k \quad (7)$$

The result obtained by equation (7) is actually a prognosis for the ability of the haulage system, working with the dumping area and the specific depot "spetsotval".

The time for one operating route is determined by (8)

$$t_p = \frac{L_{m,n}}{V_n} + \frac{L_{n,n}}{V_n} + \frac{L_{m,np}}{V_{np}} + \frac{L_{n,np}}{V_{np}} + t_{mo} + t_{moe} + t_{pazm} + t_{op.3} \quad (8)$$

where:

$L_{m,n}$  &  $L_{n,n}$  – total lengths of the sections with movable railroads and permanent railroads;

$V_n$  и  $V_{np}$  – speed of movement of the train at direction "loaded" and direction "unloaded";

$t_{m.o.}$  – time for maneuver operation;

$t_{rob}$  – time for loading;

$t_{paz1}$  – time for unloading;

$t_{op.3}$  – time for other unforeseen delays.

In Bulgarian practice special observations on the different motion routes of trains in all the five opencast mines with technological railroad transport have not been performed. However, such observations are made into underground mines and S. Irinkov [1] assumes, that time for movement for train compositions there, sufficiently for the practice, may be subordinated to the Gauss distribution. In such case the dispersion of time, in which the train occurs during operating status is [1]:

$$\begin{aligned} D(t_p) = L^2 & \left[ \frac{D(V_n^{m,n})}{V_n^4} + \frac{D(V_n^{n,n})}{V_n^4} + \frac{D(V_{np}^{m,n})}{V_{np}^4} + \frac{D(V_{np}^{n,n})}{V_{np}^4} \right] + \\ & + D(t_{mo}) + D(t_{moe}) + D(t_{pazm}) + D(t_{op.3}) \end{aligned} \quad (9)$$

The required number of courses of the trains to provide the shift productiveness  $Q_{cm}$  is:

$$n_p = \frac{Q_{cm}}{Q_{ct}} \quad (10)$$

where:

$Q_{bn} = V_{b.n.b} \cdot \gamma$  – effective weight of train, as

$n_b$  – number of cars in the train;

$V_{b.}$  – volume of a car;

$\gamma$  – bulk weight of carried rocks.

The root-mean-square deviation of time needed for movement of trains is:

$$\sigma_t = \sqrt{D(t_p) \cdot n_p} \quad (11)$$

In case of limited (caused by different reasons) number  $N$  of train compositions in the mine, the necessary time for transportation of rock mass is:

$$T_p = \frac{t_p \cdot Q_{cm}}{Q_{ct}} \quad (12)$$

The average root-mean-square deviation of flow stream of average value is;

$$\sigma_Q = \frac{m_Q \cdot \sigma_t}{T_p} \quad (13)$$

The probability for transportation of a planned for a shift volume of load can be expressed by (14)

$$P(Q) = \Phi \left( \frac{T_{cm} \cdot m_Q}{T_p} \right) \cdot \frac{1}{\sigma_Q} \quad (14)$$



## THEORETICAL INVESTIGATION OF THE APPLICABILITY MANEVICH-PAVLENKO MODEL FOR DETERMINING THE STRENGTH OF EXTRACTION OF A SINGLE TRAVERSE FROM THE BALLAST PRISM OF A MOVABLE RAILROAD

Atanas Smilianov

University of Mining and Geology  
"St. Ivan Rilski"  
Sofia 1700, Bulgaria

### ABSTRACT

Increasing the strength of movable railroads against their lateral displacement would make the operation of the technologic railroad haulage in the opencast mines much more reliable. This is related to the increasing of strength of extracting a single traverse and determining the stress while doing it.

A model is examined, which is created by Manevich-Pavlenko in the middle of the 80's of 20<sup>th</sup> century and its applicability to the above task is shown by means of the theoretical mechanics, mathematical physics and the classical mathematical analysis.

### INTRODUCTION

There is an observation of a unique phenomenon related to movable railroads - displacement in a horizontal plane during summer. One of the considerable reasons for that is their insufficient strength against lateral movement in a horizontal plane.

Relatively cost-effective opportunity without general raise of cost for the upper construction of the movable railroads is to in-build into it a metal traverse of the shape of a cross in the underrail section.

This engineering approach, realized in large scale requires immense investments. It is quite natural to question if they are reasonable and if there are any possibilities to estimate quantitatively and precisely enough the increase of strength of movable railroads in a horizontal plane. Actually the problem reduces to finding a sufficiently reliable method for calculating the strength of extracting of a single traverse from the ballast bed. This requires development of an adequate mathematical apparatus, based on a physically grounded model. The process, though, has a dynamical character. Therefore it is necessary to describe the mechanical system of three traverses (the one in the middle is supposed to be released of upholding couplings) and ballast in a moment of limited balance. i.e. a model is needed through which by the same type of equations to describe the processes of limited balance between the ballast and the traverses with a conventional and crossed shape in the under-rail cut, when the system is still at rest, however there is an initial, even though an infinitely small movement of the extracted traverse.

### BASIC MODEL

In general there are two approaches. The first one requires the establishing of an intentional model, which describes the discussed physical processes. However, this is a very difficult task, which is to be solved only by the efforts of collective teams. The second approach assumes utilizing of a physics-mathematical model, intended for other conditions, but applicable to the specific task. Its implementation demands relevant physical-mathematical arguments.

The second approach is chosen in this study. The model of Manevich and Pavlenko, developed in the beginning of 90's in (*Manevich L. et al., 1982*) is selected as a basic model. Its essence is illustrated in fig. 1, and the common scheme of thinking is as follows:

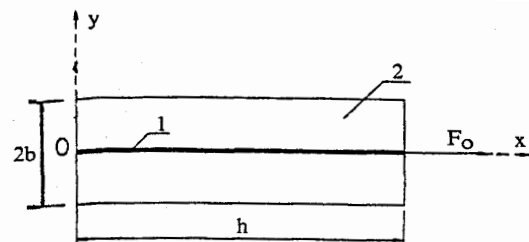


Figure 1. Basic model of Manevich and Pavlenko

Physically, the model represents a plane plate (item 2) with measurements "2.b" and "h", and a fibre is extracted out of it (item 1). The plane plate (2) represents a homogeneous medium. The fiber (1) is allocated in it and it has a structure different from ambient structure:

- non-deformable;
- rigid.

After applying an axis force "F<sub>0</sub>" on the fiber into the direction of "x" axis, extracting of the fiber (1) from the environmental medium of the plate (2) begins. For conciseness, further on the ambience of the plate will be called matrix. Within the process of extracting (extracting), the behaviour of the fiber (1) and the matrix (2) is shown by the following dependences:

- Equations of equilibrium of the matrix (2) – this a system of partial differential equations (1);
- Equation of displacement of points of fiber (1) - differential equation (2).

$$\begin{cases} B_1 \frac{\partial^2 U}{\partial y^2} + G \frac{\partial^2 U}{\partial x^2} + (v_2 B_1 + G) \frac{\partial^2 V}{\partial x \partial y} = 0 \\ G \frac{\partial^2 V}{\partial y^2} + B_2 \frac{\partial^2 V}{\partial x^2} + (v_1 B_2 + G) \frac{\partial^2 U}{\partial x \partial y} = 0 \end{cases} \quad (1)$$

$$EA \frac{\partial^2 W}{\partial x^2} = F_0 \cdot \delta(x) - 2\tau(x) \quad (2)$$

where:

z(u, v) – vector of displacing of the matrix;  
 u, v – vector components of displacing the matrix. In this case the axes x and y coincide;  
 G – rigidity of matrix to cutting;  
 F<sub>0</sub> – axis strength, applied to the fiber in the boundary point;  
 EA – geometrical characteristics of fiber when tensile stresses;  
 B<sub>1</sub>, B<sub>2</sub> – rigidity to tensile stress and compression of the matrix;  
 u<sub>1</sub>, u<sub>2</sub> – the coefficients of Poisson;  
 τ(y) – tension to cutting between fiber and matrix. It is assumed that in the contact area

$$\tau(y) = G \left. \frac{\partial U}{\partial X} \right|_{x=0} \quad \mathbf{t}(y) = 0$$

W – extraction of fiber;  
 δ(y) – delta function of Dirac. It represents integral functional and characterizes the extracting strength.

The new system of equations [(1) & (2)] has the following boundary conditions (3) – [3.1], [3.2], [3.3], [3.4].

$$[3.1] \quad \begin{cases} U = W \\ V = 0 \end{cases} \Big|_{x=0} \quad \text{- its physical meaning is that in}$$

the direction of the fiber "y", the component of solution "U" coincides with "W", which is the solution of the equation (2), i.e., if the value of "W" is known at any point of "y", then "U" (component of the vector of extracting of the matrix) has the same value. Practically that means, that the vector of displacement of the matrix for points situated on the axis "y" has its second component V=0 (the solution Z=U, 0 or Z=W, 0);

$$[3.2] \quad U = V = 0 \Big|_{y=\pm b} \quad \text{- its physical meaning is that}$$

the matrix is fastened on by its two ends in parallel to the axis "x", i.e., that immobility of the matrix is guaranteed out of points with coordinates "±b";

$$[3.3] \quad \left. \frac{\partial U}{\partial y} = V = 0 \right|_{x=0} \quad \text{- its physical meaning is that}$$

the vector of speed of displacement of the matrix on direction of axis "x" is equal to zero in the point x=0;

$$[3.4] \quad U = V = 0 \Big|_{x=\infty} \quad \text{- its physical meaning is, that}$$

when "x" is very large, than displacements in the matrix are equal to zero.

#### ANALOGICAL ADAPTATION OF THE BASIC MODEL TO THE SOLUTION OF THE TASK

The peculiarities of the model of Manevich-Pavlenko are:

- The matrix is homogeneous medium;
- The fiber has a structure, different from the structure of the matrix and carries the following characteristics:
  - It is non-deformable;
  - It is rigid;

While extracting of a steel traverse of a crossed shape from the under-rail section, released from connections and dipped to its upper edge into gravel ballast prism, the following should be observed:

- cutting up the gravel ballast along the surfaces, represented by lines 1-1 and 2-2 (fig. 2), i.e. because of the different structure, this system may be treated as follows:
  - the gravel – like a matrix;
  - the traverse – like an extracted fiber;
- cutting up the gravel along the surface, which coincides with the lower base of the traverse, i.e. if assumed that through the height of the traverse the behavior of cutting through all horizontal sections of the extracted traverse is the same, than principally the picture resembles to a level of identification of the theoretical model according to fig. 1.

In case that the traverse is situated in the gravel bed and several traverses are missing around it, from both sides, then cutting of the gravel (according the above mentioned considerations) is realized under an angle φ (fig. 3) from the farther (in relation to the direction of extracting) end of the crossed extensions onto the surface, coinciding with the surface of the lower base. The last is due to the following circumstance:

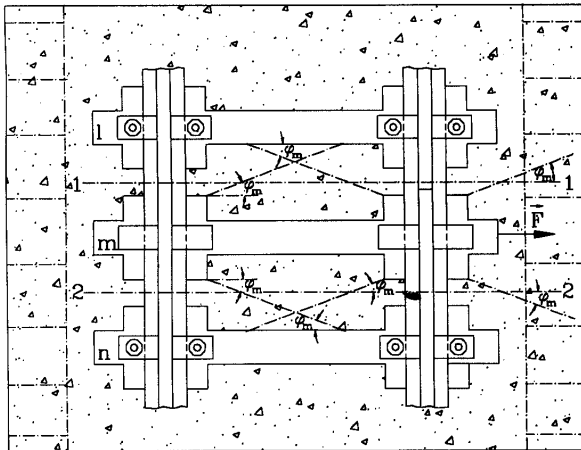


Figure 2. Lines of cutting of the gravel ballast during the extraction of a cross-shaped traverse

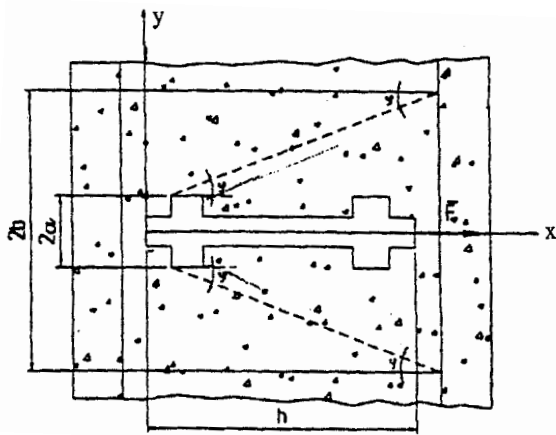


Figure 3. Illustration of cutting of gravel ballast, caused by the cross-shaped traverse

Availability of under-traverse thresholds under and near to the extracted traverse determines the larger strength of shearing of the ballast prism under angle " $\varphi$ " (of internal friction of gravel) into depth towards the ground base. At the same time, force " $F_0$ " actively operating on the axis of the traverse seeks the zone of the less strength. And it is namely onto the horizontal plane, coinciding with the lower base of the extracted traverse due to the lower degree of consistence compared to compression of gravel in the zone of under-traverse thresholds. The above mentioned considerations are logical and truthful. But they do not report and there is no way to report, that the model of Manevich-Pavlenko is created to be applied to extracting of a fiber from composite medium.

A comprehensive theoretical is needed in order to prevent suspicions in the adequacy of utilizing the basic model for the purposes of the above task.

#### BASIC PRECONDITIONS ABOUT APPLICATION OF THE MODEL

The basic preconditions, assuming validity of the theoretical background for applying of the Manevich-Pavlenko model are as follows, according to fig. 4.

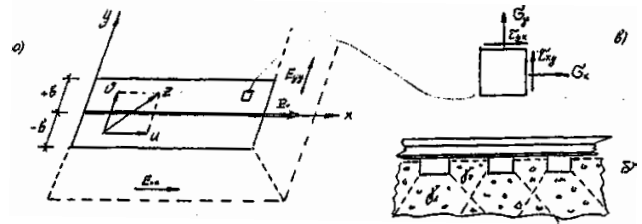


Figure 4. Initial basis for genesis of the Manevich-Pavlenko model. a) principal scheme of the movable railroad line according the Manevich-Pavlenko model; b) physical behavior of the gravel ballast bed; c) elementary segment of the compacted gravel ballast bed.

They are as follows:

FIRST: It is assumed that, a plane fragment of the gravel ballast prism and the rail-traverse frame is been treated. It is supposed that, in whatever way (by an approach up to now unknown) the traverses are compressed volumetrically to the transformation into dimensionless fibers and through extracting them from the gravel ballast prism they provoke (by an approach up to now unknown) cutting in the gravel bed onto the axis "x" (fig. 4 a).

SECOND: The components U & V of the vector z of displacement of the matrix are in parallel to the axes x and y (fig.4 a);

THIRD: The elastic moduli of the gravel ballast bed, though close to the values on axes x and y are different, i.e.,  $E_{xx} \neq E_{yy}$  (fig. 4. a), i.e. the gravel prism is orthotropic. Thus the modulus on the axis of road  $E_{yy}$  is higher than the modulus transversely to the road  $E_{xx}$ .

FOURTH: The gravel is compacted to a rate of formation of under-traverse thresholds and its compactness as a function of the bulk weight is figured out by the inequality:

$$\gamma_1 > \gamma_2 < \gamma_{cp}^{\ominus} \quad (\text{по фиг. 4 а}), \quad (4)$$

where:  $\gamma^{\ominus}_{cp}$  is the gross weight, after which it is so compressed that its behavior and characteristics are similar to the behavior of an elastic body..

FIFTH: The system is in a dynamical equilibrium, i.e. every one infinitely small element of the matrix is into an equilibrium – on (fig.4.c).

#### REASONING OF THE COMPACTION OF THE CONCRETE PRISM

In connection to the fourth precondition and dependence (5), it should be notified that, during the development of (Stoyanov D. et al. 1998; 2000) by the team of D. Stoyanov, observations were made on the loading of the operating trains on a movable railroad at the "Obrouchishte" dumping area at "Trayanovo" mine of the "Maritza Iztok" Co.

According to Ivanov G. (1981), Kostov T. (1991) etc. in Shahonyants G. (1982) etc., and general administrations of the conventional railroads in many countries assume that the gravel ballast bed of the railroad is compacted enough after passing over on it of 1,000,000 gross tons. Furthermore, it is assumed that the process goes on according to the response in fig.5.

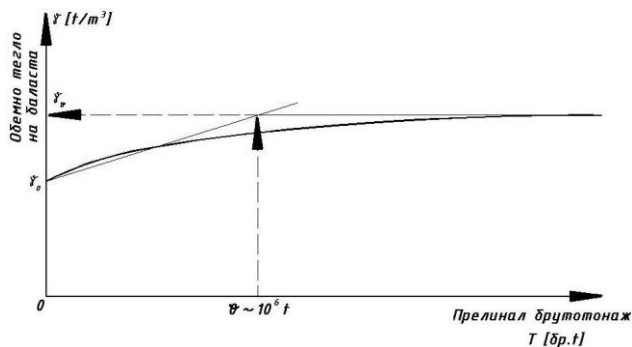


Figure 5. Illustration of the process of compacting of gravel in the gravel prism after passing over a definite gross-tonnage

A constant number of cars of 16 is assumed with the aim of safety;

- useful car volume is 40 m³ and own weight is 34 t. The transported overburden consists of different clays with average bulk weight of 2,1 t/m³ and average coefficient of swelling  $K_p = 1,45$ . Twenty nine cars are measured and an average coefficient of filling up of cars is established to  $K_n = 1,02$ .

In this case the gross weight of a train is:

$$Q_{вт} = P_{л} + \frac{n_g \cdot V_g \cdot \rho \cdot K_n}{K_p} + n_g \cdot q_T \quad (5)$$

and the loading stress requires addition of the weight of empty train –

$$P_{л} = n_g \cdot q_g$$

where:

$P_{л}$  - weight of the locomotive. For EL2-  $P_{л}$  series = 147 t;

$n_g$  - number of cars in the train. Assumed  $n_g = 16$ ;

$V_g$  - volume of the bucket of the car. For the trains of Russian and Bulgarian manufacture with dumping cars -  $V_g = 40$  m³;

$K_n$  - coefficient of filling the bucket of the car. Average coefficient in the calculation is  $K_n = 1,02$ ;

$K_p$  - coefficient on swelling. Assumed  $K_p = 1,45$ ;

$q_T$  - coefficient of the cars  $q_T \approx 34$  t.

Therefore, the loading stress of one train is 2 274 t.

For the both mines, using the "Obruchishte" dumping area there is a two-shifts regime of railroad haulage. For the aim of safety a coefficient of use is assumed as

$$K_g = 0,75;$$

- The loaded overburden spreader AS-6 accepts between 3 and 6 trains per hour. For the aims of safety it is assumed 4 trains/hour.

Therefore, for a twenty four hour period the overburden spreader AS-6 accepts:

$$N_{вт.дн} = n_{вт/h} \cdot T \cdot K_g = 4.24.0,75 = 72 \text{ trains}$$

Then the total gross tonnage for a twenty four hour period is:

$$Q_{оп.дн} = N_{вт.дн} \cdot Q_{оп} = 2274.72 = 163728t$$

This means that the gross tonnage of 1,000,000 t on the movable railroad of overburden spreader AS-6 at the "Obruchishte" dumping area is accumulated for less than 7 days.

Therefore, after 6-7 days of operating on a new track the gravel in the gravel prism of the movable railroad near the overburden spreader AS-6 is thickened through (5) and its behavior and properties are approximating to those of the elastic body.

### THEORETICAL PROVE

Since all the above is known, it is accepted that the matrix (gravel bed) is in equilibrium. Then every plane fragment of it (from first precondition) is in equilibrium. This also applies to the infinitely small element of the matrix – fig.-4.c., i.e. the conditions for equilibrium are in validity.

$$\begin{cases} \frac{\partial \sigma_x}{\partial x} + \frac{\partial \tau_{yx}}{\partial y} = 0 \\ \frac{\partial \sigma_y}{\partial y} + \frac{\partial \tau_{xy}}{\partial x} = 0 \end{cases} \quad (6)$$

Theoretical mechanics and strength of materials (Kisliakov S., 1980; Федосьев B., 1965 etc.) reveal that, the infinitely small movements of the matrix through components U and V of the vector Z (from the second precondition) may be introduced down by the equations:

$$\begin{cases} \varepsilon_{xx} = \frac{\partial U}{\partial x} \\ \varepsilon_{yy} = \frac{\partial V}{\partial y} \\ \varepsilon_{xy} = \gamma_{xy} = \frac{\partial U}{\partial y} + \frac{\partial V}{\partial x} \end{cases} \quad (7)$$

The generalized type of the Hook law is:

$$\begin{cases} \sigma_x = a_{11} \cdot \varepsilon_{xx} + a_{12} \cdot \varepsilon_{yy} + a_{13} \cdot \varepsilon_{xy} \\ \sigma_y = a_{21} \cdot \varepsilon_{xx} + a_{22} \cdot \varepsilon_{yy} + a_{23} \cdot \varepsilon_{xy} \\ \tau_{xy} = a_{31} \cdot \varepsilon_{xx} + a_{32} \cdot \varepsilon_{yy} + a_{33} \cdot \varepsilon_{xy} \end{cases} \quad (8)^*$$

\* Equations (8) represent the 2 dimensional case. If a 3-dimensional case is treated the equations are 6, and the coefficients  $a_{in-36}$ .

In the system of equations (8)  $a_{in}$  are elastic constants, characterizing the matrix (compacted gravel prism). As it is assumed (the third precondition from IV) that the matrix is orthotropic, these two coefficients, based on the theorem for interaction of operations and calculations (Федосьев В., 1965), are two by two equal.

In the Hook law a substitution is done in the conditions of equilibrium; it is differentiated by "x" and "y" and first and third and second and fourth equations are added.

$$1. \frac{\partial \sigma_x}{\partial x} + \frac{\partial \tau_{xy}}{\partial y} = 0$$

$$\frac{\partial \sigma_x}{\partial x} = a_{11} \cdot \frac{\varepsilon_{xx}}{\partial x} + a_{12} \cdot \frac{\varepsilon_{yy}}{\partial x} + a_{13} \cdot \frac{\varepsilon_{xy}}{\partial x}$$

$$\frac{\partial \tau_{xy}}{\partial y} = a_{31} \cdot \frac{\varepsilon_{xx}}{\partial y} + a_{32} \cdot \frac{\varepsilon_{yy}}{\partial y} + a_{33} \cdot \frac{\varepsilon_{xy}}{\partial y}$$

Or

$$\frac{\partial \sigma_x}{\partial x} = a_{11} \cdot \frac{\partial^2 U}{\partial x^2} + a_{12} \cdot \frac{\partial^2 V}{\partial x \partial y} + a_{13} \cdot \frac{\partial^2 U}{\partial x \partial y} + a_{13} \cdot \frac{\partial^2 V}{\partial x^2}$$

$$\frac{\partial \tau_{xy}}{\partial y} = a_{31} \cdot \frac{\partial^2 U}{\partial x \partial y} + a_{32} \cdot \frac{\partial^2 V}{\partial y^2} + a_{33} \cdot \frac{\partial^2 U}{\partial y^2} + a_{33} \cdot \frac{\partial^2 V}{\partial x \partial y}$$

Due to the assumed orthotropic type

$$a_{13} = a_{31} = a_{32} = a_{23} = 0$$

$$a_{12} = a_{21}$$

Then the first equation acquires the type by 1'

$$1'. \frac{\partial \sigma_x}{\partial x} + \frac{\partial \tau_{xy}}{\partial y} = a_{11} \cdot \frac{\partial^2 U}{\partial x^2} + a_{33} \cdot \frac{\partial^2 V}{\partial y^2} + (a_{12} + a_{33}) \cdot \frac{\partial^2 V}{\partial x \partial y}$$

$$2. \frac{\partial \sigma_y}{\partial y} + \frac{\partial \tau_{xy}}{\partial x} = 0$$

Or

Similarly, equation (2) acquires the type by 2'

$$2'. \frac{\partial \sigma_y}{\partial y} + \frac{\partial \tau_{xy}}{\partial x} = a_{33} \cdot \frac{\partial^2 V}{\partial x^2} + a_{22} \cdot \frac{\partial^2 V}{\partial y^2} + (a_{21} + a_{33}) \cdot \frac{\partial^2 U}{\partial x \partial y}$$

Or the system of equations for equilibrium (6) acquire the type of (9)

$$\left\{ \begin{array}{l} a_{11} \frac{\partial^2 U}{\partial x^2} + a_{11} \frac{\partial^2 U}{\partial x^2} + (a_{12} + a_{33}) \frac{\partial^2 V}{\partial x \partial y} = 0 \\ a_{33} \frac{\partial^2 V}{\partial x^2} + a_{22} \frac{\partial^2 V}{\partial y^2} + (a_{21} + a_{33}) \frac{\partial^2 U}{\partial x \partial y} = 0 \end{array} \right. \quad (9)$$

On the other side the generalized Law of Hook (Kisliakov S., 1980; Федосьев В., 1965 etc.) for the two-dimensional problem acquires the type of (10)

$$\left\{ \begin{array}{l} \varepsilon_{xx} = \frac{\sigma_x}{E_{xx}} - \mu_x \frac{\sigma_y}{E_{xx}} \Rightarrow \varepsilon_{xx} = \frac{1}{E_{xx}} (\sigma_x - \mu_x \cdot \sigma_y) \\ \varepsilon_{yy} = \frac{\sigma_y}{E_{yy}} - \mu_y \frac{\sigma_x}{E_{yy}} \Rightarrow \varepsilon_{yy} = \frac{1}{E_{yy}} (\sigma_y - \mu_y \cdot \sigma_x) \\ \varepsilon_{xy} = \gamma_{xy} = \frac{\tau_{xy}}{G_{xy}} = \frac{\partial U}{\partial y} + \frac{\partial V}{\partial x} \Rightarrow \tau_{xy} = G_{xy} \left( \frac{\partial U}{\partial y} + \frac{\partial V}{\partial x} \right) \end{array} \right. \quad (10)$$

where:  $\mu_x, \mu_y$  – coefficients of Poisson for interrelating transverse and lengthwise deformations;  
 $G_{xy}$  – second modulus (modulus of Young of shearing).

The first equation of (10) is multiplied by  $\mu_y$  and is added to the second, and the second is multiplied by  $\mu_x$  and is added to the first. After certain transformations (6) and (10) acquire the type as shown in (11):

$$\left\{ \begin{array}{l} \frac{E_{xx} \sigma_y}{1 - \mu_x \cdot \mu_y} \cdot \frac{\partial^2 U}{\partial x^2} + G_{xy} \cdot \frac{\partial^2 U}{\partial y} + \left( \frac{E_{xx} \sigma_y}{1 - \mu_x \cdot \mu_y} \mu_x + G_{xy} \right) \cdot \frac{\partial^2 V}{\partial x \partial y} = 0 \\ G_{xy} \cdot \frac{\partial^2 U}{\partial x^2} + \frac{E_{yy} \sigma_x}{1 - \mu_x \cdot \mu_y} \cdot \frac{\partial^2 V}{\partial y^2} + \left( \frac{E_{yy} \sigma_x}{1 - \mu_x \cdot \mu_y} \mu_x + G_{xy} \right) \cdot \frac{\partial^2 U}{\partial x \partial y} = 0 \end{array} \right. \quad (11)$$

The comparison of the system (11) and the system (1) from the basic model of Manevich – Pavlenko (Manevich L. et al., 1982) and the system (9) gives a reason to state, that:

-  $a_{11} = \frac{E_{xx}}{1 - \mu_x \cdot \mu_y}$  in the basic model is indicated by  $B_1$  and

expresses the reduced module of elasticity of the matrix on "x";

-  $a_{22} = \frac{E_{yy}}{1 - \mu_x \cdot \mu_y}$  in the basic model is indicated by  $B_2$  and

expresses the reduced module of elasticity of the matrix on "y";

-  $a_{33} = G_{xy}$  in the basic model is indicated by  $G$  and expresses the reduced second modulus (of shearing) of Young;

$$- a_{12} = a_{21} = \frac{E_{xx}}{1 - \mu_x \cdot \mu_y} \cdot \mu_x = \frac{E_{yy}}{1 - \mu_x \cdot \mu_y} \cdot \mu_y = B_1 \mu_x = B_2 \mu_y$$

Through the accomplished transformations and conclusions it is determined the applicability of the system of equations (1) from the basic model for the task. It remains to reason also the constitution of the third equation – (2) from the basic model. Considerations are as follows:

If accepted that the fiber in the modulus is subordinated to the Law of Hook for uni-dimensional stress state – tensile strength. Then the stress is:

$$\sigma_x = \frac{P}{F} \quad (12)$$

where  $F$  – the surface of the fiber.

The stress according the complete Law of Hook is expressed by (14) and (8)

$$\sigma_x = a_{11} \cdot \varepsilon_{xx} + a_{12} \cdot \varepsilon_{yy} + a_{13} \cdot \varepsilon_{xy} \quad (13)$$

however

$$a_{12} \cdot \varepsilon_{yy} = 0 \quad (14)$$

(15) comes after the uni-dimensional condition of the fiber

Then

$$a_{13} \cdot \varepsilon_{xy} = 0 \quad (15)$$

(16) following of  $a_{13}=a_{31}$  because of the orthotropic type (third basic precondition of VI)

Therefore the tension in the fiber can be expressed yet by:

$$\sigma_x = a_{11} \cdot \varepsilon_{xx} \quad (16)$$

But from the theoretical mechanics and tensile strength (Kisliakov S., 1980; Федосьев B., 1965 etc.) and the already applied equations(7), is known that:

$$\varepsilon_{xx} = \frac{\partial U}{\partial x} \quad (17)$$

Then

$$\frac{\sigma_x}{\partial x} = a_{11} \frac{\partial \varepsilon_{xx}}{\partial x} = a_{11} \frac{\partial^2 U}{\partial x^2} \quad (18)$$

On the other hand, the basic model of Manevich – Pavlenko (Manevich L. et al., 1982) treats a condition in which the extracted fiber is still in balance. In the same time by the conclusion (11)

$$a_{11} = \frac{E_{xx}}{1 - \mu_x \mu_y} \quad (19)$$

In this case by the reason of single-dimensionality of the extracted fiber  $\mu_y = 0$ , i.e.

$$a_{11} = E_{xx} \quad (20)$$

Therefore

$$\frac{\sigma_x}{\partial x} = E_{xx} \frac{\partial^2 U}{\partial x^2} \quad (21)$$

Considering the third equation (2) from the basic model in a different way and treating the second basic precondition for the components of the vector Z for displacement along axes x and y, and substitute W (displacement) with its component and comply from (22), that from (13) the surface F should be added, then finally (2) is represented as:

$$F \cdot E_{xx} \frac{\partial^2 U}{\partial x^2} = F_0 \delta(x) - 2\tau(x) \quad (22)$$

Therefore, it is assumed for a moment, that the left side of (22) is obvious and the right-handed part should be made clear.

There is the product  $F_0 \delta(x)$ , where  $F_0$  is the extracting force, and  $\delta(x)$  is delta function of Diraque. The delta function in this case is initiated in order to indicate the characteristics of the force. It  $[\delta(x)]$  is a generalized function. It does not have any physical meaning. It shows only, that the force is applied in a point (point force) and that it changes from zero to a certain value. Exactly, that final value brings to extraction. Changing from zero to the final value is subordinated to the law

$$\left. \begin{aligned} \delta(x) \Big|_{x=\pm\infty} &= 0 \\ \delta(x) \Big|_{x=0} &= \int_{-\infty}^{+\infty} \delta(x) \partial x = 1 \end{aligned} \right\} \quad (23)$$

The geometrical interpretation is shown in fig. 6.

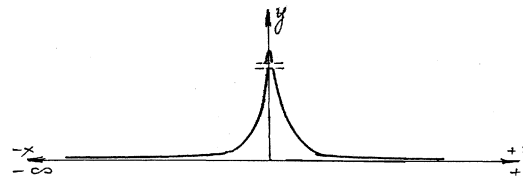


Figure 6. Geometrical interpretation of the integral from delta function of Diraque

One of the properties of  $\delta(x)$  is that its sub-integral surface is always one. This allows the treating of a series of  $\delta(x)$  of constantly narrowing interval to characterize the change of force from zero to a certain value, in which the extraction takes place. Therefore, the presence of  $\delta(x)$  in the right-hand side of the equation (22) does not change the force, it only characterizes it.

The physical sense of the last member of the right-hand of the equation (22) needs to be explained. Considerations are as follows:

The equation

$$F \cdot E_{xx} \frac{\partial^2 U}{\partial x^2} = F_0 \delta(x) \quad (24)$$

is in fact another type of the Newton's law, usually represented in the type (25).

$$\vec{F} = m \cdot \vec{a} \quad (25)$$

However, from the mathematical physics (Armanovich J. et al., 1969; Genchev T., 1976; Mechanical engineering 1982-1994; Academy of Science of the USSR, 1971—1982; Russian Academy of Science, 1985-1999 etc.) is known, that the completeness of this law includes also the strength of medium, where movement takes place (in this case – the extracted fiber) and its inertness.

If W denotes the coordinate and t the trajectory of the points of the fiber with the time and there is no strength, then the Newton's law is as follows (26)

$$m.W'' = F \quad (26)$$

where  $W$  is movement of points from extracted fiber.

Since the fiber is moving only along a straight line, the movement of a point from the fiber is a movement along a straight line, in fig. 7.

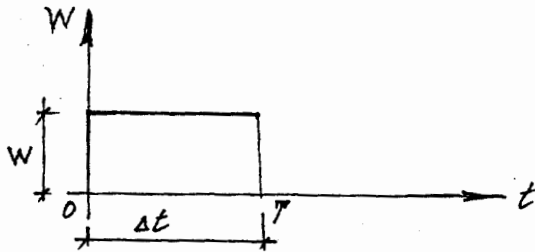


Figure 7. Geometrical representation of a uno-dimensional displacement of points of the fiber for time  $\Delta t$

In the most general case the law is non-linear, because it depends on the time  $t$ , displacement  $W$  and its second derivative. A linear solution is needed, because the mathematical physics suggests typical solutions.

Supposing that  $F$  depends linearly of displacement  $W$  and its first derivative  $W'$ , a formal mathematical record of this dependence is as follows:

$$F(W_1 + W_2, W', t) = F(W_1, W', t) + F(W_2, W', t) \quad (27)$$

That means that

$$W = W_1 + W_2 \quad (28)$$

When a function depends linearly on its first and its second argument, the solution may be presented in the following description:

$$F(W, W', t) = C_1.W + C_2.W' + F(t) \quad (29)$$

Where  $C_1$  and  $C_2$  are known integral constants.

Then the Newton law in the treated case is:

$$C_1.W'' + C_2.W' + C_3.W = F(t). \delta(x) \quad (30)$$

The physical meaning of the constants is as follows:

$C_1$  – characterizes the mass of the fiber;  
 $C_2$  – characterizes the strength (contact strength) of outside medium (matrix), in which fiber moves;  
 $C_3$  – characterizes inertness of moving fiber.

The physical meaning of these constants most clearly is illustrated and explained by one of most simple problems in mechanics – the pendulum (fig. 8).

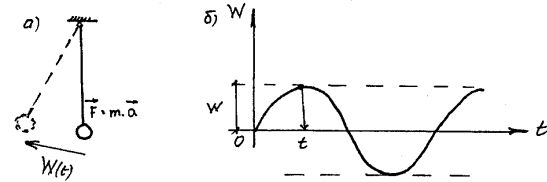


Figure 8. a) Schematic view of a waver, set in motion by a force  $\vec{F}$  and displaced at  $W$  b) Response of pendulum motion with time

Four cases are possible:

**First case:** Medium does not have any strength, force is applied only once.

In this case the equation of the pendulum is:

$$W''(t) + \omega^2.W(t) = 0 \quad (31)$$

Solution of the differential equation (31) is:

$$W(t) = C_1.\cos.\omega t + C_2.\sin.\omega t \quad (32)$$

Here  $C_i$  are constants and depend on  $A$  (the amplitude) and  $\varphi$  (the phase), and  $\omega$  is frequency.

**Second case:** Medium does not have any strength, the force  $F_0$  acts permanently according to a cosine law.

The equation of the pendulum is:

$$W''(t) + \omega^2.W(t) = F_0.\cos \omega_1 t \quad (33)$$

Solution for the differential equation (33) is:

$$W(t) = C_1.\cos.\omega t + C_2.\sin.\omega t + \frac{F_0}{\omega^2 - \omega_1^2}.\cos \omega_1 t \quad (34)$$

In this case when  $\omega_1 = \omega$  there is a resonance.

**Third case:** Medium has a strength, the force is applied only once.

The equation of the pendulum is:

$$W''(t) + a.W'(t) + \omega^2.W(t) = 0 \quad (35)$$

If there is a linear dependence between displacement " $W'$ " and time  $t$ , then solution depends on the characteristic equation (36):

$$\lambda^2 + a\lambda + \omega^2 = 0 \quad (36)$$

The discriminant  $D$  of (36) is:

$$D = a^2 - 4\omega^2 \quad (37)$$

The solution of (35) has a physical sense, when the discriminant D is negative, i.e.  $D < 0$ . Then solutions of the characteristic equation (36) are:

$$\lambda_{1,2} = \frac{-a \pm i \sqrt{a^2 - 4\omega}}{2} \quad (38)$$

and it is presented as (39):

$$\lambda_{1,2} = \alpha \pm i \beta \quad (39)$$

Then solution of the equation of pendulum (35) is:

$$W(t) = C_1 e^{\alpha t} \cdot \cos \beta t + C_2 \cdot e^{\alpha t} \cdot \sin \beta t + \Phi(t) \quad (40)$$

This is the case of gradual attenuation of amplitude and frequency – fig. 9.

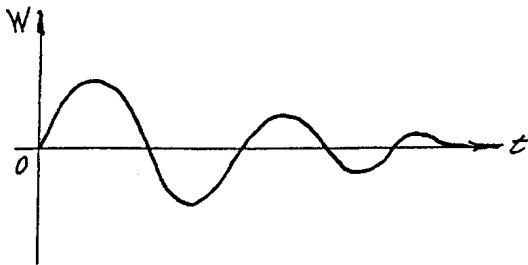


Figure 9. Gradual attenuation of amplitude and frequency of the pendulum

**Fourth case:** Medium has its own strength, the force  $F_0$  acts according to a cosine law.

The equation of pendulum is:

$$W''(t) + aW'(t) + \omega^2 W(t) = F_0 \cdot \cos \omega_1 t \quad (41)$$

Without paying attention of the solution of (41), and if analyzing it and assuming, that the mass of pendulum is normed to one, then there is a full similarity with the law of Newton and the model of Manevich-Pavlenko (Manevich L. et al., 1982) for the extracted fiber. Furthermore,:

- a) the coefficient before the second derivative of displacement  $W''$  is one. In the basic model this coefficient is  $F \cdot E_{xx}$ .
- b) the coefficient in front of the first derivative shows the strength of medium, in which the pendulum moves. In the general case this is a strength of friction.

In the basic model of Manevich-Pavlenko this is a contact strength of medium round the fiber. It is indicated by  $\tau(x)$  and it is transferred to the right-hand side of the equation, because it always counteracts to extracting force. The value of coefficient in front of  $\tau(x)$  is 2, because it is assumed that it acts simultaneously from the both sides of the fiber – fig. 10.

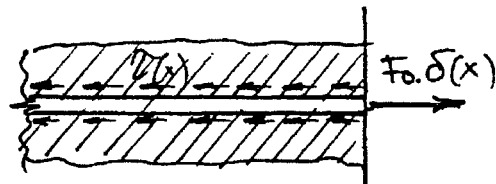


Figure 10. Illustration of contact stress  $\tau(x)$

- c) The coefficient  $\omega$  in front of displacement  $W(t)$  stands for inertia of the process, which on its own depends on weight of the moving mass.

At the basic model the coefficient  $C_3$  is zero, because the authors Manevich and Pavlenko (Manevich L. et al., 1982) presume, that uni-dimensional fiber is weightless. Finally, the equation in the basic model acquires the type (2), and namely:

$$F \cdot E_{xx} \cdot \frac{\partial^2 U}{\partial x^2} = F_0 \cdot \delta(t) - 2\tau(x)$$

This does not comprise all the peculiarities of genesis of the basic model. This is because in order to function, the three equation [system (1) and equation (2)] in one model, it is necessary to associate the system for equilibrium of the matrix (1) and the equation for movement of fiber into a dependence.

This connection of the model (Manevich L. et al., 1982) is formulate by the assigned relation (42).

$$\tau(x) = G \left. \frac{\partial U}{\partial y} \right|_{y=0} \quad (42)$$

It defines, that the contact stress in the direction  $y=0$  is proportional to the reduced second modulus of Young of the matrix. The higher G, the higher  $\tau(x)$ .

The G is just the coefficient  $a_{33}$  of the matrix.

$$G = \frac{G_{xy}}{1 - \mu_x \mu_y} \quad (43)$$

In other words, the contact stress is proportional to the elastic modulus of shearing of the matrix and, the inverse proportional to the difference  $(1 - \mu_x \mu_y)$ , where  $\mu_x$  and  $\mu_y$  are coefficients of Poisson for already compacted gravel bed onto axes x and y.

## RESULTS AND CONCLUSIONS

BASIC CONCLUSION is, that the third equation (2) of the basic model does not concern and does not affect by the type of strength, which medium (matrix) effects to the extracted fiber – friction, shearing, shearing of adhesion, shearing of friction etc. The equation only reports on the quantity of strength of medium (matrix) while extracting of the fiber. Just for that, the authors of the model define it as a “contact” and

have in mind, that it is manifested and effected simultaneously from both sides along the whole length of extracted fiber.

THE BASIC RESULT is in the proof of the correctness of application of the model, developed by Manevich and Pavlenko for determination of strength, which is applied to an extracted traverse (treated as a fiber) from the side of the gravel bed (treated as a matrix) from a movable railroad.

#### REFERENCES

- Manevich L., Pavlenko A., 1982. Applied Mathematics and Theoretical Physics.– Moscow, volume 3 (in Russian)
- Stoyanov D. *et al.*, 1998. Preventive control and repairs-reconstructive works on the movable railroads in the opencast mine “Trayanovo” at “Maritsa Iztok Mines” Co. – Project 1633/1998 at Research & Development Sector of the University of Mining and Geology. Archives of RDS at UMG (in Bulgarian)
- Stoyanov D. *et al.*, 2000. Preventive control and repairs-reconstructive works upon the movable railroads in the opencast mine “Trayanovo-north” at “Maritsa Iztok Mines” Co. – Project 1683/2000 at the Research & Development Sector at University of Mining and Geology. Archives of RDS at UMG (in Bulgarian)
- Ivanov G., *et al.*, 1981. Upper construction and maintenance of the railroad. Sofia, Technics (in Bulgarian)
- Kostov T. *et al.*, 1991. Railroad construction – Sofia, Publishing house of University of Architecture and Civil Engineering (in Bulgarian)
- Shahonyants G., 1982. Railroads. – Moscow, Transport (in Russian)
- Kisliakov S., 1980. Strength of materials. – Sofia, Technika (in Bulgarian)
- Федосъев В., 1965. Strength of materials. – Sofia, Technika (in Bulgarian)
- Armanovich I., *et al.*, 1969. Equations of mathematical physics. – Moscow, Science (in Russian)
- Genchev T., 1976. Partial differential equations. – Sofia, Science and Art (in Bulgarian)
- Mechanical engineering 1982-1994.. – New York
- Academy of Science of the USSR., 1971 – 1982. Applied mathematics and mechanics.– Moscow, Science (in Russian)
- Russian Academy of Science., 1985 – 1999. Physics of solid body– St. Petersburg, Science (in Russian).

Recommended for publication by Department  
, Faculty of Mining Electromechanics

## TECHNICAL CONDITION OF MOVABLE RAILROADS AND EFFECT ON TECHNOLOGICAL PARAMETERS OF COMBINED OPERATION OF RAILROAD HAULAGE AND BUCKET WHEEL EXCAVATORS

**Paulin Zlatanov**

University of Mining and Geology  
"St. Ivan Rilski"  
Sofia 1700, Bulgaria

**Atanas Smilianov**

University of Mining and Geology  
"St. Ivan Rilski"  
Sofia 1700, Bulgaria

**Philip Kuzmanov**

### ABSTRACT

Disadvantages of recently applied dependencies for assessment of the effect of movable railroads on the main technological parameters are analyzed. A probabilistic approach for that study is suggested and the bases of formulas, allowing the quantitative assessment are developed.

### INTRODUCTION

The following disadvantages may not be disregarded when the formulas, known from technology, are applied to a study of the effect of movable railroads on the main parameters of haulage transport and opencast mines in the combined work of railroad transport and bucket wheel excavators:

- Impossibility to read the indetermined character of processes described by those formulas;
- Not considering the probabilistic character of speed of movement of trains and movable railroads, in particular;
- Impossibility for connecting the system excavator – train + railroad in a single technological structure etc.

On the other hand, the technological condition of movable railroads depends on the actual deviation of railroads from the position, determined by the project. Factors, which effect on the value of that deviation, are many. The most important factors may be grouped as follows:

-

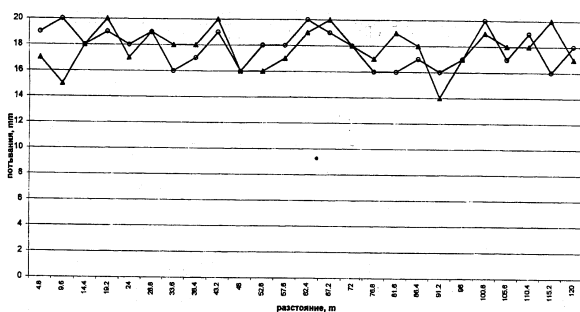


Figure 1. Response of hidden settlements of railroads in the area of bucket wheel excavator RS-2

- Visible and open settlements in the vertical plane. That brings to mudding of the ballast gravel bed immediately in or near the zone of hidden settlements, breaking of road in the zones of joint connections, loosening and breaking of joining

connections between rails and sleeves etc. Figure 1 shows the results of measured hidden settlements in a vertical plane for an excavator RS-200 at the "Trojanovo" mine and shows the results from an investigation managed by Prof. D. Stoyanov at the same mine in October 1997.

- Visible and hidden deformations in a horizontal plane. That brings to disturbing of distance between rails. (more than 1435 mm), loosening and breaking of connecting joints between rails and sleeves, intensification of lateral wearing out of rails, deviation from the axis of road (destruction) etc. Those deviations from the designed position reduce the reliability of road and require reduction of speeds of trains;

Fig. 2 illustrates the visible deformations in a horizontal plane. They were measured in October 1997 by a team managed by Prof. Stoyanov in the area of spreader AS 1600 (inventory No 3) in a curved section of the out dumping site at the "Trojanovo-sever" [2].

- Torsion of road round its axis. This is achieved due to irregular settlement (visible and hidden) in both rails simultaneously in one and the same cross-section of road, i.e. one and the same sleeve or one and the same area between sleeves.

Figure 3 shows hidden settlements in the area of the same spreader AS-1600, measured and described in the project of D. Stoyanov [2]. Hidden settlements are measured within distances, corresponding to distances between wheel axis of dump-cars. Torsion of road in the middle of the response is evident. It comprises four intervals (five measurements)

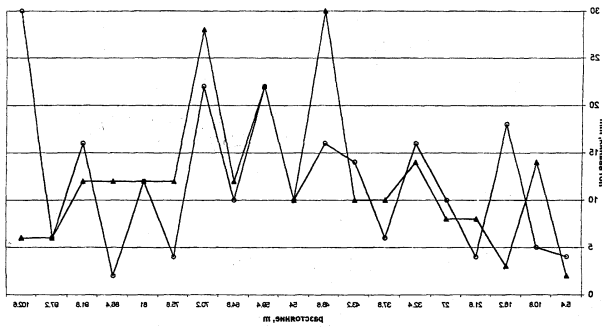


Figure 2. Response of visible settlements of rails in the area of spreader AS-1600, No 3

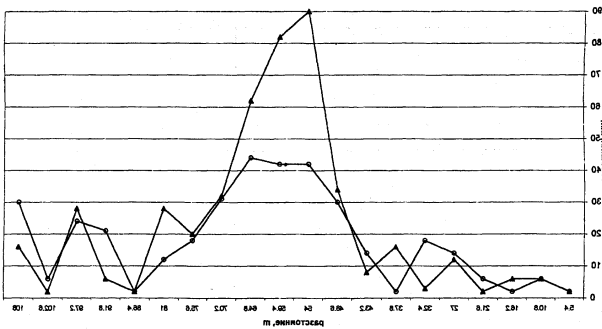


Figure 3. Response of hidden settlements of rails in the area of spreader AS-1600, No 3

Joining of first two to torsion is most often in the basis of derauling of railroad vehicles, i.e. failures of movable railroads.

On the third hand, the real technical condition of movable railroads limits the speed of movement of trains along them. In other words, speed is a synthetic factor, which is a result of all deviations (faults) of the design position of the road. Characteristics of those lines in the layout and profile allow speed up to 45 km/h (according to project of Atanas Smilianov "In-company regulations for moving, maintenance and repair of movable railroads" [3]), but in practice they are limited as follows:

- at the "Maritsa-East Mines" EAD – not more than 25 km/h;
- in the other three mines – not more than 8 km/h in the direction "full" and not more than 12 km/h in the direction "empty".

Considerations are developed below, which establish the functional connection of technical condition of movable railroads (shown by speed of movement) to the main technological parameters in case of joint work of railroad haulage with bucket wheel excavators on the basis of probabilistic approach, aiming to overcome the disadvantages, discussed in the beginning of the introduction.

### MAIN PRECONDITIONS

The discussion below presented refers to the common work of a bucket wheel excavator and railway haulage with spreader. The following preconditions are supposed to act:

#### First:

The performance of production assignment is a priority for the shift, month, year etc. for the system excavator – train – railroad, because it brings to the realization of production assignment.

#### Second:

Both the system excavator and the system train – railroad refer to the man-machine class of systems, characterized with a high rate of indetermination.

For the system excavator – the productivity is limited by a multitude of factors (constructive, mining, climatic, organization etc.), and the connection between them is different. For example, connection between productivity and constructive factors is functional and connection to other factors is stochastic.

The operator of excavator as a unit of the man-machine system works according to a fuzzy algorithm. The sense of fuzziness consists in the fact that he selects the strategy of his actions alone, which usually does not coincide with preliminary instructions.

Productivity of the system train + railroad is limited by many factors – constructive, mining, organizational etc. and connection is also different. Functional is connection only between volume of bucket of cars and their number in the train. Connection of other factors is also stochastic.

Operator of the excavator as a unit of the man-machine system also works according to a fuzzy algorithm. For example, led by feeling of technical condition of road, cars and locomotives, he changes he speed within wide ranges.

#### Third:

Treating of the technological structure excavator – train + railroad as a system of continuous transporting line is advisable for assessing its functioning. That is admissible, if the time for realization of train route, calculated in technological accounts as (1)

$$t_{\kappa} = t_m + t_{mn} + t_{nn} + t_p + t_{mexh.n} + t_{op.3} \quad (1)$$

and it is treated as a failure of the system. From a formal point of view, the above outlet is admissible, because if the excavator is served by only one train composition, then the excavator does not work during the complete route of train, i.e. the subsystem excavator does not work, it is failed.

$t_{\tau}$  – time for loading of train, h;

$t_{mn}$  – time for train movement (full and empty) along movable railroads in the mine and the dumping are for each specific route is

$$t_{mn} = l_{mn}^3 \left( \frac{1}{V_{mn.n}^3} + \frac{1}{V_{mn.np}^3} \right) + l_{mn}^H \left( \frac{1}{V_{mn.n}^H} + \frac{1}{V_{mn.np}^H} \right) \quad (2)$$

where:  $l_{mn}^3$  и  $l_{mn}^H$  are the lengths of movable railroads in the faces of the dumping area;

$V_{mn.n}^3, V_{mn.np}^3, V_{mn.n}^H$  и  $V_{mn.np}^H$  are speeds for moving of train along those sections for the full and the empty train and the are coordinated with [3];

$t_{nn}$  is time for moving of train on constant railroads on the same route from the face to the dumping site. It is shown by the expression (3),

$$t_{nn} = \sum_{j=1}^m \left( \frac{l_j}{V_n} + \frac{l_j}{V_{np}} + 0,025 \right) \quad (3)$$

where  $\sum l_j$  is the total length of constant railroads along the route;

$V_n$  and  $V_{np}$  are speeds of movement in direction "full" and direction "empty",

0,025 – factor, reading the time needed for connection to the Central Base;

$t_p$  is the time for unloading at the receiving point at hopper (power plant, dressing factory, briquetting factory) or receiving pit. It depends on the faultless work of compressors, air-conductive systems and pneumatic unloading systems. It is relatively constant for a train with constant number of cars and locomotives and follows the expression:

$$t_p = n_e \cdot t_p, h \quad (4)$$

where  $t_p$  is the time for unloading of one car,  $h$  (for the summer this is 1,5-2 min, for winter - 3 min).

$t_{тех.н}$  is the time for inevitable technological idle time and depends on the route, rail interdistance, installations and fault-free operation of the opening/closing of arrows, type of railroad transportation schemes,  $t_{np.3}$  comprises the time for other idle time of any kind. The highest is the share of idle time for removing of faults on the road, cars etc.

#### PROJECT FOR CONSTRUCTION OF PROBABILISTIC APPROACH FOR ESTIMATION

Those precondition allow the use of a set of formulas, developed in the theory of reliability and adapted to large engineering systems, like those in opencast mines ([4], [5], [6], [7] etc.), consisting of mutually interrelated individual engineering subsystems. The system of excavator – train – railroad may be treated like one of those.

The below formulas are referred to a long period of time, for example an year. Having in mind that the technical productivity of the excavator is a variable value (see part II) than the annual productivity may be expressed by (5).

$$Q_{zoo} = \sum_{i=1}^n Q_{mexh.(i)} \cdot t_{p(i)}, m^3 / a \quad (5)$$

where:

$Q_{zoo}$  - annual productivity of the excavator, given by the planned schedule ;

$Q_{mexh.(i)}$  - technical productivity of the excavator, corresponding to its  $i^{mo}$  working condition. It is a function of many factors, described in part II.

$n$  – number of possible conditions, where the excavator is during the year, characterized with the relevant productivity;

$t_p(i)$  – total duration of working time for the  $i^{mo}$  condition of the object during the calendar year.  
In fact, the times  $t_p(i)$  represent a portion or a percentage of the total annual fund of working time of the excavator, i.e..  $t_p(i) = t_p.n\%$  or

$$t_{p(i)} = t_p \cdot P[t_{p(i)}] \quad (6)$$

In (6)  $P[t_{p(i)}]$  is the probability that the excavator is in the  $i^{mo}$  condition of probability.

Then the equation (5) may be represented as follows:

$$Q_{zoo} = t_p \cdot \sum_{i=1}^n Q_{mexh.(i)} \cdot P[t_{p(i)}], m^3 / a \quad (7)$$

According to [4], [5], [6], [7] etc. the distribution of the calendar time during the year, when the bucket wheel excavator works as a technologically combined subsystem excavator – train – railroad is structured into three parts::

$t_p, h$  – total time for continuous work of the system during the calendar year (pure working time);

$t_{o6}, h$  – time for technological servicing of the system.

$$t_{o6} = t_{nnp} + t_{np.np.cm.} + t_{np}, h \quad (8)$$

Those times respectively are:

$t_{nnp.cm.}, h$  – time for planned preventive repairs;

$t_{np.np.cm.}, h$  – time for changing the shifts. Within one day this time is regulated to be 1h.;

$t_{np}, h$  – time for compulsory reviews of specific units and aggregates;

$t_e, h$  – time for recreation of the system from non-working into working condition. It consist of:

$$t_e = t_{mexh.np.} + t_{opz.np.} + t_{ae.np.} + t_{op.3} \quad (9)$$

Those time respectively are:

$t_{mexh.np.}, h$  – the excavator works but does not realize volumes, change of new positions, waiting of trains, auxiliary operations etc.

$t_{opz.np.}, h$  – idle time for various organizational reasons;

$t_{ae.np.}, h$  – idle time for removing the accidents in the subsystem excavator – train – railroad;

$t_{0.2.3}, h$  – time, for which the excavator does not produce for various reasons different from the above: strikes, misfortune etc.

In the case the following expression is valid for the following annual calendar period of time.

$$t_{\kappa} = t_p + t_{o\delta} + t_{\epsilon}, h \quad (10)$$

where:  $t_{\kappa}, t_p, t_{o\delta}, t_{\epsilon}$  are respectively the annual calendar period of time, pure working time of the sub-system, time for technological service and time for recreation.

According to the above quoted sources each large system for continuous period of time characterizes with the coefficient of readiness  $K_r$ .

$$K_r = \frac{t}{t_{\kappa} - t_{o\delta}} \quad (11)$$

where:

$t_p$  – pure working time of the subsystem excavator – train – railroad;;  
 $t_{o\delta}$  – time for servicing of the subsystem.

Time for servicing of the subsystem ( $t_{o\delta}$ ) may be represented through the coefficient of servicing:

$$K_{o\delta} = \frac{t_{\kappa} - t_{o\delta}}{t_{\kappa}} \quad (12)$$

the meaning of this is the time, for which the system is not served.

The coefficients  $K_r$  and  $K_{o\delta}$  allow the annual calendar fund of time to be expressed as:

$$\frac{t_p}{K_r} = t_p + t_{\epsilon} \quad (13)$$

When reading that from (12),  $t_{o\delta}$  may be expressed as :

$$t_{o\delta} = t_{\kappa}(1 - K_{o\delta}) \quad (14)$$

It may be easily proved that between the times for (10) and coefficients  $K_r$  and  $K_{o\delta}$  there is a connection:

$$t_p = t_{\kappa} \cdot K_r \cdot K_{o\delta} \quad (15)$$

In that case, for the annual productivity the following is valid:

$$Q_{zod} = \sum_{i=1}^n Q_{mexh(i)} \cdot t_{p(i)} \cdot t_{\kappa} \cdot K_r \cdot K_{o\delta}, m^3 / a \quad (16)$$

Expressions from (5) to (16) are in the basis of mathematical methods, studying the technological peculiarities of line systems.

In the case above described, when movement of train along the route is considered as a specific failure of the system, it is in fact transferred from cyclic into continuous. Considering the opportunities for the excavator to work in “n” massifs with “m” different characteristics (hardness, bulk weight, humidity, cohesion, angle of inner friction etc.), the equation (16) may be written as follows::

$$Q_{zod} = t_{\kappa} \cdot K_r \cdot K_{o\delta} \left( Q_{mexh(1)} \cdot m_1\% + Q_{mexh(2)} \cdot m_2\% + \dots + Q_{mexh(n)} \cdot m_n\% \right), m^3 / a \quad (17)$$

On the other hand, the readiness for work of the technological structure, consisting of consecutively related systems (like the discussed sub-system excavator – train – railroad) for significantly continuous period of time (year, for example) is expressed by the coefficient of readiness of the whole system. Its structure according to [4], [5] etc. is represented by (18).

$$K_z = \left[ \sum_{i=1}^n \frac{1}{K_{z(i)}} - (n-1) \right]^{-1} \quad (18)$$

The type of formula (18) is easily transformed into (19)

$$K_z = \frac{1}{1 + \sum_{i=1}^n \frac{1 - K_{z(i)}}{K_{z(i)}}} \quad (19)$$

which is much more convenient to work with. That is because in (19) each of the consecutively related elements in one technological structure like the structure of excavator – train – railroad acquires an individual presence by its individual coefficients of readiness. The prove is in the development of the nominator in the expressions (20):

$$1 + \sum_{i=1}^n \frac{1 - K_{z(i)}}{K_{z(i)}} = 1 + \sum_{i=1}^n \left[ \frac{1}{K_{z(i)}} - 1 \right] = 1 + \sum_{i=1}^n \frac{1}{K_{z(i)}} - \sum_{i=1}^n 1 = 1 + \sum_{i=1}^n \frac{1}{K_{z(i)}} - n = \sum_{i=1}^n \frac{1}{K_{z(i)}} + 1 - n = \sum_{i=1}^n \frac{1}{K_{z(i)}} - (n-1) \quad (20)$$

The last expression in (20) is completely adequate to the denominator in (18).

In that case the pure working time for the years of the technological structure excavator – train – railroad is:

$$t_p = t_{\kappa} \cdot \frac{t_{\kappa} \cdot K_{o\delta} \cdot 1}{1 + \left( \frac{1 - K_z^{\delta}}{K_z^{\delta}} + \frac{1 - K_z^{61}}{K_z^{61}} + \frac{1 - K_z^{mn}}{K_z^{mn}} + \frac{1 - K_z^{mn}}{K_z^{mn}} \right)} \quad (21)$$

Therefore, the main task of that paper – to reason the opportunity through the apparatus of probabilistic approach to show the effect of movable railroads on technological parameters (the example shows the annual productivity) has been fulfilled.

## ASPECTS OF THE ASSESSMENT OF EFFECT OF TECHNICAL CONDITION OF MOVABLE RAILROADS

The authors have been working on that idea for long. In spite of that there are not enough data to prove the unmeaning decisions. For that reason, below is presented the essence of the idea for assessment of technological condition and coefficient of readiness of railroads in the conventional railroads of Russia. The reason is in the high values of loading of railroads in Russia in comparison to high values of loading at the "Maritsa-East" mines Co for the movable railroads. The treated Russian approaches are adopted in Poland, the Czech Republic, Hungary, Romania and recent members of CIS.

The idea consists in the fact that technical condition of railroads is controlled and predicted through the norms of consumption of materials (rails, sleeves, joints etc.) The presumption is that expenses for those resources for current maintenance increases with the aging of the road after its previous innovation (capital repair). The approach is based on the theory of reliability and binds the number of failures of all the elements of the upper structure and general technical condition of road. The idea is laid down in [8], developed in [9], [10], [11], [12] etc. Its meaning is illustrated in fig. 4 and is used as a basis for different principles of accumulation of deformations in both media – upper and lower structure, and therefore, different intensity and different intensity of their norms of failure.

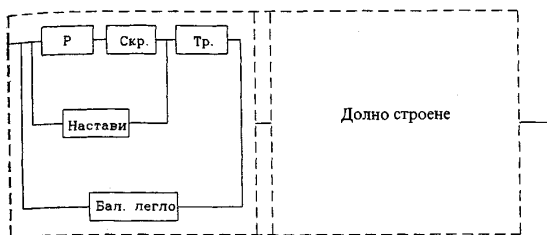


Figure 4. Illustration of binding of failures of elements of the upper structure of the railroad

It is proved in ([10], [11] etc.), precisely enough for the practice, that failures in all the structural elements of the upper structure may be described by functions of the type

$$A = B + C.T^t \quad (22)$$

where:

T – loading;

t – exponent, showing the norms of amortization for term of service of specific elements;

B, C – empirical coefficients, obtained by the root-mean-square methods after processing the statistical data for failures.

An exception is the ballast gravel bed, where A of (22) characterizes the norm of contamination for bulk weight.

It should be mentioned that (22), referred to rails and joints has a coefficient B = 0, which means that the function starts from the beginning of the coordinate system. This is related to the highest requirements for them in comparison to the other elements.

In [9], [10] and [11] the norm of failure is referred to the real one and the coefficient of reliability of elements of the upper structure is obtained. In fact this represents the probability for the system not to give a failure because of the failures of its specific elements:

$$P_{\text{жн}}(t) = P_p(t) \cdot P_{\text{скр}}(t) \cdot P_{\text{тр}}(t) \cdot P_{\text{мп}}(t) \cdot P_{\text{б}}(t) \quad (23)$$

where:  $P_{\text{жн}}(t)$  – probability for failure of construction of upper structure and the railroad;

$P_p(t)$ ,  $P_{\text{скр}}(t)$ ,  $P_{\text{тр}}(t)$ ,  $P_{\text{мп}}(t)$ ,  $P_{\text{б}}(t)$  – probabilities for failures of rails, joints, sleeves and ballast gravel, respectively.

It is worth mentioning that this part of the issue has not been developed. The reason consists in the extremely high responsibility, related to mathematical formalization of the probabilistic failure in the railroad. However, all the authors support the opinion that recent construction of upper structure has a high rate of reliability and each subsequent change has to increase the reliability without making the structure more expensive – [10], [11] etc., approximating to the reliability to one, and the risk of failure – to zero.

Furthermore, up to now there are no decisions, bringing to quantitative characteristics for determining the reliability of lower structure of railroad.

In the sense of the above mentioned, and the developed opportunity for assessment of technical condition of the system – excavator – train – railroad of (19) and in particular movable railroads in their common work with railroad haulage with bucket wheel excavators – following (21) the authors using formulas (11) and (12) derived a representative number of data from the dispatching inventory lists of mines "Trojanovo" and "Trojanovo – sever".

Data are processed according to methods of statistical modeling and the idea is to acquire preliminary information for parameters of both coefficients for each element of the subsystem excavator – train – railroad and to acquire the real value for the pure working time, according to (21).

Results will show the importance of the idea.

## CONCLUSIONS

1. Representing the effect of technical condition of movable railroads on main technological parameters of opencast mines is shown by an approach based on probabilistic methods. That will give an opportunity for more realistic planning of a technically achievable calendar fund of working time for the mining equipment – bucket wheel excavators and enhance the rate of complete utilization.
2. The ideas will be easily adopted into technological practice, if the authors make the ideas closer to classical differentiation of working time of mine equipment. That means "specifying" from a point of view of technology the expressions (8) and (9) and appearance of another member in (10), and therefore – a coefficient of the structure like (11) and (12).

REFERENCES

- Stoyanov D. et al., 1998. Preventive control and repair and maintenance of movable railroads at the "Trojanovo" opencast mine of "Maritsa-East Mines" EAD – Project 1633/1998 of the R&D S of the University of Mining and Geology. Archive of the R&D S of the University of Mining and Geology. (in Bulgarian)
- Stoyanov D. et al, 2000. Preventive control and repair and maintenance of movable railroads at the "Trojanovo" opencast mine of "Maritsa-East Mines" EAD – Project 1683/1998 of the R&D S of the University of Mining and Geology. Archive of the R&D S of the University of Mining and Geology. (in Bulgarian)
- Smilianov A. et al., 1998. In-company regulations for moving, maintenance and repair of movable railroads at the "Kremikovtsi" mine. Project 1201/1998 of the R&D S of the University of Mining and Geology. Archive of the R&D S of the University of Mining and Geology. (in Bulgarian)
- Garuzish V. et al. 1981 Automation of upper structure of opencast and underground mine openings.- Leningrad, Nedra. (in Russian)
- Irinkov S., 1986. Automation of technological process in opencast mines. – Sofia, Technika. (in Bulgarian)
- Vuchkov I,m et al. 1986. Mathematical modelling and optimization of technological objects. – Sofia, Technika. (in Bulgarian).
- Lalov I., 1996. Study of the technological bases for control and improvement of systems for control of processes of mining and transportation of mining mass by bucket wheel excavators and belt conveyance.- Sofia, Library of the University of Mining and Geology, Dissertation for acquiring a DSC degree and a summary for it. (in Bulgarian).
- Tsukalov P., 1967. Suggestions for improving the planning and use of railroad resource of the country. Moscow, Works of CSII, vol. 334, Transport. (in Russian)
- Shendrev etc al., 1976 Reliability and productivity of integrated lines for mining and transportation, Moscow, Nedra. (in Russian)
- Shulga V. et al. 1976. Roads and safety of moving along them. Moscow, Transport. (in Russian)
- Shulga et al. 1975. Exploitation approach to the railroads and joints of КБ type and sleeves of type C-56-2. Moscow, Works of MIIT, vol. 505. (in Russian)
- Shulga et al., 1975. Exploitation approach to the railroads and joints of КБ type and reinforced concrete sleeves. Moscow, Works of MIIT, vol. 505. (in Russian)
- Shulga, V 1977. Failures in the rails and sleeves in the curved portions of railroads and measures for their reduction, Moscow, Works of MIIT, vol. 556. (in Russian)
- Shulga, V 1975. Exploitation approach to the railroads and joints of КБ type and reinforced concrete sleeves. Moscow, Works of MIIT, vol. 505 (in Russian)
- Shulga et al., 1975. Effect of the application of increased strength to the failures of joint-free roads of reinforced concrete sleeves. Moscow, Works of MIIT, vol. 505 (in Russian)

*Recommended for publication by Department of  
Mine Mechanization, Faculty of Mining Electromechanics*

## SAMPLING DEVICE ADAPTABLE TO THE HIGH CAPACITY CONVEYER - BELTS

Nicolae Cristea

University of Petrosani  
Petrosani 2675  
Romania

Gheorghe Gherman

University Aurel Vlaicu  
Arad, 2900  
Romania

Georgeta Cristea

University of Petrosani  
Petrosani 2675  
Romania

### ABSTRACT

In our country, the manual sampling is the usual manner at the sub-bituminous coal furnishing to beneficiaries although this one is affected by human errors, is expensive and is not recommended by International Standards. Because the mechanical sampling endeavors failed in the conditions of big discharges of the belt conveyers in the loading points, the manual sampling is still applied. The paper analyses the various feasible procedures for sampling, with their benefits and also drawbacks. The most difficult problems are those in connection with: the device utilization in the available space in the loading points, the high material flows, the upper size of the material. The proposed solution respects the specific requirements of International Standards about mechanical sampling. The device fastening will be realized on the belt frame, thus ensuring its placement in existing space. The constitutive elements of this ensemble are: the deflector shield, the sampling device and the taking over device. Each of these elements has a fixed role for safe working conditions of the device.

### INTRODUCTION

In the current tendency of all activities harmonization with the communitarian AQ, the sub-bituminous coal furnishing from quarries to customers required a close examination concerning the safeguard of a suitable accuracy in coal sampling. The present coal loading point structure does not refer of mechanical sampling and its equipping with mechanical sampling device is impossible, for that time the manual methods of coal sampling were thought to be corresponding.

Frequently, in the long run, the manual methods of coal sampling were a disputed subject between producer and customers and a narrow place with drawbacks like:

- the manual method of coal sampling from train loads requires a lot of labour;
- the staff subjectivity determines a lot of controversies;
- the necessary time for manual sampling can determine punishment for the vehicle stopping from the transport company;
- there is outsized staffs in this activity.

All this outstanding issues in the circumstance of big moving steams and of the material granulometry don't recommend the manual methods of coal sampling.

### CASE ANALYSIS

The sub-bituminous coal analysis had in view to establish the granulometric composition, the moisture content and the minimum flowing angle for extreme conditions. Although the granulometric analysis indicated lump size higher 150mm value, we considered that this situation rose because of the shortcomings in coal preparation for delivery and the situation must be remedied.

Usually, the sub-bituminous coal granulometry is like that witch is presented in figure 1.

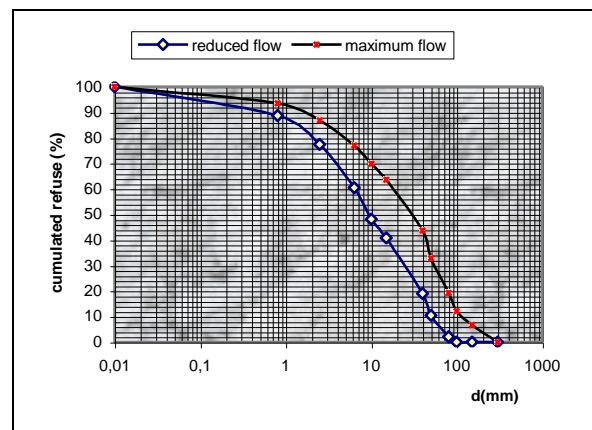


Figure 1. Granulometric limits of the delivered sub-bituminous coal

The flowing angle for coal, in extreme condition, on metallic surface, using special sample from different sectors and of different moisture contents was established at a value of 25°. The material speed in discharge point from the belt, in the impact point with deflector shield is of 6 – 7m/s. The maximum flow value on belt conveyer that feeds the loading point is 500kg/s.

The replace of manual methods of coal sampling from road or rail vehicle charges with mechanical sampling from steams moving on the high speed belt conveyers determined the subsequent problems:

- in the case of using a scrapping device for coal sampling:
  - o the repeatable stopping of the loading belt generates higher power requirement and premature wear of the belt driving system;

- the belt stops can generate shutting off in previous loading flux;
- there is a dangerous operation for belt safety to use a device that can totally take over the material from the belt; any lump that interposes between the device wall and the belt of high speed can produce the belt deterioration.
- in the case of using a sampling device with bucket that traverses the downward coal stream:
  - the bucket size has to be large because of coal granulometry and its high downward flow and also, the standard recommends that the maximum bucket load at a single passing through the coal flow has to be no more  $\frac{3}{4}$  from its volume;
  - this large buckets are inadequate in the actual sampling point;
  - in the dynamic regime, the bucket and its driving device must be mechanical oversized, thus being able to assume the whole dynamic charge of material flow of 6 – 7m/s speed value.

The mechanical sampling of the incremental sample has to be able to produce representative samples. In this sampling method, the representative coal samples are in higher quantities and therefore had to follow a mechanical preparation in order to obtain the laboratory sample. The mechanical preparation device must include a mass division stage and also a stage for the decreasing in maximum lump size. The mechanical preparation device must assure a continuously and proportionally of the reduced sample taking over and also a continuously preparation in order to avoid the introduction of a homogenisation operation.

#### SOLUTION IDENTIFICATION

In order to establish the alternative that will be applied in the concrete conditions, six basic alternatives with their advantages and disadvantages were analysed. The selected alternative has to bring together a general feasible solution and a maximum accuracy in the representative sample constitution. The sampling device can be assembled on the belt frame in the material discharge moment at the loading point and has to comply with all standard requirements concerning the representative sample constitution.

From the point of view of the constructive nature, the installation has to have:

- a device capable to assume the dynamic energy of the material that is projected from the belt and to conduct it towards the sampling device
- a device for the increment sampling capable to traverse the entire falling flow and to conduct this material to the preparation device
- a suitable tightness able to eliminate the deliberate or casual contamination of the representative sample.

#### INSTALLATION DESCRIPTION

In order to ensure all these requirements, the mechanical sampling installation was conceived of three solid connected sub-assemblies, presented in figure 2:

- the deflector shield, A
- the proper device for sampling, a chute, with its driving system, B
- the taking over device for increments, C

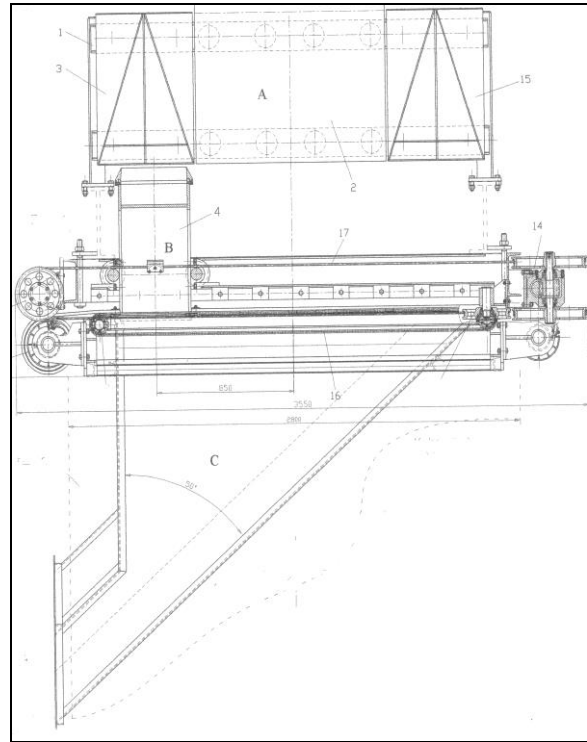


Figure 2. Sampling installation (side view)

The installation will be placed where the actual belt deflector screen is.

The deflector shield, A, is thus conceived that to be stiffened on the belt conveyer frame through the stiffening frame (1). The screen (2) of the deflector shield is attached of the stiffening frame through elastic systems. The screen is made out of rubberised metallic material, which will assure the minimizing of the impact between the material and the shield and will deflect it towards the sampling device, B, through the smallest possible area.

The proper device for sampling is in such way built that the sampling will be achieved through the material deviation from the influence zone of the drawing bucket.

The chute (4) that realizes the increment sampling traversing the entire falling flow has the following constructive specific features:

- chute width: 400mm;
- the collected and loading flow ratio, during the active runs is 1:3;
- the chute length is dictated by the material scattering zone after the impact with the deflector shield;
- the chute's side walls are equipped on the top side with cutters which protect against wear;
- the inclination angle of the device's base: 30°;

- the cutting speed of the material flow is about 12m/s and can be regulated through the driving device;
- during the crossing through material flow, the chute speed must be invariable. In this way, the proportionality principle between the quantities of charged material in chute and the transported material flow in that section is respected;
- in the representative sample constitution, the incremental mass is proportional with the material flow in the sampling moment.

In the conditions of maximum flow value, the loading time of a lot corresponding to 2400t is of 80 minutes.

If the valid standards are respected, the representative sample has to include 32 incremental sample, namely at each 150 seconds, an incremental sample must be gathered and the representative sample weight will be of 5 tonnes.

From the constructive point of view, the chute is supported through four elastic couplings from two roll axes, which slides on the supporting frame. Through the driving group, the device performs a translation movement that allows the increment sampling. The system is a carcasses building and is endowed with an auto-cleaning device for rolling way. Towards the discharge zone, the chute is tight fixed through some straps with the rubberier carpet. Thus, the collecting chute moves concomitantly with the carpet wind and rewind. At each end, the collecting chute retires under two directional screens (15), where remains during the stationed period and thus the avoidance of the particle penetration are ensured. The selected solution requires the chute sizing only like a passing device and not like an accumulating one and the taking over angle reduces the impact charge.

The incremental sample taking over device, C, consists of tight carpet and the sample taking over chute. The tight carpet moves concomitantly with the collecting chute because the same device drives them. It is maintained stretched through the two rolling cylinders (11) that are endowed with pretension spiral springs.

The belt is crosswise stiffened with metallic bands against the chain with rolls (16) and thus ensures the perfect tightness of the upper part of the taking over chute.

The taking over chute connects the chute with a sample bin or with a conveyor device that feeds the bin. There is a drive cable (17) that transmits the motion from the driving to the hydraulic (14) devices, to the collecting chute, to the tight belt and to the chain with rolls.

In order to remove the shocks that appear when the chute is starting or stopping, it is equipped with damping springs. The dynamics scheme of the installation is presented in figure 3.

Sampling interval, the interval between taking increments shall be regulated by needs, using a time relay, which acts when equal loads are achieved.

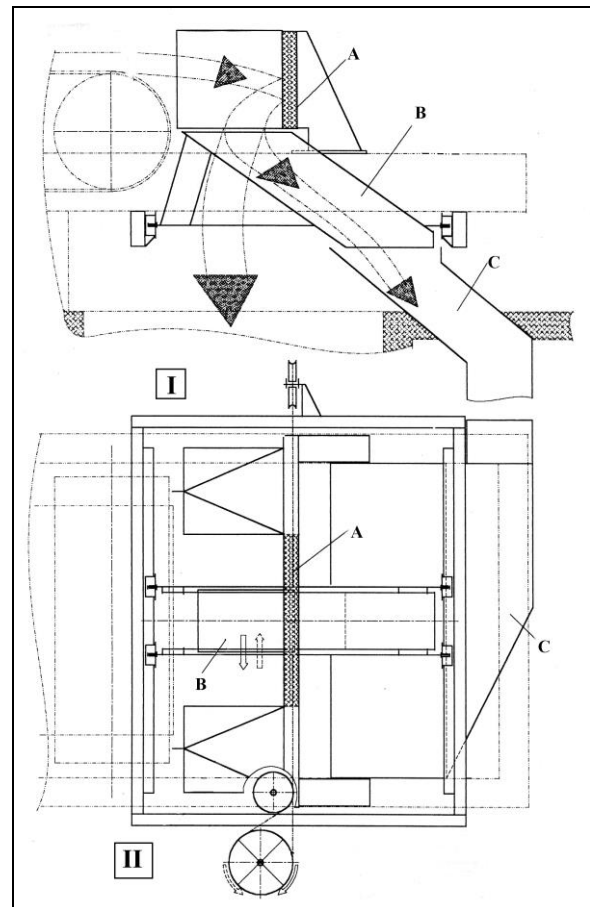


Figure 3. (I) The material and sampling trajectory. (II) Diagram and the sampling chute movement.

The representative sample will be prepared using an automatic system and thus will result the analysis sample.

## CONCLUSIONS

It is thought that the sampling installation replies to the needs for which it was realised.

This device can be applied in all loading points where the material is supplied by means of high capacity belts.

The device fulfils the standardized requirements for the representative sample accomplishment.

The requisite number of the primary increments for the representative sample accomplishment can be determined for each case depending on the coal's specific feature in order to obtain the pursued accuracy.

REFERENCES

- N. Cristea et al.. – Mechanical sampling possibilities for the sub-bituminous coal in the loading points from Jilț Sud Quarry, Contract de cercetare C8/2001 Universitatea din Petroșani;
- N. Cristea G. Cristea. - Aspecte ale prelevării și prelucrării probelor în punctele de încărcare și livrare a lignitului către beneficiari, International Symposium Universitaria ROPET 2002 Petroșani
- \*\*\* STAS SR ISO 1988/1996

*Recommended for publication by Department of  
Mine Mechanization, Faculty of Mining Electromechanics*

## VENTILATION OF ZONES OF POTENTIALLY EXPLOSIVE GAS ATMOSPHERE ВЕНТИЛАЦИЯ НА ЗОНИ С ПОТЕНЦИАЛНО ОПАСНА АТМОСФЕРА

Julian Zaimov

University of Mining and Geology "St. Ivan Rilski"  
Sofia 1700, Bulgaria

### ABSTRACT

The need for guaranteeing the low concentrations of flammable substances in manufacture, where the formation of potentially explosive gas atmosphere is possible, requires development and use of special fans. Fans should be constructed with technical and maintenance characteristics, which do not allow ignition of the explosive gas atmosphere within the fan in both regular and accidental mode of operation.

The present article reports the construction of a fan with a system for stroke protection and bearing temperature control allowing the theoretical and experimental determination of the probability for ignition of explosive gas atmosphere within its casing. A fan performed in that construction is considered as a spark-free fan.

### INTRODUCTION

In recent technologies of production, storage and use of flammable liquids, gases and powders, more and more efforts are devoted to involving approaches and methods, in which the release of flammable substances in the air will be reduced to the minimum.

Nevertheless, technological processes related to underground coal mining, production and chemical petroleum processing, painting and lacquering in both regular and accidental mode of operation are characterized with release of flammable gases, vapors or dusts.

Similar are the cases, when raw materials or products are flammable substances, which need to be transported, poured out, weighted or stored in warehouses.

Those technological processes require ventilation of premises with the aim of maintaining low concentrations of the flammable substance in the potentially explosive gas atmosphere. Fans, the technical and constructive characteristics of which do not allow them to cause fires and explosions, achieve the above objective.

There are requirements, within the regulations acting in Bulgaria and some other countries that those fans should be in a spark-free performance. However, there are no clearly defined criteria.

### REASONS FOR THE ORIGINATION OF FRICTIONAL SPARKS AND LOCAL HEATING IN THE FANS

Except for the electric motor, the explosion-proof performance of which is complied to the location of operation, sources of ignition of the explosive gas atmosphere might be frictional sparks or local heating, caused by strike or friction

between movable or immovable parts of the fan. Reasons for the appearance might be as follows:

- falling of solid particles, carried by the air flow in the body of the fan;
- axial or radial displacement in the turbine, caused as a result of damages in the bearings.

Researches showed that frictional sparks, caused by stroke or friction between movable and immovable parts of the fan may bring to establishing of real conditions for ignition of the explosive gas atmosphere, passing through the fan.

### MEASURES FOR PREVENTING THE ORIGINATION OF DANGEROUS FRICTIONAL SPARKS

Referring to recent fan construction for operation in explosive gas atmosphere, the measures applied for achieving safe operation of fans are reduced to the following:

- Use of bearing of rather high resource and improved wearing;
- Use of special lubrications;
- Use of special couple of metal for manufacturing of turbine and the inlet pipe, which are believed not to ignite the explosive gas atmosphere, passing through the body of the fan;
- Use of different plastics for the turbine and the inlet pipe.

The above constructions do not allow the determination of probability of ignition of explosive gas atmosphere neither experimentally nor theoretically.

Predicting of possible damages in the bearings of the turbine, which bring to operation of the fan in an accidental mode is also difficult. For that reason, up to now there is no unified statement or standardized requirement to define the constructive characteristic of fans for ventilation of hazardous zones, conditionally called "spark-free" (Regulation No 2).

That issue may be resolved by the introduction of a system for protection in the construction of fans, which allows theoretical and experimental determination of probability for ignition of explosive gas atmosphere. The system realizes a continuous control of the condition of fan and in case of some damages it work ceases. In that case neither dangerous sparks nor local heating is possible.

#### SYSTEM FOR PROTECTION AND CONTROL OF SPARK-FREE FAN CONDITION

The system for protection and control may be implemented in each ventilator, in spite of its construction. It consists of:

- Electrical switching of the feeding voltage of the electrical motor with the first possible stroke of turbine to any immovable part of the ventilator (confuser – the closest immovable part);
- Thermal control of bearing condition.

The electrical switching of turbine into immovable parts of the fan is done by a sensor (a metallic plate isolated from the casing of the fan), laid down between the turbine and the confuser.

In case of radial displacement of the turbine, an electrical contact takes place between the turbine and the sensor and it takes the potential of the earthing contour. This brings to switching off the electrical motor from the power supply. The number of dangerous frictional sparks, if admitted that they may originate is equal to the number of revolutions till the absolute stopping of movable parts (turbine, connecting coupling and rotor).

That system for protection by electrical switching off is analogous to the explosion-proof performance "increased safety – e", standardized for electrical appliances.

When the number of strikes is known then probability of ignition of the explosive gas atmosphere, passing through the fan, is predictable.

Thermal control of bearing is in fact a supplementary independent device for protection. It is used for continuous indirect monitoring of bearings in the period between repairs.

In case of random damages the electric motor switches off from the power supply and this prevents the long work of the fan under an accidental mode of operation.

Reasoned on specific requirements for appliances from group I and group II for operation in potentially explosive gas atmosphere, fans possessing the suggested system for protection and the additional independent device for monitoring of bearing temperature may be referred to category M1 for operation in mines and to category 1 – for the other industries (Directive 94/9/EC).

The construction of a fan, which implies the described system for protection and bearing temperature monitoring, is shown in figure 1.

Electrical circuits for implementing the switching off in case of strike and thermal monitoring are in explosion-proof performance of individual protection (spark-free performance).

To discharge possible electrostatic charges toward the earthing contour is done by a high-resistivity resistor.

The temperature monitoring of bearings and lubrications done by means of thermal sensors in the bearing box.

The described switching off may easily be adapted to all centrifugal conventional fans and thus they may be adapted into a spark-free performance.

#### DETERMINING THE PROBABILITY OF DANGEROUS FRICTION SPARKS

The commissioning of a system for protection and monitoring the temperature of bearings may bring to determining the probability of origination of frictional sparks. This is possible because number of possible strikes between the turbine and the confuser depends on known values only.

It is admitted that displacement of turbine is possible during the fan operation. After the first strike, which means after implementation of an electrical contact between turbine and immovable parts of the fan, the switching off starts to act and the electrical motor switches off from the power supply. Then number of strikes will depend only on inertial masses of rotating parts (turbine, rotor, coupling and bearings). For each couple of fan – motor, they are known in advance and therefore, number of revolutions until complete stopping is determined by the formula:

$$n = \frac{E_{K(1)}}{(dM_{TP} + dM_A + M_{CN}) \cdot 2\pi}, \text{min}^{-1} \quad (1)$$

$E_{K(1)}$  – kinetic power in the initial moment of stopping  
 $dM_{TP}$  – moment of friction in bearings

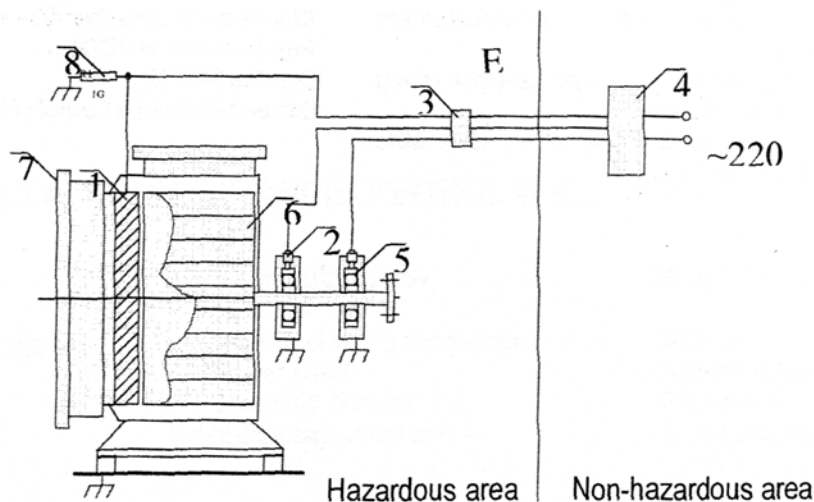
$dM_A$  – moment, created by aerodynamic resistance, which depends on the construction of working wheel and its aerodynamic characteristics.

$M_{CN}$  – stopping moment, depending on force of contact between turbine and confuser

Then the probability of ignition ( $P_{B3n}$ ) of the explosive gas atmosphere in the fan is determined as a ratio of number of strikes  $n$  towards the number of realized ignitions  $m$ , or

$$P_{B3n} = \frac{m}{n} \quad (2)$$

Laboratory tests show that the probability is with the range of  $10^{-8}$  to  $10^{-11}$ .



1. Sensor
2. Thermal
3. Coupling box in explosion-proof performance
4. Automation to the system for protection and monitoring
5. Bearing body
6. Turbine
7. Inlet pipe
8. Resistor

Figure 1. Scheme of the switching off for spark-free fan

Not only possible ignition from hazardous frictional sparks, but also local heating is considered.

In consideration of possible damages in bearings within their resource, it is accepted that current of events is precisely enough subordinated to the law of Poisson and the probability ( $P_{\text{ПБР.ПГ.}}$ ), is determined by the expression:

$$P_{\text{ПБР.ПГ.}} = 1 - e^{-\mu \cdot t} \quad (3)$$

$\mu$  – density of current of events from different damages (number of damages for a unit time);

$t$  – duration of period between repairs

For roller bearings that probability in the period between repairs is within the range of  $10^{-3}$  to  $10^{-4}$  (INA Walzlager Schaeffler KG).

Based on the above, a system for protection and additional device for monitoring the temperature of bearings, which switches the electric motor off is adapted. The probability of ignition of the explosive gas atmosphere in its casing ( $P_B$ ) is determined by the product of probabilities for appearance of hazardous frictional sparks ( $P_{\text{ВЗП.}}$ ) and probability of damage of bearings ( $P_{\text{ПБР.ПГ.}}$ ):

$$P_B = P_{\text{ВЗП.}} \cdot P_{\text{ПБР.ПГ.}} \quad (4)$$

Having in mind the above ranges of probabilities ( $P_{\text{ВЗП.}}$ ) и ( $P_{\text{ПБР.ПГ.}}$ ), and in compliance to (4) the probability ( $P_B$ ) acquires values within the range from  $10^{-11}$  to  $10^{-15}$ .

Applying the requirement for coefficient of resource  $\kappa=1.5$ , the probability ( $P_B$ ) acquires values within the range from  $10^{-6}$  to  $10^{-10}$ .

In the case of those probabilities, a fan adapted according to the above approach, may be considered a non-damageable machine.

#### CONCLUSION

The discussed construction shows a new principle for implementation of spark-free centrifugal fans, based on principles analogous to standardized explosion-proof performance "improved safety – e".

Fans, adapted accordingly, have been applied into workshops of pharmaceutical industry and workshops for painting and lacquering for more than 6 years.

There have not been any damages and accidental situations since.

REFERENCES

- BSS 9557–72. General technical requirements. Fans.  
BSS 15629–83. Explosive gas atmosphere. Classification and methods of testing  
Vaneeva B. N., 1979. Reliability of explosion-proof mining electrical equipment (in Russian)  
Kovalevska V. I., Babak, G. A., Pack, V. V., 1976. Mine centrifugal ventilators. (in Russian)
- Kravchenko, B. S., Bondaria, V. A., 1982. Explosion protection from electrical discharge and frictional sparks (in Russian).  
INA Walzlager Schaeffler KG – company catalogue  
Regulation №2 за ПСТН  
Directive 94/9/EC  
Decree №205 of the Council of Ministers of 12.09.2001

*Recommended for publication by Department of  
Electrical Engineering, Faculty of Mining Electromechanics*

## DC MAINS INSULATION RESISTANCE CONTROL IN ELECTROLYSIS SHOPS

**Kiril Djustrov**

University of Mining and Geology  
"St. Ivan Rilski"  
Sofia 1700, Bulgaria  
E-mail: justrov@mgu.bg

**Dragolyub Kostov**

University of Mining and geology  
"St. Ivan Rilski"  
Sofia 1700, Bulgaria  
E-mail drakost@hotmail.com

**Mento Menteshv**

CMC-C Ltd  
Sofia 1164, Bulgaria  
8 Krivolak St.  
E-mail cmc\_c@mail.orbitel.bg

### ABSTRACT

The paper discusses the problems related to the low insulation resistance in dc mains of electrolysis shops. An analysis is made of the reasons for the low insulation resistance in these mains, the resulting risks for the workers, electric energy losses and difficulties in measuring.

A microprocessor system has been developed and implemented in the electrolysis shop at Umicor Med, which computes the leakage currents, power and energy losses, voltages to ground and the asymmetry between them.

The electric energy supplied to electrolysis baths is converted from multiphase rectifiers (16) and distributed in the electrolysis shop by copper bus bars having a  $10^4 \text{ mm}^2$  cross-section. The voltage normally reaches up to 100 V and the current – 10 000 A.

The bus bars are opened and mounted on pedestal insulators exposed to aggressive atmosphere and the direct attack of an existing electrolyte ( $\text{H}_2\text{SO}_4$ ). This situation, combined with the insulation problems of the baths themselves to ground, determine the considerably high leakage currents. It was experimentally found that at a single-pole direct short circuit the leakage current reaches up to 240A. Normally the insulation resistance to ground varies within  $10^{-1} - 10^2 \Omega$ , beyond the range of the widely used insulation resistance control devices [1, 2]. The change in the insulation resistance as a function of time is rather dynamic.

The existing asymmetry in the voltages to ground is determined by the asymmetry of the corresponding insulation resistances to ground:

$$A = \left| \frac{U^+ - U^-}{U^+ + U^-} \right| \cdot 100, \% \quad (1)$$

It should be noted that the asymmetry A carries information about the difference in the insulation resistance values  $R^-$  and  $R^+$ , and not about their absolute values that limit the leakage current.

$$I_y = \frac{U}{R^+ + R^-} = \frac{U^+ + U^-}{R^+ + R^-} \quad (2)$$

The above-mentioned experimentally determined insulation resistance values and the leakage currents to ground that they limit create problems in relation to two aspects:

- Risks for the service personnel in case of a single-pole contact;
- Considerable losses of electric energy not related directly to the electrolysis process;

A quantitative assessment of these two problems can be made by using the diagram in Fig. 1.

The risks for the service personnel are related to the actually existing possibility for a single-pole contact – in contact with the current-conducting bus bars.

1. The bus-bar contact voltage "+" is:

$$U_h^+ = \frac{R_h \cdot R^+ \cdot U}{R^+ \cdot R_h + R^- \cdot (R^+ + R_h)} \quad (3)$$

In contact with bus-bar "-" one gets energized:

$$U_h^- = \frac{R_h \cdot R^- \cdot U}{R^- \cdot R_h + R^+ \cdot (R^- + R_h)} \quad (4)$$

The maximum contact voltages are obtained as follows:

- In contact with bus-bar "+" and  $R^- \approx 0$ ;  
 $U_h = U$
- In contact with bus-bar "-" and  $R^+ \approx 0$ ;  
 $U_h = U$

For these reasons and in compliance with Art. 1-7-36(1) of the Regulation for Electrical Systems Design (RESD), the labor safety control authorities have recommended a maximum voltage up to 100 V.

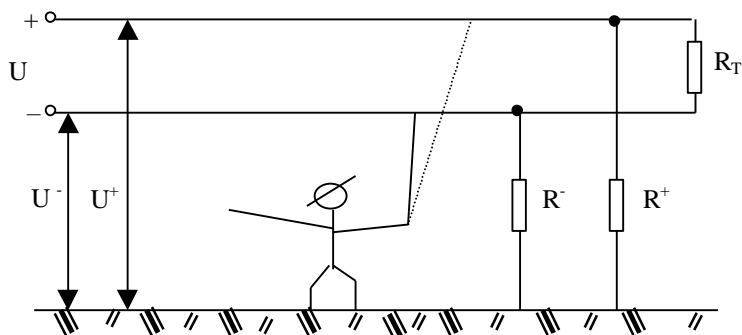


Figure 1

The supply voltage rarely reaches this value in practice since it is determined by the number of operating baths but this voltage may be exceeded thus creating real risks for humans in case of a single-pole direct contact and direct ground fault of the other bus bars. This risk situation has a very low probability but cannot be completely excluded.

Having in mind the working conditions in the electrolysis shops, it is more reasonable to adopt Art. 1-7-37 of RESD, which limits the maximum allowable contact dc voltage to 50V. This limitation is practically observed with supply voltage of 100V but only in the absence of asymmetry in the insulation conductivity to ground. This is difficult to realize in practice. In this sense, it is necessary to control both the current leaks and the voltage to ground. Since the protection switch-off is unallowable due to technological reasons, the service personnel are obliged to undertake measures with respect to the insulation resistance to ground in order to reduce the asymmetry to an extent not permitting the voltage to ground of each bus-bar to exceed 50V.

The second aspect is related to electric energy losses from leakage currents, which have a parasitic nature. From the diagram in Fig. 1 it is easy to determine the leakage current expression:

$$I_y = \frac{U}{R^+ + R^-} \quad (5)$$

and the power expression:

$$P_y = \frac{U^2}{R^+ + R^-} \quad (6)$$

At the minimum measured insulation resistance values of the order of  $10^{-1}\Omega$ , which can really occur, the power loss, calculated by (6) is of the order of  $10^2\text{kW}$ . And at insulation resistance of  $10^2\Omega$ , measured as characteristic, the leakage current power is of the order of several kW.

Due to the continuous nature of the technological process, the annual electric energy loss is within the range of  $8.6 \times 10^3$  to

$8.6 \times 10^5$  kWh, i.e. from 0.2 to several % of the energy consumed to perform the process.

The problems described above determined the need for developing an electrical device that can control the leakage currents and direct the attention to undertaking measures to equalize an insulation resistance value that can be used to limit the probability of a hazardous single-pole contact and reduce the electric energy losses.

The microprocessor device for measuring leakage currents KTU-M is designed to control and assess the conditions for safe operation and power and energy losses resulting from reduced insulation resistance to ground in powerful electric dc mains intended, for example, to supply electrolysis baths in copper refineries. The basic parameters of the designed apparatus are:

- |   |       |
|---|-------|
| 1. Mains voltage  | 125 V |
| 2. Controlled mains current                                   | 12 kA |
| 3. Control voltage  | 12 V  |
| 4. Control voltage frequency                                  | 50 Hz |
| 5. Period of scanning the indications                         | 6s    |
| 6. Periods accounting for the changes in the measured values: |       |
| -For the voltages and the current (moment values) -           | 6 s   |
| -For the power from 10 measurements -                         | 1 min |
| -For the energy from 6 measurements -                         | 6 min |
| 7. Supply voltage   | 220 V |
| 8. Output contact voltage :                                   |       |
| - 30 V dc   |       |
| - 120V ac   |       |
| 9. Output contact current                                     | 1 A   |

The block diagram of the device and the manner of connection to the controlled mains are shown in Fig. 2.

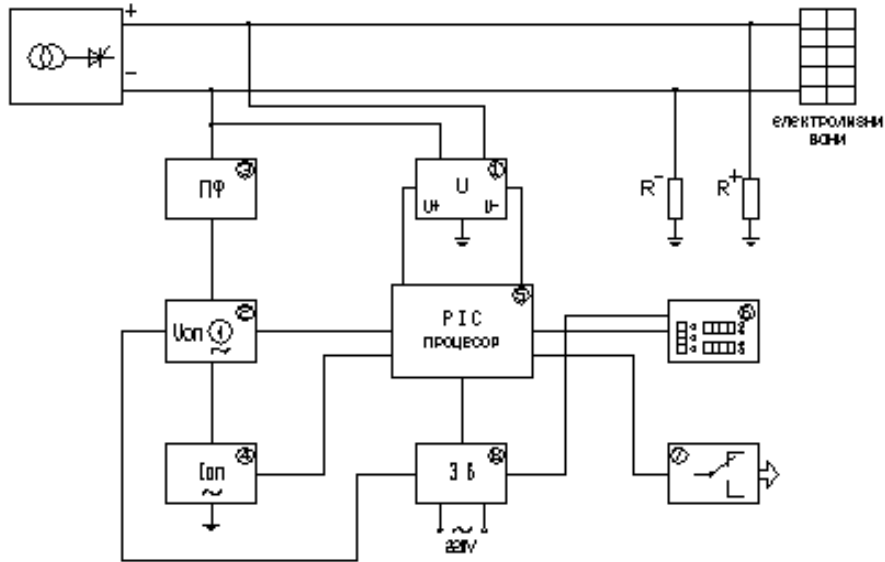


Figure 2

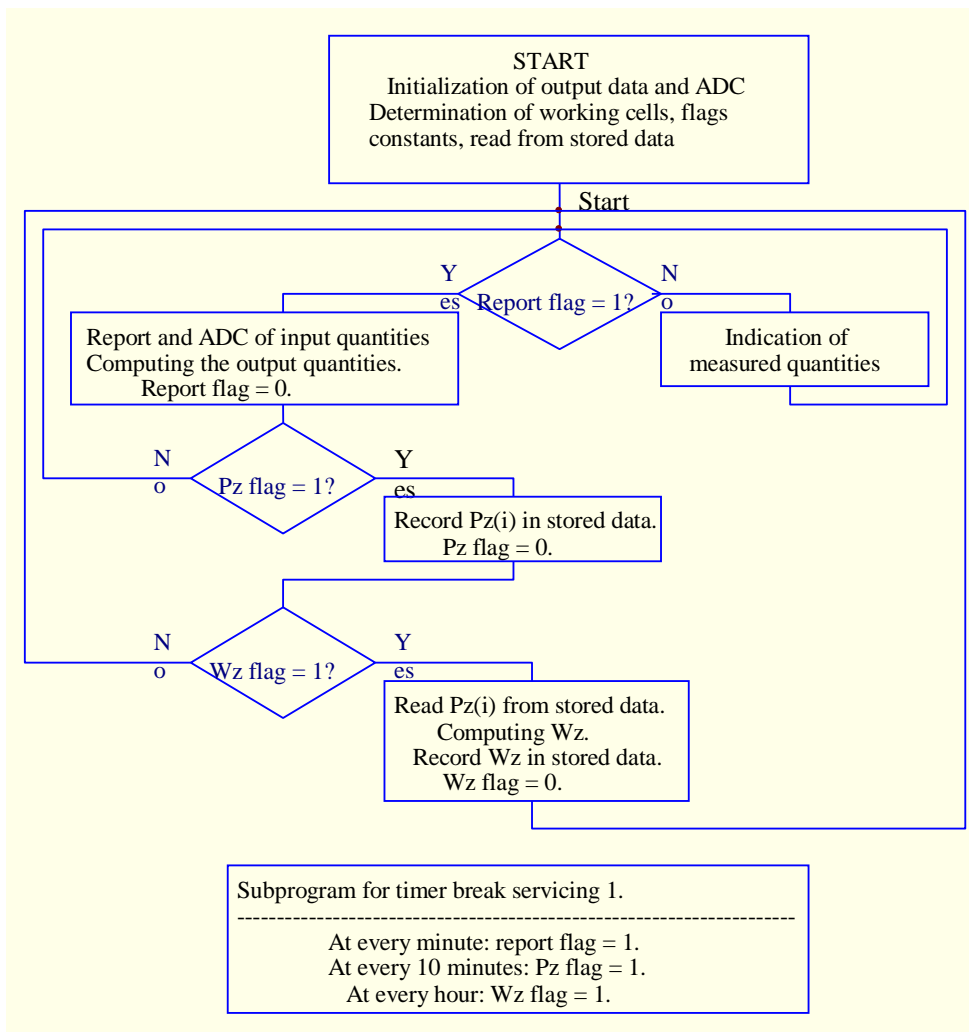


Figure 3

The basic constituent units of the apparatus are the following: Unit 1 carries out measurements of the mains voltage  $U$  and voltages to ground – of the plus bus bar “ $U +$ ”

and of the minus bus bar “ $U -$ ”. Unit 2 contains the ac control voltage source  $U_{0n}$ , connected to the controlled mains by a filter 3. The control current  $I_{0n}$ , which is a function of the

conductivity to ground, is computed in unit 4. The computing and indicating control unit 5 is built up on the basis of a PIC-processor – a new approach to the design of these devices [1, 2]. It receives data on the voltage  $U$ , voltages to ground  $U_+$  and  $U_-$ , control voltage  $U_{on}$  and control current  $I_{on}$ . It also controls the indicating unit 6 that consists of two four-element digital displays mounted on the front panel, a two-color diode ladder and variously colored diodes indicating the values from the digital panels measured at any one moment. The relay unit 7 has an outlet of three switching contacts that form signals for the leakage currents to the centralized information system. The supply unit 8, connected to the 220 V mains, provides stabilized voltages for the measuring and computing units.

The insulation resistance is computed on the basis of the measured values of the control voltage and current. The leakage current and its power are determined by introducing the mains voltage and the lost energy is computed by taking into account the time. These three quantities are scanned periodically and indicated on the upper digital panel. Fig. 3 shows the algorithm of the process involving the collection of the analog data, their conversion into digital data, computing the output quantities and their indication.

A criterion for the electrical safety of the service personnel is the magnitude of the supply voltage of the bus-bar system. The latter is controlled by a two-color diode ladder: at a voltage up to 120 V the level is measured by the yellow flashing diodes. When this value is exceeded then the red diodes flash thus warning for dangerous voltage values.

The light indication is designed for three levels of current leakage values: normal – up to 10 A, higher – from 10 to 100 A and unallowable – over 100 A. These levels are subject to quantitative correction (by adjustment) and are primarily related to the increasing electric energy losses from parasitic leak currents. The signals should initiate the corresponding actions for increasing the insulation resistance to ground: washing and drying the pedestal insulators for the bus bars, removing bath leaks, etc.

The energy calculated as a current leakage loss gives an accurate quantitative picture of the damages suffered as a result of additional costs for electric energy, which has nothing to do with the realization of the technological process in recovering electrolytic copper. The four-digit indicator makes it possible to compute up to 9999 kWh so that it is necessary to reset the indications periodically. The resetting is automatic or can be done by the reset button.

The bus-bar voltages to ground are measured and the asymmetry between them is computed in % (indicated by the lower digital panel). The data allow to assess the asymmetry in the conductivity to ground and to identify the bus bar with the higher current leakage thus directing the actions towards improving the insulation resistance: at a voltage  $U_+ < U_-$  the

higher current leakage is in bus bar “+”, at  $U_+ > U_-$  the current leakage is higher in bus bar “-”.

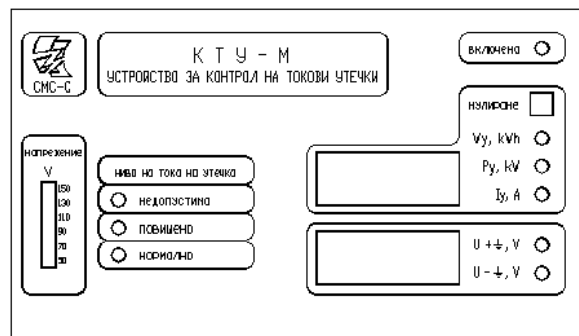


Figure 4

Fig. 4 shows the front panel of the device whose indications define fully and accurately enough the functions of the displayed elements. The asymmetry in the voltages to ground is indicated by the letter “A” preceding the corresponding number on the lower digital panel.



Figure 5

Fig. 5 shows the physical appearance of the device that is being successfully experimented at Umicor Med – Pirdop.

## REFERENCES

- Анев Г., Ментешев М., 1987. Електробезопасност в минните предприятия (Основи на електрообезопасването). София, Висш Минно-геоложки институт, 30-63.
- Hofheinz, W., 1993. Protective Measures with Insulation Monitoring, Vde-verlag gmbh, Berlin, 147-149  
Catalogue: ABB, Bender, Shneider.

## TOPOGRAPHICAL METHOD FOR SOLVING PROBLEMS OF THREE-PHASE CIRCUITS

Angel Zabchev

University of Mining and Geology "St. Ivan Rilski"  
Sofia 1700, Bulgaria

### ABSTRACT

A topographical method of drawing of alternating current circuits used for analysis and synthesis of three-phase circuits for determination of phase sequence is treated. The main point of the method is drawing of circuit diagram and all its connections and elements on a complex plane. Every node of the circuit has coordinates, which determine a complex number equal to the voltage of the node in a complex form. A simple diagram for determination of phase sequence with a negative-glow lamp is synthesised.

### INTRODUCTION

The main methods of analyse of alternating current circuit is the symbolical method. The current and voltage, which are sinusoidal quantities and are time functions, are noted as complex numbers  $Ae^{j\varphi}$  where  $A$  is the module of the complex number and is equal to the current or voltage, angle  $\varphi$  is the phase angle and  $j$  is the imaginary unit. The impedance is noted also as a complex number  $Z = ze^{j\varphi}$ . This method allows to use directly the laws and methods of calculation of direct current circuits and all calculations are made by complex numbers. If he expressions are complicated, the main difficulty is calculative, because it is necessary to convert the complex numbers in algebraic form when adding and subtracting are made and in index form when multiplication and division are made. This difficulty drop of when use calculator that could calculate complex expressions (for example TI 89). This calculator is able to calculate random complicated expressions and complex numbers could be inputted both in algebraic and index form.

As the complex numbers are represented as vectors in a complex plane, all currents and voltages could be represented as vectors. The vector diagram gives a clear idea for current state in determined values of impedance and frequency.

If we are interested in a particular vector - current or voltage and its changes as a result of change of particular element of the circuit or frequency, we should find the vector hodograph, i.e. the geometrical locus (GL) that the vertex of the vector covers in the whole diapason of change of the variable parameter.

A topographical method [3] is worked out, in which the electrical diagram is not driving in standard way but is transferred on complex plane. Every node takes defined place which coordinates that determine a complex number equal to the voltage of this node. The nodes are divided in two groups: static and mobile. In static nodes the voltage does not depend on diagram elements. Such are the clamp of electromotive

force source. All the rest elements are mobile, i.e. the voltage on them is changing.

For illustration (fig.1) is selected a RC group, connected to the voltage source  $U_{12}$  in two ways:

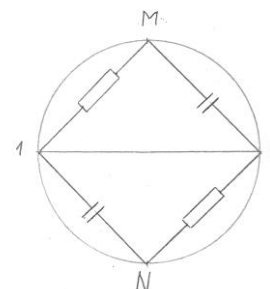


Figure 1.

Nodes 1 and 2 are static – they are connected to the voltage source. In first way resistor is connected to p.1 and capacitor to p.2. The mobile node M moves on the upper semi-circumference when the value of element or frequency is changed. That is so because the voltages  $U_{1M}$  and  $U_{2M}$ , which correspond to the segments M1 and M2 are on  $90^\circ$  one towards another. When connect the resistor to the p.2 and capacitor to p.1, the mobile node N moves on the bottom semi-circumference.

### ANALYSIS OF THE CIRCUIT IN ORDER TO DETERMINE THE PHASE SEQUENCE

When two lamps and a capacitor are connected in star connection the popular diagram for determination of phase sequence is obtained. [2]. This circuit was drawn on fig. 2 by the described topographical way.

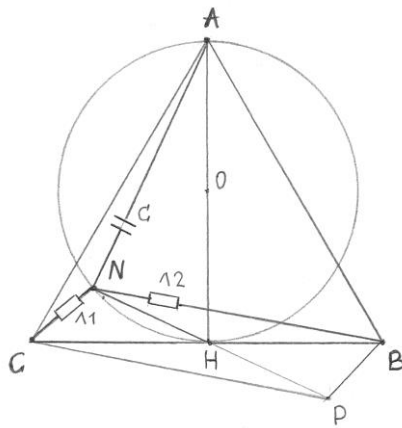


Figure 2.

Points A, B and C are static nodes, connected to the supplying three-phase voltage. The two lamps  $L_1$  and  $L_2$  are identical and have the same conductance  $Y$ . In determined scale (conditionally  $Y=1$ ) vectors of the current coincide with vectors of the voltage, because the lamp often have pure active resistance.  $\overline{NC}$  - vector of current and voltage for lamp  $L_1$ .  $\overline{NB}$  - vector of current and voltage for lamp  $L_2$ . The sum of the two currents through the lamps  $L_1$  and  $L_2$  coincide with the vector  $\overline{NP}$ .

$$\overline{NP} = \overline{NC} + \overline{NB} \quad (1)$$

NP is the diagonal in the parallelogram NBPC and passes through the middle of CB, i.e.  $\overline{NP} = 2\overline{NH}$ . Or:

$$Y.U_{NC} + Y.U_{NB} = Y.U_{NP} = 2Y.U_{NH} \quad (2)$$

Expression (2) allows to change both lamps  $L_1$  and  $L_2$  with active resistor  $R_{NH}$ , connected between p.N and p.H, which has two times higher conductance and is equal to  $2Y$ . This way the three-element diagram (star connection) becomes two-element one - resistor  $R_{NH}$  is series connected to the capacitor C. In this type of connection mobile node N moves on the left semi-circumference which diameter is AH. This conclusion is made in [1] using the analytical expressions of the circle diagram theory.

We consider the problem only geometrically and in this way it is possible to present better the motion of node N as well as to make a mechanical analogue. Two lamps and a capacitor are presented as springs, one end of which is attached respectively to points A, B и C, and another end to the mobile point N. The spring stiffness  $\kappa$  ( $f = k.x$ ) corresponds exactly to the conductance  $Y$  of the element. Point N is attached on the periphery of the rotating round the point O circle with diameter AH. So p. N of this mechanical model will stop on the place, exactly corresponding to the voltage of the node N in complex plane. The distances conform to the voltages and amperage, i.e. expressions  $I = Y.U$  and  $f = k.x$  are analogous. For example, if the capacitor capacity increases, the spring stiffness AN increases too. However the circle will turn to the clockwise and p. N will come near the p. A. The voltage on the capacitor will decrease, and voltage on the lamps – will increase.

In positive phase sequence the lamp  $L_2$  shines brighter because  $NB > NC$ . The lamps are for nominal voltage 230V. If p. N takes away from p. A, the voltage on lamp  $L_2$  will be higher than nominal voltage and the lamp will be destroyed. In the expression, solved in [2] is sat that conductance of lamps and capacitor are equal. So the voltage on lamp  $L_2$  is 330V and it will be destroyed.

Geometrically we could quickly determine the conductor capacity, in which the voltage on the lamps is secure. In corresponding scale we determine the segment NB, and this segment corresponds to the voltage 230V (segment CB corresponds to 380V). We draw the circle with centre p.B that crosses the circle on fig.2 in p. N. We should write:

$$\frac{Y_C}{Y_{NH}} = \frac{Y_C}{2Y} = \frac{NH}{AN} \quad ,$$

$$\omega C = Y_C \cdot 2Y \cdot \frac{NH}{AN}$$

$$C = \frac{2Y}{\omega} \cdot \frac{NH}{AN} \quad (3)$$

Expression (3) determines the capacitor capacity when we have chosen two identical lamps with conductance  $Y$ .

#### SYNTHESIS OF THE CIRCUIT IN ORDER TO DETERMINE THE PHASE SEQUENCE

The most important advantage of the topographical drawing of the electrical circuit of alternating current is the opportunity to create a new diagram, which working could be presented graphically.

In this report we will consider a simple circuit synthesised in order to determine the phase sequence. In described above circuit, one lamp shines brighter than another. This indication is not enough clear. The phase determination circuit should have only one lamp, which is on in positive phase sequence and is off in negative phase sequence.

The circuit consists of tow resistors R, two capacitors C, a negative-glow lamp L for 220V and limit resistor  $r = 360k\Omega$  (fig. 3a). The impedance of the resistors and capacitors is identical, i.e.  $R = \frac{1}{\omega C}$ . On fig. 3b the circuit is drawn topographically.

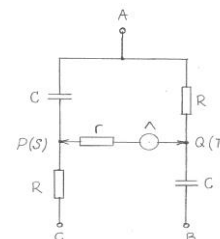


Figure 3a

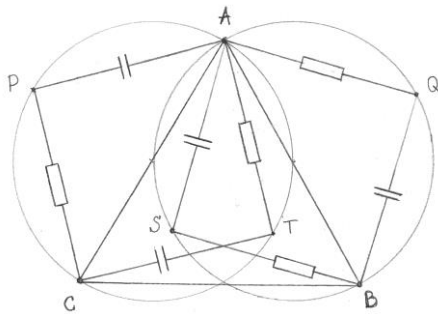


Figure 3b

On the side AC of the triangle ABC is drawn the circle with diameter AC. On the side AB is drawn another circle. Mobile node P is the vertex of the rectangular isosceles triangle ACP that lies on the circle. This way we find the mobile node Q on the second circle. Linear voltage  $U_{\pi} = 380V$  corresponds to the sector  $m$  and:

$$m=AB=BC=CA$$

$$\angle PAQ = 45^{\circ} + 60^{\circ} + 45^{\circ} = 150^{\circ}$$

$$PA = QA = \frac{m}{\sqrt{2}} = 0,7071m \quad (4)$$

$$PQ = 2PA \sin \frac{\angle PAQ}{2} = 2 \frac{m}{\sqrt{2}} \sin 75^{\circ} = 1,366m \quad (5)$$

From (5) we could determine the voltage between mobile nodes P and Q:

$$U_{PQ} = 1,366 \cdot 380 = 519,1V \quad (6)$$

In the method of connection, shown on fig.3a, the voltage on the negative-glow lamp is  $U_{PQ} = 519V$ . The negative-glow lamp is on and it is indication for the right phase sequence.

If we change the places of phases B and C as a result is the system with negative phase sequence. Mobile node T from RC group connected between p.A and p.C lies on the left circle and is the vertex of isosceles triangle ACT. Another mobile node S lies on the second circle and is a vertex of isosceles triangle ABS. Than the voltage on the negative-glow lamp is  $U_{ST}$ , and is determined by fig. 3b.  $\angle SAT = \angle SAQ - \angle TAQ$ . Angle  $\angle SAQ$  is an internal angle of the square AQBS and is equal to  $90^{\circ}$ . Angle  $\angle TAQ$  is equal to  $60^{\circ}$  because the right circle together with inscribed in it square is obtained from the left by  $60^{\circ}$  rotation round p. A. As a result of this rotation the diameter AC comes over AB, and side AT over AQ.

$$\angle SAT = 90^{\circ} - 60^{\circ} = 30^{\circ}$$

$$ST = 2SA \sin \frac{\angle SAT}{2} = 2 \frac{m}{\sqrt{2}} \sin 15^{\circ} = 0,3660m \quad (7)$$

Recommended for publication by Department of Electrical Engineering, Faculty of Mining Electromechanics

The segment ST corresponds to the voltage on the negative-glow lamp. From (7) we determine the voltage between mobile nodes S and T:

$$U_{ST} = 0,3660 \cdot 380 = 139,1V \quad (8)$$

This voltage is applied on the negative glow lamp when the phase sequence is negative. The lamp is off because the its starting voltage is 170V. Two resistors and two capacitors work under the same voltage. We determine this voltage by using of (4):

$$U_{PA} = 0,7071 \cdot 380 = 268,7V \quad (9)$$

For resistor s R we have selected  $R = 33k\Omega$ ; 2W. The power on them is  $P = 2,188W$ , and there are no problems when in short time we turn it on many times.

The capacitor capacity is  $C = \frac{1}{\omega R} = \frac{1}{100\pi 33 \cdot 10^3} = 96,46nF$ . The capacitor is polyester one and has the nominal value  $C = 100nF, U = 400V$ .

Dimensions of the plate together with all elements are 3X5 cm. The three terminals are numbered - 1,2 and 3, and when they are connected to the system with positive phase sequence the lamp is on and to the system with negative phase sequence the lamp is off.

## CONCLUSION

The diagram shown on fig.3a is realised and tested in three-phase systems with linear voltage 127V, 220V and 380V. The diagram is used for determination of phase sequence. The voltages  $U_{PQ}$  and  $U_{ST}$  are measured by using of the high-resistance voltmeter ( $10M\Omega$ ) when the negative-glow lamp is connected or is not connected. The voltage  $U_{PQ}$  decreases about 5%, and voltage  $U_{ST}$  is constant.

Presented topographical method of drawing of an alternating current circuit and the mechanical model, created on this base gives the new opportunities to understand these diagrams and to synthesise new circuits with particular applications.

## REFERENCES

- Seveke G.V., P.A.Ionkin, A.V.Netushil, S.V.Strahov, Bases of circuit theory, M. "Energia" 1965.
- Kosarov A.S., S.A.Stefanov, Theoretical bases of electrical engineering, S. "Technika" 1978.
- Musichenko A.D., A.P. Trofimenko, Topographical method of calculation of electrical circuits, K. "Naukova dumka" 1987.

## ANALYSES OF ONE ELECTROSTATIC PROBLEM AND ITS APPLICATION IN MEASUREMENT OF THE ELECTROSTATICAL FIELD PARAMETERS

**Spefan Stefanov**

University of Mining and Geology "St. Ivan Rilski"  
Sofia 1700, Bulgaria

**Angel Zabchev**

University of Mining and Geology "St. Ivan Rilski"  
Sofia 1700, Bulgaria

### ABSTRACT

In this report is considered creation of non-uniform field of point charge, in which as a sensor is introduced a conductive sphere. Two instances – earthing and isolate sphere are treated and is used popular principle that induced on the sphere surface charge could be changed with charge-image, located into the sphere volume. Analysis we made proves that two sensors, located on the sphere surface when the sphere is earthed, make measurements.

### INTRODUCTION

Most modern device designed for measurement of parameters of electrostatical fields use the effect of electrostatical induction.

Electrostatical induction causes accumulation of charges on the measuring electrode of the converter, which field is superposed on the measured field and deforms it. That is why the measuring instrument designed for measurement of parameters of electrostatical field converts the value of deformed field.

It is known that measuring instrument for electrostatical field, graduated according to the particular source is inexact when is used for measurement of the field with other dimensions and configuration [1, 2]. Most often the graduation of the measuring instrument is made in the field of plane capacitor [1]. But in real conditions should be measured parameters of non-uniform field.

It should be mentioned, that in order to use the induction meters correctly it is necessary to earthen them.

Let note the coefficients of intensity deformation as:

$$K_E = \frac{E}{E_0} \quad (1),$$

where E is the average value of intensity of deformed field on the surface of the measuring electrode and E<sub>0</sub> is intensity of measured field when the device is missing.

The indication α of the device is proportional to the field intensity on the surface of measuring electrode: α = mE, where m is the coefficient of transmission of the device. Therefore:

$$K_E = \frac{\alpha}{mE_0} \quad (2)$$

The coefficient K<sub>E</sub> depends on field deformation and on distance between source and measuring instrument. In case of ideal measuring instrument, the coefficient K<sub>E</sub> is constant for fields with different configuration and intensity.

### FIELD OF EARTH SPHERE

We treat solution of classical problem for the field of conducting medium that is in the field of point charge +q (fig.1)

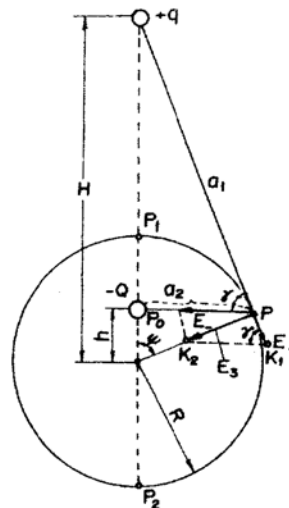


Figure 1.

The point charge +q is at distance H from the centre of earthed conducting sphere, which radius is R. Induced on the sphere surface charge could be changed with charge-image -Q, which is concentrated in point P<sub>0</sub> inside the sphere at

distance  $h$  from the centre. Charge  $-Q$  and distance  $h$  are selected so that the fields of real charge  $+q$  and charge image  $-Q$  to have a zero equipotential plane, coincided with the sphere surface. For every point of this plane is valid:

$$\varphi = 0 = \frac{q}{4\pi\epsilon_0 a_1} - \frac{Q}{4\pi\epsilon_0 a_2} \quad (3)$$

From (3) follows:

$$\frac{a_1}{a_2} = \frac{q}{Q} = k = const \quad (4)$$

In point  $p_1$  -

$$\frac{a_1}{a_2} = k = \frac{H-R}{R-h} \quad (5)$$

In point  $p_2$  -

$$\frac{a_1}{a_2} = k = \frac{H+R}{R+h} \quad (6)$$

We solve the system of equations (5) and (6) towards the unknown  $k$  and  $h$  and obtain:

$$h = \frac{R^2}{H} \quad (7)$$

$$k = \frac{H}{R} \quad (8)$$

This way the conducting surface of the sphere with the zero potential could be changed with charge image:

$$Q = -\frac{q}{k} = -q \frac{R}{H} \quad (9)$$

The resultant intensity of the field in anyone point  $p$  from the surface of the conducting sphere has two components:

a) from charge  $+q$  on the direction of the line  $a_1$  :

$$E_+ = \frac{q}{4\pi\epsilon_0 a_1^2} \quad (10)$$

b) to charge  $-Q$  on the direction of the line  $a_2$

$$E_- = -\frac{Q}{4\pi\epsilon_0 a_2^2} \quad (11)$$

The ratio of absolute values of these components is:

$$\frac{E_-}{E_+} = \frac{Q a_1^2}{q a_2^2} = k. \text{ The geometrical sum of } E_+ \text{ and } E_-, \text{ i.e. the}$$

complete value of the intensity of the field  $E_3$  in point  $p$  could be determine from similarity of triangles  $(+q)p(-Q)$  and  $pk_1k_2$  :

$$\frac{E_3}{E_+} = \frac{H-h}{a_2} \text{ from where:}$$

$$E_3 = E_+ \frac{H-h}{a_2} = \frac{q}{4\pi\epsilon_0 a_1^2} \frac{H-R}{\frac{a_1}{H/R}} = \frac{q}{4\pi\epsilon_0} \frac{H^2 - R^2}{a_1^3 R} \quad (12)$$

The intensity of deformed field  $E_3$  on the surface of earth sphere is determined by expression (12). The vector  $E_3$  has direction on normal to spherical surface.

### FIELD OF ISOLATED SPHERE

Considered sphere in general could has the arbitrary potential  $\varphi_{cp}$ , which is different form zero when the earthing is removed and the charge  $+Q'$  is located in the its centre. The charge is determined by the formula:

$$+Q' = \varphi_{cp} 4\pi\epsilon_0 R \quad (13)$$

Complete charge of the sphere is equal to:  $Q_{cp} = Q' - Q$ , where  $-Q$  is the charge image of the external charge  $+q$ .

If the sphere is isolated than its complete charge is equal to zero, therefore:

$$Q' = Q = q \frac{R}{H} \quad (14)$$

Intensity of the electrostatic field on the sphere surface in this case will have an additional component. It could be determine by charge  $+Q'$  and arithmetically is extracted from the value  $E_3$  in case of earthing sphere. i.e.

$$E_{II} = \frac{q}{4\pi\epsilon_0} \left( \frac{H^2 - R^2}{a_1^3 R} - \frac{1}{RH} \right) \quad (15)$$

The value  $E_{II}$  is zero when:  $\frac{H^2 - R^2}{q^3 R} - \frac{1}{RH} = 0$ , from

where:

$$a_1 = \sqrt[3]{H(H^2 - R^2)}.$$

According to fig.1  $a_1^2 = H^2 + R^2 - 2HR \cos \varphi$ , from where obtain, that the intensity  $E_{II}$  is zero when:

$$\cos \varphi = \frac{1}{2} \left[ \frac{H}{R} + \frac{R}{H} - \sqrt[3]{\frac{H}{R} \left( \frac{H}{R} - \frac{R}{H} \right)^2} \right]$$

We subtract (15) from (12) and obtain the component of intensity of deformed field  $E'_3$ , conditioned by the effect of earthing of the sphere

$$E'_3 = E_3 - E_{II} = \frac{q}{4\pi\epsilon_0} \frac{1}{RH} = \varphi_q \frac{1}{R} \quad (16)$$

CONCLUSION

where  $\varphi_q = \frac{q}{4\pi\epsilon_0 H}$  is the potential of the field in the centre of the sphere, created by the charge q. In expression (16) is replaced  $a=a_1$ . This way the intensity of earthed sphere is sum of two components:

$$E_3 = E_{II} + E_3' \tag{17}$$

Expression (16) is transformed:

$$E_3' = E_0 \left( \frac{H}{R} - 2 + \frac{R}{H} \right) \tag{18}$$

where  $E_0$  is intensity of the external field created by the charge q in point  $p_1$  from the sphere surface.

The intensity in  $p_1$  could be expressed by  $E_0, E_{3p1}$ :

$$E_{3p1} = \frac{q}{4\pi\epsilon_0 (H-R)^2} \left( 1 + \frac{H}{R} \right) = E_0 \left( 1 + \frac{H}{R} \right) \tag{19}$$

Intensity  $E_{II}$  for the same point is:

$$E_{IIp1} = \frac{q}{4\pi\epsilon_0 (H-R)^2} \left( 3 - \frac{H}{R} \right) = E_0 \left( 3 - \frac{H}{R} \right) \tag{20}$$

Dividing (19) and (20) to  $E_0$ , according to (1) we find the coefficients of deformation of the field on the sphere surface in point  $p_1$  respectively of earthing and isolated spheres;

$$K_{E_{3p1}} = 1 + \frac{H}{R} \tag{21}$$

$$K_{E_{IIp1}} = 3 - \frac{R}{H} \tag{22}$$

It should be mentioned, that when  $a = \sqrt{H(H^2 - R^2)}$  on the line of electrical neutral the intensity  $E_{II}$  is zero, because  $E_3 = E_3'$  [3,4]. This way by using of the intensity of line of electrical neutral of earthing sphere could be determined intensity on surface of isolated sphere.

When  $a = \sqrt{H^2 + R^2}$  intensity of earthing sphere on the line of geometrical neutral in point  $p_2$  is:

$$E_{3p2} = E_0 \frac{(H-R)^2 (H^2 - R^2)}{R(H^2 + R^2) \sqrt{H^2 + R^2}} \tag{23}$$

We extract (23) from (19) and obtain the difference of intensities in point  $p_1$  and point  $p_2$ :  $E_3'' = E_{3p1} - E_{3p2}$ . Now we find:

$$\frac{E_3''}{E_0} = 1 + \frac{H}{R} - \frac{(H-R)^2 (H^2 - R^2)}{R(H^2 + R^2) \sqrt{H^2 + R^2}} \tag{24}$$

Calculations results for  $K_{E_{3p1}}, K_{E_{IIp1}}$  and  $\frac{E_3''}{E_0}$  by using the formulas (21), (22) and (24) are given in table:

|                     |   |      |      |      |      |      |
|---------------------|---|------|------|------|------|------|
| R                   | 1 | 2    | 3    | 4    | 5    | 6    |
| H                   | 1 | 4    | 9    | 16   | 25   | 36   |
| H/R                 | 1 | 2    | 3    | 4    | 5    | 6    |
| R/H                 | 1 | 0,50 | 0,33 | 0,25 | 0,20 | 0,17 |
| $K_{E_{3p1}}$       | 2 | 3    | 4    | 5    | 6    | 7    |
| $K_{E_{IIp1}}$      | 2 | 2,5  | 2,67 | 2,75 | 2,80 | 2,83 |
| $\frac{E_3''}{E_0}$ | 2 | 2,73 | 2,99 | 3,07 | 3,10 | 3,11 |

On fig.2 are shown the dependences of coefficients of deformation according to (21) and (22) and of the ratio  $\frac{E_3''}{E_0}$ , according to (24).

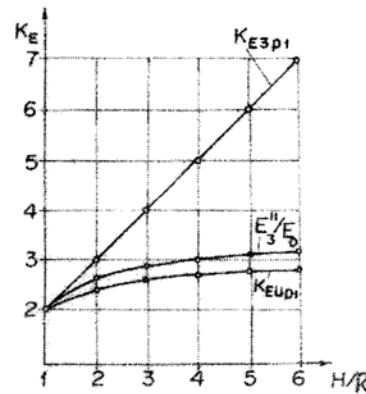


Figure 2

When the sphere is earthed, the coefficient of deformation  $K_{E_{3p1}}$  increases unlimitedly when the distance H increases. In the sphere is isolated, the coefficient of deformation  $K_{E_{IIp1}}$  aims to be constant equal to three, when the distance H increases. A special characteristic of the ratio  $\frac{E_3''}{E_0}$  is that it is insignificantly different from the coefficient  $K_{E_{IIp1}}$ , and therefore the intensity  $E_3''$  is close to intensity  $E_{IIp1}$ .

Characteristic for graphics, shown on fig.2, is that when H/R increases, functions  $K_{E_{3p1}}, K_{E_{IIp1}}$  and  $\frac{E_3''}{E_0}$  monotonously increase. When the values of H/R are small, the values of shown above functions do not decrease (they stay minimum-extremum), It could be explained with the fact that common capacity of the system conducting sphere-point charge is equal to zero.

Analysing the theoretical conclusions (21), (22) and (24) and graphics, shown on fig.2 is offered a principle of design of device for measurement of intensity of electrostatic field with optional configuration with determine precision. The principle is:

Two converters are used – the first one is located on the surface of conducting body of the converter in the area, turned to the source of field, and another one – on the line of geometrical neutral.

---

#### REFERENCES

- Imyatikov I. M. Devices and methods of investigation of atmosphere electricity, M., GITTL, 1957.
- Kversiev V.A., A.A. Zaitsev, .U.A.Ovechkin. Staticval electricity in semi-conducting industry, M. Energia, 1968
- lonkin, P.A., A.I.Darevskii etc. Theoretical bases of electrical engineering. M. Vishhaja shkola, 1976 Govorkov V.A. Electrical and magnetic fields. M. Energia 1968

*Recommended for publication by Department of  
Electrical Engineering, Faculty of Mining Electromechanics*

## TRANSFORMATION OF MINE BATTERY LOCOMOTIVE 4,5 ARP INTO A TROLLEY LOCOMOTIVE

**Venelin Tasev**

University of Mining and Geology  
"St. Ivan Rilski"  
Sofia 1700, Bulgaria  
E-mail: lvtasev@mail.bg

**Ivailo Iordanov**

University of Mining and Geology  
"St. Ivan Rilski"  
Sofia 1700, Bulgaria  
E-mail: iyordanov@mail.mgu.bg

### ABSTRACT

The article considers the reconstruction of mine battery locomotive 4,5 ARP into a trolley locomotive. All of the important changes of the motor, operations, illumination devises/lighting installation, signaling, achieving the needed cohesive mass/weight and all necessary requirements, such us motorman cab, trolley, information about the consumed current supply by the motors and the voltage at the trolley circuit. All sections of the mechanical and the braking systems are described as well as the current intensity system and the auxiliary electrical installation. There are pictures displaying the developed locomotive and results from the service tests.

The small trolley locomotives of a mass of 4-5 tons are applied in mining practice as face machines, driving machines and auxiliary equipment. In Bulgaria, in fact trolley locomotives of that mass were not manufactured and were not imported. For those reasons, wherever there is a need of trolley locomotive, battery machines were used, as a rule. The crisis, which spread over mining industry in the last years, made difficult the use of battery locomotive. Main factor for that was the high cost of the accumulator batteries. In many of the mines, where conditions did not allow utilizing of heavier machines, the reconstruction of the existing battery locomotives "4,5 ARP" to operate on a trolley circuit started on a local level, without any serious precautions of mine safety.

Due to the need of light trolley locomotives and availability of free unused battery machines with mass of 4,5 tons, the team of the Research and Development Department for mine equipment to the UMG "St. Ivan Rilski" decided to develop a practical and inexpensive trolley locomotive on the base of the existing battery "4,5 ARP" (fig.1).

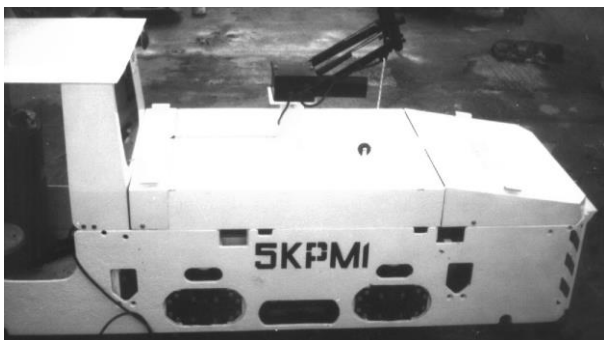


Figure 1.

The following tasks have to be solved:

1. According to the requirements of Safety Guide for operation with a trolley circuit.
  - 1.1. Availability of a cab for the motorman.
  - 1.2. Light signaling – headlight in the direction of moving and a red light in the opposite direction.
  - 1.3. Sound signaling – mechanical and electrical.
  - 1.4. Trolley
  - 1.5. Safe mechanical and electro-dynamical brake.
  - 1.6. Ensuring the necessary visibility in both directions.
2. Ensuring the necessary mass of cohesion since the accumulator battery is liquidated.
3. Adjusting the electrical equipment in conformity to its operating on trolley circuit.

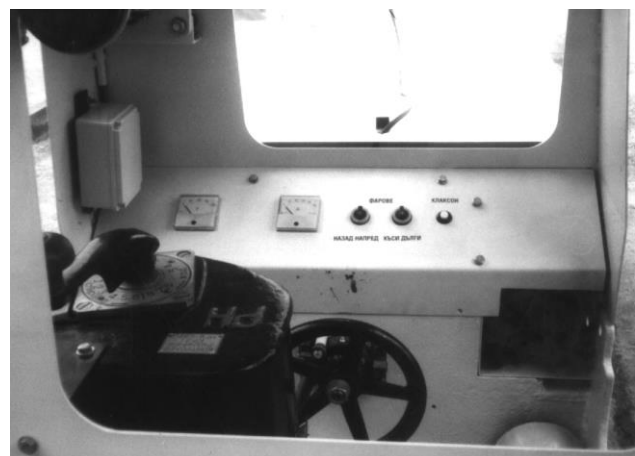


Figure 2.

The cabin (the superstructure) was designed and produced by six millimeter sheet. It is provided to be fastened to the frame by six bolts and if necessary to be in position to be easily removed. On the front and the rear side there are apertures and supports for fastening of the two headlights and the rear

lights, as well. On the front side is situated the control panel (fig.2).

There are an amper-meter and a voltmeter, which read respectively the current supply to the motors and the voltage of the circuit. There also are the different control switches for headlights and the horn. In the cabin a place is envisaged for the main switch and the voltage transformer, supplying the auxiliary devices.

To provide the necessary illumination of the road, a normal duty headlight was engineered on the basis of the optical element of VAZ 2103 automobile. The headlight is cased in aluminum alloy and it is composed by three parts – front one, in which the optical element is situated, body and rear lid. Into it a 24 volts 50/55 W bulb with two lights is mounted, which allows besides the choice of illumination of the road, also a duplicate/spare light in occasion of burning out of one of the lights.

The sound signaling is fulfilled by a mechanical bell and an electrical horn.

The trolley is similar to those used into the Russians trolley locomotives K7 and K10. Keeping in mind the small room and the higher manoeuvre ability of the machine, some changes are developed. A construction was engineered (fig.3) with only one electrically removable arm and lightened frame.



Figure 3.

Current supply is completed by an aluminium slider, and current is derived by an appropriate flexible conductor to a shoe gear.

The mechanical brake of the locomotive does not sustain any change. A very safe and convenient electro-dynamic brake is incorporated. For that purpose, the engines are set to a generating (braking) regime, and the operation is fulfilled by the controller of the locomotive driver.

Removing the battery bucket the visibility from the cabin becomes excellent and it complies with all requirements.

The ensuring of necessary cohesive mass at the release of the batteries was accomplished in the following way. A 30 millimeters thick steel plate was placed on the bottom of the cabin. The compartment for the starting resistors in the front part of the locomotive was filled with metal waste and was poured with concrete. The basic part of the extra mass was ensured by a specially prepared bucket (fig.4) It was also filled with metal waste and was poured with concrete. This was the way to be provided a cohesive mass of about 5000 kg.



Figure 4

The electrical equipment of the locomotive went through corrections in the realization of several tasks:

1. Operating on trolley circuit at significant variations of the incoming voltage.
2. Improving the operation of the locomotive in motoring and braking regime.
3. Increasing the traction possibilities and velocity of the locomotive.
4. Ensuring a stable and safe voltage for the auxiliary electrical consumers.
5. Increasing the exploiting safety of the electrical equipment.

At the trolley circuits there always exists a loss of voltage, for which compensation the voltage at the traction station increases with 20-30%. Practically, current supply of the circuits, in which locomotives "4,5 ARP" are operating, reach up to 140-150V.

The engines of these machines are designed for 80V. When voltage is increased to more than 100V, they suddenly get

worse due to the commutation of the collector and they rapidly fail.

To solve that problem and increasing the haulage and speed abilities of the locomotive, haulage motors type "EDR-7P" were amended. There were mounted two additional poles to compensate the electrical armature reaction. The rig tests done figure the following:

1. The motor remains with dark commutation at voltage 150-160 V.
2. The motor operates stable and without sparking at nominal capacity at higher velocity and higher voltage.

The consequence of introducing the additional poles is not only a considerable improvement of the commutation at higher voltages, but also increasing by 20-30% the power of the motor at the respective voltage amplification.

The battery locomotive "4,5 ARP" operates by the Russian controller of the type "GR-9M". The last ensures only seven stages for accelerating the locomotive and controlling the speed.

For improving the operation control and providing a convenient electro-dynamical brake a controller of the type "KP-1" was applied to the trolley locomotive. The controller was produced at the Research and Development Department for mine equipment. Additionally two diodes "D161-250/10" were mounted to decrease the commutation of the contacts. This controller possesses eight haulage positions and seven braking positions, as it ensures very stable operation for all modes.

The starting and restraint resistors were recalculated according to the new electromechanical characteristics of the motors. There were laid resistors of the type "BR-1", shared by heavy locomotives K7 and K10. The alteration of the degrees leads to smoother accelerating of the locomotive and helps the efficiency of the electro-dynamical brake.

A stabilizer-voltage transformer from 130V to 24V with power capacity 200W was specially invented for the current supply of the auxiliary electric consumers. It provides a stable outgoing voltage at variation of the incoming one within 40%.

The reconstruction of the motors "DR-7П", by introducing the additional poles, the laying of the controller "KR-1" and the changed starting and restraint resistors increase significantly the exploitation security of the particular elements and of the locomotive in overall.

With the so described changes, the locomotive "5KPM1" was created in the Research and Development Department for mining equipment. All functional tests, at which the machine showed satisfactory parameters, were performed there.

The locomotive was delivered in 2000 to "Lucky-Gorupso" Co where it has been operating since. The reports from the mining management are that the locomotive has excellent parameters and high exploitation safety. For the last mentioned there is a fact that speaks for itself, that until this moment it operates free of failures.

In 2002, after a request of the management of the "Lucky-Gorupso" Co two other locomotives were reconstructed, which are operating in the mine at the moment.

*Recommended for publication by Department of  
Electrical Engineering, Faculty of Mining Electromechanics*

## ABOUT THE TEMPERATURE REGIME OF AN INDUCTION MOTOR, SUPPLIED BY A CONTROLLED INVERTER

**Konstantin Trichkov**

University of Mining and Geology "St. Ivan Rilski"  
Sofia 1700, Bulgaria

**Boriana Petrova**

University of Mining and Geology "St. Ivan Rilski"  
Sofia 1700, Bulgaria

### ABSTRACT

The heating of the induction motor that aggravates its frequency control is a subject of this article. With a view the motor to be used to the highest degree when it runs in a preset frequency range, some possibilities for an optimization of the motor construction are examined.

### FORMULATION OF THE PROBLEM

The modern means of the induction motors control put a number of new problems about the losses in the motor and its heating. The value and the frequency variations in the supply voltage within very large limits require the formulation of a larger criterion of the loss optimization in the copper and the steel. As it is known in [1], when the induction motor is supplied with a rated voltage with a constant and unchanging frequency, the optimal designing requires, if the load is rated, the losses in the copper and the steel to be with close values. If the motor concerned is supplied by a controlled inverter, works in a steady-state regime and the rotation frequency is low, the heating balance changes considerably. On the one hand the losses in the steel of the motor decrease considerably, as they are approximately proportional to the square of the frequency. The square of the current, which depends on the frequency and on the value of the supply voltage, that is also liable to control, determines the losses in the copper. On the other hand, when the rotation frequency is low, the ventilation deteriorates, which leads to deterioration of the cooling, unless an independent fan is used. Consequently, in the case in question, a reevaluation of the constructionally determined losses in the motor is necessary with a view to its better use in the whole control range. In the analysis of the so put question, the maximum enhancement of the motor possibility, more exactly the mechanical work accomplished for a long period of time with different settled rotation frequencies, is accepted for criterion. Besides in this article the efficiency of the rectifier - inverter - motor system is not accepted as an additional criterion, i.e. the optimum power effectiveness of the system is not sought.

### FORMULATION OF THE OPTIMIZATION PROBLEM

The heating balance of the stator is expressed with the following formula  $P_{st} + P_{cop} = P_{cool}$ , where  $P_{st}$  and  $P_{cop}$  are the losses in the steel and the copper, and  $P_{cool}$  is the power

emitted as a result of the cooling. The frictional losses are deliberately less and they have to be ignored.

As it is known in [2] if the approximation is greater, the formulas will be the following:  $P_{st} = K_{st} \cdot U^2 \cdot f^2$  and  $P_{cop} = K_{cop} \cdot I^2$ , where  $K_{st}$  and  $K_{cop}$  depend on the motor construction.

At first the case, when an independent external fan accomplishes the cooling of the motor, will be examined and consequently  $P_{cool} = \text{const}$  does not depend on the variable frequency  $f$  of the supply voltage. In the case in question the motor can be used much better especially when the lower frequency limit value is low.

The following formula about the current can be determined with a sufficient precision from the equivalent circuit of the induction motor [2] (when the sliding is normal):

$$I = \frac{U f_n}{U_n f} I_n, \text{ where the index "n" means the rated}$$

values of the quantities.

When a substitution in the equation about the heating balance is accomplished the following formula comes out:

$$U^2 = \frac{f^2 P_{cool}}{K_{st} f^4 + K_{cop} \frac{f_n^2}{U_n^2} I_n^2}$$

The torque of the motor, when the voltage is  $U$  and the frequency  $f$ , is determined by the equation:

$$M = M_n \frac{U^2 f_n^2}{U_n^2 f^2}.$$

Because of the small value of the sliding, when the operation is normal, it can be accepted that  $f_2 \approx f_1$  and the mechanical power is:

$$P_{mec} = 2\pi f_1 M = 2\pi M_n \frac{U^2 f_n^2}{U_n^2 f^2}$$

If it is accepted that all of the frequencies  $f$  of the steady-state regime in the range between  $f_{min}$  and  $f_{max}$ , are equally possible, the motor will produce maximal mechanical work "A"

during a definite long period of time. It may happen if

$$A = \int_{t_1}^{t_2} P_{mec} dt = Max, \text{ where } (t_2 - t_1) \text{ is the service life.}$$

After some transformations the following problem can be formulated: an induction motor has to operate with different, equally possible frequencies in the range between  $f_{min}$  and  $f_{max}$ . It is based on a prototype of an induction motor with preset rated characteristics. What changes about the values of the factors have to be constructionally realized in order the following equation to be observed?

$$J = \int_{f_{min}}^{f_{max}} \frac{f P_{cool}}{K_{st} f^4 + K_{cop} \frac{I_n^2 f_n^2}{U_n^2}} df = Max.$$

### SOLUTION OF THE PROBLEM

When the overall dimensions are determined, the correlation between the cross-sections of the magnetic cores and the windings can vary. Let the cross-section of the

magnetic cores changes a little, for example  $S_{st} = \frac{S_{stn}}{1 + \epsilon}$ ,

where  $|\epsilon| \ll 1$ . With a first approximation it can be accepted that the total cross-section of the winding will receive opposite, by nature, change  $S_{cop} = S_{cop}(1 + \epsilon)$ , which leads to a relevant change in the cross-section of each conductor  $S_{con} = S_{con,n}(1 + \epsilon)$  when the number of the windings is the same. These changes affect on the factors  $K_{st}$  and  $K_{cop}$  in the following way. When the magnetic flux is constant, the magnetic induction "B" changes as follows  $B = B_n(1 + \epsilon)$ . As a result the losses in the ferromagnetic material change per unit of weight –  $P_{st} = P_{st,n}(1 + \epsilon)^2$ . On the other hand the overall weight of the magnetic core "G" changes as

well  $G = \frac{G_n}{1 + \epsilon}$ . Therefore the losses in the steel are

determined by the following equations:  $P_{st} = P_{st,n}(1 + \epsilon)$  or

$$K_{st} = K_{st,n}(1 + \epsilon). \text{ By analogy}$$

$$K_{cop} = \frac{K_{copn}}{(1 + \epsilon)}$$

It is necessary the value of  $\epsilon$  to be determined so as the equation  $J = Max$ , to be realized.

After integrating and differentiating in respect of the value  $(1 + \epsilon)$ . The derivative is reduced to zero. As a result the following formula comes out:

$$\epsilon_{max} = \frac{f_n^2}{f_{max} \cdot f_{min}} \sqrt{\frac{P_{copn}}{P_{st}}} - 1$$

The same result comes out assuming that the magnetic core is with preset parameters, but the number of the windings "w" changes. Let this number for the initial motor be "w<sub>0</sub>". In case of a new value "w" and when all of the overall dimensions are the same, the magnetic induction has got a new

value  $B = B_0 \frac{w_0}{w^2}$ . The losses in the copper depend on the

resistance R of the winding:

$P_{cop} = R \cdot I^2$ . This resistance depends on the number w of windings through both the overall length  $l = l_1 \cdot w$  and the cross-

section of the conductor  $S_{con} = \frac{\Delta}{w} K_l$ , where  $l_1$  is the average length of a winding and  $\Delta$  is the total cross-section of

the coil. Therefore  $P_{cop} = P_{cop0} \frac{w^2}{w_0^2}$ . As a result, when

the motor construction is instant, the values of the losses in the steel can increase x-times through a relevant change in the numbers of the windings and the losses in the copper decrease approximately x-times i.e. if  $P_{st} = x P_{st0}$ , then

$$P_{cop} = \frac{1}{x} P_{cop0}.$$

### CONCLUSIONS

The results obtained are achieved on the basis of some approximate suppositions. Nevertheless they correctly reflect the tendency, that has to be observed during the designing with a view to the improvement in the use of the motor. The equations shown above, also afford an opportunity an optimization to be sought when some irregular distributions of the frequencies are expected during the service life. That has been accomplished on the basis of prognosis suppositions.

### REFERENCES

- Костенко, М. П., Л. М. Пиотровский. Электрические машины – ч. I и ч. II, Энергия, 1973
- Ангелов, А., Д. Димитров. Електрически машини – част I., С., Техника, 1976 г.

## INVESTIGATION AND ESTIMATION OF HIGHER HARMONICS IN POWER NETWORK OF CHARGE STATION IN UNDERGROUND COAL MINE "IVAN ROUSEV"

**Nikolai Genadiev**

University of Mining and Geology  
"St Ivan Rilski"  
Sofia 1700, Bulgaria

**Velisar Bagarov**

University of Mining and Geology  
"St Ivan Rilski"  
Sofia 1700, Bulgaria

### ABSTRACT

Electricity consumption of electrical transport with accumulator electrical locomotives is about 10% of the total electricity consumption. The total installation capacity of charging stations on thyristor devices is commensurable with the capacity of charging transformer. Amplitudes of higher harmonics in electricity supply network of underground charging station in mine "Ivan Rousev" are measured. Measurements are realized by using of the network analyser Multiver – 3SN. An attempt for analytical calculation of influence of non-linear load of the charging stations on the other consumers is made.

### INTRODUCTION

One of the quantity indexes of electrical energy (BDS 10694-80) is the coefficient of non-sinusoidality of current or voltage, that express degree of distortion of current or voltage sinusoid. The maximal legitimate value is 5%. Distorted sinusoid could be presented as a sum of regular sinusoids with determined frequency, amplitude and initial phase, which are termed harmonic components or higher harmonic of the current or voltage.

An occasion for appearance of higher harmonic is presence of electrical consumers with non-linear current-voltage characteristic. Charging stations for accumulator locomotives are this kind of consumers because are constructed of thyristor converters. Electricity consumption in charging stations is about 10% of the total consumption.

### OBJECT OF INVESTIGATION AND DATA FROM EXPERIMENT

In mine "Ivan Rousev" are constructed two charging stations- one underground and one overground. Because of technological reasons experimental measurement is made in overground charging station. The charging devices in both stations are the same. The value of current higher harmonic generated from one charging device is measured. The value of higher harmonic in underground station with n working charging devices and its influence on the rest consumers in the network are estimated on the base of obtained results. Only the harmonics of current are measure. The voltage harmonics are different for overground and underground

stations because of different capacity of power transformers that supply the charging device. Electricity supply of underground charging system is realized by a sectional transformer substation (STS) with TKШБП-180 кVA, located near the substation and electricity supply of overground charging station is made by transformer station with transformer TM-750 кVA.

STS "Underground charging station" supplies also two drainage pumps and a fan. One-linear circuit of electricity supply of consumers is shown on fig. 1 and data for installed powers age given in table 1

Table 1. Data about consumers.

| Kind of consumer | Quality | Power<br>кW | cosφ |
|------------------|---------|-------------|------|
| ЗУК155/230/У5    | 7       | 15          | 0,76 |
| Pump             | 2       | 5,5         | 0,86 |
| Fan              | 1       | 5,5         | 0,86 |

Using electrical analyser Multiver - 3SN we made the record of levels of higher harmonic, generated from a current charging device. Measurements results show, that in the network are generated higher harmonics only with numbers 5 and 7 and their percentage concerning the main (first) harmonic is given in table 2.

Table 2. Values of measured and calculated currents.

| $I_{изм}, A$ | $I_1, A$ | $I_5, \%$ | $I_7, \%$ |
|--------------|----------|-----------|-----------|
| 42,35        | 34,95    | 42        | 18,8      |

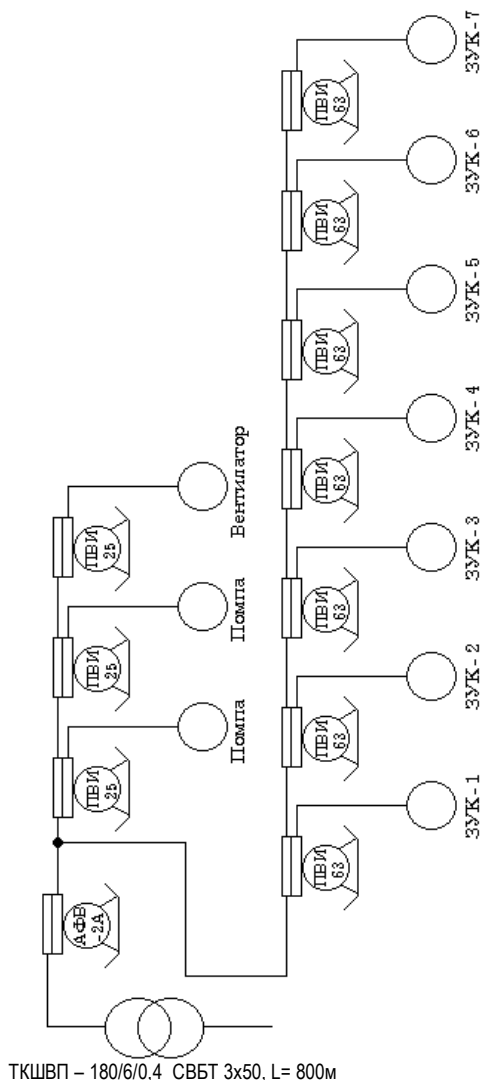


Figure 1. One-linear circuit of STS "Underground charging station".

CALCULATIONS OF COEFFICIENT OF NON-SINUSOIDALITY BY ANALYTICAL METHOD (E. DANKOV, 1991)

Using the obtained results and data about electrical network and consumers in underground charging station is calculated the degree of distortion of voltage sinusoid.

This is made for the most unfavourable real variant when three charging device and three induction motors are working simultaneously, as well as for theoretical variant when seven charge devices are working.

The equivalent circuit of the electrical network is constructed for this purpose and is shown on fig. 2 (for the first variant).

The coefficient of non-sinusoidality is determined by formula (E. Dankov, 1991):

$$K_{nc} = \frac{\kappa_{\psi} \cdot \kappa_d \cdot I_n \cdot x_e \cdot \sqrt{n_v}}{U_n} \cdot 100, \% \quad (1)$$

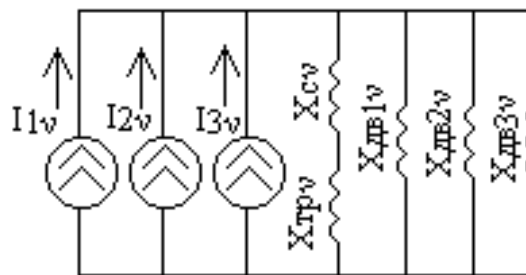


Figure 2 Equivalent circuit of the electrical network for v harmonic.

where:

- $\kappa_{\psi} = 0,9$  – is the coefficient, that gives non-coincidence of phases of the harmonics;
- $\kappa_d = 1,3$  – coefficient of presence of abnormal harmonics;
- $I_n$  – sum of nominal current of valve converters, A;
- $x_e$  – equivalent resistance of the electrical system,  $\Omega$ ;
- $U_n$  – nominal linear voltage of the network, V;
- $n_v$  – number of serial harmonics, in which the coefficient of non-sinusoidality is determined ( $n_v=2$ );

Obtained from calculations results are given in table 3.

Table 3. Calculated values of inductive resistances of the network and coefficient of non-sinusoidality.

| $X_c, \Omega$ | $X_{TP}, \Omega$ | $X_{ДВ}, \Omega$ | $X_e, \Omega$ | $K_{nc}, \%$ |
|---------------|------------------|------------------|---------------|--------------|
| 0,005         | 0,028            | 2,1              | 0,0314        | 1,74         |

The coefficient of non-sinusoidality 4,14 % is obtained as a result of calculation for the second variant with seven simultaneously working charge devices.

DETERMINATION OF ADDITIONAL LOSSES AND ACTIVE POWER CAUSED BY HIGHER HARMONICS.

Higher harmonics cause considerable damages as a result of: increase of losses of active power and energy, wearing and ageing of electrical isolation.

Additional loss of power in the windings of induction motors and transformer, caused by higher harmonics are determined by the formula (E. Dankov, 1991):

$$\Delta P = 3 \sum_{v=3}^n I_v^2 \cdot R_v \quad (2)$$

where:  $I_v$  – is the effective value of the current of v harmonic;  
 $R_v$  – active resistance for the v harmonic.

$$R_v = R \cdot \sqrt{v} \quad (3)$$

$R$  – is active resistance of the main harmonic.

Results from calculation of active resistance of the network elements and losses of active power, caused by the fifth and seventh harmonic and total losses by higher harmonics are given in table 4 and table 5.

Table 4. Calculated values of active resistances of the motors, transformer and equivalent of the network for 5 and 7 harmonic.

|             | Harmonic number |         |        |
|-------------|-----------------|---------|--------|
|             | 1               | 5       | 7      |
| $R_{дв.в}$  | 3,11            | 6,95    | 8,23   |
| $R_{тр.в}$  | 0,00427         | 0,00955 | 0,0113 |
| $R_{экв.в}$ | -               | 0,00955 | 0,0113 |

Table 5. Losses of active power caused by 5 and 7 harmonic and total losses from harmonics.

| $\Delta P_5, W$ | $\Delta P_7, W$ | $\Delta P_{\Sigma}, W$ |
|-----------------|-----------------|------------------------|
| 55,57           | 1,545           | 57,02                  |

#### DETERMINATION OF VOLTAGE OF N HARMONIC

The following formula is used for determination of levels of higher harmonics of the voltage (N. Vasilev 1991):

$$U_v = I_v \cdot Z_v, \quad V \quad (4)$$

$Z_v$  – impedance of the electrical network v harmonic,  $\Omega$ ;

$$Z_v = \sqrt{R_v^2 + X_v^2}; \quad X_v = K_x \cdot X_2 \cdot v \quad (5)$$

$K_x$  – coefficient of influence of surface effect of the current;  
 $X_2$  – inductive resistance of the negative sequence,  $\Omega$ ;

Calculation results for inductive and total resistance of network elements concerning 5 and 7 harmonic and the value of harmonics on voltage are given in table 6.

Table 6. Calculation results for  $X_v$ ,  $Z_v$  and  $U_v$ .

|                          | Harmonic number |       |       |
|--------------------------|-----------------|-------|-------|
|                          | 1               | 5     | 7     |
| $X_{2\text{дв.}} \Omega$ | 2,37            | -     | -     |
| $X_{2\text{тр.}} \Omega$ | 0,031           | -     | -     |
| $X_{дв.в} \Omega$        | -               | 9,24  | 12,94 |
| $X_{тр.в} \Omega$        | -               | 0,137 | 0,174 |
| $Z_{дв.в} \Omega$        | -               | 11,56 | 15,34 |
| $Z_{тр.в} \Omega$        | -               | 0,137 | 0,174 |
| $Z_{\Sigma.в} \Omega$    | -               | 0,132 | 0,168 |
| $U_v, V$                 | -               | 5,29  | 3,32  |

Using the obtained results for higher harmonics on voltage is calculated the coefficient of non-sinusoidality by the voltage of higher harmonics.

$$K_{hc} \approx \frac{\sqrt{\sum_{v=2}^7 U_v^2}}{U} \cdot 100, \quad \% \quad (6)$$

$$K_{hc} \approx \frac{\sqrt{(5,29)^2 + (3,32)^2}}{380} \cdot 100 \approx 1,64 \%$$

The difference 0,1% between values of  $K_{hc}$ , determined by classical method (table 3) and by the voltage of higher harmonics (when working three charge devices) allow to consider that the precision of obtained results is high. The coefficient of non-sinusoidality of the voltage when 7 charging devices are working simultaneously, calculated in the mentioned above method is 3.99%, i.e. the error is about 4 % concerning the analytical method and it is in the admissible norms.

#### CONCLUSIONS

1. Form calculations considered in the report is seen that when both with three and with seven working simultaneously charging device the harmonics of voltage do not exceed the admissible norms of standard BDS 10694 – 80, i.e. the charging station is designed according to the standard BDS concerning  $K_{hc}$ .
2. Initiated power losses, caused by higher harmonics are insignificant comparing with the power, consumed in underground charging station.
3. In mines except the charging stations there are another power consumers of electrical energy with non-linear current-voltage characteristic as some lifting devices, contact electrical locomotives etc. and their influence on the rest consumer and coefficient of non-sinusoidality of the voltage should be estimate.

#### REFERENCES

- Vasilev, N., Siderov, 1991. "Electricity supply of industrial enterprises.", S."Technika".
- Dankov, E., 1991. "Electricity supply of mining enterprises", S. "Technicka".
- Siderov, S. 1999 "Handbook in Energetics" Editor Prof. Ph.D. S. Stoyanov, v. 6, S. "ABC Technika".
- BDS 10694-80, Norms for Quality indexes of electrical energy of receivers.

## SYSTEM OF ENERGY MANAGEMENT OF ELECTRICITY CONSUMPTION IN THE CONCENTRATION PLANT "ELACITE MED"

**Velizar Bagarov**

University of Mining and Geology  
"St. Ivan Rilski"  
Sofia 1700, Bulgaria

**Jordan Stojanov**

University of Mining and Geology  
"St. Ivan Rilski"  
Sofia 1700, Bulgaria

### ABSTRACT

The concentration plant "Elacacite med", situated in the village of Mirkovo, has yearly consumption about 270 millions tones. About 30% of the cost price of production are used for payment of electrical energy. Since 2000 in the plant works a system for control and reading of electricity consumption. The system is developed and is introduced by the collective from the UMG "St. Ivan Rilski" under the guidance of Prof. M. Menteshhev.

On the base of the gained experience from exploitation of this system in this report are made proposals for expansion the ranges of utilisation of the available data. It is proposed to create a data base of generalised indexes and daily analysing of obtained results of specific energy consumption for a tone processed ore, for average night and day value of energy consumption in typical workshops and for the whole plant.

### GENERAL PRINCIPLES FOR BUILDING OF ENERGY MANAGEMENT SYSTEM

An energy management system in a plant is build in order to decrease the expenses for consumed energy. Decrease of the expenses is made in two ways: using the opportunities of rate for payment of electrical energy and by increasing of energy effectiveness.

Before development of the energy management system in particular plant it is necessary to make the energy odit (investigation). Energy odit is made in order to decrease quickly and effective the expenses for energy bearers and abstain from the unwarranted expenses for implementation of non-effective activities.

The results of energy odit could stay on the paper if a system of energy management (control system of energy resources) with corresponding responsibilities, rights and obligations of the participants, ways of financing and estimation of results is not created.

The aim on present development is to help the governing body of the "Elacite med" to decrease the expenses of energy consumption by using of opportunities of rate for payment of electrical energy. A part of proposed activities are carried out in the concentration plant, but are not controlled strictly every day. This opportunity exists because the automated system for control and reading of energy consumption works in the plant.

### ANALYSIS OF THE ENERGY CONSUMPTION OF CONCENTRATING PLANT "ELACITE MED"

The analysis of the energy consumption is made on the base of the written data by the control system of energy consumption. A year period of energy consumption is investigated. Data, read by the microprocessor system, are grouped in some units:

- "ELCAITE MED" – read values for the bushings "Murgana" and "Galabets" (110 kV) are summed and it is the whole energy consumption and financial expenses of the concentrating plane;
- MAIN CORPUS - read values for the terminals Main corpus I and II (6 kV) are summed;
- WATER AND WASTE DEPARTMENT – read values of terminals Pump Station I and II and terminal "Kalievo" (20 kV) are summed;
- CCT – the values of terminals CCT I, II and III (6 kV) are summed.

The values of the consumption of active energy and expensed for payment in three-phase zones, workshops and total plant for selected year are given in table 1. The prices of electrical energy are 0.076 lv/kW – daytime and 0.016 lv/kWh night-time and 0.112 lv/kWh –peak energy.

The biggest consumer of electrical energy is the Main corpus, where is concentrated the greatest part of production – grinding, regrinding, flotation, compression and drying. The Main corpus consumes 77.7% of the year active energy. Other consumers are the workshop CCT (12.4%) and Water and waste department (9.42 %). The rest Workshops of the plant consume very little part (0.46%) what means that

attention of the control and activities to consumption decrease should be paid on the workshops situated in the Main corpus, CCT and Pump Stations.

During treated period were consumed about 12 000 thousand tones ore, that means the specific consumption of electrical energy is 23.21 kWh/ton. The average consumption of electrical energy is 0.076 lv/kWh.

Table 1. Consumed electrical energy and expenses

|                   |                        | "Elacite med" | Main Corpus | CCT   | Water and waste dept. |
|-------------------|------------------------|---------------|-------------|-------|-----------------------|
| Electrical energy | Total Thous.kW/h       | 278 547       | 216 447     | 34586 | 26 228                |
|                   | peak energy Thous.kW/h | 66 111        | 3 697       | 6 829 | 5 194                 |
|                   | Daytime Thous.kW/h     | 116 033       | 89 933      | 14616 | 10 955                |
|                   | Night-time Thous.kW/h  | 96 403        | 72 817      | 13141 | 10 079                |
| Expenses          | Total Thous.lv         | 21 316        | 16 736      | 2 549 | 1 926                 |
|                   | peak energy Thous.lv   | 8 066         | 6 551       | 833   | 634                   |
|                   | Daytime Thous.lv       | 8 819         | 6 835       | 1111  | 833                   |
|                   | Night-time Thous.lv    | 4 431         | 3 30        | 605   | 459                   |

In a selected month are processed 997 thousands tones ore and is read consumption 23 167 000 kW/h which means the specific consumption is 23.23 kWh/ton. The average price of consumed electrical energy is 0.076 lv/kWh.

In table 2 are shown the daily quantities processed ore, daily consumption of electrical energy and achieved daily specific consumption. According to the expectation the greatest specific consumption 25.07 kWh/ton is achieved in a day with minimal quantity of processed ore, and the smallest specific consumption is achieved in a day with approximately maximal consumption. The difference between the maximal and minimal specific consumption is about 3 kWh/ton.

Table 2. Achieved specific consumption of energy

| Day | Processed ore, Ton/day | Electrical energy, kWh/day | Specific consumption, kWh/ton |
|-----|------------------------|----------------------------|-------------------------------|
| 1   | 30 727                 | 770 332                    | 25,07                         |
| 2   | 33 047                 | 742 163                    | 22,45                         |
| 3   | 35 300                 | 791 943                    | 22,43                         |
| 4   | 32 829                 | 764 037                    | 23,27                         |
| 5   | 31 004                 | 732 767                    | 23,63                         |
| 6   | 30 986                 | 727 021                    | 23,46                         |
| 7   | 35 063                 | 787 000                    | 22,44                         |

|               |         |          |       |
|---------------|---------|----------|-------|
| 8             | 34 443  | 765 079  | 22,21 |
| 9             | 33 583  | 757 194  | 22,54 |
| 10            | 34 440  | 775 077  | 22,50 |
| 11            | 33 446  | 783 705  | 23,43 |
| 12            | 30 453  | 762 951  | 25,05 |
| 13            | 31 618  | 761 602  | 24,08 |
| 14            | 32 072  | 786 803  | 24,53 |
| 15            | 34 516  | 799 616  | 23,16 |
| 16            | 34 611  | 773 684  | 22,35 |
| 17            | 34 524  | 782 609  | 22,66 |
| 18            | 34 018  | 785 128  | 23,08 |
| 19            | 33 258  | 790 412  | 23,76 |
| 20            | 33 027  | 790 016  | 23,92 |
| 21            | 32 169  | 815 905  | 24,89 |
| 22            | 33 051  | 783 843  | 23,72 |
| 23            | 32 305  | 736 274  | 22,79 |
| 24            | 33 953  | 765 191  | 22,54 |
| 25            | 33 687  | 779 157  | 23,13 |
| 26            | 33 815  | 775 649  | 22,94 |
| 27            | 34 915  | 787 247  | 22,55 |
| 28            | 33 618  | 760 531  | 22,62 |
| 29            | 33 462  | 776 106  | 23,19 |
| 30            | 33 127  | 757 854  | 22,88 |
| Average       | 33 236  | 772 230  | 23,23 |
| Month indexes | 997 067 | 23166900 | 23,23 |

When about 30 000 tones ore are processed it should be calculated that the daily consumption increases with about 100 000 kWh, respectively the expenses increases with 7 600 lv/day.

For the month period are processed the schedules for every day and the daily energy consumption and average price of consumed electrical energy are calculated. The average indexes, days with maximal and minimal energy consumption and days with achieved maximal and minimal price of consumed electrical energy are determined. Obtained results are given in table 3.

Table 3. Achieved average price of energy consumption

|                          | "Elacite med"  | Main Corpus    | CCT           | Water and waste dept. |
|--------------------------|----------------|----------------|---------------|-----------------------|
| Average consump. kWh/day | 795 554        | 612 968        | 77106         | 101 485               |
| Average price lv/kWh     | 0,07654        | 0,07739        | 0,07474       | 0,07233               |
| Maximal consump. kWh/day | <u>838 134</u> | <u>633 268</u> | <u>95 223</u> | <u>117 433</u>        |
| Min.cons. kWh/day        | <u>744 277</u> | <u>563 367</u> | <u>53 213</u> | <u>73 409</u>         |
| Price lv/kWh             | 0,07648        | 0,07754        | 0,07601       | 0,06708               |

|                     |                |                |                |                |
|---------------------|----------------|----------------|----------------|----------------|
| Max.price<br>lv/kWh | <u>0,07848</u> | <u>0,07951</u> | <u>0,08017</u> | <u>0,08839</u> |
| Consump.<br>KWh/day | 750 238        | 609 320        | 74 359         | 97 643         |
| Min.price<br>lv/kWh | <u>0,07477</u> | <u>0,07641</u> | <u>0,06969</u> | <u>0,06451</u> |
| Consump.<br>KWh/day | 768 780        | 582 935        | 80 004         | 91 236         |

Analysis of the data shown in table 3 show that because of near regular load schedule of the Main corpus, the average daily price of consumed electrical energy in "Elacite med" varies with  $\pm 2.5\%$ . Variation of the average daily price in CCT is from  $+7.2\%$  to  $-6.8\%$ , and in Water and Waste department from  $+22.2\%$  to  $-10.9\%$  from the average prices. The explanation is that in these workshops are made purposeful activities for consumption in zones with lower prices of electrical energy. The missing of dependencies between achieved prices and daily-consumed quantity of electrical energy shows that these activities are not made strictly every day.

From the made analysis follows that it is necessary to build a system for energy management, which first to observe every day the following indexes:

1. Achieved specific consumption for the last day and night.
2. Achieved average price of consumed electrical energy for the last day and night separately for the workshops CCT and for Water and Waste department and for the whole plant.

#### **Proposals for improvement of energy management in "Elacite med"**

The analysis of consumption of electrical energy shows that main attention should be paid on the daily maximal loading of mills in the Main corpus.

It is necessary to improve the work organisation in the workshop CCT and to estimate the opportunities for turning off during the evening peak. The same concerns to the pump stations. There compulsory should be made turning off during the evening peak and the aim is part of daily consumption to be made in the night.

For this purpose is necessary every day to print and analyse the data for energy consumption of these workshops in the time of morning and evening peaks separately and to calculate the average prices of consumed electrical energy in workshops. The achieved specific consumption for passed day should be calculated for the whole plant.

It is necessary to make these calculations every day in order to analyse objectively the reasons for eventual successes or unsuccesses, because after the time the real conditions are forgotten.

Using of program product EXCEL at the energetic department should preserve the following data:

1. Date (day and night)
2. Produced quantity of concentrate.
3. Processed ore
4. Consumed electrical energy, kWh
5. Expenses for payment of the consumed energy, lv.
6. Consumed electrical energy by the three zones, total by the plant, by the Main corpus, by CCT and by Water and waste department, kWh.
7. Expenses for payment of consumed electrical energy by the mentioned above days, lv
8. Achieved specific cost of consumed electrical energy during the day and night, total for the plant, for Main corpus, for CCT and for Water and waste department, lv/kWh.

Analysis and prognosis of electrical energy processes could be made using these data in the future.

## ENERGY ABSORPTION RATE AT THE MECHANICAL TREATMENT OF SPECULARITE FROM BULGARIAN DEPOSITS

Raina Vucheva

University of Mining and Geology "St. Ivan Rilski"  
Sofia 1700, Bulgaria

### ABSTRACT

Following an appropriate mechanical treatment, the specularite can serve for the manufacture of anticorrosion lacquer coatings. This ability of it is due to the flaky structure of the ground material. This presentation examines the effect of some basic parameters of the process on the energy absorption rate at the mechanical treatment of specularite on horizontal discs. The topical importance of the presentation is substantiated by the considerable amounts of specularite in Bulgarian deposits.

The specularite from the Kremikovtsi deposit has a flaky structure. The flake thickness is many times less than that of the known MIO, which is used in the chemical industry for the production of quality anticorrosion lacquers. The Kremikovtsi specularite has a very pleasant reddish colour with metallic lustre that makes it very much desired for such use. It is necessary to find a method and a regime of grinding, where the fragile thin film will be kept intact.

In order to determine the possibilities for grinding up to the qualities wanted by the chemical industry for the finished product - in terms of grain size, flaky structure and cost-effectiveness - were conducted a number of experimental investigations.

In a special test bench - a horizontal plate on which a grinding roll moves - were conducted laboratory examinations. The independent parameters were:

- The process speed:  $v = 40.2 \times 10^{-3}$  m/s. This velocity can be obtained by means of one of the standard movement drives of the slide of a combination lathe.
- The grinding roll diameter - D in mm. Rolls having diameters D = 150 mm, 200 mm and 250 mm were used. The main experiments were conducted with a D = 200 mm roll.

- The particles to be ground were selected by their typical size from 1 mm to 10 mm. No crushing was obtained with some of the particles measuring 7 and 10 mm at the adopted regimes.
- Tensioning of the rolls over the ground particles. Such tensioning was obtained by changeable weights from  $G = 243$  N to  $G = 773$  N.

To evaluate the results from the grinding were carried out sieve analyses of the finished product. At almost all the regimes the sieve analysis showed that, as far as the granulometric composition was concerned, the finished product satisfied the anticorrosion lacquer manufacturers. An analysis by microscope was carried out, too, on the condition of the flakes in the finished product.

To determine the energy absorption rate, being the principal technical and economic parameter at similar processes, were carried out measurements and some specific energy consumption rates were found (Fig.1). As is evident from the figure, the respective areas correspond to the energy put into the the crushing of the single grains. The total energy consumed for the grinding of 1 g of finished product was determined -  $E_{og}$ , J/g. The losses at the bench and the net energy applied for grinding were measured, too. The results of these measurements are presented diagrammatically.

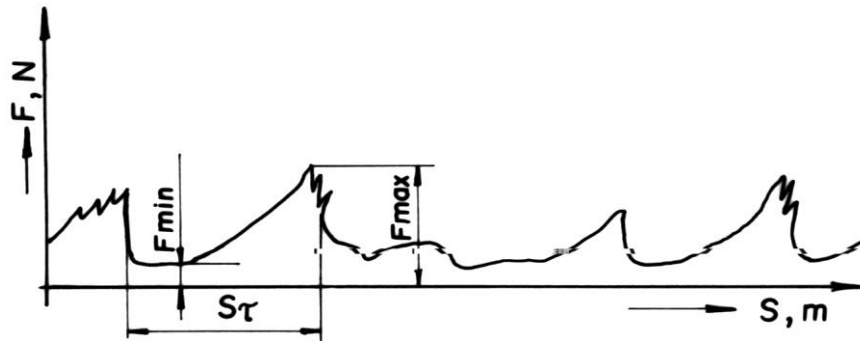


Figure 1.

Fig.2 shows the total energy applied in the comminution of specularite particles having different sizes, depending on the tension  $G$  in  $N$ . As a comparison are shown the results obtained in grinding under the same conditions of different particles of quartz (designated in the figure by  $k$ ). The data on the regime are given in the figure.

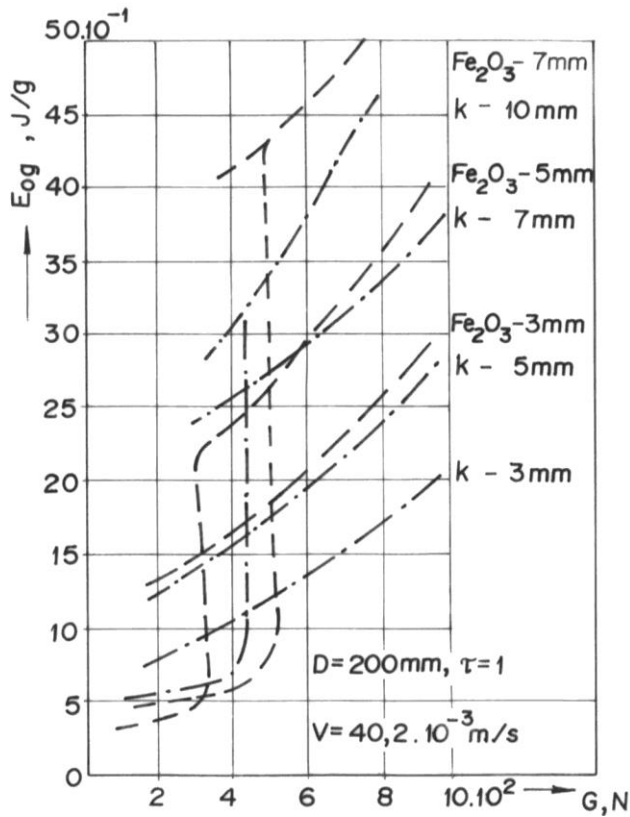


Figure 2.

Fig.3 shows the variation in the total energy applied in crushing specularite particles having different sizes, depending on the tension. The regime data are given in the figure. The vertical tracts of some regimes correspond to the transition from the strain of a particle to its crushing. Here for comparison is also shown the

energy applied for the crushing of quartz particles measuring 7 mm.

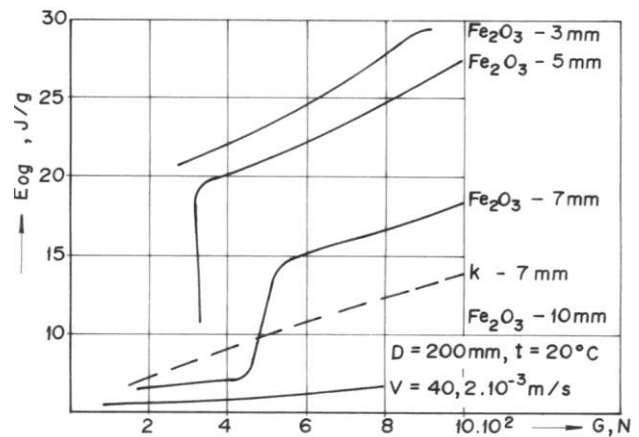


Figure 3.

Fig.4 presents the variation of the same energy, however depending on the grain size of the particles being ground, while Fig.5 indicates the variation of the net crushing energy  $E_{mg}$  depending on the tensioning  $G$  in  $N$ . The regime data and the particle sizes are shown in the figures themselves.

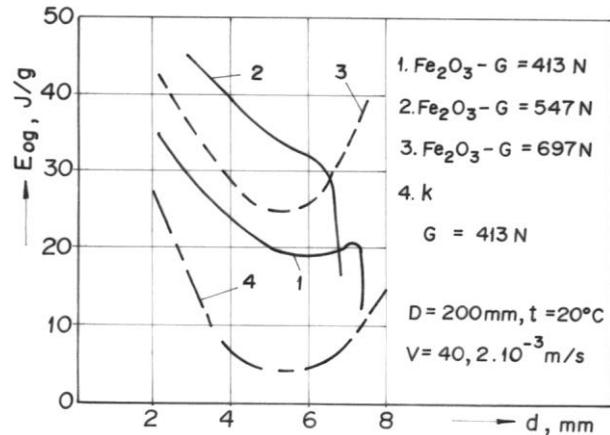


Figure 4.

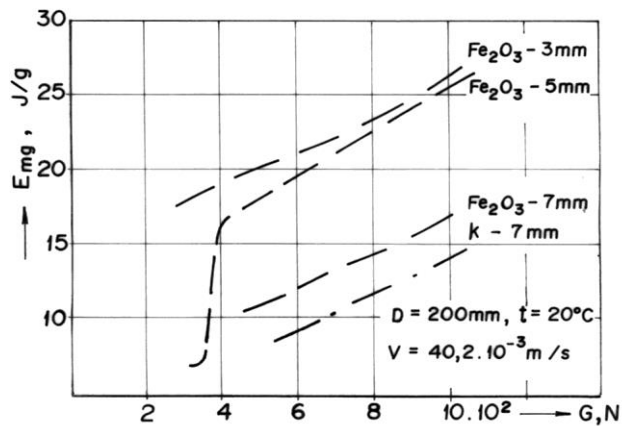


Figure 5.

To determine the flaky structure of the ground specularite were carried out investigations by microscope. It turned out that with all the regimes the flakes were crushed in over 60% of the ground material. This parameter is the most important one with such kind of materials, because it is known that its anticorrosion properties depend on the deposition of the flakes one on top of the other.

The following conclusions can be made as a result of the investigation:

1. The grinding of specularite from the Kremikovtsi deposit to a grain size as required by the chemical industry for the manufacture of anticorrosion lacquers by means of rolls is possible.
2. The regimes of the grinding process, as well as the consumed energy, are comparable with the same parameters in grinding other mineral resources.
3. The flakes of over 60% of the particles are broken as a result of the grinding. Such material is of a relatively low quality.
4. Other technologies should be employed for the production of high quality specularite aggregate from the Kremikovtsi deposit, where the single flakes will be segregated without being broken.

## REFERENCES

- Höfl, K., 1985, Zerkleinerungs und Klassiermaschinen VEB Deutscher Verlag für Grundstoffindustrie Leipzig.
- Höfl, K., Kolberg, L., Bauer, L., 1974, Beitrag zur Untersuchung von Kegelrollenmühlen, *Neue Bergbautechnik* 4.
- Irmer, K., Folgner, Th., Höfl, K., 1982, Untersuchung zur Klinkermahlung auf Wälzmühlen, Freib.Forsch.-H.A.685.

Recommended for publication by Department of Electrical Engineering, Faculty of Mining Electromechanics

## FAILURES OF THE POWER SUPPLY SYSTEM OF OPEN – AIR MINE "HRISTO BOTEV" OF MINES "BOBOV DOL" Ltd.

**Tzanko Georgiev**

Technical University, Faculty of Automatics  
Sofia 1756, Bulgaria,  
E-mail: [tzg@vmei.acad.bg](mailto:tzg@vmei.acad.bg)

**Todor Varbev**

University of Mining and Geology "St. I. Rilski"  
Sofia 1700, Bulgaria,  
E-mail: [vat@mail.mgu.bg](mailto:vat@mail.mgu.bg)

### ABSTRACT

This article deals with safety analysis of the electrical power supply systems in open - air mine "Hristo Botev" of the mines "Bobov dol" – Ltd.. The data of failures are collected and investigated for a two years time period. The failures by reason of events are classified. All statistical researches are carried out using **MATLAB** and **STATGRAPHICS** packages.

### INTRODUCTION

The open – air mine "Hristo Botev" is one of the important mines of the company "Bobov Dol" – Ltd. that exploited the coal field basin of the "Bobov Dol" area. This open – air mine includes three sections that are denoted as I<sup>st</sup> (first), II<sup>nd</sup> (second) and III<sup>rd</sup> (third).

The power supply of these sections is independent and is realized by air supply lines with conductors of type AS installed on lattice towers. The first section receives power supply from the substation "Mlamovo" by air electric power line with 6 kV – voltage realized by conductors of type AS 3x35 mm<sup>2</sup> and length of 2000 m.

The second and third sections are connected by power supply from the substation "Babino" by an air electric power line of the same type and voltage. The length of the electric power line of the II (second) section is 2300m and those of the III (third) section is 1500m.

The electric power lines supply same mobile transformer points (MTP) and mobile switching points (MSP). Electric power cable lines from these mobile points (MTP and MSP) supply the loads in the sections.

The data have been collected during the period of twenty three (23) months (about two years) from the message log journals of the substations "Mlamovo" and "Babino" and operating journals of the dispatchers.

Classification of the failures by reason of events is done and months with maximum number of failures are established. The results are: January 2001 – 31 failures, February - 37 failures, August – 35 failure, November – 27 failures, and March 2002 – 29 failures, April – 27 failures, June – 29 failures, August – 32 failures. The maximum numbers of failures classified by section are as follows: Section I – 239 failures, Section II –

173 failures, and Section III with 145 failures or the total number of the failures is 557.

The data analysis includes: investigation of the reasons of the failure events and the types of the protections that after being activated disconnect the power supply of the load sections in the mine.

It could be emphasized that: the single-phase earth – fault protection was operated for total 426 times, which is 76.5% of the total number of operation of the protections. The over – current protection and current segment (over – current without time delay) protection were operated 100 times and 31 times respectively.

The total number of these disconnections is 23.5% of the total number of failure events. It could be said that the unselective switch – off are 90.8% (506 times) of the total number of failures and as it is in other mines in Bulgaria.

The faults of instrumentations are as follows: faults of the junction boxes yield 27 failures, the electrical breakdown of cable lines yield 12 failures, excavator faults are registered 9 times and one is caused by the kit distribution unit (KDU).

### BASIC RESULTS

The results of the statistical analysis are obtained by STASTGRAPHICS package STATGRAPHICS (1996). Table below shows the estimates of the population parameters as follows.

Table 1. Summary statistics

|                     |          |
|---------------------|----------|
| Count               | 23       |
| Average             | 24,2174  |
| Median              | 23,0     |
| Geometric mean      | 23,1742  |
| Variance            | 49,4506  |
| Standard deviation  | 7,03211  |
| Standard error      | 1,4663   |
| Minimum             | 12,00    |
| Maximum             | 37,00    |
| Range               | 25,0     |
| Coeff. Of variation | 29,0374% |
| Sum                 | 557,0    |

Frequency tabulation is used for preliminary investigation of the population distribution of the failure sample. The results are represented in Table 2.

Table 2. Frequency tabulation of the failures.

| N <sup>o</sup> | Lower limit | Upper limit | Midpoint | Frequency |
|----------------|-------------|-------------|----------|-----------|
|                | -∞          | 10,0        | 0        | 0         |
| 1              | 10,0        | 15,0        | 12,5     | 3         |
| 2              | 15,0        | 20,0        | 17,5     | 4         |
| 3              | 20,0        | 25,0        | 22,5     | 5         |
| 4              | 25,0        | 30,0        | 27,5     | 6         |
| 5              | 30,0        | 35,0        | 32,5     | 4         |
| 6              | 35,0        | 40,0        | 37,5     | 1         |
|                | 40,0        | ∞           | 0        | 0         |

Table 2. Continuation.

| N <sup>o</sup> | Relative Frequency | Cumulative frequency | Cum. Rel. frequency |
|----------------|--------------------|----------------------|---------------------|
|                | 0,000              | 0                    | 0,000               |
| 1              | 0,1304             | 3                    | 0,1304              |
| 2              | 0,1739             | 7                    | 0,3043              |
| 3              | 0,2174             | 12                   | 0,5217              |
| 4              | 0,2609             | 18                   | 0,7826              |
| 5              | 0,1739             | 22                   | 0,9565              |
| 6              | 0,0435             | 23                   | 1,0000              |
|                | 0,0000             | 23                   | 1,0000              |

Frequency histogram is shown in Fig.1 based on results from table 2.

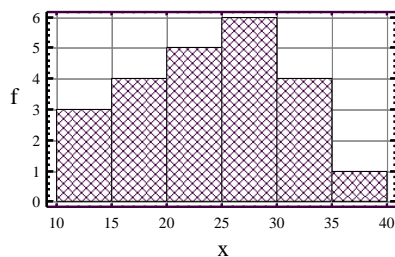


Figure 1. Histogram of the failures.

The labels in figure are: **x** – number of the failures, **f** – frequency of the failures.

It could be assumed from the preliminary calculation of the parameters by Bekeron (1975) and the shape of the histogram that the failure data comes from normal distribution, gamma or Weibull distributions.

Two tests are run to determine whether the variable of the failures can be adequately modeled by a normal distribution, gamma or Weibull distributions.

The chi-square test divides the range of the investigated variable into nonoverlapping intervals and compares the number of observations in each class to the number expected based on the fitted distribution. The Kolmogorov-Smirnov test computes the maximum distance between the cumulative distribution of the variable and the CDF (cumulative distribution function) of the fitted theoretical distribution. In this case, the following P – values are derived:

- Normal Distribution,  
Kolmogorov-Smirnov test  $P[\lambda] = 0,108506$ ,  
Pearson test  $P[\chi^2] = 0,903116$  ;
- Gamma Distribution,  
Kolmogorov-Smirnov test  $P[\lambda] = 0,11685$ ,  
Pearson test  $P[\chi^2] = 0,799386$  ;
- Weibull Distribution,  
Kolmogorov-Smirnov test  $P[\lambda] = 0,110309$ ,  
Pearson test  $P[\chi^2] = 0,319974$  .

Probability density functions are represented as follows:

- Normal Distribution,  

$$f(x) = \frac{1}{\sigma\sqrt{2\pi}} \cdot e^{-\frac{(x-\mu)^2}{2\sigma^2}}$$

where  $\mu$  is mathematical expectation (population mean),  $\sigma$  is standard deviation ;

- Gamma Distribution  

$$f(x) = \frac{\lambda^k \cdot x^{k-1}}{\Gamma_k} \cdot e^{-\lambda x}$$

- Weibull Distribution  

$$f(x) = a \cdot b^{-a} \cdot x^{b-1} \cdot e^{-\left(\frac{x}{a}\right)^b}, x \geq 0,$$

where  $a$  is scale parameter , and  $b$  is shape parameter of the distribution.

Probability density functions of discussed distribution are shown if Figs. 2,3 and 4.

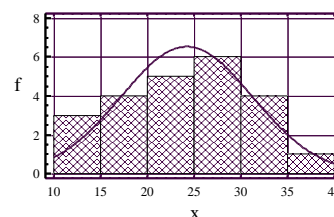


Figure 2. Approximation fit of the normal distribution.

The parameters of the distribution are:  $\mu=24,2174$ ,  $\sigma=7,03211$ .

The labels in figures are:  $x$  – number of the failures,  $f$  – frequency of the failures.

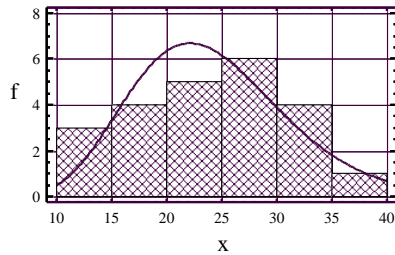


Figure 3. Approximation fit of the gamma distribution.

The parameters of this distribution are:  $\lambda=0,475705$ ,  $k=11,5203$ .

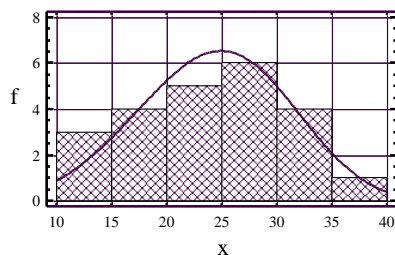


Figure 4. Approximation fit of the Weibull distribution.

The parameters of the distribution are:  $a=26,7817$ ,  $b=3,98877$

## CONCLUSIONS

The following conclusions could be drawn so far:

1. The lack of information about “unselective switches” is difficult problem for data analysis of the power supply system.
2. The largest number of the failures appears in the first section it is 239 failures or 42.9% of the total failure number.
3. The earth – fault protection is operated in 75% of the total failure number. This fact shows that the problems are due to some equipment element such as cable lines, distribution boxes, junction boxes, switching points, mobile switching point et. s.
4. The summary statistics are obtained based on the failure sample.
5. The P –value ( $P(\chi^2) = 0,903116$ ) of the chi-square test shows that the population distribution is normal with 90% confidence interval. The additional investigation of the data will reveal the usability of the other derived distributions.
6. The result from this investigation shows that the design problems of the equipment units are very important for the reliability of the power supply system.

## REFERENCES

- Magnugistics Inc., Statgraphics, User Guide, 1996.  
 Bekerov P. G., Methods of the data analysis of statistical information for reliability of the mining power supply systems, I, M., M., 1975 (in Russian)

Recommended for publication by Department of  
 Electrical Engineering, Faculty of Mining Electromechanics

## SAFETY ANALYSIS OF THE POWER SUPPLY SYSTEMS IN OPEN-AIR MINES OF BULGARIA

**Todor Varbev**

University of Mining and Geology "St. I. Rilski",  
Sofia 1700, Bulgaria,  
E-mail: vat@mail.mgu.bg

### ABSTRACT

This article deals with comparative safety analysis of the open – air mines in Bulgaria. The data of failures are collected and investigated for a long time period. Classification of failures by reason of events is presented. Distribution functions of the failures are estimated and compared. All statistical researches are carried out using **MATLAB** and **STATGRAPHICS** packages

The power supply systems of the mines are important element in structure of the industrial mining companies. Both the normal technological process and the breakdown situations depend on the safety work of these systems.

This article deals with failure analysis of the power supply systems of the open – air mines "Chucurovo", "Hristo Botev" and "Kremikovci". The first two enterprises mine coals and the third enterprise mines iron crude ore and supplies the metallurgical engineering company (having the same name), and is a structure element of this company.

The electrical power supply systems on these enterprises are similar as a type. The loads are supplied with electrical power by a general reception point denoted as general mining substation (GMS). The national power supply system is connected with the GMS by its primary high voltage side. The connection of the GMS for each mine is built as follows: substation "Babino" supplies the mine "Hristo Botev" by electrical power line with 110kV voltage, substation "Taygova" supplies the mine "Kremikovci" by the same type electrical power line. The substation "Chukurovo" is connected by electrical power lines of 35 kV and 20Kv voltage, which is risen by voltage step-up transformer to 35 kV voltages.

The loads of mines are supplied by a longitudinal scheme of connection with radial located electrical air power lines with 6 kV voltages. They are realized by conductors of type AS.

The electrical power lines of the mine transform into electrical air power lines with conductors type Cu and they supply the mobile switching points and mobile transformer points. The loads are supplied by cable lines with 6 kV or 0,4 kV voltages. The summary data of the air and cable electrical power lines are shown in Table 1.

Table 1

| LineType<br>Company | Air el. line      |                                    | Cable line     |                                    | Total length<br>km |
|---------------------|-------------------|------------------------------------|----------------|------------------------------------|--------------------|
|                     | Leng<br>th,<br>km | Type<br>Section<br>mm <sup>2</sup> | Length<br>, km | Type<br>Section<br>mm <sup>2</sup> |                    |
| "Chukuro<br>vo"     | 11,4<br>1         | AS-90                              | 3,5            | FEC-16                             | 14,91              |
| "Hr.Botev<br>"      | 5,80<br>0         | AS-35                              | 7,7            | FEC-16                             | 13,500             |
| "Kremiko<br>vci"    | 9,31<br>0         | AS-50                              | 4,740          | FEC-16                             | 14,05              |

The total lengths of the electrical power supply systems for the three mines are approximately equal. The electrical air supply lines of the mines "Chukurovo" and "Kremikovci" have length of 76,5% and 66,3% of the total length respectively.

The number of the main loads, which make the basic mining and dump formation, is uniform in these enterprises. Mines have following equipment:

- Mine "Chukurovo" – 14 excavators and 7 drillings rig of different types.
- Mine "Hrosto Botev" – 14 excavators and 6 drillings rig of different types.
- Mine "Kremikovci" - 12 excavators and 4 drilling rigs.

The terminals of the mines are as follows:

- Mine "Chukurovo" (I) – 6 terminals.
- Mine "Hrosto Botev" (II) 3 terminals.
- Mine "Kremikovci" (III) –5 terminals.

The data of failures are collected for different periods of the discussed enterprises. The statistical analysis is done by the software package STATGRAPHICS (1996). The basic sample parameters are obtained for all data collections (Varbev et. al.; 2001; Varbev et. Al. ; 2003; Georgiev et. Al. 2003).

Table 2 shows length of the time period, number of the failures, average  $\bar{X}$ , variance  $D$  and standard deviation  $S$ .

Table 2

| Mine          | Period, month | Failures    | Mean $\bar{X}$ | Variance, D | Standard deviation, S |
|---------------|---------------|-------------|----------------|-------------|-----------------------|
| "Chujur ovo"  | 48(60)        | 2502 (1437) | 52,125         | 535,984     | 23,1513               |
| "Hr.Botev"    | 23            | 557         | 24,2174        | 49,4506     | 7,03211               |
| "Kremik ovci" | 24(48)        | 519 (1156)  | 24,625         | 74,1576     | 8,61148               |

The investigation of this type was done more over 30 years ago. The results from this investigation are published in (Anev G. 1974) and may be compared with the results from this article. It could be seen that the number of the failures from the mine "Chukurovo" is increased while in the mine "Kremikovci" this value is approximately equal for the both investigations.

The articles (Varbev et. al.; 2001; Varbev et. al.; 2003; Georgiev et. al. 2003) analyze the failures, reasons of the operation of protections.

In mine "Chukurovo" the over – current protection have operated 56,53% times and single – phase earth – fault protection have operated 46,47%.

In mine "Hristo Botev" the over – current protection have operated 23,5% times and single – phase earth – fault protection have operated 76,5%. In mine "Kremikovci" the operation of the protections are: over – current protection have operated 34% times and single – phase earth – fault protection have operated 55%.

The both protections have operated in 11% of the events. Same important safety parameters of the power supply systems are estimated too. These parameters are: frequency of the failures  $\omega$ ; time between the failures  $T_{II}$ ; time of the restore of the power supply  $T_B$ ; coefficient of condition of a system  $K_{\Gamma}$ ; coefficient of the idle time  $K_{\Pi}$ .

These coefficients are calculated as follows Rosanov M.,(1987):

$$\omega = \frac{m}{n \cdot T}, \text{ year}^{-1};$$

$$T_{II} = \frac{8760}{\omega} \text{ hour};$$

$$T_B = \frac{1}{m} \sum_{i=1}^m t_i \text{ hour};$$

$$K_{\Gamma} = \frac{T_{II}}{T_{II} + T_B};$$

$$K_{\Pi} = \frac{T_B}{T_{II} + T_B},$$

where:  $m$  – number of the failures,  $n$  – number of the similar observable elements;  $T$ -time interval of the observation of events (years);  $t_i$  – time of the restore of power supply network at  $i$  – failure.

The results are represented in Table 3.

Table 3. Safety coefficients .

| Mine | $\omega(y^{-1})$ | $\omega_1$ | $T_{II}$ (h) | $T_B$ (min)    | $K_{\Gamma}$ | $K_{\Pi}$ |
|------|------------------|------------|--------------|----------------|--------------|-----------|
| I    | 625.5            | 3.469      | 14.0         | 73.91 (1h14m)  | 0.919        | 0.0809    |
| II   | 290.56           | 1.794      | 30.15        | 81.40 (1h22m)  | 0.9569       | 0.04306   |
| III  | 259.5            | 1.539      | 33.75        | 224.05 (3h44m) | 0.90014      | 0.09986   |

Failures of the three enterprises are compared by the frequency of the failures per unit length of the supply line obtained by the formula

$$\omega = \frac{m}{nL \Delta t}, \text{ failures / km.month.}$$

where:  $L$  – total length of the electrical power supply (see Table 1.);  $\Delta t$  – time period (months)

The derived data are represented in Table 3. The frequencies of the failures  $\omega$  and  $\omega_1$  are maximum number of the mine "Chukurovo". These frequencies are approximately equal for the mines "Hristo Botev" and "Kremikovci" but are two times less than failures in the mine "Chukurovo".

This fact is expressed by the time between the failures  $T_{II}$ . This time for the mine "Chokurovo" approximately two failures per 24 hours and over one failure per 24 hours for the other mines.

It could be seen from Table 3 that in the first two enterprises the failures are repaired for equal time, while for the mine "Kremikovci" this time is three times long. This fact gives influence to the coefficients  $K_{\Gamma}$  and  $K_{\Pi}$ .

The distribution of the failures is derived for the three investigated enterprises and the probability density functions are represented in (Varbev et. al.; 2001; Varbev et. al.; 2003; Georgiev et. al. 2003). The following distributions are obtained: for the mine "Chukurovo" the failures are described by the Gamma distribution. For the mine: "Kremikovci" the distribution of the failures is Normal or Weibull with significant values of the Kolmogorov test and test of the Pearson  $\lambda$  and  $\chi^2$ . For the mine "Bobov Dol" the possible choice is between the distributions Normal, Weibull and Gamma, ordered by the values of the test in decreasing sequence.

The following conclusion could be drawn so far:

1. It is difficult to analyze failure reasons in the power supply system because there is lack of the information about "unselective switches".

2. The great part of the failures appears after operation of the single – phase earth – fault protections for the mines “Hr. Botev” and “Kremikovci” while in mine “Chukurovo” the operations of the over - current protection and earth – fault protection are equal one to each other.
3. It could be emphasized for the above conclusions that the equipment of the power supply system as: cable lines, distribution boxes, junction boxes, switching points, mobile switching point, is a serious reason for the safety operation of the system.
4. The basic estimates of the summary statistics parameters are derived for the discussed mines after 30 years lack of statistical investigations.
5. It could be said that for the estimate of the failures distributions for the mines “Bonov Dol” and “Kremikovci” the additional investigation could be done.

## REFERENCES

- Magnugistics Inc., Statgraphics, User Guide, 1996.
- Varbev T., Tz. Georgiev, Failure Analysis of the Electrical Power Supply System of the Open – Air Mine, Vi – National Conference with Foreign Participations of Open Air Mining of Mineral Resources, Nesebar, 2001, pp. 373 – 378.
- Varbev T., Tz. Georgiev, P. Petkova, Data Failure Analysis Of Power Supply System In Mine “Kremikovtzi” Georgiev Tz. ,Varbev T., , Failurs Of The Power Supply System Of Open – Air Mine “Hristo Botev” Of Mines “Bobov Dol” Ltd. Anev G., Investigation of power supply networks of the open - air mines in Bulgaria and design of the safety equipments, Thesis for the “Doctor of Science” degree, Sofia, 1974 ( in bulgarian).
- Rosanov M., Safety of the Power supply Systems, Tehnika, 1987 (in bulgarian),

*Recommended for publication by Department of  
Electrical Engineering, Faculty of Mining Electromechanics*

## DATA FAILURE ANALYSIS OF POWER SUPPLY SYSTEM IN MINE "KREMIKOV TZI"

**Todor Varbev**

University of Mining and Geology  
"St. I. Rilski"  
Sofia 1700, Bulgaria  
E-mail: vat@mail.mgu.bg

**Tzanko Georgiev**

Technical University  
Faculty of Automatics  
Sofia 1756, Bulgaria  
E-mail: tzg@vmei.acad.bg

**Petay Petkova**

Municipality "Studentska"  
Sofia 1700, Bulgaria,

### ABSTRACT

This article deals with safety analysis of the electrical power supply systems in mine "Kremikovtzi". The data of failures are collected and investigated for a two years time period. Classification of failures by reason of events is presented. All statistical researches are carried out using **MATLAB** and **STATGRAPHICS** packages.

The power supply systems are important key subsystem in the structure of the industrial manufacturing companies and also in mines. The mine "Kremikovtzi" is one of basic enterprises that feed with the crude the metallurgical engineering company "Kremikovtzi". The safety of the mine power supply system is of fundamental precondition for carrying out the continuous technological process and feeding the metallurgical company with crude ore.

The mine power supply system is mixed type using air and cable lines. The electric power supply of the mine is connected with the substation "Taygova" by 6kV voltage. The national power supply system is connected with 110kV - voltage of the primary side of substation "Taygova". The mine includes two distribution substations denoted as "DS1" and "DS2". The substation "Taygova" by same air electric power lines denoted as "Mine 1", "Mine 2", "Shaft" and "Tower" supplies these distribution substations.

Lattice towers and conductors of type AS-150 with total length of 8600m build up the electric power lines. The substation "DS1" supplies the loads in the mine by radial scheme with air electrical power lines denoted as "3", "4" and "5". This substation by other terminals "8" and "9" supplies the waste banks and embankment of the mine.

The substation supplies the loads of the "mine drainage shaft" and mine drainage complex of the mine. The loads that work on the east side of the mine and goods railway station are supplied by the (air) terminal "13".

The air electrical supply lines that supply the load in the mine are two types: stationary and mobile. The stationary part of the power supply lines are built up by conductors of type AS-50 while mobile electrical lines is built up by conductors of type M-16. These electrical power lines supply the mobile transformer points and the mobile switching points. The mobile supply points are connected with the loads of the mine, excavators with 6kV voltage and drilling rids, and pumps with 0,4 kV voltage, and supply these components of the technological process. The total length of the cable lines and

air lines, coming out from the substations "DS1" and "DS2" is 14,05 km.

The investigation is done for the period 1.09.2000 - 1.09.2002 (two years). The data are collected from the message log journals of the substations "DS1" and "DS2", which apply the electrical power system of the mine.

The total number of failures of the investigated period is 591 failures classified by substation as: for "DS1" they are 382, and for the "DS2" – 209 failures. The data are represented in Table 1.

Table 1. Failures of the substations "DS1" and "DS2".

| Month | Year | Failures | Terminal | Failures |
|-------|------|----------|----------|----------|
| 09    | 00   | 26       | N°3      | 123      |
| 10    | 00   | 26       | N°4      | 42       |
| 11    | 00   | 38       | N°5      | 142      |
| 12    | 00   | 15       | N°8      | 27       |
| 01    | 01   | 18       | N°9      | 48       |
| 02    | 01   | 40       | N°13     | 153      |
| 03    | 01   | 25       | Pump N°1 | 7        |
| 04    | 01   | 30       | Pump N°2 | 0        |
| 05    | 01   | 34       | Pump N°3 | 6        |
| 06    | 01   | 34       | Pump N°4 | 1        |
| 07    | 01   | 29       | Pump N°5 | 0        |
| 08    | 01   | 20       | Pump N°6 | 24       |
| 09    | 01   | 30       | Pump N°7 | 1        |
| 10    | 01   | 15       | Pump N°8 | 17       |
| 11    | 01   | 30       |          |          |
| 12    | 01   | 6        |          |          |
| 01    | 02   | 27       |          |          |
| 02    | 02   | 19       |          |          |
| 03    | 02   | 29       |          |          |
| 04    | 02   | 27       |          |          |
| 05    | 02   | 13       |          |          |
| 06    | 02   | 11       |          |          |
| 07    | 02   | 21       |          |          |
| 08    | 02   | 28       |          |          |
| Сума  | -    | 591      |          |          |

The table shows that the maximum number of failures are obtained from the terminals "13", "5", and "3", and they are 153, 142 and 123 respectively. These numbers of the failures are 70,73% from the total number of the failures. The maximum

number of the failures was recorded in February 2001, and the minimum number of the failures was recorded in December 2001. The failures are recorded in other nine terminals but its number is less than 30% of the total number of the failures. The failures are not met for the terminals "Pump №2" and "Pump №3". The next table shows the reasons of the operation of protection for a one year period. The results are: the over – current protection was operated 199 times or 34%, while the single– phase earth – fault protection was operated 329 times or 55% of the total number of failures.

Table 2.

| N°  | Protection operation                            | 9.00 – 8.01r | 9.00 – 8.02r | Брой |
|-----|---|--------------|--------------|------|
| I   | Over-current protection                         | 148          | 51           | 199  |
| 1   | Short connection in junction box                | 6            | 4            | 10   |
| 2   | Short connection in cable separation            | 1            | -            | 1    |
| 3   | Lightning storm                                 | -            | -            | -    |
| 4   | Unselective switches                            | 138          | 47           | 185  |
| II  | Earth–fault protection                          | 160          | 169          | 329  |
| 1   | Short connection in junction box                | 15           | 11           | 26   |
| 2   | Short connection in cable separation            | 1            | 2            | 3    |
| 3   | Lightning storm                                 | -            | -            | -    |
| 4   | Unselective switches                            | 144          | 156          | 300  |
| III | Over-current protection, Earth–fault protection | 27           | 36           | 63   |
| 1   | Short connection in junction box                | 1            | 3            | 4    |
| 2   | Short connection in cable separation            | -            | 1            | 1    |
| 3   | Lightning storm                                 | -            | -            | -    |
| 4   | Unselective switches                            | 26           | 32           | 58   |

The operation of the two protections simultaneously was done 63 times, which is 11% of the total number of failures. The table 2 shows that 543 times (91,88%) the unselective switches are met in set of the failures. This fact presents one of the difficulties of the data analysis. The rest of the failures are classified as follows: "short connection in junction box" - 40 failures, "short connection in cable separation" – 4 failures and 3 failures are from "lightning storm".

The statistical analysis is done by software package STATGRAPHICS (1996). The results from the analysis is represented in Table 3.

Table 3. Summary statistics

|                          |          |
|--------------------------|----------|
| Count                    | 24       |
| Average                  | 24,625   |
| Median                   | 26,5     |
| Geometric mean           | 22,7809  |
| Variance                 | 75,1576  |
| Standard deviation       | 8,61148  |
| Standard error           | 1,75781  |
| Minimum                  | 6,0      |
| Maximum                  | 40,0     |
| Range                    | 34,0     |
| Coefficient of variation | 34,9705% |
| Sum                      | 519,0    |

Frequency tabulation is used for preliminary investigation of the population distribution of the failure sample. The results are represented in Table 4.

Таблица 4. Frequency tabulation of the failures.

| No                   | Class         | M.P.    | Frec. | Wi                           | Frec. | ΣWi    |
|----------------------|---------------|---------|-------|------------------------------|-------|--------|
| 0                    | -∞-0          |         | 0     | 0,0000                       | 0     | 0,0000 |
| 1                    | 0-8,333       | 4,1667  | 1     | 0,0417                       | 1     | 0,0417 |
| 2                    | 8,333-16,667  | 12,5    | 4     | 0,1667                       | 5     | 0,2083 |
| 3                    | 16,667-25,0   | 20,833  | 5     | 0,2083                       | 10    | 0,4167 |
| 4                    | 25,0-33,333   | 29,1667 | 10    | 0,4167                       | 20    | 0,8333 |
| 5                    | 33,333-41,667 | 37,5    | 4     | 0,1667                       | 24    | 1,0000 |
| 6                    | 41,667-50,0   | 45,833  | 0     | 0,0000                       | 24    | 1,0000 |
| 7                    | 50,0-∞        |         | 0     | 0,0000                       | 24    | 1,0000 |
| Mean Value = 24,6225 |               |         |       | Standard deviation = 8,61148 |       |        |

Frequency histogram is shown in Fig.1 based on results from table 4.

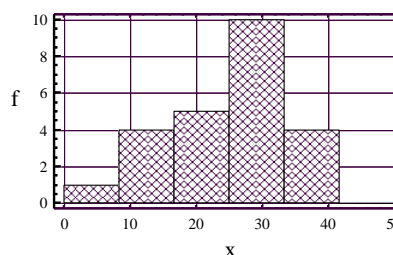


Figure 1. Histogram of the failures.

The labels in figure are: **x** – number of the failures, **f** – frequency of the failures.

It could be assumed from the preliminary calculation of the parameters by Bekerov (1975) and the shape of the histogram that the failure data comes from normal distribution, gamma or Weibull distributions.

Two tests are run to determine whether the variable of the failures can be adequately modeled by a normal distribution, gamma or Weibull distributions.

The chi-square test divides the range of the investigated variable into nonoverlapping intervals and compares the number of observations in each class to the number expected based on the fitted distribution. The Kolmogorov-Smirnov test computes the maximum distance between the cumulative distribution of the variable and the CDF (cumulative distribution function) of the fitted theoretical distribution.

In this case, the following P – values are derived:

- Normal Distribution,
  - Kolmogorov-Smirnov test  $P[\lambda] = 0,679416$ ,
  - Pearson test  $P[\chi^2] = 0,586082$  ;
- Weibull Distribution,
  - Kolmogorov-Smirnov test  $P[\lambda] = 0,658172$ ,
  - Pearson test  $P[\chi^2] = 0,586082$  .

Probability density functions are represented as follows:

$$f(x) = \frac{1}{\sigma\sqrt{2\pi}} \cdot e^{-\frac{(x-\mu)^2}{2\sigma^2}},$$

where  $\mu$  is mathematical expectation (population mean),  $\sigma$  is standard deviation .

The following estimates are obtained  $\mu = 24,625$ ;  $\sigma = 8,61148$  . The distribution is represented in Fig.2 based on the derived estimates

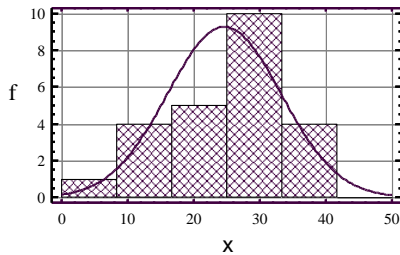


Figure 2.

The probability density functions of the Weibull distribution is

$$f(x) = a \cdot b^{-a} \cdot x^{b-1} \cdot e^{-\left(\frac{x}{a}\right)^b}, x \geq 0,$$

where  $a$  is scale parameter , and  $b$  is shape parameter of the distribution.

The estimates of the parameters are :  $a = 27.4534$ ;  $b = 3.32119$ .

Probability density functions of discussed distribution is represent in Fig. 3.

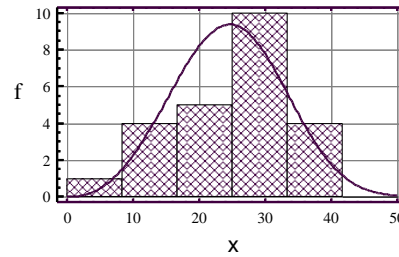


Figure 3.

The labels in figures are:  $x$  – number of the failures,  $f$  – frequency of the failures.

### CONCLUSIONS

The following conclusions could be drawn so far:

1. The lack of information about “unselective switches” is a difficult problem for data analysis of the power supply system.
2. The great part of the failures appears after operation of the earth – fault protection. This fact shows that the problems are due to some equipment element such as cable lines, distribution boxes, junction boxes, switching points, mobile switching point et. s.
3. The P – values show that two probability distributions are possible. The exact estimation of the distribution could be establishes on the next step of the investigation based on the long data sample.
4. The result from this investigation shows that the design problems of the equipment units are very important for the reliability of the power supply system for example junction boxes, cable separation boxes et. s.
5. The summary statistics parameters are calculated and investigated.

### REFERENCES

- Magnugistics Inc., Statgraphics, User Guide, 1996.  
 Bekerov P. G., Methods of the data analysis of statistical information for reliability of the mining power supply systems, I, M.,M, 1975 (in Russian)

Recommended for publication by Department of Electrical Engineering, Faculty of Mining Electromechanics

## STRUCTURE AND OPERATION OF THE MICROPROCESSOR ANALYZER OF THE ELECTROMAGNETIC COMPATIBILITY OF ELECTRICAL POWER SYSTEMS

**Sider Siderov**

**Nikolay Matanov**

**Borislav Bojchev**

**Vulchan Georgiev**

Technical University of Sofia, Sofia 1756, 8 Kl. Ohridski Blvd., Faculty of Electrical Engineering, Department of Electric Power Supply, Electrical Equipment and Electrical Transport

E-mail:  
ssiderov@tu-sofia.acad.bg

E-mail:  
matanov@bitex.com

E-mail:  
bojchev@tu-sofia.acad.bg

E-mail:  
vulchy@tu-sofia.acad.bg

### ABSTRACT

After analyzing the characteristics of the already existing analyzers manufactured by the leading companies on the market, the authors of this paper have designed a microprocessor analyzer of the electromagnetic compatibility (EMC) of electrical power systems, having nonsinusoidal and unbalance regime of the voltage and current.

The structure and functional capabilities of the designed analyzer are presented in this paper, fully revealing the operating conditions, the measured magnitudes, types of visualization, and e.t.c.

The newly designed analyzer will contribute to the practical applying of the standards of EMC of electrical power systems, currently in use in our country.

### STATUS OF THE PROBLEM OF CHARACTERISTICS CONTROL OF ELECTROMAGNETIC COMPATIBILITY

The basic electromagnetic compatibility (EMC) characteristics which are defined in (БДС EN 61000-40-7; Шидловский и др. 1977; С.Сидеров и др. 2003) are:

- Harmonic ratio of current and voltage components;
- Voltage (Current) total harmonic distortion (THD);
- Normalized THD of inductions and capacitors;
- Form factor;
- Crest factor
- Fundamental factor;
- Voltage psfometric coefficient;
- Unbalance factor;
- Voltage deviation and fluctuation;
- Frequency deviation and fluctuation.

The control and the analysis of these parameters are performing by analyzers of various manufacturers. After comparing these analyzers they can be divided into two groups according to their constructional implementation:

- Autonomous – which are developed as a independent measurement units, containing in them all necessary components for working. Companies such as GOSSEN-METRAWATT GMBH and LEM provide those types analyzers.
- Component – or parts of them are implemented as independent devices with standardized inputs and outputs and they can be configuring whole measurement systems with different facilities. Most often a personal computer is used for data processing, visualization and sometimes for supply. As separate units are offered the following:
  - primary transducers (Signal Conditioning);

- analog-digital transducer (Data Acquisition device) or card for data gathering. There is big variety both of types which offered (PCI, ISA, PCMCIA card extend of personal and portable computers; external devices connected by USB or parallel port to PC) and in technical characteristics;

- Drivers and Application Software; for personal computer

Some of the biggest manufacturers of such devices are the following companies: *National Instruments, Hewlett-Packard, Keithley, Computer Boards*, and e.t.c. Personal Engineering 1998

Comparing their functional abilities and technical characteristics it is obvious that their hardware abilities are almost equally, but the application software of the second group offers various functions of research, control and visualization. Both the groups of analyzers have their practical application. The first type is easily portable and can be used by personal in operation, while the second group is suitable for laboratories and research work.

The necessity for permanent supervision of the parameters of EMC is increased to the introduced European standards and the increasing control of their observance and because of the broad application of devices with nonlinear V-A characteristics in industry, interfering the operation of convectional loads and measurement and controlling systems. Usually the problem of application of specialized systems for parameter evaluating of EMC is their high price. Sometimes it is not very easy to use them in industrial conditions.

Bearing in mind all mentioned above the authors aimed at designing an analyzer, which of the one hand is cheap, suitable for practical application, securing necessary precision for EMC control according the standards currently in use. On

the other hand to give an opportunity of further experiments and research work.

### THE STRUCTURE OF THE ANALYZER

The block diagram of the system is shown on Figure 1. The basic elements of the system are:

#### Primary transducers

The primary transducers are essential part of each system of measuring and analysis of electric magnitudes. Often the precision and the capability of the whole device depend of them. The measured analog signal is transformed by the primary transducers to levels suitable for further analog-digital transformations.

There are high requirements to the primary transducers.

- To provide the required precision- amplitude and current mistake in given tolerance and minimum self noise.
- To provide vast enough range of the measured values – the levels of voltage in electrical supply systems are standardized and along with this the maximum voltage deviation is set to rate. It will allow the voltage transducers to be produced for constant level of 380 Veff. In the same time the primary current transducers should provide measurement in vast range of values, as with this the use of current transformers should be limited because their precision is guaranteed only for low frequencies.

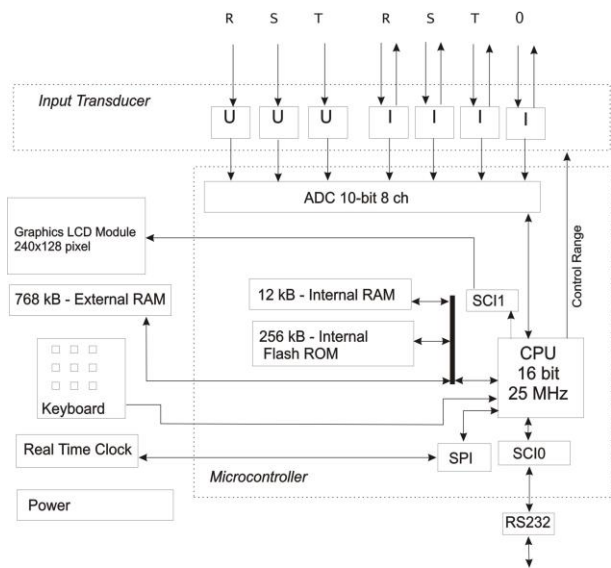


Figure 1. Block diagram of the microprocessor system

- To allow different wiring diagrams – the input transducers should allow measurement of different electrical values in single phase, three phases, DC, symmetrical and asymmetrical electric circuits.
- To provide voltaic diversion between the measurement and the power circuits. That will increase the reliability and the device safety, to give it higher resistance to the inevitable exploitation errors in connecting.
- To be on low price. This condition is often defining in choosing the necessary equipment and scheme design. Dropping down the price would inevitably bring compromise with the other parameters of the system.

**Input current transducers:** There are three basic methods in current measurement:

- Shunt – basically used for DC (there are shunts for AC with minimum inductance). Their basic faults are their big size and the lack of voltaic diversion between the measurement and the power circuits.

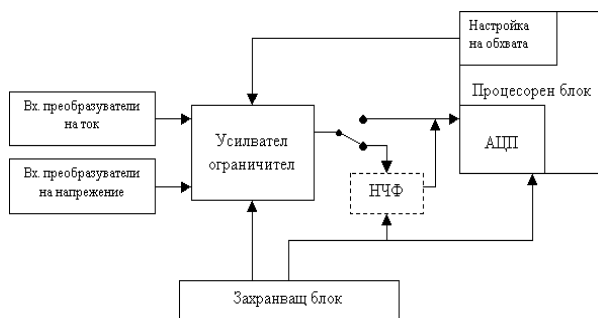


Figure 2. Block diagram primary transducers

- Voltage transformer – the secondary current is proportional to the primary. Usually in digital measurement these transformers work with a small load resistor, which transforms the secondary current to proportional to it voltage. These are the transducers most commonly used for alternating current measurement.
- Devices based on the Hall effect - there are a lot of transducers based on the Hall effect, measuring AC along with DC in very large frequency range.

Most of the manufacturers usually offer the standard transformers and those based on the Hall effect with voltage output 1mV/A, which allows both of them to be used with no change for the rest part of scheme or the algorithm of work.

**Input voltage transducers:** As a result of the fixed level of the primary voltage cheap active separators are produced. The required precision in certain exploitation conditions could be achieved with high stable resistors. Voltaic diversion is realized with linear optrones use because of providing sufficient precision with drawing down the price.

**Amplifier – limiter:** Transforms the input signals to levels suitable for ADT of the processor block. The input signal is increased with 2,5V so that the negative half-wave could be transmitted. The amplitude is limited at 5,1V. The precision is increased by the possibility for digital amplification control.

**Low-pass filter.** The low frequency filter is a-binding part of each system for harmonic analysis. It can be realized like analog, digital or combination of analog and digital and both of the two methods have advantages and disadvantages. The analog filter limits noise of measured signal before its converting into digital. So it can remove irregular peaks that can't be removed from digital filters. According to highly spread opinion analog filters are suitable for fast systems, where they decrease the signal processing time.

An opportunity for using both types filters is provided.

### Microcontroller

The authors looked for following common characteristics by choose of the controller according to the given tasks: good calculate abilities, communicate capabilities (various interfaces); possibility for external addressing according to extended memory; fast enough, multichannel ADC (opportunity for external ADC remain for following development of the analyzer); cheap; enough inputs and outputs with general purpose, often times in electro supply systems performing control function is required and достъпна развойна среда.

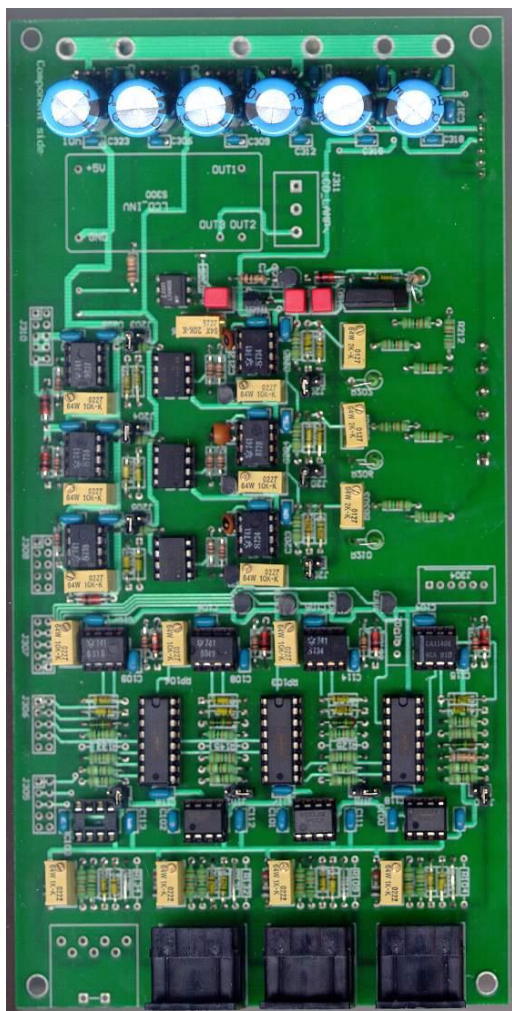


Figure 3. Primary transducers - PCB

These are the reasons why we use 16-bit processor of *Motorola* with the following characteristics:

- 25 MHz bus operations at 5V for 40 nsec minimum instruction cycles time and C optimized architecture produce extremely compact code.
- Dedicated serial debug interface, on-chip breakpoints and read/write memory and registers while running at full speed.
- Integrated 256 K Flash EEPROM. Programming, reading and erasing with 5V trough debug interface.
- Two 8-channel A/D transducers 7  $\mu$ sec, 10-bit single conversion time and scan mode available.
- 8-channel 16-bit with input capture, output compare and pulse accumulator 16-bit modulus down counter.
- 8-bit or 16-bit pulse-wide modulation.

- Asynchronous communication between the MCU and a terminal, computer or a network of microcontrollers (SCI)
- High-speed synchronous communication between multiple MCUs or between MCU and serial peripherals (SPI).
- Inter IC bus (I2C).
- Modules implementing the CAN 2.0 (Controller Area Network) A/B protocol.

We don't use all the capabilities of the single chip computer, because they are not necessary for our tasks and the other will be used in the future development of the system. The first serial communicational interface (SCI0) is used for connection with graphic LCD for control of the visualization. The second (SCI1) is used for connection of the analyzer with PC by RS232. This allows controlling the analyzer by the PC; transfer all the data from analyzer to PC for storing, processing and analysis. The serial peripheral interface (SPI0) is used for communication with real clock timer (RTC) build into analyzer. One of the inputs of the timer module is used for measuring of the voltage frequency.

### Memory

This passage concerns both Random access memory RAM for variables and data used in the programs, and the memory for the program codes (ROM) Solving such problems usually engages a good deal of memory because a lot of data is being processed and stored. As the controller memory is insufficient in this case external RAM is added.

### Keyboard

It is used for choosing and setting-up of different operation modes of the measuring system, for controlling of visualization of results, for input of parameters and e.t.c.

### Module for visualization

It consists of graphic LCD with resolution 240/128 and controllers.

### Supply unit and battery

They provide for all necessary supply voltages of the separate system elements and allow saving of operation memory content when there isn't external supply (for example when transporting measuring device).

### Communication unit (RS232)

It is used for connection with PC, which allows us to foresee opportunities for additional processing of measured data by our software, for preparation of data for using by other standard analysis application, for control of the measuring process and more detail various visualization of results.

### Real time clock (RTC)

It is used to register date and time of each measurement and control the implementation of set in advance operations by analyzer according to defined timetable.

### Functional abilities and operation modes

On the basis of measured voltages and currents the analyzer calculate the active, reactive and apparent power, energies and other magnitudes connected with qualitative and quantitative parameters of electric power. When the voltage values are less than 400 V, connecting to the voltage inputs of

the device are direct while to the current inputs - by ampere clamps. Additional options such as digital outputs and PC interface are also provided.

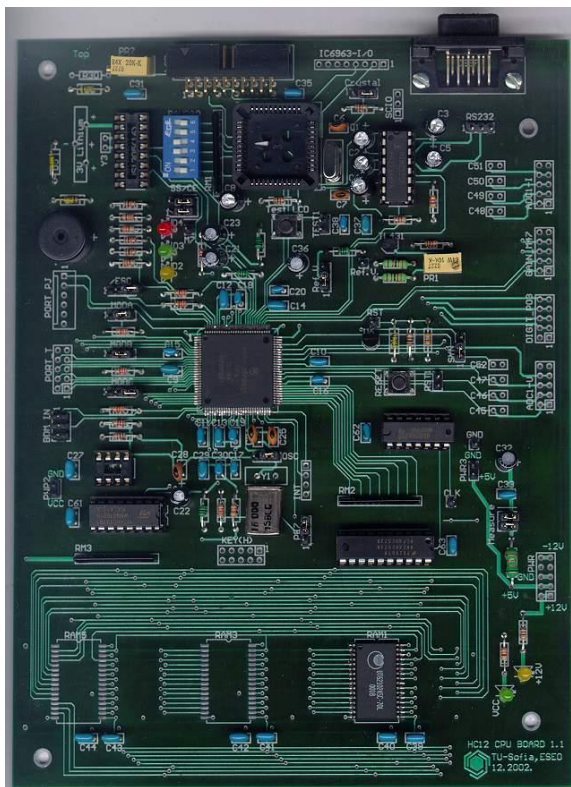


Figure 4. Microprocessor system - PCB

**Operation modes and measured magnitudes:** The analyzer has several operation modes, which are chosen by the user. The following modes and options are offered:

- **Measurement** – under this mode on the basis of the measured values of voltage and current the following basic electric magnitudes of each phase are calculated:
  - Effective value of voltage - Urms and current - Irms;
  - Maximum values of voltage -  $U_m$  and current -  $I_m$ ;
  - Active power – P;
  - Reactive power – Q;
  - Apparent power – S;
  - Power factor;
  - Frequency of voltage –  $f_1$  (phase 1);
  - Deviation of voltage frequency;
  - Deviation of voltage.
- **Harmonic analysis** – under this mode on the basis of Fast Fourier Transform (FFT) harmonic analyses of voltage and current is carried out up to 50<sup>th</sup> harmonic. The following values of each phase and each harmonic can be visualized:
  - R.m.s. values of voltage and current for each harmonic in named and relative units (harmonic coefficient);
  - Initial phases of harmonics;
  - Voltage and current THD;
  - Form factor;
  - Fundamental factor;

- Active, reactive, apparent and deformation powers;  
Information can be shown in tables or charts.

- **Transient processes** – on the basis of the discrete values of voltage and current for given time interval fluctuation of voltage and peak value of the current is calculated. The curves of voltage and current are visualized by phases. There are three possibilities to start of the measuring – manually (from button in the front panel) or automatically in preliminary adjusted time.
- **Statistics** – under this mode for given time interval the measured magnitudes are stored into the memory or sent to PC (see measuring mode). After that some statistic parameters of stored information are calculated.
- **Energy** – under this mode the analyzer operates like electric meter. It calculates active and reactive power. There is a possibility to adjust time zones according to prices of energy, to input the prices currently in use and to calculate and visualize the amount due. The visualization includes displaying of active and reactive power by phases and as a whole in tables or load timetable.
- **Compensation of reactive loads** – on the basis of measured magnitudes calculation of necessary capacitor banks for specific nodes of electro supplying system is provided for.
- **Unbalance** - under this mode the characteristics connected with unbalance in three - phase systems are analyzed and calculate.
- **Test and Set-Up** – this option is for testing and setting up of some characteristics and functions of the analyzer like:
  - Transformation coefficients of power and current transformers (if there are any connected);
  - Calibration of primary transducers;
  - Setting of real time clock;
  - Setting and testing of communication with PC;
  - Determination of sequence of phase connection. It includes vector diagram visualization on the display.



Figure 5. Common view of Analyzer

It is important to be marked out that because of complexity and variety of the solved theoretical and practical problems we have to elaborate many of the set tasks and algorithms. This will make our system very useful for both practical application

and for continuation and extension of research in the field of electromagnetic compatibility in electric power systems.

#### REFERENCES

БДС EN 61000-4-7

Сидеров С., Н.Матанов, Б.Бойчев, В.Георгиев, 2003.  
Алгоритъм за оценка на основни показатели на

електромагнитна съвместимост в електроснабдителни системи с микропроцесорен анализатор. – Юбилейна международна научна сесия 50 години МГУ "Св.Иван Рилски" 14-14 май 2003, София.

Шидловский А.К., Б.П.Борисов. Симметрирование однофазных и двухплечевых электротехнических установок, Киев, 1977.

*Recommended for publication by Department of  
Electrical Engineering, Faculty of Mining Electromechanics*

## ALGORITHM FOR EVALUATING THE BASIC CHARACTERISTICS OF THE ELECTROMAGNETIC COMPATIBILITY OF ELECTRICAL POWER SYSTEMS BY DIGITAL ANALYZER

**Sider Siderov**

**Nikolay Matanov**

**Borislav Bojchev**

**Vulchan Georgiev**

Technical University of Sofia, Sofia-1756, .8 Kl.Ohridski Blvd., Faculty of Electrical Engineering, Department of Electric Power Supply, Electrical Equipment and Electrical Transport

E-mail:  
ssiderov@tu-sofia.acad.bg

E-mail:  
matanov@bitex.com

E-mail:  
bojchev@tu-sofia.acad.bg

E-mail:  
vulchy@tu-sofia.acad.bg

### ABSTRACT

An algorithm for evaluating the basic characteristics of electromagnetic compatibility (EMC) such as harmonic and asymmetrical components, nonsinusoidal, unbalance coefficients (factors) of voltage and current in specific nodes of the electrical power systems, providing for some specific distorting big loads is presented in this paper.

This algorithm is designed for digital analyzer for control of electromagnetic compatibility of electrical power systems.

In addition, it will allow a certain research work to be carried out, concerning the methods and the precision of evaluation of electromagnetic compatibility.

An approach for determination the characteristics of electromagnetic compatibility (EMC) in electrical power system are discussed in the paper. This approach is used in digital analyzer developed by the authors. The structural scheme and functional abilities of the analyzer are discussed in retile in Сидеров *и др.* (2003).

$$k_{hc I} = \frac{\sqrt{\sum_{v=2}^{50} I_v^2}}{I_1} \cdot 100 = \sqrt{\sum_{v=2}^{50} k_{Iv}^2}, \% \quad (4)$$

- Normalized THD of inductions and capacitors:

### BASIC CHARACTERISTICS OF EMC

The basic EMC characteristics are subject of many standards and publication such as Шидловски *и др.* (1977). These characteristics are critical for electrical power quality and are related to evaluation of non-sinusoidal current and voltage, unbalance in three phase power systems, voltage variation (deviation) and fluctuation.

The basic characteristic of non-sinusoidal current and voltage are:

- Harmonic ratio of current and voltage components

$$k_{Iv} = I_{v*} = \frac{I_v}{I_1} \cdot 100, \% \quad (1)$$

$$k_{Uv} = U_{v*} = \frac{U_v}{U_1} \cdot 100, \% \quad (2)$$

- Voltage (Current) total harmonic distortion (THD)

$$k_{hc U} = \frac{\sqrt{\sum_{v=2}^{50} U_v^2}}{U_1} \cdot 100 = \sqrt{\sum_{v=2}^{50} k_{Uv}^2}, \% \quad (3)$$

$$k_{hc,ind} = \frac{\sqrt{\sum_{v=2}^{50} \left( \frac{U_v^2}{v^\alpha} \right)}}{U_1} 100, \% \quad (5)$$

$$k_{hc,cap} = \frac{\sqrt{\sum_{v=2}^{50} (vU_v)^2}}{U_1} 100, \% \quad (6)$$

where

$U_v$  and  $I_v$  are voltage and current harmonics;

$v$  - harmonic order;

$\alpha$  - a parameter taking value 1 or 2.

The current and voltage harmonics ratios are used for choosing power filters, estimating the overload power system elements and for control of the units that generate harmonics.

Harmonic distortions are intended for evaluating of heating and extra active power losses in the elements of electric power system:  $k_{hc U}$  and  $k_{hc I}$  - for power transformers, cables and airlines;  $k_{hc,ind}$  - for asynchronous motor coils;  $k_{hc,cap}$  - for directly connected capacitors, without protective inductors.

There are some more coefficients (factors), defined in the electrical engineering, which characterize the form of current and voltage:

- Form factor (sine wave -  $k_f = 1.11$ )

$$k_{fU} = \frac{U}{U_{cp}}; \quad k_{fI} = \frac{I}{I_{cp}}; \quad (7)$$

- Crest factor (sine wave  $k_a = \sqrt{2}$ )

$$k_{aU} = \frac{U_{max}}{U}; \quad k_{aI} = \frac{I_{max}}{I}; \quad (8)$$

- Fundamental factor

$$k_{DU} = \frac{U_1}{U}; \quad k_{DI} = \frac{I_1}{I}, \quad (9)$$

where

$U$  and  $I$  are r.m.s. value of the voltage and current taken for one phase and period  $T=2\pi f$  ( $f$  is the fundamental frequency);

$U_{cp}$ ,  $I_{cp}$  – average voltage and current values for the fundamental component for one phase and period  $T$ ;

$U_1$ ,  $I_1$  – voltage and current r.m.s. values for fundamental component;

$U_{max}$ ,  $I_{max}$  – the maximal (peak) voltage and current values in period  $T$ .

The distortion of the current and voltage curves (forms) can be evaluated by comparing form and crest factors derived from measurements and these calculated for sine wave.

The unbalance in three-phase system is characterized by unbalance factor that can be determined to be:

$$\varepsilon_u = \frac{U_{neg}}{U_{pos}} \cdot 100 = \frac{\sqrt{\sum_{v=1}^{40} U_{neg,v}^2}}{\sqrt{\sum_{v=1}^{40} U_{pos,v}^2}} 100, \% ; \quad (10)$$

$$\varepsilon_i = \frac{I_{neg}}{I_{pos}} \cdot 100 = \frac{\sqrt{\sum_{v=1}^{40} I_{neg,v}^2}}{\sqrt{\sum_{v=1}^{40} I_{pos,v}^2}} 100, \% , \quad (11)$$

where

$U_{pos}$  and  $I_{pos}$  are r.m.s. values of positive sequence components of voltage and current;

$U_{neg}$  и  $I_{neg}$  - are r.m.s. values of negative sequence components of voltage and current;

$U_{pos,v}$ ,  $U_{neg,v}$ ,  $I_{pos,v}$ ,  $I_{neg,v}$  - are r.m.s. values of positive and negative sequence components of voltage and current harmonics with order  $v$ .

The degree of unbalance of a three-phase system is often characterized by unbalance factor of voltage and current which is determined as:

$$\alpha_u = \frac{U_0}{U_{pos}} \cdot 100 = \frac{\sqrt{\sum_{v=0}^{40} U_{0,v}^2}}{\sqrt{\sum_{v=1}^{40} U_{pos,v}^2}} 100, \% ; \quad (12)$$

$$\alpha_i = \frac{I_0}{I_{pos}} \cdot 100 = \frac{\sqrt{\sum_{v=0}^{40} I_{0,v}^2}}{\sqrt{\sum_{v=1}^{40} I_{pos,v}^2}} \% , \quad (13)$$

where

$U_0$  and  $I_0$  are r.m.s. values of direct sequence components of voltage and current;

$U_{0,v}$  и  $I_{0,v}$  - r.m.s. values of direct sequence components of voltage and current harmonics with order  $v$ .

The voltage deviation amplitude for each phase can be defined by the expression

$$V(t) = \frac{U(t) - U_H}{U_H} 100, \% , \quad (14)$$

where

$U(t)$  is wrapping curve of the voltage r.m.s. values;

$U_H$  – the nominal voltage of the power system.

The average and r.m.s. amplitude as well as average and r.m.s. voltage deviation can be determined from  $V(t)$ .

In analogical manner the fundamental frequency deviation can be determined. The voltage and frequency fluctuation are not subject of this paper.

The voltage and current harmonic calculation are necessary to determine the basic EMC characteristics. Direct positive and negative component are estimated in three-phase unbalance systems.

When current and voltage are non-sinusoidal and unbalance, first the Fourier transformation has to be done and after that the direct, positive and negative sequence component are calculated for each harmonic. The algorithm discussed in this paper considers the way of determination of the above quantities.

## OPERATION ALGORITHM

This paragraph considers the main algorithm and it's heaviest part – harmonic analysis that will be discussed in details. All possible operation modes are described in Сидеров *и др.* (2003).

**General operation algorithm**

Generalized flowchart of the operation algorithm is given in *Figure 1*. The following basic steps are shown:

- Initializing the system resources assigning initial values to all variables, configuration I/O interface and data memory check.
- Operation mode choosing. The desired mode has to be selected in accordance with the client task.
- Measurement. At this point all quantities related to chosen mode are measured and acquired data are put into computation routines.
- Visualization (Show) of the results in the LCD.
- Returning to operation mode choice.

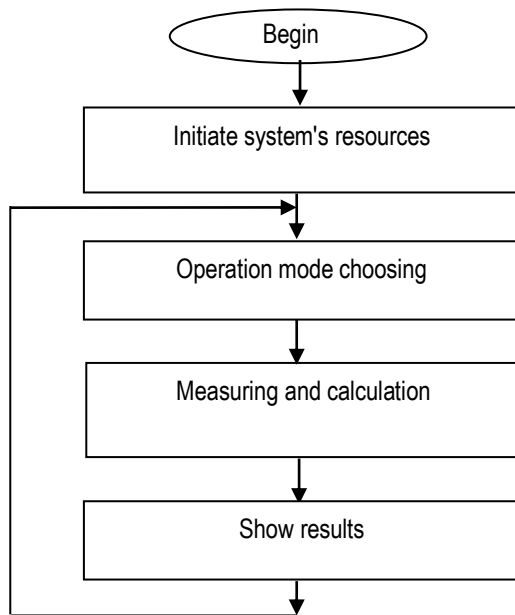


*Figure 1. Flowchart of general operation algorithm*

**Algorithm in harmonic analysis mode**

A flowchart describing working sequence is given in *Figure 2*. The main steps are:

- Choice of the external connection scheme. After each change a checking subroutines is started to reassume absence of mistakes.
- Setup of the basic measurement and calculating parameters. The user can select some measurement parameters as: sample rate, the kind of window function, the kind of anti-aliasing filter, the maximum harmonic

order (the upper bound of the harmonic order depends on the previously setup parameters)

- Performing the actual measurement with ADC.
- Filtering the acquired data and saving in the memory.

As it is well known the input signals has to be limited in the frequency domain in order to receive correct results from Fast Fourier Transform (FFT). A digital filter is used to prevent the aliasing of out-of-band noise and interference. A Finite Impulse Response (FIR) filter is chosen because of its simplicity and suitable characteristics.

The digital FIR filter is linear discrete system with single input and single output. It has constant (according to time) parameters. In that way the system reactions is independent from the input signal initial time. Any linear system can be unambiguously determined by its reaction to the series of normalized pulses, each of which can be defined by the following expression Иванов (1997):

$$\delta(k) = \{1, 0\}, k = 0, k \neq 0. \quad (15)$$

If we mark the filter input with  $\{u_n\}$  and its reaction (i.e. output) with  $\{y_n\}$ , the input can be presented as a sum of normalized pulses

$$u(n) = \sum_{k=-\infty}^{\infty} u(k)\delta(n-k) \quad (16)$$

And the filter output is expressed by

$$y(n) = L\left\{\sum_{k=-\infty}^{\infty} u(k)\delta(n-k)\right\}. \quad (17)$$

For the linear, time invariant systems, equation (17) can be written as

$$y(n) = \sum_{k=-\infty}^{\infty} u(k)h(n-k), \quad (18)$$

where  $\{h_k\}$  is impulse response of the filter. In practice the input sequence is constrained, so if the number of input points is  $N$ , the FIR filter output will be

$$y(n) = \sum_{k=0}^{N-1} u(k)h(n-k) = \sum_{k=0}^{N-1} h(k)u(n-k). \quad (19)$$

This sum is called convolution and can be written in the next way

$$\{y_n\} = \{u_n * h_n\}. \quad (20)$$

If the number of discrete input values is equal to the number of filter coefficient, it is realized by the mathematical operation

ring shrinkage (circular shrinkage) but if not aperiodic shrinkage is used.

The filter response in the z-domain is

$$Y(z) = H(z)U(z), \tag{21}$$

Where  $H(z)$  is the filter transfer function

$$H(z) = \sum_{k=-\infty}^{\infty} h(k)z^{-k} \tag{22}$$

The phase response of this kind of filters is a linear function of the frequency, which is a big advantage of such kind of applications. The linearity is achieved only for the filter coefficients are symmetrical around the central coefficient (i.e. the first and the last coefficients has to be equal). The linear filter delay is  $(N - 1)/Fs$ , where  $Fs$  is the sampling frequency, and  $N$  is the number of points. For instance for 21 point and 1 kHz sampling rate the delay will be 20 ms. In practice the frequency response is given by (22).

The "windowing" approach is accepted in filter design. The initial impulse response is multiplied by "window" function. The convolution realized in that way leads to smoothing in the frequency response. The user can chose between rectangular window and Hanning window. The last one is required by standard EN 61000-4-7.

In filter design the following sequence is accepted: first the sampling rate is set; the pass band and the hold band are set, after that the transition band with and normalized cutting frequency are calculated. Finally filter order and filter coefficient are defined. The results after filtration can be obtained by using equation (19).

- Performing Fast Fourier Transformation (FFT) and determine current and voltage harmonic ratio.

When the signals are captured experimentally but are not given as analytical expressions, there are two common methods for their processing:

- In the first one a function approximation is done, followed by numerical integration.;
- In the second method continuous Fourier Transformation is replaced by Discrete Fourier Transformation (DFT). This approach suits better to our tasks. The FFT is always preferred than directly applying DFT because of reducing mathematical operations. For example DFT with 512 samples requires  $1,5 \cdot 10^6$  mathematical operations, while by FFT this number can be reduced to about  $2,5 \cdot 10^4$  mathematical operations for same number of samples. In general FFT requires  $N \cdot \log_2 N$  complex multiplications, where  $N$  is the number of samples Донева и др. (1999).

The abbreviation FFT represents not single method but set of algorithms that speed up the process. One widely used algorithm is called "time decimation". It can be generally described with the following equations:

$$F(n) = \sum_{k=0}^{N-1} f(k)W^{nk}, \quad n = 0, 1, 2, \dots, (N - 1); \tag{23}$$

where

$F(n)$  is coefficients row of DFT;

$f(k)$  – input data sequence (the index  $k$  associated with the time),  $W = e^{-j2\pi/N}$ .

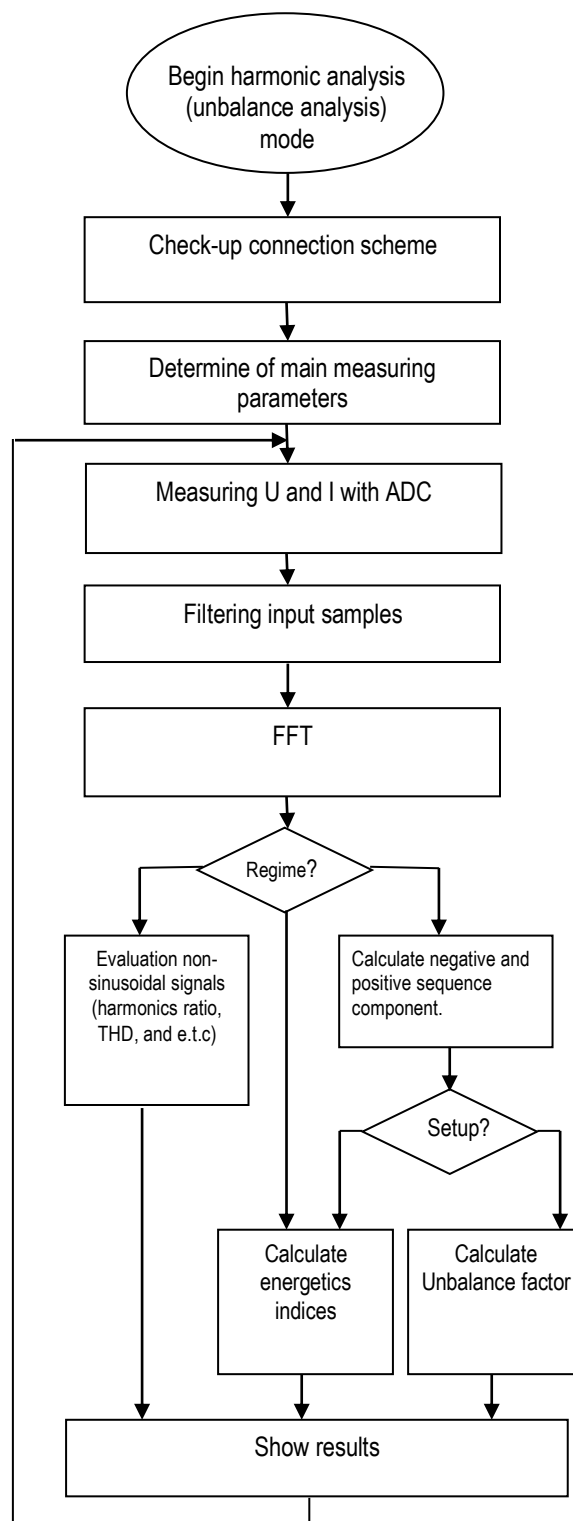


Figure 2. Flowchart for harmonic analysis mode

If the number of samples  $N$  can be divided by 2, the initial DFT can be decomposed in two shorter subsequences – the first one containing all samples with even indexes  $f(2k)$ , and the second one comprised by all samples with odd indexes  $f(2k+1)$ , where  $k=0,1,2,\dots,(N/2-1)$ . Each of these two new rows of data is decomposed in to parts in its turn. In that way the current and voltage harmonics are evaluated for all three phases at the same time. In this case the sum (23) can be represented by four subsumes given by (24).

$$\begin{aligned}
 F(n) = & \sum_{k=0}^{N/4-1} f(4k)(W^n)^{2k} + \\
 & + \sum_{k=0}^{N/4-1} f(4k+1)(W^n)^{(4k+1)} + \\
 & + \sum_{k=0}^{N/4-1} f(4k+2)(W^n)^{(4k+2)} + \\
 & + \sum_{k=0}^{N/4-1} f(4k+3)(W^n)^{(4k+3)}.
 \end{aligned} \tag{24}$$

This formula can be written in other way

$$\begin{aligned}
 F(n) = & \sum_{m=0}^3 \sum_{k=0}^{N/4-1} f(4k+m)(W^n)^{(4k+m)} = \\
 = & \sum_{m=0}^3 \sum_{k=0}^{N/4-1} f(4k+m)(W^n)^{4k} (W^n)^m
 \end{aligned} \tag{25}$$

The time decimation process continues until initial and final values for  $k$  become equal to 0 and 3.

- In dependence on the current mode of operation either non-sinusoidality characteristics are calculated by expressions (1) - (9) or unbalance parameters are calculated in accordance to the equations (10) - (13).

- The analyze is completed by visualization of the results. In stand-alone regime of operation the results are shown in graphics LCD module. If the analyzer is connected to PC specially developed software capture the data and gives much more possibilities for data processing and visualization.
- The algorithm loops with measurement of the next current and voltage periods.

The analyzer can evaluate a wide variety of EMC characteristics. In addition active and reactive power for a user-supplied interval can be measured. In such way observation of the load variation could be performed.

During the last few years the requirements concerning EMC became stronger and stronger. Such requirements are included in the new standards. This means that the question for fast and cheap measuring devices is its importance.

## REFERENCES

- Доневска С., Б.Доневски. Бързо преобразуване на Фурие. - *Технически Университет-София, 1999.*
- Иванов Р.С. Цифрова обработка на едномерни сигнали. – *Габрово, ТУ-Габрово, 1997.*
- Сидеров С., Н. Матанов, Б. Бойчев, В. Георгиев. Структура и работа на микропроцесорен анализатор на електромагнитна съвместимост. – *Юбилейна международна научна сесия 50 години МГУ "Св.Иван Рилски" 14-14 май 2003, София.*
- Шидловский А.К., Б.П.Борисов. Симетрирование однофазных и двухплечевых электротехнических установок, - *Киев, 1977.*

## SYSTEM FOR MEASURING CONTROL AND MONITORING OF POWER CONSUMPTION AT THE DRESSING PLANT OF THE "ELATSITE-MED" Co

Ivan Stoilov

Kiril Djustrov

Mento Menteshhev

Anton Trapov

University of Mining and Geology  
"St. Ivan Rilski"  
Sofia 1700, Bulgaria  
E-mail: stoilov@mgu.bg

University of Mining and Geology  
"St. Ivan Rilski"  
Sofia 1700, Bulgaria  
E-mail: justrov@mgu.bg

"SMS – S" Ltd.  
Sofia 1164, Bulgaria  
8 Krivolak Str.  
E-mail: cmc\_c@mail.orbitel.bg

ComSystems Ltd.  
30 Vrabcha Str.  
Sofia, Bulgaria  
E-mail: ComSystems@ttm.bg

### ABSTRACT

A microprocessor system for measuring all the values, characterizing the power consumption of the whole enterprise is commissioned. The active and reactive power of at all the inlets and outlets of the GPP 110/20/6 kV are visualized. Daily and monthly record of consumed power and the power factor for different rate zones for each outlet and for the whole enterprise is printed automatically. Power consumption is evaluated for different outlets of the enterprise and for the enterprise, as a whole, according to relevant regulations. A load schedule is printed for specific workshops and for the enterprise as a whole.

With the commissioning of the automated system an opportunity is established for optimum regulation of loads in the specific rate zones, which is a precondition for reduction of power consumption. Control of electric power consumption in the specific departments of the enterprise is improved. The needed technical preconditions for observation of the requirements of the power producing company and avoiding penalties is absolutely possible.

### STRUCTURE OF THE SYSTEM

The linear scheme of the main sub-station (fig. 1) shows the zones, which control power and power consumption. At both ends of the ORU 110 kV there are three three-phase transformers for active power, for reactive (inductive) power, for reactive (capacity) power. Two three-phase transformers for active and for reactive power are mounted at all the outlets of the KRU 20 kV and 6 kV. Outgoing direct current unified signals 0 – 5 mA from all transformers (totally 32 transformers) are brought to the microprocessor system by multiple screened cables. They enter a converter, where current signals are transformed into voltage: from 0 – 5 mA into 0 – 10 V. Signals are scanned and identified from the controller and then they are supplied consecutively to the computer, which process them in real time.

Consumed power of voltage 110 kV, of voltage 20 kV and voltage 6 kV are visualized selectively on the background of linear schemes shown in the monitor (fig. 2, fig. 3, fig. 4).

Information about consumed power, calculated by the data of all transformers, is printed in an appropriate layout at certain given intervals of time. Data for each day, for each month and for the whole year are printed automatically. The system is incorporated to a circuit of 220 V by an uninterrupted power supply (UPS), which guarantees work without supplied voltage for 15 min.

### APPARATUS

The microprocessor system is constituted of modern elements.

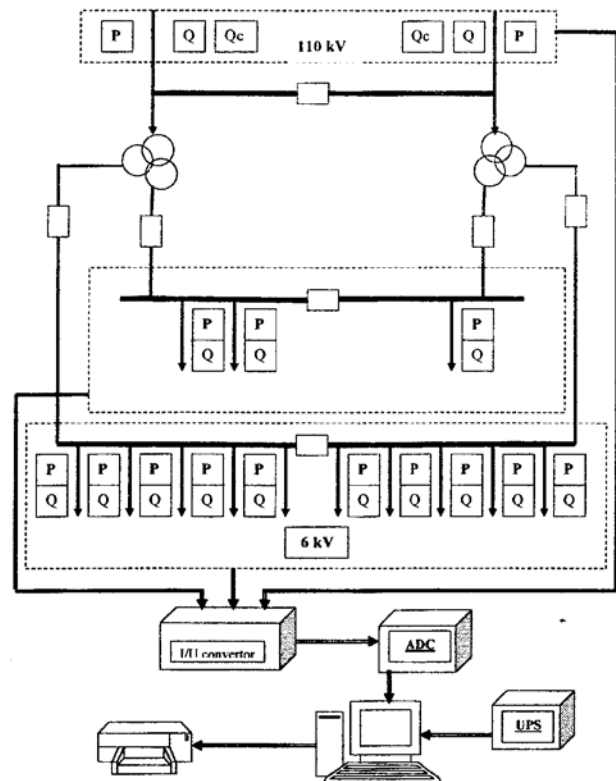


Figure 1.

#### Preliminary transformers for power:

- for active power – type E 829/1
  - for reactive power – type E 830/1
- with parameters at the inlet: voltage: 100 V; current 2,5/5 A;  
 outgoing current: direct current 0 - 5 mA;  
 Maximum resistance of charges  $R_T$  3 k $\Omega$ ;  
 Class of precision 1,0;

**Converter current-voltage I/U**

Type: PCLD 880; Voltage at the outlet for inlet 5 mA - 10V;  
Resistance of load - 2 kΩ; Precision of resistors - 0,1%;  
Number of active inlets 32

**Controller microprocessor**

Type: PCL 813B; Number of channels 32; A/D convertor 12 bits;  
Inlet voltage: Bipole ± 5V; ± 2,5V; single pole 0-10V; 0

- 5V; 0 - 2,5V; 0 - 1,25V; Time for converting 25 μs; Resistance at inlet > 10 MΩ; Ambient temperature: - 20 + 65°C; Precision ± 0,01%

**Computer configuration**

There is a computer configuration of standard elements: processor, monitor, printer and uninterrupted power supply - "APC" Back UPS 300 MI

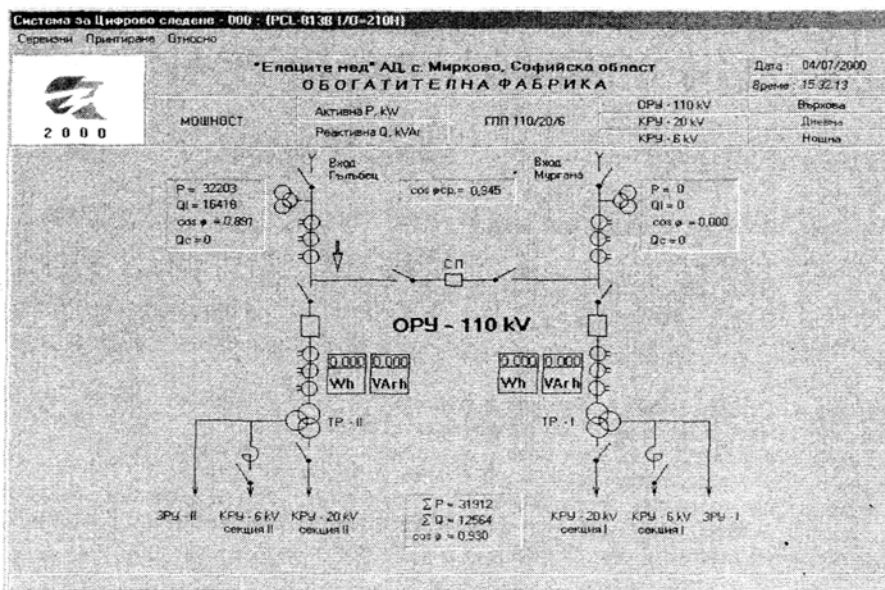


Figure 2.

**Software**

**General characteristic**

The software of the system is constituted hierarchically. The operational media is WINDOWS '98

At the first level of selective scanning of data from the 32 preliminary transformers of power (15 for active power and 17 for reactive power) and their addressing into the PC

apply the software products Activ DAQ and Visi DAQ and Ver 11 - installation.

A specialized software program "ELATZITE" is developed for the second level of processing of information and calculation.

All the installed software products are authorized.

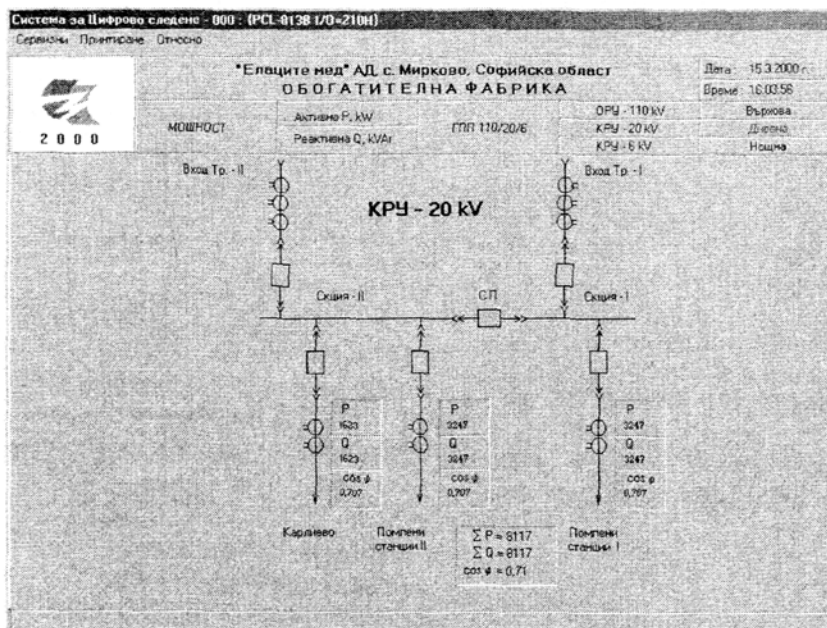


Figure 3

The basic requirements towards the software uniting both levels in WINDOWS media correspond to the relevant principles.

They are as follows:

**The system** acquires, processes and stores information in real time.

**Scope of the system**

- Inlets for measuring at 110 kV:

- "Murgana" and "Galabets"
- Outlets for 20 kV:
- Pumping plant "Benkovski I", pumping plant "Benkovski II", pumping plant "Karlievo"
- Outlets of workshops for 6 kV:
- Workshop medium and fine crushing 1 (CCT 1)
- Workshop medium and fine crushing 2 (CCT 2)
- Workshop medium and fine crushing 3 (CCT 3)

- Crushing-flotation department (Main building 1)
- Crushing-flotation department (Main building 2)
- Mechanical-repairing workshop (PMЦ 1)
- Mechanical-repairing workshop (PMЦ 2)
- Boiler heating department
- Electrical repairing department (EPL)
- Administration

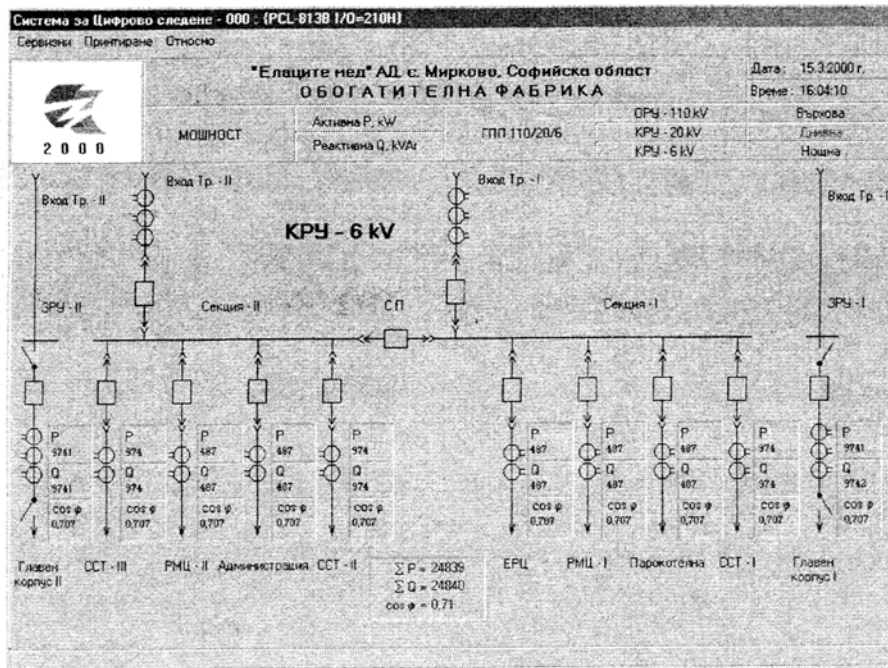


Figure 4

**Directly measured and calculated values:**

- Active power P – for all inlets and outlets, values are obtained as:

$$P = k_I \cdot k_U \cdot k_P \cdot m,$$

where:  $k_I$  is a factor of transformation of the current transformer

$k_U$  - factor of transformation of voltage transformer

$k_P$  - factors of transformation of power transformation

$m$  - digit, read by AЦП

- Reactive power Q – calculated according to the same way, including:

- with inductive character  $Q_L$  – for all the inlets and outlets;
- with capacity character  $Q_C$  - only for two inlets (110 kV).

**Calculated values:**

- power: average values are calculated for intervals of time 5s and 30min
- Average values for  $\cos \varphi$  - for 5 s and for 30 min

Remark: The average power for 5 s is considered and visualized as a momentum value:

- Power:

active  $W_a = \sum P_i \cdot t_i$

reactive  $W_L = \sum Q_{Li} \cdot t_i$  и  $W_C = \sum Q_{Ci} \cdot t_i$

- Cost of electric power is determined according to acting regulations for evaluation and rates of electric power. Daily, monthly and annual cost of electric power for the peak, daily and night rate zones and the backward reactive capacity power in the system.

- Normed limits. When certain limits are introduced for specific values  $L_{(x)}$ , the percentage of consumed portion is calculated

$$N_{(x)}:$$

$$L_{\%} = \frac{N_{(x)}}{L_{(x)}} \cdot 100, \%$$

- Measurements and calculations of all the parameters is done according to zones of different rates:

- power, energy and currency expenses:
  - peak – subdivided for two parts of the day
  - daily – subdivided into three parts in the day (from the peak zones)
  - nightly
- average values of  $\cos \varphi$  for the day and the month:
  - daily (calculated by the total power consumed in the peak and the daily zones):

| <br>2000 | "Елаците мед" АД с. Мирково, Софийска област<br>ОБОГАТИТЕЛНА ФАБРИКА |                     |                    |                     |                    |                     | Дата: 10/07/2002   |       |                       |
|---|--|---------------------|--------------------|---------------------|--------------------|---------------------|--------------------|-------|-----------------------|
|   | КОНСУМИРАНА ЕЛЕКТРИЧЕСКА ЕНЕРГИЯ                                     |                     |                    |                     |                    |                     | Време: 06.00.37    |       |                       |
| Период от 10/06/2002 до 10/07/2002  |  |                     |                    |                     |                    |                     |                    |       |                       |
| ВХОД / ИЗХОД  | Консумирана енергия по зони  |                     |                    |                     |                    |                     | cosφ <sub>ср</sub> |       | Върната енергия, kVAh |
|   | Върхова  |                     | Дневна             |                     | Нощна              |                     | дневен             | нощен |                       |
|   | W <sub>a</sub> kWh   | W <sub>r</sub> kVAh | W <sub>a</sub> kWh | W <sub>r</sub> kVAh | W <sub>a</sub> kWh | W <sub>r</sub> kVAh |                    |       |                       |
| 110 kV  | 194040   | 85116               | 320291             | 141450              | 260657             | 116113              | 0,915              | 0,913 | 4                     |
| Гълъбец   | 0  | 0                   | 0                  | 0                   | 0                  | 0                   | 0,000              | 0,000 | 4                     |
| Миргана   | 194040   | 85116               | 320291             | 141450              | 260657             | 116113              | 0,915              | 0,913 | 0                     |
| 20 kV   | 11339  | 7177                | 18913              | 12313               | 19508              | 12504               | 0,841              | 0,842 | 0                     |
| Помпени станции I   | 11259  | 7177                | 18778              | 12312               | 19401              | 12503               | 0,839              | 0,841 | 0                     |
| Помпени станции II  | 11   | 0                   | 20                 | 1                   | 13                 | 0                   | 1,000              | 1,000 | 0                     |
| Общо Помпени станции  | 11269  | 7177                | 18798              | 12313               | 19414              | 12504               | 0,839              | 0,841 | 0                     |
| Карлиево  | 70   | 0                   | 116                | 1                   | 95                 | 1                   | 1,000              | 1,000 | 0                     |
| 6 kV  | 167172   | 58550               | 276408             | 97531               | 221507             | 77934               | 0,943              | 0,943 | 0                     |
| Гл. корпус I  | 75596  | 8754                | 125892             | 14924               | 100809             | 12510               | 0,993              | 0,992 | 0                     |
| Гл. корпус II   | 80480  | 18172               | 133902             | 32355               | 108256             | 26557               | 0,973              | 0,971 | 0                     |
| Общо Гл. корпус   | 156075   | 26926               | 259793             | 47279               | 209065             | 39067               | 0,984              | 0,983 | 0                     |
| ССТ I   | 693  | 17530               | 1115               | 29050               | 881                | 23100               | 0,039              | 0,038 | 0                     |
| ССТ II  | 9735   | 13897               | 14348              | 20635               | 10727              | 15266               | 0,572              | 0,575 | 0                     |
| ССТ III   | 0  | 0                   | 0                  | 0                   | 0                  | 0                   | 1,000              | 0,000 | 0                     |
| Общо ССТ  | 10427  | 31428               | 15464              | 49685               | 11607              | 38366               | 0,304              | 0,290 | 0                     |
| РМЦ I   | 0  | 0                   | 0                  | 0                   | 0                  | 0                   | 1,000              | 1,000 | 0                     |
| РМЦ II  | 154  | 93                  | 291                | 211                 | 210                | 168                 | 0,825              | 0,782 | 0                     |
| Общо РМЦ  | 154  | 93                  | 291                | 211                 | 211                | 168                 | 0,826              | 0,782 | 0                     |
| ЕРЦ   | 24   | 14                  | 40                 | 26                  | 34                 | 18                  | 0,853              | 0,888 | 0                     |
| Парокотелна   | 48   | 90                  | 119                | 176                 | 131                | 162                 | 0,533              | 0,629 | 0                     |
| Администрация   | 443  | 100                 | 700                | 154                 | 460                | 154                 | 0,976              | 0,948 | 0                     |

Figure. 5

**Storage of information**

Momentum values of the active, reactive power and cosφ (average for 5s) are saved for 30 min.

All the average data for 30 min are saved for a period of time not less than 5 years.

**Constants**, that should be introduced by the operative staff (in case of relevant protection).

- factors of transformation of measuring transformers, current transformers  $k_I = x/5$  A and voltage transformers  $k_U = x/100V$ ;

- factors of transformation of power transformers  $k_P$  and  $k_Q$

- rate zones in astronomic time (hours) for the power: peek, daily, nightly rate zones;

- rate zones in astronomic time (hours) for cosφ: peek plus daily and nightly rate zones;

- given limits (if there are any)

- data for correction of the factor for payment of reactive energy depending on the average monthly values of  $COS\phi_{мес}$ .

- data for cost of electric power: peek, daily, nightly;

- corrections for dates and astronomic time;

- corrections for time for reading and processing of data (scanning, average, visualization, record etc.).

**Visualization**

A linear scheme of OPY 110 kV, KPY 20 kV and KPY 6 kV is shown in a main and two additional menus. The screen has a window for visualizing the rate zone in the moment of measuring.

For all the inlets and outlets there is a visualization of the momentary values of the active power P, reactive power Q and cosφ.

In the main menu the backward reactive power  $Q_c$  in the system is also visualized, combined with a sound signal.

The main menu indicates also the  $cos\phi_{ср}$ , calculated from the beginning of the month till the moment of observation..

The window "ADMINISTRATOR" organizes and visualizes all the service programs and records for printing at the printer.

-

|  |  |                  |
|--|--|------------------|
| <br>2 0 0 0 | <b>"Елаците мед" АД с. Мирково, Софийска област</b><br><b>ОБОГАТИТЕЛНА ФАБРИКА</b> | Дата: 10/05/2002 |
|  | МЕСЕЧНИ РАЗХОДИ ЗА ЕЛЕКТРИЧЕСКА ЕНЕРГИЯ  | Време: 16.49.24  |

Период: 2002 година

| ВХОД / ИЗХОД | За консумирана енергия по зони общо,<br>лв. |        |        |         | Санкция,<br>лв.      |                                   | Премия,<br>при $\cos\phi < 0,7$ ,<br>лв. | Всичко,<br>лв. |
|--------------|---|--------|--------|---------|----------------------|-----------------------------------|--|----------------|
|              | Върхова                                     | Дневна | Нощна  | ОБЩО    | При $\cos\phi < 0,9$ | От върнатата<br>капац.<br>енергия |  |                |
| Януари       | 734377                                      | 777274 | 403147 | 1914798 | 0                    | 15                                | 0  | 1914813        |
| Февруари     | 669074                                      | 723850 | 371630 | 1764555 | 0                    | 19                                | 0  | 1764574        |
| Март         | 718980                                      | 781786 | 400163 | 1900929 | 0                    | 20                                | 0  | 1900948        |
| Април        | 700472                                      | 749488 | 377619 | 1827580 | 0                    | 42                                | 0  | 1827622        |
| Май          | 711389                                      | 764388 | 391459 | 1867235 | 0                    | 19                                | 0  | 1867254        |
| Юни          | 685076                                      | 723937 | 377465 | 1786478 | 0                    | 15                                | 0  | 1786493        |
| Юли          | 585322                                      | 634251 | 324249 | 1543822 | 0                    | 16                                | 0  | 1543838        |
| Август       | 683159                                      | 729256 | 362380 | 1774795 | 0                    | 13                                | 0  | 1774808        |
| Септември    | 675936                                      | 711624 | 366049 | 1753610 | 0                    | 19                                | 0  | 1753629        |
| Октомври     | 101442                                      | 114861 | 59917  | 276221  | 0                    | 3                                 | 0  | 276224         |
| Ноември      | 0   | 0      | 0      | 0       | 0                    | 0                                 | 0  | 0              |
| Декември     | 0   | 0      | 0      | 0       | 0                    | 0                                 | 0  | 0              |

Figure 6

### Documentation

-the following records are printed each day at 6.00 h:

- "Consumed electric power", which includes all the inlets and outlets, energy for different rates, average values for:  $\cos\phi_{cp}$  - daily (peak + daily zones) and nightly and returned capacity power – fig..5
- "Cost of electric power" – expenses in leva, including all inlets and outlets for zones and a total
- "Daily loading schedule", which includes data for hour active and reactive power, totally for the enterprise and for all the outlets of КРУ 20 and КРУ 6 for the substation.

-each month is printed the following:

- "Monthly consumption of electric power" for different rate zones, with calculated  $\cos\phi_{cp}$  – daily and nightly rates and returned capacity power.
- "Annual expenses for electric power" for the zones with a calculation of different rates according to relevant regulations for cost and rates – fig. 6.

### Assembly

The complete system is positioned at one of the fields of the central panel of the sub-plant.

The micro-processing system is commissioned in March 2000 and has been working since.

Records for consumed electric power, expenses in leva and daily schedule are presented to the professionals from the power supply department of the enterprise. Analysis of information provides an option for in-time activities and effective power management. Having in mind that the dressing plant of "Elaците мед" Co is a power consuming enterprise (the average power consumption is nearly 30 MW) the skillful management of power consumption brings to significant savings of currency.

### REFERENCES

- Danailov D. 1985, Rational use of electric power in mining enterprises – Sofia, Technika (in Bulgarian)
- Pachamanov, A. 2002, Planning, control and management of power consumption – Sofia, King (in Bulgarian)
- Stepanov V. 1984, Analysis of improvement of power technologies – Novosibirsk, Science (in Russian)
- Solution Guide Vol. 91, 1999, PC-based Automation – Advantech

Recommended for publication by Department of  
Electrical Engineering, Faculty of Mining Electromechanics

## STRUCTURE OF POWER CONSUMPTION OF DRESSING PLANT AT THE "ELATSITE – MED" Co

**Ivan Stoilov**

University of Mining and Geology  
"St. Ivan Rilski"  
Sofia 1700  
e-mail: stoilov@mgu.bg

**Dobri Tsvetkov**

"Elatsite Med" Co  
Mirkovo 2086,  
Sofia district  
e-mail: elatzite@mbox.digsys.bg

**Evtim Filipov**

"ASA" Ltd.  
Sofia 1111  
7-13 "Shipchenski prohod" Str.  
e-mail: evtimf@engineer.bg

### ABSTRACT

Data about power consumption of the "Elatsite - Med" is analyzed for a period of one year, one month and one typical working day. Structure of power cost is determined for different workshops and for different rate zones. Characteristics for qualitative estimation of efficiency of the activities for power saving are suggested. The options for more rational distribution of power among the different rate zones are discussed. Organizational and technical decisions for reducing the specific power consumption are also suggested.

"Elatsite – Med" Co. mines and processes more than 12 million tones of low-grade copper-containing ore. Mining and coarse crushing is carried out at the open pit of the "Elatsite". Crushed ore (class 0-200 mm), loaded on a belt conveyer is fed from the mine to open-air hopper #2 above the department for medium-size and fine crushing (MFC). Medium-size crushing is realized by cone crushers of the type KSD and "Kubria" 210-35, and fine crushing in cone crushers of "Kubria" 210 –15 type. Crushed ore of the class of "-15mm" (86%) from the interim hoppers is fed to the milling department. Grinding of ore is carried out in ball crushers of central unloading of the type of МШЦ – 4500x6000, operating under a single-stage system of grinding with a control classification in a hydrocyclon ГЦ-1000 and "KREBS". The milled product enters a flotation cell, where the main flotation is done by machines of Denver 500 type. The froth product from the main flotation, enters for re-grinding in a mill МШЦ 2000x4500. Mills work in a closed cicle with the hydrocyclon "KREBS". The concentrate, after 3 (4) scavenge operations in the flotation machines is fed into condensers СП-30, and then into a pressing filter БОУ-40-3 for drying. The ready concentrate has an average copper content of nearly 25% and moisture content of 9-11%.

Pumping plants of three stages of pumping of circulation water are constructed for the needs of circulation water supply.

Electric power is supplied to the dressing plant through the main substation by two three-coiled transformers 50 MVA, 110/20/6 kV. A voltage of 20 kV supplies the pumping plants, and a voltage of 6 kV supplies the dressing departments. Annual power consumption is more than 260 millions kWh.

According to a decision of the State Committee of Energy Regulation of November 1<sup>st</sup> 2002 the company pays the power consumed in holidays with a certain discount from working days and night rates.

In 2000 a modern micro-processor system for measuring, regulation and control of power consumption (Stoilov, Djustrov et al., 2003). The system prints out records of data about consumed active, reactive electric power and factor of power. Those data, referred to specific rate zones, comprise each department and the company as a whole. A record of expenses in leva is also printed for specific departments and the whole company as well, according to stipulations of the Regulation for applying the prices and rates for power consumption. All the data about power consumption, the average for a period of 30 min are stored in the system for a period of 5 years.

An analysis of the structure of power consumption is prepared for a period of one year (May 2000 – April 2001), for one month (June 2000) and a typical working day (June 16<sup>th</sup> 2000).

Fig. 1 represents the annual distribution of consumed active electric power from the company for different rate zones.

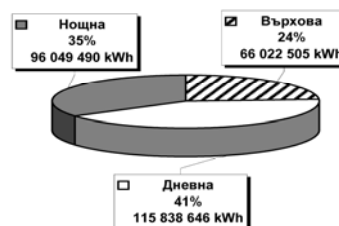


Figure 1

Compared to the case when the average consumed power in all the zones is equal (peak – 25%, daytime – 41,66% and nighttime – 33,33%) it is evident that efforts are paid for limiting consumption in the peak and daytime consumption on the account of the nighttime. In June 2000 a monthly distribution of consumed active power is achieved, which is 1% less in the peak zone on the account of

the day-time zone. This represents reserves, which in fact are available for better distribution of power in different rate zones.

Fig. 2 shows distribution of annual currency expenses for power in different rate zones.

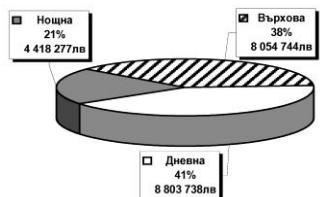


Figure 2

Significant portion of funds are paid for power consumed in the peak zones – 38%. The equality in the percent distribution of power and expenses for it (41 %) for the day-time zone is interesting.

Distribution of consumed active power for specific departments is shown in fig.3.

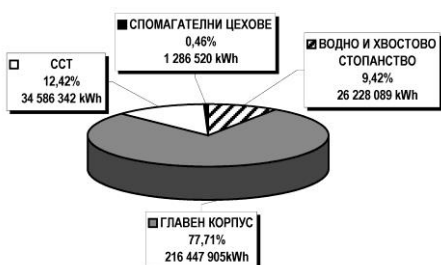


Figure 3

The consumer of the highest consumption is the MAIN BUILDING, where the main portion of production is concentrated – grinding, fine grinding, flotation, compression and filtering. The MAIN BUILDING uses 77,7% of the power, Department for medium and fine crushing – 12,42%, water circulation and tailings – 9,42%.

The other auxiliary departments – mechanical repairing department, heating department, electrical repairing department and administration – 0,46%.

Production process in the departments of MAIN BUILDING is continuous. The process grinding is the most power-consumable. There are 10 mills, driven by synchronous motors of 2, MW power. Annual and month distribution of electric power, consumed by the MAIN BUILDING is: peak zone - 25%, day-time zone – 41%, night-time zone – 34%. Therefore, the average hour power is almost constant for all the rate zones.

The schedule of work of the department for medium and fine crushing is subjected to the objective of reducing consumption of power in the peak zone. As a rule the department interrupts operation for technical servicing during the morning peak zone. The availability of a hopper with a large enough volume between the Department for medium-size and fine crushing and the MAIN BUILDING provides the option of interrupting the Department for crushing during the evening peak zone, in case of future enhancement of its productivity. Below is presented the annual distribution for different zones: peak zone – 20%, day-time zone – 42%, night-time zone – 38%. There is a real opportunity for achieving a better distribution, which is evident from the data obtained for June: peak zone – 18%, day-time zone – 43%, night-time zone 39%.

Circulation water supply and delivery of fresh water to the plant occupies a share of 9,42 % of the power consumption of the company. In case of the existing scheme of circulation water supply (pumping stations, water-collecting basins and schemes of work) the distribution of consumed power is as follows: peak zone – 20%, day-time zone – 42%, night-time zone – 38%. In June 2000 the distribution was better: peak zone – 16 %, day-time zone - 41%, night-time – 43%, and on June 16: peak zone – 12%, day-time zone – 37%, night-time zone – 51%. It is evident that much better distribution of electric power consumption for different rate zones may be realized for the cycles of water supply.

Annual expenses of the company distributed for specific departments and rate zones is shown in fig.4.

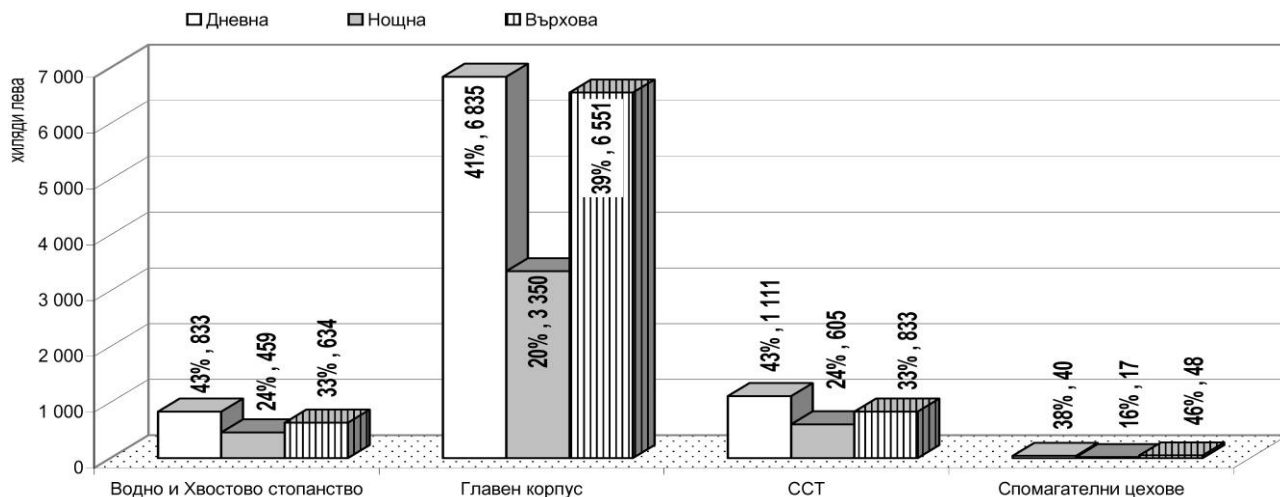


Figure 4

Percentage distribution of annual expenses for electric power for specific departments is as follows: MAIN BUILDING – 77,27%, MEDIUM-SIZE AND FINE CRUSHING – 13,27%, WATER SUPPLY AND TAILINGS – 8,95% and supplementary departments – 0,51%.

Expenses are minimum in the month of June due to the better distribution of electric power within the different zones. Therefore, characteristics achieved for that month may be considered as a norm.

Operative control of power consumption of the whole company is done by the person-in-charge in the main sub-station on the basis of visual data from the micro-processing system. Planning and reading of power consumption is done on the basis of records from daily power consumption. Each day professionals from the power department determine the following characteristics, generally for the company and for the departments of MAIN BUILDING, Medium-size and fine crushing and water supply and tailings:

- specific power consumption;
- average specific consumption for the current day of the month;
- percentage distribution of consumed power supply for each day for specific zones;
- implementation of the schedule for power consumption, in kWh and in leva for specific rate zones.
- percentage implementation of schedule for each day and for the current day of the month.
- average factor of power for the day-time and the peak zones -
- for each day and from the beginning of the current month.

Each month data are summarized and a record is prepared for consumed electric power and expenses in (eva) for rate zones for each department of the company, including the supplementary departments.

The criterion for analysis of power consumption, namely – the specific power consumption does not provide an objective assessment of the effect of redistribution of loading in the different rate zones and expenses. The other criterion – daily determination of percentage power distribution in the rate zones provides a certain opportunity for comparative assessment, however the logical analysis is difficult due to the large scope of data. For that reason we suggest the involvement of a differential reading of power specific consumption for rate zones. A better view of the distribution of funds may be presented by the parameter “C” – levas for the electric power spent for 1 ton of processed ore (leva/ton). That parameter shows completely the main factors, effecting on

expenses for electric power – quantity of used electric power, ratio of cost of power in the different rate zones and possible financial penalties from the power supplying company. Below are presented the bases for that suggestion:

- technological process in the MAIN BUILDING, where more than 77% of the total power is consumed, is continuous;
- daily productivity of the plant is rather constant and for the year 2002 it is within the range of: minimum: 32299 tones, maximum 34420 tones and average 33247 tones. The above presented is a reason for accepting, with a certain approximation, that the daily, respectively monthly productivity is proportionally distributed in a ratio corresponding to the percentage distribution of rate zones – peak rate 25 %, day-time rate 41,66% and night-time rate 33,33%. The Department for medium-size and fine crushing works with interruption during the morning peak zone, and the Water supply and tailings department reduces loading during the two peak zones. A reduced specific electricity consumption is determined for those departments as a consumed power for the respective rate zone referred to the quantity of dressed ore of the MAIN BUILDING. Having in mind that the month coefficient of motion of the mills is within the range 95% - 99% and for the year the average-weighted value is 97,22%, we consider that its reading is not necessary for comparing the month characteristics for specific consumption of electric power.

The establishing of a scheme for determining the structure of power consumption for each month is advisable. Table 1 shows the comparison of suggested parameters for months January and month December of 2002. The selected months belong to the winter period, which allows not to read the coefficient of season. The specific power consumption for January is – 23,376 kWh/ton, and for December 23,01 kWh/ton. The table covers the whole structure of power consumption, reading all the factors – changes in the regulation for cost of electric power, effects of the activities for saving of energy, and what are the departments of the company and what is the approach for achieving that effect. For example, for dressing of one ton of ore in January the enterprise paid 1,788 BGL for power, and for December - 1,695 BGL. For a conditional average month productivity of one million ton, in case of the above ratio, expenses for electric power will be reduced with 93 000 BGL. A portion of the reduction is due to preferential costs for December for the day-time and night-time power during the weekends and holidays. However, there are other factors that are evident from the suggested structure in table 1.

Table 1

| zones<br>months | peak zone         |              |                   |              | day-time zone     |            |                   |            | night-time zone   |            |                   |            | total             |              |                   |              |
|-----------------|-------------------|--------------|-------------------|--------------|-------------------|------------|-------------------|------------|-------------------|------------|-------------------|------------|-------------------|--------------|-------------------|--------------|
|                 | I                 |              | XII               |              | I                 |            | XII               |            | I                 |            | XII               |            | I                 |              | XII               |              |
|                 | $\omega$<br>kWh/t | c<br>BGL/t   | $\omega$<br>kWh/t | c<br>BGL/t   | $\omega$<br>kWh/t | c<br>BGL/t | $\omega$<br>kWh/t | c<br>BGL/t | $\omega$<br>kWh/t | c<br>BGL/t | $\omega$<br>kWh/t | c<br>BGL/t | $\omega$<br>kWh/t | c<br>BGL/t   | $\omega$<br>kWh/t | c<br>BGL/t   |
| PP              | 22,41             | <b>2,734</b> | 21,21             | <b>2,59</b>  | 22,996            | 1,748      | 23,10             | 1,68       | 24,578            | 1,131      | 24,25             | 1,04       | 23,376            | <b>1,788</b> | 23,01             | <b>1,695</b> |
| FP              | 17,88             | 2,181        | 17,93             | 2,188        | 17,971            | 1,366      | 18,28             | 1,332      | 18,007            | 0,828      | 18,596            | 0,798      | 17,96             | 1,39         | 18,299            | 1,368        |
| AFC             | <b>2,448</b>      | 0,299        | <b>1,689</b>      | 0,206        | 2,878             | 0,219      | 2,683             | 0,195      | 3,385             | 0,156      | 2,997             | 0,129      | <b>2,939</b>      | 0,218        | <b>2,539</b>      | 0,176        |
| WST             | 1,896             | <b>0,231</b> | 1,387             | <b>0,169</b> | 1,982             | 0,151      | 3,059             | 0,144      | 3,038             | 0,140      | 2,517             | 0,108      | 2,312             | 0,167        | 2,008             | 0,138        |

For example, for the peek zone, when the cost of power was not changed, 2,734 BGL were paid for January, while 2,59 BGL were paid for December for the dressing of 1 ton of ore. In that case, the reduction of expenses is due to the more-rational management of power consumption. The specific consumption of power in the peek zone for the Department of Medium-size and fine crushing is reduced from 2,448 kWh/ton to 1,689 kWh/ton. Therefore, a significant reduction of loading during the peek zone is achieved on the account of the night-time zone. That is a result of strict observation of the regime of work at the department – excluding the whole period of the morning peek, implementation of planned repairs in the peek zones of the working days, maximum loading in the weekends and holidays. There is a positive tendency in the general specific consumption for the Department for Medium-size and fine crushing from 2,939 kWh/ton is reduced to 2,539 kWh/ton for December. The automated system for control of the technological process, which optimizes the work of crushers and limits the idle work contributes to the power consumption reduction (Voloshtenko, N.E., Ostrovski et al, 1990r.)

At the Water supply and tailings Department a more rational distribution of the specific power consumption in the respective rate zones is realized in December. That brings to reduction of expenses for circulation water supply in the peek zone from 0, 231 BGL to 0,169 BGL for ton of dressed ore.

The month elaboration of the suggested table gives an opportunity for discovering the structure of main parameters, characterizing the power consumption. Comparison of suggested parameters for individual months provides the option for qualitative assessment of applied measures for saving of power.

Professionals from the enetprise achieved the following positive long-term effects on the basis of data about distribution of power consumption:

1. Precise planning of consumed electrical power for a quarter of year without any corrections.
2. Lack of penalties for the low average month values of the factor of power.
3. Lack of penalties for returned in the system reactive power.
4. Satisfactorily distribution of consumed power among the rate zones for the technological processes.
5. Tendencies for increase of consumed power in day-time and night-time zones in the weekends and the holidays..

II. In respect of saving the power:

1. Voltage of major consumers is maintained close to the maximum to the nominal one. For that purpose, digital volt-meters and a device for sound signaling of the deviation of voltage from given values are mounted in the sub-station.

2. Excitation of synchronous motors is optimized to a level that their common work with condenser batteries is realized with an average-month factor of power of 0.9 - 0.91. A regulation of the factor of power by changing the voltage by Jansen regulators of transformers is allowed, however within narrow boundaries, determined by experimental investigation (Menteshev, Stoilov et al., "Report", 1994)

3. Regime of work of air electrical ducts and transformers in the pumping stations of the circulation water supply is optimized. Losses of power are calculated for three versions and the most economic one is selected. The pumping plant for fresh water works only three nights in the week, two of them in the weekends or in the holidays, if possible. In all the other time the transformer – 1600 kVA/20/6kV is also switched out.

Expenses for electric power occupy the highest share of the expenses of the company. The issue of reduction becomes more and more up-to-date, due to the tendency of rise of power cost. The schedule of loading, constructed for a typical working day (fig. 5) illustrates the character of electrical loading.

I. In respect of acting rates for paying the power:

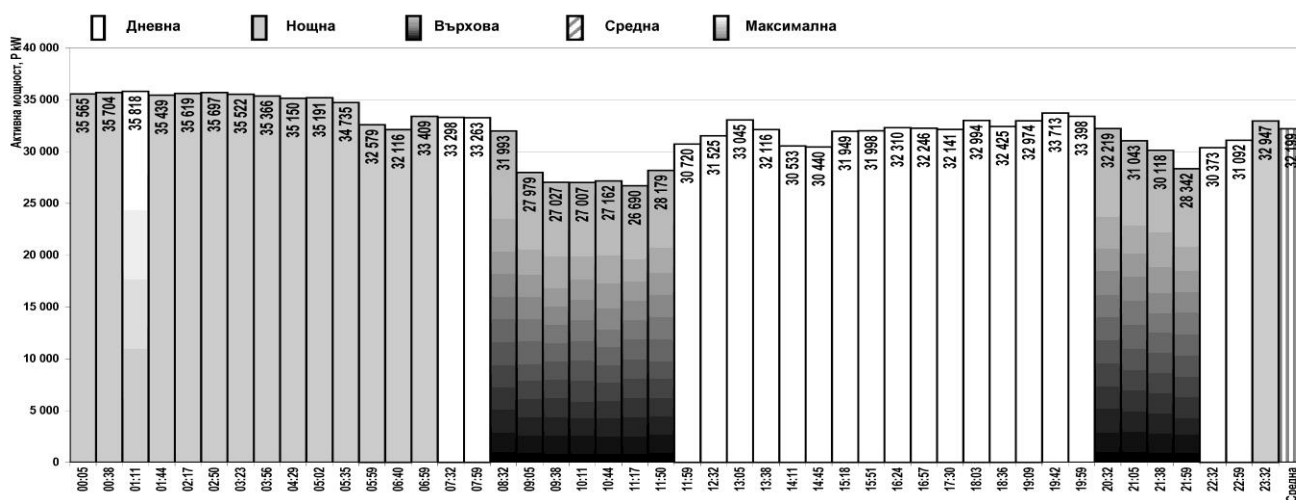


Figure 5

Evidently, opportunities for reduction of expenses through more optimal distribution of power among the rate zones have already been exhausted. For that reason, measures of larger

scale are undertaken to use more rationally the opportunities of payment rate of electric power:

1. Water-collecting basins for circulation water on the territory of the plant are reconstructed. Their volume is increased with 3000 m<sup>3</sup>, which will allow an unloading of peak zones with nearly 2100kW.

2. A project is developed for increase of the productivity of Departemnt for Medium-size and fine crushing to 2000 t/hour. Its implementation will make possible the interrupting of operation of the evening-time peak zone. This will bring to: reducing the loading of the company during the evening peak with nearly 4000kW.

The main criterion for effective use of power supply in the technological processes is the specific consumption. In the MAIN BUILDING the type of loading is determined by the ball mills. They consume more than 70% of the power. The following energy characteristics of power  $P=4,41.A + 18762$  and specific power consumption  $\omega = 4,41 + 187622/A$  (Danailov D., 1985) are derived with the aim of determining the regularities of power consumption at the department, (data of power and productivity refer to June 2000). Fig. 6 illustrates the above dependencies.

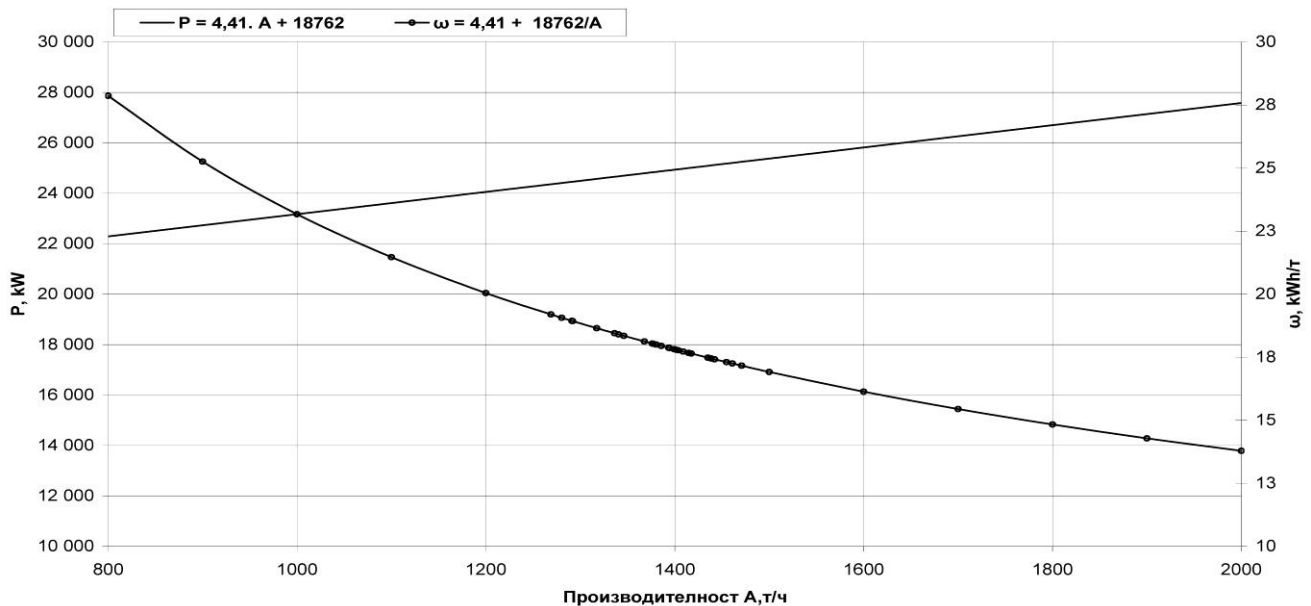


Figure 6

As it is known, specific power consumption for grinding in ball mills is closely related to the technological process and depends on a number of factors: weight of ball loading, density of slurry, size of feeding material, mechanical properties of ore, productivity of the mill, granular composition of milled product etc. Experimental investigations showed that the main power in the ball mill is used for rise of the ball loading – nearly 80% (Stepanov V.S., 1984). Increase of mill productivity brings to insignificant increase of used power. Considering that ball mills are a decisive factor in the structure of power consumption, the intention for increase of mill productivity and respective reduction of specific power consumption is logical. For that purpose, the flowsheet of the Department for medium-size and fine crushing comprises a set – cone crusher, sieving machine and a shaft crusher. Milling aggregates are to be fed with ore, in which the class “-15mm” is 95%, i.e. through reducing the size of ore fed for milling to improve the productivity of mills. This, on its own behalf will bring to reduction of the specific power consumption for the process of grinding. The mounting of two new sets is forthcoming. On the other flows for fine crushing the class “-15mm” will be controlled with sieving machines only.

Productivity of the depends on the correct selection of the ball loading. Both the enhancement and the reduction of ball

loading bring to reduction of mill productivity, and therefore rise of specific power consumption. Size of grinding bodies (balls) also effects productivity of milling process. An investigation for optimizing the diameter of grinding bodies (balls) is needed, when the provided granular composition of incoming ore (95% class “-15mm”) is achieved. That is why an automatic system for dosing the balls in the mill is in a process of testing. It is typical that feeding of balls is a continuous process, which improves the structure of ball loading. It is expected that with the optimization of ball loading, in both quantity and structure, the productivity of the mill will be enhanced and parameters of outgoing product will be improved.

The determination of structure of power consumption at the dressing plant through differential into the rate zones for specific consumption of power  $\omega_i$  and expenses for power for a ton of the processed ore are a pre-condition for:

- more rational control of power consumption;
- effective control over the departments for the observation of determined regimes of operation;
- precise quantitative assessment of the efficiency of activities for saving of power;
- reasoned determination of the differential norms for power consumption for individual departments.

For the "Elatsite-med" Co. the conclusion of a contract, as a privileged consumer, with the power supplying company is forthcoming. Based on the data of structure of power consumption, professionals from the company will be able too negotiate attractive costs and parameters, if they are supplied with the respective option.

#### REFERENCES

- Voloshtenko N.I., E. P. Ostrovski et al, 1990. Effective use of electric power in coal mining, Nedra Moscow, (in Russian)
- Danailov D. 1985, Rational use of electric power in mining. Technika, Sofia (in Bulgarian)
- Report – Development and commissioning of technical and organizational means for minimizing the expenses for paying electric power by the "Elatsite" according to the new rate (SJ No 26/29.03.1994) – *Mingeouniverse engineering, archieve of MGU, Sofia* (in Bulgarian)
- Stepanov V. S., 1984 Analysis of energetic improvement of technological processes, Nauka, Novosibirsk (in Russian)
- Stoilov I., K. Djustrov et al. 2003 System for measuring, control and management of power consumption at the "Elatsite Med" Co. Annual of the University of Mining and Geology "St. Ivan Rilski", volume 46, 2003, Publishing house "St. Ivan Rilski"

*Recommended for publication by Department of  
Electrical Engineering, Faculty of Mining Electromechanics*

## INNOVATIONS IN CMC-C ELECTROENGINEERING

**Stephan Chobanov**

CMC – C Ltd  
Pirdop 2070, Bulgaria  
St.St. Kiril I Methodi St. 5  
E-mail: [cmc\\_c@mail.bg](mailto:cmc_c@mail.bg)

**Mento Menteshv**

CMC – C Ltd  
Sofia 1164, Bulgaria  
8 Krivolak St.  
E-mail: [cmc\\_c@mail.orbitel.bg](mailto:cmc_c@mail.orbitel.bg)

### ABSTRACT

CMC-C EOOD is an electrical engineering company established in 1995, which develops activities mainly in the mining and metallurgical industries. These activities involve expert assessments, consultancy services, design and implementation of electricity supply and electrical equipment of electrical systems up to 35 kV, design and manufacturing of switchboards, LV and MV electrical systems and special control and protection devices.

A Quality Control System was introduced in 2001 in compliance with the ISO 9001 standard.

Innovations are priority activities in the company. By using its own investigation results and with the active participation of university lecturers, the company has proposed, developed and implemented new engineering and technological designs at the request of our clients in this country and abroad. These designs are in the field of efficient utilization of electric power, updating of the electrical equipment of mine battery locomotives, electrical safety, electric devices, electricity supply and electrical equipment.

CMC – C EOOD was established in 1995 and provides full engineering services in the field of electricity supply and electrical equipment of industrial, public and household sites. The activity is mainly focused on the mining and metallurgical industries.

The basic company activities involve research, design, construction, manufacturing, erection, adjustment, maintenance, repair and reconstruction of cable and aerial lines, distribution switchgear and substations, lightning protection and earth wiring systems, electric power equipment, indoor electrical systems, material-handling equipment, automatic control of technological units and processes.

The company has been certified under ISO 9001-94. A type-C Control Section has been set up at CMC-C and certified by the Bulgarian Accreditation Agency.

A priority in the all-round activity of the company is the application of the most modern electrical devices, equipment and technologies as well as the development of original new designs for solving practical problems.

In the field of innovations the company works in collaboration with university lecturers and specialists. Its strongest connections are with the University of Mining and Geology and, primarily, with the Departments of Mining Electrification and Electrical Engineering. Contacts have also been established with the Department of Electrical Devices at the Technical University.

It is worth mentioning in advance that all innovatory engineering and technological designs have been implemented and introduced in practice and very well accepted by our clients.

### *Updating of MV switchgear*

Our company is one of the first in this country (1995) that developed and implemented a technology for updating obsolete and outdated switchgear by replacing the electromechanical protections with multifunctional microprocessor ones and the oil-minimum breakers with sulfur and vacuum ones (Fig. 1). The updating thus performed offers functional possibilities and reliability corresponding to new switchgear but at 2–2.5 times lower prices (Navan-Chelopech).



Figure 1

### *Electric switchboards and LV distribution switchgear*

General and special purpose switchboards and switchgear are designed and manufactured by using modern components and technologies including the Schneider Electric PRISMA system.

**Lightning-discharge protectors with active lightning arresters**

Active lightning arresters have been designed and manufactured (Fig. 2). The protected area is tens of times larger than that protected by lightning pointed rods with considerably higher reliability (Umicor Med, petrol stations, gas stations, public buildings in Sofia, Koprivshitsa, Turgovishte).



Figure 2

**Integrated moving electrical systems.**

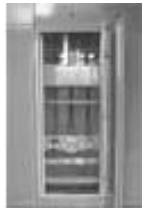
An integrated moving electrical system has been designed (Fig.3) which consists of a steel container (a) integrating switch and protection apparatus for 6 kV (b), for low voltage 0.4 kV (c) and an automated management and control system (d). This original engineering design has been applied for the electrical equipment of the Sever Shaft fan at Chelopech Mine.



a



b



c



d

Figure 3

**Updating of the electrical equipment of mine battery electric locomotives**

CMC-C integrates the efforts of specialists from the University of Mining and Geology "St. Ivan Rilski", the Technical University, Energia AD, Tzar Kaloyan CRP for updating the mine battery locomotives by:

- Replacing the alkaline traction storage batteries with lead-acid ones.
- Introducing modern technology for battery charging.
- Applying static control of the electric locomotive dc drive.

This combination allows for the locomotive to be completely updated at the cost of the alkaline batteries only with considerably higher energy efficiency, convenient operation and facilitated explosion protection.

This concept has been realized by the substantial support of the manufacturers of lead-acid traction batteries – Energia AD in Turgovishte; of battery chargers - Tzar Kaloyan CRP in Razgrad. The concept has been fully implemented at Malamovo Mine (Bobov Dol) and partially at Marbas and the Elatsite Med Tunnel.

Mass implementation in the Ukraine coal mines at Donetsk started in 2000 in active collaboration with NPP Energia.

**Updating of the electrical equipment of machine tools**

Modernization of the electrical equipment of machine tools has been carried out which involves replacement of the electric machines of Г-Д groups with static controllable rectifiers and all switch and control apparatus with modern designs characterized by smaller overall dimensions, higher precision as well as reliability and performance.



Figure 4

**12 000A circuit breaker.**

A dc circuit breaker has been designed, manufactured and put into operation in collaboration with ET Metalplast and intended for shunting of electrolysis baths. It has the following characteristics:

- Voltage 100 V
- Rated current 12 000 A
- Remote control, electric motor drive
- Contact bodies: Ag -Cu

The circuit breakers (Fig. 5) have been applied in the electrolysis shop at Umicor Med, Pirdop.



Figure 5

**Plug connector with a high level of protection from external actions**

A plug connector has been designed with the following parameters:

- Voltage 1000V
- Rated current 250A
- Number of poles 3+1
- Level of protection IP54

It has been applied in connecting powerful mining machines at Chelopech Mine (BIMAK). It is manufactured as an individual item or supplied with an automatic switch (Fig. 6)



Figure 6

#### **Earth leak protection devices (ELPD) in mains of up to 220V**

The company manufactures a variety of earth leak protection relays for IT systems (with sources insulated to ground) based on own designs in compliance with BSS 10880-83. Basic parameters:

- Mains voltage 110; 127; 220V;
- Type of mains current – dc/ ac
- Natural actuation time <100ms

Various types of earth leak protection relays (Fig. 7) have been applied successfully in shovels and spreaders – AZU 127 and AZU 220 V, in substations AZU 110, AZU 220 V, in chargers for traction batteries (AZU-120 Ex), etc.



Figure 7

#### **Current leak control device LCD-M**

The current leak control device LCD-M is a special-purpose apparatus used for bus systems and electrolysis baths. The dc mains in the electrolysis shops are characterized by low insulation resistance -  $10^{-1}$ - $10^3\Omega$ . The current leak control is related mainly to limiting electric energy losses.

The device has been designed especially for Unicor Med-Pirdop (Fig. 8) and is used to control:

- Leakage current, A
- Leakage power, kW
- Energy lost from leakage currents, kW/h
- Asymmetry of voltage to ground, %

The device contains a PIC processor that computes and scans the quantities listed above by means of digital indicators. The light signalization, doubled by remote control, indicates three levels of leakage current: “normal”, “higher” and “unallowable” thus requiring measures for limiting the losses.



Figure 8

#### **Electricity demand control and management systems**

Electricity demand control, measuring and management systems have been developed and put into service. The system implemented at Elatsite Med AD in 2000 (Fig. 9) can perform the following functions:

- Measuring the active and reactive power at the input and outputs;
- Determining the consumed active energy in three zones: peak zone, day zone and night zone;
- Determining the moments of the mean values of  $\cos \varphi$  in the day and night zones as of the beginning of the month;
- Determining the reactive energy returned to the mains with a possibility to signal its generation;
- Daily, monthly and yearly information about the consumed electric energy by tariff zones. The information contains the electricity costs corrected in relation to  $\cos \varphi$  and the reactive energy returned to the mains;
- Possibility for extracting daily, monthly and yearly load curves by terminals and generally at the input, including a choice of random periods within up to 3 years back;
- Automatic print-out of daily, monthly (on every first day of the month) data on energy consumption and the amounts paid for electricity;



Figure 9



Figure 10

**Indication of short circuits in electrolysis baths**

An indicator has been designed for identifying short circuits between the anodes and cathodes in electrolysis baths for recovering copper. The needle instruments, strongly vulnerable in an aggressive environment, as well as digital instruments causing sight fatigue, have been replaced with original engineering designs. The indicator indicates the occurrence of a short circuit by a light-emitting diode mounted in the upper base of the cylinder (tube). The sensor is positioned in the lower widened part of the measuring instrument (Fig. 10).

The indicator has been applied at Umicor Med AD, Pirdop.

A short-circuit centralized control system is being developed as a prerequisite for shortening the duration of a short circuit and hence, improving the efficiency of the electrolytic process.

**Flameproof units for remote control of explosion-protected mine starters**

Flameproof units for remote control of PVI mine starters in Exdil design have been developed and manufactured.

The units are completely interchangeable with the original RC units of the starters but have been designed and manufactured by using modern electronic components in integral design.

The units have been certified as flameproof.

Recommended for publication by Department of Electrical Engineering, Faculty of Mining Electromechanics

## SCHEME AND TECHNICAL MEANS FOR AUTOMATED CONTROL OF THE COMPRESSOR STATION IN QUARRY FIRST OF MAY – MARBLE AND GRANITE CORPORATION

**Neli Stefanova**

University of Mining and Geology  
"St. Ivan Rilski"  
Sofia 1700, Bulgaria

**Angel Zabchev**

University of Mining and Geology  
"St. Ivan Rilski"  
Sofia 1700, Bulgaria

**Matei Mateev**

University of Mining and Geology  
"St. Ivan Rilski"  
Sofia 1700, Bulgaria

### ABSTRACT

The paper treats the means for automated control of the compressor station exploited under the conditions of quarry FIRST OF MAY - MARBLE AND GRANITE CORPORATION

Until recently a large dimensions extraction of granite blocks has been realized in the quarry FIRST OF MAY of the MARBLE-GRANITE Ltd., which is situated in the western slopes of the VITOSHA MOUNTAIN. For next machining (cutting into slabs and grinding) the blocks have been transported in the stone cutting and grinding workshops built in the village VLADAJA.

Considerable amounts of sets, free stone and elements for granite lining have been produced on the quarry territory.

Drilling and blasting operations has been carried out for uncovering and partially for extraction realization and for separation from the mass - drilling operations providing hydraulic wedges use.

The quarry has had several production sections, its own transformer station and pneumatic management including an air conduit long about 2-3 km and compressed air consumers (jack hammers and pneumatic picks, set presses and sharpener).

Initially, the compressor station has been equipped with five two-stage reciprocal compressors type BORETZ 10/8, which have fed a shared air tank (receiver) with a blow valve by a manifold pipe.

Each compressor drive consists of a three-phase squirrel-cage induction motor AM-92-6 (power 75kW, rotation frequency 950 min<sup>-1</sup> and voltage 380V) and a V-belt transmission.

The compressors cooling are provided by a shared water tank in an open scheme with gravitation liquid flow.

The manual motors control (start and stop) and their overload protection have been realized by automatic oil-filled star-delta starters АПМ3Т - 500/200.

The participation of the input, medial and executive starter elements in the power and driving circuit is respectively shown in figures 1a and 1b.

In principle, the motor-compressor unit basic configuration is shown in fig. 2.

The manual start of each compressor is realized as follows:

- A. At no excessive pressure of the air in the tank (i.e. after a long pause of the pneumatic energy consumers operation or after a compressed air deliberately emission in the atmosphere through the cocks K<sub>2</sub> and K<sub>1</sub>) the motor starting process goes off at closed cock K<sub>1</sub> and opened K<sub>2</sub>.
- B. At a high (i.e. close to the operational) air pressure in the tank the motor starting process is preceded by the cock K<sub>2</sub> closing and K<sub>1</sub> opening. After the end of the process closing of the cock K<sub>1</sub> and opening of K<sub>2</sub> have to start simultaneously.

Usually, the compressors have been in continuously operation during the whole shift and the compressed air high consumption and the possibility for the number of the compressors in use to be changed have prevented the blow valve 8 (adjusted for bound pressure 0,65MN/m<sup>2</sup>) actuation as well as the rise of the respective undesirable pneumatic energy losses.

For several years quarry FIRST OF MAY lands in the extended borders of the NATIONAL PARK VITOSHA, so the production and extraction activities have got more complicated due to the intolerable realization of blasting operations.

At this stage, the quarry extraction is brought to oversized blocks dragging out of its own old dumps and the production activity - to production of sets and free stone. This has also led to a sharp decrease in the quarry pneumatic management, which is now presented by two compressors (an operating and a reserve), an air conduit long about 600m and several

jack hammers and pneumatic picks. The maintenance personnel number has been reduced as well and the only man, who is in charge of the compressor, is also responsible for the pneumatic management rest components maintenance.

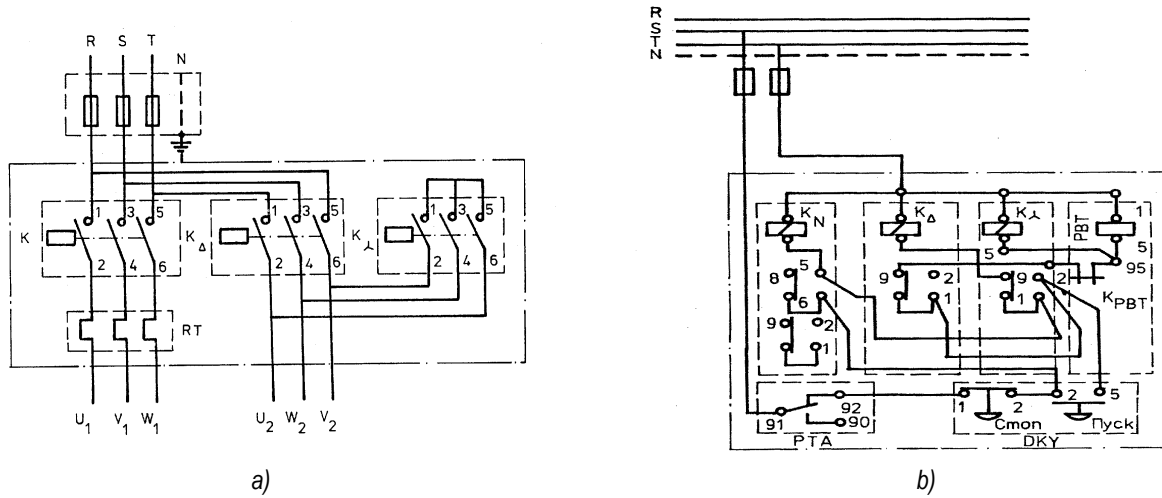


Figure 1

The attempt for decrease in the electric power consumption for the compressed air production by reduction of the compressor operation time ( $t_1$ ) during the working shift to tree hours has not brought acceptable results because at the restricted consumers number and comparatively high compressor output (30 m<sup>3</sup>/min) even small changes in the operating pneumatic picks number lead to the blow valve actuation and the compressed air emission to the atmosphere.

At the state of affairs, worsen by the continuous increase of the electric power price in the country, the governing body of MARBLE-GRANITE has assigned (by a contract with the Scientific-research Sector of the University of Mining and Geology "St. Ivan Rilski") to the team of the authors the implementation of automatic control of the quarry FIRST OF MAY compressor station.

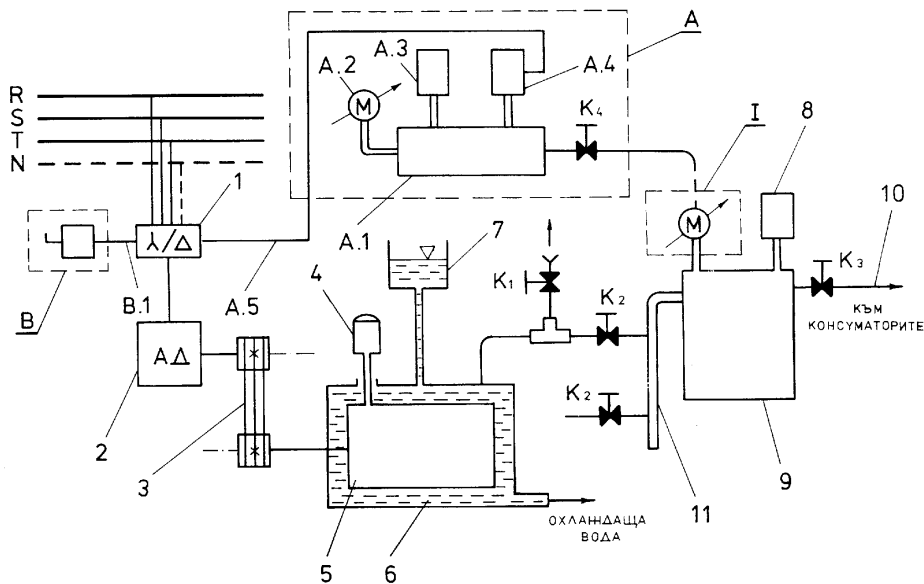


Figure 2. 1 - starter АПМ-3Т-500V/200А; 2 - induction motor; 3 - V-belt transmission; 4 - air filter; 5 - compressor; 6 - cooling water jacket; 7 - water tank; 8 - blow valve; 9 - air tank (receiver); 10 - main air conduit; 11 - manifold pipe; А - control-measuring pneumatic device; А.1 - body-distributor; А.2 - manometer; А.3 - blow valve; А.4 - pressure regulator; В - duty switch changer; А.5 and В.1 - lines supplying control electric signals to the starter 1; I - manometer; K<sub>1</sub>, K<sub>2</sub>, K<sub>3</sub> and K<sub>4</sub> - manually controlled stop cocks.

The restricted corporation finances predetermined the realization of partial (in accordance with the criterion of compressed air pressure) compressor control automation at a maximal preservation of the existing compressor station configuration. The restricted contract price did not allow the transmission reconstruction by implementation of starting clutches, respectively the back valves delivery or remote controlled cocks substitution for the cocks  $K_1$ ,  $K_2$  and  $K_3$  as well as the basic starting electric equipment replacement.

Under these circumstances the following changes (fig. 2) have been done in the motor-compressor set configuration:

1. The manometer I (see fig. 2) is removed;
2. Two new units supplying control electric signals to the АПМ3Т – 500/200 are implemented:
  - A duty switch changer B (fig. 2) consisting of medial relay and two-position switch;
  - A control - measuring pneumatic device A (fig. 2) consisting of a body-distributor A.1, manometer A.2, blow valve A.3, pressure regulator A.4 and stop cock  $K_4$ .

The general view of the unit A is shown in fig. 3 and the subunit A.4 (pressure regulator PH) mechanical diagram – in fig. 4. Both of them (i. e. A.3 and A.4) are components of the German industrial locomotives EL-2 pneumatic brake system. The former subunit A.3 has been calibrated and adjusted in laboratory conditions for bound pressure  $0,67 \text{ MN/m}^2$ , so in case of failure to repeat the action of the basic blow valve 8. The latter (A.4) has been subjected to a reconstruction, which finds expression in replacement of the coil spring  $\Pi_1$  (see fig. 4) and readjustment of the regulating screws  $B_1$  and  $B_2$ , respectively of the left supporting plate 4. As a result the pressure regulator PH maximal switch range is increased from  $0,2 \text{ MN/m}^2$  to  $0,4 \text{ MN/m}^2$ . By the regulating screw  $B_2$  and the adjustable right supporting plate 4 an upper bound of PH actuation exceeding to  $0,6 \text{ MN/m}^2$  (PH allows  $p_{\text{max}}=0,9 \text{ MN/m}^2$ ) is measured in laboratory conditions.

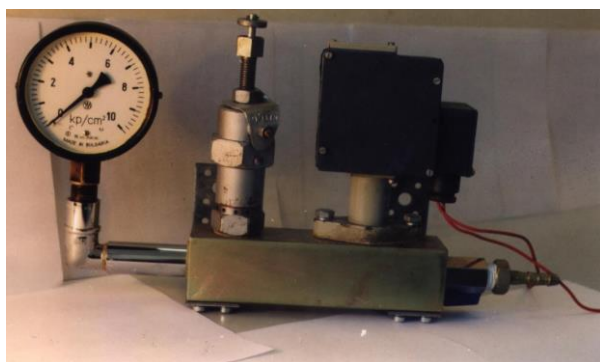


Figure 3

By the compressor test starts, carried out in industrial conditions by the available starter АПМ3Т – 500/200, but at different excessive pressure values in the receiver, has been ascertained that the upper pressure bound at which the starting process still ends successfully is  $0,35 \text{ MN/m}^2$ .

The changes in the starter АПМ3Т – 500/200 driving circuit and the whole compressor control circuit diagram are shown in fig.5.

The diagram provides two control regimes – manual and automatic, which could be chosen and switched by the switch II.1.

At a choice of the first regime the switch has to be put in position “0” (this diagram position is shown in fig. 5) and the connection between the clamps 4 and 5 is restored by the movable contact  $\Pi K_1$  of II.2. In manual control regime the compressor start and stop are realized by corresponding starter АПМ3Т – 500/200 buttons regardless of the III.1.1 and III.2 contacts condition. At this control regime a normal compressor operation is provided in cases, when preventive maintenance or repair works in the rest of the diagram components are carried out.

At a choice of automatic control regime the switch II.1 has to be put in position “I”. At this, the АПМ3Т – 500/200 buttons Start and Stop are shunted by the movable contact  $\Pi K_2$  of II.2 and the compressor start and stop are transferred to the pressure regulator III.1.

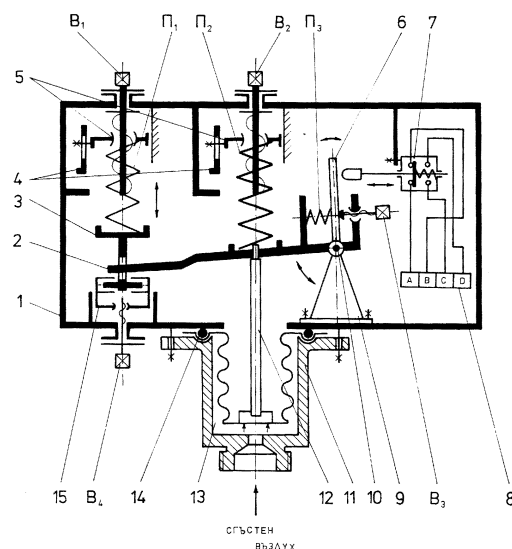


Figure 4. 1 – body; 2 – hinged frame; 3 – adjustable thrust; 4 – restrictive adjustable supports; 5 – tightening movable cross arms; 6 – hinged arm; 7 – limit switch; 8 – clamps; 9 – hinged prop; 10 – hinged axle; 11 – nipple-inlet for the compressed air; 12 – a stem transmitting the compressed air pressure to the hinged frame 2; 13 – corrugated metal sleeve; 14 – sealing ring; 15 – a movable frame changing the thrust 3 position;  $B_1$ ,  $B_2$ ,  $B_3$  u  $B_4$  – regulating screws;  $\Pi_1$ ,  $\Pi_2$  u  $\Pi_3$  – coil springs with adjustable pressure force.

The automatic control aims at the compressor operation discontinuation when the air pressure in the receiver has reached to  $0,6 \text{ MN/m}^2$  and switches it on again, when the latter has fallen to  $0,25 \text{ MN/m}^2$  (the bounds have been coordinated with the corporation specialists). The compressed air emission from the receiver to the atmosphere is prevented by a choice of the upper pressure bound with  $0,5 \text{ MN/m}^2$  lower than the actuation level of the air tank blow valve and corresponds to the compressed air rated pressure for the manual pneumatic tools in use.

When the switch II.2 is in position "I" the contactor PM is actuated because 0 is supplied to the clamp 3 and to the clamp 2 – the phase R along the circuit : point 92 from I, the clamps 4,1, B, the closed switch of PH, clamps A and 2. The contactor PM closes its contact  $K_{PM}$  connected with the

clamps 4 and 5. The phase R reaches the point 5 from I through the clamp 4, the contact  $K_{PM}$ , the clamp 5, the movable contact  $\Pi K_2$  and clamp 6 as a result of that the motor starts.

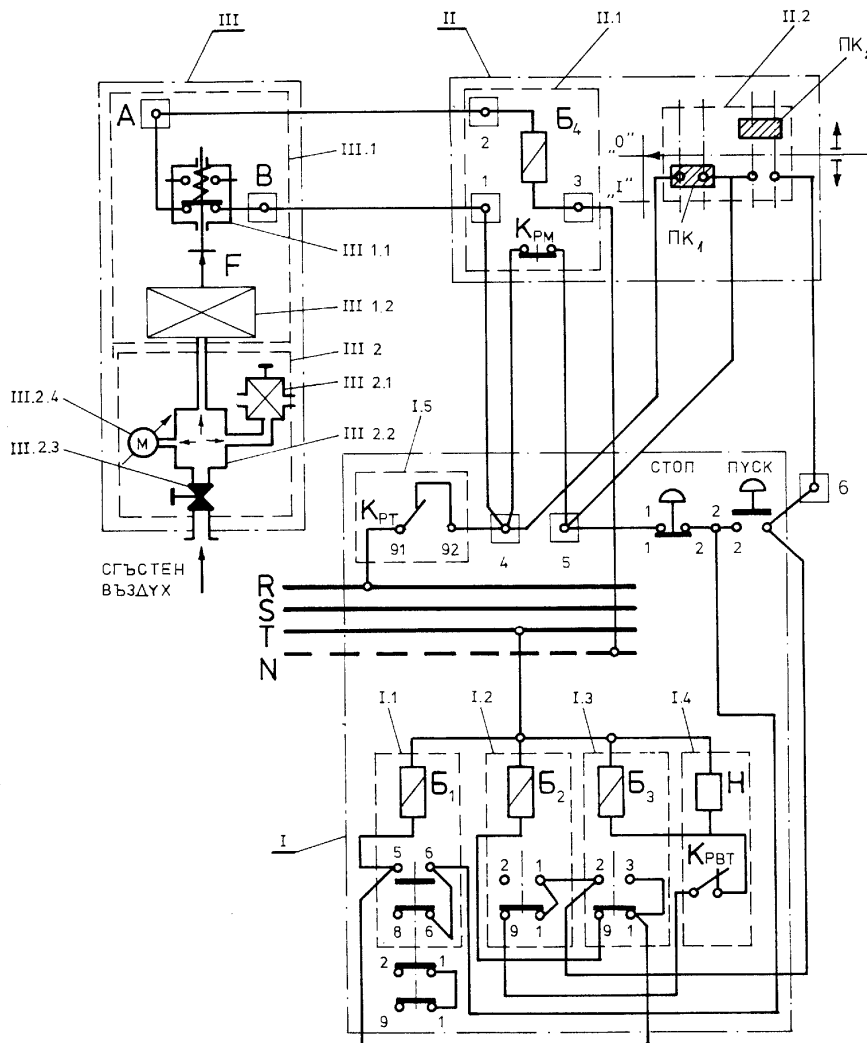


Figure 5. I – star-delta starter АПМ3Т – 500/200; I.1 – main starter contactor ( $K_N$ ); I.2 and I.3 – starter switching contactors ( $K_S$  and  $K_D$ ); I.4 – thermal timer (PBT); I.5 – thermal relay; II – duty switch changer; II.1 – medial relay (PM); II.2 – bistable switch; III. – control-measuring pneumo-electric block; III.1 – pressure regulator (PH); III.1.1 – limit switch; III.1.2 – regulator mechanical part; III.2 – pneumatic part of the block III; III.2.1 – blow valve; III.2.2 – body-distributor; III.2.3 – cock; III.2.4 – manometer;  $B_1, B_2, B_3$  u  $B_4$  – coils of the contactors  $K_N, K_S, K_D$  and PM; H – PBT heating element; - clamps of the clamp-rows II and III; F – total force created by the pressure regulator mechanical part.

At the pressure increase to  $0,6 \text{ MN/m}^2$  the PH switches off the contactor KM coil by the circuit disconnection between the clamps A and B. The contact  $K_{PM}$  switches off and breaks the phase to point 5 from the starter I, which causes the motor turning off.

At the pressure fall to  $0,25 \text{ MN/m}^2$  PH closes its contact and actuates the contactor PM, which by the contact  $K_{PM}$ , supplies the phase to the point 5 and the motor starts. The process continues in an automatic regime controlled by the pressure change in the receiver.

In order the operating compressor to be emergency stopped in an automatic regime the bistable switch has to be turned to "0" (i.e. the manual control to be switched over) and next the Stop button to be pressed.

During the November, 2002, 72-hour recording test (by a recording instrument WATTREG 10) of the power consumed by the motor (N) has been carried out in order the technical means and the diagram operability to be determined.

A wattmeter record of the dependence  $N=f(t)$  at the compressor drive automatic control and absence of operating compressed air consumers is presented in fig. 6, and fig. 7

shows the graphic expression of the dependence  $p=f(t)$ , constructed according to the manometer indications, which have been read at the same load and compressor control

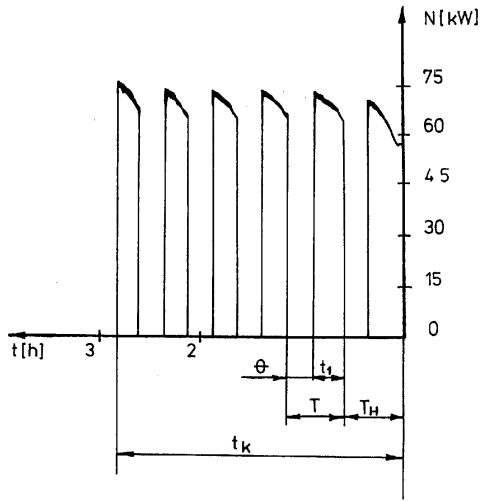


Figure 6

type. The two curves illustrate the normal operation of the diagram and equipment, realizing the compressor drive automatic control. In fig. 7 it could be seen that the compressor start and stop are steadily realized at reaching respectively the upper ( $p_{max}=0,6 \text{ MN/m}^2=6\text{at}$ ) and the lower ( $p_{min}=0,26\text{MN/m}^2=2,6\text{at}$ ) values of the pressure in the receiver.

Fig. 7 shows that after the initial cycle ( $T_H$ ) completion the rest of the time for the compressor use during the working shift ( $t_k$ ) is divided in equal cycles ( $T$ ). At this, the relation between  $t_1$  and  $\theta$  (these are the compressor operation and idle times during a cycle) is unchangeable.

The compressor automatic system has been delivered for exploitation in industrial conditions after the test completion (6<sup>th</sup>, November, 2002) and it has not shown any defects.

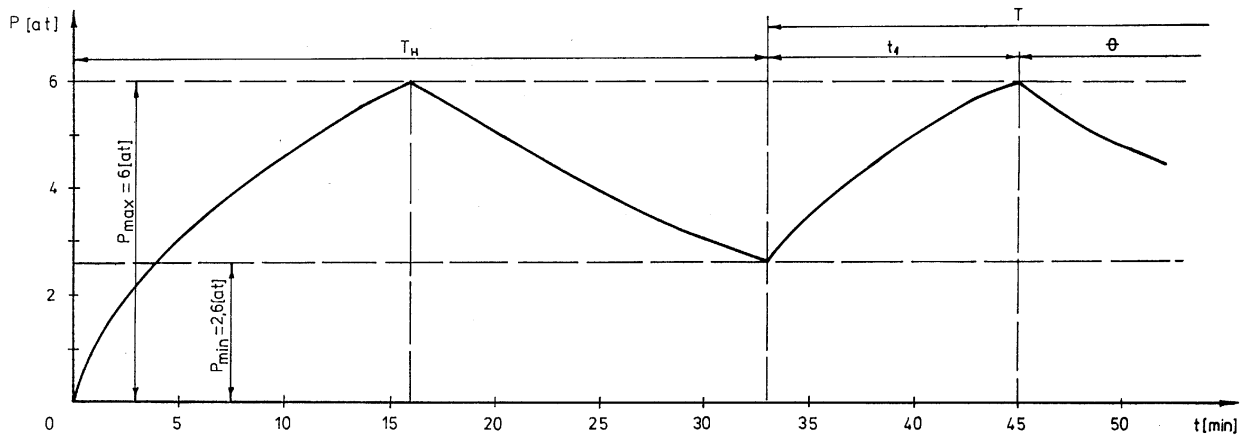


Figure 7

Recommended for publication by Department of Electrical Engineering, Faculty of Mining Electromechanics

## MATHEMATICAL MODELS WITH IMPROVED CHARACTERISTICS IN THE CONTROL SYSTEMS OF WHEEL EXCAVATORS

**Diana Tasheva**

University of Mining and Geology  
St Ivan Rilski  
Sofia 1700, Bulgaria  
E-mail: iliev@mgu.bg

**Zdravko Iliev**

University of Mining and Geology  
St Ivan Rilski  
Sofia 1700, Bulgaria  
E-mail: iliev@mgu.bg

### ABSTRACT

Determining the parameters of main working motions in the systems for programmed control of wheel excavators utilizes complex mathematical relationships requiring calculation of direct and inverse trigonometric functions. The minimization of computing operations may be achieved by using mathematical models. A basic problem in searching for such models consists in the circumstance that the initial information is acquired through constant-step scanning. This results in the occurrence of multicollinearity, which leads to finding coefficients of strongly differing orders. This impedes the program realization, decreases the reliability in verifying the model adequacy, and worsens the accuracy of forecasting.

In this article the results of applying three approaches to finding models with improved characteristics, namely those of factor normalization, regressor standardization and use of ridge-regression analysis, are presented.

### FORMULATION OF THE PROBLEM

The wheel excavator work is connected with performing a cyclic sequence of motions. Their programmed control is performed on the basis of preset reference coordinate points within the face space. This allows determining the motion parameters with the aid of mathematical relationships.

The use of analytically derived expressions (Iliev, 2001; Iliev 2002) is connected with multifold calculation of radicals and multiple direct and inverse trigonometric functions, which does not allow meeting the requirements for fast response. For this

reason it is necessary to seek other approaches to modelling in order to determine the parameters of main working motions with virtually satisfactory accuracy by carrying out a minimum number of computing operations.

A good solution proposed by Iliev (2002) consists in finding regression models estimated by the method of least squares (LSM). Using these methods not only permits building unified algorithms for programmed control that are invariant with respect to the excavator kinematic specificities, but also leads to a multifold increase in the required number of computing operations (see Table 1).

Table 1

| Number of "multiplication" operations                    | Analytical relationships | Mathematical models | Analytical relationships | Mathematical models |
|--|--------------------------|---------------------|--------------------------|---------------------|
|  | SRs 1200                 |                     | SRs 2000                 |                     |
| Determining the parameters of cut sickles                | 4                        | 7                   | 4                        | 6                   |
| Determining the number of layers                         | 30                       | 4                   | 29                       | 3                   |
| Determining the maximal depth of the block               | 131                      | 4                   | 109                      | 7                   |
| Forming the cut-sickle thickness                         | 203                      | 6                   | -                        | -                   |
| Determining the angle of swinging of the wheel boom      | 112                      | 16                  | -                        | -                   |
| Determining the parameters for transition to a new layer | 424                      | 29                  | 124                      | 29                  |

A characteristic feature of the mathematical description obtained is the wide range of varying the coefficients in regression equations. It is a normal phenomenon to find coefficients lesser than  $10^{-5}$  that cannot be assumed insignificant as their rejection will lead to considerable worsening of the models forecasting properties. Another

problem is connected with the fact that the coefficient estimates are sought with the aid of computers and in a programming environment that differs considerably from those used in real industrial control systems. For instance, MATLAB operates with numbers represented by 16 significant digits and an order of  $10^{\pm 308}$ . Presetting the regression coefficients in

such a form is virtually unrealizable for programmed control systems. However, the experience gained shows that the diminishment of the number of digits used for representing these coefficients leads to essential worsening of forecasting accuracy. This requires the application of other approaches to modelling the main working motions of wheel excavators, through which a smaller coefficient variation range will be provided and the sensitivity to changes in the number of digits representing the coefficients will be lessened in order to preserve the forecasting properties of models.

APPROACHES TO IMPROVING THE CHARACTERISTICS OF MATHEMATICAL DESCRIPTIONS OF THE MAIN WORKING MOTIONS OF WHEEL EXCAVATORS

The search for mathematical models describing the main working motions of wheel excavators is connected with the following specificities:

- An asymmetry of the factor space as a result of the essential differences in factor variation ranges;
- A presence of correlation between the columns of the augmented matrix from the experimental plan  $F$ , which is caused by the way of forming the input data.

This imposes the use of specific approaches to the information processing.

Working with normalized variables.

Input data for estimating the models that describe the main working motions of wheel excavators are obtained by scanning with a constant step. As a result there emerge significant correlations of the type  $r(x_i, x_i^2)$ ,  $r(x_i, x_i x_j)$ ,  $r(x_i x_j, x_i^2)$ ,  $r(x_i, x_i^3)$ , although the factors  $x_i$  and  $x_j$  are independent. This is the cause for bad conditionality of the information matrix  $G = F^T F$ , and leads to problems in using the least-squares method, discussed by Vuchkov and Boyadjieva (1987).

In this case it is useful to perform factor centering and normalizing before proceeding with the search for regression coefficients. This approach was investigated and promoted by D. Marquardt (1980):

$$x_{i,j}^o = \frac{x_{i,j} - \bar{x}_i}{\bar{x}_i - \min_j x_{i,j}}, \quad i = 1, \dots, m, \quad j = 1, \dots, N \quad (1)$$

where  $m$  is the number of factors,  $N$  the number of experiments, and  $\bar{x}_i = \frac{1}{N} \sum_{j=1}^N x_{i,j}$ .

As  $X^o$  has a zero mathematical expectation, the theoretical correlation coefficients also become equal to zero. Actually, they are small numbers and in the general case matrix  $G$  is well stipulated.

Standardization of regressors.

This approach finds application when the factors have diverse physical senses and dimensions, as it is also the case of modelling the working motions of wheel excavators..

The values of standardized regressors are determined in accordance with the relationship:

$$f_{ji-1}^o = \frac{f_{ji} - \bar{f}_i}{\sqrt{\sum_{u=1}^N (f_{ui} - \bar{f}_i)^2}}, \quad i = 2, \dots, k, \quad j = 1, \dots, N \quad (2)$$

where  $\bar{f}_i$  is the arithmetic mean value of the  $i^{th}$  column of  $F$ , and  $k$  the number of estimated coefficients.

The model is sought by applying the least-squares method, using the standardized information matrix.

Regularization

For the first time the regularization methods were proposed by Tikhonov (1979). They are an efficient means for estimating the models as regards the presence of multicollinearity (linear relationship between columns in the augmented matrix of the experimental plan). Obenchain (1997) demonstrated on the basis of the comparative analysis he had carried out that the most widespread and most frequently used method of this group is the ridge-regression analysis, in which the coefficient estimates are determined by the relation:

$$\bar{B}_p = (F^T F + P)^{-1} F^T Y \quad (3)$$

where  $Y$  is a column-vector with the output data, and  $P$  is a positive definite matrix with dimension  $(k \times k)$ . Most frequently  $P$  is in the form  $P = pE$ , where  $E$  is a unit matrix, and  $p$  represents parameter regularization.

Hoerl and Kennard (2000) have shown that for the problems with multicollinearity it is possible to find a value  $p^*$ , for which the estimates  $\bar{B}_p$ , although displaced, are much closer to the theoretical coefficients in comparison to those obtained by using the classical least-squares method.

A basic problem of the application of ridge-regression analysis consists in finding the optimal value  $p^*$ . Selecting the parameter for regularization cannot be done uniquely because the degree of displacement of estimates  $\bar{B}_p$  and the generalized root-mean-square error depend on the unknown theoretical regression coefficients  $\bar{\beta}$ . For this reason a large number of optimality criteria are proposed.

The determined criterion of Vinod is used for finding mathematical description of the main working motions of wheel excavators. For this criterion  $p^*$  is found from the condition for minimum of the function:

$$Q = \sum_{i=1}^{k-1} \left( \frac{(k-1)\delta_i^2}{\lambda_i \theta} - 1 \right)^2, \tag{4}$$

where  $\delta_i = \frac{\lambda_i}{\lambda_i + p}$ , and  $\theta = \sum_{i=1}^m \frac{\lambda_i}{(\lambda_i + p)^2}$ .

The eigen-values of standardized information matrix  $G^o$  are designated by  $\lambda_i$ ,  $i = 1, \dots, k-1$ .

According to the author the ridge-estimates found by using this criterion are the closest to those that would be obtained for an orthogonal matrix of the experimental plan.

### RESULTS AND CONCLUSIONS

The considered approaches to finding models with improved characteristics have been realized by programming in MATLAB

environment. They have been applied to estimating the coefficients in polynomials intended for determining the maximal depth of the block  $T_b$  in working with wheel excavators Rs 2000 and the maximal ratio between the thickness and width of the cut sickle  $i_{max}$  for excavators with fixed boom.

The programs developed have allowed to obtain and examine models of 1<sup>st</sup>, 2<sup>nd</sup> and 3<sup>rd</sup> orders, the search having been accomplished through the classical least-squares method as well as by using the approaches proposed in Section II.

The coefficients found in regression equations that describe, respectively,  $T_b$  as a function of the inclination angle of the wheel boom and the position of the taking-out mechanism, and  $i_{max}$  as a function of the layer height and the preset productivity are shown in Tables 2a/ and 2b/.

Table 2a/

| Linear model                   | LSM               | Method II.1       | Method II.2      | Method II.3      |
|--------------------------------|-------------------|-------------------|------------------|------------------|
| $b_0$                          | 0.03609986366880  | 5.56141309867896  | 5.561413098679   | 5.561405439806   |
| $b_1$                          | 0.00008969398502  | -0.73771673156166 | 0.033977331725   | -0.039940763667  |
| $b_2$                          | 0.92088553916836  | 5.52531323501016  | 106.301467997969 | 106.151626946256 |
| $b_{12}$                       | -0.00616258842718 | -0.73951061126207 | -16.341320754085 | -16.255017200151 |
| Model of 2 <sup>nd</sup> order | LSM               | Method II.1       | Method II.2      | Method II.3      |
| $b_0$                          | 0.00507252211393  | 5.58698392508998  | 5.561413098679   | 5.561411631555   |
| $b_1$                          | 0.00008969398502  | -0.73771673156166 | 0.033977331725   | 0.019696060482   |
| $b_2$                          | 0.93975159515699  | 5.52531323501016  | 108.479251622126 | 108.036482643396 |
| $b_{12}$                       | -0.00616258842718 | -0.73951061126207 | -16.341320754085 | -16.324665484406 |
| $b_{11}$                       | -0.00003666142207 | -0.01466456882859 | -0.146843984164  | -0.146804288370  |
| $b_{22}$                       | -0.00157217133239 | -0.05659816796589 | -2.254689792396  | -1.826529515609  |
| Model of third order           | LSM               | Method II.1       | Method II.2      | Method II.3      |
| $b_0$                          | 0.00514132179850  | 5.58698392508998  | 5.561413098679   | 5.561412084968   |
| $b_1$                          | 0.00108172470731  | -0.71787611711594 | 0.409772396745   | 0.398801996160   |
| $b_2$                          | 0.93967486402001  | 5.52544022889438  | 108.470394242832 | 106.880356392369 |
| $b_{12}$                       | -0.00616258842718 | -0.73951061126207 | -16.341320754085 | -16.329580483659 |
| $b_{11}$                       | -0.00003666142207 | -0.01466456882859 | -0.146843984164  | -0.146816554023  |
| $b_{12}$                       | -0.00155585520166 | -0.05659816796589 | -2.231290425768  | 1.476569651841   |
| $b_{111}$                      | -0.00000393975664 | -0.03151805313061 | -0.409863290312  | -0.408954989081  |
| $b_{222}$                      | -0.00000090645171 | -0.00019579356881 | -0.015057558788  | -2.218628073790  |

Table 2b/

| Linear model                   | LSM               | Method II.1       | Method II.2        | Method II.3        |
|--------------------------------|-------------------|-------------------|--------------------|--------------------|
| $b_0$                          | -0.00000000000123 | 3.16399958250370  | 3.16399958250370   | 3.16397577899822   |
| $b_1$                          | 0.00000000000000  | -1.22797028612256 | 0.00000000000004   | -0.74220702702786  |
| $b_2$                          | 0.99485433987013  | 0.48676916653903  | 7.20840452332031   | 6.84410426289174   |
| $b_{12}$                       | -0.00018774509869 | -0.18891850555732 | -8.50261808612360  | -7.67371750385568  |
| Model of 2 <sup>nd</sup> order | LSM               | Method II.1       | Method II.2        | Method II.3        |
| $b_0$                          | 3.26557591923311  | 2.98961806240783  | 3.16399958250370   | 3.16399918012368   |
| $b_1$                          | -0.00254223182584 | -1.22797028612256 | -15.87272198086817 | -15.82707525497650 |

|                      |                   |                   |                    |                    |
|----------------------|-------------------|-------------------|--------------------|--------------------|
| b <sub>2</sub>       | 0.99485433987700  | 0.48676916653903  | 7.20840452332028   | 7.16398037221861   |
| b <sub>12</sub>      | -0.00018774509869 | -0.18891850555732 | -8.50261808612352  | -8.50623610455675  |
| b <sub>11</sub>      | 0.00000046969641  | 0.47558596389783  | 15.95243667561529  | 15.91003156851794  |
| b <sub>22</sub>      | -0.00000000000051 | 0                 | 0.00000000000019   | 0.04594250197596   |
| Model of third order | LSM               | Method II.1       | Method II.2        | Method II.3        |
| b <sub>0</sub>       | 6.51871367108561  | 2.98961806240783  | 3.16399958250370   | 3.16399956929197   |
| b <sub>1</sub>       | -0.00638907760531 | -1.10692038572146 | -39.89095388965000 | -39.40273896827786 |
| b <sub>2</sub>       | 0.99485433947461  | 0.48676916653903  | 7.20840452340212   | 6.82934750530163   |
| b <sub>12</sub>      | -0.00018774509869 | -0.18891850555732 | -8.50261808612335  | -8.50371837352500  |
| b <sub>11</sub>      | 0.00000193561560  | 0.47558596389783  | 65.73987925325532  | 64.73479444587571  |
| b <sub>12</sub>      | -0.0000000010559  | 0.00000000000000  | 0.0000000017701    | 0.76367381508999   |
| b <sub>111</sub>     | -0.0000000018056  | -0.18396641398343 | -26.00208805321579 | -25.47955791244682 |
| b <sub>222</sub>     | 0.0000000000634   | 0.00000000000000  | 0.0000000002746    | -0.38491847157070  |

The impact of the maximal number of digits representing the model coefficients upon the accuracy of forecasting has been examined with the purpose of evaluating the applicability of models obtained to systems for programmed control of wheel excavators. That is why, using diverse degrees of rounding, the model-forecast values of the parameter examined  $\hat{y}_i, i = 1, \dots, N$  have been determined, and:

- the residual sums of the squares  $Q_o = \sum_{i=1}^N (\hat{y}_i - y_i)^2$  and
- the maximal absolute error from forecasting  $\Delta_{max} = \max_i |y_i - \hat{y}_i|$

have been calculated.

Table 3a/

| Maximal absolute errors for a model of finding the maximal depth of the block for a wheel excavator SRs 1200 |                  |                  |                  |                  |
|--|------------------|------------------|------------------|------------------|
| Linear model   | LSM              | Method II.1      | Method II.2      | Method II.3      |
| 3  | 0.95469138888250 | 0.09274441086981 | 0.07869054142926 | 0.07499479568782 |
| 4  | 0.13074441086981 | 0.09074441086981 | 0.09187473548691 | 0.09001067201056 |
| 5  | 0.08364441086981 | 0.09224441086980 | 0.09218422742794 | 0.08826960345126 |
| Model of 2 <sup>nd</sup> order   |                  |                  |                  |                  |
| 3  | 1.16469138888250 | 0.05274441086981 | 0.04159556525676 | 0.05115751837770 |
| 4  | 0.08830861111750 | 0.04474441086981 | 0.04730690651268 | 0.05074082135723 |
| 5  | 0.04613441086981 | 0.04654441086980 | 0.04660969825073 | 0.05279765663714 |
| Model of third order   |                  |                  |                  |                  |
| 3  | 1.16469138888250 | 0.04274441086981 | 0.03708861367869 | 0.03618193969953 |
| 4  | 0.10830861111750 | 0.03274441086981 | 0.03606557766521 | 0.02936596718147 |
| 5  | 0.06784441086981 | 0.03474441086981 | 0.03479828338201 | 0.02873311174606 |

Table 3b/

| Maximal absolute errors for a model of finding $i_{max}$ for a wheel excavator SRs 2000. |                  |                  |                  |                  |
|--|------------------|------------------|------------------|------------------|
| Linear model   | LSM              | Method II.1      | Method II.2      | Method II.3      |
| 3  | 4.90456363636364 | 0.43418823529412 | 0.44058991490449 | 0.46110764298111 |
| 4  | 4.94206363636364 | 0.43618823529412 | 0.43654528567511 | 0.45580572074388 |
| 5  | 0.62743636363636 | 0.43648823529412 | 0.43653283449078 | 0.45579175205944 |
| Model of 2 <sup>nd</sup> order   |                  |                  |                  |                  |
| 3  | 8.17456363636364 | 0.12418823529412 | 0.13464448464654 | 0.14236019941366 |
| 4  | 4.24732000000000 | 0.13418823529412 | 0.13571774888725 | 0.13538822073170 |
| 5  | 6.64308636363637 | 0.13528823529412 | 0.13527839506169 | 0.13586465479281 |

|                      |                  |                  |                  |                  |
|----------------------|------------------|------------------|------------------|------------------|
| Model of third order |                  |                  |                  |                  |
| 3                    | 27.0083200000000 | 0.06418823529412 | 0.06962886333570 | 0.07336275142821 |
| 4                    | 12.1318200000000 | 0.07118823529412 | 0.07285499375310 | 0.07419283840457 |
| 5                    | 17.8687363636364 | 0.07238823529412 | 0.07243248658507 | 0.07369985095839 |

Table 3c/

| Maximal absolute errors for a model of finding the maximal depth of the block for a wheel excavator SRs 1200 |                  |                  |                  |                  |
|--|------------------|------------------|------------------|------------------|
| Linear model   | LSM              | Method II.1      | Method II.2      | Method II.3      |
| 3  | 104.568184126320 | 0.42995879717320 | 0.51225155028232 | 0.51274988623360 |
| 4  | 0.58032784002766 | 0.41815138703630 | 0.41805920814596 | 0.43012376376252 |
| 5  | 0.42708363599184 | 0.41788069583451 | 0.41788278686114 | 0.44279995114598 |
| Model of 2 <sup>nd</sup> order   |                  |                  |                  |                  |
| 3  | 117.467975043315 | 0.08086797254300 | 0.28429311321500 | 0.07526384405400 |
| 4  | 0.79513754222256 | 0.05561947979853 | 0.05602753337193 | 0.07238815930581 |
| 5  | 0.05581125225909 | 0.05543295352681 | 0.05543347721596 | 0.06845674125306 |
| Model of third order   |                  |                  |                  |                  |
| 3  | 117.467975043315 | 0.05278344276400 | 0.25679269149700 | 0.07167215451700 |
| 4  | 1.19287264013240 | 0.02889645867371 | 0.02973880317474 | 0.05829324927401 |
| 5  | 0.18277354255024 | 0.02866642911099 | 0.02866600400534 | 0.05852915786512 |

Table 3d/

| Maximal absolute errors for a model of finding $i_{max}$ for a wheel excavator SRs 2000. |                  |                  |                  |                  |
|--|------------------|------------------|------------------|------------------|
| Linear model   | LSM              | Method II.1      | Method II.2      | Method II.3      |
| 3  | 1198.15646527233 | 2.68050471573000 | 2.67978859755000 | 2.68646370927000 |
| 4  | 1220.85745805931 | 2.67809889041000 | 2.67809637444000 | 2.68465299462000 |
| 5  | 7.85199363013467 | 2.67809602165858 | 2.67809593143896 | 2.68465526220022 |
| Model of 2 <sup>nd</sup> order   |                  |                  |                  |                  |
| 3  | 4567.10695196704 | 0.14253097003000 | 0.14359871766000 | 0.14307270693000 |
| 4  | 392.409447372075 | 0.14119791902900 | 0.14116723562000 | 0.14119198275700 |
| 5  | 1711.51674750314 | 0.14116323378000 | 0.14116321259000 | 0.14118564599000 |
| Model of third order   |                  |                  |                  |                  |
| 3  | 34343.5368087833 | 0.03700908270000 | 0.03940754570000 | 0.03833278750000 |
| 4  | 5228.47454898258 | 0.03577750966000 | 0.03575057723000 | 0.03579117847000 |
| 5  | 14382.7828136771 | 0.03574242620000 | 0.03574237840000 | 0.03578639630000 |

- The approach used for estimating regression models exerts virtually no effect on the maximal absolute error and the value of the residual sum of the squares.
- For the linear models the best results are obtained when working with centered factors, but for cubic regression the ridge-regression analysis should be preferred because of the pronounced multicollinearity.
- In all cases decreasing the number of digits used for the presentation of coefficients in the models found by the least-squares method leads to an inadmissible increase not only in  $Q_o$ , but also in  $\Delta_{max}$ . This tendency becomes stronger with increasing the order of the model.
- Modifying the number of digits in the presentation of coefficients found by using the approaches described in Section II does not lead virtually to any change in the forecasting properties of models.

All the investigations performed have shown that the use of ridge-regression analysis or standardization of factors or regressors leads to finding such models describing the basic

working parameters of wheel excavators, which have improved characteristics in comparison with those obtained through the least-squares method. They can be successfully used in the systems for programmed control without any need of imposing special requirements regarding the control system hardware.

## REFERENCES

- Вучков И.Н., Л. Бояджиева, Е. Солаков. 1987, Прикладной линейный регрессионный анализ., Москва, Финансы и статистика.
- Илиев З. А., 2002, Определяне параметрите на работните движения при роторните багери с помощта на математични модели, *Международна конференция "Автоматика и информатика '02", Сборник доклади том 1* (бълг., резюме на англ.), 237 – 240.
- Илиев З. А., 2001, Метод за оптимизиране параметрите на стружката при роторен багер SRs 2000, *Международна научна сесия "Управление на природни и техногенни рискове", Сборник доклади* (бълг., резюме на англ.), 317-319.

Тихонов А. Н., В. Арсенин., 1979, Методы решения некорректной задачи., Москва, Наука.  
Hoerl, A. E., R. W. Kennard., 2000, Ridge Regression Biased Estimation for Nonorthogonal Problems., *Technometrics*, Vol 42, No. 4, 80-87.

Obenchain, R. L., 1997, Shrinkage Regression: Ridge, BLUP, Bayes and Stein, *Technometrics*, Vol 39.  
Marquardt D., 1980, You should standardize the predictor variables in your regression models. *J. Amer. Stat. Assoc.*, V 75, pp 87-91.

*Recommended for publication by Department of  
Mine Automation, Faculty of Mining Electromechanics*

## E-ENGINEERING: A PROJECT FOR MECHANICAL CONSTRUCTIONS DESIGN OVER INTERNET

**Veselin Christov**

University of Mining and Geology "St. Ivan Rilski"  
Sofia 1700, Bulgaria  
E-mail: V\_Christov@abv.bg

**Stephan Garabito**

Technical University  
Sofia, Bulgaria  
E-mail: StefanG@vmei.acad.bg

### ABSTRACT

A project of independent information resource for mechanical constructions producers and users is examined. The project include following modules: (i) a web site - it is used for receiving user requests and for returning base parameters of finishing solution, a full documentation of the solution is sent by e-mail, (ii) a design module what is used for automated design, (iii) an administrative module – it controls user requests and (iv) databases – for mechanical constructions, for mechanical construction producers, for clients and for client requests. The main purpose of the project is to specify: information that has to be included in the web site, information that has to be required from the user, programming language of the system, exactly which mechanical constructions has to be included in the design module and their parameters, and data bases organization. This project is the first stage of developing of the E-engineering – a machine elements distance design.

### INTRODUCTION

With Internet help it began possible to be developed the projects in which to take part designers and engineers from all over the world. In this way an open development has realized. Everyone can take part and develop a dial from one joint project, Amor D. (2000).

The main purpose of the current project is to build up a system for machine element design over Internet. Because of huge variety of different kinds of such elements we at first concentrate on reduction gears. On the other hand the high difficulty of the task for automation of the design process and its dependence from local factory standards, used particular machines and materials for designed element producing make us for now to take care of the task only for choosing certain type of reduction gear according to the user request. After development of a first system version the kinds of machine elements and the design process range eventually will be expanded

The problems, which have to be solved, are:

- ◆ Modules and databases from which the system will consist of;
- ◆ Kinds and parameters of reduction gears and their possible producers;
- ◆ Method of user request setting;
- ◆ Appearances of the result and ways for receiving it by the user;
- ◆ Control of the users and the implementation stages of their requests;

### SYSTEM ARCHITECTURE

The system will be based on the standard Internet service - World Wide Web. It will be implemented to certain Web site, and its users, administrator and assistant designer will connect to it with Web browser. The system will be developed mainly by PHP language that is becoming more and more popular, is supported by most of the Web servers and permits easy work with databases. The system will consist of following parts as shown on Figure 1:

**Web site.** It serves as a main instrument for connection of the users, administrator and assistant designer with the system. It includes static and generated by the system Web pages that is used by the users to set their requests, to communicate with the assistant designer and to receive the results. The administrator also uses the site to control the system and the stages of the user requests, and the assistant designer uses it to help for task solving.

**Design module.** It will be developed mainly by PHP. Eventually its parts could be developed by C++, if it becomes necessary any more difficult processing. As well it is possible to become necessary linking this module to a CAD system, may be Mechanical Desktop. The module will communicate by the Web site mainly with the users and the assistant designer. After receiving a user request it will do a choice for corresponding reduction gear, will compute its base parameters, will generate schemes of the gear and recommendations for its preparation and will choose eventual producers. If in the design period any difficulties arise, the module will connect by e-mail to the assistant designer.

**Administrative module.** It also will be developed by PHP. Its main function is to control the system by the administrator. This module makes user and request registration. It will control payments and request stages. The module communicates only with the administrator through the Web site.

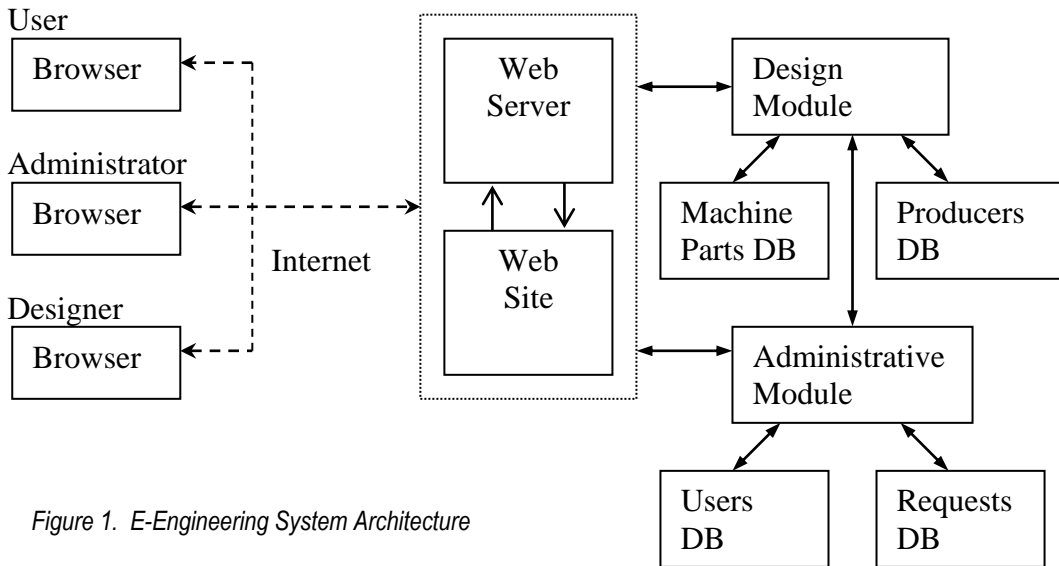


Figure 1. E-Engineering System Architecture

**Databases.** There will be following bases in the system:

- for mechanical constructions – for every reduction gear will contain: component parts and their parameters, schemes, recommendations for preparing. It is supported and updated by the assistant designer through the Web site.
- for producers. It will contain address, phone numbers, **nomenclature**, prices. The base is supported and updated by the assistant designer through the Web site.
- for users. It contains user information, request number, payment. The base is updated automatically by the administrative module and is supported by the administrator.
- for requests. For every task it contains number, description, implementation stage, problems. The base is updated automatically by the administrative module and is supported by the administrator.

The system will be supported, controlled and updated by:

**Administrator** His task is supporting the overall functioning of the system. In addition he cares for the implementation of the user requests and their payment.

**Assistant designer.** He controls and gives assistance for the technical solution of user requests, updates the database for producers and expands the system by including new mechanical elements and design process extending

#### PROCESSING OF THE REQUESTS

To set a request the user of the system has to register. This includes him into the database for users. While registering he has to enter certain amount of personal data. A problem arises here for incorrect users who do not wait finishing their requests or do not pay.

In that stage he will determine a method of payment and result delivery. Five different methods are possible in Bulgaria for now:

- ◆ in the firm office – the user has to go there;
- ◆ delivery by an express service – payment by the courier;
- ◆ delivery by a postal package - the user has to go to the post office and pays by cash on delivery;
- ◆ e-delivery through Internet – payment by bank transfer;
- ◆ e-delivery through Internet – by the Bulgarian e-payment system “e-Pay”.

After registration the client has to enter his request parameters. After receiving a request from the system it is included into the corresponding database. The system sends e-mail to the administrator and starts to process the request by its design module. During processing it is possible to send to the user some additional questions. If the system meets any difficulties, it generates a message by e-mail to the assistant designer.

He on his turn can also to send questions to the user and to make own decision what to do with the request.

After the request has been finished, the system sends a message to the administrator to initialize the process of payment and result delivery.

The communication with the user will be done mainly through the Web site. Complete history of the request will be saved in the database for requests. The result can be sending on paper, disk or by e-mail as the user likes.

#### MODIFICATIONS AND PARAMETERS OF REDUCTION GEAR

While the dialog is running the user is necessary to specify the following parameters, MECD (1972):

- ◆ Relatively lay of the shafts
- ◆ Magnitude of the transmission power
- ◆ Torque
- ◆ Desired efficiency
- ◆ Transmission ratio
- ◆ Speed of rotation
- ◆ Restriction at the rate
- ◆ Restriction at the mass

To specify reducer technicalities some possibility solutions have to be shown to the client:

- ◆ Cylindrical reducer
  - Planetary gear
  - Spur gear
- ◆ Bevel gear
- ◆ Worm Gear

- ◆ Mixture
  - Bevel +Worm
  - Worm+ Bevel
  - Worm+ Cylindrical

He has to make more precise following parameters:

- ◆ Number of gear transmission
  - Single-step gear
  - Double-step gear
  - Triple-step gear
  - Four-step gear
- ◆ Relatively lay of the shafts
  - Parallel
  - Coaxially
  - Intersect axes
  - Lay crosswise axes
  - Horizontally axes
  - Vertically axes
    - Come out upwards
    - Come out downwards
    - Come in upwards come out downwards
    - Come out upwards come in downwards
  - Horizontally come out and vertically come in
    - Come out upwards
    - Come out downwards
  - Vertically come out and horizontally come in
    - Come out upwards
    - Come out downwards
- ◆ One-sided layer
- ◆ One come in and two come out
- ◆ Worm gear
  - Upper worm
  - Lower worm
  - Lateral worm
  - Horizontal shaft
  - Vertical come in shaft
  - Vertical come out shaft

The assistant designer has to consider with some standards:

- ◆ Standard for center-line distance 7466—69
- ◆ Standard for transition number 7553-69
- ◆ Standard for number of gear
- ◆ Standard for coefficient for gear length
- ◆ Standard for gear declination angle
- ◆ Standard for worm size and worm gear
- ◆ Standard for gear reducer height 7155-68
- ◆ Standard for gear precision
- ◆ Standard for lateral gap and association 3296-72, 3535-71

So received requirements is used to search the database for standard reducers. Closest standard design in example form shown on the figures 2, 3 and 4 will be sending to the client for approval.

### CONCLUSIONS

The proposed in this article project for e-engineering is only the first approximation to development a real system. The purpose is to be outlined main ideas, solution approaches and

difficulties.

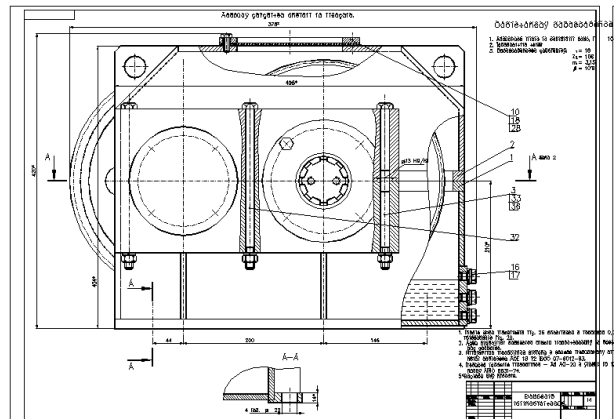


Figure.2 Cylindrical reduction gear (I projection)

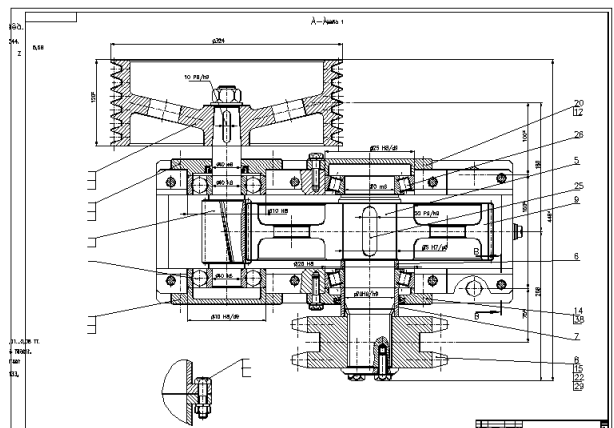


Figure.3 Cylindrical reduction gear (II projection)

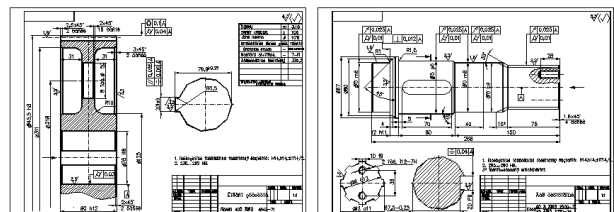


Figure.4 Typical cylindrical reduction gear parts

The main problem behind building a helpful and efficient system is automated design implementation (the design module in our model). A full realization of this task as we mentioned in the introduction is almost impossible. The task is too large and difficult and would require a large team and great financial support. For that reason we have chosen the approach of step-by-step growth.

The existing widespread CAD systems do not offer Web interface and are difficult for distant control, but we think that it is not impossible.

Another direction for development of the system is its transformation to high competent mediator between the users of mechanical constructions and their producers. Thus it will cover entire process from determination of wanted construction, finding the producer, to its production and delivery.

#### REFERENCES

- Amor D., The E-Business (R)evolution. – Hewlett Packard Company, 2000.
- Reference book "Machine Element Calculation and Design" – State publisher "Techika", 1972 (in Bulgarian).

*Recommended for publication by Department of  
Mine Automation, Faculty of Mining Electromechanics*

## APPLYING MULTIFACTOR LOGICO-PROBABILISTIC FUNCTIONS IN LOCAL ECOLOGICAL MONITORING

Teodora Kissiova

University of Mining and Geology "St Ivan Rilski"  
Sofia 1700, Bulgaria  
E-mail: teodora@mgu.bg

### ABSTRACT

The ecological monitoring involves the activities of observing, analyzing, and controlling. The purpose of the present report is to propose a system for observing a natural water reservoir within the boundaries of a settlement. The quantity and quality of hazardous emissions according to the productivity of local enterprises and changes in atmospheric conditions will be monitored. The plant considered is a multifactor and stochastic one. For this purpose multifactor logico-probabilistic functions have been used.

### INTRODUCTION

The ecological monitoring is a system of observing, analyzing, and controlling the impact of one or more pollutants on the state, properties, and modifications of biosphere parameters. It is important to measure the quantitative values and control the qualitative indicators that characterize the environment components: water, air, soil, landscape, flora, and fauna. These components are basic for the subsystems of ecological monitoring – water, soils, radioactive pollution, noise and vibrations, non-ionizing emissions, forest subsystems, preserved natural sites, air, etc.

In settlements with developed industry it is especially important to monitor these parameters and to define in time the level of pollution. There exists a hierarchical system for ecological monitoring, in which the environment pollution data are forwarded by the Regional Inspection for Natural Environment Protection (RINEP) to the Ministry of Environment and Water (MEW) and the Central Dispatching Station [3]. There are still some problems that are as follows:

- Low level of automation in monitoring the environment parameters [4];
- All technical devices for measurement should have unified metrological characteristics [4];
- Low level of the communication system [4];
- Lack of system approach to the investigation of ecological plants [4];
- Sudden large-volume release of pollutants performed by industrial enterprises.

All factors listed so far define the processes of polluting the environment as stochastic and non-linear. Furthermore, in a given region there are more than one enterprises releasing pollutant substances. This leads to multifactoriness of the problem for forecasting the possible pollution.

The local ecological monitoring involves considering the extent of water pollution in a settlement. The output level  $y(t)$

will be forecasted for preset varying input or disturbing actions,  $x(t)$  or  $z(t)$  respectively. All these have unknown probabilistic characteristics.

The objective consists in determining the logic functions of the relationship between input and output parameters, taking into account the disturbances. In such a way this relationship will allow forecasting the behavior of the plant, which in this case is the water pollution of a natural water source in a settlement.

### PROBLEM DESCRIPTION

The generalized technological diagram of the processes of releasing hazardous substances into the river is shown in Fig. 1.

The input factors are:  $x_1(t)$  representing various types of organic pollutants from the first enterprise, given in mg/l,  $x_2(t)$  representing various types of inorganic pollutants from the first enterprise, also given in mg/l,  $x_3(t)$  being the water flow rate from this enterprise,  $x_4(t)$  the organic pollutants from another company in mg/l,  $x_5(t)$  inorganic pollutants,  $x_6(t)$  being the flow rate. The factors listed above depend on the company's productivity rate as well as on the qualitative change of the raw materials being used. For instance, in the cosmetics and chemical industries the qualitative characteristic of released hazardous substances depends on the type of products being manufactured at the corresponding point.

Of course, the input flows of materials can be generated by several enterprises if there are such in the region of investigation. Moreover, the probability that RINEP does not acquire data for pollutants from any large or small enterprises should be also taken into consideration. In such cases it will be useful to examine the activities of small companies and workshops in order to find out the approximate qualitative and quantitative compositions of released pollutants.

An important factor affecting essentially the model being developed is the detection of the place where polluted water is poured out into the river. In most Bulgarian cities there are separated industrial zones where all manufacturing enterprises are located on a territory appointed for these purposes. There are also places where these are located all over the settlement. When there are industrial collectors at different locations, in some cases exceeding the acceptable limit values will be prevented.

Besides, the time point of waste release should be taken into account as well. In cyclic technological processes more hazardous substances are released at the end of each cycle. This is the case with the pharmaceutical and cosmetics companies where various containers are washed at the end of shifts. Respectively, in enterprises having a waste water treatment station the occurrence of this event is well known and an increased amount of reagents is added at that moment.

Disturbing factors acting upon the pollution of the ecological plant, i. e. the river, turn out to be:  $z_1(t)$  being the amount of precipitation during the period of sampling,  $z_2(t)$  the water temperature, and  $z_3(t)$  the water speed in the river. These factors are of stochastic nature and influence to a great extent the output parameters. Precipitations increase the river flow rate, and level of hazardous component content, measured in mg/l. becomes lower. On the other hand, it should be taken in mind that in time of raining many companies discharge polluted water for then it is almost impossible for the inspections to corner such offenders. The temperature is an essential parameter because some substances decompose more quickly with its increase. The speed of water movement exerts the same effect: rapid waters have a higher content of oxygen and volatile substances decompose faster.

Output factors to be forecasted are:  $y_1(t)$  being the water flow rate in the river,  $y_2(t)$  the quantity of hazardous components in the river, and  $y_3(t)$  the water turbidity.

The main links between input and output flows are also shown in Fig. 1. The effect exerted by disturbing factors has not been added intentionally because these influence all the outputs.

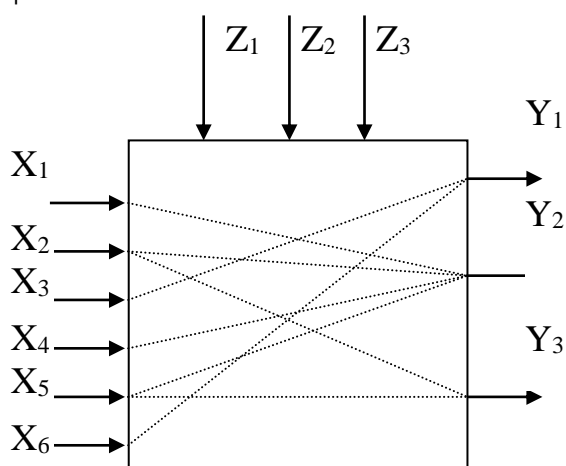


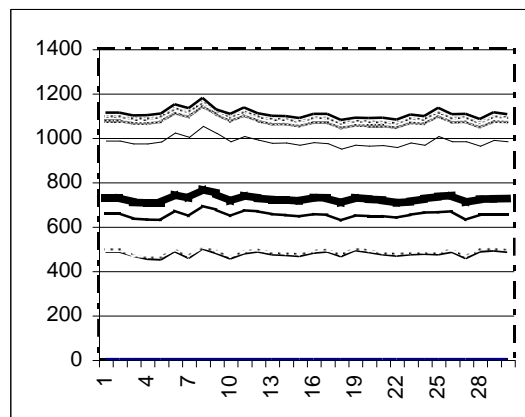
Figure 1

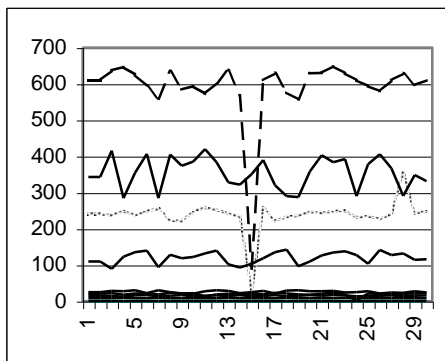
POSSIBILITIES PROVIDED BY THE MULTIVALUED LOGICAL PROBABILISTIC FUN

Analyzing the parameters listed above shows that they are multiple and that it is difficult to elaborate a precise mathematical model of river pollution resulting from the operation of several enterprises, provided that production and climate conditions are changing incessantly, i. e. the plant is characterized by stochasticity and multifactoriness. There are some possible ways of solving this problem:

1. Applying mathematical models to modeling the processes of plant pollution. Using these models leads to complex sets of equations, which, in some cases, do not express all the links existing between the factors. This is the so-called principle of non-compatibility between the plant's complexity and the possibility of achieving high accuracy in its mathematical description.
2. Composing a logico-probabilistic model (LPM) when a large set of plant's inputs and outputs is known. In such a LPM will demonstrate the logical links between the individual variables. However, the extent of interaction between them will not be expressed quantitatively. For multiple changes of a part of the quantities measured or of all of them, when not all feasible possible outputs are known, it is possible to use learning systems (neuron nets).
3. Composing a LPM again and using the simulation product MATLAB represent another possible method of generating the probable outputs.
4. Unfortunately, it is difficult to find out some of the logical relations between factors in the ecological object considered. This is due to the fact that some of the factors do not influence one another. That is why it can be generalized that the object considered is characterized by fuzzy and stochastic non-determination. As a result it is not possible to apply autonomously methods of the fuzzy logic or those of the probabilistic distributions. [2]

In supporting the above statements data for the inorganic pollutants from two mines are presented as an example:





The plotted graphs clearly demonstrate that in the first graph there are peaks on two of the values that do not depend on the rest of the values. There could be several causes for this phenomenon: due to season precipitations the quantity of filtrated water is higher and the concentration of ingredients is lower; an error in taking and preserving the sample; incorrect method of analysis or device failure; unintentional mixing of samples, etc. Under other unpredictable conditions it is possible that this influence will be expressed in other components or in all of them at the same time.

On the second graph it can be seen that the values of pollutants exhibit certain regularity and are not affected by random influences.

In such cases it is expedient to apply complex methods combining features of the methods mentioned above. Such are the multivalued logical probabilistic functions (MLPF). In these functions, each parameter assumes several definite linguistic values depending on the accuracy required. The values of the logical arguments are of qualitative character, for instance: very low, low, medium, high, and very high values, i. e.  $\kappa = 5$ , which is the exponent of the possible solutions of this problem. In the  $\kappa$ -value logical system each element of the argument domain is associated with  $\kappa$  elements from  $Y_j, j = 1 \div \kappa$ , for  $Y = f(X,W)$ .

Determining the logical values of arguments always takes into consideration the real variation limits of the corresponding quantities. These limits are related to the supposed most probable values that can be assumed by the plant under specific conditions. In some cases, when this is imposed by the real conditions, it is allowed that they exceed the maximal acceptable values or are very close to these values. The degree of membership of each linguistic variable is assumed in accordance with these probable values. Furthermore, when MLPF are formed, technological specialists in the respective area always take part with their expert statement in determining the mutual influence of individual parameters. Table 1 is an exemplary table containing logico-linguistic values of the variables, i. e. of the arguments and function. Only a small part of the feasible combinations is shown in this table.

Table 1.

| s  | I  | II | III | IV | V  | VI | VII | VIII | IX | X  | XI | XII |
|----|----|----|-----|----|----|----|-----|------|----|----|----|-----|
| x1 | VL | L  | M   | B  | VB | VL | L   | m    | B  | VB | VL | L   |
| x2 | VL | VL | L   | L  | M  | M  | B   | B    | VB | VB | VL | VL  |
| x3 | VL | VL | VL  | L  | L  | L  | M   | M    | M  | B  | B  | B   |
| x4 | VL | VL | VL  | VL | L  | L  | L   | L    | M  | M  | M  | M   |
| x5 | VL | VL | VL  | VL | VL | L  | L   | L    | L  | L  | M  | M   |
| x6 | VB | VB | VB  | B  | B  | B  | M   | M    | M  | L  | L  | L   |
| w1 | VB | B  | M   | L  | VL | VB | B   | M    | L  | VL | VB | B   |
| w2 | VB | VB | B   | B  | M  | M  | L   | L    | VL | VL | VB | VB  |
| w3 | VB | VB | VB  | VB | B  | B  | B   | L    | M  | M  | M  | M   |
| y1 | VL | VL | L   | M  | M  | M  | M   | M    | M  | M  | M  | M   |
| y2 | L  | VL | M   | L  | L  | L  | L   | M    | B  | B  | L  | M   |
| y3 | VL | VL | M   | VL | VL | VL | L   | M    | B  | M  | VL | Mc  |

The set of arguments  $X_i$ , for  $i = 1 \div n$ ,  $W_s$ , for  $n \leq s = 1 \div l$  and the set of function  $Y_j$ , for  $j = 1 \div k$  have values in the  $\kappa$ -element set of logical values  $A_\kappa (a_1, a_2, a_3 \dots a_\kappa)$ . [1]  
 Using probability matrix  $P = [p_{sj}]$  the probabilistic correspondence between arguments  $X_i$ , for  $i = 1 \div n$ ,  $W_s$ , for  $s = 1 \div l$  and the values of function  $Y_j$ , for  $j = 1 \div k$ , where  $s = 1 \div M$  is the number of the set, is preset. The number of possible sets is  $M = \kappa^n$ . The function assumes the form:  
 $y=f(X,W)/P\{X,W\}$

transformed into analytical one. A set of relationships is obtained:

$$\begin{aligned}
 Y_{i1} &= f_1(X_1, X_2, X_3 \dots X_n, W_1, W_2, W_3 \dots W_l) \\
 Y_{i2} &= f_2(X_1, X_2, X_3 \dots X_n, W_1, W_2, W_3 \dots W_l) \\
 Y_{i3} &= f_3(X_1, X_2, X_3 \dots X_n, W_1, W_2, W_3 \dots W_l) \\
 Y_{iu} &= f_u(X_1, X_2, X_3 \dots X_n, W_1, W_2, W_3 \dots W_l)
 \end{aligned}$$

The functional relationships can be used for making an evaluation of the probabilities of its realization according to the argument values. In such a way, in accordance with the probability laws the logical probabilistic function assumes the form of a logical function. Here follows an example for a possible functional relationship:

In such a way the MLPF expresses the links between individual input, disturbing and output variables, and it will help establishing the logical connection between them. Matrix  $P\{F(X,W)\}$  is represented in the form of a table (Table 2). The table values are based on the variants in Table 1.

2. The relationships between the functions and arguments  $Y=f(X,W)$  are derived from Table 2, i. e. the table form is

$$Y_{i1} = f_1(X_1, \overline{X_2} \vee W_1, W_2) \vee X_3 \wedge \overline{X_5}$$

The minimal and maximal feasible probabilities are determined from the table with the set of arguments. Based on derived logical functions it is analyzed when they are minimally or maximally probable.

#### CONCLUSIONS

The method described can be used for forecasting the behavior of a multifactor plant characterized by non-determination and stochasticity. In the case considered the pollution of a local plant, namely the river, is forecasted in accordance with the productivity rate of enterprises in that region and the local climate conditions.

The MLPF written in table form provides a lighter variant of searching for the relationships between the input and output as well as of finding possible controlling actions upon the process. For the plant described these are the stoppage of water with norm-exceeding ingredients and its purification in water treatment stations, knowing in advance the necessary amounts of reagents. It is possible to design a system of taking

determinate samples that influence one another, which will enhance the reliability of MLPF.

It is appropriate to use the graphs as a basis for forecasting the ecological monitoring in a given settlement. The most effective approach is the MLP one as it permits embracing completely all the factors influencing the environment. Using this approach an accurate and relatively long-term forecast can be achieved.

#### REFERENCES

- Gegov, Emil 1993. "Logico-Probabilistic Method of Modeling Complex Plants and Systems", Proceedings of St Ivan Rilski University of Mining and Geology, No. 3, Sofia.
- Gegov, Emil 1997. "Investigating Multifactor Plants and Control Systems in Conditions of Non-Determination by Using a Multivalued Probabilistic Logic" – National Conference on Automation and Informatics'97, Conference Proceedings, Vol. 5, SAI, Sofia, pp. 1 - 5.
- Radulov, Georgui 1998. "Instruments for Ecological Monitoring and Automation of Polluted Media Purification", Sofia.
- Videnova, I., Stoenchev, S., Todorov, Ch., Karastoyanov, D., Petrov, I., 1997. "Microprocessor Devices for Ecological Monitoring", SAI, No. 3.

*Recommended for publication by Department of  
Mine Automation, Faculty of Mining Electromechanics*

## OPPORTUNITIES FOR IMPLEMENTATION OF WEB INTERFACE IN DATA BASE WORKS IN THE MINING INDUSTRY

### Nikolay Janev

University of Mining and Geology  
"St. Ivan Rilski"  
Sofia 1700 , Bulgaria

### Kancho Ivanov

University of Mining and Geology  
"St. Ivan Rilski"  
Sofia 1700, Bulgaria

### Volin Karagiozov

American University in Bulgaria  
Blagoevgrad, Bulgaria

### Iskra Starbanova

University of Mining and Geology  
"St. Ivan Rilski"  
Sofia 1700, Bulgaria

### Yordanka Anastasova

University of Mining and Geology  
"St. Ivan Rilski"  
Sofia 1700, Bulgaria

### ABSTRACT

The necessity for the creation of software working in the mining is increasing along with the implementation of market principles in the ore output. The complexity of the issues and tasks needed to be solved requires highly specialized software. Due to the specifics of the mining enterprises, the usage of Internet is the best solution for ensuring of access for random clients to the information data basis of the enterprise. The present article regards the characteristics of a Web interface and its application in the mining for the extraction of operative information from the data base, related to the carrying-out of the production indicators, as well as daily the indicators for a past production period. For this purpose, an existing DB on FoxPro has been used and has been transformed in MySQL to meet the requirement for a Web-SQL based interface. The relation between the web-pages and the DBs is carried out by the use of cgi-php scripts in compliance with the requirements of the client/server technology for processing of information. The concrete usage of this technology in the mining is a contribution to the automation of the mining production. The regarded realization has been done on a freeware software – MySQL as a server for DB and PHP as a language for relation to the DB. Another of its advantages are: scalability, portability, usage of customized queries and etc. interment to the Web-SQL based interface. The developers efforts are aimed at the implementation of this software the mining enterprises.

### INTRODUCTION

At the end of the XX century, the use of information technologies and the stored in the WWW multimedia data has increased tremendously. This is due to the fact there is a constantly increasing need for information and for an interactive access to this information. Internet has turned into a mechanism for a global spread of information and into a mean for cooperation between the people and their computers not accounting for their location. Its influence affects not only the field of computer communications, but society as a whole, taking into consideration the ever more greater development in the means for e-trade, the acquiring of information, as well as the social processes. Its significant advantage in the case appears in the fact that the information process is a dynamic and two-sided one, so that the acquired by one side information is consequently returned into the net, enriched with new elements.

Internet has changed the flow of the business transactions both between the computers and the companies and the final consumer, offering the following key advantages:

- A fast market cycle;
- Increased turnovers and reduced costs.

The necessity for the creation of software working in the mining is increasing along with the implementation of market principles in the ore output. The complexity of the issues and tasks needed to be solved requires a highly specialized software. The mining companies are situated on large areas, sometimes on the territories of separate states and the sole solution for the DB to be accessible from every point of the enterprise and to clients from all over the world is the usage of intranet or Internet.

### DIVIDED INFORMATION SYSTEM – WWW

After its publishing in 1992, WWW (World Wide Web) is presently the most used application of Internet. WWW is a universal mean for accessing to different in structure and character data divided between a large number of computer systems in a TCP/IP based network, which by the help of hypertext provide access to different type of Internet protocols through a common interface. The selection of documents requires searching finding of the machine (*the Web server*), which contains the desired information establishing of connection to it, transfer of information to a local machine through a client program (*browser*), which interprets and visualizes the documents[12].

The WWW information system is based on a hypertext technology. A word in a hypertext document can serve as a hyperlink.

The basic principle in the work of the WWW information system is that the client send query in a particularly specified format to the server, which processes it and the result from it is send back to the client. The exchange of data between the server is usually realized according to the HTTP protocol (a standardized protocol allowing work with structural divided data, described by the HTML language).

Here are some of the advantages of the client/server technology:

- Decreased service costs;
- The net load is reduced;
- An improved integration of the data due to their centralized storing;
- A big number of operation system cam work together on condition that a common net protocol is used.

On Fig.1 are given the functions of the WWW client and WWW server programs:

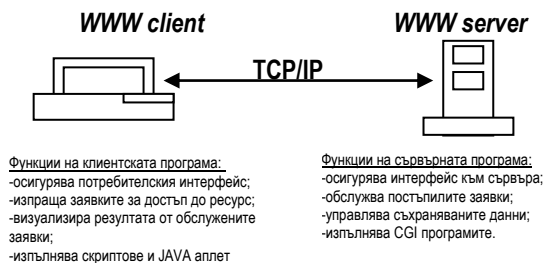


Figure 1. Functions of the WWW client and WWW server programs

An important advantage of the Web technology is the possible that large data volumes to be divided to smaller in volume documents, called Web pages. They incorporate different elements, the more important of which are:

- Formatted and non-formatted text;
- Graphics, sound, animations;
- Hyperlinks – references to other information resources;
- Execute programs;
- JAVA scripts or JAVA applets.

Web pages can be:

- Static – they are only extracted by the browser and are stored in a ready form in the Web site
- Dynamic – they are generated as a result of query by the client.

A great part of the pages in WWW are written in a program language, called HTML(HyperText Markup Language). The code, written on HTML, is interpreted by the WWW browser and is viewed on the screen of the computer. The HTML language has been developed on the basis of SGML – a language for presentation and exchange of data between different companies. Today, the HTML contains more that 100 commands (tags), which makes it a comparatively complex one [3].

XML (eXtensible Markup Language) has been developed to refer to this disadvantages. This is a simple standard, which is almost as powerful as SGML and in the same time is easy for

usage just as HTML. XML makes two main changes in HTML[6]:

- It close not define preliminary any tags;
- He is more strict.

The stored in the WWW multimedia data increase quite rapidly. This has lead to the appearance of programs designated to serve users queries, related to the searching of particular data in the file structure of the Web server, as well as for the providing of access through Internet to the DB and for processing and systematizing, of the information send by the server to the client. To solve all these problems the CGI (Common Gateway Interface) was adopted, which allowed programs, created on high-level programming language (C, C++ and etc.), to be executed under the management of the Web server. The most popular language for writing on CGI is Perl[4].

One of the most important application of CGI is the processing of HTML forms. The forms are used mainly for two things: first, to collect information for the user and second – to ensure interactive connection between the server and the user.

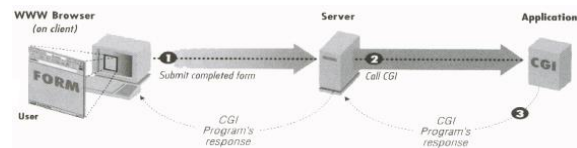


Figure 2. CGI interface

Describing the above figure, one can explain visually the principle of work of the CGI interface. The Web-pages which is seen on the browser, contains blank form with fields which need to be filled in and send back to the server after pressing the "Submit" button. The filled-in information send to the server, which has to process it. The server calls the CGI-script, which in fact is a program, installed on the Web server for processing of the sent information. It resends this information to the computer of the client, who watches it through her/his Web browser.

A considerable disadvantage of CGI is that here to independent applications are considered – every time when a user refer to the script, a new place is separated within the memory and a new copy of the program is executed. This becomes a problem for example when in one and the same moment several hundred people refer to the script – the server separates too much memory and processor time and its work may considerably be delayed. Nevertheless CGI is very suitable for sites, which do not envisage the above – mentioned extreme number of visits.

The above – shown problems of CGI are being solved by the use of applications, which utilize server API (applicable program interface). The idea of these applications is that they are in bodied in the server itself and this means that they use one and same place within the memory and the most important in each new users turning to the script connected with the given application, a new niche is created in the server process.

The most popular API are PHP, ASP, Java Server Pages (JSP) and Server-Side JavaScript (SSJS). Among them the leading is the role of PHP. The major advantages of PHP are[7]:

- PHP can be executed as a separate CGI script or can be incorporated in the HTML page itself, which brings an opportunity to the server itself to generate a part of the html code;
- PHP support the greatest quantity of DBs;
- PHP is extremely suitable for web. For example Php has a built-in support of sessions, automatically processes the input information from the forms and etc.

### SERVER FOR DATABASE

The necessity for generating of dynamic pages on the basic of some information, for storing of orders for buying of goods and so on requires within the most of Web sites to have DBs created as well as the respective data basis management system (DBMS).

The most often used model of DB is the relational one. The relational model offer a high degree data independence. An advantage of the relational model is the one and same representing of classes of objects and the relations between them[8].

In a relational DB the data are stored in two – dimension tables – each table contains non-ordered rows and named columns and each column has a unique name attribute – the type of data contained in it. A DB usually includes more that one table with mutually related information. In this way, it becomes possible the carrying – out of more complex and effective operations with the data.

The systems, which in the greatest extend cover the requirements for the DBMS are the DBMS, which use the relational data model. These systems are called relational data basis management systems.

The access to the relational data is provided with the help of the relational languages. They are divided into two major categories - *languages of the relational algebra* and *languages of the relational calculation*. Beside the two categories of languages there are also the so-called *intermediate relational languages*, which have abilities of the relational calculus and the relational algebra. The most widely spread language of such type is SQL (Structured Query Language)[9].

For the realization of the particular DBMS today are used neither the relational algebra, nor the relational calculations. In the fact the standard access to relational data is provided by the SQL language. The SQL language is a mixture of operators of the relational algebra, expression of relational calculations and expanded additional capacities, not present in the relational algebra and the relational calculations SQL are a non-procedural, platform and product independent language. Actually, this is the standard language used for manipulation and extraction of data from relational DB[10].

The connection between the relational data model, the SQL standard and its different realization can be formally represented by the following pyramid[11]:

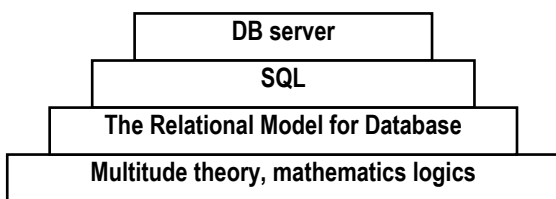


Figure 3. The connection between the relational data model, the SQL standard and its different realization

At the moment the most DBMSs provide opportunities for integration of Web-based applications such as: SQL Server 2000, Oracle, Progress, Informix and etc. From the other hand many program languages allow integration of DBMS, from one side and of Web-based applications from another side.

For the development of such applications a three-layer structure is used:

- First layer – web client (for example web browser);
- Second layer – web server, CGI scripts and APIs for connection with DBs;
- Third layer – database server.

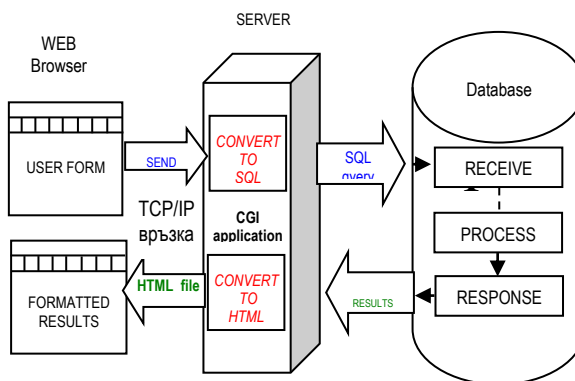


Figure 4. Three-layer structure

MySQL is a small, compact and easy for use server for DB. It is made on the client/server model and is accessible for both UNIX and Window platforms SQL 92 and ODBC 0-2. It is not to disregard the fact that MySQL has an open code and is freeware. Among the other advantages the MySQL are its rapidness, punctuality, as well as it well-developed system of privileges. The system of privileges of MySQL allows every user to make exactly what is permitted for her/him. MySQL is available on the two most popular program languages for server applications – Perl and PHP. And exactly because of such qualities, in the present report, this server for DB has been preferred instead of the commercial DB servers such as DB2, Microsoft SQL Server and Oracle. It is true that they provide greater potentialities that MySQL, but their prices are considerably height (DB2 – 20 000\$, Oracle – 40 000\$, Microsoft SQL Server – 20 000\$), and they, similarly to MySQL, are SQL based, so that the transition from MySQL to a commercial server for DB shall not be a considerable difficulty.

MySQL keep every table as a separate file in the directory for DB. The maximum size of a table can be from 4GB to the maximum size of a file supported by the used operational system. The maintenance of the saved procedures, transactions sub-SELECT and UNION (the fields within which the MySQL has suffered numerous criticism) has been added in the 4.0 version of MySQL of November, 2002. This version is still in a beta type[14].

In MySQL there are missing some of the capacities in comparison to the commercial DB servers[5]:

- **triggers** – they are stored procedures which are executed in the appearance of certain conditions;

- **views** – a view is an ordered by the user presentation of tables (or from other views). A view accept the returned result from a query and treats it as a table;
- **foreign keys** – this is a column or group of columns in table A, which are not a primary key in this table, but are a primary key in table B. They are part of the rules for the completeness of the data;
- **inherent support of XML** – the XML support is present in Perl and PHP;
- **in MySQL the access is limited only to a command row** – there are instruments with open exit code offering a graphic design of administration – MySQL Manager 1.0 and WinMySQLadmin 1.3

Despite of all these disadvantages MySQL remains the most widely spread server for small and medium sized DBs in Internet.

REALIZATION OF WEB INTERFACE FOR EXTRACTION OF OPERATIVE INFORMATION

This article aims to represents the realization of a DB with Web interface in the mining and in automation of the mining production. For that purpose a relation DB was create, which can be filled through Internet by the use of a Web-SQL based interface. The choice for SQL has been made due to the fact, that it is the standard that has been proved itself over for the past several years. SQL is used in all products for creation and processing of DB. It has been created and developed also an appropriate interface for searching and visualization in the data basis. The connection between the web-pages and the data basis is carried out by the use of cgi-perl/php scripts.

The “Operational Extraction” data basis will be daily used for putting, in of data as per working places, blasting fields, excavators, shifts or as per other production units regarding the way of reporting and recording. There will be sustained models entitling numbers or names of excavators, which will represent dumpers with different volumes of their baskets, as well as tables with volume weight, which can be updated on any time. The daily quantity of oar and metal as per working places excavators, blasting fields and etc. will be automatically calculated and be visualized. The software will provide a potentiality for an automatic operative tracking of the ready oar balance, as per blasting fields for example.

After the initial input of the quantities and the qualities of the mined mass as per blasting fields, an every day recording and reporting of the extraction as operational data will start. In every moment it will be possible an inquire to be made for the current situation of the ready oar of quantity and quality as per fields sections, horizons and for the whole mine..

The “dobiv” data basis contains the tables **main**, **bager**, **samosval** and **indicators**.

Table 1. Description table **main**:

| Field | Type        | Attribute             | Null | Default |
|-------|-------------|-----------------------|------|---------|
| IDnum | Tinyint(3)  | Primary Key, UNSIGNED | No   |         |
| name  | Varchar(10) |                       |      |         |

It contains information about the section, in which works are done.

Table 2. The contents of table **main** is:

| № | Name       |
|---|------------|
| 1 | Кет        |
| 2 | Насипище   |
| 3 | План-шихта |

The tables **bager** and **samosval** contain information about the excavators and draggers, which are being used.

Table 3. Description table **bager**:

| Field    | Type        | Attribute             | Null | Default |
|----------|-------------|-----------------------|------|---------|
| Number_b | Tinyint(3)  | Primary Key, UNSIGNED | No   |         |
| name_b   | Varchar(10) |                       |      |         |

Table 4. Description table **samosval**:

| Field    | Type        | Attribute             | Null | Default |
|----------|-------------|-----------------------|------|---------|
| Number_s | Tinyint(3)  | Primary Key, UNSIGNED | No   |         |
| name_s   | Varchar(10) |                       | No   |         |
| obem_s   | int(10)     | UNSIGNED              | No   |         |
| Kursove  | Tinyint(3)  | UNSIGNED              |      |         |

Table 5. Description table **indicators**:

| Field    | Type            | Attribute | Null | Default |
|----------|-----------------|-----------|------|---------|
| Idnum    | Tinyint(3)      | UNSIGNED  | No   |         |
| Za       | Enum('за','до') |           | No   | 3a      |
| day      | Tinyint(3)      | UNSIGNED  | No   | 0       |
| Number_b | Tinyint(3)      | UNSIGNED  | No   | 0       |
| Z        | Smallint(5)     | UNSIGNED  | No   | 0       |
| Cu       | float(5,3)      |           | No   | 0.000   |
| Obem     | int(10)         | UNSIGNED  | No   | 0       |
| obt      | float(4,2)      |           | No   | 0.00    |
| Ruda     | float(9,1)      |           | No   | 0.0     |
| Cut      | float(9,1)      |           | No   | 0.0     |

It contains 10 fields:

*IDnum* – this field is an foreign key from table **main** it shows for which section belong the entered parameters;

*za* – this field has two possible values “за” or “до” and shows whether the inquiry is being made for a particular day or for a group of days;

*day* – number of the day the inquiry is being made;

*bager* – the number of the excavator. The field is an foreign key from table **bager** ;

*z* – horizon;

*Cu* – Copper contains;

*obem* – the volume of the excavate mass, it is calculated on the basis of the indicators “kursove” and “obem\_s” from table **samosval**;

*obt* – volume weight;

*ruda* – oar quantity;

*Cut* – Copper quantity.

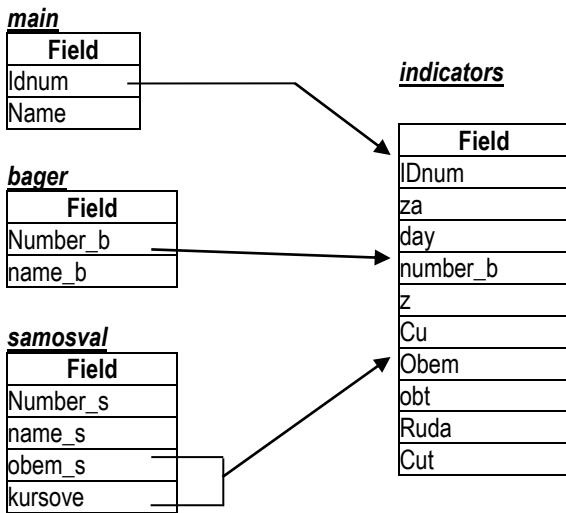


Figure 5 Description of relations between the tables

The Web interface for extraction from the data basis of operative information about the implementation of the production indicators for daily production, as well as for production for a past period, is done through PHP. And as a server for DB is used MySQL. The choice for PHP is provoked by the fact that for the last several year it has become the most widely used language for creation of Internet application and has replaced Perl (as CGI programming language) and ASP (as API). Beside this, PHP can work as CGI or other module to the Web server, avoiding in such a way the disadvantages of CGI. With its fastness, high reliability and open code MySQL has proved itself as a leading server for DB for small and medium sized Internet applications. The mutual work of PHP and MySQL responds to and meets also the requirements of the Internet programming and the client/server processing of information:

- A full Internet support;
- The fastest possible market circle;
- A full scalability both upstreaming and downstreaming;
- Portability.

The application contains three major scripts. The first is **index.php**. This is the initial page of the site.



Figure 6. Page index.php

To make a query to the data basis, the system requires the user to identify her/himself. For that purpose she/he, must enter her/his name and a password. By pressing the "LOG IN" button a call is made to the data basis whether such an user exists. If the answer is YES, the script

**create\_cquery\_select.php** is activated. Otherwise, an error message is viewed. Here the user can by the help of application form buttons can compose its query. Although the query is in SQL format, it is not necessary for the user to know the SQL syntax or the DB structure. All these is in concern of the PHP script. The access to this page is allowed only after the identification of the user – by **index.php**. Every other attempt to make a query will be rejected.

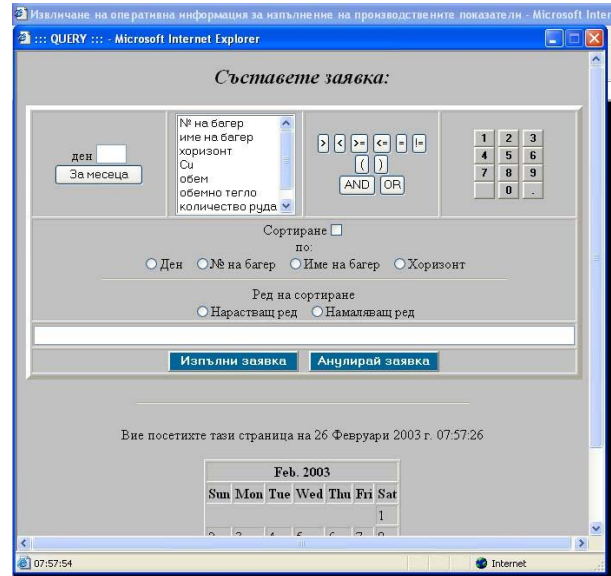


Figure 7 Page create\_cquery\_select.php

For the carrying out of the connection of the Web server to the server for the MySQL data basis, by the use of a PHP script several stages are needed:

1. A connection is created to the MySQL server.
2. A SQL query is sent to the MySQL server and a result is received.
3. The applicable program interfaces are used for extracting of data from the result received from (2).
4. A HTML page is generated to present the contents.

Two often used functions - **DisplayErrMsg** – a function for displaying of a message for error and **authenticateUser** – the function making the connection with MySQL are given in a separate file - **functions.php**

Besides the application form the page shows the hour in which it is activated the current hour (in Status Bar) and a calendar with the current month. For the creation of all these things a JavaScript. For a great view ability and clarity the JavaScript and the cascade styles are moved in separate files - **query\_javascript.js** and **query\_style.css**.

After sending of the query, the third major script - **create\_cquery.php** is activated. Its tasks are to compose and to send query to the server for DB in compliance with the data provided by the user, as well as to visualize the returned by the server answer. For this purpose, two queries are executed - the one created by the user in **create\_cquery\_select.php** and the query requiring a providing of data the relevant day or group of days. The result of these queries is visualized by the PHP command **mysql\_fetch\_object**. It will return the next row

of the given set of results as an object, or as a "false", if there are no more rows.

The screenshot shows a web browser window titled "Microsoft Internet Explorer" displaying a page with two tables. The first table is titled "Оперативна информация за изпълнение на производствените показатели за ден:" and contains 7 columns: "za/do", "Ден", "Номер на багер", "Име на багер", "Хоризонт", "Cu %", "Обем", "Обемно тегло", "Количество руда", and "Количество Cu". It lists 7 rows of data. The second table is titled "Обобщена оперативна информация за изпълнение на производствените показатели за дни:" and contains 5 columns: "za/do", "Ден", "Багер", "Количество руда", "Количество Cu", and "% Cu". It lists 4 rows of data. A "Print" button is visible at the bottom left of the page.

Fig. 8 Page create\_cquery\_select.php

The access to this page is possible only and only after the identification of the user – by *index.php* Every other try to take answer from the query will be reject. It is envisaged also an option for printing of the result – by pressing of the Print button. This option is realized by JavaScript.

The filling in of the data basis is not a subject of this development. One of the possible ways is the usage an additional module (provided by the official site of MySQL – [www.mysql.com/contrib](http://www.mysql.com/contrib)) for transforming of a table from dbf format – a format used by FoxPro, into frm – the format used by MySQL Or in other words, after the updating of the data basis in FoxPro the contents of the table is to be extracted in a text file and then a small script is to be executed, containing the SQL command - LOAD DATA INFILE "file name" ...

## CONCLUSION

The created software for extracting of operative information besides the advantages of the Web-SQL based software – scalability, portability, preparation of queries from the DB by the request of the user an etc., has also another big advantage – it is created by a freeware software - MySQL as a server for data base and by PHP as a language for connection with the data base.

Recommended for publication by Department of Mine Automation, Faculty of Mining Electromechanics

It is expected that the developed project of DB with a Web interface to grow in the future into a compete system, which shall take into accounting the objective and subjective factors in the automation of the mining, as well as shall analyze the data and support the decision – taking in the management of the mining enterprise.

The authors expectations are that it will be implemented in one of the mining enterprises functioning in Bulgaria.

## REFERENCES

- Тодоров Ю., Щърбанова И., М. Трифонова, GTMdata – български софтуер за планиране, управление и отчитане на добива, използван в ПК Елаците и Асарел-Медет АД .
- Karagiozov V., at. al., 1998. Networking the Third Millennium: The Third CEENet Workshop on Network Technology - Zagreb; Vienna; Skopje: Formica - pp.380, ISBN 9989-769-07-9 (book);
- Айзенменгер Р., 1999. HTML4, ИнфоДар;
- Gundavaram Sh., 1996. CGI programming on the WWW, O'reilly;
- ДюБоа П., 2002. MySQL, ИнфоДар;
- Колектив на издателство СофтПрес, 2001. Програмиране с XML, СофтПрес;
- Castagetto J., Rawat H., Schumann S., Scollo C., Veliath D., 2000. Professional PHP Programming, Wrox Press;
- Codd E. F., 1990. The Relational Model for Database Management, Addison-Wesley Publishing Company
- Майер Д., 1987. Теория реляционных баз данных, Мир;
- Грубер М., 2001. SQL – Професионално издание, СофтПрес;
- Кузнецов С.Д., Основы современных баз данных, Центра Информационных Технологий ;
- [www.w3.org](http://www.w3.org);
- [www.isoc.org](http://www.isoc.org);
- [www.mysql.com](http://www.mysql.com).

## ORGANIZATIONS AND MANUFACTURERS IN FIELD OF LASER

Miroslav Radovanovic

University of NIS  
Faculty of Mechanical Engineering

### ABSTRACT

Today, laser make up a multi-billion EUR industry. Industrial manufacturers have developed innovative ways to use lasers to increase manufacturing efficiencies and product quality. At present time every year over 3000 laser machines for industrial application are installed in the world. In many countries they are formed laser associations or organizations. These laser associations or organizations assist the manufacturing industries by providing technical, product and service information. All of these associations and organizations promote lasers and laser applications. Web-sites of laser associations and organizations contain: news, promote of lasers, industrial product catalogs and links, laser applications and safety, a list of events and a directory of services. Many of these associations and organizations support research in laser technology on a non-profit basis. They are several manufacturers of lasers, and many manufacturers of laser machines and equipments.

### INTRODUCTION

Laser is undoubtedly the most promising and constructive invention of the second half of the 20<sup>th</sup> century. The laser is a young invention and it has found a wide range of applications in all the sectors such as telecommunications, measurement techniques and the processing of metal and non-metal materials. The laser have been accepted globally by the engineering sector as an accurate and economical product. Laser based technologies are increasingly accepted as a competent substitute in component manufacturing on account of improvements in efficiency, quality and productivity at affordable cost. Laser processing is fast becoming essential in nearly all manufacturing industries. Today, laser make up a multi-billion EUR industry. At present time every year over 3000 laser machines for industrial application are installed in the world.

The first laser, a ruby laser, was invented 1960 by T. Maiman, the first He-Ne laser was invented 1961 by A. Jovan, D. Herriot and W. Bennett, the first Nd:YAG laser was invented 1964 by Geusic, the first CO<sub>2</sub> laser was invented 1964 by C.K.N. Patel, the first excimer laser was invented 1976. The first industrial application of a laser was making holes in diamonds used a beam from ruby laser. Since that beginning, the use of laser technology has continued to be an impressive and successful story. The term LASER is an acronym for Light Amplification by Stimulated Emission of Radiation. A laser is a cavity, with mirrors at the ends, filled with material such as crystal, glass, liquid, gas or dye. It is a device that produces an intense beam of light with the unique properties of coherence, collimation and monochromaticity. Typical lasers use electricity to create coherent light. Laser light can be different colors of the visible light spectrum, or can be invisible when the light is ultraviolet or infrared.

From laser surgery to CD players and grocery-store checkout scanners, our daily lives are enhanced by a basic discovery that was originally thought by some to have no practical uses

whatsoever. Lasers are used in almost all important sectors of industry, such as automotive industry, electrical industry, metal-working industries and others. In USA, the automotive industry and the metal-working industries are the biggest customers for lasers. In Asia, the electrical and semiconductor industry is the laser supplier's most important customer. In Europe, the metal-working industry and automotive industry are the biggest customers for lasers. Typical areas for applications of lasers are: printing technology, soldering, marking, drilling, cutting non-metals, cutting metals, sintering, heat condition welding, polymer welding, welding metals, hard soldering, hardening, heating, brazing, cladding. Some of these applications can be performed by lasers alone, but for many the justification is purely economic. For many applications, laser processing is the most precise, economical method available. For some, laser processing is the only method. Given the speed, flexibility and precision of laser processing, the cost savings are dramatic and the payback rapid.

In Germany, in 1989. year, it is investigated in laser equipment 804.5 milion EUR. From this in laser equipment for: material processing 222.5 milion EUR, research and development 143 milion EUR, information technique 141.5 milion EUR, communication 135 milion EUR, medicine 118 milion EUR, measure technique 34.5 milion EUR and printer technique 10 milion EUR. Figure 1 shows the percentages of investigation in laser equipment.

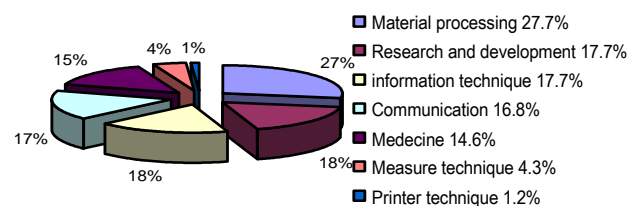


Figure 1. Percentages of investigation in laser equipment

Many types of lasers have been developed, but very few may be employed in a practical sense by industry. In laser equipment it is installed: semiconductor lasers 30%, CO<sub>2</sub>-lasers 22%, solid-state lasers 17%, ion lasers 13%, He-Ne lasers 7%, excimer lasers 4%, dye lasers 3% and other lasers 4%. Figure 2 show the percentages of installed lasers.

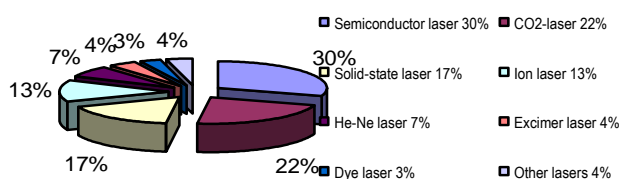


Figure 2. Percentages of installed lasers

The two most commonly used lasers are the CO<sub>2</sub> lasers and the Nd:YAG lasers. It is probably fair to say that of these two,

the CO<sub>2</sub> laser is the most versatile. Today, there is no doubt that the CO<sub>2</sub> laser is the most useful one for metalworking.

## LASER ASSOCIATIONS AND ORGANIZATIONS

In many countries they are formed laser associations or organizations. They assist the manufacturing industries by providing technical, product and service information. All of these associations and organizations promote lasers and laser applications. Web-sites of laser associations and organizations contain: news, promote of lasers, industrial product catalogs and links, laser applications and safety, a list of events and a directory of services. Many of these associations and organizations support research in laser technology on a non-profit basis. In table 1 is shown some of these associations and organizations and their web-sites. In table 2 are shown laser institutes, in table 3 are shown laser centres, and in table 4 are shown laser laboratories.

Table 1. Laser associations and organizations

| No | Laser associations  | Web-site          |
|----|---|-------------------|
| 1  | American Welding Society (AWS)                                | www.aws.org       |
| 2  | European Laser Applications Network (ELAN)                    | www.ailu.org.uk   |
| 3  | International Laser Display Association (ILDA)                | www.ilda.wa.org   |
| 4  | International Society for Optical Engineering                 | www.spie.org      |
| 5  | Japan Laser Processing Society (JLPS)                         | www.jlps.gr.jp    |
| 6  | Laser and Electro-Optics Manufacturer's Association (LEOMA)   | www.sfo.com       |
| 7  | Lasers and Laser Engineering                                  | www.lasers.org.uk |
| 8  | Optical Soc. of America (OSA)                                 | www.osa.org       |
| 9  | Optronics Ireland   | www.tcd.ie        |
| 10 | Russian Federal Research Center RAMET                         | www.girmet.ru     |
| 11 | The Association of Industrial Laser Users                     | www.ailu.org.uk   |
| 12 | The Entertainment Laser Association                           | www.ela.org.uk    |
| 13 | The International Society for Optical Engineering (SPIE)      | www.spie.com      |
| 14 | The Laser & Electro-optics Manufacturer's Association (LEOMA) | www.sfo.com       |
| 15 | UK Laser and Electro-Optics Trade Association                 | www.ukleo.org     |

Table 2. Laser institute

| No | Laser institute  | Web-site                  |
|----|--|---------------------------|
| 1  | Arizona State University – MEMS                                    | www.eas.asu.edu           |
| 2  | Beckman Laser Institute  | www.bli.uci.edu           |
| 3  | Columbia University – MRL  | www.mrl.columbia.edu      |
| 4  | Edison Welding Institute (EWI)                                     | www.ewi.org               |
| 5  | Fraunhofer Institute for Laser Technology (ILT)                    | www.ilt.fhg.de            |
| 6  | Institute of Optics – Rochester                                    | www.optics.rochester.edu  |
| 7  | Institute of Electronic Structure and Laser (IESL)                 | http://safety.web.cern.ch |
| 8  | ISLT TU Vienna   | www.tuwien.ac.at          |
| 9  | Laser Institute of America (LIA)                                   | www.laserinstitute.org    |
| 10 | Laser Palace – Lawrence University                                 | www.pkal.org              |
| 11 | Rice University – Laser Science                                    | www.ruf.rice.edu          |
| 12 | Rockwell Laser Institute   | www.rli.com               |
| 13 | The Welding Institute (TWI)  | www.twi.co.uk             |
| 14 | UMIST University of Manchester Institute of Science and Technology | www.me.umist.ac.uk        |
| 15 | University of Twente (WB)  | www.wa.wb.utwente.nl      |
| 16 | University of Wisconsin  | www.engr.wisc.edu         |
| 17 | University St Etienne  | www.univ-st-etienne.fr    |
| 18 | Lund university – Lund laser centre (LLC)                          | www.llc.fysik.lth.se      |
| 19 | Masquarie university – Centre for lasers and applications          | www.mpec.mq.edu.au        |
| 20 | Oklahoma State University – Laser Center                           | www.okstate.edu           |

|    |  |                             |
|----|--|-----------------------------|
| 21 | Umea University – Laser Physics Group                  | www.phys.umu.se             |
| 22 | Lulea University of Technolofy                         | www.mb.luth.se              |
| 23 | Michigan state university-MSU laser laboratory         | http://photon.cern.msu.edu  |
| 24 | Optics and Laser Group, Adelaide University, Australia | www.physics.adelaide.edu.au |
| 25 | tsinghua University                                    | www.tsinghua.edu.cn         |

Table 3. Laser centres

| No | Laser centres  | Web-site                     |
|----|--|------------------------------|
| 1  | Australian National University Laser Physics Centre    | http://laserspark.anu.edu.au |
| 2  | Center for Research and Education in Optics and Lasers | http://lorien.creol.ucf.edu  |
| 3  | Fraunhofer Center for Laser Technology (CLT)           | www.clt.fraunhofer.com       |
| 4  | Laser Physics Centre ANU - Canberra                    | http://laserspark.anu.edu.au |
| 5  | Laser Science Centre - Queensland                      | www.physics.uq.edu.au        |
| 6  | Laser Spectroscopy Center – Wisconsin at Madison       | www.chem.wisc.edu            |
| 7  | Laser zentrum Hannover                                 | www.lzh.de                   |

Table 4. Laser laboratories

| No | Laser laboratories                                 | Web-site                     |
|----|--|------------------------------|
| 1  | Bell laboratories                                  | www.bell-labs.com            |
| 2  | Lapeeuranta University of Technology               | www.lut.fi                   |
| 3  | Laser and Electro-Optics Research Laboratory (BYU) | www.ec.byu.edu               |
| 4  | Laser Laboratory – Hope College                    | www.chem.hope.edu            |
| 5  | Laser Laboratory – Hunter College                  | www.ph.hunter.cuny.edu       |
| 6  | Laser Laboratory – Lawrence College                | www.lawrence.edu             |
| 7  | Laser Laboratory – Lynchburg College               | www.lynchburg.edu            |
| 8  | Laser Laboratory – Western Maryland College        | www.wmc.car.md.us            |
| 9  | Laser Optics&Spectroscopy Group                    | www.lsr.ph.ic.ac.uk          |
| 10 | Lawrence Berkeley National Laboratory              | http://efssun.lbl.gov        |
| 11 | Penn State's Applied Research Lab.                 | www.arl.psu.edu              |
| 12 | Semiconductor Laser Laboratory                     | http://sll.ccsm.uiuc.edu     |
| 13 | Ultrafast Laser Laboratory (BNL)                   | www.inst.bnl.gov             |
| 14 | Berkelet-Laser Manufacturing Laboratory            | http://enler.me.berkeley.edu |

## LASER MANUFACTURERS

There are several manufacturers of lasers, and many manufacturers of laser machines. In table 5 are shown manufacturers of lasers. Industry leaders of laser manufacturers are: Coherent Laser Group, Ferranti Photonics, Rofin-Sinar, Spectra-Physics and Trumpf. Laser machines are product of high technology. They present complexe hardware and software equipment. Manufacturers of machines

incorporate laser, optical system for laser beam transmission, and processing head in mechanical machines with CNC unit and build laser machines. In table 6 are shown the most known manufacturers of laser machines and their web-sites. Industry leaders of laser manufacturers are: Amada, Bystronic, Cincinnati, ESAB, Hahn%Kolb, Lumonics, Mazak, Messer. Prima Industrie, Rofin, Salvagnini and Trumpf.

Table 5. Laser manufacturers

| No | Laser manufacturers        | Web-site                  | No | Laser manufacturers    | Web-site               |
|----|----------------------------|---------------------------|----|------------------------|------------------------|
| 1  | Aculight                   | www.aculight.com          | 23 | Melles Griot           | www.mellesgriot.com    |
| 2  | Alpha Lasers               | www.alphalas.com          | 24 | Metrologic Instruments | www.metrologic.com     |
| 3  | Big Sky Laser Technologies | www.bigskylaser.com       | 25 | Optlectra              | www.optlectra.com      |
| 4  | Blue Sky Research          | www.blueskyreseach.com    | 26 | Opto Power Corporation | www.optopower.com      |
| 5  | Bonneville Technologies    | www.bonnevilletech.com    | 27 | Oxford Lasers          | www.oxfordlasers.com   |
| 6  | Cilas                      | www.cilas.com             | 28 | Parallax Technology    | www.parallax-tech.com  |
| 7  | Coherent                   | www.cohr.com              | 29 | Photonics Industries   | www.photonix.com       |
| 8  | Continuum                  | www.ceoi.com              | 30 | Photonics Solutions    | www.psplc.com          |
| 9  | Cutting Edge Optronics     | www.ceolaser.com          | 31 | Positive Light         | www.poslight           |
| 10 | EKSPL                      | www.ekspla.com            | 32 | Power Technology       | www.powertechology.com |
| 11 | Ferranti Photonics         | www.ferrantiphotonics.com | 33 | PRC Laser              | www.prcclaser.com      |
| 12 | Lambda Physik              | www.lambdaphysik.com      | 34 | Q-Peak                 | www.qpeak.com          |
| 13 | LASAG Industrial Lasers    | www.lasag.com             | 35 | Quantronix             | www.quantron.com       |

|    |                         |                      |    |                        |                             |
|----|-------------------------|----------------------|----|------------------------|-----------------------------|
| 14 | Laser Labs              | www.laserlabs.com    | 36 | Resonetics             | www.resonetics.com          |
| 15 | Laser Physics           | www.laserphysics.com | 37 | Rockwell Lasers        | www.rli.com                 |
| 16 | Laser Power Corporation | www.laserpower.com   | 38 | Rofin-Sinar            | www.rofin-sinar.com         |
| 17 | Latronix AB             | www.latronix.se      | 39 | Spectra-Physics        | www.splasers.com            |
| 18 | Lee Laser               | www.leelaser.com     | 40 | Spectron Laser Systems | www.spectron.co.uk          |
| 19 | Lexel Laser             | www.lexellaser.com   | 41 | Synrad                 | www.synrad.com              |
| 20 | Liconix                 | www.liconix.com      | 42 | Trumpf                 | www.haas-laser.com          |
| 21 | Light Solutins          | www.lightsol.com     | 43 | TRW                    | www.trw.com                 |
| 22 | LumenX Technologies     | www.dyelaser.com     | 44 | Unitek Miyachi Lasers  | www.unitekmiyachilasers.com |

Table 6. Laser machine manufacturers

| No | Laser machine manufacturers  | Web-site                  | No | Laser machine manufacturers | Web-site                       |
|----|------------------------------|---------------------------|----|-----------------------------|--------------------------------|
| 1  | Amada                        | www.amada.com             | 28 | Mazak                       | www.mazaklaser.com             |
| 2  | Arnold                       | www.arnold-rv.de          | 29 | Mecanumeric                 | www.mecanumeric.fr             |
| 3  | Baasel Lasertech             | www.baasel.de             | 30 | Messer Cutting Systems      | www.messer-cs.de               |
| 4  | BLM-ADIGE USA                | www.blmgroupp.com         | 31 | Mitsubishi Laser            | www.mitsubishi-world           |
| 5  | Bystronic Laser.             | www.bystronic.com         | 32 | Modern Machine Tool         | www.modernmachinetool.com      |
| 6  | Cheval Freres                | www.cheval-freres.fr      | 33 | Motoman                     | www.motoman.com                |
| 7  | Cielle                       | www.ciellecnc.com         | 34 | Omega Laser                 | www.a1.nl/omega-laser-systems/ |
| 8  | Cincinnati Incorporated      | www.cincinnati-tools.com  | 35 | OTO Mills USA               | www.otomills.com               |
| 9  | Convergent Prima             | www.convergentprima.com   | 36 | Photonics Spectra           | www.photonicspectra.com        |
| 10 | Cutting Edge Optronics       | www.ceo-laser.com         | 37 | Precitec                    | www.precitec.com               |
| 11 | Edwards Pearson              | www.edwards-pearson.co.uk | 38 | Prima Industrie             | www.primaindustrie.com         |
| 12 | Electrox                     | www.electrox.com          | 39 | Profile 600                 | www.profile600.co.uk           |
| 13 | Embassy Machinery            | www.embassy-mach.co.uk    | 40 | Pullmax                     | www.pullmax.com                |
| 14 | ESAB                         | www.esab.com              | 41 | Rofin                       | www.rofin.com                  |
| 15 | FANUC Robotics North America | www.fanucrobotics.com     | 42 | RPA Limited                 | www.rpaservices.com            |
| 16 | Ferranti Photonics           | www.ferrantiphotonics.com | 43 | Salvagnini                  | www.salvagnini.it              |
| 17 | Franek Laser&Fab Systems     | www.franeklaser.com       | 44 | SEI                         | www.seispa.com                 |
| 18 | GSI Lumonics                 | www.gsilumonics.com       | 45 | Sondronic Automotive        | www.sondronic.com              |
| 19 | Haco                         | www.haco.com              | 46 | Strippit/LVD                | www.lvdgroup.com               |
| 20 | Hahn&Kolb                    | www.hklaser-systems.com   | 47 | Thinklaser                  | www.thinklaser.com             |
| 21 | Hana Laser                   | www.hanalaser.com         | 48 | Trotec                      | www.trotec.net                 |
| 22 | Koike                        | www.coikeox.co.jp         | 49 | Trumpf                      | www.trumpf.com                 |
| 23 | Lasag AG                     | www.lasag.com             | 50 | Yamazaki Machinery UK       | www.mazakeurope.com            |
| 24 | LaserCut                     | www.lasercutinc.com       | 51 | Universal laser systems.    | www.ulsinc.com                 |
| 25 | LPKF Laser&Electronics       | www.lpkf.com              | 52 | Virtek Industrial Laser     | www.virtek.ca                  |
| 26 | Lumonics                     | www.lumonics.com          | 53 | Wightman Stewart            | www.wightmanstewart.co.uk      |
| 27 | Marbach                      | www.marbach.com           | 54 | Whitney                     | www.wawhitney.com              |

## CONCLUSION

Today, industrial lasers are now classed as "conventional" technology in many sectors of industry. There are several manufacturers of lasers, and many manufacturers of laser machines. Industry leaders of laser manufacturers are: Coherent Laser Group, Ferranti Photonics, Rofin-Sinar, Spectra-Physics and Trumpf. Industry leaders of laser manufacturers are: Amada, Bystronic, Cincinnati, ESAB, Hahn%Kolb, Lumonics, Mazak, Messer. Prima Industrie, Rofin, Salvagnini and Trumpf. Laser associations and organizations assist the manufacturing industries by providing technical, product and service information. All of these associations and organizations promote lasers and laser applications.

## REFERENCES

Radovanovic M., Laser cutting cost considerations, International scientific conference "UNITECH'02", Technical

University of Gabrovo, Gabrovo, Bulgaria, 2002, p.362-366.

Radovanović M., Lazarević D., Laser-machines and Laser-robots for Cutting Thin Sheet, International Conference on Mechanical Transmissions and Mechanisms MTM '97, Tianjin University, Tianjin, China, 1997, p. 867-870.

Radovanović M., Application of Lasers in Manufacturing, 4<sup>th</sup> International Conference on Accomplishments of Electrical and Mechanical Industries, Faculty of mechanical engineering, Banja Luka, Bosna&Hercegovina, 2001, p. 169-174.

Radovanovic M., Laser cutting machines, 5<sup>th</sup> International conference DEMI 2002, University of Banja Luka, Faculty of mechanical engineering, Banja Luka, Bosna&Hercegovina, 2002, p. 173-178.

Radovanovic M., Laser cutting machines for 3-D thin sheet parts, 8<sup>th</sup> International Conference "University's day", University "Constantin Brancusi", Faculty of engineering, Targu Jiu, Romania, 2002, CD

- Radovanović M., CO<sub>2</sub> laserske mašine za sečenje, 28.  
Savetovanje proizvodnog mašinstva Jugoslavije, Mašinski  
fakultet Kraljevo, Kraljevo, Jugoslavija, 2000, str. 3.13-3.18
- Introduction to Industrial Laser Materials Processing, Rofin-  
Sinar Laser, Hamburg, 2000
- Konig W., Fertigungsverfahren, VDI-Verlag, Dusseldorf, 1990.
- Dilthey U., Schweißtechnische Fertigungsverfahren, Schweiß  
und Schneidtechnologien, VDI-Verlag, Dusseldorf, 1994.
- Steigende Dynamik in Lasermarkt, Laser-Praxis, Jun, 1990,  
LS.4
- [www.laserspot.com](http://www.laserspot.com)  
[www.franeklaser.com](http://www.franeklaser.com)  
[www.pcs-usa.com](http://www.pcs-usa.com)  
[www.synova.ch](http://www.synova.ch)  
[www.directindustry.com](http://www.directindustry.com)  
[www.connectexpress.com](http://www.connectexpress.com)  
[www.iwb.tum.de](http://www.iwb.tum.de)  
[www.thefabricator.com](http://www.thefabricator.com)  
[www.e4production.net](http://www.e4production.net)

*Recommended for publication by Department of  
Mine Automation, Faculty of Mining Electromechanics*

## NEUTRAL EQUATIONS WITH POLYNOMIAL NONLINEARITIES ARISING IN TRANSMISSION LINES

Vasil Angelov

University of Mining and Geology  
"St. Ivan Rilski"  
Sofia 1700, Bulgaria  
E-mail: angelov@staff.mgu.bg

ABSTRACT: An existence theorem for neutral equations with polynomial nonlinearities is proved.

### INTRODUCTION

It is known that in the theory of nonlinear circuits  $V-I$  characteristic curve can be approximated by various nonlinear functions (cf. [1]-[3]) - polynomials, exponential functions, hyperbolic functions and their combinations. In [4]-[7] the authors in their endeavour to investigate the lossless transmission lines considers the hyperbolic system

$$\frac{\partial u}{\partial x} = -L \frac{\partial i}{\partial t} \quad \text{и} \quad \frac{\partial i}{\partial x} = -C \frac{\partial u}{\partial t}, \quad (1)$$

where  $i = i(t, x)$ ,  $u = u(t, x)$  are the current and the voltage respectively, while  $L$  is the series inductance, and  $C$  is the parallel capacitance per unit length of the line. The line is shorted at  $x=0$  which implies  $u(0, t) = 0$  and it is connected with a nonlinear element (for instance tunnel diode) at  $x=l$  ( $l$  is the length of the line), that is,  $i(l, t) = f(u(l, t) + E)$ , where  $E$  is the bias voltage, and  $I = f(V)$  is the  $V-I$  characteristic curve. In many cases  $f(V)$  is third degree polynomial of the type  $f(V) = -aV + V^3$  (cf. [4]-[7]) or polynomial of higher order [1], [2]. If the parallel capacitance  $C_0$  is considered in the circuit the above boundary value condition becomes

$$i(l, t) = f(u(l, t) + E) + C_0 \frac{\partial u(l, t)}{\partial t}.$$

Then the mixed initial-boundary problem for system (1) can be replaced by a pure initial value problem for a functional differential equation of neutral type ([4]-[7]) while in the first one obtains only functional equations. The general theory of neutral equations can be found in [8]-[11] but the polynomial nonlinearities only in particular cases are considered [4]-[7].

The main purpose of the present paper is to formulate conditions for the existence and uniqueness of solutions of

neutral functional differential equations with polynomial nonlinearities in the right-hand sides in general case. Our investigations are based on fixed point approach obtained in [12]-[13].

Let us consider an initial value problem for the neutral functional differential equation of first order

$$\begin{aligned} \dot{u}(t) &= F(u(\Delta_1(t)), \dots, u(\Delta_m(t)), \dot{u}(\gamma_1(t)), \dots, \dot{u}(\gamma_n(t))), t > 0, \\ u(t) &= \varphi(t), \dot{u}(t) = \dot{\varphi}(t), t \leq 0 \end{aligned} \quad (2)$$

where  $F(u_1, \dots, u_m, v_1, \dots, v_n) : R^{m+n} \rightarrow R^1$ ,

$$\varphi(t), \dot{\varphi}(t) : R_-^1 \rightarrow R^1, R_+^1 = [0, \infty), R_-^1 = (-\infty, 0],$$

$$\Delta_i(t) : R_+^1 \rightarrow R^1 \quad (i = 1, 2, \dots, m),$$

$$\gamma_k(t) : R_+^1 \rightarrow R^1 \quad (k = 1, 2, \dots, n) \text{ are prescribed functions.}$$

Usually when one look for global solution of (2)  $F$  has to satisfy the condition of the type

$$|F(u_1, \dots, u_m, v_1, \dots, v_n)| \leq a \left[ \sum_{k=1}^m |u_k| + \sum_{s=1}^n |v_s| \right] \quad (3)$$

Our goal is to include in the consideration the right-hand sides of general type:

$$\begin{aligned} F(u_1, \dots, u_m, v_1, \dots, v_n) &= \sum_{s=1}^{k_1} a_s^{(1)} u_1^s + \sum_{s=1}^{k_2} a_s^{(2)} u_2^s + \dots \\ &+ \sum_{s=1}^{k_m} a_s^{(m)} u_m^s + \sum_{k=1}^n b_k v_k \end{aligned} \quad (4)$$

where  $a, a_s^{(l)}, b_k$  are prescribed constants.

The equations obtained in [4] - [7] are particular cases of (4):

$$C_0[\dot{u}(t) + K\dot{u}(t-h)] + \left(\frac{1}{z} - g\right)u(t) - K\left(\frac{1}{z} + g\right)u(t-h) = -u^3(t) - Ku^3(t-h),$$

where  $C_0, K, \frac{1}{z}, g$  and  $h$  are prescribed constants.

EXISTENCE THEOREM

As usually we put  $y(t) = \dot{u}(t)$  for  $t > 0$  and  $\psi(t) = \dot{\varphi}(t)$  for  $t \leq 0$ . Then (2) becomes assuming  $y(0) = \varphi(0) = 0$ ):

$$y(t) = F\left(\int_0^{\Delta_1(t)} y(s)ds, \dots, \int_0^{\Delta_m(t)} y(s)ds, y(\gamma_1(t)), \dots, y(\gamma_n(t))\right), t > 0$$

$$y(t) = \psi(t), t \leq 0. \tag{5}$$

Indeed  $y(t-t_0) = u(t) - \varphi_0 - \varphi_0'(t-t_0)$  satisfies

Condition

s

$$y(0) = y(t_0 - t_0) = u(t_0) - \varphi_0 = 0 \text{ and}$$

$$y'(0) = u'(t_0) - \varphi_0' = 0 \text{ (} u(t_0) = \varphi_0, u'(t_0) = \varphi_0' \text{)}.$$

**Theorem 1.** Let the following conditions be fulfilled:

- 1.1 Functions
- 1.2

$$\Delta_i(t), \gamma_k(t) : \mathbb{R}_+^1 \rightarrow \mathbb{R}^1 \text{ (} i = 1, \dots, m; k = 1, \dots, n \text{)}$$

are continuous and  $\Delta_i(0) \leq 0, \gamma_k(0) \leq 0$ , and

$$t - \Delta_i(t) \geq \Delta_0 > 0, t - \gamma_k(t) \geq \gamma_0 > 0,$$

where  $\Delta_0$  and  $\gamma_0 > 0$  are constants;

- 1.3 the function

$$F(u_1, \dots, u_m, v_1, \dots, v_n) : \mathbb{R}^{m+n} \rightarrow \mathbb{R}^1$$

is continuous and satisfies the conditions:

1.3.1  $\psi(t) = \dot{\varphi}(t)$  is continuous and satisfies conformity

condition

1.3.2

$$\psi(0) = F\left(\int_0^{\Delta_1(0)} \psi(s)ds, \dots, \int_0^{\Delta_m(0)} \psi(s)ds, \psi(\gamma_1(0)), \dots, \psi(\gamma_n(0))\right);$$

$$1.2.2 \quad |F(u_1, \dots, u_m, v_1, \dots, v_n)| \leq$$

1.2.3

$$\leq a_1 \left( \sum_{s=0}^{k_1} |u_1|^s + \dots + \sum_{s=0}^{k_m} |u_m|^s \right) + a_2 \sum_{s=1}^n |v_s|,$$

where  $a_1$  and  $a_2$  are positive constants;

1.2.3

$$|F(u_1, \dots, u_m, v_1, \dots, v_n)| - |F(\tilde{u}_1, \dots, \tilde{u}_m, \tilde{v}_1, \dots, \tilde{v}_n)| \leq$$

$$\leq b_1 \left( \sum_{s=1}^{k_1} |u_1^s - \tilde{u}_1^s| + \dots + \sum_{s=1}^{k_m} |u_m^s - \tilde{u}_m^s| \right) + b_2 \sum_{s=1}^n |v_s - \tilde{v}_s|$$

Then (5) has a unique continuous solution.

**Proof.** Consider the set  $X$  of all continuous functions  $f(t) : [0, T_0] \rightarrow \mathbb{R}^1$  which coincide with  $\psi(t)$  for  $t \leq 0$ .

Introduce a family of pseudometrics

$$\mathcal{A} = \{\rho_\lambda(f, \tilde{f}) : \lambda \in [0, \infty)\}, \text{ where}$$

$$\rho_\lambda(f, \tilde{f}) = \sup\{e^{-\lambda t} |f(t) - \tilde{f}(t)| : t \in [0, T_0]\}.$$

Recall that for  $t \leq 0$   $f(t) = \psi(t)$  and  $\tilde{f}(t) = \psi(t)$ .

Then the set  $X$  endowed with the family  $\mathcal{A}$  becomes a uniform space  $(X, \mathcal{A})$ .

Introduce the set

$$M = \{f \in (X, \mathcal{A}) : |f(t)| \leq Ae^{\lambda t}, t \in [0, T_0]\},$$

where  $A$  is a fixed constant which does not depend on  $f$ .

It is easy to verify that  $(Tf)(t)$  is a continuous function on  $\mathbb{R}^1$ .

First we show that the operator  $T$  defined by the right-hand side of (5) is contractive:

$$(Tf)(t) = \begin{cases} F\left(\int_0^{\Delta_1(t)} f(s)ds, \dots, \int_0^{\Delta_m(t)} f(s)ds, f(\gamma_1(t)), \dots, f(\gamma_n(t))\right), t \in [0, T_0] \\ \psi(t), t \leq 0. \end{cases}$$

Indeed for every  $f, \tilde{f} \in M$  we have  $t \in [0, T_0]$  for which  $\Delta_k(t) > 0$ :

$$|(Tf)(t) - (T\tilde{f})(t)| \leq b_1 \left[ \sum_{s=1}^{k_1} \left| \left( \int_0^{\Delta_1(t)} f(\tau)d\tau \right)^s - \left( \int_0^{\Delta_1(t)} \tilde{f}(\tau)d\tau \right)^s \right| + \dots + \sum_{s=1}^{k_m} \left| \left( \int_0^{\Delta_m(t)} f(\tau)d\tau \right)^s - \left( \int_0^{\Delta_m(t)} \tilde{f}(\tau)d\tau \right)^s \right| \right] + b_2 \sum_{s=1}^n |f(\gamma_s(t)) - \tilde{f}(\gamma_s(t))| \leq$$

$$\begin{aligned} &\leq b_1 \left[ \sum_{s=1}^{k_1} \left| \int_0^{\Delta_1(t)} f(\tau) d\tau - \int_0^{\Delta_1(t)} \tilde{f}(\tau) d\tau \right| s \left| \int_0^{\Delta_1(t)} \tilde{f}(\tau) d\tau \right|^{s-1} + \dots + \right. \\ &+ \sum_{s=1}^{k_m} \left| \int_0^{\Delta_m(t)} f(\tau) d\tau - \int_0^{\Delta_m(t)} \tilde{f}(\tau) d\tau \right| s \left| \int_0^{\Delta_m(t)} \tilde{f}(\tau) d\tau \right|^{s-1} + \\ &+ b_2 \sum_{s=1}^n e^{-\lambda \gamma_s(t)} |f(\gamma_s(t)) - \tilde{f}(\gamma_s(t))| e^{\lambda \gamma_s(t)} \leq \\ &\leq b_1 \left[ \sum_{s=1}^{k_1} s A^{s-1} \left| \int_0^{\Delta_1(t)} e^{\lambda \tau} d\tau \right|^{s-1} \left| \int_0^{\Delta_1(t)} |f(\tau) - \tilde{f}(\tau)| e^{-\lambda \tau} e^{\lambda \tau} d\tau \right| + \dots \right. \\ &+ \sum_{s=1}^{k_m} s A^{s-1} \left| \int_0^{\Delta_m(t)} e^{\lambda \tau} d\tau \right|^{s-1} \left| \int_0^{\Delta_m(t)} |f(\tau) - \tilde{f}(\tau)| e^{-\lambda \tau} e^{\lambda \tau} d\tau \right| + \\ &+ b_2 \rho_\lambda(f, \tilde{f}) \sum_{s=1}^n e^{-\lambda \gamma_s(t)} \leq \\ &\leq b_1 \rho_\lambda(f, \tilde{f}) \left[ \sum_{s=1}^{k_1} s A^{s-1} \left| \int_0^{\Delta_1(t)} e^{\lambda \tau} d\tau \right|^s + \dots + \sum_{s=1}^{k_m} s A^{s-1} \left| \int_0^{\Delta_m(t)} e^{\lambda \tau} d\tau \right|^s \right] + \\ &+ b_2 \rho_\lambda(f, \tilde{f}) \sum_{s=1}^n e^{-\lambda \gamma_s(t)} \leq (k = \max\{k_1, k_2, \dots, k_m\}) \\ &\leq b_1 \rho_\lambda(f, \tilde{f}) \left[ \sum_{s=1}^{k_1} s A^{s-1} \left| \frac{e^{\lambda \Delta_1(t)} - 1}{\lambda} \right|^s + \dots + \sum_{s=1}^{k_m} s A^{s-1} \left| \frac{e^{\lambda \Delta_m(t)} - 1}{\lambda} \right|^s \right] + \\ &+ b_2 \rho_\lambda(f, \tilde{f}) \sum_{s=1}^n e^{-\lambda t + \lambda \gamma_s(t)} e^{\lambda t} \leq \\ &\leq \rho_\lambda(f, \tilde{f}) \left[ b_1 \left( \sum_{s=1}^{k_1} s A^{s-1} e^{\lambda s t} \left( \frac{e^{-\lambda t + \lambda \Delta_1(t)}}{\lambda} \right)^s + \dots \right. \right. \\ &+ \left. \sum_{s=1}^{k_m} s A^{s-1} e^{\lambda s t} \left( \frac{e^{-\lambda t + \lambda \Delta_m(t)}}{\lambda} \right)^s \right) + e^{\lambda t} b_2 \sum_{s=1}^n e^{-\lambda \gamma_0} \leq (-\lambda t + \lambda \Delta_i(t) \leq -\lambda \Delta_0) \\ &\leq \rho_\lambda(f, \tilde{f}) \left[ b_1 m \sum_{s=1}^k s A^{s-1} \frac{e^{-\lambda \Delta_0 s}}{\lambda^s} e^{\lambda s t} + n e^{\lambda t} b_2 e^{-\lambda \gamma_0} \right]. \end{aligned}$$

We multiply the previous inequality with  $e^{-\lambda t}$  and then  $e^{-\lambda t} |(Tf)(t) - (T\tilde{f})(t)| \leq$

$$\begin{aligned} &\leq \rho_\lambda(f, \tilde{f}) \left[ b_1 m \sum_{s=1}^k s A^{s-1} \frac{e^{-\lambda \Delta_0 s}}{\lambda^s} e^{\lambda(s-1)T_0} + n b_2 e^{-\lambda \gamma_0} \right] \leq \\ &\leq \rho_\lambda(f, \tilde{f}) \left[ b_1 m \frac{e^{-\lambda \Delta_0}}{\lambda} \sum_{s=1}^k s \left[ \frac{A e^{-\lambda \Delta_0 + \lambda T_0}}{\lambda} \right]^{s-1} + n b_2 e^{-\lambda \gamma_0} \right] \equiv \\ &\equiv \rho_\lambda(f, \tilde{f}) B(\lambda) \Rightarrow \rho_\lambda(Tf, T\tilde{f}) \leq B(\lambda) \rho_\lambda(f, \tilde{f}). \end{aligned}$$

For sufficiently large  $\lambda$  one can see that  $B(\lambda) < 1$  provided  $T_0 - \Delta_0 \leq 0$ . This implies that  $T$  is contractive.

We show  $f \in M \Rightarrow Tf \in M$ . Indeed  $(\Delta_k > 0)$ :

$$\begin{aligned} |(Tf)(t)| &\leq a_1 \left( \sum_{s=1}^{k_1} \left| \int_0^{\Delta_1(t)} f(\tau) d\tau \right|^s + \dots + \sum_{s=1}^{k_m} \left| \int_0^{\Delta_m(t)} f(\tau) d\tau \right|^s \right) + \\ &+ a_2 \sum_{s=1}^n |f(\gamma_s(t))| \leq \\ &\leq a_1 \left( \sum_{s=1}^{k_1} A^s \left( \frac{e^{\lambda \Delta_1(t)} - 1}{\lambda} \right)^s e^{\lambda s t} + \dots + \sum_{s=1}^{k_m} A^s \left( \frac{e^{\lambda \Delta_m(t)} - 1}{\lambda} \right)^s e^{\lambda s t} \right) + \\ &+ a_2 e^{\lambda t} \sum_{s=1}^n e^{-\lambda t + \lambda \gamma_s(t)} A \leq \\ &\leq a_1 m \sum_{s=1}^k \left( \frac{A}{\lambda} \right)^s \left( e^{-\lambda \Delta_0 + \lambda T_0} \right)^s + a_2 e^{\lambda t} A n e^{-\lambda \gamma_0}. \end{aligned}$$

Multiply the last inequality  $e^{-\lambda t}$ :

$$\begin{aligned} e^{-\lambda t} |(Tf)(t)| &\leq \\ &\leq a_1 m \sum_{s=1}^k \left( \frac{A}{\lambda} \right)^s \left( e^{-\lambda \Delta_0 + \lambda T_0} \right)^s e^{-\lambda t} + n a_2 A e^{-\lambda \gamma_0} \leq \\ &\leq a_1 m \sum_{s=1}^k \left( \frac{A}{\lambda} \right)^s \left( e^{-\lambda \Delta_0 + \lambda T_0} \right)^s + n a_2 A e^{-\lambda \gamma_0} \leq A, \end{aligned}$$

which is always satisfied for sufficiently large  $\lambda$  and  $T_0 - \Delta_0 \leq 0$ .

In order to be satisfied all conditions of the fixed point theorem [12] we have to find such an element  $x_0$  that

$$\rho_{j^k(\lambda)}(x_0, Tx_0) \leq Q < \infty \quad (k = 1, 2, \dots)$$

Here the map  $j : A \rightarrow A$  (cf. [12]) is  $j(\lambda) = \lambda$ . One can choose  $x_0$

$$x_0(t) = \begin{cases} \psi(0), & t \geq 0 \\ \psi(t), & t \leq 0 \end{cases}.$$

Then we obtain

$$\rho_{j^k(\lambda)}(x_0, Tx_0) = \\ = \sup \{ |\psi(0) - F(\Delta_1(t)\psi(0), \dots, \Delta_m(t)\psi(0), \psi(0), \dots, \psi(0))| e^{-\lambda t} : t \in [0, T_0] \} < \infty$$

The last supremum exists because

$$|\Delta_i(t)| \leq |t - \Delta_0| \text{ and consequently}$$

$$e^{-\lambda t} \sum_{s=1}^{k_i} (|\Delta_i(t)| \psi(0))^s < \infty, \quad (i = 1, 2, \dots, m).$$

Therefore  $T$  has a unique fixed point [12], which is a solution of (5).

#### REFERENCE

- Matkhanov P. N. Analysis of electrical circuits-nonlinear circuits. *Visha schola*, Moscow, 1977 (in Russian).
- Andreev V. S., B.I. Popov, A.I. Fedorov, H.H. Fomin. Generators of harmonic oscillations with tunnel diodes. *Energia*, Moscow, 1972 (in Russian).
- Starr A. T., Radio and Radar Technique. I. Pitman&Sons, London, 1958.
- Nagumo J., M. Shimura. Self-oscillation in a Transmission Line with a Tunnel Diode. *Proceeding of the IRE*, v.49, (1961), 1281-1291.
- Shimura M. Analysis of Some Nonlinear Phenomena in a Transmission Line. *IEEE. Transactions on Circuit Theory*, v.14, N1, (1967), 60-68.
- Brayton R. K. Bifurcation of periodic solutions in a nonlinear difference-differential equations of neutral type. *Quarterly of Applied Mathematics*. v.24, N3, (1966), 215-224.
- Brayton R. K. Nonlinear oscillations in a distributed network. v.24, N4, (1968), 289-301.
- Hale J. K. Theory of functional differential equations, *Springer Verlag*, 1977.
- Myshkis A. D. Linear differential equations with retarded argument, *Nauka*, Moscow, 1972 (in Russian).
- El'sgoltz L. E., S. B. Aiorkin, Introduction in the theory of differential equations with deviating argument. *Nayka*, Moscow, 1971 (in Russian).
- Kamenskii G. A., Skubachevskii A. L. Linear boundary value problems for differential-difference equations, Moscow, 1992 (in Russian).
- Angelov V. G. Fixed point theorem in uniform spaces and applications. *Czechoslovak Math. J.*, v. 37 (112), (1987), 19-33.
- Angelov V. G.. On the Sygne equations in a three-dimensional two-body problem of classical electrodynamics. *J. Math. Anal. Appl.*, v.151, N2 (1990), 488-511.

Recommended for publication by Department of Mine Automation, Faculty of Mining Electromechanics

## ON THE NEUTRAL LOSSLESS TRANSMISSION LINE EQUATIONS WITH TUNNEL DIODE AND A LUMPED PARALLEL CAPACITANCE

**Vasil Angelov**

University of Mining and Geology "St. Ivan Rilski"  
Sofia 1700, Bulgaria  
E-mail: angelov@staff.mgu.bg

**ABSTRACT**

By means of a fixed point approach an existence theorem for neutral equations arising in transmission lines is proved.

The present paper continuous investigations on lossless transmission lines equations with nonlinear resistive elements.

In a previous paper [1] we have studied neutral equations ([2]-[4]) with nonlinearities caused by a nonlinear  $V-I$  characteristic which is of polynomial type. Here we consider an initial value problem for neutral equations with an exponential nonlinearity in the right-hand side. Such a problem is equivalent (cf. [5]-[7], [2]) to an initial-boundary value problem for linear hyperbolic system with a nonlinear boundary conditions. Indeed in some cases the approximation of the  $V-I$  characteristic curve generated by the diffusion current in semiconductors [8]-[9] can be fitted by an exponential function. The relation between the diffusion current and the voltage is of the type  $i(u) = (Ae^{\alpha u} - 1)$ , where  $A$  and  $\alpha$  are constants. It is known that such type nonlinearities have also another applications (cf. [10], [11]).

Therefore formulating the initial value problem

$$\dot{u}(t) = F(u(\Delta_1(t)), \dots, u(\Delta_m(t)), \dot{u}(\gamma_1(t)), \dots, \dot{u}(\gamma_n(t))), \quad t > 0$$

$$\begin{aligned} u(t) &= \varphi(t), \quad t \leq 0 \\ \dot{u}(t) &= \dot{\varphi}(t), \quad t \leq 0, \end{aligned} \tag{1}$$

we have to impose such conditions on the right-hand side of (1),  $F(u_1, \dots, u_m, v_1, \dots, v_n)$ , in order to include exponential nonlinearities. For instance  $F$  can be chosen of the type

$$F(u_1, \dots, u_m, v_1, \dots, v_n) = A \sum_{k=1}^m (e^{\alpha_k u_k} - 1) + B \sum_{s=1}^n v_s.$$

We reduce the problem (1) to the following one (putting  $y(t) = \dot{u}(t)$  for  $t > 0$  and  $\psi(t) = \dot{\varphi}(t)$  for  $t \leq 0$  assuming  $\varphi(0) = 0$ ):

$$y(t) = F \left( \int_0^{\Delta_1(t)} y(\tau) d\tau, \dots, \int_0^{\Delta_m(t)} y(\tau) d\tau, y(\gamma_1(t)), \dots, y(\gamma_n(t)) \right), t \in [0, T_0]$$

$$y(t) = \psi(t), \quad t \leq 0. \tag{2}$$

We make the following assumptions (C):

**(C1)** functions  $\Delta_i(t), \gamma_s(t) : R_+^1 \rightarrow R^1$

( $i = 1, \dots, m; s = 1, \dots, n$ ) are continuous and  $t - \Delta_i(t) \geq \Delta_0 > 0, t - \gamma_s(t) \geq \gamma_0 > 0$  for some constants  $\Delta_0, \gamma_0$ .

**(C2)** the functions  $F(u_1, \dots, u_m, v_1, \dots, v_n) : R^{m+n} \rightarrow R^1$  and  $\psi(\cdot) : R_+^1 \rightarrow R^1$  are continuous and satisfies the condition

$$\begin{aligned} \psi(0) &= F \left( \int_0^{\Delta_1(0)} \psi(s) ds, \dots, \int_0^{\Delta_m(0)} \psi(s) ds, \psi(\gamma_1(0)), \dots, \psi(\gamma_n(0)) \right) = \\ &= F(0, \dots, 0, \psi(0), \dots, \psi(0)). \end{aligned}$$

**(C3)**  $|F(u_1, \dots, u_m, v_1, \dots, v_n)| \leq A \sum_{k=1}^m |e^{\alpha_k u_k} - 1| + B \sum_{s=1}^n |v_s|$

where  $A, B$  are positive constants.

**(C4)**  $|F(u_1, \dots, u_m, v_1, \dots, v_n)| - |F(\bar{u}_1, \bar{u}_2, \dots, \bar{u}_m, \bar{v}_1, \dots, \bar{v}_n)| \leq$

$$\leq A_1 \sum_{k=1}^m |e^{\alpha_k u_k} - e^{\alpha_k \bar{u}_k}| + B_1 \sum_{s=1}^n |v_s - \bar{v}_s|.$$

where  $A_1$  and  $B_1$  are positive constants.

(C5)  $A \sum_{k=1}^m \frac{2|\alpha_k|T_0}{2-|\alpha_k|P_0T_0} + nB \leq 1$ , where  $P_0 > 0$  is chosen

such that  $|\alpha_k|P_0T_0 < 2$ .

**Theorem 1.** Under assumption (C) the initial value problem (2) has a unique continuous solution.

**Proof.** Consider the set  $X$  consisting of all continuous functions  $f(t) : [0, T_0] \rightarrow R^1$ , ( $T_0 > 0$ ) whose restrictions on  $(-\infty, 0]$  coincide with  $\psi(t)$ . It becomes a uniform space endowed with the following saturated family of pseudometrics (metrics) (cf. [13]-[14]):

$$\rho_\lambda = \{ \rho_\lambda(f, \tilde{f}) : \lambda \in [0, \infty) \},$$

$$\rho(f, \tilde{f}) = \sup \{ e^{-\lambda t} | f(t) - \tilde{f}(t) | : t \in [0, T_0] \}.$$

Introduce the following subset  $M$  of  $X$  :

$$M = \{ f(\cdot) \in (X, \rho_\lambda) : | f(t) | \leq P_0, t \in [0, T_0] \},$$

where  $P_0$  is a constant which does not depend on  $f$ . It is easy to see that  $M$  is bounded and closed set. Define the operator  $T : (X, \rho_\lambda) \rightarrow (X, \rho_\lambda)$  by right-hand side of (2):

$$(Tf)(t) = \begin{cases} F \left( \int_0^{\Delta_1(t)} f(s) ds, \dots, \int_0^{\Delta_m(t)} f(s) ds, f(\gamma_1(t)), \dots, f(\gamma_n(t)) \right), & t \in [0, T_0] \\ \psi(t), & t \leq 0. \end{cases}$$

Obviously  $(Tf)(t)$  is a continuous function.

In what follows we show that  $T$  maps the set  $M$  into itself. Indeed let  $f \in M$ . Then in view of (C3) we have

$$| (Tf)(t) | \leq A \sum_{k=1}^m \left| e^{\alpha_k \int_0^{\Delta_k(t)} f(s) ds} - 1 \right| + B \sum_{s=1}^n | f(\gamma_s(t)) | \leq$$

$$\leq \left[ A \sum_{k=1}^m (e^{|\alpha_k|P_0|\Delta_k(t)|} - 1) + nBP_0 \right].$$

It is know that for  $0 < w < 2$  we have:

$$e^w - 1 = w + \frac{w^2}{2!} + \frac{w^3}{3!} + \dots < w \left( 1 + \frac{w}{2} + \left(\frac{w}{2}\right)^2 + \dots \right) = \frac{2w}{2-w}.$$

Therefore

$$\left| \alpha_k \int_0^{\Delta_k(t)} f(s) ds \right| \leq |\alpha_k| P_0 |\Delta_k(t)| \leq |\alpha_k| P_0 T_0$$

and then

$$\left[ A \sum_{k=1}^m (e^{|\alpha_k|P_0|\Delta_k(t)|} - 1) + nBP_0 \right] \leq A \sum_{k=1}^m \frac{2|\alpha_k|P_0T_0}{2-|\alpha_k|P_0T_0} + nBP_0 \leq P_0,$$

provided  $A \sum_{k=1}^m \frac{2|\alpha_k|P_0T_0}{2-|\alpha_k|P_0T_0} + nB \leq 1$  which is (C5).

It remains to show that  $T$  is contractive operator. Indeed for every  $f$  and  $\tilde{f} \in M$  and in view of the inequalities

$$t - \Delta_0 \geq \Delta_k(t) \geq \frac{|\alpha_k|P_0\Delta_k(t)}{\lambda} \quad (\text{for sufficiently large } \lambda > 0) \Rightarrow -\lambda t + |\alpha_k|P_0\Delta_k(t) \leq -\lambda\Delta_0$$

we have for  $t \in [0, T_0]$  for which  $\Delta_k(t) > 0$  :

$$| (Tf)(t) - (T\tilde{f})(t) | \leq A_1 \sum_{k=1}^m \left| e^{\alpha_k \int_0^{\Delta_k(t)} f(s) ds} - e^{\alpha_k \int_0^{\Delta_k(t)} \tilde{f}(s) ds} \right| +$$

$$+ B_1 \sum_{s=1}^n | f(\gamma_s(t)) - \tilde{f}(\gamma_s(t)) | \leq$$

$$\leq A_1 \sum_{k=1}^m |\alpha_k| e^{\alpha_k \int_0^{\Delta_k(t)} \hat{f}(s) ds} \left| \int_0^{\Delta_k(t)} f(s) ds - \int_0^{\Delta_k(t)} \tilde{f}(s) ds \right| +$$

$$+ B_1 \sum_{s=1}^n e^{-\lambda \gamma_s(t)} | f(\gamma_s(t)) - \tilde{f}(\gamma_s(t)) | e^{\lambda \gamma_s(t)} \leq$$

$$\leq A_1 \sum_{k=1}^m |\alpha_k| e^{\alpha_k P_0 \Delta_k(t)} \left| \int_0^{\Delta_k(t)} e^{\lambda s} ds \right| \rho_\lambda(f, \tilde{f}) +$$

$$+ B_1 \sum_{s=1}^n e^{\lambda \gamma_s(t)} \rho_\lambda(f, \tilde{f}) \leq$$

$$\leq e^{\lambda t} \left[ A_1 \sum_{k=1}^m |\alpha_k| e^{-\lambda t + \alpha_k P_0 \Delta_k(t)} \left| \frac{e^{\lambda \Delta_k(t)} - 1}{\lambda} \right| + \right.$$

$$\left. + B_1 \sum_{s=1}^n e^{-\lambda t + \lambda \gamma_s(t)} \right] \rho_\lambda(f, \tilde{f}) \leq$$

$$\leq e^{\lambda t} \rho_\lambda(f, \tilde{f}) \left[ A_1 \sum_{k=1}^m |\alpha_k| \frac{e^{-\lambda \Delta_0} e^{\lambda t}}{\lambda} + B_1 n e^{-\lambda \gamma_0} \right] \leq$$

$$\leq e^{\lambda t} \rho_{\lambda}(f, \bar{f}) \left[ \frac{A_1 e^{-\lambda \Delta_0} e^{\lambda T_0} \sum_{k=1}^m |\alpha_k|}{\lambda} + B_1 n e^{-\lambda \gamma_0} \right].$$

Consequently

$$\rho_{\lambda}(Tf, T\bar{f}) \leq \left[ A_1 \sum_{k=1}^m |\alpha_k| \frac{e^{\lambda T_0 - \lambda \Delta_0}}{\lambda} + n B_1 e^{-\lambda \gamma_0} \right] \rho_{\lambda}(f, \bar{f}).$$

But for sufficiently large  $\lambda$  the expression in the bracket is smaller than 1 (if  $T_0 - \Delta_0 \leq 0$ ) and therefore  $T$  is contractive operator.

Finally we have to choose an initial approximation. Indeed let

$$x_0(t) = \begin{cases} \psi(t), & t \leq 0 \\ \psi(0), & t > 0 \end{cases}.$$

Then

$$|(Tx_0)(t) - x_0(t)| = \begin{cases} 0, & t \leq 0 \\ |F(0, \dots, 0, \psi(0), \dots, \psi(0))|, & t > 0 \end{cases}$$

The map  $j : A \rightarrow A$  in this case is  $j(\lambda) = \lambda \Rightarrow$

$$\Rightarrow j^k(\lambda) = \lambda, \text{ i.e.}$$

$$\rho_{j^k(\lambda)}(x_0, Tx_0) \leq |F(0, \dots, 0, \psi(0), \dots, \psi(0))| < \infty \quad (k = 1, 2, \dots).$$

Therefore  $T$  has a unique fixed point which a solution of (2). Theorem is thus proved.

## REFERENCES

- Angelov V.G., On the neutral equations with polynomial nonlinearities arising in lossless transmission lines. (ibid)
- Hale J. K. Theory of functional differential equations, *Springer Verlag*, 1977.
- Myshkis A. D. Linear differential equations with retarded argument, *Nauka*, Moscow, 1972 (in Russian).
- Kamenskii G. A., Skubachevskii A. L. Linear boundary value problems for differential-difference equations, Moscow, 1992 (in Russian).
- Brayton R. K. Bifurcation of periodic solutions in a nonlinear difference-differential equations of neutral type. *Quarterly of Applied Mathematics*. v.24, N3, (1966), 215-224.
- Brayton R. K. Nonlinear oscillations in a distributed network. v.24, N4, (1968), 289-301.
- Lopes O. Forced oscillations in nonlinear neutral differential equations. *SIAM J.Appl. Math.*, v.29, N1, (1975), 196-207.
- Bessonov L.A. Nonlinear electrical circuits. Moscow, 1977.
- Andreev V.S., V.I. Popov, A.I. Fedorov, ets. Generators of harmonic oscillations on tunnel diodes. Moscow, 1972.
- M. Kauda, Analytical and numerical techniques for analyzing an electrically short dipole with a nonlinear load. *IEEE Trans. Antennas Propag.* v.28, (1980), 71-78.
- J. Ladbury, D. Camell, Electrically short dipoles with a nonlinear load, a revisited analysis. *IEEE Trans. Electromagnetic Compatibility*. v.44, N1, (2002), 38-44.
- Jankowski T., M. Kwapisz. On the existence and uniueness of solutions of systems of differential equations with a deited arguments. *Annales Polonici Mathematici*. v.26, (1972), 253-277.
- Angelov V.G. Fixed point theorem in uniform spaces and applications. *Czechoslovak Math. J.* v.37, (1987), 19-33.
- Kelley J.L. General Topology D. Van Nostrand Company, New York, 1959.

Recommended for publication by Department of Mine Automation, Faculty of Mining Electromechanics

## NONLINEAR CIRCUITS WITH POLYNOMIAL RESISTIVE ELEMENTS

**Vasil Angelov**

University of Mining and Geology  
"St. Ivan Rilski"  
Sofia 1700, Bulgaria  
E-mail: angelov@staff.mgu.bg

**Dafinka Angelova**

"Lu.Karavelov"  
Civil Engineering Higher School  
Sofia 1373, Bulgaria  
E-mail: angelova@vsu.bg

**Ljubomir Georgiev**

University of Mining and Geology  
"St. Ivan Rilski"  
Sofia 1700, Bulgaria  
E-mail: lubotal@abv.bg

**ABSTRACT**

Sufficient conditions for existence and uniqueness of a bounded solution of a class of functional equations are obtained. The result is applied to the equilibrium equation of a parallel-consecutive nonlinear circuit with resistive elements.

**INTRODUCTION**

The nonlinear circuits and devices have many applications in the electric technique, radio technique, automatics and other fields of science and practice. The work of many important mechanisms is based on properties and phenomena inherent only to nonlinear circuits. The phenomena in the nonlinear devices are very complicated and different from the linear ones and not to be available usual methods for their analysis. Even for circuits, consisting of one type of elements (resistive, inductive and capacitive) usual methods can not found. As a rule, any concrete problem for a nonlinear circuit can be solved by different methods. Here we consider nonlinear circuits with resistive elements, whose  $V-I$  characteristics are of polynomial type. Using the Banach fixed point principle for contraction mapping we prove an existence and uniqueness of a bounded solution of the obtained functional equation.

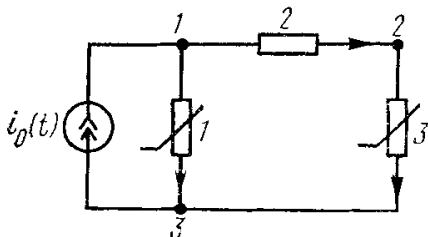


Figure 1

For the simplest parallel in series nonlinear circuit provided by current source  $i_0(t)$ , presented on fig.1 (see [1]), it is assumed the second branch to be linear and the first and the third ones- nonlinear. The graph of the circuit (fig.2) has 4 branches and 3 knots (junctions), so that the number of the independent junctions is 2 and the number of the independent contours is 2, too. To obtain independent equations for the junctions, connecting the variable branches of the circuit, it is used a graph in the form of a tree, presented on fig.3. It is reported the kind of the elements and the way of definition of the resistive elements characteristics. (The current spring and the third branch, presented by noncontinuous lines, are junction branches, the second branch - branch of the tree and the first branch, corresponding to the nonlinear element - the lacking branch of the tree. The number of the variables into the

equations of the junctions is equal to the double number of the branches. One of these quantities (the current source) is a given function of (the time)  $i_0(t)$ .

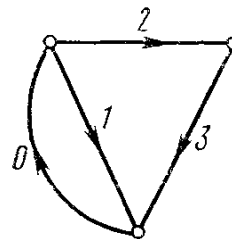


Figure 2

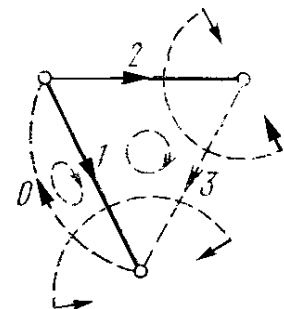


Figure 3

The equilibrium equations of the currents in the first and the second knots (on the number of tree branches) are  $-i_0 + i_1 + i_3 = 0, i_2 - i_3 = 0$ . The equilibrium equations of the voltages in the null and the third contours (on the number of the junction branches) are  $-u_0 + u_1 = 0, -u_1 + u_2 + u_3 = 0$ . From the equations of the junctions it follows the source voltage is equal to voltage of the first element and the current of the second element is equal to the current of the third element, i.e.  $u_0 = u_1, i_2 = i_3$ . So we obtain the system

$$\begin{cases} i_1 = A_1 u_1^{\frac{1}{3}} \\ u_2 = A_2 i_2 \\ u_3 = A_3 i_3 + A_4 i_3^3 \\ i_1 + i_3 = i_0 \\ i_2 = i_3 \\ u_1 = u_0 \\ u_1 = u_2 + u_3 \end{cases} \Rightarrow \begin{cases} u_1 = (A_2 + A_3)i_3 + A_4 i_3^3 \\ \frac{1}{3} \\ A_1 u_1^{\frac{1}{3}} + i_3 = i_0 \\ -u_1 + A_2 i_2 + A_3 i_3 + A_4 i_3^3 = 0 \\ -u_1 + A_2 i_3 + A_3 i_3 + A_4 i_3^3 = 0 \\ A_1 [(A_2 + A_3)i_3 + A_4 i_3^3]^{\frac{1}{3}} + i_3 = i_0 \end{cases} \quad (1)$$

The solving of this system can be reduced to the solving of a single nonlinear functional equation for one of the unknown

functions. After proper transformations (see.[1]) we get the equation

$$i_3(t) = i_0(t) - A_1[(A_2 + A_3)i_3(t) + A_4i_3^3(t)]^{\frac{1}{3}}, \quad (2)$$

where  $i_0(t)$  is a given function, and  $i_3(t)$  is an unknown function. The right hand side of (2) generates an operator  $\Phi$ , acting on some function space which can be defined as follows:

$$(\Phi i)(t) := i_0(t) - A_1[(A_2 + A_3)i(t) + A_4i^3(t)]^{\frac{1}{3}}.$$

Let us denote by  $C[0, \infty)$  the space of bounded continuous functions on the interval  $[0, \infty)$ . This space becomes a metric one, if we introduce a distance (a metric) between any two its elements (functions) in the following way:

$$\rho(i, \bar{i}) = \sup_{t \in [0, \infty)} |i(t) - \bar{i}(t)|.$$

To apply the fixed point theorem for contraction mappings [3], we must find the partial derivative in  $i$  of the right hand side of (2), i.e. of the function

$$f(t, i) = i_0(t) - A_1[(A_2 + A_3)i + A_4i^3]^{\frac{1}{3}}$$

and to estimate it from above. Since

$$\begin{aligned} \frac{\partial f}{\partial i} &= -\frac{A_1}{3}[(A_2 + A_3)i + A_4i^3]^{-\frac{2}{3}}(A_2 + A_3 + 3A_4i^2) = \\ &= -\frac{A_1(A_2 + A_3 + 3A_4i^2)}{3[(A_2 + A_3)i + A_4i^3]^{\frac{2}{3}}}, \end{aligned} \quad (3)$$

we must find a constant  $M > 0$ , such that  $|\frac{\partial f}{\partial i}| \leq M$  for any

$t \in [0, \infty)$  and any function  $i(t) \in C[0, \infty)$ . Since  $i$  is in the nominator of (3), and in the case of alternative current the nominator can nullify for some  $t$  then such constant  $M$  does not exist. This difficulty can overcome easily, when solve the system (1) in relation to another variable, for instance  $i_2$  in the following way. From the first equation of (1) we express

$$u_1 = \frac{i_1^3}{A_1^3} \text{ and replace with this expression and the}$$

expressions for  $u_2$  and  $u_3$  (from the second and third equation of (1)) into the last equation of (1) and obtain

$$\frac{i_1^3}{A_1^3} = A_2i_2 + A_3i_3 + A_4i_3^3.$$

From the fifth equation of (1) we have  $i_3 = i_2$ , and from the fourth one we get  $i_1 = i_0 - i_2$ . Then

$$\frac{(i_0 - i_2)^3}{A_1^3} = A_2i_2 + A_3i_2 + A_4i_2^3 \Rightarrow i_2 = \frac{(i_0 - i_2)^3 - A_1^3A_4i_2^3}{(A_2 + A_3)A_1^3}.$$

We can write the last equation in the form

$$i(t) = \frac{1}{(A_2 + A_3)A_1^3} [i_0^3(t) - 3i_0^2(t)i(t) + 3i_0(t)i^2(t) - (1 + A_1^3A_4)i^3(t)]. \quad (4)$$

Here we wrote  $i(t)$  instead of  $i_2(t)$ . We recall  $A_i (i = 1, 2, 3, 4)$

are known constants, and  $i_0(t)$  is a given function (of the current source). From physical considerations we can assume  $A_1 > 0, A_2 > 0$  and  $|i_0(t)| \leq \bar{i}_0$ , where  $\bar{i}_0$  is an upper bound of  $i_0(t)$  and  $t \geq 0$ .

### MAIN RESULT

By the Banach fixed point principle for contraction mapping we prove an existence and uniqueness of a bounded solution of the obtained functional equation.

For this purpose we consider the set

$$M = \{i(t) \in C[0, \infty) : |i(t)| \leq I_0\} \subset C[0, \infty),$$

where  $I_0 > 0$  is an arbitrary constant. This is a natural restriction since the currents in a circuit can not be the infinite. Further we suppose  $I_0 = \bar{i}_0$ .

The right hand side of (4) generates an operator  $T$ , that can be defined as follows:

$$(Ti)(t) := \frac{1}{(A_2 + A_3)A_1^3} [i_0^3(t) - 3i_0^2(t)i(t) + 3i_0(t)i^2(t) - (1 + A_1^3A_4)i^3(t)].$$

Firstly we prove the operator  $T$  maps the set  $M$  into itself, e.i. If the function  $i(\cdot) \in M$ , then  $(Ti)(\cdot) \in M$  or  $T : M \rightarrow M$ .

Really by the definition of  $T$  it is clear  $(Ti)(t) \in C[0, \infty)$ .

It is easy to see that

$$\begin{aligned} |(Ti)(t)| &\leq \frac{1}{|A_2 + A_3|A_1^3} [\bar{i}_0^3 + 3\bar{i}_0^2I_0 + 3\bar{i}_0I_0^2 + \\ &+ |1 + A_1^3A_4|I_0^3] = \frac{(7 + |1 + A_1^3A_4|)I_0^3}{|A_2 + A_3|A_1^3} \end{aligned}$$

and if

$$\frac{(7 + |1 + A_1^3A_4|)I_0^3}{|A_2 + A_3|A_1^3} \leq I_0, \quad (5)$$

then  $|(Ti)(t)| \leq I_0$ . Since  $|A_2 + A_3|A_1^3 > 0$ , we can transform the inequality (5) in the form

$$(7 + |1 + A_1^3A_4|)I_0^3 \leq I_0|A_2 + A_3|A_1^3 \Rightarrow$$

$$I_0[(7 + |1 + A_1^3A_4|)I_0^2 - |A_2 + A_3|A_1^3] \leq 0 \Rightarrow$$

$$I_0 \left( 7 + |1 + A_1^3A_4| \right) \left( I_0^2 - \frac{|A_2 + A_3|A_1^3}{7 + |1 + A_1^3A_4|} \right) \leq 0. \quad (6)$$

But  $I_0(7 + |1 + A_1^3A_4|) > 0$ . Hence the inequality (6) is fulfilled for

$$I_0 \leq \sqrt{\frac{|A_2 + A_3|A_1^3}{7 + |1 + A_1^3A_4|}}. \quad (7)$$

So if the inequality (7) holds the operator  $T$  satisfies the condition  $|(Ti)(t)| \leq I_0$  for arbitrary function  $i(t) \in M$ , i.e. the operator  $T$  maps the set  $M$  into itself.

Now we prove the operator  $T$  is contractive.

In fact let us suppose  $i(\cdot), \bar{i}(\cdot) \in M$  be arbitrary functions.

Then

$$\begin{aligned} & |(Ti)(t) - (T\bar{i})(t)| \leq \\ & \leq \frac{1}{|A_2 + A_3|A_1^3} [3I_0^2|i(t) - \bar{i}(t)| + 3I_0 \cdot 2I_0|i(t) - \bar{i}(t)| + 3|1 + A_1^3A_4|I_0^2|i(t) - \bar{i}(t)|] \leq \\ & \leq \frac{9 + 3|1 + A_1^3A_4|}{|A_2 + A_3|A_1^3} I_0^2 \rho(i, \bar{i}). \end{aligned}$$

Since the right hand side of the last inequality does not depend on  $t$ , we conclude

$$\rho(Ti, T\bar{i}) \leq \frac{3(3 + |1 + A_1^3A_4|)}{|A_2 + A_3|A_1^3} I_0^2 \rho(i, \bar{i}).$$

If we suppose

$$\frac{3(3 + |1 + A_1^3A_4|)}{|A_2 + A_3|A_1^3} I_0^2 < 1,$$

i.e. if

$$I_0 < \sqrt{\frac{|A_2 + A_3|A_1^3}{3(3 + |1 + A_1^3A_4|)}} \tag{8}$$

then it follows the operator  $T$  is contractive with a constant

$$k = \frac{3(3 + |1 + A_1^3A_4|)}{|A_2 + A_3|A_1^3} I_0^2.$$

Comparing (7) and (8), we immediately see

$$\sqrt{\frac{|A_2 + A_3|A_1^3}{3(3 + |1 + A_1^3A_4|)}} < \sqrt{\frac{|A_2 + A_3|A_1^3}{7 + |1 + A_1^3A_4|}},$$

i.e. condition (7) holds on condition that (8) is fulfilled.

So the conditions of the Banach fixed point theorem [3] are satisfied and according to it there exists a unique function  $i^*(t) \in M$ , such that  $(Ti^*)(t) = i^*(t)$ , i.e. there exists a unique solution of the equation (4).

As a matter of fact, we proved the following

**THEOREM.** Let  $A_i$  ( $i=1,2,3,4$ ) be known constants and  $A_1 > 0, A_2 > 0$ . Let the function  $i_0(t) : [0, \infty) \rightarrow (-\infty, \infty)$  be bounded, i.e.  $|i_0(t)| \leq I_0$ , where  $I_0$  is a constant satisfying the inequalities

$$0 < I_0 < \sqrt{\frac{|A_2 + A_3|A_1^3}{3(3 + |1 + A_1^3A_4|)}}.$$

Then there exists a unique solution  $i^*(t) \in C[0, \infty)$  of equation (4) such that  $|i^*(t)| \leq I_0$  for  $t \geq 0$ .

The solution is a uniform limit of the sequence of consecutive approximations  $\{i^{(n)}(t)\}$  and

$$\rho(i^*, i^{(n)}) \leq \frac{1}{2^n k^n} \rho(i^{(1)}, i^{(0)}), \tag{9}$$

where  $i^{(0)}(t) \in C[0, \infty) : |i^{(0)}(t)| \leq I_0$  is an arbitrary initial approximation and

$$k = \frac{3(3 + |1 + A_1^3A_4|)}{|A_2 + A_3|A_1^3} I_0^2.$$

**Example.** Let us choose  $A_1 = 1, A_2 = 5, A_3 = -\frac{3}{2}, A_4 = \frac{1}{4}$ .

Then

$$\begin{aligned} I_0 & < \sqrt{\frac{|A_2 + A_3|A_1^3}{3(3 + |1 + A_1^3A_4|)}} = \sqrt{\frac{|5 - \frac{3}{2}|}{3(3 + |1 + \frac{1}{4}|)}} = \sqrt{\frac{\frac{7}{2}}{\frac{51}{4}}} = \\ & = \sqrt{\frac{14}{51}} \approx \sqrt{2,7 \cdot 10^{-1}} \approx 0,5, \end{aligned}$$

$$k = \frac{51}{56}$$

and the equation (4) takes the form

$$i(t) = \frac{2}{7} [i_0^3(t) - 3i_0^2(t)i(t) + 3i_0(t)i^2(t) - \frac{5}{4}i^3(t)]. \tag{10}$$

The relation between  $i^{(1)}(t)$  and  $i^{(0)}(t)$  is given by the formula

$$i^{(1)}(t) = \frac{2}{7} \{i_0^3(t) - 3i_0^2(t)i^{(0)}(t) + 3i_0(t)[i^{(0)}(t)]^2 - \frac{5}{4}[i^{(0)}(t)]^3\}.$$

For initial we take  $i^{(0)}(t) = 0$  and obtain

$$i^{(1)}(t) = \frac{2}{7} i_0^3(t).$$

Then the second approximation is

$$\begin{aligned} i^{(2)}(t) & = \frac{2}{7} \{i_0^3(t) - 3i_0^2(t)i^{(1)}(t) + 3i_0(t)[i^{(1)}(t)]^2 - \frac{5}{4}[i^{(1)}(t)]^3\} = \\ & = \frac{2}{7} i_0^3(t) [1 - \frac{6}{7}i_0^2(t) + \frac{12}{49}i_0^4(t) - \frac{10}{343}i_0^6(t)]. \end{aligned}$$

The distance between  $i^{(1)}(t)$  and  $i^{(0)}(t)$  is

$$\rho(i^{(1)}, i^{(0)}) = \sup \left\{ \left| \frac{2}{7} i_0^3(t) - 0 \right| : t \in [0, \infty) \right\} = \frac{2}{7} I_0^3.$$

The estimate (9) takes the form

$$\rho(i^*, i^{(n)}) \leq \frac{1}{2^n \left(\frac{51}{56}\right)^{\frac{n}{2}}} \rho(i^{(1)}, i^{(0)}).$$

Then

$$\begin{aligned} \rho(i^*, i^{(1)}) &\leq \frac{1}{2^1 \left(\frac{51}{56}\right)^{\frac{1}{2}}} \frac{2}{7} I_0^3 < \frac{\left(\frac{14}{51}\right)^{\frac{3}{2}}}{7 \left(\frac{51}{56}\right)^{\frac{1}{2}}} \approx \frac{1}{8} = \\ &= \frac{1}{\sqrt{51.56}} \approx 0,02 = 2 \cdot 10^{-2}, \end{aligned}$$

$$\begin{aligned} \rho(i^*, i^{(2)}) &\leq \frac{1}{2^2 \frac{51}{56}} \frac{2}{7} I_0^3 < \frac{4}{51} \cdot \left(\frac{14}{51}\right)^{\frac{3}{2}} \approx \frac{4}{51} \cdot \frac{1}{8} = \\ &= \frac{1}{102} \approx 0,01 = 10^{-2}, \end{aligned}$$

$$\begin{aligned} \rho(i^*, i^{(3)}) &\leq \frac{1}{2^3 \left(\frac{51}{56}\right)^{\frac{3}{2}}} \frac{2}{7} I_0^3 < \frac{1}{28} \cdot \left(\frac{56}{51}\right)^{\frac{3}{2}} \left(\frac{14}{51}\right)^{\frac{3}{2}} \approx \frac{1}{28} \left(\frac{56}{51}\right)^{\frac{3}{2}} \cdot \frac{1}{8} = \\ &= \frac{\sqrt{56}}{204 \sqrt{51}} \approx 0,005 = 5 \cdot 10^{-3} \end{aligned}$$

and so on.

In such a way we can apply the above theorem to equation (10) and find the solution (it is only one!) by the step by step method. Some more we obtain a high exactitude of the solution with the first and the second approximations.

#### REFERENCES

- Mathanov P. N. Principles of the analysis of electrical circuits. Nonlinear circuits. "Vishaia shkola", Moscow, 1977 (in Russian).
- Bessonov L. A. Nonlinear electrical circuits Нелинейные электрические цепи. "Vishaia shkola", Moscow, 1977 (in Russian).
- Kollatz L. Functional analysis and numerical mathematics. Mir, Moscow, 1969 (in Russian).

Recommended for publication by Department of Mine Automation, Faculty of Mining Electromechanics

## AUTOMATIC RECOGNITION OF SCALES, GRIDS AND TABLES IN SCANNED MECHANICAL DRAWING

**Julian Dimitrov**

University of Mining and Geology "St. Ivan Rilski"  
Sofia 1700 Bulgaria

### ABSTRACT

Complete solution for advanced automated conversion from paper copy of mechanical drawing to electronic format is still missing. In this paper the method for recognizing the elements scales, grids and tables from symbolic set of a mechanical drawing are discussed. It uses an automatic description of functional dependencies. Key words: Image recognition, mechanical drawing, scale, grid, table

### INTRODUCTION

For the purposes of technical documentation are used electronic copy of plan the received by scanning the paper. The raster graphical formats of mechanical drawings contain defects and they are not appropriated for processing. It is necessary a transformation of the image as recognition elements of drawing and at the final result the presentation is received in vector format.

There exist many program products, which transform from raster to vector format but it is carried out with participation of operator. At the same time there is a lot of publication that contain great number of methods and algorithms for recognition of graphical image (Dimitrov J., 2001). They can be used as basis for receiving of hybrid decisions of task for recognition of elements of the mechanical drawing.

### THE PURPOSE

To present in this paper an algorithm for processing of images of scales, grids and tables of scanned copy of mechanical drawing.

To discuss and realized an appropriated method for automatically recognition of this elements and analytical description of the functional dependencies that are given graphically with diagram.

### METHOD FOR RECOGNITION OF SUCCESSION OF PARALLEL SEGMENTS OF LINES

The projection elements of mechanical drawing consist basically from segments of line and arcs of circle. Exclusions make diagrams that can express more complicated functional dependencies.

After contouring of given element of the image and description of contour with basic vectors with definite length, the image can be put to the following processing (Dimitrov J., 2002).

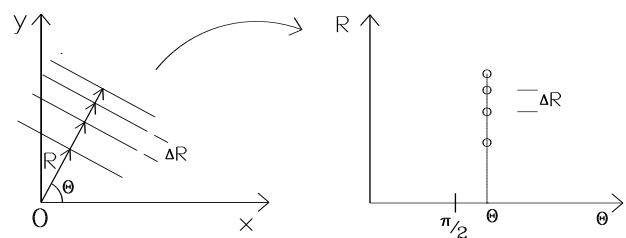


Figure 1: Succession of parallel segments of lines and their Hough transformation

We consider an element of the image consisted from alternatively parallel segments of line. Such configuration meets in the nets and in the tables, where are used two mutually orthogonal systems from such segments of lines. For the recognition we will use Hough transformation, such as this is madden in Dimitrov J., 2002. for stroked lines. The algorithm is added with determination of the functional dependence that describes the alteration of the distance  $\Delta R$  between the parallel lines. The distance  $\Delta R$  is accounted by secondary axis in  $(\theta, R)$  space. A final result of recognition is the information in  $(\theta, R)$  area complemented with analytical description of the dependence for  $\Delta R$ , the as the method for its description is discussed bellow.

### RECOGNITION OF THE SCALES, GRIDS AND TABLES

The basic part of these elements consists from segments of lines. The symbols and signs that are used have typical shape.

- They have not big parts of the contour with rectilinear form or form near to arc of circle.

- The length of the enveloped contour is small.
- The symbols are recognizing by OCR programs. So the basic part of element is separated as the symbols are recognized and them appropriate coordinates and associated with its destination.

In the case of the scale we have straight line that is presenting number axis and it is intersected by the stroke. This configuration is recognized as succession of parallel straight lines and together with recognized symbols of the sign includes the whole information lines and together with recognized characters of the sign includes the whole information.

On fig.2 is presented a logarithmic grid received after determination of the sign and its Hought transformation.

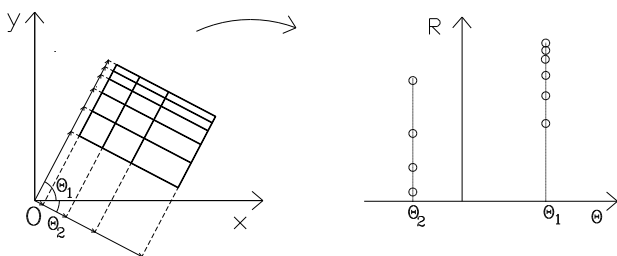


Figure 2: Logarithmic grid and its Hought transformation

APPROXIMATION OF THE FUNCTIONAL DEPENDENCE

The element scale, grid and diagram of mechanical drawing contain graphical description of dependencies, to which is necessary to give analytical expressions. There uses a transformation reducing

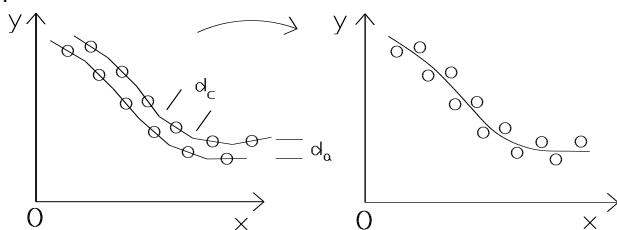


Figure 3: A Transformation that follows basic vectors to points and a approximation of dependence

the basis vectors from contour to points (fig.3). Two contrary contours of the graphic of dependence are processed for more exact presentation. Optimum speed of the processing receives with appropriate choice of the length of basic vector.

The received image of the drawing is approximated with functions given with parameters from sort

$$y = \sum_{k=0}^n a_k \varphi_k(x), \tag{1}$$

as polynomial or another that are linear functions of the parameters. This procedure can be executed and with partial

intervention of operator with introducing suitable structural description of the formula of the dependence and if is necessary to delete the drawing on parts for approximation every part individually.

The choice of appropriate formula for approximation and the precision of analytical presentation makes or from the operator, or automatically. The precision of graphic presentation  $\varepsilon$  of the dependence is restricted from the thickness of the image of the drawing  $d_a$  and from the length of basic vector  $d_c$ . Let

$$\Delta x_i = x_{i+1} - x_i \tag{2}$$

are the differences for the chosen points for approximation and  $m$  is their number, then for the precision  $\varepsilon$  we have

$$\varepsilon \geq \frac{2}{d_a d_c} \sqrt{\sum_{i=1}^m \left( \frac{1}{\Delta x_i} \right)^2} \geq \frac{m d_a d_c}{2(b-a)}, \tag{3}$$

Where  $b-a$  is the length of the interval on the axis  $x$  where is performing approximation. After giving the accuracy of the approximation  $\varepsilon$  choices a most simple formula for approximation as it is possible so that

$$\min_{a_k} \frac{1}{m} \sum_{j=1}^m \left[ \sum_{k=0}^n a_k \varphi_k(x_j) - y_j \right]^2 \leq \varepsilon^2. \tag{4}$$

As have in mind, that most frequently meted are the linear and logarithmic dependence. Than the recognizing must begin from them.

The procedure for recognition of dependence follows in next sequence:

- Recognition of linear dependence  
Program module for analytical presentation at first attempts to determine linear dependence;
- Recognition of the logarithmic dependence  
If in attempt for approximation with linear function the precision  $\varepsilon$  is overstepped then uses the change of the variables

$$\begin{aligned} x' &= \ln(x) \\ y' &= y \end{aligned} \tag{3}$$

and verifies for linear dependence - verifies for dependence from sort:

$$y = C \cdot \ln(x) + D \tag{4}$$

- Recognition of another dependencies  
Can be envisage verification and for another functional links as  $y = \frac{1}{x}$ ,  $y = \sqrt{x}$ ,  $y = x^2$  and another.

The possibility for automated testing for linear and logarithmic dependence can be used in description of the strokes of scales and lines in most often nets.

The transformation that is illustrated with fig.3 can be chosen and as that the middle of the basic vectors depicts in a properly selected parameter space and in it to perform approximation.

REALIZATION AND CONCLUSIONS

An experiment is performed with scanned paper-copy in 300dpi (fig.4, fig.5 and fig.6).

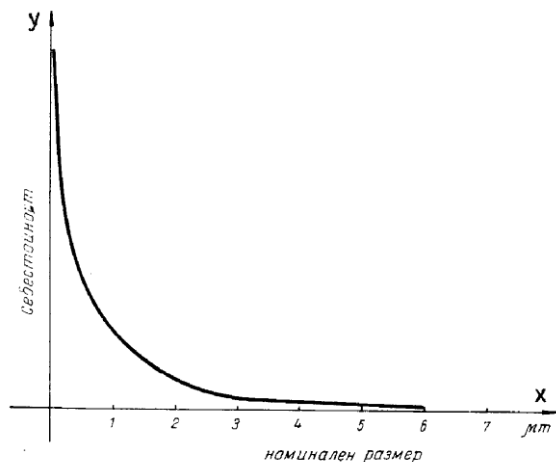


Figure 4: Scanned copy of diagram

There are realized the algorithms contouring, depicting of the contour with basic vectors, recognition of scales and succession of parallel segments of lines, separation of symbol and receiving formulas for analytical dependencies. As a result are received the dependencies  $y = 1.1/x$  for the drawing on fig.4 and  $C_{HO} = 2 - 0.41/(h - 1)$ ,  $C_a = 3.7h$  for fig.5. Is received and information for respective succession of parallel segments of lines and recognized symbols.

On fig.7 and fig.8 are depicted the results from making in vector format of the grid from fig.5 and the table from fig.6.

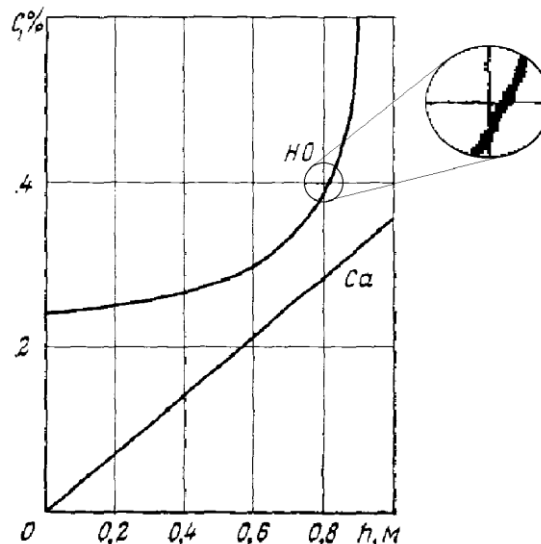


Figure 5: Copy of uniform grid with two diagrams

| $\bar{x}_i$ | $n_i$ | $\delta_i$ | $\delta_i n_i$ | $\delta_i^2 n_i$ | $\delta_i^3 n_i$ | $\delta_i^4 n_i$ |
|-------------|-------|------------|----------------|------------------|------------------|------------------|
| 1,75        | 1     | -1,51      | -1,51          | 2,2801           | -3,4450          | 5,2020           |
| 2,25        | 2     | -1,01      | -2,02          | 2,0402           | -2,0606          | 2,0812           |
| 2,75        | 9     | -0,51      | -4,59          | 2,3409           | -1,1939          | 0,6089           |
| 3,25        | 14    | -0,01      | -0,14          | 0,0014           | 0                | 0                |
| 3,75        | 8     | 0,49       | 3,92           | 1,9208           | 0,9412           | 0,4612           |
| 4,25        | 3     | 0,99       | 2,97           | 2,9403           | 2,9109           | 2,8818           |
| 4,75        | 1     | 1,29       | 1,29           | 1,6641           | 2,1467           | 2,7692           |
|             |       |            | -0,08          | 13,1878          | -0,7007          | 14,0043          |

Figure 6: Scanned copy of table

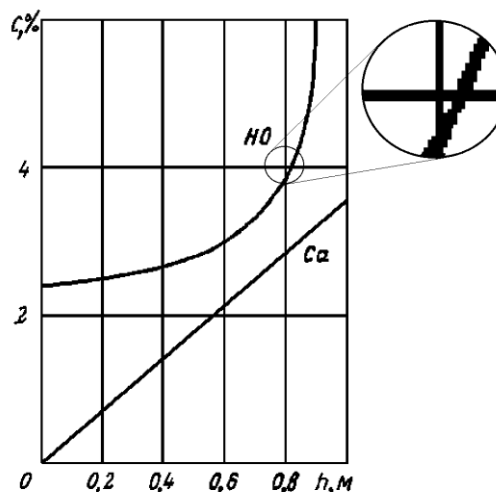


Figure 7: Copy of grid in vector format

The realized software product finds application as a part of a program for automatic recognition of mechanical drawing. It can be used and for receiving of formulas on given diagrams from publications with scientific purpose.

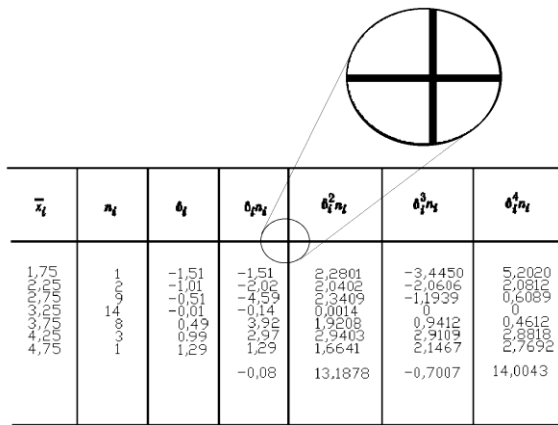


Figure 8: Copy of table in vector format

The discussed method can be use for creating program for processing and another sorts of diagrams, tables and schemes in dependence of the area of application.

Гочев Г., Компютърно зрение и невронни мрежи, София, 1998.

Головцов Г., П. Скачков, Г. Романияк, Алгоритъм за синхронна компресия на линеаризирани двойни линии, Годишник МЕИ, 1979.

Димитров Ю., Автоматизирана реконструкция на сканирано изображение на машиностроителен чертеж, Годишник МГУ, том 44-45, св. 3, 2002.

Димитров Ю., М. Чалашканов, Автоматизирана обработка на сканирано изображение на чертеж на центробежно ролкова мелница, сб. "Управление на природни и технологични рискове – МГУ", 2001

Димитров Ю., Ст. Иванов, Автоматично разпознаване на размерните линии в сканирано копие на машиностроителен чертеж, Трета научна конференция "Смолян - 2001", 2001.

Pavlidis T., Algorithms for graphics and image processing, Computer science press, 1986.

Cheng F., M. Chen, Recognition of Hahdwriten Chinese Characters by Modified Hough Transform Techiques, IEEE Trns. Pattern Anal. Machine Intell., vol. 11, 1989.

Sount Er., Symbolic Construction of 2-D Scale-Space Image, IEEE Trns. Pattern Anal. Machine Intell., vol. 12, 1990.

Recommended for publication by Department of Mine Automation, Faculty of Mining Electromechanics

## ELECTRIC POWER SUPPLY OF UNDERGROUND MINES FOR MACHINE PRODUCTION OF COAL

**Evtim Kartselin**  
**Roumen Istalianov**

"St Ivan Rilski" University of Mining and  
Geology, Sofia 1700, Bulgaria  
E-mail: [rgi@mgu.bg](mailto:rgi@mgu.bg)

**Petar Petrov**  
**Sashko Vasilev**

Bobov dol Mines Co.,  
Bobov dol

**Lyudmil Todorov**  
**Nikolay Nikolov**

Minproekt Co., Sofia

### ABSTRACT

The report summarizes results of many years of experience gained in the development and operation of the electric power supply system of machine complexes for underground coal production in the conditions of the Babino Mine belonging to Bobovdol Mines Co. at the town of Bobovdol.

### INTRODUCTION

The today's mine for underground production of mineral resources is characterized by a high degree of machine implementation and automation of technological processes, big power consumers installed, large-scale concentration of operating personnel, high costs of investment construction, and a considerable amount of existing risks. The risk level is especially high in underground mines for machine production of coal.

The Babino Mine of Bobovdol Mines Co. at the town of Bobovdol is a modern mine where machine production of coal to a depth of 400 m has been carried out for more than 30 years.

During this period a considerable production experience was gained and many research and design solutions in different areas of the mining science were verified under real operating conditions.

One of the main factors being of crucial importance for the rhythmical, efficient and safe realization of production processes at the Babino Mine is the electric power system that supplies all consumers along the whole technological chain.

The report contains information about: today's achievements of the mining science and the industry that produces electrical equipment for up-to-date high-performance mining machines; a most general characteristic of the electric power consumers in the Babino Mine and the power supply circuit is presented; data for the basic electric equipment of a mechanized face with a Klöckner-Becorit complex are given; the main directions of the scientific support of Bobovdol Mines Co. provided by the Department of Mine Electrification are summarized. Some problems of urgent importance for the further development of the power supply system of the Babino Mine are defined as conclusion of the report.

### 1. Latest achievements regarding the electric equipment of machine complexes for underground coal production.

Table 1 contains technical data for electric motors used for driving of modern coal getters manufactured by world-famous companies and demonstrated at an international exhibition in 2000.

Table 1 imposes the following conclusions:

1. The motors used are intended for voltages of 500, 1000, 1100, 3300, 5000, or 6000 V, respectively.

2. Motors of power 300 kW each are mounted on both drums of the EDW-300LN coal getter (the company manufacturing the motors is Siemens from Germany), and motors of power 500 kW each are mounted on both drums of the EDW-450/1000 coal getter (the company manufacturing the motors is Eickhoff from Germany). Motors of type F-37 with a power of 300 kW are used on the ACE coal getters (of British Jeffrey Diamond Co., U.K.). British coal getters of series AM 500 made by Anderson Co. are equipped with one or two motors of types 2K1 or 2R1, and the coal getters of the Electra series produced by the same company are provided with electric motors of the EL type. Polish coal getters KGU of Famur Co. use electric motors manufactured by Celman Works (Poland).

3. The power of electric motors used on combined coal getters in Babino Mine is 230 kW or 350 kW, and the supplied voltage is 1000 V.

In 1991 91 combined coal getters operated in the USA, their power-oriented classification being shown in Table 2.

Australia occupies a leading position as concerns the development and implementation of most advanced machines for underground coal production. The design performance of coal getters for long faces has been increased from 800 t/h to 2500 t/h. The power installed of electric motors for coal getters is 750 kW, and the working feed rate is 10 – 12 m/s. The average 24-hour output from a face attains 10,000 t/h. At the present time design solutions connected with putting into implementation a complex with a new generation of combined coal getters are being prepared for realization. The Ulan complex involves a coal getter of Eickhoff Co. with a shearing

Table 1.

| Parameters                        | Type of coal getter (motor) |                       |           |                      |           |           |              |            |
|-----------------------------------|-----------------------------|-----------------------|-----------|----------------------|-----------|-----------|--------------|------------|
|                                   | EDW-300LN Siemens           | EDW-400/1000L Siemens | ACE F37   | Electra 500 EL12A006 | AM500 2K1 | AM500 2R1 | Electra 1000 | KGU Celman |
| Thickness of coal seam, m         | 0.8 - 1.7                   | 2.4 – 4.4             | Up to 1.2 | 1.2 - 6              | 2.6 - 3   | 2 - 3     | 1.3 – 4.5    | -          |
| Motor power, kW                   | 300                         | 500                   | 300       | 230 X 2              | 375       | 450 X 2   | 375 X 2      | 132        |
| Voltage, V                        | 1000                        | 3300 – 5000           | 1100      | 1140                 | 1100      | 6000      | Up to 3300   | 1000       |
| Rotational speed, s <sup>-1</sup> | 1450                        | 1500                  | 1500      | 1500                 | 1500      | 1500      | 1500         | 1440       |
| Insulation class                  | F                           | -                     | F         | H                    | H         | H         | H            | H          |

drum and motor of power 1000 kW and a face conveyer with electric drive power 1050 kW. The powered support of working strength of 800 t is provided by Dowty Co. The complex output is 2500 t/h, and coal is transported by a belt conveyer with belt width of 1600 mm.

Table 2

| No | Working conditions                | Type of coal getter                   | Motor power, kW |
|----|-----------------------------------|---------------------------------------|-----------------|
| 1  | Flat seams of thickness 1.4 – 3 m | Electra 550<br>EDW-2L-2W              | 350 – 500       |
| 2  | Flat seams of thickness 1.5 – 4 m | AM 500<br>Electra 1000<br>EDW-380/760 | 500 – 1000      |

A modern power supply system of voltage 10 kV for an underground coal mine has been developed and put into operation in Germany. It is expected that in near future there will emerge new electric equipment for even higher voltage.

## 2. Power supply network of the Babino Mine.

A main surface substation (MSS) for a voltage of 110/20/6 kV is built for supplying power to the Babino Mine and other mines of Bobovdol Mines Co. Two power transfer lines of 110 kV supply the substation. One of the power lines is 25 km long and connects the Babino substation with the Republika Thermal Power Station in the town of Pernik, and the other is 9 km long and makes a connection with the Bobovdol Thermal Power Station.

To supply powerful consumers located at considerable distances from MSS Babino, at the corresponding sites there have been built substations supplied with a voltage of 20 kV through overhead power transfer lines. Such are the substations of ventilation shafts VS-1, VS-2, VS-3, and that in the pithead of the main cage shaft (MCS). The near consumers are supplied directly with cables from MSS Babino. Such powerful consumers are the mine hoist winders (MHW) of the MCS, MHW of the main skip shaft (MSkS), nitrogen station, and ventilation installation of MSkS. To supply electric power to the underground consumers of the Babino Mine, on the principal horizon of the mine (level 292) there has been built a central underground substation (CUS) in the area of the shaft bottom of MCS and 7 section transformer substations (STS) located in different parts of the underground mine.

The most generalized characteristic of the power supply network of underground mine Babino is shown in Fig. 2. It can be reduced to the following:

1. Deep input of high voltage 6 kV into the underground mine that reaches production faces at a distance of up to 150 m.

2. Direct two-side power supplying from MSS Babino to CUS - at level 292 – and to STSs that are connected in a ring.

3. To improve the reliability of the power supply network, three rings have been formed: one for CUS at level 292, one for STS-2 and STS-9, and one for STS-6, 7, 8, 8A.

4. To supply electric power to underground consumers in the area of VS-1, there has been built an STS that is supplied by the central distribution substation CDS-VS-1. At certain moments the ventilation stream is directed upward. In order to meet the requirement of Regulations [6], an anti-leakage protection device of type RZEZS-1 developed by a team with the Department of Mine Electrification at MGU "St Ivan Rilski, led by Prof. G. Anev, Dr.Tech.Sc., has been mounted.

5. CUS at level 292 and STSs are provided with a switchgear KRU for 6 kV in which low-oil circuit breakers of type RVD-6 are mounted.

6. The mobile transformer substations are of types TKShVP, TSVP, and Siemens.

7. With certain small exceptions the power supply of all consumers is carried out at a voltage of 660 V.

8. Voltage of 1000 V is used for the operation of some of the electric motors at the mechanized production face where the complex of Klöckner-Becorit GmbH is working, namely the motors of the coal getter (1 pc.), face chain conveyer (2 pcs.), crusher (2 pcs.), and transfer conveyer (2 pcs.).

9. Voltage of 1000 V is also supplied to the same types of electric motors in the mechanized complex of Dowty Co.

10. Transformer substations of 6/1 kV are manufactured by Siemens AG.

11. CUS at level 292 and STSs are equipped with 85 low-oil circuit breakers of type RVD-6 and 43 mobile transformer substations of types TKShVP and TSVP.

12. 25,000 m of cables of type SVBT-6 with cross-sections 3 X 185 mm<sup>2</sup>, 3 X 150 mm<sup>2</sup>, 3 X 70 mm<sup>2</sup>, and 3 X 50 mm<sup>2</sup> have been laid for the realization of the Babino Mine cable network for 6 kV.

## 3. Power capacities installed in the underground mine

Irrespective of the non-interrupted development of the mine after its first commission in 1974, two main periods should be considered as concerns the field of electric power supply, namely till 1986 and after 1986, when mechanized complexes for coal production from seams of thickness up to 5.5 m were put into operation after entire reconstruction of the transportation scheme and electric power supply network.

Table 3. Installed power capacities at Babino Mine

| No. | Sites   | Power installed, kW |              |
|-----|---|---------------------|--------------|
|     |   | Till 1986.          | After 1986   |
|     | A) Surface premises                                 | 6 900               | 16 950       |
| 1.  | Mine hoist winches                                  | 3200                | 6000         |
| 1.1 | MHW of ventilation shaft No. 1 – 1 pc.              | 320                 | 400          |
| 1.2 | MHW of ventilation shaft No. 2 – 1 pc.              | 320                 | 400          |
| 1.3 | MHW of ventilation shaft No. 3 – 1 pc.              | -                   | 400          |
| 1.4 | MHW of main skip shaft – 2 pcs.                     | 1700                | 3400         |
| 1.5 | MHW of main cage shaft – 2 pcs.                     | 700                 | 1400         |
| 2.  | Ventilation installations                           | 2000                | 5650         |
| 2.1 | Main ventilation installation of VS-3               | -                   | 2500         |
| 2.2 | Ventilation installation of VS-1                    | 1000                | 1000         |
| 2.3 | Ventilation installation of VS-2                    | 1000                | 1000         |
| 2.4 | Ventilation installation of MSkS                    | -                   | 1000         |
| 2.5 | Degassing installation of VS-3                      | -                   | 150          |
| 3.  | Nitrogen station                                    | -                   | 3500         |
| 4.  | Machine-repairing workshop                          | 750                 | 750          |
| 5.  | Administration complex                              | 950                 | 950          |
| 6.  | Coal slurry facilities                              | -                   | 100          |
|     | B) Underground premises                             | 5100                | 10410        |
| 1.  | Water-drainage installation                         | 1100                | 1520         |
| 1.1 | Main water-drainage installation at level 292       | 900                 | 900          |
| 1.2 | Water-drainage installation of the structural basin | -                   | 200          |
| 1.3 | Sump water drainage of 5 shafts                     | 100                 | 220          |
| 1.4 | Water-drainage installation at level 484 of MCS     | 100                 | 200          |
| 2.  | Sections of mechanized coal production              | 1200                | 4200         |
| 2.1 | First section                                       | 400                 | 1300         |
| 2.2 | Second section                                      | 370                 | 1100         |
| 2.3 | Third section                                       | 430                 | 1100         |
| 2.4 | Fourth section                                      | -                   | 700          |
| 3.  | Preparation sections                                | 1700                | 2490         |
| 3.1 | Fifth preparation section                           | 500                 | 700          |
| 3.2 | Sixth preparation section                           | 600                 | 820          |
| 3.3 | Seventh preparation section                         | 500                 | 650          |
| 3.4 | Eighth section – Investment construction            | 100                 | 320          |
| 4.  | Horizontal transportation                           | 1100                | 2200         |
|     | <b>Total A + B</b>                                  | <b>12000</b>        | <b>27360</b> |
|     | Recapitulation                                      |                     |              |
|     | A) Surface premises                                 | 6 900               | 16 950       |
| 1.  | Mine hoist winches                                  | 3200                | 6000         |
| 2.  | Ventilation installations                           | 2000                | 5650         |
| 3.  | Nitrogen station                                    | -                   | 3500         |
| 4.  | Machine-repairing workshop                          | 750                 | 750          |
| 5.  | Administration complex                              | 950                 | 950          |
| 6.  | Coal slurry facilities                              | -                   | 100          |
|     | B) Underground premises                             | 5100                | 10410        |
| 1.  | Water-drainage installations                        | 1100                | 1520         |
| 2.  | Sections of mechanized coal production              | 1200                | 4200         |
| 3.  | Preparation sections                                | 1700                | 2490         |
| 4.  | Horizontal transportation                           | 1100                | 2200         |
|     | <b>Total A + B</b>                                  | <b>12000</b>        | <b>27360</b> |

Data about power capacities installed in the underground mine of Babino are given in Table 3 with the purpose of making comparison with world trends in power supply and electric drives of mining machines.

The transformer capacity installed in substations through which electric power is being supplied to the Babino Mine is given in Table 4.

Table 4

| No. | Substations                | Transformers installed   |
|-----|----------------------------|--|
| 1.  | Main surface substation    | No. 1 – 25,000 kVA, 110/20/6 kV<br>No. 2 – 16,000 kVA, 110/20/6 kV   |
| 2.  | CDS –VS-1                  | No. 1 – 2500 kVA, 20/6 kV<br>No. 2 – 2500 kVA, 20/6 kV<br>No. 3 – 100 kVA, 6/0.4 kV<br>No. 4 – 100 kVA, 6/0.4 kV   |
| 3.  | CDS – VS-2                 | No. 1 – 1800 kVA, 20/6 kV<br>No. 2 – 1800 kVA, 20/6 kV<br>No. 3 – 100 kVA, 6/0.4 kV<br>No. 4 – 100 kVA, 6/0.4 kV   |
| 4.  | CDS – VS-3                 | No. 1 – 4000 kVA, 20/6 kV<br>No. 2 – 4000 kVA, 20/6 kV<br>No. 3 – 630 kVA, 6/0.4 kV<br>No. 4 – 630 kVA, 6/0.4 kV<br>No. 5 – 160 kVA, 6/0.4 kV<br>No. 6 – 160 kVA, 6/0.4 kV |
| 5.  | CDS of pithead             | No. 1 – 1000 kVA, 20/6 kV<br>No. 2 – 1000 kVA, 20/6 kV<br>No. 3 – 1000 kVA, 20/6 kV<br>No. 4 – 630 kVA, 6/0.4 kV   |
| 6.  | CDS of mechanical workshop | No. 1 – 400 kVA, 6/0.4 kV<br>No. 2 – 400 kVA, 6/0.4 kV<br>No. 3 – 1000 kVA, 6/0.4 kV<br>No. 4 – 1000 kVA, 6/0.4 kV   |

Table 5 shows the electric equipment of a section for mechanized coal production with a complex of Klöckner-Becorit GmbH.

Table 5

|    | Electric motors of mining machines                              | Installed capacity |      |                |
|----|---|--------------------|------|----------------|
|    |   | Unit power         | Qty. | Total power    |
| 1. | Coal getter   | 380 kW             | 1    | 380 kW         |
| 2. | Face chain conveyer   | 132 kW             | 2    | 264 kW         |
| 3. | Chain transfer conveyer   | 75 kW              | 2    | 150 kW         |
| 4. | Oil station   | 75 kW              | 2    | 150 kW         |
| 5. | GTL Gvarek - 1000   | 95 kW              | 2    | 190 kW         |
| 6. | Crusher   | 75 kW              | 2    | 150 kW         |
| 7. | Additional equipment  | -                  | -    | 116 kW         |
|    | <b>Total power</b>  |                    |      | <b>1400 kW</b> |
|    | Power train of composition:                                     |                    |      |                |
| 1. | Siemens underground transformer, $U_1 = 6000$ V, $U_2 = 1000$ V | 630 kVA            | 2    |                |
| 2. | Control station of type $L_{11} - U_H = 1000$ V, $I_H = 1200$ A |                    | 1    |                |
| 3. | Control station of type $L_{12} - U_H = 1000$ V, $I_H = 400$ A  |                    | 2    |                |

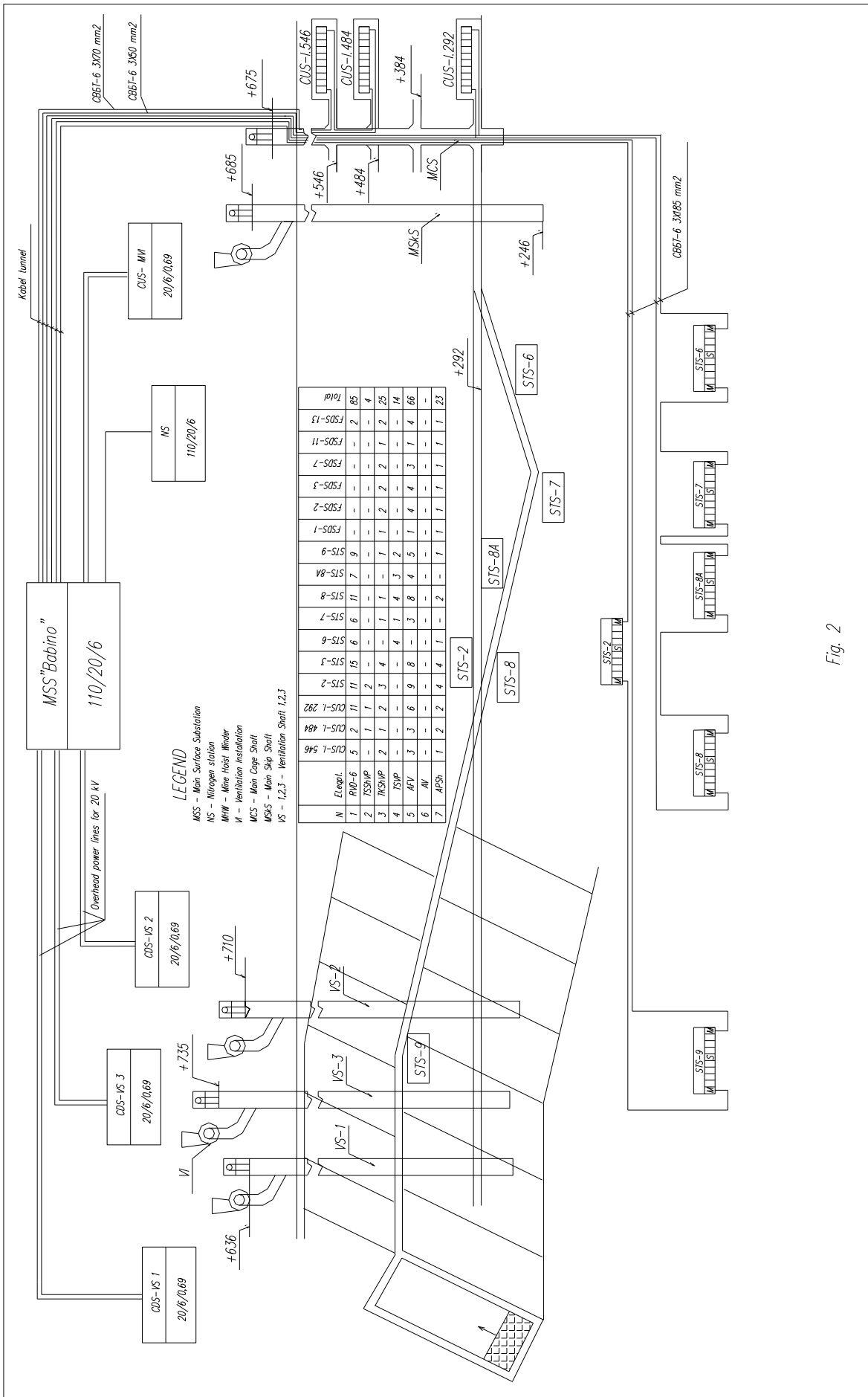


Fig. 2

#### **4. Scientific support of the activities of Bobovdol Mines Co provided by the Department of Mine Electrification.**

In connection with the exceptional importance of this issue it should be considered and analyzed individually. For this reason only some basic moments and trends in the scientific collaboration of many years between MGU "St Ivan Rilski" and Bobovdol Mines Co. will be pointed out in this report.

This collaboration could be generalized in the following basic directions:

1. Training of higher education specialists with a bachelor or master degree.
2. Improving the qualification of the chief executive personnel.
3. Participation of MGU's researchers and teachers in expert committees discussing issues, problems and tasks connected with the development of Bobovdol Mines Co.
4. Regular periodic revisions of the Regulations on Technical Safety of Coal Production in Underground Manner (V-01-01-01).
5. Development and implementation of leakage protection devices for 6-kV cable network.
6. Re-designing existent leakage protection devices for cable networks of 1140 V.
7. Performing tests of electric equipment with explosion-proof design for mines.
8. Making expert assessments and providing consultations on diverse issues in the field of electric power supply and relay protection.

#### **5. Important problems to be examined and solved in the field of electric power supply to the Babino Mine.**

The production experience gained during the many years of operating the power supply system of the Babino Mine of Bobovdol Mines Co. shows there are many unsolved issues that limit and in certain cases reduce the effectiveness and safety of the underground mechanized coal production.

1. The optimization problem providing a scientifically substantiated relationship between mine conditions of coal seams in Babino Mine, necessary installed capacities of mining machines and rated network voltage has not been solved yet.
2. The task of determining the reliability of the power supply system depending on the productivity of production and preparation faces and the provision of technical means for its practical realization is of prime importance.
3. Substantiation, development and implementation of advanced systems of electric drive and control for various machines and mechanisms as a principal source of realizing considerable savings of electric power and increasing their working capacities.
4. Implementation of modern starting equipment with increased information resources, which should be understood as improving their structural scheme for providing continuous diagnostic information about their condition.
5. Optimization of repairing cycles of the electric mine equipment as well as of the amount of their preventive maintenance; development and implementation of an efficient program of technical maintenance and repair works for the entire complex of electrical and mechanical equipment with

the purpose of providing maintenance according to the "technical condition", and not in connection with failures as it is the case for the time being.

6. It can be easily explained why for the conditions of an underground mine of the type of Babino the requirements of the Regulations of Labor Safety [6] for verification of the faultless condition of devices for non-interruptible insulation monitoring and for protective turning off of the power supply network "before the beginning of each shift" cannot be accepted any more as a solution improving the safety in using electric power in underground coal mines. Finding a new, up-to-date solution of this problem is one of the topical tasks to be performed.

7. The electric power became the main driving force in the underground coal production in nearly all countries of developed mining industry. At the same time the statistical data demonstrate that the electrical power is one of the main causes of fire and explosion occurrences in underground coal mines and of electric current accidents.

In their majority the existent regulation documents concerning technical and labor safety are based on a qualitative approach in determining the conditions of safe application of electric power in underground coal mines, not defining quantitatively the level of safety. This represents an up-to-date problem of critical importance that is being studied by many research and university teams in countries of developed mining industry.

8. Development and implementation of protection devices against leakages in electric networks supplying power to regulated thyristor drives. Development of new means for protection against short-circuit currents in applications connected with the use of regulated thyristor drives.

9. Selection and realization of solutions for substantial reduction of the total mining consumption of electric power as well as of the power consumption of individual technological processes.

## CONCLUSIONS

Based on the presentation above the following conclusions have been derived:

1. If compared to latest achievements of mining science and practice there are modern solutions implemented in the Babino Mine as far as the installed equipment and power supply system used are concerned, but lagging behind the tendencies of today can be observed as well.

2. As regards the rated supply voltage of electric motors in the Babino Mine a considerable lagging is found in comparison with today's achievements and trends.

3. Evaluating comprehensively the experience gained in many years of designing and operating electric power systems for underground coal mines, including those in the Babino Mine, imposes also the obligatory conclusion that today's requirements of mining organization and production have led to the formation of a number of new problems and tasks demanding urgent investigations and solutions.

These problems are even more urgent as concerns such high-risk production processes as underground coal mining.

REFERENCES

- Anev G.A. Investigation of 6-kV Power Distribution Networks in Bulgarian Open Mines and Development of Protection Devices for These Networks (in Bulgarian). – Author's Synopsis of a Dissertation Thesis for Acquiring the Scientific Degree of Doctor of Technical Sciences. Sofia, 1975
- Voloshchenko N.I. et al. Power Supply and Electric Equipment in Coal Mines Abroad (in Russian). Moscow, Nedra, 1983.
- Kuzmich I.A. et al. Foreign Companies Manufacturing Mining Equipment. A Handbook (in Russian), Moscow, Nedra, 1997.
- Kartselin E.R. et al., Developing and Implementing a Regulated Electric Drive for Chain Conveyers in Underground Coal Mines (in Bulgarian), Yearbook of MGU "St Ivan Rilski", Vol. 44-45, Scr. III, Sofia, 2002.
- Kartselin E.R. Mathematical Models for Investigating Mine Power Supply Systems (in Bulgarian), Yearbook of MGU "St Ivan Rilski", Vol. 44-45, Scr. III, Sofia, 2002.
- Regulations on Labor Safety in Underground Coal Mines (V-01-01-01) (in Bulgarian), Sofia, 1992.
- Shutskiy V., Anev G., Dankov E. Electrical Safety in Mining Enterprises (in Bulgarian), Sofia, Tekhnika, 1980.
- Bikov A.I. et al. Electrical Apparatuses for 1140-V Voltage (in Russian), Moscow, Energoatomizdat, 1983.
- Shutskiy V., Shishov S. Analysis of the Operational Reliability of PMVI Magnetic Starters at Bobovdol Mines Co. (in Bulgarian), J. of Mining, 1990, No. 5.

*Recommended for publication by Department of  
Electrical Engineering, Faculty of Mining Electromechanics*

## RISING A LEVEL OF SAFETY WORK OF MINERS – THE MAIN DIRECTION OF ACTIVITY OF THE PUBLICLY HELD COMPANY "KRASNY METALLIST"

**A. Kotlyarov  
N. Matvienko**

PHC "Krasny Metallist"  
Ukraine

**E. Kartselin  
R. Istalianov**

University of Mining and Geology "St Ivan Rilski"  
Sofia 1700, Bulgaria  
E-mail: [rgi@mgu.bg](mailto:rgi@mgu.bg)

The Publicly Held Company "Krasny Metallist" is the only enterprise in Ukraine specializing in the production of:

- systems and devices of control of methane content in mine atmosphere;
- systems and means of early detection and suppression of methane and coal-dust explosions;
- carbon monoxide gas analyzers;
- mine stationary plants and transport automations systems (main water drainage, ventilation and air-heater plants, mine-rail transport) ;
- systems of automation, travel control and protection of hoisting plant moving vessel;
- signalling and communication systems, including transmission of information through a rope from the moving vessel on the hoisting plants;
- actuating mechanisms, starting and adjusting equipment, breast and column drills.

Lately the PHC "Krasny Metallist" has been paying great attention to the development and putting into production the devices, means and systems ensuring rising of level of safety work of miners. Thus during the last three years more than ten kinds of new products have been developed and put into production. These are:

- methane alarm combined with a caplamp(СМГ.1);
- portable methane analyzer "Сигнал.5", which ensures methane volume part concentration measurement from 0 to 100%, with simultaneous remembering the extreme values of methane concentrations for the period of continuous operation(function of "black box");

- explosion-proof mine lighting device of increased safety with extended functional abilities(СМГ.1.01);
- modernized automated explosion localization system (СЛВА);
- blind working ventilation equipment (АКТВ);
- mine atmosphere dust content meter(ИЗША);
- piezoelectric audible signalling devices(СЗВ.1 and СЗВ.2), etc.

At present time the enterprise is conducting production tests of complex of means for alarming about the accident in mine by a signal from the surface and sending a radiobeacon signal during search of victims, remaining under the fallen rock. The complex consists of:

- accident alarm generator(apparatus "Вызов");
- apparatus "Зонд" intended for remote detection, radio search of the miner, remaining under the fallen rock;
- signaling device(СМГ.3) intended for alarming the miner, remaining under the fallen rock by a signal from the surface and sending a radiobeacon signal during his search. The СМГ.3 signaling device is combined with a caplamp.

The complex of such means will be put into serial production in the third quarter of 2003.

The PHC "Krasny Metallist" is performing a great deal of work on ensuring high quality and safety of its production. One of the main directions of such works is conducting of product tests on a high technical level. Tests are being conducted at the company's testing center, which is accredited to technical competence in Certification system UkrSEPRO.

## TWO-PHASE TURBULENT FLOWS. METHODS FOR DESCRIPTION AND NUMERICAL MODELING

Ivan Antonov

Technical University, Sofia, Bulgaria

### ABSTRACT

The article is about modern methods for a mathematical description and a numerical modeling of two-phase turbulent flows, which are worked out of the collective through the last 10-15 years. It is given results from a numerical experiment for a kind of jet non-isothermal two-phase flows.

Two-phase turbulent flows are basically used in the energetics, the chemistry, the dry technologies and in the food technologies. Their studying is at a great interest from scientific and practical point of view. Therefore, the current article is about one of these methods for numerical investigation of flows of such kind.

### MATHEMATICAL MODEL

It is known two ways for mathematical interpretation of the two-phase (of course and poly-phase) flows. The statistic method is based on the Boltzman's theory of gas mixtures. Because of the complex mathematical description its use is very difficult. That makes the second method – phenominal, more convenient and more accessible than the first one, the second method uses Newton's equations, which are well known from engineers.

I won't describe here the method of passive mixtures, because it is physically ungrounded and because it isn't fit with the real picture of the flow [1], [2].

Two-fluid (or poly-fluid) method examines each of the phases as separate fluid with its own velocity, density and temperature. The mixture phase doesn't have its own tensor of inner pressures P, i.e. its own viscosity and pressure. That means the state equation can't be used for them. On the other hand they have their own turbulence, and their own tensor of turbulent pressures. That is explained with the fact the turbulence is not quality of the fluid, but it is a characteristic of the flow.

It is accepted that the losses of the quantity of movement and the energy are consequence from the between-phase interaction, the hits between particles and so on, and these losses are compensated from the quantity of movement and the energy of the carrier phase. The forces of between-phase interaction in the equations of movement for the gas phase are with mark "-," and with mark "+" for the mixture phase. The basic forces are determined when the physical picture of the flow is done.

The mixture phase is regarded as "rare multitude of particles", i.e. the time between two hits between particles is much more than the time for relaxation after its own hit.

The Reynolds's equation for the two phase of the two-dimensional flow are:

$$1. \frac{\partial}{\partial x} [y^j U_g \rho_g] + \frac{\partial}{\partial y} [y^j V_g \rho_g] = 0$$

$$2. \frac{\partial}{\partial x} [y^j U_p \rho_p] + \frac{\partial}{\partial y} [y^j V_p \rho_p] = 0$$

$$3. [y^j U_p] \frac{\partial \rho_p}{\partial x} + [y^j V_p] \frac{\partial \rho_p}{\partial y} = - \frac{\partial}{\partial y} [y^j \rho_p V'] - \overline{\rho_p V_p'}$$

$$4. [y^j \rho_g U_g] \frac{\partial U_g}{\partial x} + [y^j \rho_g V_g] \frac{\partial U_g}{\partial y} = - \frac{\partial}{\partial y} [y^j \rho_p \overline{U_g V_g'}] - F_x y^j$$

$$5. [y^j \rho_p U_p] \frac{\partial U_p}{\partial x} + [y^j (\rho_p V_p + \overline{\rho_p V_p'})] \frac{\partial U_p}{\partial y} = - \frac{\partial}{\partial y} [y^j \rho_p \overline{U_p V_p'}] + F_x y^j$$

6.

$$[y^j \rho_g U_g] \frac{\partial h_g}{\partial x} + [y^j \rho_g V_g] \frac{\partial h_g}{\partial y} = - \frac{\partial}{\partial y} [y^j \rho_g \overline{h_g V_g'}] - [y^j \rho_g \overline{h_g V_g'}] \frac{\partial U_g}{\partial y} - Q y^j + F_x y^j (U_g - U_p) + F_y y^j (V_g - V_p) - \sum_{i=1}^3 \overline{F_i V_{pi}'} + 2.R_j . \pi . \overline{\rho_g} . (T_2 - \overline{T_g}) \overline{V_g} - 2.R_j . \pi . \overline{\rho_g} . \frac{\overline{V_{ig}}}{Pr_t} . \frac{\partial \overline{T_g}}{\partial y}$$

$$7. [y^j \rho_p U_p] \frac{\partial h_p}{\partial x} + [y^j (\rho_p V_p + \overline{\rho_p V_p'})] \frac{\partial h_p}{\partial y} = - \frac{\partial}{\partial y} [y^j \rho_p \overline{h_p V_p'}] + Q y^j +$$

$$+ 2.R_j . \pi . \overline{\rho_p} . (T_2 - \overline{T_p}) \overline{V_p} - 2.R_j . \pi . \overline{\rho_p} . \frac{\overline{V_{ip}}}{Pr_t} . \frac{\partial \overline{T_p}}{\partial y}$$

$$8. P = \rho_g . R . T_g$$

where: subscripts *g* and *p* are for the carrier phase and for the mixtures; *j* = 0 is for the plane flows; *j* = 1 is for the axes-symmetric flows; *F<sub>x</sub>* - the forces of between-phase interaction.

METHODS FOR SOLUTION. MODELING OF  
TURBULENT PRESSURES

The integral methods. The integral methods are used for researching of turbulent jets and this method brings the system of private differential equation to the system of integral conditions, which are ordinary differential equations. These equations can be solved by using the alikeness of the velocity and temperature of the jet flows. The method is convenient and exact for engineering problems [3], [4], [5].

The numerical methods. The equations for movement and model equations for the turbulence are exchanged with differential schemes in the numerical methods, with using the method of final differences. The most used scheme in our solutions is open, and it is Duffert-Frankel's type [6].

The turbulent pressures are modeled with models from 1<sup>st</sup> row, which is  $k - \varepsilon$  model with its own modification for the two phases of the flow. The modification used from us [6], [7], which is  $k_g - k_p - \varepsilon$ , makes use of three model equations about turbulent energy of the gas phase and of the mixtures and one equation about the dissipation of the energy of the mixtures. The turbulent alongside pressures are, according to the Kolmogorov's theory:

$$9. \overline{v_{tg}} = C_\mu \cdot \frac{\overline{K_g^2}}{\varepsilon}; \overline{v_p} = C_\mu \cdot \frac{\overline{K_p^2}}{\varepsilon}$$

$$10. \overline{\varepsilon} = C_D \cdot \frac{\overline{K_g^{1.5}}}{L}$$

where:  $C_\mu = 0.09$  is empirical coefficient.

The methods, which are given above, are one modern direction for solving the equations of movement [8], [9], but they required very powerful computers and much time.

## THE RESULTS FROM NUMERICAL EXPERIMENT

For illustration of described possibilities of the numerical methods for investigating of the two-phase flows are given results received by  $k_g - k_p - \varepsilon$  model. The numerical experiment is hold with the next initial conditions for the two-phase turbulent jet:

mixtures' concentration –  $\chi = 1.00$

mixtures' diameter –  $D_p = 0.000145m$

velocity of the gas phase –  $u_{g0} = 35m/s$

velocity of the mixtures –  $u_{p0} = 35m/s$

temperature of the gas phase –  $T_{g0} = 300K$

temperature of the mixtures –  $T_{p0} = 400K$

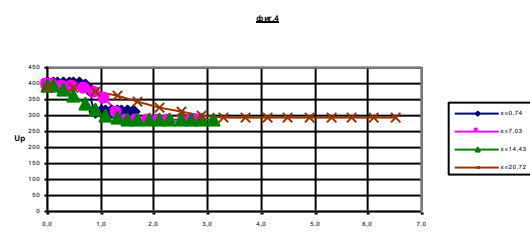
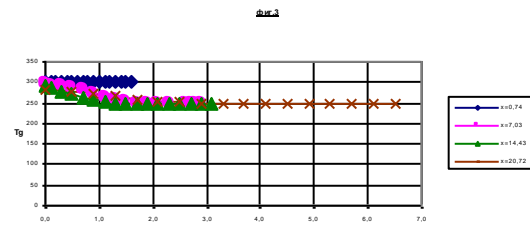
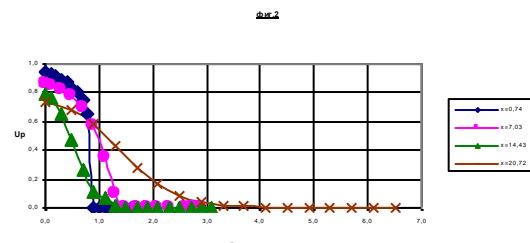
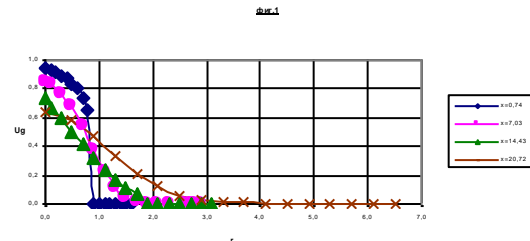
density of the gas phase –  $\rho_{g0} = 1.04kg/m^3$

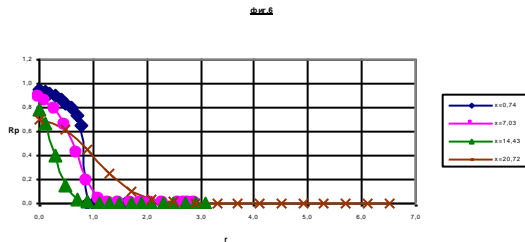
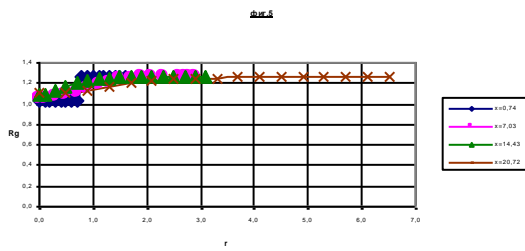
density of the mixtures –  $\rho_{p0} = 800kg/m^3$

temperature of the environment –  $T_2 = 200K$

On fig. 1÷6 are shown the transverse distribution of velocities, temperatures and densities correspond to the gas phase and admixtures for cut  $x=20,72$  (the last one). The results show the workability of the chosen method and its numerical realization for the two-phase turbulent jets.

The lack of enough space in the current article is the cause that the other numerical results are not shown





## REFERENCES

- Nigmatulin R.I., Основы механики гетерогенных сред, М., Nauka, 1978  
 Lojcianskii L.G. "Механика жидкости и газа", Nauka, М., 1970

- Antonov, I.S., N.T.Nam, H.D.Lien, Two-Phase Turbulent Jet. Integral Method, Procc. of the 4<sup>th</sup> Workshop of Applies Mechanics, on 28.04.1994, HVT, HCM, Vietnam, p.p. IX-1 – IX-8  
 Antonov I.S., M.S.Angelov, Integral methods for investigation of two dimensional two phase turbulent jets 10<sup>th</sup> inter. Conference "SAER'96", sept. 27-29, 1996, st. Konstantin ,Bulgaria p.p.156-160.  
 Antonov, I.S., H.D.Lien , E.P.Agontzev ,Integral method for investigation of non-isothermal two phase jets, 11<sup>th</sup> international conf. "SAER'97" sept.20-21, 1997, st. Konstantin ,Bulgaria p.p.145-151.  
 Antonov, I.S., N.T.Nam, Numerical methods for modeling of two phase turbulent swirling jets ,HADMAR'91 Procc., vol1, 34-1-34-5.  
 Antonov, I.S., H.D.Lien , E.P.Agontzev, Numerical investigation of two phase non isothermal jet by three parameter turbulent model, 11<sup>th</sup> international conf. "SAER'97" sept.20-21, 1997, st. Konstantin ,Bulgaria p.p.145-151.  
 Antonov, I.S., N.P.Petkov, L.A.Elenkov, Numerical model of a two dimensional two-phase turbulent jets, Год. на МГУ , т.38, св2, 1992, стр.95-104.  
 Antonov, I.S., M.S.Angelov, Direct Numerical modeling of two phase turbulent axially symmetrical jets ,The 25<sup>th</sup> Israel conf. of mech. Engin., Technion ,Haifa ,25-26 may , 1994

Recommended for publication by Department of  
 Mine Automation, Faculty of Mining Electromechanics

## STATIONARY STREAM OF VISCOSE FLUID IN A PIPE WITH FINITE LENGTH

Veselina Dimova

Utrecht University  
Department of Applied Geophysics

Petko Lalov

University of Mining and Geology "St. Ivan Rilski"  
1700, Sofia, Bulgaria

### ABSTRACT

A finite length pipe, filled with viscose fluid, with bases rotating in opposite directions with constant angle velocities, dragging the fluid, is looked over. The velocity field is defined.

Finite cylinder with radius  $R$  and length  $l$ , filled with viscose fluid which has up and down bases rotating in opposite directions with angle velocities of  $\omega$  and  $-\omega$  respectively (see Fig.1), is considered. Defining the velocity field is the target of the present paper.

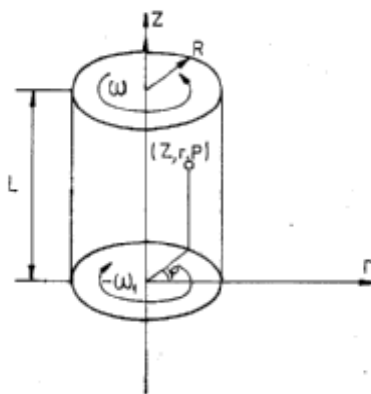


Figure 1

Basic equations of hydromechanics of viscose fluids in this case are set to

[1]

$$\rho \frac{v_\varphi^2}{r} = \frac{\partial}{\partial r} (p + \Omega) = 0 \quad (1a)$$

$$\mu \left( \frac{\partial^2 v_\varphi}{\partial r^2} + \frac{1}{r} \frac{\partial v_\varphi}{\partial r} - \frac{v_\varphi}{r^2} + \frac{\partial^2 v_\varphi}{\partial z^2} \right) = 0 \quad (1b)$$

$$\frac{\partial}{\partial z} (p + \Omega) = 0 \quad (1c)$$

where  $p$  is the pressure (scalar),  $\Omega$  is the potential of volume powers,  $\rho$  is the coefficient of viscosity of the fluid and  $v_\varphi$  is the tangent velocity.

The basic problem is brought to finding the solution of the equation (1b) with the following limit conditions:

$$\begin{aligned} v_\varphi(0, z) = v_\varphi(R, z) &= 0, & 0 \leq z \leq l \\ v_\varphi(r, 0) &= -\omega_1 r, & 0 \leq r \leq R \\ v_\varphi(r, l) &= \omega r, & 0 \leq r \leq R \end{aligned} \quad (2)$$

where  $v_\varphi$  is the tangent velocity.

Applying the method of Fourier, i.e putting

$$v_\varphi(r, z) = f(r) \cdot g(z) \quad (3)$$

from (3) and (1b) is obtained

$$\frac{r^2 \frac{d^2 f}{dr^2} + r \frac{df}{dr} - f}{fr^2} = \frac{d^2 g}{dz^2} = \lambda, \quad (-\lambda = a^2) \quad (4)$$

or

$$\begin{aligned} \frac{d^2 g}{dz^2} + \lambda g &= 0 \\ \frac{d^2 f}{dr^2} + \frac{1}{r} \frac{df}{dr} + \left(-\lambda - \frac{1}{r^2}\right) f &= 0 \end{aligned} \quad (5)$$

where

$$\begin{aligned} g(z) &= C_1 \text{sh}az + C_2 \text{ch}az \\ f(r) &= AJ_1(ar) + BY_1(ar) \end{aligned} \quad (6)$$

where  $J_1$  is a cylindric function (Bessel функция) of first type and first row,  $Y_1$ - cylindric function (Weber function) of second type and first row.

From (6) and from the first condition (2) it comes that the function  $v_\varphi(r,z)$  can be sought in the following appearance

$$v_\varphi(r, z) = \sum_{i=1}^{\infty} (A_i sha_i z + B_i cha_i z) J_1(a_i z) \quad (7)$$

where  $a_i = \frac{\xi_i}{R}$ ,  $\xi_i$  – zeros of  $J_1(r)$ ,  $i=1,2,3,\dots$ , and from the last two conditions (2) is obtained the following system

$$\sum_{i=1}^{\infty} B_i J_1(a_i r) = -\omega_1 r \quad (8a)$$

$$\sum_{i=1}^{\infty} (A_i sha_i l + B_i cha_i l) J_1(a_i r) = \omega r \quad (8b)$$

Putting  $r = Rx$  ( $0 \leq x \leq 1$ ,  $0 \leq r \leq R$ ) (8a) takes the appearance

$$-\omega_1 Rx = \sum_{i=1}^{\infty} B_i J_1(\xi_i x),$$

then multiplying this equation to  $xJ_1(\xi_k x)$  and integrating it in the limits from 0 to 1 is obtained

$$\omega_1 R \int_0^1 x^2 J_1(\xi_k x) dx = \sum_{i=1}^{\infty} B_i \int_0^1 x J_1(\xi_k x) dx$$

and in finite

$$B_k = -\frac{2\omega_1}{a_k J_2(\xi_k)}, \quad k = 1,2,3,\dots$$

where  $J_2$  is a cylindric function of first type and second row.

In absolutely the same way, designating

$$\beta_i = A_i sha_i l + B_i cha_i l$$

is obtained

$$\beta_k = \frac{2\omega}{a_k J_2(\xi_k)}, \quad k = 1,2,3,\dots$$

so getting to the system

$$\begin{aligned} A_k sha_k l + B_k cha_k l &= \frac{2\omega}{a_k J_2(\xi_k)} \\ B_k &= -\frac{2\omega_1}{a_k J_2(\xi_k)} \end{aligned} \quad (9)$$

which has the solution leading to

$$\begin{aligned} A_k &= \frac{2(\omega_1 cha_k l + \omega}{a_k J_2(\xi_k) sha_k l} \\ B_k &= -\frac{2\omega_1}{a_k J_2(\xi_k)} \end{aligned}$$

and finally is written

$$v_\varphi(r, z) = \sum_{k=1}^{\infty} \frac{2\omega_1 sha_k(z-l) + 2\omega sha_k z}{a_k J_2(\xi_k) sha_k l} J_1(a_k r) \quad (10)$$

Equation (10) is a solution of the basic problem just defined. It becomes evident that if  $|\omega| = |\omega_1|$  area  $z=l/2$  remains unmovable. The numeric experiments show that if  $|\omega| \neq |\omega_1|$  the field of the tangent velocities  $v_\varphi = v_\varphi(r, z)$  has the appearance turbulence.

It should be stressed that the problem just solved arises in global Earth sciences too.

#### REFERENCES

- Litwiniszyn J-A certain Problem of stationary laminary Flow of a Viscous Liquid , Bull. Polon.Sci. Letters , v.1 № 4, 1951

## RISK ANALYSIS OF MINE EQUIPMENT

**Michael Michaylov**

University of Mining and Geology  
"St. Ivan Rilski"  
Sofia 1700, Bulgaria  
mihailov@mgu.bg

**Nikola Marhov**

University of Mining and Geology  
"St. Ivan Rilski"  
Sofia 1700, Bulgaria

**Elena Vlaseva**

University of Mining and Geology  
"St. Ivan Rilski"  
Sofia 1700, Bulgaria  
elena@mgu.bg

**Zahari Dinchev**

University of Mining and Geology  
"St. Ivan Rilski"  
Sofia 1700, Bulgaria  
zdinchev@mgu.bg

### ABSTRACT

The issue is discussed of contemporary stringent requirements to ensuring of safe labor conditions for mine workers. Risk assessment of mine equipment breakdowns and failures is reviewed in more detail. Risk assessment of a raise driving complex is presented as an example.

### THE ISSUE OF INDUSTRIAL SAFETY

It is well known that in the last decades, in industrial countries, concern about working conditions and safety of industrial personnel has been increasing. The importance of these issues has both human and social and economic aspects. For example, nearly 120 mill labor accidents are reported in the world each year, representing approximately 40 accidents per 1000 workers per year. Those accidents result in the death of approximately 200 000 people per year making, or 8 fatal accidents per 100 000 workers/a. The number of temporarily disabled people as a result of labor accidents is much greater. This is the price the public pays for the continuous strive towards life quality improvement. It is obvious that living standards should not be raised at the expense the health and lives of the people that work to achieve it.

### RISK IN THE MINING INDUSTRY

World over, approximately 1% of industrial personnel is working in the mining industry. Specific labor conditions in this branch predetermine a risk of accidents and occupational diseases 8 times higher than average industrial one. The situation in our country is similar to that.

Considering the above-said, it is necessary to answer the radical question, why does modern society accept the high risk for mining industrial personnel? The answer seems simple and obvious, but for considerations of comfort and consumption, modern society is too willing to look away from the truth about prodigal utilization of material resources. And the truth is that only a small portion of materials resources come from the flora and fauna, the rest mining industry extracts from the earth.

The price society is paying for better life quality is the higher risk of mining activity. It is unfair, but still a fact that such higher risk only concerns miners and not the entire society.

The risk (possible danger) is always related to a hazard. Рискът (възможната опасност). In industrial activity, a hazard means every source of potential damage, injury or potentially damaging situation. Substances, materials, energy, methods, work technologies, systems, equipment, etc., all could be hazardous.

The risk has two components: the probability for a certain hazard to become real and the consequences of the hazard that has become real. The probability for one or more people to be injured during exposure to hazard depends on the probability for this hazard to be realized in work environment and on exposure frequency and duration.

The magnitude of consequences depends on their severity and is defined by the degree of injury (temporary or permanent disability or death) and on the number of affected persons.

Professional risk for miners is defined by the probability of suffering consequences of different severity in respect of their health and safety in mines. This risk differs for each mine and depends on labor conditions in each mine. For example, labor accidents and occupational diseases in opencast mining are two or three times less in number that in underground mining. This means that risks for opencast mine workers are smaller that for underground miners. It should be pointed out that risks associated with opencast mining are still greater than those associated with most industrial activities.

It is known that mining technology is implemented in complex and changing geological and technical conditions, with specific risks for miners, but here only the risk of mining equipment is discussed.

### SOME TERMS RELATED TO MINING EQUIPMENT AND ITS SAFETY

**Mining equipment**– the totality of machines, mechanisms, facilities, devices and apparatuses for various applications used in

the usual implementation of main and independent technological procedures in mining.

**Machine – mechanical device**, comprising components in coordinated operation and performing specific purposeful movements to convert energy into work.

Facility – a functional combination of one or more machines with the so-called **equipment**. The most characteristic mining equipment includes winding, compressor, ventilation and other facilities.

**System – a network of components (subsystems)**, които performing as one whole piece for achieving a certain objective. Generally, the system is defined as a set of objects and events. The mining equipment employed in a mine or section thereof can be presented as a system as well.

**Machine serviceability** - defined by the status that at any given time corresponds both to the main parameters of machine availability and to secondary parameters relating to safety and other factors.

Fault – defined by the machine condition that at any given time does not comply even with one single requirement of either main or secondary parameters.

**Breakdown**- event resulting in making the machine non-operable.

**Failure** - event resulting in making the machine non-operable. Each failure is a breakdown but not every breakdown is a failure.

#### RISK FILE OF MINE EQUIPMENT

This file must record the hazards, which the machine creates during performance and inherent machine hazards and also the measures planned to reduce the risk of such hazards happening. The file must also contain all information about realized and potential risks of the equipment and its systems.

The main document introducing the risk accent is the Law on Healthy & Safe Working Conditions, enforced in our country. In this aspect, machine risk files must include two major analyses – of technological risks and of technical risks of equipment. These analyses should contain appropriate measures for avoiding and minimization of technological risks of machine-performed operations and of technical risks of breakdowns and failures of equipment functional and structural subsystems.

Generally, risk assessment should include:

- Work processes;
- Work equipment;
- Work places;
- Labor organization;
- Utilization of raw materials;
- Other factors that could present risk

The two key analyses for the files should systematize hazards (including those created by materials used, extracted and transported by the equipment) of individual operations in their technological sequence, measures to avoid such hazards (including organizational ones) and should assess residual risks.

#### EXAMPLE RISK ANALYSIS OF KPV-4 RAISE DRIVING COMPLEX

Mechanized raise driving is associated with risks for miners inherent to driving technology and technical condition of complex subsystems (platform and monorail):

- Gas inhaling while miners work in poorly ventilated faces;
- Injuries and traumas of various degree while working in unsafe face;
- Fatalities in case of non-compliance with blasting regulations;
- Silicosis disease from blast hole boring with insufficient water flush.

The main technological operations in one driving cycle (raise driving) are:

- Driving of chamber for the complex;
- Complex installation;
- Inspection of platform technical status at shift start;
- Taking of air samples from the face;
- Platform advance to face;
- Making the face safe
- Monorail extension;
- Drilling of blast holes;
- Charging of blast holes;
- Moving platform to chamber;
- Blasting and ventilating of face;
- Technical inspection and maintenance of complex;
- Dismantling of complex.

Example analysis of technological risks associated with certain operations is presented in table 1. Potential mechanical risks are associated with unsatisfactory technical conditions of the complex and the following hazards are possible:

- Injuries of different severity during operations for remedying breakdowns and failures of the complex;
- Fatalities in case of failure of complex undercarriage.

In order to identify potential technical hazards, it is recommended to split the complex into functional systems and subsystems. For example, the complex on fig. 1 comprises the following systems:

- Hose winch;
- Power supply block;
- Pneumatic system;
- Monorails;
- Platform;
- Signaling & communication system.

Complex risk file would analyze all systems but here we only focus on platform – the most important one. For risk assessment of breakdowns (failures) of the system, it would be necessary to analyze all subsystems, starting from the most important (most hazardous) one and ending with the least risky one. For example, the platform system comprises several subsystems, the most closely associated with miners' safety being: driving mechanism, manual brake and automatic arrestor (eccentric safety clutch), all shown on fig. 2.

Breakdown risk analysis should assess technical condition of important structural system elements at any given time, as well as define boundary admissible wear of important working surfaces of system and subsystem components. It is recommended to describe in words particularly responsible actions.

Here, risk analysis is performed of the drive mechanism subsystem, for the operations "platform hoist" and "platform lowering", as shown in table 2.

The drive mechanism subsystem operates in the following way: reversible pneumatic motor 1, via gear 2, drives shaft 3, which in turn, via cylindrical wheels 4 and 5, drives shaft 6. Screws 7 and 8 are mounted on shaft and drive two parallel units:

- -first: screw 7, via screw wheel 9, shaft 11 and wheel 13, interlocked with monorail 15 and via support rollers 17, the platform moves forward;
- - second (similar to first unit): via the sequence screw 8, screw wheel 10, shaft 12 and wheel 14, interlocked with monorail and via alignment rollers 18, the platform moves forward.

This drive system with two parallel power chains was designed solely for safety purposes. For example, in case a monorail component falls out, the system will continue its uninhibited movement in the specified direction.

Similarly, if there is a faulty component in one drive unit, the other unit will implement movement. However, if there is a faulty component from pneumatic motor 1 to shaft 6, the platform is secured against free downward gravitational movement because screws 7 and 8 in this case are self-braking, i.e. these serve as platform brakes.

If compressed air supply is discontinued, the platform could be emergency-lowered through manual operation of flywheels 37

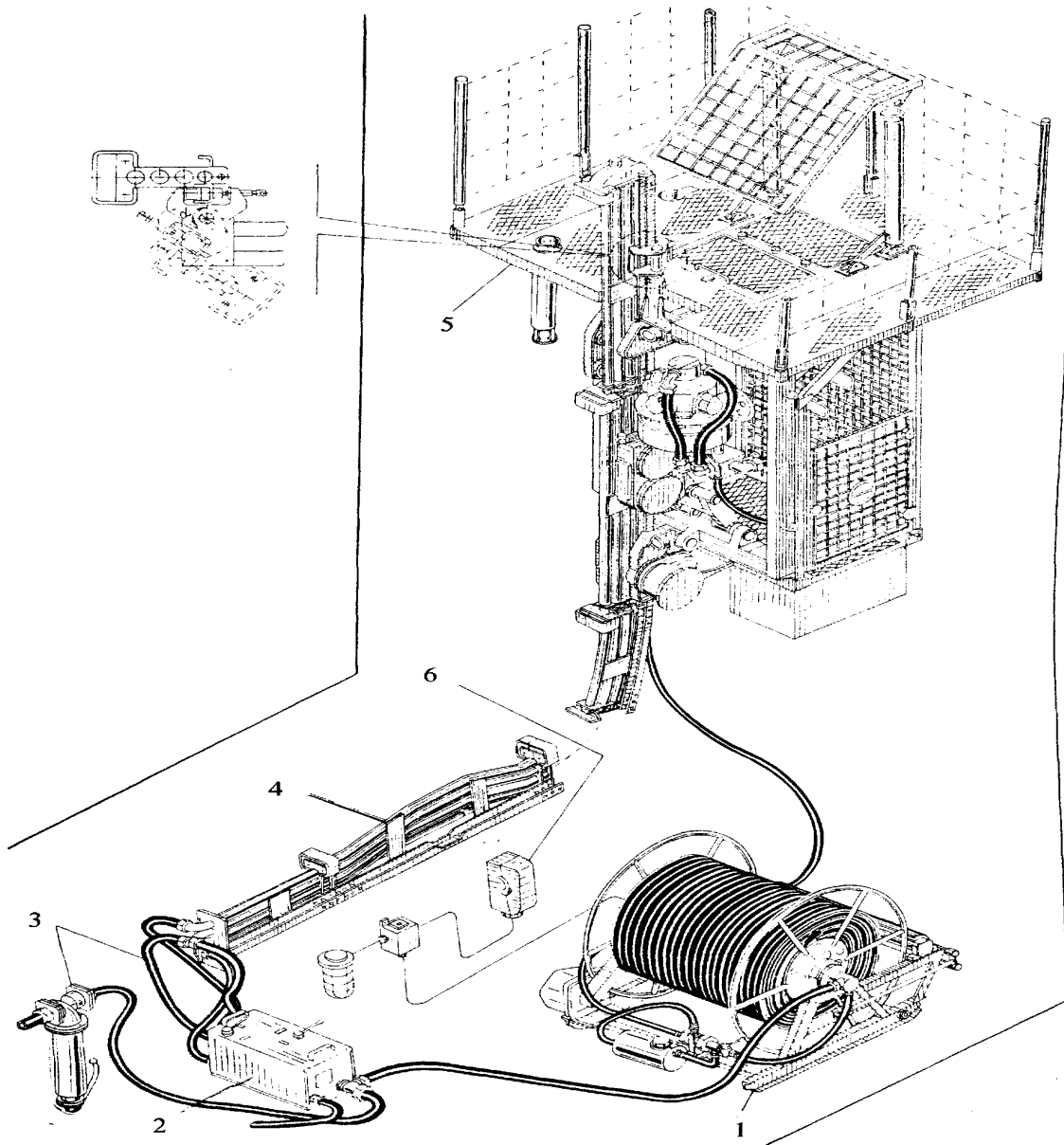


Figure 1. General arrangement of KPV-4 complex

Table 1. TECHNOLOGICAL RISK ANALYSIS Raise driving with KPV-4 Complex

| OPERATION                        | POTENTIAL HAZARD  | RECOMMENDED SAFETY MEASURES   | SAFETY EQUIPMENT             | RESIDUAL RISK |   |   |
|----------------------------------|---|---|------------------------------|---------------|---|---|
|                                  |   |   |                              | F             | C | R |
| 7. Monorail extension            | 7.A. 1. Insecure and improper installation of monorail section creates risk of platform failure and hazard for miners.            | 7.A.1. New monorail section must be installed by two miners in compliance with the following requirements:<br><ul style="list-style-type: none"> <li>- Linearity (alignment) of section with monorail track;</li> <li>- Secure section support;</li> <li>- Distance between upper section end and face should be greater than 1 m.</li> </ul> | Hard hat                     |               |   |   |
|                                  |   | 7.A.2. For the purpose of ensuring sufficient robustness and stability of vertical monorail section, each 10 <sup>th</sup> section should be reinforced.  |                              |               |   |   |
| 8. Blast hole drilling           | 8.A. Breach of technology and technical requirements creates hazard of injury and sickness for miners                             | 8.A.1. Drilling in old holes is strictly forbidden.   | Hard hat, gloves             |               |   |   |
|                                  |   | 8.A.2. In the presence of so-called "pixes" the minimal spacing of holes should be observed.  | Hard hat, gloves             |               |   |   |
|                                  |   | 8.A.3. At the beginning of hole drilling, so-called "flushing", the assistant miner must support the drill end to face.   | Hard hat, gloves             |               |   |   |
|                                  |   | 8.A.4. Hole drilling with insufficient water supply is not allowed, i.e. dry drilling mode.   | Hard hat, gloves             |               |   |   |
| 9. Blast hole charging           | 9.A. Breach of hole charging requirements creates real hazard for miners' safety. Such hazards almost always have lethal outcome. | 9.A.1. On commencement of hole charging, lighting and telephone systems must be switched off.   |                              |               |   |   |
|                                  |   | 9.A.2. Blast holes must be loaded in strict compliance with Safety Regulations.   |                              |               |   |   |
| 10. Platform movement to chamber | 10.A. Breach of technical requirements for platform downward movement creates hazard for miners.                                  | 10.A.1. During platform lowering and occurrence of excessive speed and operation of automatic safety clutch (arrestor), manual brake must be operated immediately.  | Hard hat                     |               |   |   |
|                                  |   | 10.A.2. Platform should be lowered only with operating safety clutch.   |                              |               |   |   |
|                                  |   | 10.A.3. Blocking of safety clutch as strictly forbidden after being operated for the purpose of faster movement of miners in chamber.   |                              |               |   |   |
| 11. Face ventilation             | 11.A. Insufficient face ventilation after blasting creates hazard for inhaling gases by miners.                                   | 11.A.1. Face must be ventilated with water-air mixture for 30 min.  | Breathing device – isolating |               |   |   |

Table 2 RISK ANALYSIS OF BREAKDOWNS - Machine: Raise driving complex; System: Platform; Subsystem: Driving

| Identification mark | Operation Function            | Possible fault                             | Possible consequences   | Severity C <sub>m</sub> | Possible reasons for breakdown   | Probability P <sub>m</sub> | Indication (finding)  | Finding probability D <sub>m</sub> | Risk R <sub>m</sub> | Additional safety measures  | Responsible person | Period of implementation day/month/year | Result                      |                                |   |                              |
|---------------------|-------------------------------|--|---|-------------------------|--|----------------------------|---|------------------------------------|---------------------|---|--------------------|---|-----------------------------|--------------------------------|---|------------------------------|
|                     |                               |  |   |                         |  |                            |   |                                    |                     |   |                    |   | New severity C <sub>n</sub> | New probability P <sub>n</sub> | New probability of finding D <sub>n</sub> | Residual risk R <sub>n</sub> |
| 0                   | 1                             | 2  | 3   | 4                       | 5  | 6                          | 7   | 8                                  | 9                   | 10  | 11                 | 12                                      | 13                          | 14                             | 15  | 16                           |
|                     | Platform hoisting             | Irregular and non-smooth platform movement | Increased impact load of wheels (pos. 13 и 14) and teeth of 15 of monorail, creating hazard of breaking and disruption of interaction between platform and monorail | 7                       | Wear of wheel teeth (pos. 13 и 14) or enlarged gaps between drive wheels, alignment rollers and monorail components  | 4                          | Unusual noise and vibration and characteristic "beat" of wheels 13 and 14 interlocked with monorail | 4                                  | 112                 | Inspection and measurement of machine component wear. Instruction on fault warning signs. | Section mechanic   | One week                                | 7                           | 3                              | 2   | 42                           |
|                     | Platform hoisting or lowering | One driving unit not operating             | Lower safety level of system and increase of load on the other unit   | 6                       | Wheel breaking off conic shaft end 11 or 12 because of damaged fasteners (nuts) or deformation of splint and splint grooves of wheel or shaft. или вага shaft. | 3                          | Low vibration and characteristic noise with smaller intensity. Visual inspection of drive wheels.   | 9                                  | 162                 | Stopping of platform operation until drive unit is restored. завеHO                       | Section mechanic   | During the shift                        | 6                           | 2                              | 5   | 60                           |

and 38, conic wheels 39 and 40, and through brake device 19 driving shaft 3, platform, respectively.

System analysis leads to the conclusions that this mechanism is very secure against platform self-lowering. Theoretically, it could be accepted that system safety is very high. However, several years (15) of experience with the driving complex in our country show certain weak points of the system in real conditions of raise driving. For example, the two parallel driving units create certain difficulties for platform movement. This is due to the circumstance it is hard to drive that raise walls with small plane deviations, which makes alignment of monorail components with strata difficult.

This circumstance is the reason for inhibited upward movement of the platform when passing from one monorail component to another. Sometimes, poor alignment of monorail components may cause blockage of upward platform movement.

In such cases, platform operators would purposefully dismantle the wheel interlocked with monorail thus resolving the problem at the expense of system safety.

Risk analysis of breakdowns (table 2) includes measures for component safety control as well as quantitative assessment of such measures according to M. Michaylov's methodology (2001).

## CONCLUSION

The risk file documents the sequence of logic steps ensuring systematic identification, assessment and management of risks associated with mining equipment operation so that such risks could be reduced to acceptable levels. To this end, the risk files has the following goals:

- To assist employer in adopting adequate program of engineering and administrative solutions for risk management of mine equipment. Measures should be consistent with state of the art of safety and with risk specifics and magnitude, as well as with available resources. The measures included in analyses represent an optimization technical – economic task.
- To create a basis for improvement of safety culture of equipment operators. This would require additional knowledge – knowledge of hazards and measures for risk minimization, application of such knowledge, change in attitude to safety and achieving of quantitatively new safety level in equipment operation.
- To establish the basis of a unified and manageable system of mine equipment safety. Implementation of unified targeted policy of safe equipment operation is only possible on the basis company standards and procedures for safety and specific risk management.

Creation and keeping of up-to-date risk files of mine equipment would require consistent application of general rules in relation to team formation, source document compiling, carrying out of analyses, file storage, use and updating. These general rules should be personified for the experts employed by the company.

## REFERENCES

- Michaylov M., N. Marhov, E. Vlasseva. 2001. Risk diagnostics of mine equipment. Publishing House of St. Ivan Rilski University of Mining & Geology, Sofia, 284.

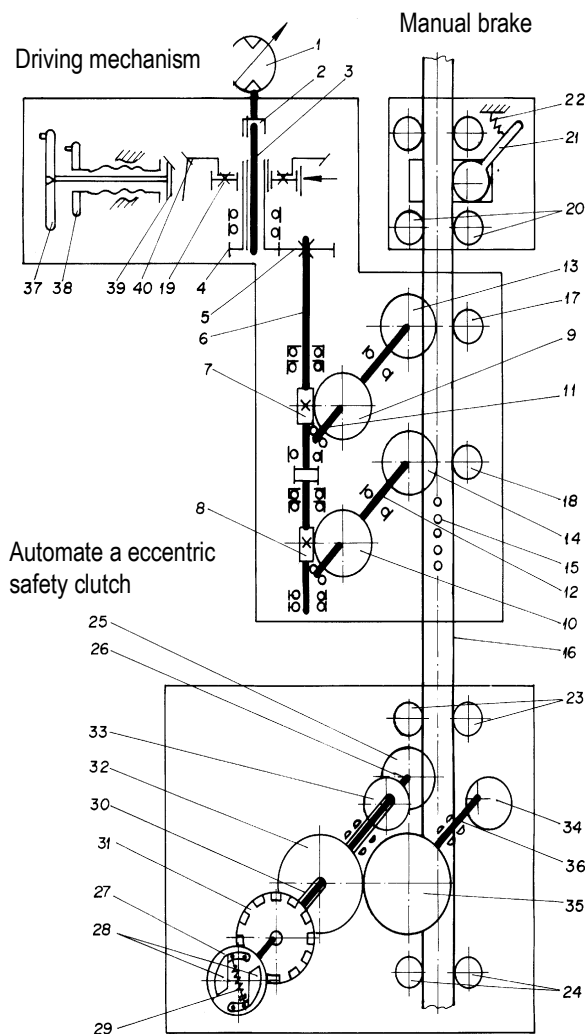


Figure 2 Kinematical charts of driving mechanism, manual brake and eccentric safety clutch subsystems

Recommended for publication by Department of Mine ventilation and occupational safety, Faculty of Mining Technology

## MODELING OF GAS JET DISTRIBUTION IN POROUS ENVIRONMENT

Michael Michaylov

University of Mining and Geology St. Ivan Rilski  
 Sofia, 1700 Bulgaria

### ABSTRACT

Preventive and operative nitrogen injection against spontaneous combustion of coal in gob areas is the most expensive technology of prevention and extinguishing sponcom fires employed in modern underground coalmines. However, this method does not always produce the desired preventive and quenching effect due to insufficient data on nitrogen jet distribution in porous environment and on the basic gas-air flow in inaccessible gob areas. Efficiency and optimization analysis of nitrogen injection parameters requires new knowledge about the process of inert gas distribution in above described conditions – porous environment in a rectangular area with two solid and two porous boundaries; basic flow, aerodynamic reversal of basic and injected flows. The paper presents a physico-mathematical model of gas jet semi-restricted by the coal seam that flows out and disseminates together with the basic flow. Model solution provides assessment of interaction among porous environment parameters, injection and basic flows all of which in turn allow evaluation of jet parameters.

### INTRODUCTION TO PROBLEM

Gas environment inertization in gob areas for the purpose of reducing natural methane release [1,5], has restricted impact on small sections therein. Nitrogen injection in the porous gob environment has been widely employed during the last fifteen years [2,6] in mining of coal seams highly prone to spontaneous combustion. The strictly empirical approach to justification of nitrogen inertization prevails both in world and Bulgarian mining practice. Such approach does not allow prediction of necessary nitrogen quantities for gob inertization because no surveys are available on injection sites, on the way nitrogen flows and disseminates, on the efficiency of application or on the relationship of all those factors with methane release in gob areas. Lack of research results and engineering tools is particularly strongly felt whilst employing the method for sponcom fire prevention. A comprehensive picture of nitrogen utilization dynamics in Babino Mine could be obtained from the data shown on fig.1. There is a nearly functional relationship between nitrogen consumption and monthly coal production. Increase of monthly production from 20000 to 45000 t results in reduction of nitrogen consumption per t coal produced by 2.5 times. (fig.1b). Power cost is the dominating element in the production cost of  $1 Nm^3$  nitrogen, the latter being slightly lower than the cost of 1 kWh electricity.

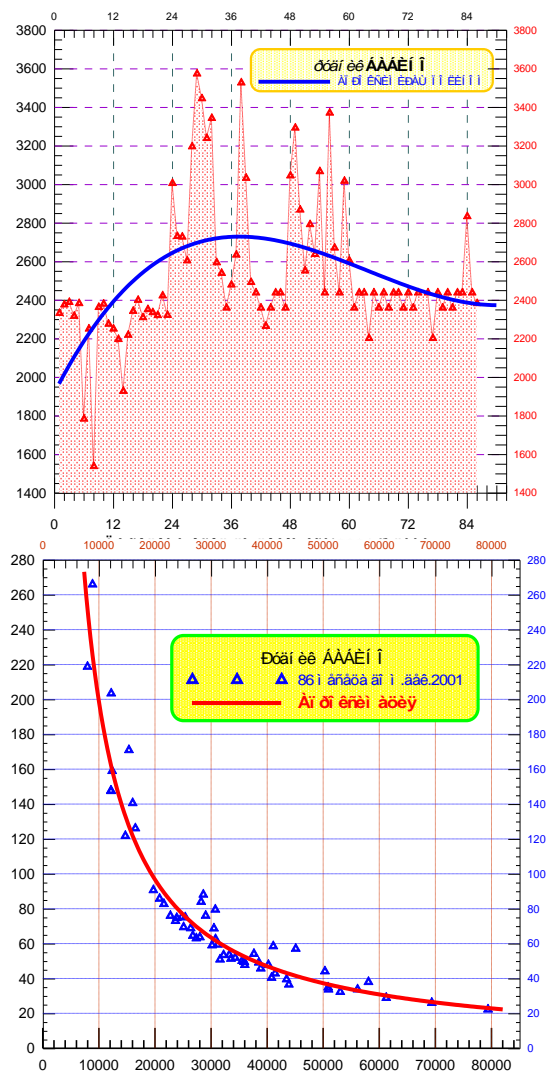
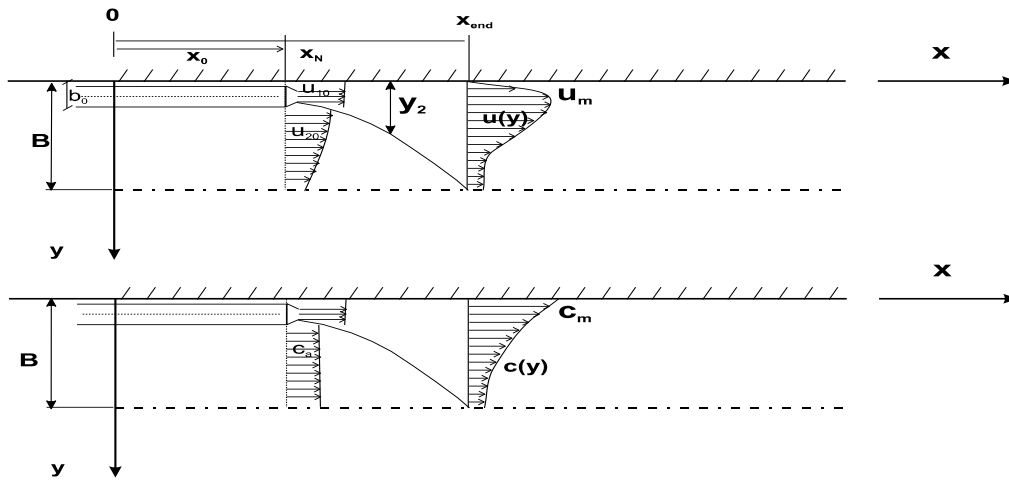


Figure 1. Nitrogen inertization parameters in Babino Mine



West - gob porous boundary  $X=0, Y \in (0..B)$        $Y_2$  - jet expansion       $X_0$  - nitrogen flow  
 North-pillar of intane gallery  $Y=0, X \in (X_0..X_N)$        $U_m$  - maximal velocity       $b_0$  - injector size

Figure 2. Physic al model of nitrogen jet distribution

Nitrogen distribution in porous gob environment and in the main methane-air flow is a complex aerodynamic problem. Its physical nature requires modeling in two zones with different energy characteristics – a jet zone wherein the nitrogen jet preserves its identity and a flow zone wherein the nitrogen mixes with the main flow and continues to disseminate as a flow and not as a jet. [1]. Jet zone end is the initial boundary of the flow zone representing the natural interaction between the two. [2].

FLOW MODEL

Physico-mathematical model formulation is based on the interaction of semi-restricted flat nitrogen jet (fig.2) and the main filtration air flow, and used for solving specific engineering tasks in specific conditions.. There are big contrasts between mechanical energies of air and nitrogen flows. The differences in internal energies of the two flows are insignificant. In the initial section of the nitrogen jet, air infusion is very small and concentrated in a narrow area around external jet boundary. This is due to the higher pressure inside the jet as compared to external porous enviroment.

Scale ratio of N- jet and its mixing with main flow allows investigation to concentrate on the main section of jet flow. The initial section can be ignored because of its small length. The flow can be described by the main conservation laws: of mass flow, of momentum, of kinetic energy, and of admixture mass. These equations are, as follows (for N-jet on fig.2):

$$\int_0^{y_2} u dy + \int_{y_2}^B u_2 dy = b_0 u_{10} + (1 - k_1 X)(B - b_0) u_{20} \quad (1)$$

$$\rho \int_0^{y_2} u^2 dy + \rho \beta \int_{y_2}^B u_2^2 dy + \int_0^{y_2} (p - p_2) dy = \rho b_0 u_{10}^2 + \quad (2)$$

$$\rho(B - b_0)(1 - k_1 X)u_{20}u_{20} - \tau_0 X - \xi_m \frac{\rho}{2} \int_0^{y_2} u^2 dy$$

$$\frac{\partial}{\partial X} \left[ \int_0^{y_2} \rho_g u(u - u_2)^2 dy + 2a \int_0^{y_2} (u - u_2) p dy \right] = \quad (3)$$

$$-2 \int_0^{y_2} \rho_g v_{tg} \left[ \frac{\partial u}{\partial y} \right]^2 dy - \frac{\rho}{2} \int_0^{y_2} \xi_m u^3 dy$$

$$\frac{\partial}{\partial X} \int_0^{y_2} (\rho_g v u) dy = 0 \quad (4)$$

Hydraulic jet pressure and energy losses in (2) and (3) are described by the following expressions:

$$\Delta p = \xi_m \frac{\rho}{2} u^2; \quad E_1 = \Delta p u = \xi_m \frac{\rho}{2} u^3$$

Local resistance factor of the porous environment is calculated, as follows:

$$\left| \begin{aligned} \frac{\partial p}{\partial X} &= \xi_m \frac{\rho u^2}{2} \\ \frac{\partial p}{\partial X} &= a_x \rho v u + \beta_x \rho u^2 = \rho u (a_x v + \beta_x u) \end{aligned} \right. \quad (5a)$$

On equalization of the right sides and subsequent division by  $\rho u$ , the following expression is obtained for the local resistance factor of the porous environment:

$$\xi_m = \left( \frac{a_x v}{u} + \beta_x \right) \quad (5)$$

where:  $\alpha_x$  and  $\beta_x$  are the coefficients respectively of viscous and inertial resistance of porous environment [1], increasing with gob depth.

For crosswise distribution of velocity profiles along jet flow, two similarity functions are taken in the equation system:

- For wall-adjacent boundary layer [3]:

$$f' = \xi^{1/N} \tag{6}$$

where  $f' = u/u_{20}$ , respectively  $f' = u/u_m$ ,  $N = f(\text{Re})$

The model accepts  $N=9$ .

- For jet boundary layer [4]:

$$f = f(\eta) = 1 - 3\eta^2 + 2\eta^3 \tag{7}$$

where:  $\eta = \frac{y - y_m}{y_2 - y_m}$

Jet kinetic energy equation (3) velocity distribution follows Abramovich [7]:

$$\frac{u}{u_m} = 1.48 \xi^{1/7} [1 - \text{erf}(0.68\xi)] = f_1 \tag{7}$$

where:  $\xi = \frac{y}{y_2}$

Jet outflow into porous environment allows the assumption that crosswise pressure distribution follows a model similar to velocity distribution one (6):

$$\frac{p_{\max} - p}{p_{\max} - p_2} = f(p) = 1 - 3\xi^2 + 2\xi^3 \tag{8}$$

Velocity similarity function in hydro-dynamic boundary layer:

$$f_1 = 1.48 \xi^{1/7} [1 - \text{erf}(0.68\xi)] \tag{7a}$$

after transformation and sensitivity analysis gives the expression:

$$f_1 = 1.48 \xi^{1/7} - 1.136 \xi^{8/7} + 0.175 \xi^{29/7} - 0.0243 \xi^{36/7} \tag{7b}$$

which defines the velocity profile shown on fig.3.

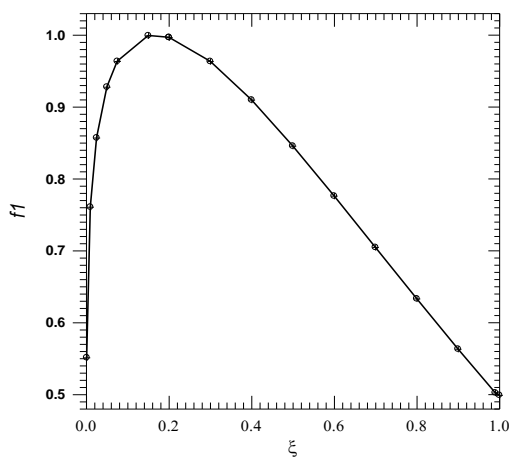


Figure 3

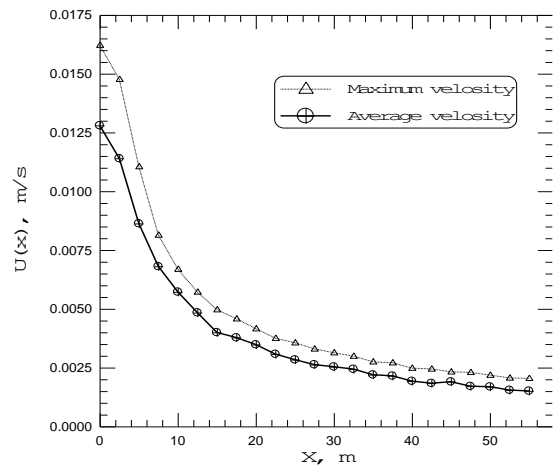


Figure 4

With accepted similarity of crosswise velocity and pressure distribution, the equations 2-5 are solved. Second integrals in (1) and (3) are solved using approximation of the solution for air leak velocity distribution in the zone  $x \in (0,70)$ ,  $y \in (0,15)$ , obtained on the main flow model [5]. Average and maximum velocity profiles are shown on fig.4, whereof characteristic factors in (2) and (3) have values, as follows:

- Boussineq factor  $\beta = \bar{u}_2 / u_{2\max} = 0.64$ ;
- Coriolis factor  $\beta = \bar{u}_2^2 / u_{2\max}^2 = 0.8$ .

After transformation of the four (2-5) integral equations, the following system results:

$$\begin{cases} A_{11} \bar{y}_2 \bar{u}_m + A_{12} \bar{y}_2 = A_{13} & (9) \\ A_{21} \bar{y}_2 \bar{u}_m^2 + A_{22} \bar{y}_2 \bar{u}_m + A_{23} \bar{y}_2 \Delta p + A_{24} \bar{y}_2 = A_{25} & (10) \end{cases}$$

$$\frac{d}{dx} [A_{31} \bar{y}_2 \bar{u}_m^3 + A_{32} \bar{y}_2 \bar{u}_m \Delta p] + A_{33} \bar{y}_2 \bar{u}_m^2 + A_{34} \bar{y}_2 \bar{u}_m + A_{35} \bar{y}_2 \bar{u}_m^3 = 0 \tag{11}$$

$$\bar{y}_2 \bar{u}_m \bar{s}_m = A_{41} \tag{12}$$

where dimensionless values are unknown:

- ♦ Maximal velocity of main N-jet -  $\bar{u}_m = u_m / u_{10}$
- ♦ Jet width -  $\bar{y}_2 = y_2 / B$
- ♦ Maximal pressure difference -  $\Delta p = \frac{P_m - P_2(x)}{\rho u_{10}^2}$
- ♦ Maximal nitrogen concentration -  $\bar{s}_m(x)$ ,

Valid for any cross section of the jet flow along X. Coefficients  $A_{ij}$  and integrals  $\varphi_{mn}$  therein are given in the denotation list.

Equations 9-12 are of different types and direct solution of the system is not possible. Moreover, the third equation if a differential one in respect of  $\Delta p$ . The equation system (9-12) is solved by consecutive iterations in respect of unknown parameters and alternating exchange of unknown values with approximate values resulting from previous iterations/equations. First, we express  $\bar{y}_2$  from (9) and substitute the resulting expression including  $\bar{u}_m$ , in (10). The latter is solved as a square power equation in respect to  $\bar{u}_m$  and thus its first approximation is obtained. The approximate

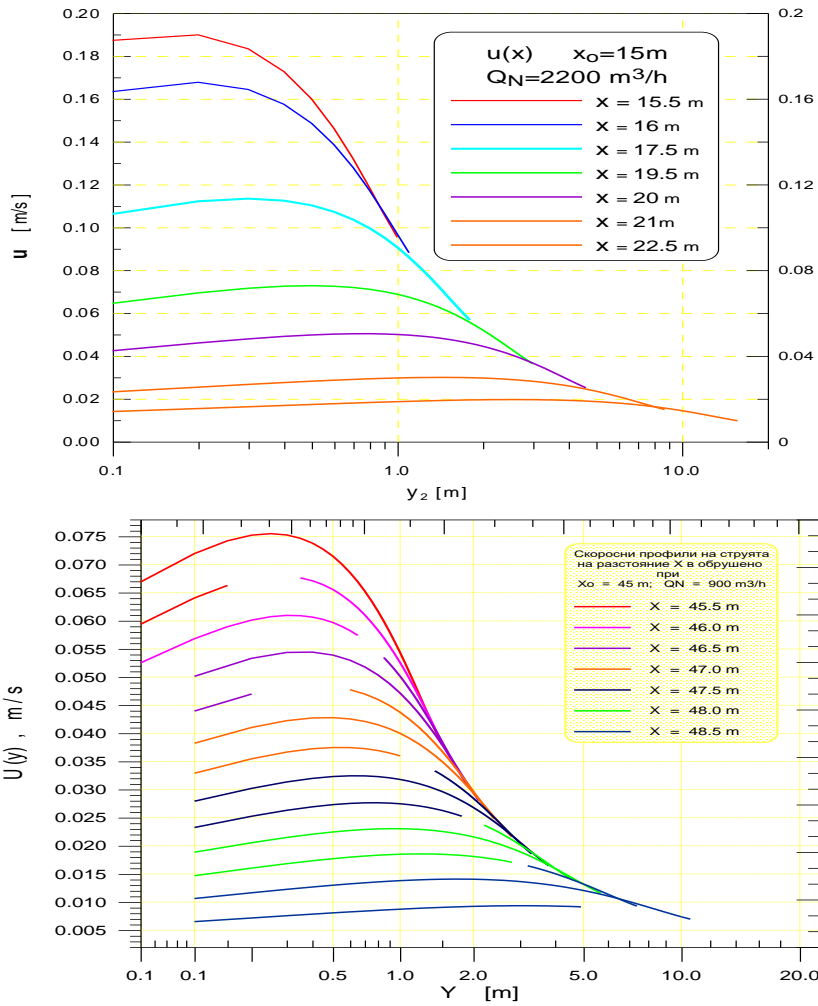


Figure 5. Velocity profiles during N-injection of  $Q_N$  at depth  $X_0$

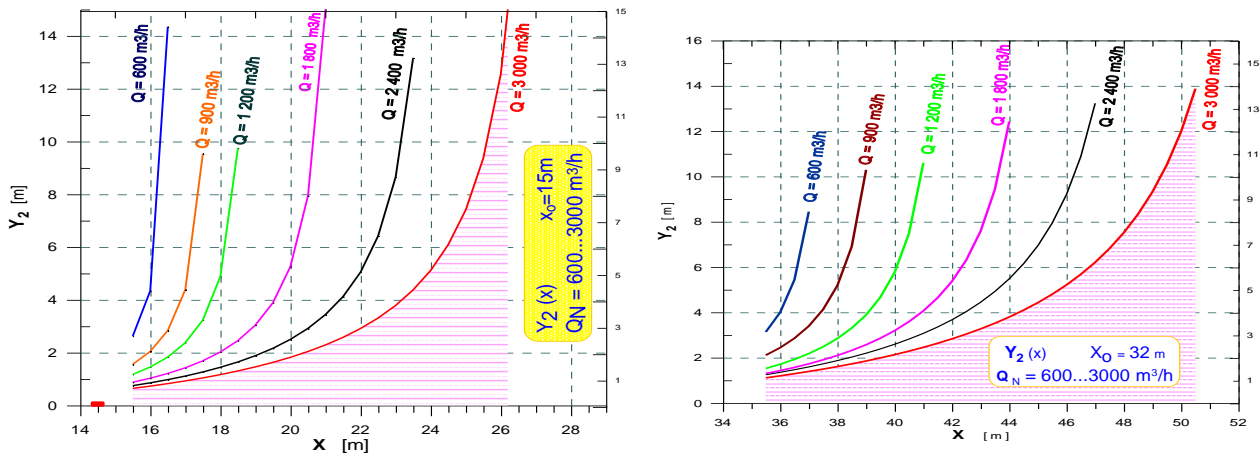


Figure 6. N-jet expansion  $Y_2$  during injection of  $Q_N$  at depth  $X_0$

values of  $\bar{u}_m$  and  $\bar{y}_2$  are substituted in (11) and this is numerically solved for  $\Delta p$ . Resulting values are substituted back in source equations and the procedure is repeated until the required accuracy for  $\bar{u}_m$  is achieved. The solution of (9-

12) follows flow direction in steps of  $\Delta x = 1$  until the set expansion zone  $y_2 = B$  is achieved by means of NitroJet software [6].

EXPERIMENTAL RESULTS

Numerical experiments were carried out for retreat longwall face. Face length is  $L_f = 100m$ , extracted seam thickness is  $m = 3m$ . Ventilation air flow is  $Q_f = 8 m^3/s$  with methane concentration  $C_{in} = 0.2\%$ . Of this flow,  $Q_l = 0.892 m^3/s$  leak into the gob. Methane of  $Q_m = 0.06 m^3/s$  is released in the gob and carried out by air leakages ( $Q_l + Q_m$ ) in the tailgate section of the face. Gob resistance varies as described in [1].

At these initial modeling conditions, variation of N-jet parameters is studied with injection rates  $Q_N$  from  $600 m^3/h$  to  $3000 m^3/h$ , at six-level variation (0.17, 0.25, 0.33, 0.5, 0.61 и  $0.83m^3/s$ ); and injection into the gob along intake road at depths of  $x_N$  (fig.1) 15m, 25m, 35m и 45m .

The wide variation range of injection parameters was chosen to obtain general conclusions and trends for N-jet distribution [2,6]. Within the framework of research [6], some results whereof are presented herein, 24 variants were solved in the above-shown variation range for  $x_N$  and  $Q_N$ . Some modeling results are shown on fig. 5 – fig.8.

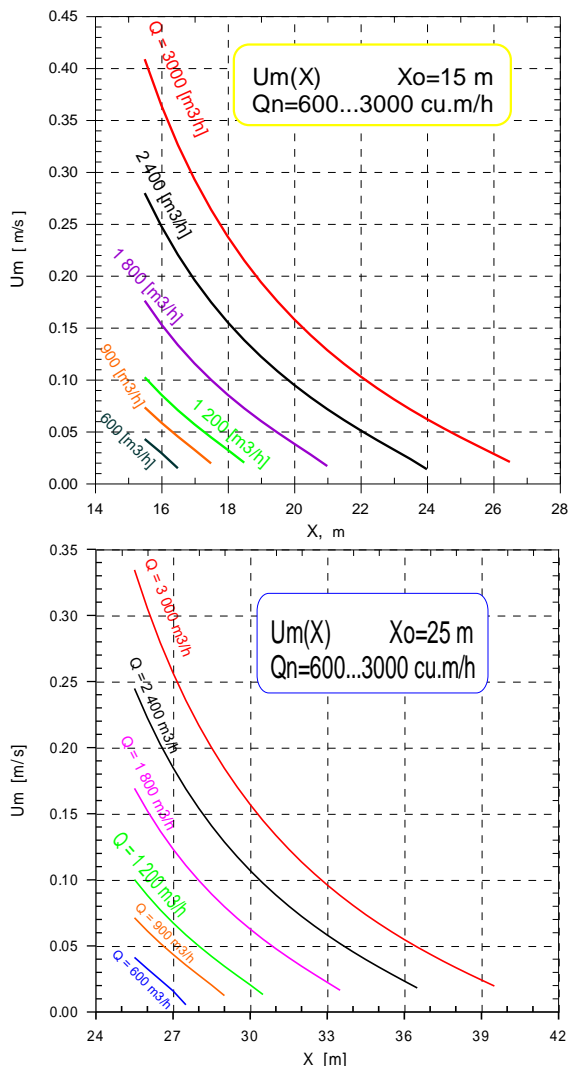


Figure 7. Maximal jet velocity variation

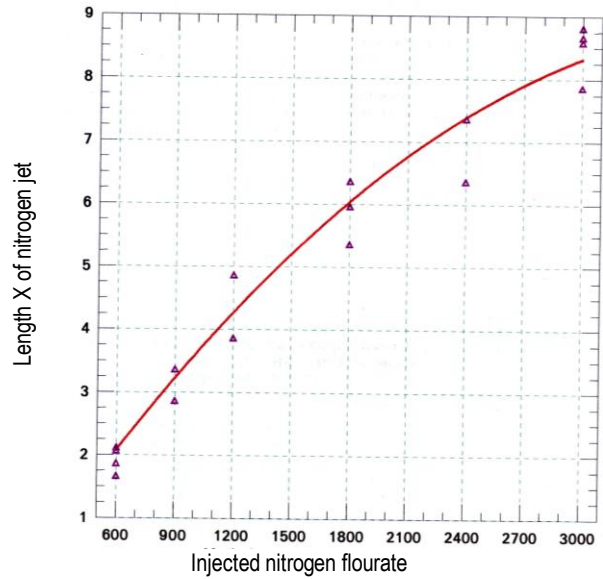


Figure 8. Nitrogen jet length

DISCUSSION

Research of nitrogen jet distribution in porous environment should provide answers to the following important issues:

- ⇒ Variation of main hydrodynamic parameters – velocity and expansion of jet flow; impact of variable porous characteristics, of main airflow and its initial velocity, on the resultant jet flow;
- ⇒ Distributions of nitrogen jet velocity and concentration at jet section end. These distributions are boundary conditions for investigation of N-jet impact in the remaining larger gob portion;
- ⇒ Efficiency of inertization with the method presently employed. The negative answer to this issue would require looking for alternative decisions in order to optimize technology including decisions that allow combined use of other methods for prevention and extinguishing of sponcom gob fires.

**Variation of main hydrodynamic jet flow parameters .** In the above-resolved variants, nitrogen flow is 18.4% to 93.5% of air leakage flow into gob area. Initial N-jet outflow velocity at injection tube end varies from 21 m/s to 106 m/s. Immediately after leaving the pipe, the jet hits the porous environment at a height of 1 m from gob floor and the velocity is sharply reduced whilst expanding in width and height. Numerical experiments show leap-wise expansion until the first 5 injector diameters ( $5b_0$ ) in flow direction

Jet expansion along gob height ( $z$ ) takes place a lot faster that along gob area because of the resistance around the intake gate pillar ( $y=0$  on fig.1). On completion of expansion in height, maximal velocity is reduced to 7...35 m/s, for injected quantities of  $Q_{N_2}$ . This reduction is accompanied by significant and fast increase of static pressure thus making injection of large nitrogen quantities near the face inefficient. This inefficiency involves premature outflow of injected

nitrogen from the gob before the atmosphere has been neutralized. Such outflow ("shortcut") practically takes place in the first third of face length. Injected nitrogen can not reach even the danger zone [2,6] in the vicinity of gob balance line. Another inefficiency of large volume injecting is related to the ejection phenomenon involved in outflow of high-velocity jet. Area expansion of the nitrogen jet (fig.6), semi-restricted by the intake gate pillar ( $y=0$  on fig.1) ends at 15 to 80 injector diameters in flow direction. Considering flow filtration nature and the relationship between environment porosity  $\varepsilon$  and extracted seam thickness, we believe that seam thickness is the more important factor. In relation to seam thickness, jet decomposition takes place at 0,55.m 2,93.m, where "m" is extracted seam thickness.

Semi-restricted nitrogen jet in the porous gob environment (fig.8) disintegrates a lot faster than a similar jet in free air and in main flow [6]. On the other hand, the jet disintegrates less but slower in non-uniform environment than in uniform one ( $d_e = \text{const}$  and  $\varepsilon = \text{const}$ ). This can be explained by naturally varying characteristics of porous environment presented in the flow model by  $\alpha_{xy}$  and  $\beta_{xy}$ . In the expansion zone, filtration resistance is increasing faster crosswise than longitudinally that is why the expansion (fig.6) takes place significantly slower than in uniform porous environment. This is the reason why the jet disintegrates more slowly in natural non-uniformity.

Velocity profiles on fig. 5 show displacement of maximal velocity from 0.1m to 2m from restricting pillar. At jet flow end, velocity is approximately 1 cm/s, i.e. significantly higher than undisturbed main flow velocity in the same profile.

With increase of initial nitrogen outflow velocity, the rate of maximal velocity reduction also increases (fig.7). The graph clearly show the impact of viscous and inertia losses in porous environment on these changes. Maximum velocity reduction shown on the figures, is almost linear for small quantities  $Q_N=600 \text{ m}^3/\text{h}$  and  $Q_N=900 \text{ m}^3/\text{h}$  and parabolic at  $Q_N=3000 \text{ m}^3/\text{h}$ . The curves on the figures follow from numerical modeling without additional approximation. Deeper into the gob ( $x_0 \uparrow$ ) maximal velocity  $U_m(x)$  reduction rate slows down (fig.7). Gob compaction, through change of  $\varepsilon$ , increases  $\alpha_{xy}$  and  $\beta_{xy}$ . This leads to increase in outflow velocity but also to significantly greater pressure losses in flow direction. As a result, maximal velocity reduction rate  $\left(\frac{dU_m}{dx}\right)$  slows down (fig.7).

With injected quantity increased, jet expansion angle decreases (fig.6). However, velocity gradient increases, between jet and main flow in the hydrodynamic boundary layer. This is one precondition for jet ejection factor increase.

With injector lagging behind face retreat ( $x_0 \uparrow$ ), gob resistance increases ( $\alpha_{xy} \uparrow, \beta_{xy} \uparrow$ ) behind outflow point ( $x > x_0$ ). Additional ejection of air from nitrogen jet, due to increase of outflow velocity, is an adverse effect, which, in

addition to causing inert substance concentration decrease, also slows down main filtration flow outside jet distribution zone ( $x \in 0 \dots B$ ). As a result, in the adjacent zone ( $B < x < 0.5L_f$ ), heat exchange conditions favoring sponcom become significantly better.[6].

## CONCLUSIONS AND RECOMMENDATIONS

### Advantages and weak points of employed injection method.

Injection method – through a single pipe left in the gob at a height of 1 m above floor, has the following advantages:

- ⇒ In jet influence zone, oxygen concentration remains low thus preventing and suppressing coal oxidation;
- ⇒ The jet provides convective cooling to coal due to temperature gradient and high outflow velocity;
- ⇒ high outflow velocity ensures deeper penetration of nitrogen along gob contour, which is very important because of the coal left in pillars until first roof break;
- ⇒ simple injecting equipment.

The major weak points of conventional injection method, borrowed from Charbonnage de France, are as follows:

- ⇒ air ejection from the N-jet has adverse effect on injection both near the face and in gob depth;
- ⇒ nitrogen backflow during injection near the face (small  $x_0$ ) in large quantities ( $Q_N$ );
- ⇒ high-velocity nitrogen outflow ( $w_{10}$ ) leads to excessive coal drying in the jet influence zone. It could be assumed that such drying causes micro-fissures and additional structural damage of coal;
- ⇒ jet zone covers a too small portion (2-6%) of gob area, making jet suppression of sponcom fires with increased nitrogen quantities  $Q_N$  non- cost effective. Attempts for nitrogen quantity increase become ridiculous where coal is left throughout the entire gob area and particularly where  $y < 1/3L_f$  - i.e. 1/3 of face length adjacent to intake gate;
- ⇒ it becomes inherently impossible to discontinue nitrogen injection without undertaking any other fire prevention measures. Any termination of nitrogen injection impacts negatively jet influence zone wherein:

*the temperature rises most*

*convective heat transfer radically worsens because of manifold reduction of velocity and temperature gradient; coal is most dried up thus shortening the sponcom time- the stage of moisture evaporation[8] is missed.*

Lack of theoretical and field research on nitrogen distribution is the reason why in recent year inertization has been thought a panacea for oxidation process suppression. Though such thinking has been refuted many times, it still exists in Babino Mine. Increase of nitrogen injection, even to hazardous quantities leading to oxygen deficiency in the face, has caused more than once isolation of mining areas rather than prevention of sponcom.

### Efficient change of nitrogen injection mode.

Not all weak point can be avoided. Some of those are inherent to nitrogen injection method. Others, however, can be minimized and even avoided as shown in [6] and

evidenced by the results from numerical experiments of jet distribution.

First, it is necessary to reduce initial nitrogen outflow velocity  $w_{10}$ . This can be accomplished by:

⇒ injection through several pipes (increase of jet number).  
The issues of pipe rotation has also been analyzed as alternative;

⇒ linear distribution of outflow;

⇒ area distribution of outflow;

Possible technology solutions are merit listed in [6]. A variant was selected based on comparative analysis, theoretical and practical considerations. Possibilities were also taken into account of combined application of other methods for sponcom prevention and suppression. On the basis of such analysis, in [6] an injector configuration is proposed along intake road. The proposed configuration ensures outflow velocity  $w_{10}$  decrease via splitting nitrogen quantity  $Q_N$  into three jets and locating outflows along height ( $z$ ) and length ( $x_0$ ). This in turn ensures three-phase increase of gradient ( $u_{10}$ - $u_{20}$ ) between jet and main flows with sufficient horizontal and vertical spacing of injector holes for more uniform velocity. Three-phase injection is an important precondition for reducing jet and main flow mixing distance. Hole location promotes three-phase static pressure increase, this pressure being the highest at the most remote injector from caving line. This injector is subjected to load from previous two pressure phases thus preventing air injection from face junction ( $x=0, y=0$ ) with air intake gate.

Moreover, injection zone processing should be mandatory prior to and after injection. Prior to injection, foam pulp may be applied, and after injection - foaming substances' injection or flooding with pulp depending on gob incline in the pillar area and injection depth. The opportunity for more efficient foam pulp and pulp injection is an important advantage of three-point nitrogen injection.

Changes in nitrogen injection mode are necessary in terms of injection start point and quantity. Our research shows that injection at  $x_0 < 15m$  is inadmissible, and at  $x_0 = 20m$  - undesirable of quantities  $Q_N > 1200m^3/h$ .

The model allows optimization of nitrogen injection parameters in the jet flow zone. Model solution is applied successfully for specifying boundary and initial conditions in the nitrogen flow distribution model in the main air leakage flow [2], the latter model supplementing the nitrogen inertization picture for the entire gob area.

DENOTATIONS

$$A_{11} = \varphi_{10} \quad A_{12} = -\bar{u}_2$$

$$A_{13} = \bar{b}_0 + (1 - k_1 x_0)(1 - b_0)m - \bar{u}_2$$

$$A_{21}(1 + \beta_x)\varphi_{11} \quad A_{22} = \frac{\alpha_x \varphi_{10} v}{u_{10}}$$

$$A_{25} = \bar{b}_0 + (1 - k_1 x_0)(1 - b_0)m^2 - 0.64 \bar{u}_2^2 - \tau_o \bar{x}$$

$$A_{23} = -\varphi_{p1} \quad A_{24} = -0.64 \bar{u}_2^2$$

$$A_{31} = \varphi_{12} \quad A_{32} = 2 \varphi_{21} \alpha \quad A_{33} = 2 \frac{v}{u_{10}} \varphi_{22}$$

$$A_{34} = \varphi_{11} \frac{v \alpha_x}{u_{10}} \quad A_{35} = \varphi_{12} \beta_x$$

$$A_{41} = \frac{1}{\varphi_x} \bar{b}_0 \frac{\rho_a}{\rho_g}$$

$$\varphi_{10} = \int_0^1 f_1 d\xi = 0.795 \quad \varphi_{11} = \int_0^1 f_1^2 d\xi = 0.560 \quad \varphi_{12}$$

$$= \int_0^1 f_1^3 d\xi = 0.565 \quad \varphi_{21} = \int_0^1 f_1 f_p d\xi = 0.450$$

$$\varphi_{22} = \int_0^1 \left[ \frac{\partial}{\partial \xi} (f_1) \right]^2 d\xi = -0.738 \quad \varphi_p = \int_0^1 f_p d\xi = 0.500$$

$$\varphi_N = \int_0^1 f_1 \sqrt{f} d\xi = 0.524 \quad f = \left( 1 - \xi^{\frac{3}{2}} \right)^2$$

$$\alpha_x = \begin{cases} 3a 0 \leq x_0 \leq 10 \Rightarrow \alpha_x = 2615938 \\ 3a x > 10 \Rightarrow \alpha_x = 1,57 \times 10^6 + 161132 \otimes x_0 - \\ - 3372,76 \otimes x_0^2 + 34,069 \otimes x_0^3 - 0,128 \otimes x_0^4 \end{cases}$$

$$\beta_x = \begin{cases} 3a 0 \leq x_0 \leq 10 \Rightarrow \beta_x = 895,4167 \\ 3a x_0 > 10 \Rightarrow \beta_x = 78,876 + 126,329 \otimes x_0 - \\ - 1,35163 \otimes x_0^2 + 0,0596 \otimes x_0^3 \end{cases}$$

$$\text{erf}(0.68\xi) = 0.7675\xi - 0.1183\xi^3 + 0.0164\xi^5$$

REFERENCES

Michaylov M., E. Vlasseva. Modeling of Methane Distribution in a Gob Area of Coal Face. Proceeding of 1<sup>st</sup> International Symposium of Mine Environmental Engineering, Turkey, July 1996.

Michaylov M., E. Vlasseva. Modelling of Gob Inertization with Nitrogen, 8<sup>th</sup> US Mine Ventilation Symposium, June 11-17 1999, Rolla Missouri.

Луицянский Л.Г. Механика жидкости и газа. М.Наука. 1987.

Маджирски В. Гидродинамика. София. Техника, 1995.

Michaylov M., E. Vlasseva. Моделиране на разпределението на метан в обрушеното пространство. Доклад 3.2 по дог.123-3 "Теоретични изследвания върху ендеогенната пожароопасност на обрушеното пространство". Архив НИС на МГУ, декември 1997.

Michaylov M., E. Vlasseva. Моделиране на разпространението на азот в обрушеното пространство-експерименти за определяне на благоприятното масто и режим на инжектиране. Доклад 3.3 по дог.123-3 "Теоретични изследвания върху ендеогенната пожаро-

опасност на обрушеното пространство". Архив НИС на МГУ, септември 1998.  
Теория турбулентных струй. Под.ред. Абрамовича Г.Н. М.Наука, 1984.

Markov Chr., M. Michaylov, (1989), Study of Self-heating Liability of Coal Seams of Bobov Dol Coal Field. *NITI "Minproject" RI, v. XXVII.*

*Recommended for publication by Department of Mine Ventilation and Occupational Safety, Faculty of Mining Technology*

## ISSUES OF NOISE OF MINE FANS

Nikolay Nikolov

University of mining and Geology "St. Ivan Rilski"  
Sofia 1700, Bulgaria  
E-mail: ustra@abv.bg

### ABSTRACT

Non-stationary processes, related to the operation of mine fans are the major source of their noise. They are aerodynamic, related to the operation of mine fans or mechanical, related to vibrations of construction. Aerodynamic components prevail in the noise spectrum of well-constructed and correctly used fans, and mechanical components prevail in the other cases.

Empirical investigations show that noise of the most widely distributed fans exceed significantly the regulations for working places and working zones of enterprises (table 1)

Practice reveals that different activities may be undertaken to reduce noise of mine fans: constructive decisions, for example optimizing the number, shape and inclination of fan blades, use of noise dampers, aerodynamic decisions like suitable profile of channels, correct use of the ventilation set.

Mine ventilation is an important process in the functioning of underground mines. However, continuously working fans bring not only the life-giving airflow but continuous noise, as well.

As it is well-known, noise is a multitude of sounds of irregularly distributed frequencies and phases, from the point of view of "listeners" it is each unwanted sound.

The main source of noise of fans are the non-stationary processes related to their operation. They might be aerodynamic, related to operation of fans, or mechanical, related to vibration of constructions.

Aerodynamic processes might be classified into the following groups:

1. Whirl noise, which appears between blades, or it is caused by whirls, which originate in the casing of a fan.
2. Periodical pulsation caused by non-homogeneous flow of limited number of blades or certain obstacles on the flow.
3. Pulsation of speed and sound pressure in the boundary layer of the casing of the fan.
4. Low speeds bring to the origination of sounds of the interconnection fan-ventilation ducts.

Mechanical noises in the fans appear in bearings, in the pipe sleeves and in the gears.

A strict consideration shows that noise of the motor and reducer does not refer directly to the fan, although that they compose a significant portion of the noise of the integration fan + motor (ventilation set).

Aerodynamic components prevail in the noise of well-constructed and correctly used fans, and mechanical components – in the other cases.

Distribution of noise in the area is determined by the type of source. Fig. 1 shows a diagram of the relative change of sound depending on the deviation from the axis of fan. The average value of all directions is accepted as one.

The hearing system of the human is sensitive for values of sound pressure –

$$I = 20 \lg \frac{P}{P_0}, \quad (1)$$

and a threshold pressure of  $p_0 = 2 \cdot 10^{-5}$  Pa for normal atmospheric conditions corresponds to a threshold of intensity

$$I_0 = \frac{p_0^2}{\rho_0 c_0}, \quad (2)$$

where  $\rho_0 c_0$  is the acoustic resistance of medium (410 Pa.s/m). Accepted threshold intensity is  $I_0 = 10^{-12}$  W/m<sup>2</sup>.

Main mine fans are characterized with significant productivity and pressure. Noise from them is significant and effects on everything, which is temporarily or constantly close to ventilation workings. As far as low frequencies are prevailing – from 63 to 250 Hz (fig. 2), noise for certain conditions may be distributed to 2-3 km.

One or two discrete frequencies are separated in the spectrum of noise of axial fans. –

$$f = \frac{m \cdot n \cdot z}{60}, \quad (3)$$

where  $m = 1, 2, 3, \dots$   
 $n$  is the number of revolutions for 1 min;  
 $z$  – number of blades.

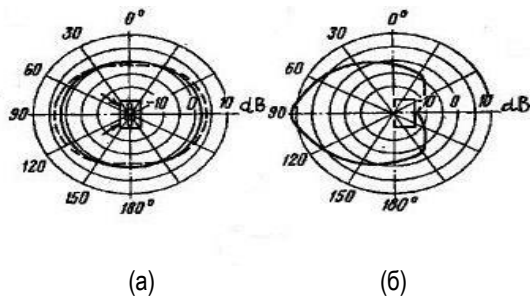


Figure 1. Distribution of noise from different sources: axial fan (a) and main fan (b) [3]

That makes the noise especially unpleasant for people.

Empirical investigations [3], show that noise from the most widely distributed fans exceeds significantly the regulations for constant working places and working zones in the enterprises (table 1).

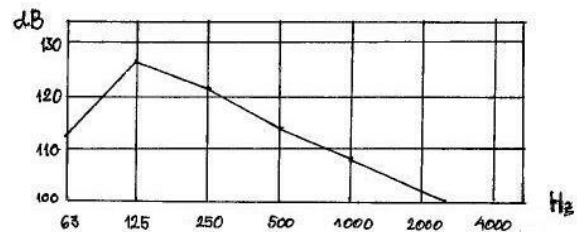


Figure 2. Average characteristic of noise from a fan main ventilation for 750 rev/min.

Table 1

|   | Sound pressure dB, for frequency of sound Hz |         |        |        |        |        |        |        |
|---|--|---------|--------|--------|--------|--------|--------|--------|
|   | 63   | 125     | 250    | 500    | 1000   | 2000   | 4000   | 8000   |
| According to regulations                        | 94   | 87      | 81     | 78     | 75     | 73     | 71     | 69     |
| Measured values for axial fans                  | 103-135                                      | 100-141 | 92-133 | 98-128 | 95-124 | 85-118 | 80-114 | 76-111 |
| Measured values for centrifugal fans            | 76-89  | 76-82   | 74-82  | 66-86  | 61-79  | 60-75  | 58-68  | 54-66  |
| Measured values for fans for local ventilation. | 63-84  | 58-81   | 59-86  | 74-92  | 82-91  | 74-95  | 72-98  | 62-94  |

Centrifugal main fans are not only more economical but also possess better aerodynamic characteristics and are less noisy. Their noise is within low frequencies and it is not so irritating (see table 1).

Fans for local ventilation are widely applied when mine workings are driven in the stopes. Number of fans for local ventilation depend on topology of workings. Their overall productivity may exceed the productivity of the main fan.

Fans for local ventilation need to be applicable for assembly in narrow places, economical, possessing working characteristics covering wide range of exploitation modes. For that reason, they have small diameter of the working wheel but high speed of rotation (up to 3000 rev/min). That brings to noise with unpleasant impact.

Noise is emitted from suction and compressive orifices of the casing of the fan. The main source of noise is one of the orifices of the fan, as the other is fastened to the ventilation pipe.

Empirical data for the level of noise at a distance of 10 km from fans for local ventilation are given in table 1. There is a

dependence between sound pressure and mode of operation – enhancement of the value for maximum productivity and pressure and minimum noise for use of fan with maximum efficiency.

Pneumatic fans for local ventilation have worse characteristics for force and spectrum of noise. The pneumomotor is an additional source of noise with high frequency, brought by a flow of compressed air between the blades. That noise overlapping with the noise of the fan itself and noise of outgoing compressed air.

Practice reveals that reduction of noise of mine fans involves varied measures. First of all, those are constructive decisions like optimization of number, shape and inclination of blades. Revolutions of the fan are also important.

A similar decision is the use of noise dampers. Most often those devices damp the noise from the casing of fan. Reduction of noise of the inlet, especially outlet flow is achieved by aerodynamic decisions – suitable profiles of channels.

Use of ventilation sets also has a varied effect on the enhancement or decrease of noise, for example:

- Use of mode of maximum productivity (high revolutions) involves much more load and unpleasant noise.
- in the case, when nevertheless of noise and vibrations the fans is still going to be used, there is a bad circle and harmful effects are enhanced;
- Non-professional performed repairs and adjustments do not limit but in some cases enhance the noise.

Unfavorable effects on health are known for humans, exposed to continuous loud noise, especially noise of prevailing high frequencies. That requires the drawing of

special attention of mining managers, of different rank, on that issue.

#### REFERENCES

- Babak, G. A., Bazrov, K. П. et al., 1982. Ventilation sets for mine workings used for the main ventilation.-Handbook. – Moscow, "Nedra" Publishing Institute (in Russian).
- Gerov V., B. 1972. PUmPs. Compressors, Ventilators- Sofia, Publishing house "Technika".
- Judin, E. J., Terehin, A. C. 1985. Against the noise of mine ventilators. - Moscow, Publishing house "Nedra".

*Recommended for publication by Department of  
Mine Ventilation and Occupational Safety, Faculty of Mining Technology*

## REVERBERATIONS\* IN LARGE AREAS

Nikolay Nikolov

University of Mining and Geology "St. Ivan Rilski"  
Sofia 1700, Bulgaria  
E-mail: ustra@abv.bg

### ABSTRACT

Reverberation is one of the most important physical phenomena related to distribution of sound in closed halls. The dependence between number of sound reflections (N) of the form, proportions and dimensions of industrial halls is determined on the basis of a theoretical model, and therefore the reverberation.

Reverberation is the presence of a gradually damping sound in an in-door hall after the cease of sound from the principal source. That phenomenon is observed in last closed areas, including processing plants, premises for repair of heavy-duty mechanization etc. Practically, it is established that in all the cases time for reverberation depends on a number of factors, primarily the size and shape of premise.

The time of reverberation is calculated by the formula of Airing–

$$T = - \frac{13.81}{N \ln(1 - \alpha)}, \text{ s}, \quad (1)$$

where N is the number of reverberations for unit time;  
 $\alpha$  - average coefficient of sound adsorption;

It is accepted that in the case of diffuse sound field, the average number of reflections 1s is:

$$N = \frac{cS}{4V}, \quad (2)$$

where c is the speed of sound, m/s;  
s – total area of inner walls of the premise, m<sup>2</sup>;  
V – volume of the premise, m<sup>3</sup>.

We will consider the case of a point source, the model of which is similar enough to real conditions.

Premises in industrial buildings most often are of the shape of a rectangular parallelepiped, their inner walls are practically plain and sound reflecting.

Then (fig.1)

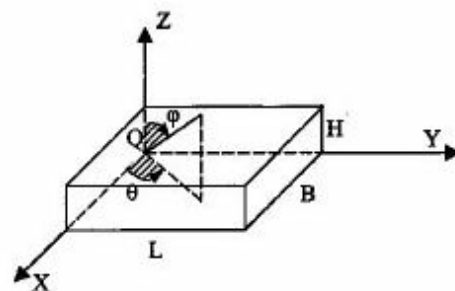


Figure 1.

$$V = B.L.H, \text{ m}^3, \\ S = 2(L.H + B.H + B.L), \text{ m}^2,$$

where L, B and H are the lengths, width and height of the premise, m.

If in the point Q there is a non-directed sound source, the sound rays going out from that point with the speed c have the following projections of the vector of speed on the three axes (X, Y and Z in fig.1):  $c \cdot \sin\varphi \cdot \cos\theta$ ,  $c \cdot \sin\varphi \cdot \sin\theta$  and  $c \cdot \cos\varphi$ . The angles  $\theta$  and  $\varphi$  may be denoted as azimuth and positioned vertical angle in the generally accepted terminology..

Number of reverberations of the bundle of rays for 1s is:

$$N = \frac{c}{B} \sin \varphi \cdot \cos \theta + \frac{c}{L} \sin \varphi \sin \theta + \frac{c}{H} \sin \varphi \quad (3)$$

\* From Latin reverberate – reflect

The total number of reverberations (from many bundles) is acquired by integration of (3) –

$$N_1 = \int_0^{\pi/2} \int_0^{\pi/2} \left( \frac{c}{B} \sin \varphi \cdot \cos \theta + \frac{c}{L} \sin \varphi \cdot \cos \theta + \frac{c}{H} \sin \alpha \right) \sin \varphi \cdot d\varphi \cdot d\theta = \frac{\pi c}{4} \cdot \frac{(L.H + B.H + B.L)}{L.B.H} = \frac{\pi c}{8} \frac{S}{V} \quad (4)$$

The formula (4), shows that in case the other conditions are equal (speed of sound and coefficient of sound adsorption), the number of reverberations is determined by the shape, proportions and sizes of the premise.

For example, for an industrial premise of dimensions 100x50x15m (V=75 000 m³)

$$N_1 = \frac{\pi c}{8} \frac{S}{V} = \frac{\pi c}{8} \frac{14500}{75000} \approx 26 \text{ rev/s.} \quad (5)$$

If the proportions are changed, however the volume is the same – for example L=200, B=37.5, H=10, number of reflections will be:

$$N_1 = \frac{\pi c}{8} \frac{19750}{75000} \approx 35 \text{ rev/s} \quad (6)$$

When one of the dimensions is significantly extended, for example (L) and the other two dimensions are approximately equal (B≈H) – a tunnel-like premise, the number of reverberations is as follows:

$$N_1 = \frac{\pi c}{8} \frac{2L.B + B^2}{L.B^2} \approx \frac{\pi c}{4\sqrt{P}}, \text{ reverb/s,} \quad (7)$$

where P is the cross section, m².

When the technological process involves industrial premises of inclined floor (fig. 2).

Then the boundaries within the integral (4) are changed (4)

$$N_1 = \int_0^{(n/2+\gamma)} \int_0^{n/2} \left( \frac{c}{B} \sin \varphi \cdot \cos \theta + \frac{c}{L} \sin \varphi \cdot \cos \theta + \frac{c}{H} \sin \alpha \right) \sin \varphi \cdot d\varphi \cdot d\theta \quad (8)$$

If the angle of slope is 15° (1/12 π), then

$$N_1 \approx \frac{\pi c}{6} \frac{L.H + B.H + B.L}{L.B.H} = \frac{\pi c}{6} \frac{S}{V}, \text{ rev/s}$$

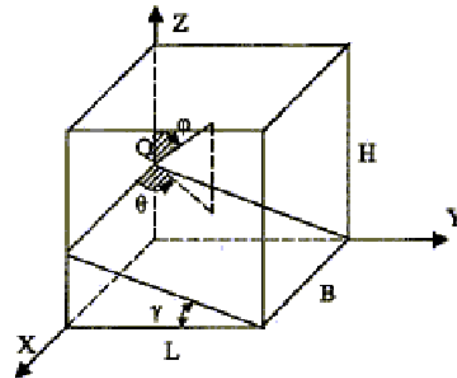


Figure 2.

In spite of the evident idealization of the accepted model, the investigations show that shape (proportions) of premises exert significant impact on the number of reflections of sound and therefore – reverberations.

REFERENCES

Conturie, L. 1960. Acoustics in civil engineering (translation from French), Moscow, Gosstroyizdat.  
 Makrinenko, L., Nikolov, N. 1984. On the effect of shape of premises on the time for reverberation. *Civil Engineering*, 1984/5.

Recommended for publication by Department of Mine Ventilation and Occupational Safety, Faculty of Mining Technology

## DYNAMICS EVALUATION OF RISK FACTORS

Vladimir Tomov

Angel Kanchev University of Rousse

Rousse 7017 Bulgaria E-mail: [vtomov@ru.acad.bg](mailto:vtomov@ru.acad.bg)

### ABSTRACT

In conventional studies of risk, the risk factors are assumed to be determined or random values. By the probabilistic method of study the statistical laws of distribution and the relevant numerical values are established. Nevertheless it takes into account the random character of risk factors, this approach is static and does not take into account their time dynamics.

In this work risk factors are analyzed as random processes on the basis of their continuous realizations.

It establishes: mathematical expectation and their dispersion; correlation function and its normalized value; spectral density and its normalized value.

The use of this approach allows evaluation of their time dynamics.

By applying the theory of random ejection two criteria are introduced – numbers of exceeding of the limit values per unit of time and duration of exceeding. On the basis of these criteria, as well as on the basis of the above-described characteristics, summarized evaluation of risk factors is made. The introduced criteria are established under specific confidence level, which is specified depending on the significance and degree of certainty of the examination. By this method the objective character of variation of risk factors is taken into account and evaluation of their dynamics is made.

Currently the methods of examination of risk factors are based on discrete measurements in time. Arithmetical mean values are determined and then they are compared to the limit values. On the basis of this comparison conclusions are made for the degree of compliance with the standard values.

In fact risk factors are dynamic processes that feature significant variations. The discrete measurements are not able to report that dynamics and so their evaluation is not objective.

In order to eliminate the mentioned disadvantages of discrete measurements, probabilistic-statistical method of analysis and evaluation is experimentally applied. It is based on the theory of random processes [1].

Continuous risk factors with normal distribution are examined. Function and density of distribution are used as its basic statistical characteristics [1].

Their probabilistic characteristics are derived:

- mathematical expectation  $m_x(t)$ ;
- dispersion  $\sigma_x^2(t)$ ;
- correlation function  $R(\tau)$ ;
- spectral density  $S(\omega)$ .

Verification for stationariness and ergodicity is made:

Stationariness is examined in its wide sense, characterized with the equalities:

- $m_x(t) = m_x = \text{const.}$ ,
- $\sigma_x^2(t) = \sigma_x^2 = \text{const.}$ ,
- $R_x(t_1, t_2) = R_x(t_2 - t_1) = R_x(t)$ .

Ergodicity is accepted on the basis of coincidence of the statistical characteristics, calculated according to the numbers of realizations, with those, calculated for continuous enough and averaged in time realization of immissions. As a result determination of probabilistic characteristics is simplified:

$$m[x] = \lim_{T \rightarrow \infty} \frac{1}{T} \int_0^T x(t) dt;$$

$$\sigma_x^2[t] = \lim_{T \rightarrow \infty} \frac{1}{T} \int_0^T [x(t)]^2 dt;$$

$$R_x(t) = \lim_{T \rightarrow \infty} \frac{1}{T} \int_0^T x(t) x(t + \tau) dt,$$

where  $\overset{\circ}{x}(t) = x(t) - m(x)$  is the centred realization of random processes.

Correlation function and spectral density are applied to find out the internal structure of processes of risk factors. They are related to the transformations:

$$R_x(\tau) = \int_0^{\infty} S_x(\omega) \cos \omega \tau d\omega;$$

$$S_x(\omega) = \int_0^{\infty} R_x(\tau) \cos \omega \tau d\tau.$$

Practically the aim is that through the correlation function  $R_x(\tau)$  to be established the process links and the character of progress as a function of time, and through the spectral density its  $S_x(\omega)$ -frequency composition.

The normalized correlation functions  $\rho(\tau)$  and the normalized spectral densities  $\sigma(\omega)$  for the whole period of observation are established, as well as their characteristics: time  $\tau_0$  of correlation drop; the average half-period  $\tau_p$ ; attenuation frequency  $\omega_p$  of correlation function; cutting frequency  $\omega_c$ ; frequency  $\omega_0$  of the maximum value of spectral density; spectral width  $\Delta\omega$ .

The modeling of continuous risk factors is made through the typical correlation function [1]

$$R(\tau) = \sigma_x^2 e^{-\mu|\tau|} \left( \cos\beta\tau + \frac{\mu}{\beta} \sin\beta|\tau| \right)$$

where  $\mu, \beta$  are coefficient of the function.

According to the valid standards emissions and immissions of a part of the risk factors are limited one-sidedly by maximum value (sound pressure level, concentrations of harmful substances, etc.) or by minimum value (for example illuminance).

Another part of risk factors are standardized two-sidedly by maximum and by minimum value. Such are temperature, relative humidity, air speed, etc.

The carried out examinations, as well as examinations of other authors show that the continuous risk factors feature normal law of distribution.

By using these results for evaluation of emissions and immissions of risk factors, we apply the theory of random ejection [2,3].

We bring the task to determination of numbers of exceeding of standard values and duration of exceeding.

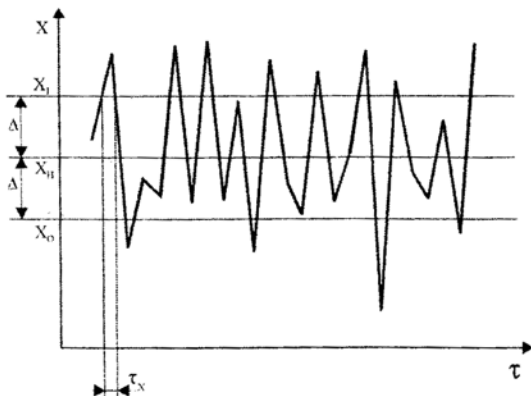


Figure 1. One-sided and two-sided limitation of hazardous values

We designate with  $X$  the characteristics of risk factors, and with  $X_0$  – the limit values that shall not be exceeded one-sidedly.

The condition not to exceed  $X_0$ , expressed through the probability  $P$  the value  $X$  to be less than  $X_0$  may be written as

$$P[X < X_0] < \alpha$$

where  $\alpha$  is the level of confidence.

The level of confidence is assumed depending on the nature of the risk factor and the degree of its influence on the particular objects ( $\alpha = 0,95; 0,99; 0,999; 0,9999$ ).

We designate the mathematical expectation with  $m_x = \langle x \rangle$  and the dispersion with  $G_x^2 = D(x)$ .

Based on the normal law of distribution the level of confidence  $\alpha$  will be:

$$\alpha = 0,5 \left[ 1 + \Phi \left( \frac{X_0 - m_x}{\sigma_x} \right) \right] \tag{1}$$

where  $\Phi(x)$  is the Laplas's function, defined as:

$$\Phi(x) = \sqrt{\frac{2}{\pi}} \int_0^x e^{-\frac{t^2}{2}} dt \tag{2}$$

From (2) follows that

$$\Phi \left( \frac{X_0 - m_x}{\sigma_x} \right) = 2\alpha - 1 \tag{3}$$

We accept the designation

$$t_{2\alpha-1} = \Phi^{-1}(2\alpha - 1) \Rightarrow \frac{X_0 - m_x}{\sigma_x} = t_{2\alpha-1} \tag{4}$$

where  $t_{2\alpha-1}$  is the quantity of the inverse function of Laplas.

From here we derive the basic condition for the limitation

$$X_0 - m_x \geq t_{2\alpha-1} \sigma_x \tag{5}$$

The values  $2\alpha-1$  and  $t_{2\alpha-1}$  are given in table 1.

Table 1 The quantity of values  $2\alpha - 1$  и  $t_{2\alpha-1}$  as a function of  $\alpha$  for emissions and immissions of risk factors with one-sided limitation:

|                 |       |      |       |        |
|-----------------|-------|------|-------|--------|
| $\alpha$        | 0,95  | 0,99 | 0,999 | 0,9999 |
| $2\alpha-1$     | 0,886 | 0,98 | 0,998 | 0,9998 |
| $t_{2\alpha-1}$ | 1,96  | 2,33 | 3,09  | 3,72   |

The condition for one-sided limitation of mathematical expectation  $m_x$  is expressed as:

$$x_0 - m_x \geq t_{2\alpha-1}\sigma_x,$$

or

$$m_x \leq x_0 - t_{2\alpha-1}.$$

For two-sided limitation the following condition is to be kept:

$$x_0 \leq x < x_1$$

where  $x_0$  and  $x_1$  are respectively lower and upper limit.

The condition for keeping these limits is:

$$P[x_0 \leq x < x_1] = \alpha. \quad (6)$$

From the condition for normal distribution follows:

$$0,5 \left[ \Phi \left( \frac{x_1 - m_x}{\sigma_x} \right) - \Phi \left( \frac{x_0 - m_x}{\sigma_x} \right) \right] = \alpha \quad (7)$$

We assume  $m_x = (x_0 + x_1)/2$ , from where

$$\Phi \left( \frac{x_1 - x_0}{2\sigma_x} \right) = \alpha \text{ or } \frac{x_1 - x_0}{2\sigma_x} = t_\alpha \Rightarrow \sigma_x = \frac{x_1 - x_0}{2t_\alpha}$$

where  $t_\alpha = \Phi(\alpha)$  is the argument of Laplas (tabl.2).

Table 2 The values of  $t_\alpha$  for emissions and immissions of risk factors with two-sided limitation

|            |      |      |       |        |
|------------|------|------|-------|--------|
| $\alpha$   | 0,95 | 0,99 | 0,999 | 0,9999 |
| $t_\alpha$ | 1,42 | 2,58 | 3,29  | 3,9    |

Therefore, for risk factors with two-sided limitation the following condition shall be kept:

$$\sigma_x \leq \frac{x_1 - x_0}{2t_\alpha} \quad (8)$$

From the above two basic conclusions follow:

- The one-sided limitation of risk factors leads to limitation of their average value – the mathematical expectation;
- The two-sided limitation of hazardous values leads to limitation of their dispersion characteristics – the root-meansquare deviation.

The mentioned conclusions provide grounds to define the tolerance  $\Delta$ , which is to be introduced for specific examinations of emissions and immissions:

$$\Delta_{HX} = |x_H - m_x| \text{ и } \sigma_x = \sigma_H + \Delta_\sigma,$$

where  $x_H$  и  $\sigma_H$  are the standard values of the mathematical expectation and the root-meansquare deviation.

We examine the limitations  $x_H$  and  $\sigma_H$  with reference to the limitations of the values of characteristics of emissions and immissions of risk factors.

For one-sided limitation we get:

$$x_H \leq x_0 - t_{2\alpha-1}(\sigma_H + \Delta_\sigma) - \Delta_{HX} \quad (9)$$

Through normalization with the values  $x_H$  and  $\sigma_H$  the relative tolerances are obtained:

$$\bar{\Delta}_\sigma = \frac{\Delta_\sigma}{\sigma_H}; \quad \bar{\Delta}_x = \frac{\Delta_{HX}}{x_H}. \quad (10)$$

Then we obtain

$$\frac{x_0}{x_H} \geq 1 + t_{2\alpha-1}(1 + \bar{\Delta}_\sigma)\bar{\sigma}_H + \bar{\Delta}_x \quad (11)$$

where:  $\bar{\sigma}_H = \frac{\sigma_H}{x_H}$  is the relative root-meansquare deviation by nominal values. It is related to the variance coefficient through the relation

$$V_x = \frac{\sigma_x}{m_x},$$

Finally the limitation for the normalized parameter is obtained:

$$x_H \leq \frac{x_0}{1 + t_{2\alpha-1}(1 + \bar{\Delta}_\sigma)\bar{\sigma}_H + \bar{\Delta}_x} \quad (12)$$

The regularities of variation of ratio  $x_H/x_0$  as a function from  $\bar{\Delta}_x$  when  $\bar{\Delta}_\sigma = 0$  and different  $\bar{\sigma}_H$  for hazardous values with one-sided limitation are shown on fig. 2.

In case of two-sided limitations after introduction of tolerances we may express  $\alpha$  as follows:

$$\alpha \leq \frac{1}{2} \left\{ \Phi \left[ \frac{x_1 - (x_H + \Delta_{HX})}{\sigma_H \pm \Delta_\sigma} \right] - \Phi \left[ \frac{x_0 - (x_H \pm \Delta_{HX})}{\sigma_H \pm \Delta_\sigma} \right] \right\} < 1$$

When choosing the sign we put the condition not to be violated in the more dangerous case, i.e.:

$$\alpha \leq \frac{1}{2} \left\{ \Phi \left[ \frac{x_1 - (x_H + \Delta_{HX})}{\sigma_H + \Delta_\sigma} \right] - \Phi \left[ \frac{x_0 - (x_H - \Delta_{HX})}{\sigma_H - \Delta_\sigma} \right] \right\} < 1.$$

Since  $\alpha$  tends to one, the addends will also tend to one by absolute value. The determinant value will be the one with smaller argument. On that basis we obtain

$$-\Phi \left[ \frac{x_0 - (x_H - \Delta_{HX})}{\sigma_H - \Delta_\sigma} \right] = \Phi \left( \frac{x_H - (x_0 - \Delta_{HX})}{\sigma_H - \Delta_\sigma} \right) \cong 1$$

So the expression gets the form

$$2\alpha \leq 1 + \Phi\left(\frac{x_1 - x_H - \Delta_{HX}}{\sigma_H + \Delta_\sigma}\right) < 2 \quad (13)$$

Taking into account the lower and upper limitation

$$x_H = \frac{x_1 + x_0}{2} \quad (14)$$

we get

$$\Phi\left(\frac{\frac{x_1 - x_0}{2} - \Delta_{HX}}{\sigma_H + \Delta_\sigma}\right) \geq 2\alpha - 1 \quad (15)$$

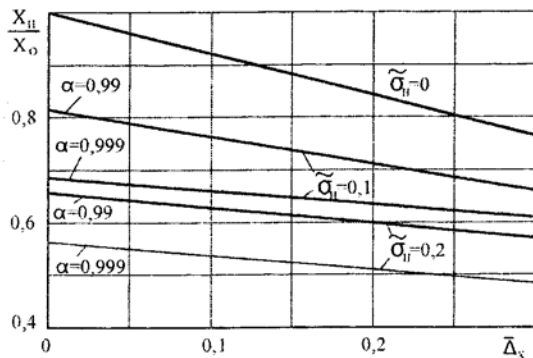


Figure 2. Regularities of variation of  $x_H/x_0$  as a function of  $\Delta_x$  for risk factors with one-sided limitation

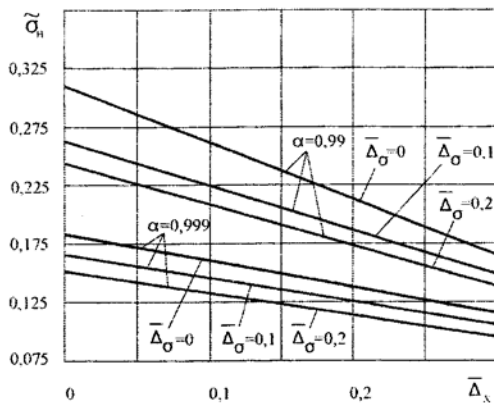


Figure 3. Regularities of variation of  $\bar{\sigma}_H$  as a function of  $\Delta_x$  for risk factors with two-sided limitation.

Thereof follows that

$$\Phi\left(\frac{\frac{x_1 - x_0}{2} - \Delta_{HX}}{\sigma_H + \Delta_\sigma}\right) \geq 2\alpha - 1 \quad (15)$$

The relative tolerance will be

$$\bar{\sigma}_H \leq \frac{\bar{\delta}_x - \bar{\Delta}_x}{(1 + \Delta_\sigma)t_{2\alpha-1}} \quad (16)$$

where  $\bar{\delta}_x = (x_1 - x_0)/(x_1 + x_0)$  is the relative value of the field of limitation of the risk factor.

The regularity of variation of  $\bar{\delta}_x$  when  $\bar{\delta}_x = 0,7$  and different  $\bar{\Delta}_\sigma$  and  $\alpha$  for risk factors with two-sided limitation is shown on fig. 3.

Exceeding of risk factors out of the area of limitations will be characterized as follows:

On the basis of the assumption that the risk factor  $x$  is a random, stationary process with mathematical expectation  $m_x$  and with the above-mentioned correlation function:

- The average numbers of exceeding  $n_{x_0}$  above  $x = x_0$  in case of one-sided tolerance is

$$n_{x_0} = \frac{\sqrt{\mu^2 + \beta^2}}{2\pi} e^{-\frac{(x_0 - m_x)^2}{2\sigma_x^2}}$$

- The average duration  $\tau_{x_0}$  of one ejection above the limit  $x_0$  is

$$\tau_{x_0} = \frac{\pi}{\sqrt{\mu^2 + \beta^2}} e^{-\frac{(x_0 - m_x)^2}{2\sigma_x^2}} \left[ 1 - \Phi\left(\frac{x_0 - m_x}{\sigma_x}\right) \right]$$

The characteristics  $x_H$  and  $\bar{\sigma}_H$  of emissions and immissions of risk factors are chosen in such a way that the probability to violate the conditions of limitation to be lower than the level of confidence  $\alpha$ .

For that reason when calculating the characteristics of exceeding the more hazardous case will be taken into account i.e. for one-sided tolerance, the following equality will be valid:

$$x_0 - m_x = t_{2\alpha-1}\sigma_x;$$

and for two-sided tolerance

$$m_x - x_0 = x_1 - m_x = t_\alpha\sigma_x.$$

Then the average numbers of exceeding  $n_{x_0}$  and their average duration  $\tau_{x_0}$  will be:

- For risk factors with one-sided limitation

$$n_{x_0} \leq \frac{\sqrt{\mu^2 + \beta^2}}{2\pi} e^{-\frac{t_{2\alpha-1}^2}{2}};$$

$$\tau_{x_0} \leq \frac{2\pi}{\sqrt{\mu^2 + \beta^2}} e^{-\frac{t_{2\alpha-1}^2}{2}} (1 - \alpha);$$

- for risk factors with two-sided limitation

$$n_{x_0} \leq \frac{\sqrt{\mu^2 + \beta^2}}{\pi} e^{-\frac{t_\alpha^2}{2}};$$

$$n_{x_0} \leq \frac{\pi}{\sqrt{\mu^2 + \beta^2}} e^{-\frac{t_\alpha^2}{2}} (1 - \alpha).$$

The analysis of the derived dependencies shows the influence of the selection of a level of confidence  $\alpha$ . The values of the expressions  $n_{x_0} / \sqrt{\mu^2 + \beta^2}$  and  $\tau_{x_0} \sqrt{\mu^2 + \beta^2}$ , which are given in Table 3 depend on it.

Table 3 The values of  $n_{x_0} / \sqrt{\mu^2 + \beta^2}$  and

$\tau_{x_0} \sqrt{\mu^2 + \beta^2}$  depending on the level of confidence  $\alpha$

| Level of confidence $\alpha$ | One-sided limitation               |                                     |
|------------------------------|------------------------------------|-------------------------------------|
|                              | $n_{x_0} / \sqrt{\mu^2 + \beta^2}$ | $\tau_{x_0} \sqrt{\mu^2 + \beta^2}$ |
| 0,99                         | 0,01054                            | 0,94853                             |
| 0,999                        | 0,001344                           | 0,7439                              |
| 0,9999                       | 0,0001573                          | 0,6356                              |
| Level of confidence $\alpha$ | Two-sided limitation               |                                     |

|        | $n_{x_0} / \sqrt{\mu^2 + \beta^2}$ | $\tau_{x_0} \sqrt{\mu^2 + \beta^2}$ |
|--------|------------------------------------|-------------------------------------|
| 0,99   | 0,01141                            | 0,8761                              |
| 0,999  | 0,001421                           | 0,704                               |
| 0,9999 | 0,0001585                          | 0,6309                              |

The presented data provide opportunity to determine the numbers of exceeding and its average duration. By other side their analysis shows that upon increase of the level of confidence by one order, the time during which one limit exceeding occurs also increases approximately with an order.

The presented approach allows:

- To establish the probabilistic characteristics of risk factors, as well as the links of the process of progress;
- To determine their frequency composition;
- To evaluate the numbers and duration of exceeding of limit values in case of one-sided and two-sided limitation;
- To evaluate completely the dynamics of risk factors, which complies with their objective progress in time.

#### REFERENCES

- Бендат Д., А. Пирсон. Измерение и анализ случайных процессов. Пер. с англ. Москва, Мир, 1983.
- Тихонов В. Выбросы случайных процессов. Москва, Наука, 1970.
- Фомин Я. Теория выбросов случайных процессов. Москва, Связь, 1980.

Recommended for publication by Department of  
Mine Ventilation and Occupational Safety, Faculty of Mining Technology

## ACCIDENT RISK ASSESSMENT AT THE ELECTRICAL ENGINEERING OBJECTS ON THE LINGUISTIC

Yuliya Podobna, Pavlo Molchanov, Tetyana Holyeva

Department of Environment Safety and Industrial Protection  
Vinnytsia State Technical University  
95 Khmelnytske shose, Vinnytsia, 21021, Ukraine  
E-mail: [envrisk@vstu.vinnica.ua](mailto:envrisk@vstu.vinnica.ua)

### ABSTRACT

The method of accident risk assessment at the electrical engineering objects that including significant uncertainty of the input data is presented in this paper. The expert linguistic evaluation of the parameters of the electrical engineering object with the use of fuzzy sets is offered in the given task. It is suggested to use the method of risk-events when analyzing the risk of the electrical engineering objects. This method allows to get characteristic of the event risk together with the probability of the event occurrence at each stage of accident development. The risk-event method is based on the calculation s of the generalized tree of risk-events.

*Keywords:* risk assessment, expert linguistic evaluation, fuzzy probability, tree of risk-events

### INTRODUCTION

Recently actual and complex problem is the estimation of risk of accidents at the atomic power plants. Safety of operation of the reactor installation is very important for a radiation safety at the atomic power plant. The failure analysis of the equipment of generating sets for several years, including the period of mastering of generating sets, shows that the down time of generating sets is arranged as follows: because of turbo-installation 35,4 %, because of electrical generators - 31,3 %, because of pipelines - 14,6 %, because of an armature-13,6 %, because of transformers -3,8 %, because of reactor - 1,3 % [1].

The probability of an emergency brake of one of units of the reactor contour is rather small. Nevertheless, it is necessary to take into account the risk of rejection of the reactor, which can significantly exceed the risk of rejection of some other element of atomic plant. The solution of the given problem is complicated as many parameters of electric equipment have the large uncertainty. In such case the use of classical models of risk assessment (e.g. Monte Carlo method) [2] gives the result with uncertainty which exceeds the value of this result.

Instead of parameters with large uncertainty it is offered to use the expert linguistic logic evaluation of the parameters of the electrical engineering objects. The results of simulation have shown that the use of the Fuzzy Sets Theory [3] combined with the expert linguistic logic evaluation of the parameters the electrical engineering objects in a number of cases allows to get the risk assessment with the same accuracy as when using accurate numerical data.

### STRUCTURAL IDENTIFICATION OF THE SIMULATION OBJECT

The nuclear reactor is used as the object of simulation in this work. Reactor installation consists of the main contour, reactor contour and the contour of circulation of the heat-carrier. A number of auxiliary systems relates to reactor. These systems and the reactor contour create the first contour: the system of volume compensation, system for clearing the water of reactor, the system of replenishment and damping of the reactor, the system of drains, the system of gaseous blowings, also the system of gaseous completion of reactor laying and the system of periodical disactivation of reactor installation.

Generalized diagram of the possible accident development for the above-described object is represented on the Figure1.

Designing of the structural diagrams of the development of possible accidents at the blocks of this structure represents detail study of the research object with taken into account all the factors that influence the object safety as a whole. The forecasting problem of the development of accidental situation comes to the object identification with one output and many inputs. The particularity of the linguistic evaluation is presentation of variables interdependence "input-output" in the form of expert statements: IF <inputs>, THEN <output>, which are fuzzy knowledge bases.

The basic characteristics of the object, that may course the accident is specified. The input variables is taken as the factors that influence the output event, i.e. the factors influence the accident occurrence. The output variable is the accident occurrence probability. Structural identification of the object "input-output" is made with the help of these variables and their linguistic evaluations based on the logical operations.

When developing the structural diagram of the occurrence and development of accident, the following actions have been done:

1. Collection and investigation of the technological factors that influence to the object safety as a whole.
2. Collection and investigation of the technical factors, such as damage of heat-producing element.
3. Collection and investigation of the human factors in the object's control system.
4. Collection and investigation of the factors which relate to the environment influence on the general safety of the object.
5. Study of the logical links between the influencing factors and its consequences.

As a matter of fact, the identification of the collected factors is the source of information for the development of the event tree of the investigated object.

PRINCIPLES OF THE LINGUISTIC SIMULATION

The logic eventual model of presentation of the input information is used for the determination of fuzzy probability of accident development. This evaluation of presentation of the fuzzy information is the most acceptable as it allows to formalize experts' knowledge represented in the form of linguistic evaluation in convenient and simple way. The basic principles of identification of the objects on the basis of fuzzy databases are represented [4,5]:

**1. The principle of linguisticability** of the input and output variables. According to this principle, the object's inputs and its output are considered as linguistic variables, which are evaluated by the qualitative terms.

**2. The principle of structure formation** of the "input-output" dependence in form of the fuzzy knowledge base. The fuzzy knowledge base is the totality of rules IF "inputs" THEN "output" which reflect the expert's experience and his/her understanding of the cause-and-effect relations for the decision making (forecast) of the investigated problem.

**3. The principle of databases hierarchy.** The development of system statements about the unknown dependency "inputs-output" becomes difficult, when there are large quantity of the input variables. Due to that, it is reasonable to classify the input variables and, according to the classification, construct an output tree, which specifies the system of nested statements.

**4. The principle of the two-stage tuning of the fuzzy knowledge.** According to this principle, the model making is done in two stages. These are the stages of structural and parametrical identification. Development of the fuzzy knowledge base based on evaluation of experts corresponds to the structural identification stage. However, the tweaking of fuzzy model can be done in concordance with experimental data for complete coincidence of the expert evaluation with the experimental data. The tuning is the selection of such fuzzy "IF"-"THEN" rules and such parameters of the membership functions that minimize the difference between experimental and simulated behavior of the object.

LINGUISTIC APPROXIMATION

The analytic-linguistic approximation is used to formalize cause-and-effect relations between the "input-output" variables, which are described in natural language with the help of linguistic variables. For this purpose, indefinite parameter q, which may correspond to the probability, reliability or to other characteristic, is transformed into a fuzzy number  $\tilde{q}$ . I.e., its membership function is specified. Having the expert information about the parameter: title of the parameter q; range [q, q] of alternation of the values of parameter q; number of linguistic terms to evaluate the parameter q; title for each linguistic term; its membership function is constructed. For the triangular form of the fuzzy number q:

$$\tilde{q} = \left\langle \underline{q}, \bar{q}, \hat{q} \right\rangle, \tag{1}$$

where:  $q(\bar{q})$  is the lower (upper) boundary of the fuzzy number  $\tilde{q}$  at zero level;  $\hat{q}$  is the value of the fuzzy number  $\tilde{q}$  at a single level.

When the number of input variables is large, construction of the fuzzy knowledge base becomes difficult. That is why it is reasonable to do the classification of variables and according to it to build the inference tree, which determines a system of nested fuzzy knowledge bases tied with cause-and-effect relations. Stepwise information's about the logical connections between the events that influence the final result and calculation formulas of the probability of these events are placed into the Table 1.

Table 1: Stepwise calculation

| INPUT VARIABLES | OUTPUT EVENTS | LOGICAL OPERATION | FORMULAS OF CALCULATIONS  |   |
|-----------------|---------------|-------------------|---|---|
|                 |               |                   | $\tilde{P}$   | $\tilde{R}$   |
| $x_1, x_2, x_3$ | A             | AND               | $\tilde{P}_A = \tilde{P}_{x_1} \cdot \tilde{P}_{x_2} \cdot \tilde{P}_{x_3}$                       | $\tilde{R}_A = \sum_{i=1}^3 A_{X_i} \cdot M_{ij} + A_{X_2} \cdot M_{ij} - A_{X_3} \cdot M_{ij}$ |
| $x_4, x_5, x_6$ | B             | OR                | $\tilde{P}_B = 1 - (1 - \tilde{P}_{x_4}) \cdot (1 - \tilde{P}_{x_5}) \cdot (1 - \tilde{P}_{x_6})$ | $\tilde{R}_B = \max(A_{X_4}, A_{X_5}, A_{X_6}) \cdot M_{ij}$                                    |
| <b>A, B</b>     | T             | OR                | $\tilde{P}_T = 1 - (1 - \tilde{P}_{x_A}) \cdot (1 - \tilde{P}_{x_B})$                             | $\tilde{R}_T = \max(A_A, A_B) \cdot M_{ij}$   |

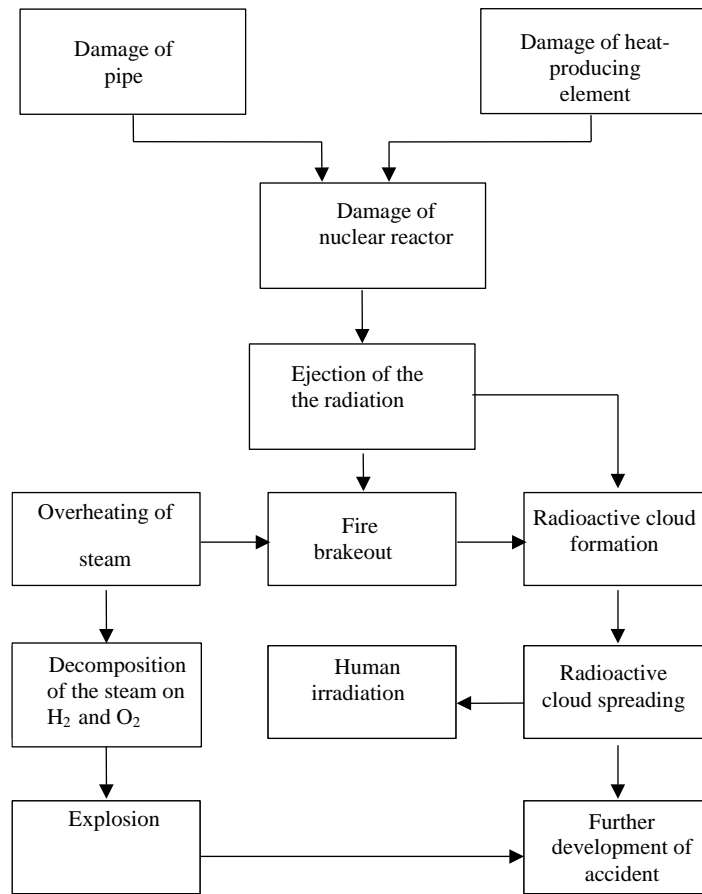


Figure 1. Generalized diagram of the possible accident development

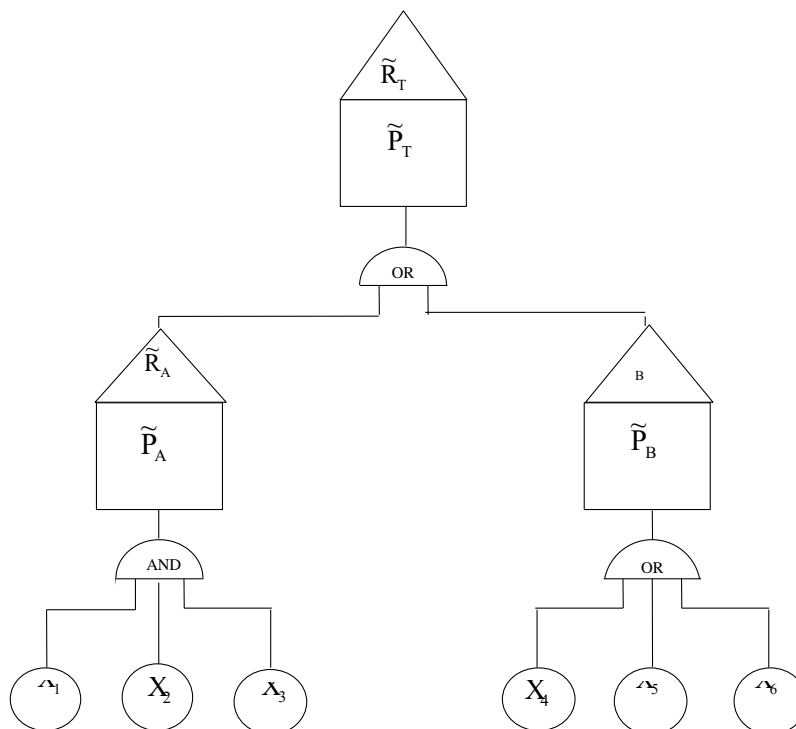


Figure 2. Fragment of the generalized tree of risk-events:  
 where:  $X_1$ - $X_6$  are basic events determined by the expert evaluation.

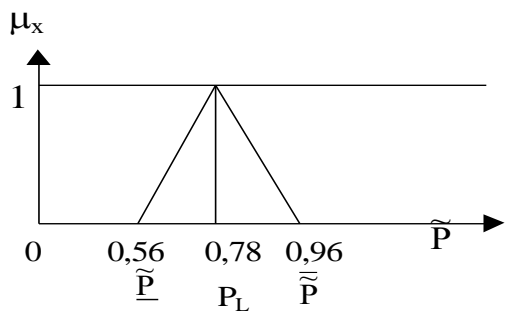


Figure 3. Membership function for  $\tilde{P}$ .

Hierarchical interconnection between the input variables, classes of input variables and the output variable is presented in the form of generalized tree of logical inference [3]. The obtained logical structure is described by the mathematical model, which takes into account the logical structure of the tree and number of its levels:

$$\tilde{P}_n = \left[ \left( \bigcup_{i=1}^k \tilde{P}_{n-1}^i \right) \vee \left( \bigcap_{i=1}^k \tilde{P}_{n-1}^i \right) \right], \quad (2)$$

where:  $\tilde{P}_n$  is the fuzzy probability of the event occurrence at n-th level;  $\tilde{P}_{n-1}^i$  is the fuzzy probability of occurrence of the i-th event at level n-1;  $\cup, \cap$  is the signs of intersection and union of the sets;  $\vee$  is the sign of the logical function "OR"; n is the number of the level at which probability is determined;  $i = 1 \dots k$  is the number of events at the given level, "~"- sign of fuzziness.

### GENERALIZED TREE OF RISK-EVENTS

The generalized tree of logical inference allows to follow up cause-and-effect relations of the accident development. It allows to analyze various scenarios of the accident development and evaluating the occurrence probability of various emergencies. However, in order to make decision about closing an accident - power engineering object or about measures of minimizing the accidental risk, it is necessary to evaluate the greatest eventual risk and accident development scenario, which is connected with it. The generalized tree of the logical inference does not provide the decision of calculation of the risk for the concrete scenario of the accident development, e.g., for the scenario that has the greatest probability and minor losses, or for the scenario that has small probability and major losses. That is why the authors suggested to introduce an additional vertex of risk applied to all basic intermediate and vertex events [5]. It is offered to call the obtained structure as event-risk method. The mathematical model that describes "AND-OR" structure of accident development and risk for the event is represented as follows:

$$\tilde{R} = \begin{cases} \sum_{k=1}^m (\tilde{A}_k \circ M_{ij}^k) \\ (\max \tilde{A}_k) \circ M_{ij}^k \end{cases}, \quad (3)$$

where:  $k = 1-m-i$  is the number of factors, which influence to the risk;  $M_{ij}^k$  is the relations matrix;  $\tilde{A}_k$  is the fuzzy losses (expenditures),  $\circ$  is the composition of fuzzy sets.

The fragment of the generalized tree of risk-events is given in Figure 2.

The advantage of the offered method is that it allows at each level of the accident development, together with the probability of the event occurrence, to get characteristic of the event risk. As a result:

- foremost, we are able to determine the event that has the greatest risk and to make appropriate decision concerning it.
- the second, when maximum of the risk is determined at each hierarchical level we can find a scenario that leads to the event with greatest risk and take measures to prevent it.
- the third when scenario of the greatest risk is known it is possible to minimize the volume and, hence, the cost of calculations which should be undertaken before decision making.

### ADEQUACY EVALUATION OF THE OBTAINED RESULT

Calculation of the fuzzy probability of the accident occurrence has to the following result:

$$\tilde{P} = (0,56; 0,96; 0,78) \quad (4)$$

The membership function, which reflects the obtained result is represented in Figure 3.

The obtained result can be interpreted as follows: the lower evaluation boundary of the accident occurrence -  $\tilde{P} = 0,56$ ; the upper -  $\tilde{P} = 0,96$ ; mean value, which corresponds to the linguistic assessment -  $\tilde{P} = 0,78$ . Thus, the span of the accident occurrence is located within 0.56 to 0.96 with the most probable value 0.78.

To evaluate the obtained result, it is necessary to calculate the degree of equality of the fuzzy sets: the set specified by the expert and the set obtained as a result of calculations. The degree of equality  $\mu(\tilde{A}, \tilde{B})$  of the fuzzy sets ( $\tilde{A}$  and  $\tilde{B}$ ) is described with the following expression [3]:

$$\mu(A, B) = \&_{x \in X} (\mu_A(x) \leftrightarrow \mu_B(x)),$$

where: " $\leftrightarrow$ " - operation of equivalency of fuzzy sentences; " $\&$ " - operation of conjunction.

If  $\mu(\tilde{A}, \tilde{B}) \geq 0,5$ , then sets  $\tilde{A}$  and  $\tilde{B}$  are fuzzy equal. Meanwhile if  $\mu(\tilde{A}, \tilde{B}) \leq 0,5$ , then sets are not fuzzy equal.

A fuzzy set specified by an expert and such that corresponds to the evaluation "High" (it means high probability of the risk of the accident occurrence) - (0,8/0,57; 0,6/0,52; 0,1/0,9). The fuzzy set obtained as a result of calculation: (0,3/0,57; 0,6/0,59; 0,7/0,72).

$$X = \{x_1, x_2, \dots, x_5\}, \quad (5)$$

$$A = \{\langle 0,8/x_1 \rangle, \langle 0,6/x_2 \rangle, \langle 0,1/x_3 \rangle\}, \quad (6)$$

$$B = \{\langle 0,3/x_1 \rangle, \langle 0,6/x_2 \rangle, \langle 0,7/x_3 \rangle, \langle 0,2/x_4 \rangle, \langle 0,3/x_5 \rangle\} \quad (7)$$

Therefore it is possible to make a conclusion about equality of fuzzy sets:  $\tilde{A} = \tilde{B}$ ;  $\mu(\tilde{A}, \tilde{B}) = 0,65$ .

### CONCLUSIONS

It is offered to use the expert linguistic logic evaluation of parameters of the power-engineering object when evaluating the risk of the objects with large uncertainty of input data. Use of the Fuzzy Sets Theory combined with expert linguistic logic evaluation of parameters of the power engineering object in many cases allows to get the risk assessment degree practically with the same uncertainty as when using accurate numerical data. It is suggested to use the risk-event method when analyzing the risk of the electrical engineering objects. The risk-events method is based on the calculations of the generalized tree of risk-events. The advantage of the suggested method is that it allows to get characteristic of the

event risk together with the probability of the event occurrence at each stage of development of the accident. As a result:

- we can determine the event that has the greatest risk and make appropriate decision regarding it;
- when maximal risk is determined at each hierarchic level, we can specify a scenario that leads to the event with greatest risk and take measures to prevent the event;
- when scenario of the greatest event risk is known it is possible to minimize the volume of calculation and, hence, time and cost of calculations to do the decision making.

### REFERENCES

- Petrosyants A. Atomic Science and Technique (1987). Moscow, 312 pp.
- Dennis C. Bley. (May 4, 2000). Accident Risk Assessment. Presented at NATO ASI : Risk Activities for the Cold War Facilities and Environmental Legacies. Bourgas, Bulgaria.
- Gene Whelan, James G. Droppo. (May 4, 2000) Advantages/Disadvantages of Multimedia Assessments. Presented at NATO ASI : Risk Activities for the Cold War Facilities and Environmental Legacies. Bourgas, Bulgaria.
- Zadeh L.A. (1965). Fuzzy Sets. Ing. Control. Vol. 18, pp.338-353.
- Rotshtayn A.P. (1999). Intellectual Technologies of Identification: Fuzzy sets, Genetic Algorithm, Neural Nets. Vinnytsia, Universum-Vinnytsia, 320 p.
- Filinyuk N.A., Molchanov P.A., Dudatiev A.V. (July 1-3, 1998). A Comprehensive Estimator of Industrial Vehicle Safety. *Int. Conf. On Advances in Vehicle Control and Safety*. Amiens-France.

•

## SPEED CONTROL SYSTEMS OF THE ELECTRICAL MOTORS WHICH ARE DRIVING THE MECHANISM OF THE ERC PORT-WHEEL EXCAVATORS

**Luminița Popescu**

"Constantin Brâncuși" University  
Str. Geneva, nr. 3  
Târgu Jiu, 1400  
Romania

**Onisifor Olaru**

"Constantin Brâncuși" University  
Str. Geneva, nr. 3  
Târgu Jiu, 1400  
Romania

**Florin Grofu**

"Constantin Brâncuși" University  
Str. Geneva, nr. 3  
Târgu Jiu, 1400  
Romania

### ABSTRACT

Due to the constructive complexity of the ERC 1400 excavators, the number of the electrical driving and their diversity is very large.

In the technological process from open pits of lignite exploitations, the excavating process takes an important role. Until the present, the most reliable ways of excavation were the excavators with port-grab wheel, which are equipments with continuous driving.

The fact that in a technological line, line composed from ERC - TMC – MH (excavator with large capacity belt rotor-conveyor – dump machines) from a day exploitation, the ERC excavator with port-wheel is the basic element, makes his safe functioning to have a primordial importance and for the other

equipments from the technological line, found in downstream from the excavator.

In table 1 are indicated some of the technical characteristics of the ERC, used in the lignite mineshafts from the Oltenia's coal basin.

Table 1

| Nr. crt. |                                       | U/M           | Excavator Type |           |           |           |
|----------|---------------------------------------|---------------|----------------|-----------|-----------|-----------|
|          |                                       |               | SRS 470        | SRS 1300  | SRS1400   | SRS 2000  |
| 1.       | Theoretical capacity                  | mc afin/h     | 1690           | 2800-3500 | 3280-3860 | 4600-6000 |
|          |                                       | mc viu/h      | 1200           | 2000-2500 | 2340-2750 | 3280-4280 |
| 2.       | Maximum cutting force                 | daN/cm        | 70/50          | 75/60     | 85/65     | 95/60     |
| 3.       | Length of the device                  | m             | 58             | 125       | 121,2     | 147       |
| 4.       | Optimal width of the excavation block | m             | 18             | 40        | 45        | 55        |
| 5.       | Excavation height                     | UP            | 15             | 26        | 30        | 30        |
|          |                                       | DOWN          | 3,5            | 3,5       | 7         | 7         |
| 6.       | Nr. of unloads – minimum              |               | 60             | 67/84     | 39/46     | 70/91     |
| 7.       | Total weight                          | tone          | 680            | 2010      | 2050      | 2933      |
| 8.       | Ground specific weight                | daN/cmp       | 1,15           | 1,10      | 1,07      | 1,13      |
| 9.       | Power supply                          | kV            | 6              | 6         | 6         | 20        |
| 10.      | Rotor installed power                 | kW            | 400            | 500       | 630       | 2x500     |
| 11.      | Maximum admitted slope - during work  |               | 1:30           | 1:33      | 1:25      | 1:33      |
|          |                                       | - in movement | 1:20           | 1:20      | 1:20      | 1:20      |
| 12.      | Total installed power                 | kW            | 1275           | 2540      | 2950      | 5110      |

The component parts of an excavator with a wheel with grabs are indicated in figure 1

The excavation device at ERC (the wheel with grabs) is droved in present with asynchronous motors with the wired rotor (with rings), with starting metallic rheostat in 3-4 steps, motors with the following characteristics: 630 kW, 6 kV, 71 A, 988 rot/min. The tuning scheme with the best results, used for this mechanism, is presented in figure 2

The working program of the pivoting excavator's pivoting mechanism with the port-grabs wheel is characterized by repeated rotations and variable rotation speeds.

In the present, for driving the pivoting mechanism, are used the following electrical engines:

- continuous current motors, in generator-motor system (figure 3) and in rectifier-motor system (figure 4);
- asynchronous motor with rotor in short-circuit (figure 5)

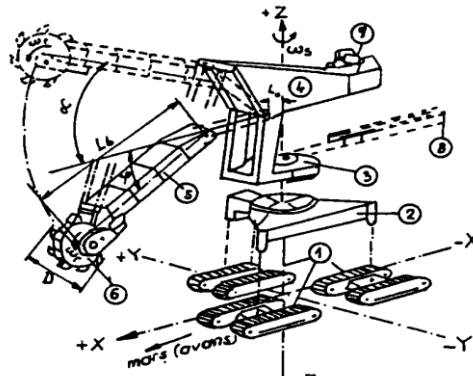


Figure 1

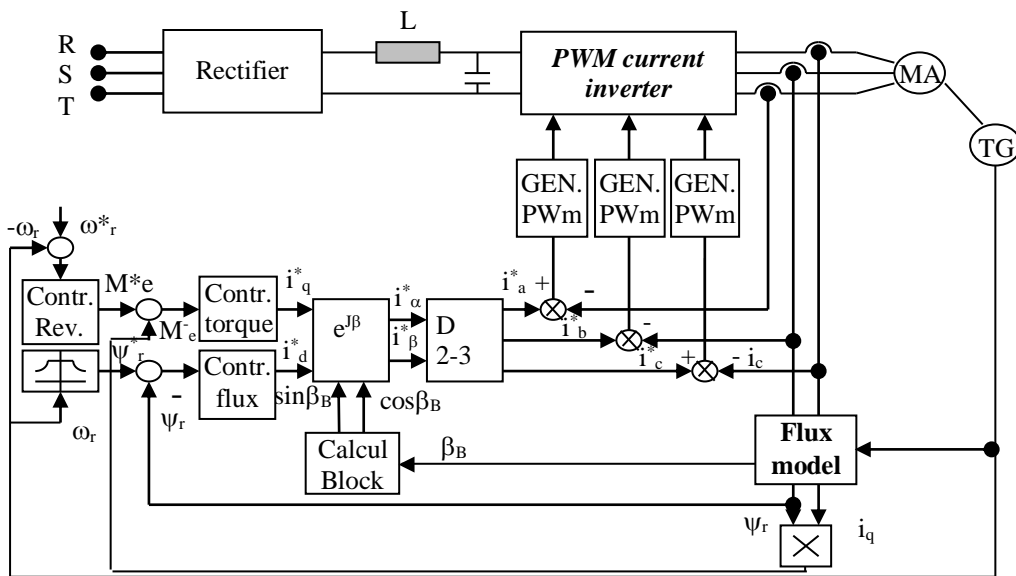


Figure 2

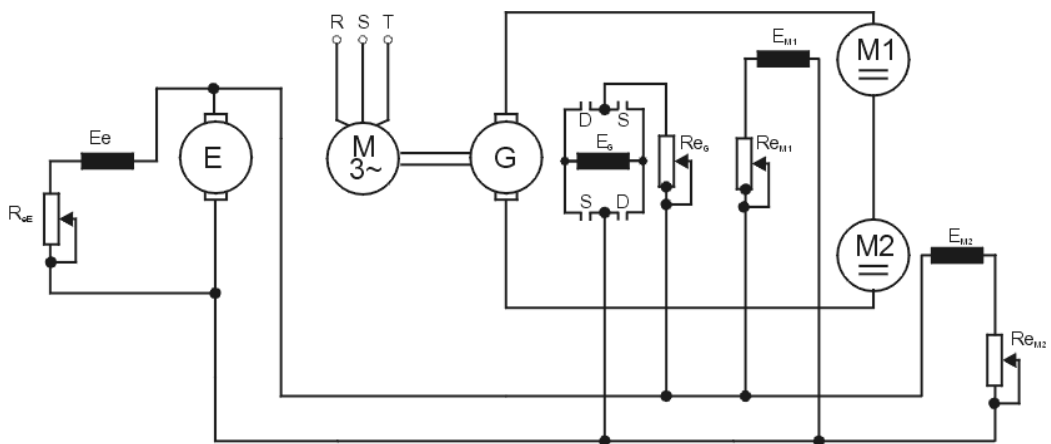


Figure 3

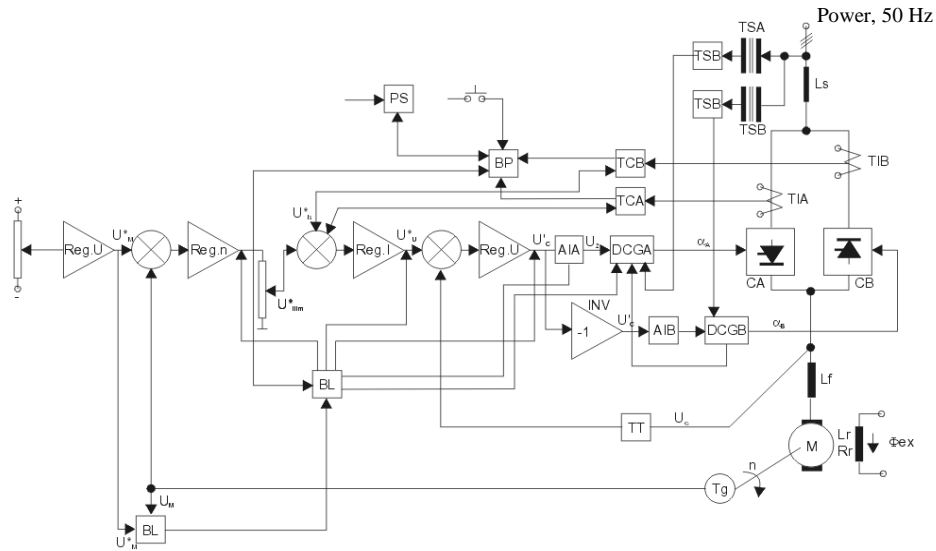


Figure 4

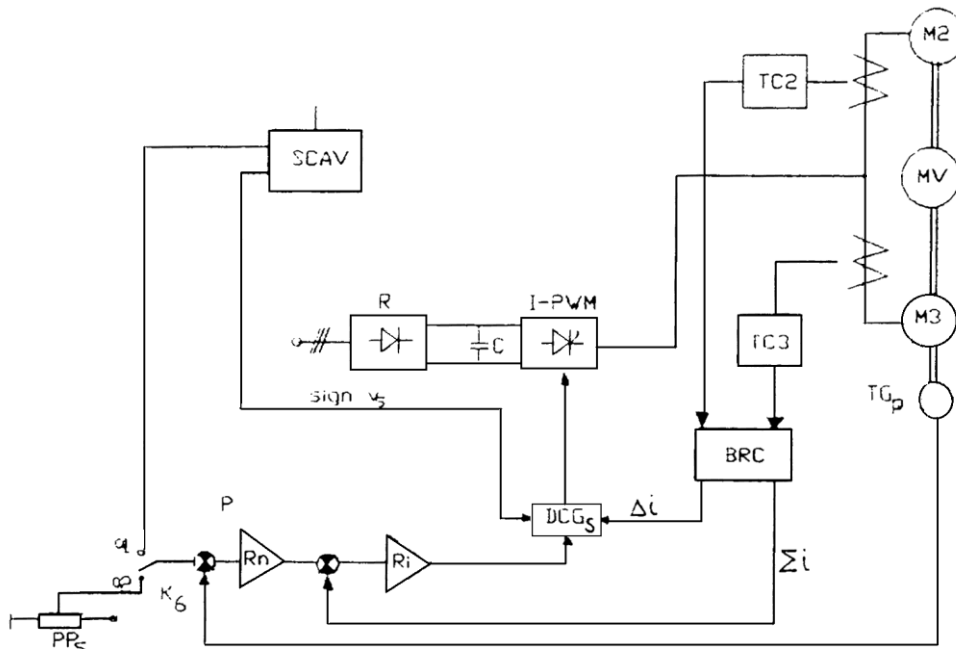


Figure 5

In the case in which is proposed the problem of maintaining a constant rapport between the grabs wheel speed and the pivoting speed, is used the electrical scheme from figure 6, where the tuning of the two speeds can be realized with the help of the two potentiometers pp<sub>s</sub> respectively pp<sub>r</sub>, or in

automatically mode, by passing the switches K<sub>5</sub> on the position a<sub>1</sub> and K<sub>6</sub> on the position a<sub>2</sub>, case in which the wheel with grabs driving motor and the superstructure driving motor will adjust the speed according with the command law of the command equipment.

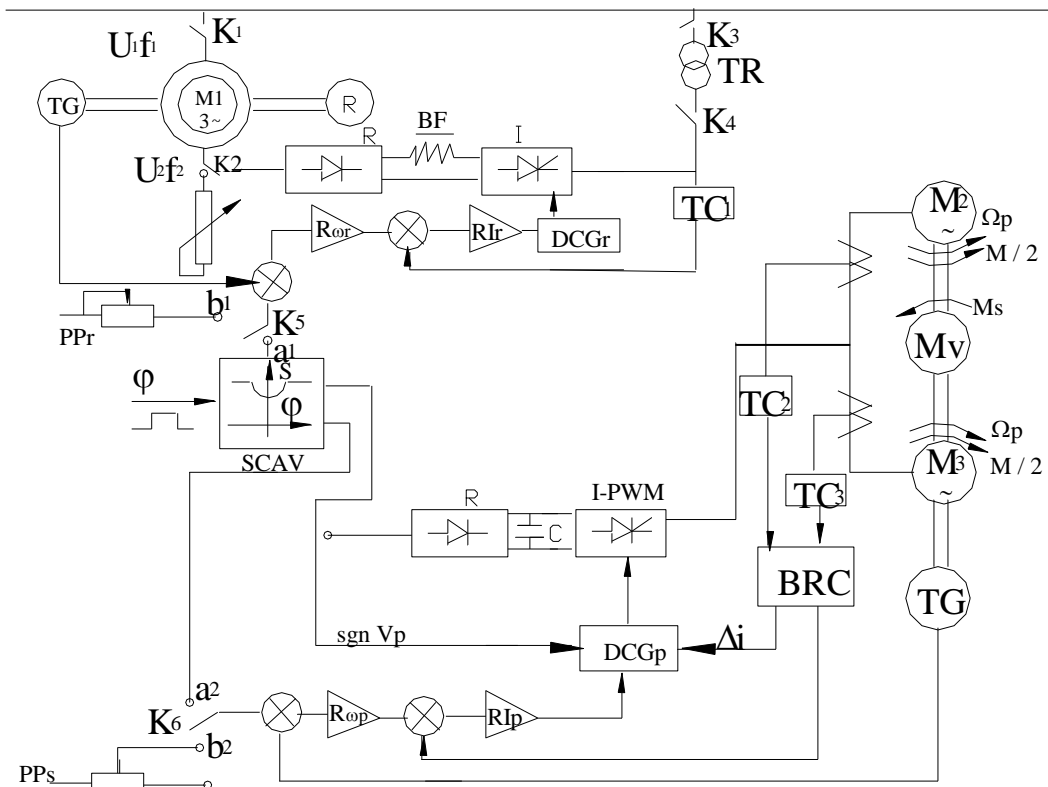


Figure 6

The lifting and descending winches of the rotorical arms from the excavators and of the halting belts at are driven by

asynchronous motors with the wired rotor with metallic rheostat starting in 3 – 4 steps (figure 7), with the driving period of 60%.

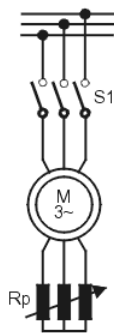


Figure 7.

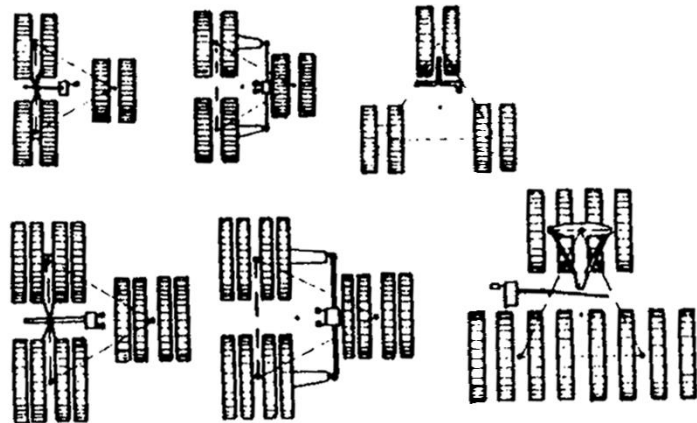


Figure 8.

According with the capacity (productivity) of the excavator (respectively of the machine), the movement system can be with two or more caterpillars groups, each of them having his own driving motor (motors) (figure 8).

The movement mechanisms at excavators with medium and large capacity rotors are driven with continuous current motors, in generator-motor system (figure 3), and at the small capacity excavators, with asynchronous motors with wired rotor and metallic rheostat starting in 3 – 4 steps (figure 7) with  $P_N = 90$  kW,  $U_N = 380V$ .

CONCLUSION

The port-grabs wheel excavator is the “leading” element in a technological line, line which also contains TMC, MH, of which functioning is depending the good functioning of all the downstream equipments.

To realize a maximum productivity with minimum power consumption is necessary to maintain a correlation between the grab wheel speed and the pivoting mechanism. To realize this desideratum is imposed to use static frequency conveyors, to supply the asynchronous motors.

REFERENCES

- L. Popescu, Improvement of commands for electrical driving in open pits for lignite exploitations, PhD. theses, Petroșani, 2000.
- N. Bercea, Trends and modernizations world wide in electrical driving domain of mining machines, Mining Magazine, no. 12, 1997

## APPLICATIONS OF STEPPING MOTORS IN MINING APPLIANCES

**Onisifor Olaru**

"Constantin Brâncuși" University  
Str. Geneva, nr. 3  
Târgu Jiu, 1400  
Romania

**Luminița Popescu**

"Constantin Brâncuși" University  
Str. Geneva, nr. 3  
Târgu Jiu, 1400  
Romania

**Gabriel Gîdei**

"Constantin Brâncuși" University  
Str. Geneva, nr. 3  
Târgu Jiu, 1400  
Romania

### ABSTRACT

The development of the hardware command structures of the stepping motors and the compatibility of these motors with the numerical technique have opened new perspectives to the control systems with stepping motors, from the point of view of appliance domains, but also from the point of view of the achieved performances. In the following article is presented the control of the ventilator's flow capacity using a stepping motor.

### CONTROLLING THE VENTILATOR'S FLOW CAPACITY

For the mining's main aeration, according with the flux capacity and with the pressure, it can choose axial or radial ventilators. Theirs action can be aspiring or refulant, and according with the necessities, some of them have the possibility to change the way of working.

To control the radial ventilators flow capacity at modern ventilators stations is used a ring-shaped device with vertical window blinds. This device is mounted at the aspiring plug of the ventilator and his driving can be realized with a stepping motor or with an electro-hydraulic stepping motor.

The principle scheme of the ring-shaped device driving with vertical window blinds with electro-hydraulic stepping motor is shown in figure 1. The stepping motor modifies the angular position of the vertical window blinds thru the medium of a mechanical system composed from: cam – lever – lighting – control cable.

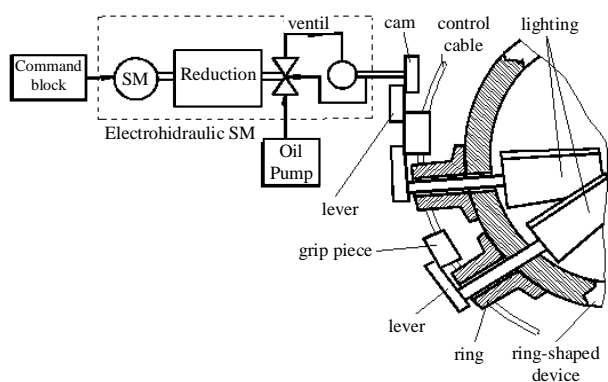


Figure 1.

Axial ventilators presents, comparing with the radial ones, numerous advantages [1].

One of these is referring to the way in which is realized the flow capacity and the pressure. This tuning is made by modifying the position angle of the pales, in the hypothesis that this angle's values are found in the execution limits of the ventilator. In the case of the axial ventilators the values necessary for the flow capacity and for pressure consists the functioning static point coordinates of the ventilator.

Automatic guidance of the aeration process [2] imposes the modification of the palette's position angle,  $\alpha$ , in the purpose of realizing the static point of functioning of the ventilator.

In the context of calculating the aeration, for establishing the coordinates of the ventilator's static point of functioning, there are necessary it's technical characteristics. They show the dependence of the pressure  $H$  from the flow capacity, for a certain value of the  $\alpha$  angle and are given by the relation:

$$H = f(Q)_{\alpha=\text{const}} \quad (1)$$

These characteristics don't allow the determination of the tuned parameter  $\alpha$ , of the ventilator, corresponding to the static point of functioning obtained by calculating the aeration, parameter necessary to establish the reference value of the ventilator's aeration system.

In consequence, it's imposed to determine the equations of the static characteristics family of the following form:

$$H = f(Q, \alpha) \quad (2)$$

The explicit form of the static characteristics [2] is given by the relation:

$$H = A(\alpha)Q^2 + B(\alpha)Q + C(\alpha) \quad (3)$$

where the coefficients  $A$ ,  $B$ ,  $C$  are square functions that depend of  $\alpha$ .

For a axial ventilator with the controllable  $\alpha$  angle (in the domain  $15^\circ - 45^\circ$ ) were obtained [2] the following expressions for the coefficients A, B, C:

$$\begin{aligned} A(a) &= 0,00033a^2 + 0,0137a - 0,09 \\ B(a) &= - 0,059a^2 + 3,415a - 30,91 \\ C(a) &= 1,628a^2 + 95,02a + 291,51 \end{aligned} \quad (4)$$

Knowing the A, B, C coefficients and the equation [3] can be determined the  $\alpha$  angle, for a given static point. Between the two resulted values for  $\alpha$  is chosen the one that is in the interior of the interval, the one for which the reported error at the static point is minimum.

The automatic guidance of the aeration process considers knowing the transfer function that characterizes the dynamic régime behavior of the ventilator.

Considering the axial ventilator as oriented object, having as output value the flow capacity Q and as input value the  $\alpha$  angle, his transfer function  $H_V(s)$  is defined as being:

$$H_V(s) = \frac{Q(s)}{\alpha(s)} \quad (5)$$

The block scheme of the ventilator, corresponding to this transfer function, is given in figure 2:

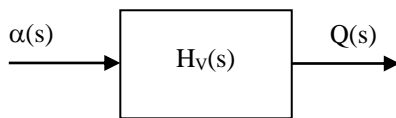


Figure 2.

For an axial ventilator, corresponding to the representation from figure 2, it was established [2] the following expression for the transfer function:

$$H_V(s) = K_V(\alpha) \quad (6)$$

The expression of the transfer function [6] leads to adopting an adaptive tuning system for the ventilation system, where modifying the slope angle of the palettes controls the flow capacity.

Changing the position angle of the palettes can be realized with a electro-hydraulic stepping motor 4, figure 3, with mounted gearing on the ventilator's hub, rotating with the ventilator. Engaging the palettes 1, to modify the position angle, is realized thru a conical transmission and a device with endless screw 3, which is functioning with a palettes command ring 2, which, thru a system of small balls with belt, is realizing the rotation of the palettes axes. Piece 5 is an equilibration table.

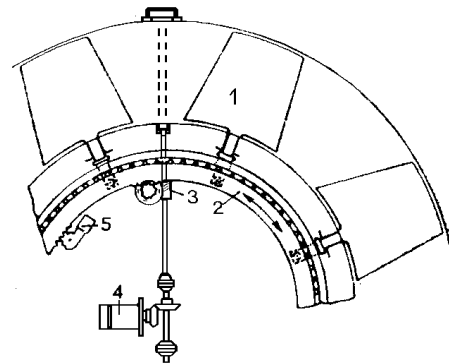


Figure 3.

The command block of the motor is realized according with [3].

## CONCLUSIONS

Stepping motor is used with good results in applications in witch the torque is constant. The advantage of that is the use of simple command schemes witch don not use reaction loops for position control.

## REFERENCES

- Popa A., - Engineering Mining Manual, vol. V, Ed. Tehnică, București, 1989.
- Poantă A., Contributions on mining ventilation process control, Petroșani University, 1990
- Kenjo Takashi., Stepping Motors and their Microprocessor Controls, Oxford University, Press, 1985

## DYNAMIC BEHAVIOR OF SERVO CONTROLLED HYDROSTATIC POWER TRANSMISSION SYSTEM WITH LONG TRANSMISSION LINE

Novak Nedić, Radovan Petrović, Ljubisa Dubonjić

University of Kragujevac, Faculty of Mechanical Engineering Kraljevo, 36 000Kraljevo, Serbia  
 e-mail: nedic.n@maskv.edu.yu , petrovic.r@maskv.edu.yu , dubonjic.lj@maskv.edu.yu

### ABSTRACT

Hydrostatic power transmission systems with long transmission line between pump and motor have more complex dynamic behavior than normal. Moreover, including closed loop in such systems it demands that design must be very careful in selection of control parameters and transmission line. The paper presents modeling and simulation analysis of dynamic behavior of servo hydrostatic power transmission system with long transmission line in frequency and time domen.

Keywords: servo hydrostatic power transmission systems, dynamic behavior, long transmission line

### INTRODUCTION

The pump is connected to the motor via line (pipe, tube) that could in some applications, such as mining, construction machines, heavy machines and remote control systems, be very long. In accordance with their strong behavior demands, for example, a motor is commanded to change to a different speed (from very low speed to very high speed and vice-versa) for short time. In such case the dynamics of the system must to be considered, that is, the dynamics of the all elements coupled in the system (pump, line, motor etc.) must to be considered. Moreover, having servo control of that system, the dynamics of the coupled system becomes more important. Authors of this paper assumed usual type of a servo hydrostatic power transmission system with a variable-displacement pump and a fixed- displacement motor as shown in Fig.1. The coupled subsystem pump-line-motor is shown in Fig.2.

The modeling of fluid transmission line has received a great deal of attention over the past few decades (from about 1950) [1-3] and there are several hundreds publication that could be quoted relating to different theories and applications for air, water and oil hydraulic systems [4-6]. The effect of transmission line dynamics on the dynamic behavior of fluid power systems was studied by J. Watton [7]. Simulation and experimental analysis of dynamics and control of pump controlled motor are presented in [8-10]. Some results in regard to dynamics of pump controlled motor with long transmission line were presented in [11-13]. This paper presents analysis on dynamic behavior of servo pump controlled motor with long transmission line based on different mathematical line models in frequency and time domen.

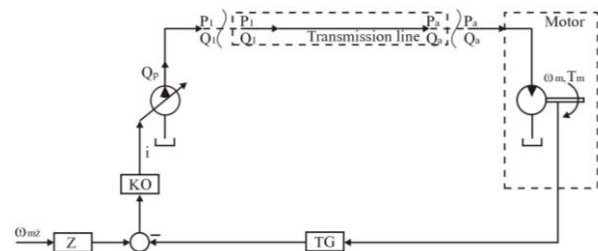


Figure 1. Symbolic diagram of the servo pump controlled motor

### DYNAMICAL MATHEMATICAL MODELS OF THE COUPLED SYSTEM PUMP - TRANSMISSION LINE - MOTOR

The structure diagram of the coupled system pump-transmission line- motor is given in Fig.2.

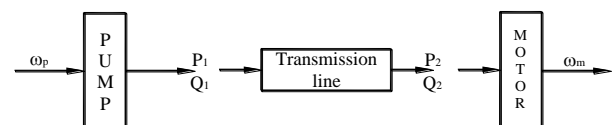


Figure 2. The structure diagram of the coupled subsystem

The fundament of the different developed dynamical models of the coupled system was presented in the [7].

According to the aim of this paper, here are given the transfer functions of the model with distributed parameters and lumped parameters ("T" and "π" model).

For the model with distributed parameters, the transfer function has form:

$$\frac{\bar{\omega}_m}{\bar{\omega}_p}(s) = \frac{1}{\left[1 + \frac{Z_T}{R_p} + \frac{Z_T}{R_m}\right] \text{ch}(\Gamma l) + \left[\frac{Z_T}{Z_c} + \frac{Z_c}{R_p} + \frac{Z_c Z_T}{R_p R_m}\right] \text{sh}(\Gamma l)} \quad (1)$$

For the "T" model, the transfer function has form:

$$\frac{\bar{\omega}_m}{\bar{\omega}_p}(s) = \frac{1}{\left[Y + \frac{1}{R_p} \left(1 + \frac{YZ}{2}\right)\right] Z_T + \left[\frac{Z}{R_p} \left(1 + \frac{YZ}{4}\right) + \left(1 + \frac{YZ}{2}\right)\right] \left[1 + \frac{Z_T}{R_m}\right]} \quad (2)$$

For the "π" model, the transfer function has form:

$$\frac{\bar{\omega}_m}{\bar{\omega}_p}(s) = \frac{1}{\left[Y \left(1 + \frac{YZ}{4}\right) + \frac{1}{R_p} \left(1 + \frac{YZ}{2}\right)\right] Z_T + \left[\frac{Z}{R_p} + \left(1 + \frac{YZ}{2}\right)\right] \left[1 + \frac{Z_T}{R_m}\right]} \quad (3)$$

$$\Gamma l = \sqrt{ZY}; Z_c = \sqrt{\frac{Z}{Y}}; Z = R + Ls; Y = Cs;$$

Where:

$$R_T = \frac{B_v}{D_m^2}; L_T = \frac{J_m}{D_m^2}; Z_T = R_T + L_T s$$

$$L = \frac{\rho l}{A}; R = \frac{128 \mu l}{\pi d^4}; C = \frac{Al}{E}; R_{ref} = \frac{P_{ref}}{Q_{ref}} \quad (5)$$

DYNAMICAL MATHEMATICAL MODELS OF THE SERVO PUMP CONTROLLED MOTOR

Based on the previous models and the pump dynamical model [14], including measurement and control parameters is obtained the open loop transfer function of the servo system.

For the servo system with distributed parameters, the transfer function has from:

$$W_{ok} = \frac{K}{\left[ \frac{s^2}{\omega_n^2} + \frac{2\xi}{\omega_n} s + 1 \right] \cdot \left\{ \left[ 1 + \frac{Z_T}{R_p} + \frac{Z_T}{R_m} \right] \text{ch}(\Gamma l) + \left[ \frac{Z_T}{Z_c} + \frac{Z_c}{R_p} + \frac{Z_c Z_T}{R_p R_m} \right] \text{sh}(\Gamma l) \right\}}$$

For the servo system with "T" line model, the transfer function has from:

$$W_{ok} = \frac{K}{\left[ \frac{s^2}{\omega_n^2} + \frac{2 \cdot \xi}{\omega_n} s + 1 \right] \cdot \left\{ \left[ Y^1 + \frac{1}{R_p} \left(1 + \frac{Y^1 Z^1}{2}\right) \right] Z_T + \left[ \frac{Z^1}{R_p} \left(1 + \frac{Y^1 Z^1}{4}\right) + \left(1 + \frac{Y^1 Z^1}{2}\right) \right] \cdot \left[ 1 + \frac{Z_T}{R_m} \right] \right\}}$$

For the servo system with "π" line model, the transfer function is given by:

$$W_{ok} = \frac{K}{\left[ \frac{s^2}{\omega_n^2} + \frac{2 \cdot \xi}{\omega_n} s + 1 \right] \cdot \left\{ \left[ Y^1 \left(1 + \frac{Y^1 Z^1}{4}\right) + \frac{1}{R_p} \left(1 + \frac{Y^1 Z^1}{2}\right) \right] Z_T + \left[ \frac{Z^1}{R_p} + \left(1 + \frac{Y^1 Z^1}{2}\right) \right] \left[ 1 + \frac{Z_T}{R_m} \right] \right\}}$$

Where:  $Y^1 = Y \cdot l, Z^1 = Z \cdot l, K = \frac{K_a K_{TG} k_p k_{li} \omega_p}{D_m}$

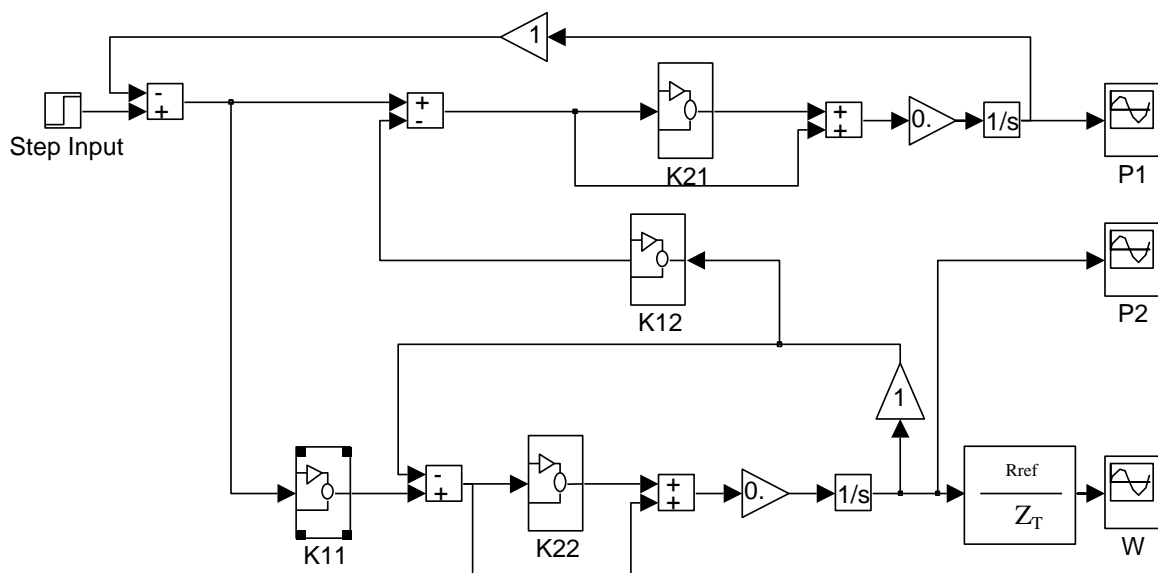


Figure 3. The Simulation model in MATLAB – Simulink

THE SIMULATION ANALYSIS IN FREQUENCY AND TIME DOMEN

For the analysis of dynamic behavior for the servo system authors of this paper developed the simulation modal based on MATLAB - SIMULINK (Fig.3. ). The subsystems K11, K12, K21 and K22 are determined by the model method and given by:

$$K_{21} = K_{22} = \frac{1}{ch(\Gamma)} = \frac{1}{\alpha} \sum_{i=1}^n \frac{a_i \bar{s} + b_i}{\bar{s}^2 + 2\xi_i \omega_{ni} \bar{s} + \omega_{ni}^2}$$

$$K_{11} = K_{12} = \frac{Z_c ch(\Gamma)}{Z_{ca} sh(\Gamma)} = \frac{1}{D_n \bar{s}} \left[ 1 + \sum_{i=1}^n \frac{\frac{D_n a_i}{Z_{ca}} \bar{s}^2 + \frac{D_n b_i}{Z_{ca}} \bar{s}}{\bar{s}^2 + 2\xi_i \omega_{ni} \bar{s} + \omega_{ni}^2} \right]$$

The values of the parameters are as follows:

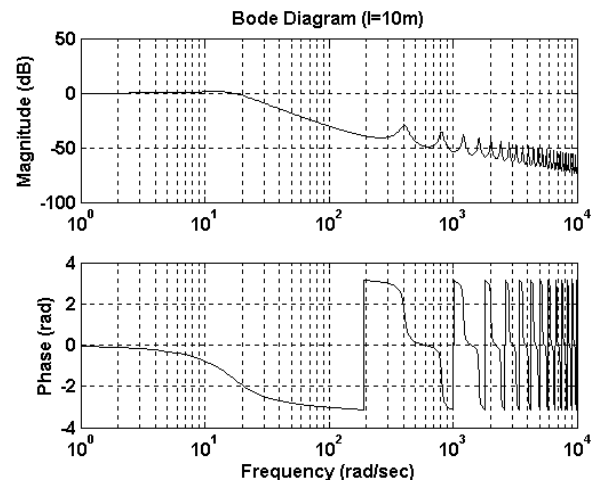
- $E = 1,43 \cdot 10^9 \text{ N/m}^2; \rho = 860 \text{ kg/m}^3; \eta = 0,033 \text{ Ns/m}^2;$
- $R_p = R_m = 1 \cdot 10^{11} \text{ Nm}^{-2} / \text{m}^3 \text{ s}^{-1}; i = 3 \text{ mA}; p_{ref} = 100 \text{ bar};$
- $Q_{ref} = 5 \cdot 10^{-4} \text{ m}^3 / \text{s} = 30 \text{ l/min}; d = 15 \cdot 10^{-3} \text{ m}; l = 10 \text{ m};$
- $c = 1290 \text{ m/s}; D_m = 2.61 \cdot 10^{-5} \text{ m}^3 / \text{rad}; B_v = 0.2 \text{ Nms};$
- $I_m = 2 \text{ kgm}^2; I_m = 0,02 \text{ kgm}^2; \omega_n = 100 \text{ rad/s}; \xi = 0.628$

The load motor inertia effect on dynamic behavior of the coupled system pump-line-motor is shown in Fig.4. in frequency domen. Domination of the motor inertia on dynamic behavior the coupled system over the domination of the hydraulic line dynamic is obvious only for very high the motor inertia (Fig.4.).

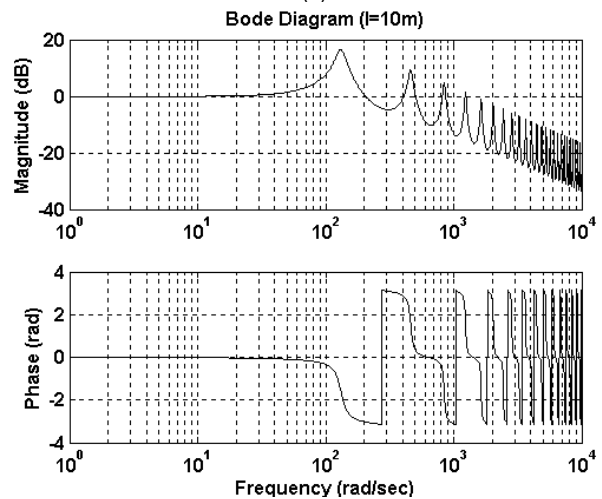
Comparative analysis of the coupled model with distributed parameters and with lumped parameters in frequency and time domen (Fig.5.-Fig.7.) shows that:

- Dynamic of the long coupled system with the transmission line model with distributed parameters is very complex,
- behavior the long coupled system with the transmission line model with lumped parameters is not authentic and
- "π" Transmission line model is more reliable than "T" model.

Comparative analysis of stability of the servo system with and without the transmission line model with distributed parameters (Fig.9.-Fig.10.) in frequency domen shows that the stability conditions of the servo system with the transmission line model with distributed parameters be fulfilled for much more amplification ( $K < 0,25$ ), then for the servo system with transmission line model with lumped parameters ( $K < 20$ ).



(a)



(b)

Figure 4. Amplitude and frequency characteristics of the coupled system with distributed parameters (a)  $I_m = 2 \text{ kgm}^2$  (b)  $I_m = 0.02 \text{ kgm}^2$

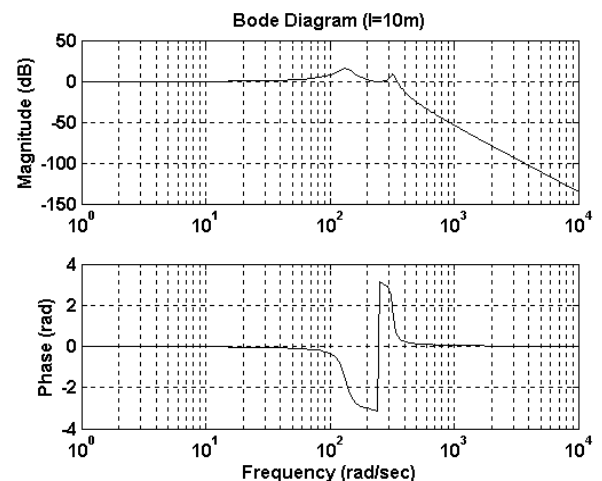


Figure 5. Amplitude and frequency characteristics of the coupled system with fixed parameters "II"  $I_m = 0.02 \text{ kgm}^2$

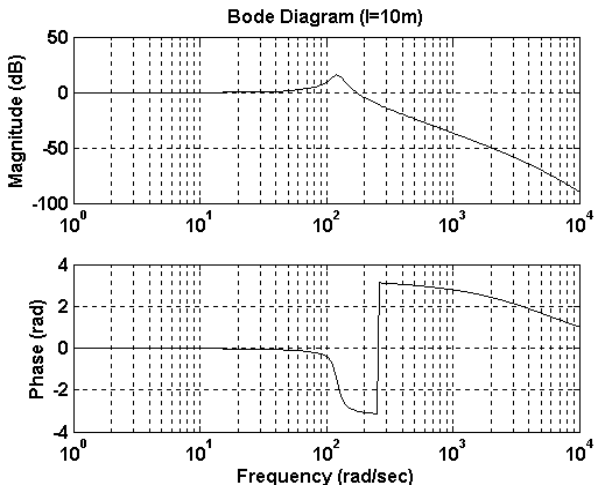
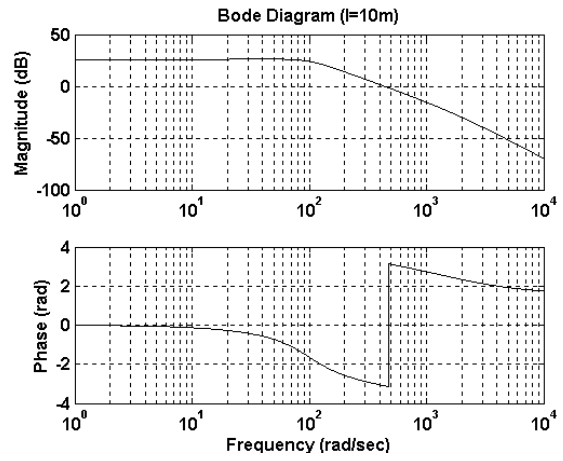


Figure 6. Amplitude and frequency characteristics of the coupled system with fixed parameters  $T'' I_m = 0.02 \text{ kgm}^2$



(a)

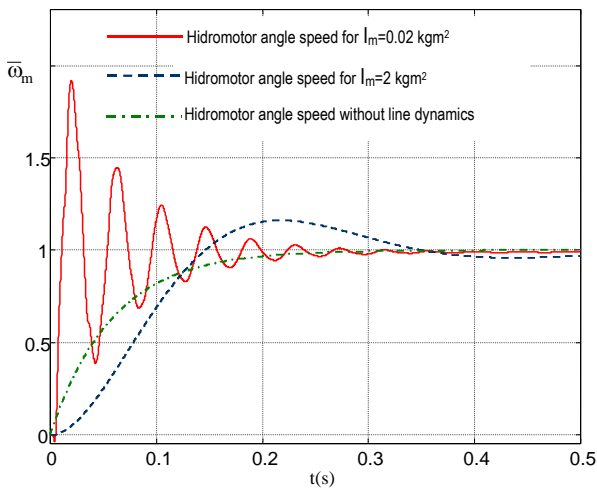
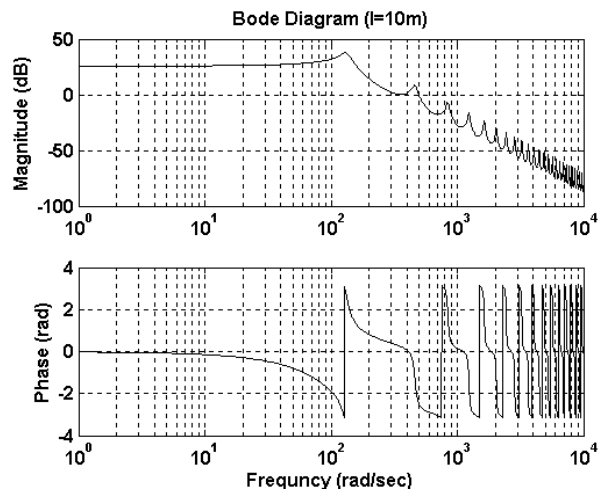


Figure 7. Transient relative motor speed, variation with time



(b)

Figure 9. Amplitude and frequency characteristics of open-loop servo system with distributed parameters (a) without line dynamics (b) with line dynamics

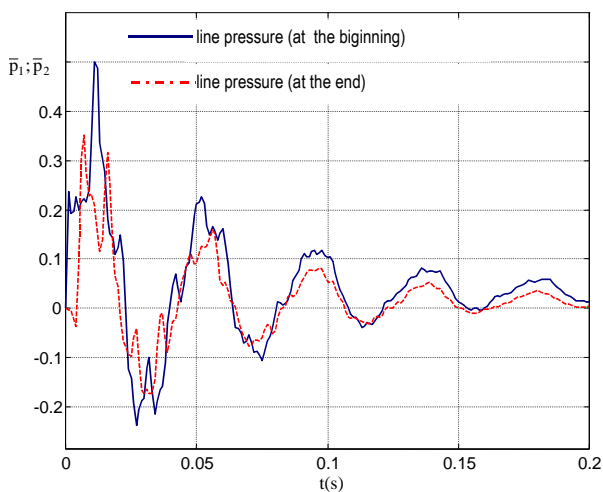


Figure 8. Transient relative line pressure variation with time (at the beginning and the end)

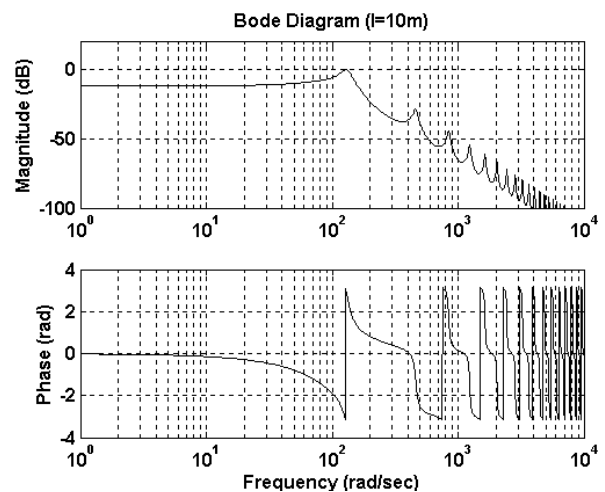


Figure 10. Amplitude and frequency characteristics of open-loop servo system with distributed parameters for  $K=0.25$ .

## CONCLUSIONS

Analysis of dynamic behavior of servo controlled hydrostatic power transmission system with long transmission line given in this paper shows:

- The long transmission line model with distributed parameters has significant effect on dynamic behavior of the servo systems.
- The stability conditions are much more rigorous for the servo system with long transmission line than for the servo system with short transmission line (this is obvious for  $l > 10$  m).
- A good the servo system design demands are that dynamics of the components and the coupled system pump- transmission line – motor must to be included.

## NOTATION

A – rod cross-sectional-area  
 $B_v$  – friction viscosity  
 C –line capacitance  
 d- line diameter  
 $D_m$  – displacement motor  
 $D_p$  – displacement pump  
 $D_n$  –dissipation number  
 E – modulus of elasticity  
 $K_a$  - coefficient current-voltage  
 $k_{1i}$  - coefficient of current application  
 $J_m$  – momentum inertia  
 l – line length  
 n – number of modes  
 $P_1, P_2$  –line pressure at inlet and outlet  
 $P_{ref}$  – simulation reference pressure  
 $Q_{ref}$  - reference flow rate  
 R - fluid resistance  
 $R_{ref}$  – simulation reference resistance  
 $R_p$  - leakage pump resistance  
 $R_m$  – leakage motor resistance  
 s- Laplace operator  
 $Q_1, Q_2$  – line flow rates at inlet and outlet  
 Z – series impedance  
 $Z_c$  – characteristic impedance  
 $Z_T$  – motor impedance  
 Y – shunt admittance  
 $\Gamma$  - Propagation operator  
 $\rho$  - Fluid density  
 $\mu$  - Fluid viscosity

$\xi$ - Damping ratio  
 $\omega_n$ - natural frequency  
 $\bar{\omega}_m$  - non dimensional motor angular speed  
 $\bar{\omega}_p$  – non-dimensional pump angular speed

## REFERENCES

- Tarko L.M., "Volnovie procesi v truboprovodah gidromehanizmov" Gosudarstvenoe naučno-tehničeskoe izdatelstvo mašinstroitelnoj literaturi, Moskva, 1963.
- Korobočkin B.L., Komitovski M.D., "O peredatočnih funkcijah truboprovodov gidrosistem v sosredotočnih i raspredeljenih parametrah", Mašinovedenie, No4, 1968.
- Hsue C.Y., Huulender, D.A., "Modal approximations for the fluid dynamics of hydraulic and pneumatic transmission lines", Fluid Transmission line dynamics, published by ASME, 51-77.pp., 1983.
- Merritt N.E., "Hydraulic Control systems", John Wiley & Sons, 1967.
- Blackburn J.F., Reethof G., Shearer, J.L., "Fluid Power Control", M.I.T. Press.
- McCloy D., Martin H.R., "Control of fluid power", Ellis Horwood Ltd.
- J.Watton, "Fluid Power Systems", Prentice Hall, 1989.
- N.N.Nedić, Z. Bučevac, D. Prsic "Experimental analysis and identification of piston- axial pump BVP 100, International Conference Heavy Machinery HM '96, Kraljevo 28-30 June, 1996, 531-536 pp. (in Serbian)
- N.N.Nedić, D.H.Pršić, "Time Variable Speed Control of a Pump Controlled Motor Using Natural Tracking Control", Conference on Control of Industrial Systems, IFAC-IFIP IMACS, 20-22 May, Belfort, France, 1997, 197-202 pp.
- R.S.Petrović, N.N. Nedić, "Mathematical Modeling and Experimental Research of Characteristic Parameters Hydrodynamic Processes of a Piston Axial Pump", VII International SAUM Conference, V.Banja, September 26-28, 2001.
- N.N.Nedić, Lj.M.Dubonjić, "Ways of modelling and simulation of a pump controlled motor coupled by long transmission line", VII International SAUM Conference, V.Banja, September 26-28, 2001.
- Lj.M.Dubonjić, "Dynamical analysis of electrohydraulic control systems with long transmission line", Master thesis, Faculty of Mechanical Engineering, Kraljevo, Dec. 2002. (in Serbian).
- Nedić N.N., Dubonjić Lj.M., "Dynamical Model of Variable Displacement Piston Axial Pump with Shwashplate" HIPNEF 2000, Beograd 2000, 28-33 pp. (in Serbian)

## THE POSSIBILITY OF APPLYING THE SELSINES IN COMMANDING THE CUPE WHEEL EXCAVATORS

**Orban Maria Daniela**

University of Petrosani  
Petrosani 2675  
Romania

**Cozma Vasile**

"Constantin Brancusi" University Tg-  
Jiu Tg-Jiu 1400  
Romania

**Pîrlea Ovidiu**

S.C. Solatron S.A.  
Timisoara,  
Romania

### ABSTRACT

It was considered the obtaining of a horizontal hearth as well as realizing judicious by chosen excavating works, with obtaining a continuous visualisation of the excavation height, which is obtained by tangent with the port-bucket wheel of the surface where is the bucket wheel excavator. It was also watched the using of installations level for determining the lateral repose angle in the transversal plain of the advancing direction, which is made by rotating with 90° against the walk direction of port buckets arm and tangent the terrain with the port buckets wheel. Another application of installation is to determine, when the excavator is on horizontal plane, of the cant angle, angle which is start from the front part of the director caterpillar (frontal repose angle), and determining the height or depth of excavation. It must be considered that the system has as a reference a gravitational pendulum mounted on the port-wheel arm with buckets.

### CONCEIVING AND REALISING OF THE INSTALLATION FOR DETERMINING THE HEIGHT OF EXCAVATION AND OF THE SLOPE

The installation was conceived and realised for the BWE-1400-30/7 excavator, but can be adapted, by changing the

indicator dial at all types of BWE used in the mine-shafts from C.N.L. Oltenia.

The dimensions determined at calculating the height of the inferior bucket facing the heart's plane, considered horizontal are given in figure 1, where:

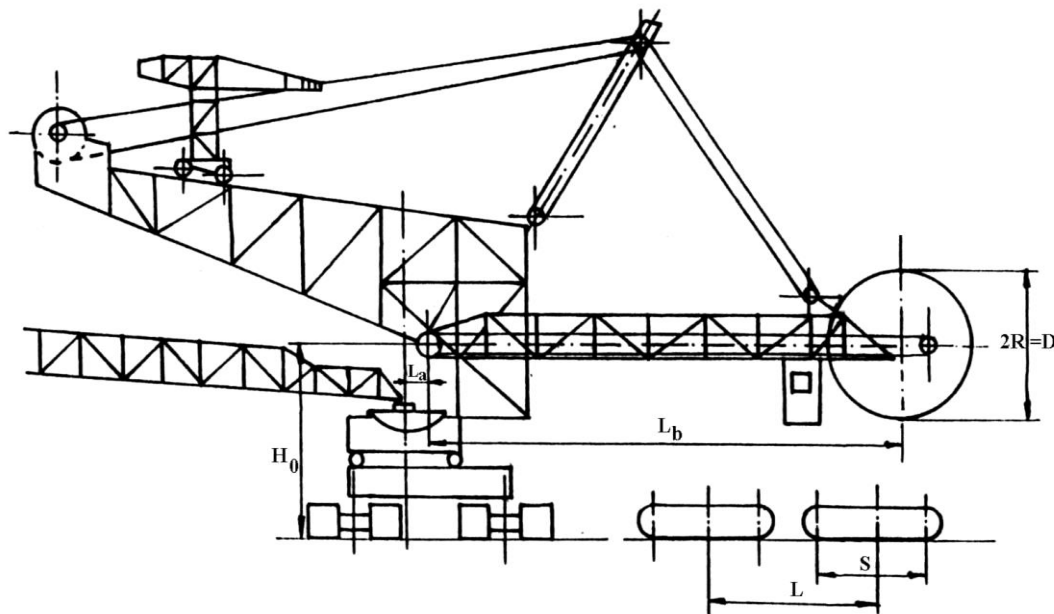


Figure 1.

S = 8 m – the length on which is stepping a caterpillar on ground.

$H_0 = 13,7$  m – the height where is the arm's articulation;  
 $R = 5,75$  m – the exterior radius of the port buckets wheel;  
 $L_b = 36,2$  m – the length of the port wheel arm from the centre of the wheel to arm articulation;  
 $L_a = 1,5$  m – the distance between the pivoting axle of the excavator's platform and the arm's articulation;  
 $L = 12,975$  m – the distance between the turning caterpillar axles;

It was mounted a pendulum on the port-wheel arm, and the couple which is activating is:

$$M \cdot g \cdot l \cdot \sin \alpha,$$



From  $D_c = 110$  mm is obtaining a length of 8 mm which is corresponding in (medie) to a meter of excavation from the 37 m, and on this length of 8 mm can be traced the 4 marks representing each of the 25% from a meter.

MEASURING THE HEIGHT AN DEPTH OF EXCAVATION ( $\Delta H$ )

The strictly necessary condition is to put the excavator on a horizontal plane, when:

$$\Delta H = h_{\text{excavation}} - h_{\text{hearth}} \quad (4)$$

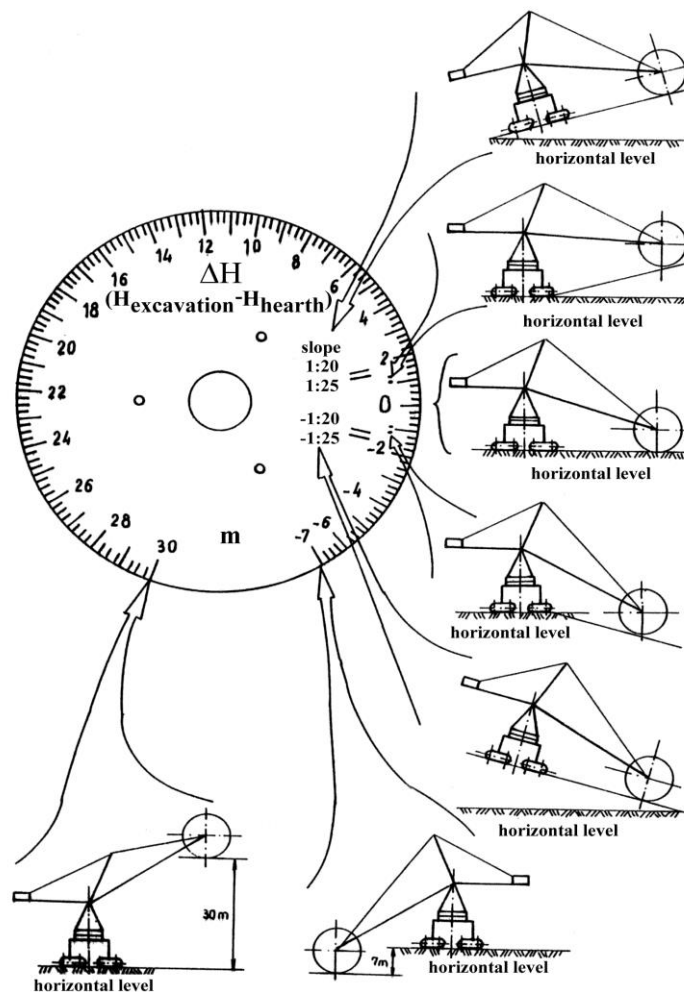
Due to the fact that the relation between the angle made by the pendulum with the arm and the height of excavation is non-

linear led to the calculating from 25 to 25 cm of centre corresponding angle.

Figure 4 contains the values of the heights, real angles, amplified angles and their positions depth, respectively to the height of 30 m; also, fig.4 shows the correspondence of the excavating height at DR which exists in the excavator man cabin.

MEASURING THE SLOPE

For measuring the slope, the strictly necessary condition is that the plain must be continuous and of the same slope.



The slope represents the connection rapport between the level difference between two points, and it's projection on horizontal.

The slope is given for an ERC-1400-30/7:

- a) Work slope, max.  $\pm$  (1:25);
- b) Marsh slope, max.  $\pm$  (1:20).

On the indicator dial the slope is indicated in two situations:

- a) The excavator is situated on a cant (fig.5a). The arm is brought so that the wheel port buckets to tangent hearth. The

Figure 4.

needle indicates the slope on which the excavator is situated. The reading is made using continuous red gradations from the indicator dial.

b) The excavator is situated on a perfect horizontal plain, (fig. 5b). From the contact point of first director caterpillar of the ERC with the hearth the cant begin. It brings the arm so that the port buckets wheel to tangent the cant. The needle is indicating the slope of the cant on which the excavator will be engaged. The reading is made using the red doted gradation

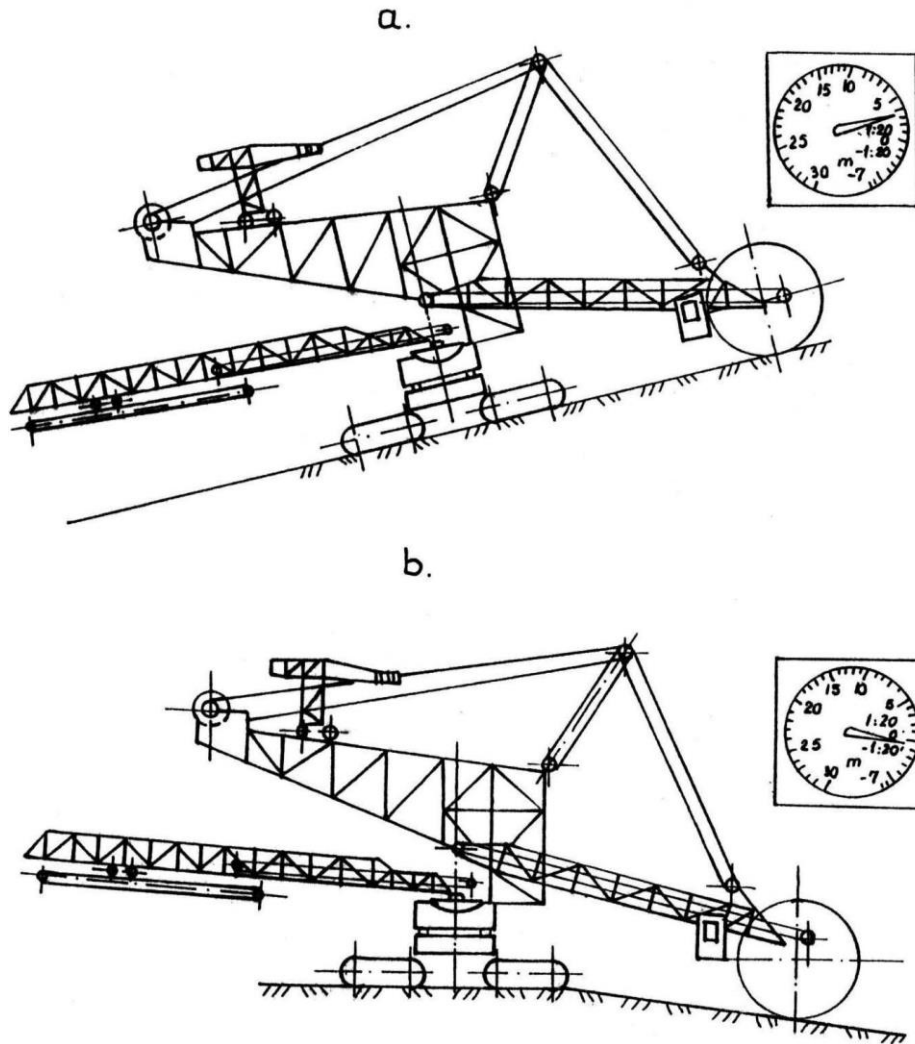


Figure 5.

**a) Determining the position of the gradations from the indicator dial (continuous red lines)**

The excavator is situated on a cant of  $\delta$  angle (fig.6)

Because the emitting device (DE) is accorded on the vertical position of that place, he makes a  $\delta$  angle with the machine's vertical. So, as angles with perpendicular sides, the angle of

the cant is equal with the angle of the pendulum of the emitting device with the vertical machine:

**Slope  $\pm$  (1:20):**

$$\text{tg} \delta = \frac{1}{20} ; \delta = \arctg \frac{1}{20} = 2,86^\circ \quad (5)$$

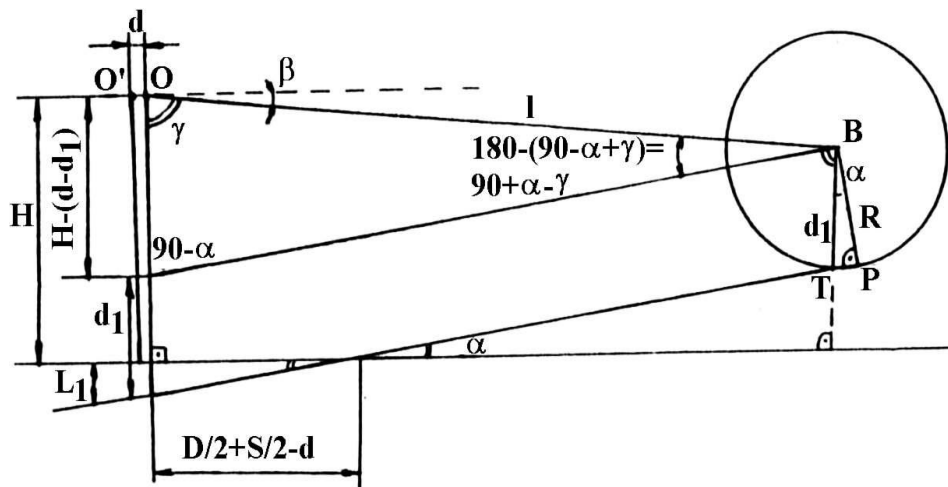


Figure 6.

The correspondence on the indicator dial, if the multiplying factor 5 is taken consideration, is:  $2,85^\circ \times 5 = 14^\circ 19'$ .

So for the slope + (1:20):  
 $\beta_{1:20} = 58^\circ 32' + 14^\circ 19' = 72^\circ 51'$ .  
 So for the slope - (1:20):  
 $\beta_{-1:20} = 58^\circ 32' - 14^\circ 19' = 44^\circ 18'$ .

**Slope ± (1:25):**

$$\operatorname{tg} \delta = \frac{1}{25}; \delta = \operatorname{arctg} \frac{1}{25} = 2,2906^\circ \quad (6)$$

The correspondence on the indicator dial, if multiplying factor 5 is taken into consideration, is:  $2,2906 \times 5 = 11^\circ 27'$ .

Determining the respective angles was possible by applying the sinus theorem.

So, for the slopes (1:20) and (1:25) figure 7 was used for determining the respective angles.

The sinus theorem:

$$\frac{L_b}{\sin(90 - \alpha)} = \frac{H_0 - d_1 + l_1}{\sin(90 + \alpha - \gamma)}$$

$$\operatorname{tg} \alpha = \frac{l_1}{\frac{L}{2} + \frac{S}{2} - L_a} \quad \text{From triangle BTP results } \cos \alpha = \frac{R}{d_1};$$

$$d_1 = \frac{R}{\cos \alpha}; \quad l_1 = \left( \frac{L}{2} + \frac{S}{2} - L_a \right) \operatorname{tg} \alpha$$

$$\frac{L_b}{\sin(90 - \alpha)} = \frac{H_0 - \frac{R}{\cos \alpha} + \left( \frac{L}{2} + \frac{S}{2} - L_a \right) \operatorname{tg} \alpha}{\sin(90 + \alpha - \gamma)} \quad (7)$$

**b) Determining the position of the gradation from the indicator dial (the red dots from indicator dial) (fig.7)**

The plain of the caterpillar perfectly horizontal is considered and the slope (1:20) and (1:25).

In triangle OBN (BN || MP):

The sinus theorem:

The slope (1:20) and for the slope (1:25) resulted, the correspondence on DR indicator dial is showed in fig. 7.

**THE ELECTRICAL WIRING DIAGRAM FOR CONNECTING THE EMITTING DEVICE WITH THE TWO RECEIVING DEVICE**

Three selsines were used, with the nominal data for the exciting winding of 220V, 50Hz, and the connecting scheme is showed in fig.8.

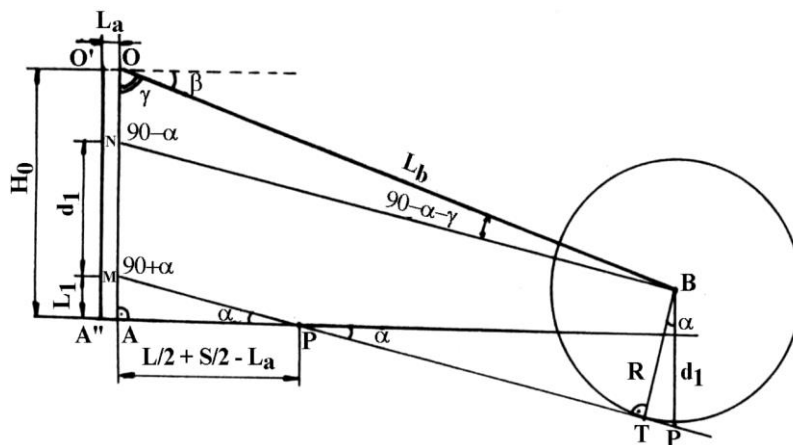


Figure 7.

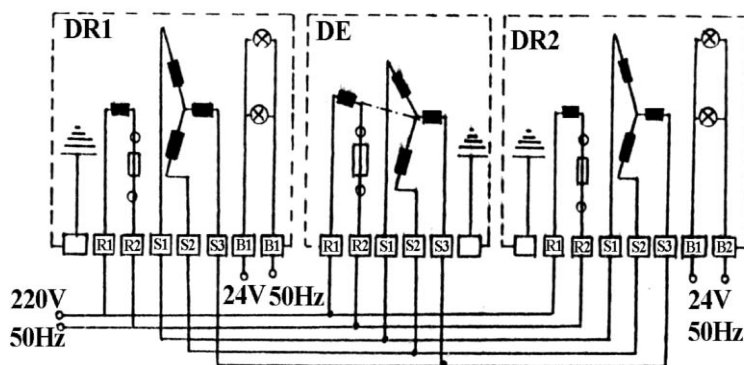


Figure 8.

Table 1. The values of resistors:

| Hubs                             | DE                           | DR                           | DE; DR1; DR2 connected     |
|----------------------------------|------------------------------|------------------------------|----------------------------|
| $R_1R_2$                         | 61 $\Omega$ ...75 $\Omega$   | 127 $\Omega$ ...156 $\Omega$ | 31 $\Omega$ ...39 $\Omega$ |
| $S_1S_2$ or $S_2S_3$ or $S_3S_1$ | 32,4 $\Omega$ ...40 $\Omega$ | 279 $\Omega$ ...341 $\Omega$ | 26 $\Omega$ ...33 $\Omega$ |

Table 2. The value of absorbed current at 220V, 50Hz by the exciting winding  $R_1R_2$  are:

| DE         | DR          | DE; DR1; DR2; connected |
|------------|-------------|-------------------------|
| Max.360 mA | Max. 150 mA | Max.660 mA              |

### CONCLUSIONS

By applying the respective installation at BWE-1400-30/7, an improvement functioning, especially were observed nighttime, an improvement fiability and of work security in the mineshafts.

### REFERENCES

Stochitoiu, A.D., Orban, M. Obtaining an Optimal Control Rule for the Bucket Wheel Excavators, ICAMC-95, International

Conference on Automation in Mining, Glivice, Poland 13-15sept. 1995

Stochitoiu, A.D., Orban, M., Marcu, M. About the possibility of Using Some Control rules of the Bucket Wheel Excavators, ICAMC-95, International Conference on Automation in Mining, Glivice, Poland 13-15sept. 1995

Cozma, Vasile Contributii privind reducerea consumului de energie electrica la actionarile transportoarelor cu banda, cu motoare de curent alternativ. Teza de doctorat. Petrosani 2000

## ABOUT THE MAGNETICAL CHARACTERISTICS OF THE SYNCHRONOUS MOTOR, PROPOSED IN ACTIVATING THE CONVEYORS FROM THE LIGNITE MINE SHAFTS

Cozma Vasile

"Constantin Brancusi" University Tg-Jiu  
Tg-Jiu 1400  
Romania

Orban Maria Daniela

University of Petrosani  
Petrosani 2675  
RomaniAbstract

### ABSTRACT

In this paperwork, the authors present the results obtained by making a program in the Borland Pascal language, to obtain the partial magnetical characteristics, used to determine the excitation solenation at nominal duty of the synchronous motor with appearing polls and in the combined variant, proposed in activating the transport tools from the lignite mine-shafts. This is done in the purpose of implementing some new types of controllable activations mend to contribute at reducing the electrical power consumption of the tools mentioned above, according with the realizations obtained in this way by the countries with tradition and experience in the domain of the extraction, transporting and depositing the useful and sterile.

### INTRODUCTION

For activating the large capacity belt conveyors from the mine shafts is proposed the synchronous motor with the rotor in the constructive combined variant, with longitudinal-transversal silencer completely made from Cu-Cu, with the following nominal data's: 777,4 kVA/630 kW, 6kV, 1000 rot/min. (fig. 1)

In the purpose of quick determining the magnetical characteristics, the program determines the main dimensions

of the motor, the electrical and magnetical solicitations of the motor, the parameters of the notches and the windings, establishes the values of the magnetical tensions in different portions of the magnetical circuit (in the main inter-iron, in the teeth and in the ladle shank of the stator, in the big tooth of the rotor, in the area of the rotorical notches and in the inductor's ladle shank)

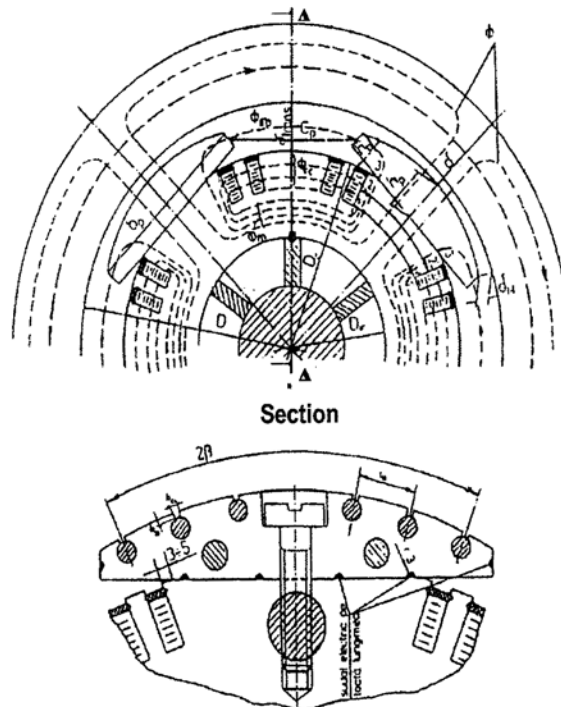


Figure 1. Synchronous motor with rotor in combined

Construction of magnetical characteristics and determination of solenation for nominal excitation of synchronous motor with rotor in combined constructive variant with nominal parameters: 777.4 kVA/630 kW; 6kV; 1000 rot/min and longitudinal-transversal complete dumping from Cu-Cu and Am-Cu

Table Nr.

| $E = \frac{E}{U_{INM}}$                                     | UF | 0.55     | 0.70     | 0.85     | 1(U <sub>INM</sub> ) | K <sub>e</sub> (E <sub>NM</sub> ) | 1.15     | 1.26     | 1.28     | 1.30     |
|---|----|----------|----------|----------|----------------------|-----------------------------------|----------|----------|----------|----------|
| Relation  | V  | 1905.2   | 2424.8   | 2944.4   | 3464                 | 3654                              | 3983.6   | 4360.72  | 4433.92  | 4503.2   |
| $\phi = \frac{E}{4K_B K_w I_{ver}}$                         | 2  | 3        | 4        | 5        | 6                    | 7                                 | 8        | 9        | 10       | 11       |
| $B_6 = \frac{\phi_{ON}}{\alpha_i \tau I_i}$                 | Wb | 0.042    | 0.053    | 0.065    | 0.076                | 0.080                             | 0.087    | 0.096    | 0.097    | 0.099    |
| $U_{m6} = \frac{2}{\mu_0} B_6 K_c \delta$                   | T  | 0.420    | 0.534    | 0.648    | 0.763                | 0.805                             | 0.877    | 0.960    | 0.976    | 0.992    |
| $B'_{dmax} = \frac{t l_{i1} B_6}{K_{Fe1} I_{Fe1} b_{dmin}}$ | A  | 4028.950 | 5127.755 | 6226.559 | 7325.364             | 7727.159                          | 8424.168 | 9221.669 | 9376.466 | 9522.973 |
| $B'_{dmed} = \frac{t l_{i1} B_6}{K_{Fe1} I_{Fe1} b_{dmed}}$ | T  | 9.521    | 12.118   | 14.714   | 17.311               | 18.260                            | 19.907   | 21.792   | 22.158   | 22.504   |
| $B'_{dmin} = \frac{t l_{i1} B_6}{K_{Fe1} I_{Fe1} b_{dmax}}$ | T  | 0.832    | 1.059    | 1.286    | 1.513                | 1.596                             | 1.740    | 1.905    | 1.937    | 1.967    |
|   | T  | 0.681    | 0.867    | 1.052    | 1.238                | 1.306                             | 1.424    | 1.559    | 1.585    | 1.610    |

$$K_{d1} = \frac{b_{cl} I_i}{K_{Fe1} I_{Fe1} b_{dmax}} = 0.791 \quad K_{d2} = \frac{b_{cl} I_i}{K_{Fe1} I_{Fe1} b_{dmed}} = 0.893 \quad K_{d3} = \frac{b_{cl} I_i}{K_{Fe1} I_{Fe1} b_{dmin}} = 10.214$$

|  |      |          |          |          |          |          |          |           |           |           |
|--|------|----------|----------|----------|----------|----------|----------|-----------|-----------|-----------|
| $H_{dmax}$   | A/cm | 2.250    | 5.025    | 15.500   | 90.000   | 140.000  | 170.000  | 760.000   | 880.000   | 1000.000  |
| $H_{dmed}$   | A/cm | 2.000    | 3.400    | 6.000    | 20.000   | 35.000   | 95.000   | 150.000   | 200.000   | 250.000   |
| $H_{dmin}$   | A/cm | 1.500    | 2.250    | 2.750    | 5.250    | 6.500    | 9.500    | 17.500    | 25.000    | 34.000    |
| $H_{d1} = \frac{1}{6}[H_{dmax} + 4H_{dmed} + H_{dmin}]$  | A/cm | 1.958    | 3.479    | 7.042    | 29.208   | 47.750   | 93.250   | 229.583   | 284.167   | 339.000   |
| $U_{md1} = 2h_{el} H_{d1}$   | A    | 18.408   | 32.704   | 66.192   | 274.558  | 448.850  | 876.550  | 2158.083  | 2671.167  | 3186.600  |
| $B_{j1} = \frac{\phi}{2K_{Fe1} I_{Fe1} h_{j1}}$  | T    | 0.703    | 0.895    | 1.086    | 1.278    | 1.348    | 1.470    | 1.609     | 1.636     | 1.662     |
| $H_{j1}$   | A/cm | 1.500    | 2.250    | 3.250    | 6.000    | 7.500    | 12.500   | 25.000    | 37.500    | 49.000    |
| $U_{mj1} = \xi_1 L_{j1} H_{j1}$  | A    | 38.745   | 56.272   | 77.285   | 118.080  | 138.375  | 194.750  | 328.000   | 476.625   | 602.700   |
| $U_{mdj1} = U_{m6} + U_{md1} + U_{mj1}$  | A    | 4086.103 | 5216.731 | 6370.036 | 7718.002 | 8314.384 | 9495.468 | 11707.752 | 12524.257 | 13312.273 |
| $\phi_{\sigma p} = \lambda_{\sigma p} U_{mdj1}$  | Wb   | 0.001    | 0.002    | 0.002    | 0.003    | 0.003    | 0.003    | 0.004     | 0.004     | 0.004     |
| $B_{dRmin} = \frac{\phi + \phi_{\sigma p}}{K_{Fe2} I_{Fe2c} b_{DRmax}}$                              | T    | 0.642    | 0.817    | 0.993    | 1.169    | 1.234    | 1.347    | 1.481     | 1.509     | 1.536     |
| $U_{md\delta j1\delta imb} = \frac{2}{\mu} B_{dRmin} \delta_{imb}$                                   | A    | 153.317  | 195.149  | 237.008  | 279.093  | 294.602  | 321.676  | 353.653   | 360.309   | 366.626   |
| $U_{md\delta j1\delta imb} = U_{mdj1} + U_{md\delta imb}$  | A    | 4239.420 | 5411.881 | 6607.044 | 7997.095 | 8608.986 | 9817.145 | 12061.405 | 12884.567 | 13678.899 |
| $\phi_{\sigma c} = \lambda_{\sigma c} U_{md\delta j1\delta imb}$                                     | Wb   | 0.003    | 0.004    | 0.004    | 0.005    | 0.006    | 0.006    | 0.008     | 0.008     | 0.009     |
| $\phi_m = \phi + \phi_{\sigma p} + \phi_{\sigma c}$  |      |          |          |          |          |          |          |           |           |           |
| $\sigma = \frac{\phi_m}{\phi}$   | Wb   | 0.046    | 0.058    | 0.071    | 0.084    | 0.088    | 0.097    | 0.107     | 0.110     | 0.112     |
| $\phi_{\sigma} = \phi_{\sigma c} + \phi_{\sigma p}$  | Wb   | 1.098    | 1.098    | 1.098    | 1.101    | 1.103    | 1.108    | 1.122     | 1.128     | 1.134     |
| $B_{dRmed} = \frac{\phi + \frac{1}{2}\phi_{\sigma c} + \phi_{\sigma p}}{K_{Fe2} I_{Fe2c} b_{DRmed}}$ | T    | 0.763    | 0.971    | 1.180    | 1.390    | 1.468    | 1.606    | 1.772     | 1.809     | 1.844     |
| $B_{dRmax} = \frac{\phi_m}{K_{Fe2} I_{Fe2c} b_{DRmin}}$  | T    | 0.927    | 1.180    | 1.433    | 1.690    | 1.786    | 1.956    | 2.167     | 2.216     | 2.262     |

$$K_{dRmax} = \frac{\left( \alpha_p \frac{Z^2}{2p} - N_D \right) b_{c2} I_i}{K_{Fe2} \left[ \alpha_p \frac{Z^2}{2p} (t_{rmin} - b_{c2}) + N_{D2} b_{c2} \right] I_{Fe2}} = 0.346 \quad K_{dRmed} = \frac{\left( \alpha_p \frac{Z^2}{2p} - N_D \right) b_{c2} I_i}{K_{Fe2} \left[ \alpha_p \frac{Z^2}{2p} (t_{Rmed} - b_{c2}) + N_{D2} b_{c2} \right] I_{Fe2}} = 0.287$$

$$K_{dRmin} = \frac{\left( \alpha_p \frac{Z^2}{2p} - N_D \right) b_{c2} I_i}{K_{Fe2} \left[ \alpha_p \frac{Z^2}{2p} (t_{Rmax} - b_{c2}) + N_{D2} b_{c2} \right] I_{Fe2}} = 0.245$$

| 1   | 2    | 3        | 4        | 5        | 6        | 7        | 8         | 9         | 10        | 11        |
|---|------|----------|----------|----------|----------|----------|-----------|-----------|-----------|-----------|
| $H_{dRmin}$   | A/cm | 1.500    | 2.000    | 2.400    | 4.500    | 6.500    | 8.600     | 19.000    | 25.000    | 27.500    |
| $H_{dRmed}$   | A/cm | 1.750    | 2.500    | 4.500    | 10.500   | 19.500   | 50.000    | 100.000   | 140.000   | 190.000   |
| $H_{dRmax}$   | A/cm | 2.250    | 4.750    | 9.750    | 86.000   | 125.000  | 280.000   | 950.000   | 1000.000  | 1600.000  |
| $H_{dR} = \frac{1}{6} (H_{dRmax} + 4H_{dRmed} + H_{dRmin})$ | A/cm | 1.792    | 2.792    | 5.025    | 22.083   | 34.917   | 81.433    | 228.167   | 264.167   | 397.917   |
| $U_{m0R} = 2I_{Fe2} H_{dR}$                                 | A    | 23.292   | 36.292   | 65.325   | 287.083  | 453.917  | 1058.633  | 2966.167  | 3434.167  | 5172.917  |
| $B_{j2} = \frac{\phi_m}{2I_{Fe2} k_{Fe2} h_{j2}}$           | T    | 0.743    | 0.945    | 1.149    | 1.355    | 1.432    | 1.568     | 1.737     | 1.776     | 1.813     |
| $H_{j2}$  | A/cm | 1.850    | 2.500    | 4.750    | 9.500    | 18.500   | 40.000    | 100.000   | 130.000   | 190.000   |
| $U_{mj2} = L_{j2} H_{j2}$                                   | A    | 33.419   | 45.160   | 85.805   | 171.609  | 334.187  | 722.566   | 1806.416  | 2348.341  | 3432.190  |
| $U_{mR} = U_{m0R} + U_{mj2} + U_{m0mb}$                     | A    | 210.027  | 276.601  | 388.138  | 737.786  | 1082.706 | 2102.876  | 5126.235  | 6142.816  | 8971.733  |
| $\sum U_{mi} = U_{mR} + U_{m0dj1}$                          | A    | 4296.131 | 5493.333 | 6758.174 | 8455.788 | 9397.090 | 11598.344 | 16833.988 | 18667.074 | 22284.006 |
| $\phi = \phi / \phi_{0N}$                                   | ur   | 0.550    | 0.700    | 0.850    | 1.000    | 1.055    | 1.150     | 1.259     | 1.280     | 1.300     |
| $\phi_m = \phi_m / \phi_{0N}$                               | ur   | 0.604    | 0.769    | 0.934    | 1.101    | 1.164    | 1.275     | 1.412     | 1.444     | 1.474     |
| $\phi_\sigma = \phi_\sigma / \phi_{0N}$                     | ur   | 0.054    | 0.069    | 0.084    | 0.101    | 0.109    | 0.125     | 0.153     | 0.164     | 0.174     |
| $\sum U_{mi} = \sum U_{mi} / U_{m0N}$                       | ur   | 0.508    | 0.650    | 0.799    | 1.000    | 1.111    | 1.372     | 1.991     | 2.208     | 2.635     |
| $U_{m0dj1} = U_{m0dj1} / U_{m0N}$                           | ur   | 0.483    | 0.617    | 0.753    | 0.913    | 0.983    | 1.123     | 1.385     | 1.481     | 1.574     |
| $U_{mR} = U_{mR} / U_{m0N}$                                 | ur   | 0.025    | 0.033    | 0.046    | 0.087    | 0.128    | 0.249     | 0.606     | 0.726     | 1.061     |

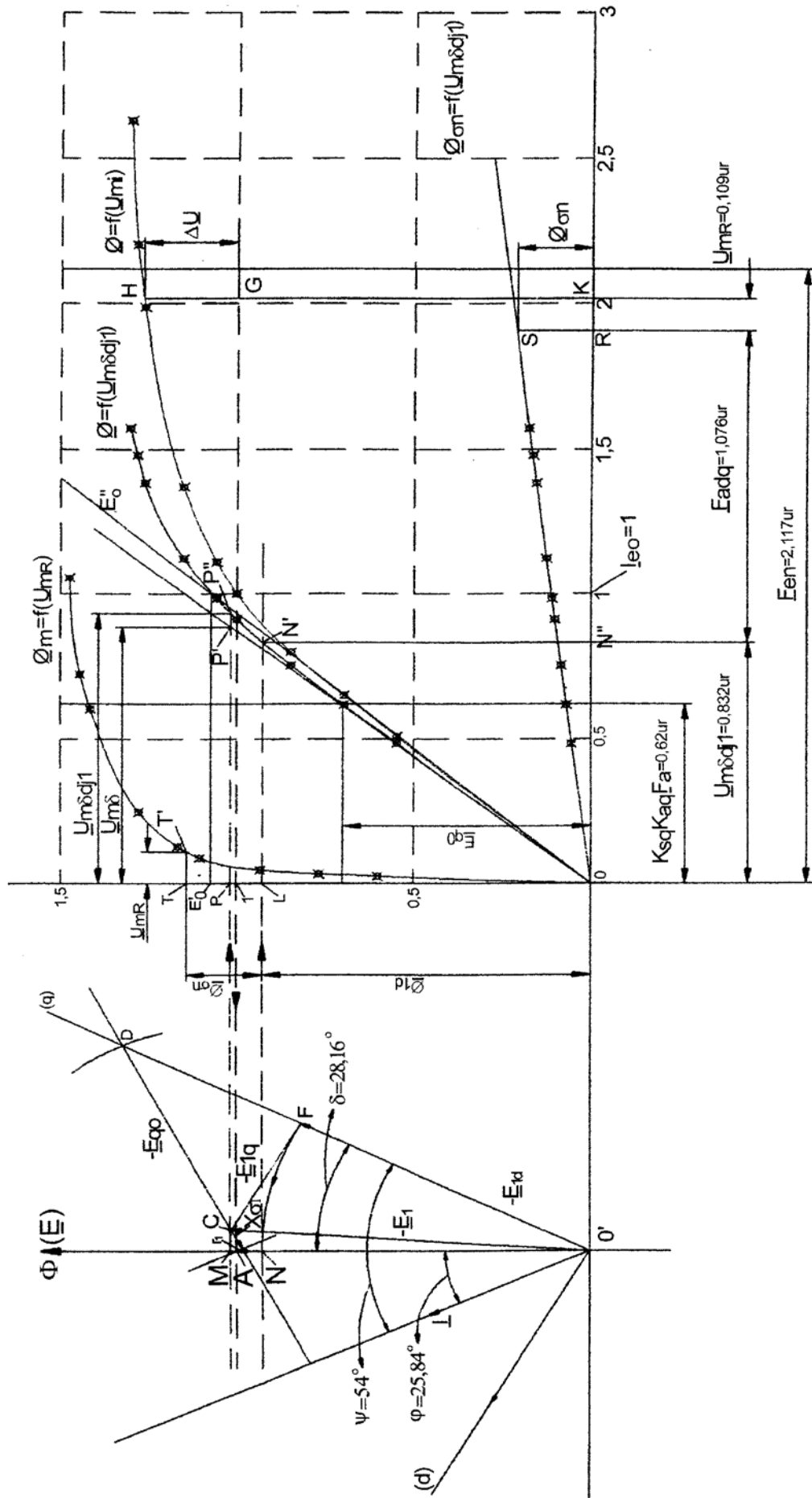


Figure 2

THE CONSTRUCTION OF THE MAGNETICAL CHARACTERISTICS AND DETERMINING THE SOLENIATION EXCITATION AT NOMINAL DUTY

Based on the data's obtained in table 1 by the conceived program, for different values of the electro-motor tension (0,55 ; 0,70 ; 0,80 ; 1 ; 1,05 ; 1,15 ; 1,26 ; 1,28 ; 1,3 )  $U_{1NM}$ , is determined the values of the flux ( $\Phi$ ) and also the magnetical tensions and is built:

- the magnetization characteristic at running on empty  $\Phi = f(\sum U_{mi})$  or  $E = f(I_e)$ ;
- partial magnetical characteristics;
  - $\Phi = f(U_{m\delta dJ1})$  - of the stator;
  - $\Phi = f(U_{mR})$  - of the rotor;
  - $\Phi_{\sigma} = f(U_{m\delta dJ1})$  - of the magnetical flux of slipping between polls.

All these magnetical characteristics (functioning unloaded and partial for motor, in u.r.) are traced by a special program in figure 2, and serve at determining the excitation solenation at nominal duty thru the method of the partial magnetical characteristics, which remembers the demagnetized effect of the inducted reaction, using the following operations:

- construction of fazorial diagrams for resulting t.e.m.  $E_1$ , in u.r. for motor regimes (and if  $r_1 \ll X_1$ , this value is neglecting);
- determining of saturation rapport corresponding of

following relations: 
$$\frac{U_{m\delta dJ1}}{U_{m\delta}} = \frac{PP''}{PP'} \quad (1)$$

- determining of coefficients  $k_{sd}$ ,  $k_{sq}$ ,  $k_1$  like mathematical functions of saturation, resulted before, from variation of inter-iron, for  $i_M/i=1,5..2,5$ ;
- establishing transversal solenation with magnetical saturation influence, according to following relations:

$$k_{sq} k_{aq} F_a = k_{sq} k_{aq} \frac{F_a}{U_{m0N}} \quad [u.r.] \quad (2)$$

where:

$$F_a = 0.9m \frac{W_1 K_{w1}}{p} I_{1NM} [A] \quad (3)$$

$$U_{m0N} = \sum U_{mi} \text{ for } U_{1NM} \quad (4)$$

- establishing fictive t.e.m.  $E_{q0} = \overline{CD}$  corresponding of solenation  $k_{sq} k_{aq} F_a$  from partial magnetical characteristic of stator,  $\phi = f(U_{m\delta dJ1})$ ;

- determining of transversal direction ( $q$ ), the line  $\overline{OD'}$ , which guiding t.e.m.  $E_{1d} = \overline{O'F}$ ;

- determining rotor magnetical tension (t.m.) corresponding of resulting t.e.m.,  $U_{m1dJ1} = \overline{ON''}$  [u.r.]

- establishing  $\theta$  angle from fazorial diagram and "effective" rotor reaction solenation,  $\overline{N''R} = \overline{F'_{adq}}$  for  $i_M/i=1,5..2,5$ ;

- determining of dispersion flux  $\Phi_{\sigma} = \overline{RS}$  [u.r.] and rotor magnetical tension  $\overline{U_{mR}} = \overline{TT'}$  [u.r.], resulting rotor solenation for nominal duty  $\overline{OK} = \overline{F'_{eN}}$  [u.r.];

For looseness work, due to digressions from magnetization curves or little modify at constructive dimensions, sue to increasing obtained value with approx.4-6%, resulting:

$$\overline{F'_{eN}} = (1,04 \div 1,06) \cdot \overline{F'_{eN}} \quad [u.r.] \quad (5)$$

respectively:

$$F_{eN} = \overline{F'_{eN}} \cdot U_{m0N} [A] \quad (6)$$

CONCLUSIONS

The presented method have the great advantage because allow to use modern technique of calculation and, in this way, could be known permanently the variation of excitation solenation, respectively the excitation circuit could be dimensioned optimally.

REFERENCES

1. I.Cioc, C. Nica Proiectarea masinilor electrice, Editura Didactica si Pedagogica Bucuresti 1994
2. V. Cozma Contributii privind reducerea cosumului de energie electrica la actionarea transportoarelor cu banda cu motoare de curent alternativ Teza de doctorat, 2000 Universitatea din Petrosani